Université de Montréal

Études de l'effet tunnel des spins quantiques macroscopiques

par
Solomon Akaraka Owerre

Département de physique
Faculté des arts et des sciences

Thèse présentée à la Faculté des études supérieures
en vue de l'obtention du grade de Philosophiæ Doctor (Ph.D.)
en Faculté des arts et des sciences

October, 2014

© Solomon Akaraka Owerre, 2014.

Université de Montréal
Faculté des études supérieures

Cette thèse intitulée:

Études de l'effet tunnel des spins quantiques macroscopiques

présentée par:

Solomon Akaraka Owerre

a été évaluée par un jury composé des personnes suivantes:

Andrea Bianchi,	président-rapporteur
Manu Paranjape,	directeur de recherche
Luc Vinet,	membre du jury
André-Marie Tremblay,	examinateur externe
Véronique Hussin,	représentant du doyen de la FES

Thèse acceptée le: . . . . . .

ABSTRACT

This thesis presents recent theoretical analyses together with experimental observations on macroscopic quantum tunneling and quantum-classical phase transitions of the escape rate in large spin systems. We consider biaxial ferromagnetic spin systems. Using the coordinate dependent spin coherent state path integral, we obtain the quantum phase interference and the energy splitting of these systems. We also present a lucid exposition of tunneling in antiferromagnetic exchange-coupled dimer, with easy-axis anisotropy. Indeed, we obtain the ground state, the first excited state, and the energy splitting, for both integer and half-odd integer spins. These results are then corroborated using perturbation theory and the coordinate independent spin coherent state path integral. We further present a lucid explication of the effective potential method, which enables one to map a spin Hamiltonian onto a particle Hamiltonian; we employ this method to our models, however, in the presence of an applied magnetic field. This method enables us to investigate quantum-classical phase transitions of the escape rate of these systems. We obtain the phase boundaries, as well as the crossover temperatures of these phase transitions. Furthermore, we extend our analysis to one-dimensional anisotropic Heisenberg antiferromagnet, with N periodic sites. For even N, we show that the ground state is non-degenerate and given by the coherent superposition of the two Neél states. For odd N, however, the Neél state contains a soliton; as the soliton can be placed anywhere along the ring, the ground state is, indeed, N-fold degenerate. In the perturbative limit (weak exchange interaction), quantum fluctuation stemming from the interaction term lifts this degeneracy and reorganizes the states into a band. We show that this occurs at order $2s$ in (degenerate) perturbation theory. The ground state is non-degenerate for integer spin, but degenerate for half-odd integer spin, in accordance with Kramers' theorem [72].

Keywords: Perturbation theory, effective potential, antiferromagnet, single molecule magnets, instanton, soliton, energy splitting, phase transition, path integral.

RÉSUMÉ

Dans cette thèse, nous présentons quelques analyses théoriques récentes ainsi que des observations expérimentales de l'effet tunnel quantique macroscopique et des transitions de phase classique-quantique dans le taux d'échappement des systèmes de spins élevés. Nous considérons les systèmes de spin biaxial et ferromagnétiques. Grâce à l'approche de l'intégral de chemin utilisant les états cohérents de spin exprimés dans le système de coordonnées, nous calculons l'interférence des phases quantiques et leur distribution énergétique. Nous présentons une exposition claire de l'effet tunnel dans les systèmes antiferromagnétiques en présence d'un couplage d'échange dimère et d'une anisotropie le long de l'axe de magnétisation aisé. Nous obtenons l'énergie et la fonction d'onde de l'état fondamentale ainsi que le premier état excité pour les systèmes de spins entiers et demi-entiers impairs. Nos résultats sont confirmés par un calcul utilisant la théorie des perturbations à grand ordre et avec la méthode de l'intégral de chemin qui est indépendant du système de coordonnées. Nous présentons aussi une explication claire de la méthode du potentiel effectif, qui nous laisse faire une application d'un système de spin quantique vers un problème de mécanique quantique d'une particule. Nous utilisons cette méthode pour analyser nos modèles, mais avec la contrainte d'un champ magnétique externe ajouté. La méthode nous permet de considérer les transitions classiques-quantique dans le taux d'échappement dans ces systèmes. Nous obtenons le diagramme de phases ainsi que les températures critiques du passage entre les deux régimes. Nous étendons notre analyse à une chaine de spins d'Heisenberg antiferromagnétique avec une anisotropie le long d'un axe pour N sites, prenant des conditions frontière périodiques. Pour N paire, nous montrons que l'état fondamental est non-dégénéré et donné par la superposition des deux états de Néel. Pour N impair, l'état de Néel contient un soliton, et, car la position du soliton est indéterminée, l'état fondamental est N fois dégénéré. Dans la limite perturbative pour l'interaction d'Heisenberg, les fluctuations quantiques lèvent la dégénérescence et les N états se réorganisent dans une

bande. Nous montrons qu'à l'ordre $2s$, où s est la valeur de chaque spin dans la théorie des perturbations dégénérées, la bande est formée. L'état fondamental est dégénéré pour s entier, mais deux fois dégénéré pour s un demi-entier impair, comme prévu par le théorème de Kramer[72].

Mots clés: théorie des perturbations, potentiel effectif, antiferromagnétique, instanton, soliton, de l'enchevêtrement, transition de phase, intégrale de chemin.

CURRICULUM VITÆ

Education

2014	Ph.D., in Physics; Université de Montréal
2011	M.Sc., in Physics; Perimeter Institute for Theoretical Physics (University of Waterloo)
2010	M.Sc., in Mathematical Sciences; African Institute for Mathematical Sciences (University of Cape Town)
2008	B.Sc., in Physics; Michael Okpara University of Agriculture

Publications

I) S. A. Owerre and M. B. Paranjape: "*Haldane-like antiferromagnetic spin chain in the large anisotropy limit*". Phys. Lett. A, **378**, 3066 (2014)

II) S. A. Owerre and M. B. Paranjape: "*Phase transition between quantum and classical regimes for the escape rate of dimeric molecular nanomagnets in a staggered magnetic field*". Phys. Lett. A, **378**, 1407 (2014)

III) S. A. Owerre and M. B. Paranjape: "*Macroscopic quantum tunneling and phase transition of the escape rate in spin systems*". To be published in Physics Reports. ArXiv:1403.4208 (2014)

IV) S. A. Owerre: "*Rotating Entangled States of an Exchange-Coupled Dimer of Single-Molecule Magnets*". J. Appl. Phys. **115** , 153901 (2014)

V) S. A. Owerre and M. B. Paranjape: "*Quantum-classical transition of the escape rate of a biaxial ferromagnetic spin*". J. Magn. Magn. Mater. **93**, 358, (2014)

VI) S. A. Owerre and M. B. Paranjape: "*Coordinate (in)dependence and quantum interference in quantum spin tunnelling*". Submitted to Physica B. ArXiv:1309.6615 (2014)

VII) S. A. Owerre and M. B. Paranjape: "*Macroscopic Quantum Tunnelling of Two Interacting Spins*". Phys. Rev. B, **88**, 220403(R) (2013)

VIII) S. A. Owerre: "*Spin Wave Theory of XY Model with Ring Exchange Interaction on a Triangular Lattice*". Can. J. Phys. **91**, 542 (2013)

IX) S. A. Owerre: "*Effects of Magnetic field on Macroscopic Quantum Tunnelling*". Can. J. Phys. **91**, 722, 2013

CONTENTS

LIST OF FIGURES

LIST OF APPENDICES

LIST OF ABBREVIATIONS

SMMs	Single molecule magnets
SQUID	Superconducting quantum interference devices
RHS	Right hand side
EP	Effective potential
WZ	Wess Zumino
Re	The real part of a complex function
WKB	Wentzel–Kramers–Brillouin
TAT	Thermally assisted tunneling

NOTATION

$\mathrm{sn}(x,\lambda), \mathrm{cn}(x,\lambda), \mathrm{dn}(x,\lambda)$	Jacobi elliptic functions
μ_m, μ_B, and μ	Magnetic moment, Bohr magneton and reduced mass respectively
ω_p, ω_b, and ω_0	Periodic instanton, sphaleron and vacuum instanton frequencies
$\mathcal{T}$, T, and $\mathtt{T}$	Time-ordered operator, temperature, and kinetic energy respectively
S_E, $\mathcal{S}_p$ and B	Euclidean, periodic instanton and vacuum instanton actions respectively
$\mathcal{K}(\lambda)$ and $F(\varphi,\lambda)$	Complete and incomplete elliptic integrals of the first kind
$\Pi(\gamma^2;\lambda)$	Complete elliptic integral of the third kind
λ and α	Dimensionless anisotropy and magnetic field parameters
L_E and L	Euclidean and Minkowski Lagrangian respectively
$\mathcal{P}_E$ and $\mathcal{P}$	Euclidean and Minkowski propagators respectively
$\delta(p-p')$	Dirac delta function
$\mathscr{S}^2$	2-sphere
$\mathscr{H}$	Hilbert space
τ	Euclidean or imaginary time
β	Inverse temperature (period of oscillation)
$\mathcal{E}$	Energy of a particle
U	Potential energy
$\hat{x}$	Position operator
$\hat{p}$	Momentum operator
$\hat{H}$	Hamiltonian operator
η	Frictional constant
$\mathbb{Z}$	Set of integers

I dedicate this thesis to my mother, Charity Owerre and my late father, Mark Chinyere Owerre

ACKNOWLEDGMENTS

First and foremost, I would like to thank God for His unprecedented grace and providence. His infinite mercies have been indispensable during my studies. The success of completing my Ph.D. degree program is not a personal achievement, rather it is a collective one. It will be an unforgivable act not to appreciate the people that contributed immensely to this successful journey.

This journey started back in 2010 at the African Institute for Mathematical Sciences (AIMS), Cape Town, South Africa, where I met my supervisor Prof. Manu Paranjape, when he gave his specialized course on instantons and tunneling. At this time it never came to my mind that I would be his Ph.D. student. Fortunately, I met him again at Perimeter Institute for theoretical Physics (PI), where he is a member. When I finished my masters at PI in 2011, he offered me a Ph.D. position in his group at the Université de Montréal. It was indeed a great change of scenery, and a reminiscent of his approach of teaching at AIMS, which I have invariably admired. He has a great decency and good sense of humour; he cares about his students' welfare; he pays attention to their complaints and he gives good advice like a father. I am grateful for working with him as a student and I greatly appreciate all his kindness towards me.

It goes without saying that the prestigious AIMS paved the way for this international collaboration. I would like to appreciate the support of Prof. Neil Turok during my stay at PI. Of course, it goes without saying that I benefited from the financial support of Natural Sciences and Engineering Research Council of Canada (NSERC), through my supervisor's grant, for the whole period of my studies, and from the Faculté des études supérieures et postdoctorales (FESP) and the department of physics. In the course of my Ph.D., I got some publications with my supervisor; I would like to appreciate the inputs of Prof. Sung-Sik Lee, Prof. Ian Affleck, and Prof. Richard Mackenzie, whom my supervisor conversed with, concerning my research and publications.

I'm indebted to all my friends, who were indispensable during the course of my

program. I appreciate useful discussions with Joachim Nsofini, in many areas of physical activities. He has been a very good friend since our stay at PI. I would like to appreciate a lovely lady, Kesha Fatmata Senessie, who has supported me since the beginning of my program. I would also like to thank my office mates, Gendron Marsolais Marie-Lou and Saoussen Mbarek, for their immense contribution to my student life.

Last but not least, I greatly appreciate all the support and the parental care from my family. I'm grateful for the support of my mother, Charity Owerre; my late father, Mark Chinyere Owerre; my aunt and her husband, Mr Chikezie and Dr. Mrs. Nkem Ogbonna; all my siblings, whom I cannot list their names without exceptions. Needless to say, you played a decisive role in my academic pursuit. You really inspired me. You motivated me. You continued to pray for me. I love you all and I pray that God will continue to enrich us with His divine blessing.

CHAPTER 1

INTRODUCTION

> Anyone who is not shocked by the quantum theory has not understood it.
>
> Niels Bohr

1.1 The concept of quantum tunneling

Quantum tunneling, being one of the most remarkable manifestations of quantum mechanics, is a ubiquitous phenomenon in physics. It involves the presence of a potential barrier, that is the region where the potential energy is greater than the energy of the particle. Classically, tunneling of a particle through this barrier is prohibited, as it requires the particle to have a negative kinetic energy. However, quantum mechanically, one finds a nonzero probability for finding the particle in the classically forbidden region. Thus, a quantum particle can tunnel through the barrier. The fundamental concept of this phenomenon is based on two formalisms: path integral formalism (instanton techniques) [33, 34, 39, 40, 61, 62, 64, 78, 116, 117] and Wentzel-Kramers-Brillouin (WKB) formalism [76] . In one-dimensional systems, the tunneling amplitude (whose modulus squared gives the probability) is usually computed by these two fundamental formalisms. For particle in a double well potential with two degenerate minima, the basic understanding is that in the absence of tunneling, the classical ground states of the system, which correspond to the minima of the potential, remain degenerate. Tunneling between these minima lifts the degeneracy; the true ground state and the first excited state become the symmetric and the antisymmetric linear superposition of the classical ground states respectively, with an energy splitting between them[34, 76]. In general, the two minima of the potential are not degenerate; the state with lower energy is the

true vacuum, while the state with higher energy is the false vacuum. The false vacuum is rendered unstable due to quantum tunneling; thus, the interesting object to compute is the decay rate of the false vacuum[32, 33]. Such a scenario plays a vital role in cosmology, especially in the theory of early universe and inflation. Besides, in some quantum systems, tunneling does not involve the splitting of the classical ground states or the decay of the false vacuum, but rather a dynamic oscillation of the (phase) difference between two macroscopic order parameters [35], which are separated by a thin normal layer, through tunneling of the macroscopic effective excitations, such as Cooper pairs as in Josephson effect[38, 65].

1.2 Quantum tunneling in single molecule magnets

In the last few decades, the phenomenon of macroscopic quantum tunneling has been extended to other branches of physics. Quantum tunneling of spins has been predicted in molecular magnets, such as $MnAc_{12}$, Mn_{12}, and Fe_8[24, 87, 136, 140, 145]. These single molecule magnets (SMMs) are composed of several molecular magnetic ions, whose spins are coupled by intermolecular interactions, giving rise to an effective single giant spin, which can tunnel through its magnetic anisotropy barrier; hence the name "macroscopic quantum spin tunneling[1]". The study of macroscopic quantum tunneling in these systems stems from the work of Hemmen and Sütő [136]. They studied the tunneling in a uniaxial ferromagnetic spin model with an applied magnetic field, using the WKB method. Enz and Schilling [87] considered a biaxial ferromagnetic spin model with a magnetic field via the instanton technique. Subsequently, Chudnovsky and Gunther [24] studied many ferromagnetic spin systems comprehensively, by solving the instanton trajectory of the Landau Lifshitz equation. These studies were based upon a semiclassical description, that is by representing the spin operator as a unit vector parameterized by

[1] In most literatures, macroscopic quantum tunneling refers to tunneling in a bias (metastable) potential, while macroscopic quantum coherence refers to tunneling in a potential with degenerate minima [81]. In this thesis we will use the former to refer to both systems.

spherical coordinates.

In this description, the spin is considered as a particle on a two-dimensional sphere $\mathscr{S}^2$, however, in the presence of a topological term, called the Berry's phase term or Wess-Zumino action [12, 146, 147], which effectively corresponds to the magnetic field of a magnetic monopole at the centre of the two-sphere. Based on this semi-classical description, it was predicted serendipitously, that for integer spins tunneling is allowed, while for half-odd integer spin tunneling is completely suppressed at zero (external) magnetic field [56, 86]. The vanishing of tunneling for half-odd integer spins is understood as a consequence of destructive interference between tunneling paths, which is directly related to Kramers' degeneracy[72, 95], due to the time reversal invariance of the Hamiltonian. In the presence of a magnetic field applied along the spin hard axis, Garg [1] showed that the tunneling splitting does not vanish for half-odd integer spins, rather it oscillates with the field, only vanishes at a certain critical value of the field. In this case, suppression of tunneling is not related to Kramers' degeneracy due to the presence of a magnetic field. These serendipitous theoretical predictions were subsequently observed experimentally in Fe_8 molecular cluster [125, 140, 142]. As the semiclassical approach is valid for large spin systems, an exact mapping of spin systems onto a particle problem was considered by Scharf *et al* [123] and Zaslavskii [148, 150]. They studied the exact mapping of a spin Hamiltonian onto a particle Hamiltonian, which has a mass and a potential field (Schrödinger equation). This method is called the "effective potential method". It gives the possibility of investigating spin tunneling akin to tunneling in one-dimensional double well potential. Recently, the problem of a rotating molecular magnet has attracted considerable attention. A theoretical study of this problem has been investigated for ferromagnets [29, 67], and for antiferromagnets [102].

1.3 Quantum-classical phase transitions of the escape rate

The possibility of quantum tunneling requires a very low temperature, $T \to 0$. This leads to a temperature independent transition amplitude, governed by $\Gamma = \mathcal{A}e^{-B}$, where B is the instanton action and $\mathcal{A}$ is a pre-factor. At high temperature, quantum tunneling becomes inconsequential; then the particle has the possibility of crossing over the barrier, a process called classical thermal activation, which dates back to the work of Kramers [73], for the diffusion of a particle over the barrier. A review on this subject for both particles and spin systems can be found in many literatures[31, 109, 127]. The transition amplitude for a classical thermal activation is governed by the Van't Hoff-Arrhenius Law [109], $\Gamma = \mathcal{B}e^{-\beta\Delta U}$, where ΔU is the height of the potential barrier, β is the inverse temperature, and $\mathcal{B}$ is a pre-factor.

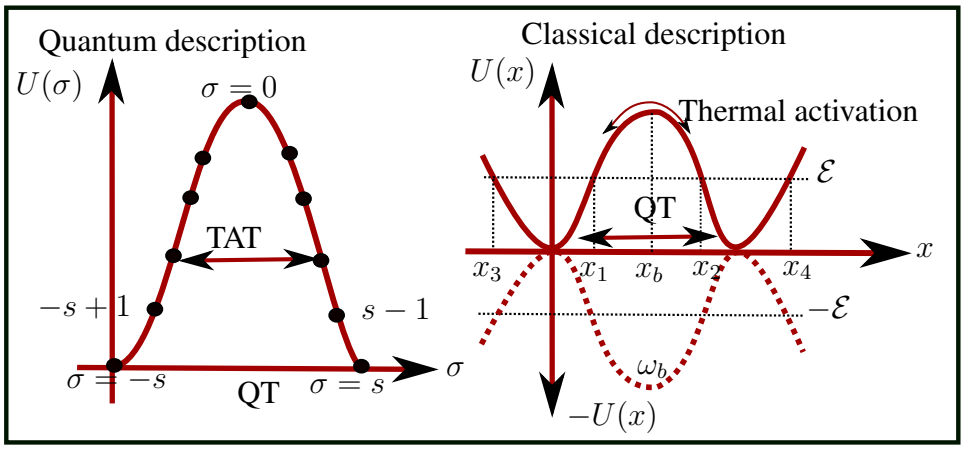

Figure 1.1: Left: Quantum description of a single spin Hamiltonian of the form $\hat{H} = -D\hat{S}_z^2 + \hat{H}_\perp$, where $D > 0$ and $\hat{H}_\perp$ is quadratic in $\hat{S}$. The free term gives a potential of $U(\sigma) = -D\sigma^2$ using the state $|\sigma\rangle$. The presence of the perturbative term $\hat{H}_\perp$ splits the two lowest degenerate ground states $\sigma = \pm s$ via quantum tunneling (QT). Transitions between existed states occur via thermal assisted quantum tunneling (TAT). Right: The description of the same Hamiltonian using instanton technique via semiclassical methods (spin coherent state path integral or the effective potential method).

The basic understanding of quantum-classical phase transitions of the escape rate is as follows: for a particle in a metastable cubic potential or double well quartic parabolic

potential, denoted by $U(x)$, with no environmental influence (dissipation), transition at finite temperature is dominated by thermon (periodic) instanton trajectory[2], whose action is denoted by $\mathcal{S}_p(\mathcal{E})$ [20], where $\mathcal{E}$ is the energy of the particle in the inverted potential $-U(x)$. The escape rate is defined by taking the Boltzmann average over tunneling probabilities at finite energy, weighed by the exponential of $\mathcal{S}_p(\mathcal{E})$ [6]. At the bottom of the barrier we have $\mathcal{S}_p(\mathcal{E}) \to S(U_{\text{min}})$, where $S(U_{\text{min}})$ is the action at the bottom of the barrier, while at the top of the barrier, $\mathcal{S}_p(\mathcal{E}) \to \mathcal{S}_0 = \beta\Delta U$, which is the action of a constant trajectory at the top of the barrier. Now, if we compare the plot of the thermon action $\mathcal{S}_p$, and that of the thermodynamic action $\mathcal{S}_0$, against temperature[20], the "critical temperature T^c" at the intersection defines the crossover or phase transition temperature from thermal regime to quantum regime.[3] If this intersection is *sharp*, T^c can be thought of as a first-order "phase transition" (crossover) temperature, from classical (thermal) to quantum regimes. At $T^c \equiv T_0^{(1)}$, there is a discontinuity in the first-derivative of the action $\mathcal{S}_p$[50]. The approximate form of this crossover temperature can be estimated by equating the quantum action $S(U_{\text{min}})$, at the bottom of the barrier, and that of the classical action at the top of the barrier $\mathcal{S}_0$, [127]:[4]

$$T_0^{(1)} = \frac{1}{\beta_0^{(1)}} = \frac{\Delta U}{S(U_{\text{min}})} = \frac{\Delta U}{2B}. \tag{1.1}$$

For a particle with a constant mass, the physical understanding for the occurrence of a sharp first-order phase transition is that the top of the barrier should be flat [27]. This condition is not generally accepted. It has been argued that the necessary condition for the occurrence of a sharp first-order phase transition is that the top of the barrier should be wider so that tunneling through the barrier from the ground state is more auspicious than that from the excited states[155]. For a particle with a position dependent mass,

[2]This is simply the solution of the imaginary time classical equation of motion with an energy $\mathcal{E}$.

[3]The thermodynamic action usually decays faster then the thermon action.

[4]Actually, the thermon action is defined over the whole period of oscillation of a particle in the inverted potential. In other words, the particle crosses the barrier twice. Thus, $B = S(U_{\text{min}})/2$ as the vacuum instanton is defined by half of the whole period.

the necessary condition for the occurrence of a sharp first-order phase transition requires the mass of the particle at the top of the barrier to be heavier than that at the bottom of the barrier. In this case tunneling from higher excited states is inauspicious. Consequently, thermal activation competes with ground state tunneling, leading to first-order phase transition. Thermally assisted tunneling (TAT), that is tunneling from excited states which reduces to ground state tunneling at $T = 0$, occurs for temperatures below $T_0^{(1)}$. In this case the particle tunnels through the barrier at the most auspicious energy $\mathcal{E}(T)$, which goes from the top of the barrier to the bottom of the barrier as the temperature decreases [27]. However, if the intersection of the $\mathcal{S}_p$ and $\mathcal{S}_0$ is *smooth*, the critical temperature is said to be of second-order, with $T^c \equiv T_0^{(2)}$. The second derivative of the thermon action has a jump at $T_0^{(2)}$. The exact form of this crossover temperature is defined as [48, 49]

$$T_0^{(2)} = \frac{1}{\beta_0^{(2)}} = \frac{\omega_b}{2\pi}, \tag{1.2}$$

where ω_b is the frequency of oscillation at the bottom of the inverted potential $-U(x)$, i.e., $\omega_b^2 = -\frac{U''(x_b)}{m}$. This formula follows from equating the Van't Hoff-Arrhenius exponential factor $\beta\Delta U$, at finite nonzero temperature, and the approximate form of the WKB exponential factor $2\pi\Delta U/\omega_b$, at zero temperature. Using functional integral approach, it was demonstrated [6, 79, 80] that in the regime $T < T_0^{(2)}$, there is a competing effect between thermal activation and quantum tunneling, which leads to TAT. For $T \gg T_0^{(2)}$, quantum tunneling is suppressed, and the assisted thermal activation becomes the dominant factor in the escape rate. For $T \approx T_0^{(2)}$, the two regimes smoothly join with a jump of the second derivative of the escape rate. Thus, $T_0^{(2)}$ corresponds to the crossover temperature from thermal regime to TAT. In term of the potential, for a constant mass particle a smooth second-order crossover is favourable with a potential with a parabolic barrier top. An alternative criterion for the first- and the second-order quantum-classical phase transitions was demonstrated by Chudnovsky [20] based on the shape of the po-

tential. He showed that for a first-order phase transition, the period of oscillation $\beta(\mathcal{E})$ is a nonmonotonic function of $\mathcal{E}$; in other words, $\beta(\mathcal{E})$ has a minimum at some point $\mathcal{E}_0 < \Delta U$ and then rises again, while for second-order phase transition, $\beta(\mathcal{E})$ is monotonically increasing with decreasing $\mathcal{E}$. Müller *et al* [97] derived a general criterion formula for investigating first- and second-order phase transitions, which is similar to the criterion formula derived by Kim [51].

1.4 Quantum tunneling in one-dimensional antiferromagnetic molecular magnets

The study of antiferromagnetic quantum spin chain is one of the most enthralling studies in quantum magnetism. Many techniques that exist in condensed matter physics today emanate from the study of quantum spin chains. The Bethe ansatz exact solution [13, 59] for a one-dimensional antiferromagnetic spin one-half chain is one of the fascinating results ever achieved in quantum magnetism. This renowned result paved the way for more theoretical and experimental studies in quantum magnetism. It also led to the development of spin wave theory for the study of the low-energy excitations in one-, two- and three-dimensional systems [8, 101], and numerous computational techniques, ranging from quantum Monte Carlo to density matrix renormalization group have been developed as a result of investigating quantum spin chains. Semiclassical methods and quantum field theory, such as spin coherent state path integral and nonlinear sigma model [54, 55] have also been applied in the study of this system.

Recently, the one-dimensional antiferromagnetic large spin ($s \gg 1$) chains (molecular magnets) has captivated researchers in this field. This system is being considered as a good candidate for investigating macroscopic quantum tunneling. Interestingly, it can be studied as an even or odd spin chain with remarkably different results. The even spin chain has been studied extensively by many authors [54, 55, 92, 94], with application to quantum computing. Quite recently, the odd spin chain has also been studied by a different approach [107]; however, in the large easy-axis anisotropy or perturbative limit. In

this case the system is frustrated, giving rise to a soliton mode as the fully anti-aligned Néel state contains a defect. In recent years, spin tunneling has been observed in many SMMs such as Fe_8 [122], $Mn_{12}Ac$ [45, 132, 153], ferrimagnetic nanoparticles [141], antiferromagnetic particles [9, 47, 130], antiferromagnetic exchange coupled dimer $[Mn_4]_2$ [121, 134], and antiferromagnetic ring clusters with even number of spins [92, 94, 129]. These molecular magnets also play a decisive role in quantum computing [83, 131].

CHAPTER 2

PATH INTEGRAL

> If you think you understand
> quantum mechanics, you don't
> understand quantum mechanics.
>
> Richard Feynman

2.1 Introduction

In this chapter we commence with the basic tools that will be essential in order the tackle most of the problems in this thesis. This chapter forms the basis of most of the analyses that will be presented. The path integral formulation of quantum mechanics will be an indispensable tool for understanding most of the analyses. This formulation is an elegant alternative method of quantum mechanics. It replicates the Schrödinger formulation of quantum mechanics, and the principle of least action in classical mechanics. In this method the classical action enters into a quantum object — the transition amplitude, thereby allowing for a quantum interpretation of a solution of the classical equation of motion.

The part integral formulation can be understood as follows: classically, there is a unique trajectory or path for a particle; quantum mechanically, a particle follows an infinite set of possible trajectories to go from an initial state, say $|x\rangle$ at $t = 0$ to a final state, say $|x'\rangle$ at time $t = t'$. The sum over all the possible paths (histories of the particle) appropriately weighted, determines the quantum amplitude of the transition. The weight for each path is exactly the phase corresponding to the exponential of the classical action of the path, multiplied by the imaginary number i in units of $\hbar$. In this chapter we will derive this quantum transition amplitude as a path integral. This chapter is organized as

follows: the path integral formulation of quantum mechanics will be derived in Sec.(2.2), from the first principle using position and momentum eigenstates. A direct application of this formalism to the tunneling of a particle in a double well potential will be reviewed in Sec.(2.2.2). As the original path integral formalism is infeasible for spin systems, we will derive the appropriate path integral for spin systems in Sec.(2.3.1). This path integral will be derived in two forms: the coordinate independent form and the coordinate dependent form. Finally, we will present a concluding remark.

2.2 Position state path integral

Let us begin by considering the Lagrangian of a single particle in one dimension:

$$L = \frac{1}{2}m\left(\frac{dx}{dt}\right)^2 - U(x), \tag{2.1}$$

where x is the position coordinate of the particle, m is the mass of the particle, and $U(x)$ is the potential energy of the particle. The first term in Eqn.(2.1) is the kinetic energy term which will be denoted by $\mathtt{T}$; in other words, the Lagrangian is given by $L = \mathtt{T} - U(x)$. For a classical particle, the unique path is determined from the Euler-Lagrange equation of motion:

$$\frac{d}{dt}\left(\frac{\partial L}{\partial \dot{x}}\right) - \frac{\partial L}{\partial x} = 0; \quad \dot{x} = \frac{dx}{dt}. \tag{2.2}$$

Quantum mechanical systems are customarily described with Hamiltonian functions; the corresponding Hamiltonian via Legendre transformation is given by

$$\hat{H} = \frac{\hat{p}^2}{2m} + U(\hat{x}). \tag{2.3}$$

In quantum mechanics, the position $\hat{x}$ and the momentum $\hat{p}$ operators form a complete, orthonormal set of states, defined as

$$\hat{x}\,|x\rangle = x\,|x\rangle\,; \quad \hat{p}\,|p\rangle = p\,|p\rangle\,; \tag{2.4}$$

$$\langle x'|x\rangle = \delta(x'-x); \quad \langle p'|p\rangle = \delta(p'-p). \tag{2.5}$$

It is easy to show that:

$$\langle x|p\rangle = e^{ipx/\hbar}, \tag{2.6}$$

which follows from the position state representation of the momentum operator $\hat{p} = -i\frac{d}{dx}$. The resolution of identities are:

$$\int dx\,|x\rangle\,\langle x| = \hat{\mathbf{I}} = \int \frac{dp}{2\pi\hbar}\,|p\rangle\,\langle p|\,. \tag{2.7}$$

The transition amplitude (propagator) of a particle that starts at the point x at $t = 0$ to the final point x' at some time $t = t'$ is given by

$$\mathcal{P}(x',t';x,0) = \langle x'|e^{-i\hat{H}t'/\hbar}|x\rangle\,. \tag{2.8}$$

The above amplitude can be written as a sum over all paths, by partitioning the time interval into N slices. This is reminiscent of Riemann integral. Indeed, the unitary operator $e^{-i\hat{H}t'}$ can be expressed as $[e^{-i\hat{H}t'/N}]^N = [e^{-i\hat{H}\epsilon}]^N$, where $\epsilon = t'/N$. One can now write Eqn.(2.8) as

$$\mathcal{P}(x',t';x,0) = \langle x'|[e^{-i\hat{H}\epsilon/\hbar}]^N|x\rangle = \langle x'|\underbrace{e^{-i\hat{H}\epsilon/\hbar}e^{-i\hat{H}\epsilon/\hbar}\cdots e^{-i\hat{H}\epsilon/\hbar}}_{\text{N times}}|x\rangle\,. \tag{2.9}$$

Inserting the position complete set of states, Eqn.(2.7) between each exponential in Eqn.(2.9), one obtains

$$\begin{aligned}
\mathcal{P} &= \langle x'|e^{-i\hat{H}\epsilon/\hbar}\int dx_{N-1}|x_{N-1}\rangle\langle x_{N-1}|e^{-i\hat{H}\epsilon/\hbar}\int dx_{N-2}|x_{N-2}\rangle\langle x_{N-2}| \\
&\cdots\int dx_2|x_2\rangle\langle x_2|e^{-i\hat{H}\epsilon/\hbar}\int dx_1|x_1\rangle\langle x_1|e^{-i\hat{H}\epsilon/\hbar}|x\rangle, \\
&= \int dx_1 dx_2\cdots dx_{N-1}\,\langle x'|e^{-i\hat{H}\epsilon/\hbar}|x_{N-1}\rangle\,\langle x_{N-1}|e^{-i\hat{H}\epsilon/\hbar}|x_{N-2}\rangle \\
&\cdots\langle x_1|e^{-i\hat{H}\epsilon/\hbar}|x\rangle\,, \\
&= \int\prod_{j=1}^{N-1}dx_j\Big[\prod_{j=0}^{N-1}\mathcal{P}_{x_{j+1},x_j}\Big];\quad x'=x_N; x_0=x;
\end{aligned} \tag{2.10}$$

where $\mathcal{P}_{x_{j+1},x_j}$ is the propagator for a sub-interval given by

$$\mathcal{P}_{x_{j+1},x_j} = \langle x_{j+1}|e^{-i\hat{H}\epsilon/\hbar}|x_j\rangle = \langle x_{j+1}|1-i\hat{H}\epsilon/\hbar+O(\epsilon^2)|x_j\rangle\,, \tag{2.11}$$

$$= \langle x_{j+1}|x_j\rangle - \frac{i\epsilon}{\hbar}\langle x_{j+1}|\hat{H}|x_j\rangle + O(\epsilon^2). \tag{2.12}$$

Inserting the complete set of momentum states, Eqn.(2.7) on the second term in Eqn.(2.12) and using Eqn.(2.6) one obtains

$$\begin{aligned}
\mathcal{P}_{x_{j+1},x_j} &= \int\frac{dp_j}{2\pi}e^{ip_j(x_{j+1}-x_j)/\hbar}\left(1-\frac{i\epsilon}{\hbar}\left(\frac{p_j^2}{2m}+U(\bar{x}_j)\right)+O(\epsilon^2)\right), \\
&= \int\frac{dp_j}{2\pi}e^{ip_j(x_{j+1}-x_j)/\hbar}e^{-\frac{i\epsilon}{\hbar}H(p_j,\bar{x}_j)}(1+O(\epsilon^2)),
\end{aligned} \tag{2.13}$$

where $\bar{x}_j = \frac{1}{2}(x_{j+1}+x_j)$. Substituting Eqn.(2.13) into Eqn.(2.10) yields

$$\mathcal{P}(x',t';x,0) = \int\prod_{j=1}^{N-1}dx_j\int\prod_{j=0}^{N-1}\frac{dp_j}{2\pi}\exp\frac{i\epsilon}{\hbar}\sum_{j=0}^{N-1}(p_j\dot{x}_j - H(p_j,\bar{x}_j)), \tag{2.14}$$

where $\dot{x}_j = (x_{j+1} - x_j)/\epsilon$. In the limit of infinite interval points $N \to \infty$, Eqn.(2.14) becomes

$$\mathcal{P}(x', t'; x, 0) = \int \mathcal{D}p(t)\mathcal{D}x(t) \exp i \int_0^{t'} dt(p\dot{x} - H(p, x)), \tag{2.15}$$

where $\mathcal{D}p(t) = \lim_{N\to\infty} \prod_{j=0}^{N-1} \frac{dp_j}{2\pi}$ and $\mathcal{D}x(t) = \lim_{N\to\infty} \prod_{j=1}^{N-1} dx_j$. Eqn.(2.15) defines the phase space (p, x) path integral. For a Hamiltonian system that is quadratic in p, such as defined in Eqn.(2.3), the momentum integration in Eqn.(2.15) is a Gaussian integral, which can be easily performed. Thus, one finally arrives at the configuration space path integral [39, 40]:

$$\mathcal{P}(x', t'; x, 0) = \langle x'|e^{-i\hat{H}t'/\hbar}|x\rangle = \int \mathcal{D}x(t)\, e^{iS[x(t)]/\hbar}, \tag{2.16}$$

where $\mathcal{D}x(t)$ is the measure for integration over all possible classical paths $x(t)$ that satisfy the boundary conditions: $x(0) = x$; $x(t') = x'$. The classical action is given by

$$S[x(t')] = \int_0^{t'} dtL, \tag{2.17}$$

where L is the Lagrangian of the system, defined in Eqn.(2.1). We have written down the path integral for a one-dimensional particle, generalization to higher dimensions is straightforward. The left hand side of Eqn.(2.16) corresponds to a quantum object, while the right hand side contains a classical integrand — the classical action. The well-known classical equation of motion in Eqn.(2.2) can be recovered in a very simple way from Eqn.(2.16). In the semiclassical limit, *i.e.*, $\hbar \to 0$, the phase $e^{iS[x(t)]/\hbar}$ oscillates very rapidly in such a way that nearly all paths cancel each other. The main contribution to the path integral comes from the paths for which the action is stationary, *i.e.*, $\delta S[x(t)] = 0$, which yields the classical equation of motion Eqn.(2.2).

2.2.1 Imaginary time path integral formalism

The main motivation of imaginary time propagator comes from the partition function in statistical mechanics, which is given by

$$Z = \text{Tr}(e^{-\beta \hat{H}}), \tag{2.18}$$

where $\beta = 1/T$ is the inverse temperature of the system. Inserting the position resolution of identity in Eqn.(2.7) into the RHS of Eqn.(2.18) gives

$$Z = \int dx \mathcal{P}(x, \beta; x, 0), \tag{2.19}$$

where

$$\mathcal{P}(x, \beta; x, 0) = \langle x | e^{-\beta \hat{H}} | x \rangle \, . \tag{2.20}$$

Suppose we consider the time in Eqn.(2.16) to be purely imaginary, which can be written as $t' = -i\beta$, where β is real. Then, substituting into Eqn.(2.16) we obtain the propagator evaluated at imaginary time [89, 116, 139]:

$$\mathcal{P}_E = \langle x' | e^{-\beta \hat{H}/\hbar} | x \rangle = \int \mathcal{D}x(\tau) \, e^{-S_E[x]/\hbar}, \tag{2.21}$$

where the action is now given by the appropriate analytical continuation of the action, nominally defined as

$$S_E[x] = \int_0^{-i\beta} dt \left[\frac{1}{2} m \left(\frac{dx}{dt} \right)^2 - U(x) \right]. \tag{2.22}$$

Indeed, setting $x' = x$ in Eqn.(2.21) yields the partition function Eqn.(2.20). Thus, the propagator continued to imaginary time gives the partition function. This method is expedient in finding the ground state of a physical system in statistical and condensed

matter physics. The analytical continuation is obtained by defining a real variable $\tau = it$, which is called the "imaginary or Euclidean time"; we see that τ and t are related as follows: $t : 0 \to -i\beta$, $\tau : 0 \to \beta$. Thus, $S_E[x(\tau)] = -iS[x(t \to -i\tau)]$. Typically, if $S[x(t)] = \int dt(\mathtt{T} - U)$, the Euclidean action is given by $S_E[x(\tau)] = \int d\tau(\mathtt{T} + U)$, as the kinetic energy changes sign with the continuation to imaginary time. The Euclidean action and the Lagrangian are

$$S_E[x(\tau)] = \int_{-\beta/2}^{\beta/2} d\tau L_E; \quad L_E = \frac{1}{2}m\left(\frac{dx}{d\tau}\right)^2 + U(x), \tag{2.23}$$

using time translation invariance. The boundary conditions for the imaginary time propagator are $x(-\beta/2) = x$ and $x(\beta/2) = x'$. This analysis of imaginary time propagator plays a decisive role in tunneling problems such as that of a particle in a one dimensional double well potential, since the period of oscillation or the momentum of the particle is imaginary in the tunneling region $\mathcal{E} < \Delta U$[76, 139], which is neatly compensated by the imaginary time. Thus, it is almost always convenient to use imaginary time corresponding to the replacement $t \to -i\tau$ [116, 139] when considering tunneling problems.

2.2.2 Instantons in the double well potential

In many textbooks of quantum mechanics, tunneling (barrier penetration) is usually studied using the WKB method. In this case the WKB exponent is imaginary; the wave function in the tunneling region becomes

$$\psi(x) \propto \frac{1}{\sqrt{|p|}} \exp\left[-\int_{-x_1}^{x_1} \frac{|p|}{\hbar} dx\right], \tag{2.24}$$

where $p = \sqrt{2m(U(x) - \mathcal{E})}$ and $\pm x_1$ are the momentum and the classical turning points $U(\pm x_1) = \mathcal{E}$ respectively. At the ground state, the energy splitting is given by [76, 139]

$$\Delta = \frac{\hbar\omega}{\sqrt{e\pi}} \exp\left[-\int_{-a}^{a} \frac{|p|}{\hbar} dx\right], \tag{2.25}$$

where $\pm a$ are such that $U(\pm a) = \mathcal{E}_0$. The instanton approach, however, uses the imaginary time formulation of path integral to find this ground state energy splitting. If we consider the classical equation of motion in imaginary time $\delta S_E = 0$ we get

$$m\ddot{x} = \frac{dU(x)}{dx}, \quad \text{where} \quad \ddot{x} \equiv \frac{d^2x}{d\tau^2}, \tag{2.26}$$

which is the equation of motion with $-U(x)$. In other words, it describes the motion of a particle in an inverted potential as shown in Fig.(2.1). Upon integration, one finds that the analog of the total "energy" is conserved:

$$\mathcal{E} = \frac{1}{2}m\left(\frac{dx}{d\tau}\right)^2 - U(x). \tag{2.27}$$

There are at least three possible solutions of this equation of motion. The first solution

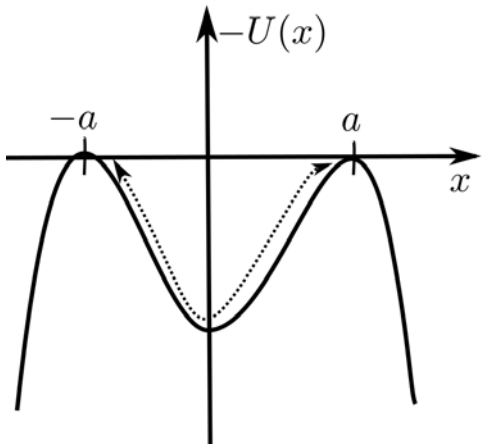

Figure 2.1: A sketch of an inverted double well potential with two minima at $\pm a$. There are two trivial solutions corresponding to a fixed motion of the particle at the top of the left or right hill of the potential. Tunneling is achieved by a nontrivial solution in which the particle starts at the top of the left hill at $\tau \to -\infty$ and roll through the dashed line and emerges at the top of the right hill at $\tau \to +\infty$. Such a solution is called an instanton.

corresponds to a particle sitting on the top of the left hill in Fig.(2.1) $x = -a$; the second solution corresponds to a particle sitting on the top of the right hill $x = a$. These are

constant solutions which do not give any tunneling. However, there is a third solution in which the particle starts at the left hill at $\tau \to -\infty$, rolls over through the dashed line, and finally arrives at the right hill at $\tau \to \infty$. This solution corresponds exactly to the barrier penetration in the WKB method. Such trajectory mediates tunneling and it is called an instanton. Quantum mechanically, the propagator for this instanton trajectory is given by

$$\mathcal{P}\left(-a, -\frac{\beta}{2}; a, \frac{\beta}{2}\right) = \langle a|e^{-\beta\hat{H}/\hbar}|-a\rangle\,. \tag{2.28}$$

For instance, the potential could be taken to be

$$U(x) = \frac{\omega_0^2}{4}(x^2 - a^2)^2, \tag{2.29}$$

but it is actually not necessary to make a specific choice, just the general form pictured in Fig.2.1 needs to be satisfied. Tunneling between the two minima of $U(x)$ requires the computation of the transition amplitudes

$$\langle \pm a|e^{-\beta\hat{H}/\hbar}|-a\rangle\,. \tag{2.30}$$

In order to calculate this amplitude, one has to know the solution of the classical equation of motion that obeys the boundary condition of Eqn.(2.21) as $\beta \to \infty$. There are two trivial solutions corresponding to no motion with the particle fixed at the top of the left or right hill of the potential. Tunneling is achieved by a nontrivial solution in which the particle starts at the top of the left hill at $\tau \to -\infty$, roll through the dashed line in Fig.(2.1), and emerges at the top of the right hill at $\tau \to +\infty$. This nontrivial solution has zero "energy" $\mathcal{E} = 0$ since initially it starts at the top of the hill at $-a$ where the potential is zero and its kinetic energy is zero. The solution of Eqn.(2.27) corresponding

to the explicit potential Eqn. (2.29), is given by [89, 116]

$$x(\tau) = a \tanh[\frac{\omega_0}{2}(\tau - \tau_0)]; \quad \omega_0^2 = \gamma a^2/m; \tag{2.31}$$

where τ_0 is an integration constant which corresponds to the time at which the solution crosses $x = 0$. The action for the solution is

$$\begin{aligned} B &= \int_{-\infty}^{\infty} d\tau \left[\frac{1}{2} m \left(\frac{dx}{d\tau} \right)^2 + U(x) \right], & (2.32) \\ &= m \int_{-\infty}^{\infty} d\tau \left(\frac{dx}{d\tau} \right)^2 = \frac{2\sqrt{2m}}{3} \omega_0 a^2, & (2.33) \end{aligned}$$

where $\mathcal{E} = 0$ from Eqn.(2.27) is used in the second line, together with Eqn.(2.31). In the method of steepest descent, the path integral, Eqn.(2.21) is dominated by the path which passes through the configuration for which the action is stationary, *i.e.*, Eqn.(2.31); the integral is given by the Gaussian approximation about the stationary point. Then, the one instanton contribution to the transition amplitude is [33, 34]

$$\langle a | e^{-\beta \hat{H}/\hbar} | -a \rangle \propto e^{-B/\hbar} [1 + O(\hbar)]. \tag{2.34}$$

Indeed, one must consider other critical points which correspond to a dilute instanton gas. The justification of the dilute instanton gas approximation is beyond the purview of this thesis, we refer the reader to lucid expositions of the subject in [33, 34]. The upshot is that one must sum over all sequences of one instanton followed by any number of anti-instanton/instanton pairs; the total number of instantons and anti-instantons is odd for the transition $-a \leftrightarrow a$, but even for the transition $-a \rightarrow -a$ ($a \rightarrow a$). The result of this summation yields [34]

$$\langle \pm a|e^{-\beta\hat{H}/\hbar}|-a\rangle = \mathcal{N}\frac{1}{2}[\exp(\mathscr{D}\beta e^{-B/\hbar}) \mp \exp(-\mathscr{D}\beta e^{-B/\hbar})], \tag{2.35}$$

where $\mathcal{N}$ is the overall normalisation including the square root of the free determinant, which is given by $Ne^{-\beta\mathcal{E}_0}$, where $\mathcal{E}_0 = \frac{1}{2}\hbar\omega_0$ is the unperturbed ground state energy and N is a constant from the ground state wave function. $\mathscr{D}$ is the ratio of the square root of the determinant of the operator governing the second order fluctuations about the instanton excluding the time translation zero mode, and that of the free determinant. It can in principle be calculated. A zero mode occurring because of time translation invariance, is not integrated over, and is taken into account by integrating over the Euclidean time position of the occurrence of the instanton giving rise to the factor of β. The left hand side of Eqn.(2.35) can also be written as

$$\langle \pm a|e^{-\beta\hat{H}/\hbar}|-a\rangle = \sum_n \langle \pm a|n\rangle \langle n|-a\rangle e^{-\beta\mathcal{E}_n}, \tag{2.36}$$

where $\hat{H}|n\rangle = \mathcal{E}_n|n\rangle$. Taking the upper sign on both sides of Eqns.(2.35) and (2.36) and comparing the terms, one finds that the non-perturbative energy splitting between the ground and the first excited states is given by

$$\Delta = \mathcal{E}_1 - \mathcal{E}_0 = 2\hbar\mathscr{D}e^{-B/\hbar}. \tag{2.37}$$

In a similar fashion, by comparing the coefficients one obtains symmetric ground state

$$|\mathcal{E}_0\rangle = \frac{1}{\sqrt{2}}\left(|a\rangle + |-a\rangle\right), \tag{2.38}$$

and an antisymmetric first excited state

$$|\mathcal{E}_1\rangle = \frac{1}{\sqrt{2}}\left(|a\rangle - |-a\rangle\right). \tag{2.39}$$

2.3 Spin coherent state path integral

2.3.1 Coordinate independent form

In this section we will derive the path integral formulation that is applicable to spin systems. The basic idea of path integral formulation will be retained, however, instead of the orthogonal position $|x\rangle$ and momentum $|p\rangle$ basis, a convenient way to derive the spin path integral is to introduce spin coherent states [71, 84, 115, 119]. Let $|s, s\rangle$ be the highest weight vector in a particular representation of the rotation group, taken as its simply connected covering group $SU(2)$. This state is an eigenstate of the operators $\hat{S}_z$ and $\hat{\mathbf{S}}$:

$$\hat{S}_z\,|s,s\rangle \;\; = s\,|s,s\rangle\,; \quad \hat{\mathbf{S}}^2\,|s,s\rangle = s(s+1)\,|s,s\rangle\,. \tag{2.40}$$

The spin operators $\hat{S}_i$, $i = x, y, z$ form an irreducible representation of the Lie algebra of $SU(2)$,

$$[\hat{S}_i, \hat{S}_j] = i\epsilon_{ijk}\hat{S}_k, \tag{2.41}$$

where ϵ_{ijk} is the totally antisymmetric tensor symbol and summation over repeated indices is implied in Eqn.(2.41). The coherent state in $2s+1$ dimensional Hilbert space is defined as[43, 44, 71, 84, 115, 152]

$$|\hat{\mathbf{n}}\rangle = e^{i\theta\hat{\mathbf{m}}\cdot\hat{\mathbf{S}}}\,|s,s\rangle = \sum_{m=-s}^{s} \mathcal{N}^s(\hat{\mathbf{n}})_{ms}\,|s,m\rangle\,, \tag{2.42}$$

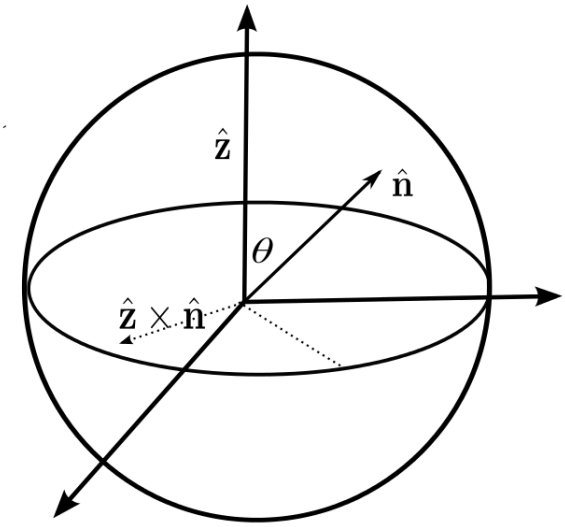

Figure 2.2: The directions of the unit vectors $\hat{\mathbf{z}}$ and $\hat{\mathbf{n}}$ on a two-sphere .

where $\hat{\mathbf{n}} = (\cos\phi\sin\theta, \sin\phi\sin\theta, \cos\theta)$ is a unit vector, *i.e.*, $\hat{\mathbf{n}}^2 = 1$, and $\hat{\mathbf{m}} = (\hat{\mathbf{n}} \times \hat{\mathbf{z}})/|\hat{\mathbf{n}} \times \hat{\mathbf{z}}|$ is a unit vector orthogonal to $\hat{\mathbf{n}}$, where $\hat{\mathbf{z}}$ is the quantization axis pointing from the origin to the north pole of a unit sphere and $\hat{\mathbf{n}} \cdot \hat{\mathbf{z}} = \cos\theta$ as shown in Fig.(2.2). This state corresponds to a rotation of $\hat{S}_z$ state, *i.e.*, $|s, s\rangle$, to a state with a quantization axis along $\hat{\mathbf{n}}$ on a two-dimensional sphere $\mathscr{S}^2 = SU(2)/U(1)$. The matrices $\mathcal{N}^s(\hat{\mathbf{n}})$ satisfy the relation

$$\mathcal{N}^s(\hat{\mathbf{n}}_1)\mathcal{N}^s(\hat{\mathbf{n}}_2) = \mathcal{N}^s(\hat{\mathbf{n}}_3)e^{-i\mathcal{G}(\hat{\mathbf{n}}_1,\hat{\mathbf{n}}_2,\hat{\mathbf{n}}_3)\hat{S}_z}, \tag{2.43}$$

where $\mathcal{G}(\hat{\mathbf{n}}_1, \hat{\mathbf{n}}_2, \hat{\mathbf{n}}_3)$ is the area of a spherical triangle with vertices $\hat{\mathbf{n}}_1$,$\hat{\mathbf{n}}_2$, and $\hat{\mathbf{n}}_3$, as shown in Fig.(2.3). Eqn.(7.50) is however not a group multiplication, thus the matrices $\mathcal{N}^s(\hat{\mathbf{n}})$ do not form a group representation. Unlike the position and momentum eigenstates in Eqn.(2.5), the inner product of two coherent states are non-orthogonal:

$$\langle\hat{\mathbf{n}}'|\hat{\mathbf{n}}\rangle = e^{-is\mathcal{G}(\hat{\mathbf{n}},\hat{\mathbf{n}}',\hat{\mathbf{z}})}[\frac{1}{2}(1 + \hat{\mathbf{n}} \cdot \hat{\mathbf{n}}')]^s. \tag{2.44}$$

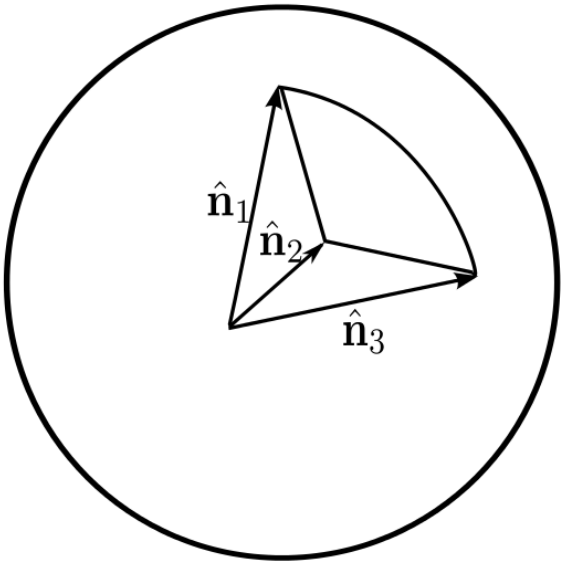

Figure 2.3: The directions of the unit vectors $\hat{\mathbf{n}}_1, \hat{\mathbf{n}}_2, \hat{\mathbf{n}}_3$ forming the area of a spherical triangle.

It has the following property:

$$\hat{\mathbf{n}} \cdot \hat{\mathbf{S}} \left|\hat{\mathbf{n}}\right\rangle = s \left|\hat{\mathbf{n}}\right\rangle \Rightarrow \left\langle\hat{\mathbf{n}}\right|\hat{\mathbf{S}}\left|\hat{\mathbf{n}}\right\rangle = s\hat{\mathbf{n}}. \tag{2.45}$$

The resolution of identity is given by

$$\hat{\mathbf{I}} = \frac{2s+1}{4\pi} \int d^3\hat{\mathbf{n}}\delta(\hat{\mathbf{n}}^2 - 1) \left|\hat{\mathbf{n}}\right\rangle \left\langle\hat{\mathbf{n}}\right|, \tag{2.46}$$

where $\hat{\mathbf{I}}$ is a $(2s+1) \times (2s+1)$ identity matrix, and the delta function ensures that $\hat{\mathbf{n}}^2 = 1$. For any spin Hamiltonian, $\hat{H}(\hat{\mathbf{S}})$, the imaginary time propagator can be written as

$$\mathcal{P}(\hat{\mathbf{n}}', \beta; \hat{\mathbf{n}}, 0) = \left\langle\hat{\mathbf{n}}'\right|e^{-\beta\hat{H}(\hat{\mathbf{S}})}\left|\hat{\mathbf{n}}\right\rangle. \tag{2.47}$$

The derivation of path integral follows as usual by discretizing the time into N slices and inserting the completeness relation Eqn.(2.46). This yields

$$\mathcal{P}(\hat{\mathbf{n}}', \beta; \hat{\mathbf{n}}, 0) = \int \prod_{j=1}^{N-1} d\chi_j \Big[\prod_{j=0}^{N-1} \langle \hat{\mathbf{n}}_{j+1} | e^{-\epsilon \hat{H}(\hat{\mathbf{S}})} | \hat{\mathbf{n}}_j \rangle \Big], \tag{2.48}$$

$$= \int \prod_{j=1}^{N-1} d\chi_j \Big[\prod_{j=0}^{N-1} \langle \hat{\mathbf{n}}_{j+1} | \hat{\mathbf{n}}_j \rangle - i\epsilon \langle \hat{\mathbf{n}}_{j+1} | \hat{H} | \hat{\mathbf{n}}_j \rangle + O(\epsilon^2) \Big], \tag{2.49}$$

with $\hat{\mathbf{n}}' = \hat{\mathbf{n}}_N$; $\hat{\mathbf{n}}_0 = \hat{\mathbf{n}}$; $d\chi_j = \frac{2s+1}{4\pi} d^3\hat{\mathbf{n}}_j \delta(\hat{\mathbf{n}}_j^2 - 1)$. We have that

$$\frac{\langle \hat{\mathbf{n}}_{j+1} | \hat{H} | \hat{\mathbf{n}}_j \rangle}{\langle \hat{\mathbf{n}}_{j+1} | \hat{\mathbf{n}}_j \rangle} \approx \langle \hat{\mathbf{n}}_j | \hat{H} | \hat{\mathbf{n}}_j \rangle ; \quad \langle \hat{\mathbf{n}}_{j+1} | \hat{\mathbf{n}}_j \rangle = e^{-is\mathcal{G}(\hat{\mathbf{n}}_j, \hat{\mathbf{n}}_{j+1}, \hat{\mathbf{z}})} [\frac{1}{2}(1 + \hat{\mathbf{n}}_j \cdot \hat{\mathbf{n}}_{j+1})]^s. \tag{2.50}$$

In the continuum limit $N \to \infty$, $\epsilon \to 0$, Eqn.(2.49) becomes [43, 152]

$$\mathcal{P}(\hat{\mathbf{n}}', \beta; \hat{\mathbf{n}}, 0) = \lim_{N \to \infty} \int \mathcal{D}\hat{\mathbf{n}} e^{-S_E(\hat{\mathbf{n}})}, \tag{2.51}$$

where $S_E(\hat{\mathbf{n}})$ is given by

$$-S_E(\hat{\mathbf{n}}) = -is \sum_{i=0}^{N-1} \mathcal{G}(\hat{\mathbf{n}}_j, \hat{\mathbf{n}}_{j+1}, \hat{\mathbf{z}}) + s \sum_{i=0}^{N-1} \ln \left(\frac{1}{2}(1 + \hat{\mathbf{n}}_j \cdot \hat{\mathbf{n}}_{j+1}) \right) - \epsilon \sum_{i=0}^{N-1} U(\hat{\mathbf{n}}_j), \tag{2.52}$$

where $U(\hat{\mathbf{n}}_j) = \langle \hat{\mathbf{n}}_j | \hat{H} | \hat{\mathbf{n}}_j \rangle$.

For any closed path on $\mathscr{S}^2$, the first term in Eqn.(2.52) which is imaginary is the sum of the areas of the N contiguous spherical triangles. It leads to the history of the spin trajectory. It is the total area of the topological half-sphere $\frac{1}{2}\mathscr{S}^2$, with cap Σ, bounded by the trajectory Ω, parameterized by $\hat{\mathbf{n}}(\tau)$. There are two caps Σ^+ and Σ^- on $\mathscr{S}^2$, whose

areas differ by 4π, *i.e.*

$$\mathcal{A}(\Sigma^+) = 4\pi - \mathcal{A}(\Sigma^-) = \lim_{N\to\infty} \sum_{j=0}^{N-1} \mathcal{G}(\hat{\mathbf{n}}_j, \hat{\mathbf{n}}_{j+1}, \hat{\mathbf{z}}), \tag{2.53}$$

$$= \int_{\frac{1}{2}\mathscr{S}^2} d\tau d\xi\, \hat{\mathbf{n}}(\tau,\xi) \cdot [\partial_\tau \hat{\mathbf{n}}(\tau,\xi) \times \partial_\xi \hat{\mathbf{n}}(\tau,\xi)] \equiv S_{WZ}, \tag{2.54}$$

This term is called the Wess-Zumino (WZ) action [43, 44, 100, 146, 147]. It is reminiscent of the Berry phase in condensed matter terminology or the Chern-Simons term in high energy physics. $\hat{\mathbf{n}}(\tau)$ has been extended over a topological half-sphere $\frac{1}{2}\mathscr{S}^2$ in the variables τ, ξ. In the topological half-sphere we define $\hat{\mathbf{n}}$ with the boundary conditions

$$\hat{\mathbf{n}}(\tau,0) = \hat{\mathbf{n}}(\tau); \quad \hat{\mathbf{n}}(\tau,1) = \hat{\mathbf{z}}; \tag{2.55}$$

so that the original configuration lies at the equator and the point $\xi = 1$ is topologically compactified by the boundary condition. This can be easily obtained by imagining that the original closed loop $\hat{\mathbf{n}}(\tau)$ at $\xi = 0$ is simply pushed up along the meridians to $\hat{\mathbf{n}}(\tau) = \hat{\mathbf{z}}$ at $\xi = 1$. The Wess-Zumino term S_{WZ} originates from the non-orthogonality of spin coherent states in Eqn.(2.44). Geometrically, it defines the area of the closed loop on the spin space, defined by the nominally periodic, original configuration $\hat{\mathbf{n}}(\tau)$. The ambiguity of modulo 4π in Eqn.(2.53), which corresponds to different ways of pushing the original configuration up, can give different values for the area enclosed by the closed loop as one can imagine that the closed loop englobes the whole two sphere any integer number of times, but this ambiguity has no physical significance since $e^{i4\pi s} = 1$ for integer and half-odd integer s. Consequently, in the continuum limit, the action becomes

$$S_E[\hat{\mathbf{n}}] = isS_{WZ} + \int d\tau U(\hat{\mathbf{n}}(\tau)); \quad U(\hat{\mathbf{n}}(\tau)) = \langle \hat{\mathbf{n}}|\hat{H}|\hat{\mathbf{n}}\rangle\,; \tag{2.56}$$

where the Wess-Zumino (WZ) action, S_{WZ} is given by Eqn.(2.54)[1]. The action, Eqn.(2.56)

[1] An alternative way of deriving this equation can be found in [15].

is valid for semiclassical spin systems whose phase space is $\mathscr{S}^2$. It is the starting point for studying macroscopic quantum spin tunneling between the minima of the energy $U(\hat{\mathbf{n}})$.

2.3.2 Coordinate dependent form

Most often a coordinate dependent version of Eqn.(2.56) is used in condensed matter literatures. In this section we will show how one can use any coordinate system of interest. In subsequent chapters, we will show that the coordinate independent form can, indeed, replicate all the known results in quantum spin tunneling. Since the spin particle lives on a two-sphere, the most convenient choice of coordinate are spherical polar coordinates. The unit vector in these coordinates can be parameterize as $\hat{\mathbf{n}}(\tau,\xi) = (\cos\phi(\tau)\sin\theta_\xi(\tau), \sin\phi(\tau)\sin\theta_\xi(\tau), \cos\theta_\xi(\tau))$, with $\theta_\xi(\tau) = (1-\xi)\theta(\tau)$, which satisfies the boundary conditions, Eqn.(2.55) at $\xi = 0$ and $\xi = 1$. Then

$$\partial_\tau \hat{\mathbf{n}} = \hat{\boldsymbol{\theta}}\dot{\theta}_\xi(\tau) + \hat{\boldsymbol{\phi}}\sin\theta_\xi(\tau)\dot{\phi}(\tau), \tag{2.57}$$

and

$$\partial_\xi \hat{\mathbf{n}} = \hat{\boldsymbol{\theta}}(-\theta(\tau)), \tag{2.58}$$

where $\hat{\boldsymbol{\theta}}$ and $\hat{\boldsymbol{\phi}}$ are the usual polar and azimuthal unit vectors which form an orthogonal triad with $\hat{\mathbf{n}}$ such that $\hat{\boldsymbol{\theta}} \times \hat{\boldsymbol{\phi}} = \hat{\mathbf{n}}$ (and cyclic permutations). Thus, we find the triple product in the WZ term becomes

$$\hat{\mathbf{n}}(\tau,\xi)\cdot(\partial_\tau\hat{\mathbf{n}}(\tau,\xi)\times\partial_\xi\hat{\mathbf{n}}(\tau,\xi)) = \dot{\phi}(\tau)\theta(\tau)\sin\theta_\xi(\tau). \tag{2.59}$$

Thus, the WZ term, Eqn.(2.54) simplifies to [68, 103]

$$S_{WZ} = \int d\tau \int_0^1 d\xi\, \dot{\phi}(\tau)\theta(\tau)\sin\theta_\xi(\tau) = \int d\tau\, \dot{\phi}(\tau)(1-\cos\theta(\tau)). \tag{2.60}$$

This is the coordinate dependent form of WZ term or Berry phase [12], which is the expression found in most condensed matter literatures. It corresponds to the area of the two-sphere with radius s, swept out by $\hat{\mathbf{n}}(\tau)$ as it forms a closed path on $\mathscr{S}^2$. To understand this explicitly, one can think of the integral in Eqn.(2.60) as a line integral of a gauge field, which only has a ϕ component, integrated over a closed path on the two sphere, parametrized by τ. We denote the closed path as $\mathcal{C}$, and it is the boundary of a region $\mathscr{S}$, with evidently $\mathcal{C} = \partial\mathscr{S}$, then

$$\int d\tau\, \dot{\phi}(\tau)(1 - \cos\theta(\tau)) = \oint_{\mathcal{C}} A_\phi d\phi. \tag{2.61}$$

Then using Stokes theorem, we have

$$\oint_{\mathcal{C}} A_\phi d\phi = \int_{\mathscr{S}} d(A_\phi d\phi), \tag{2.62}$$

written in the notation of differential forms. However, the gauge field or Berry connection $\vec{A} = A_\phi\hat{\boldsymbol{\phi}} = (1 - \cos\theta)\hat{\boldsymbol{\phi}}$ corresponds exactly to the gauge field of a magnetic monopole located at the centre of the sphere. Such a gauge field was first described by Dirac [37], and gives rise to a constant radial magnetic field, apart from a string singularity, which is a gauge artefact, located at the south pole. The non observability of this string singularity in quantum mechanics was the seminal observation by Dirac. Explicitly, the corresponding magnetic field is simply $d(A_\phi d\phi) = \partial_\theta A_\phi d\theta \wedge d\phi = \sin\theta d\theta \wedge d\phi$, which is the area element in spherical polar coordinates on the unit two sphere. Thus $\oint_{\mathcal{C}} A_\phi d\phi = \int_{\mathscr{S}} d(A_\phi d\phi) = \int_{\mathscr{S}} \sin\theta d\theta \wedge d\phi = \text{area}\,(\mathscr{S})$.

The general form of the Euclidean action in coordinate dependent formalism is then

$$S_E = is \int d\tau\, \dot{\phi}(\tau) + S_0, \tag{2.63}$$

where

$$S_0 = \int d\tau[\, -is\dot{\phi}(\tau)\cos\theta(\tau) + U(\theta(\tau), \phi(\tau))]. \tag{2.64}$$

The first term in Eqn.(2.63) is a boundary term; it is unaffected by the classical equation of motion. It can be integrated out as

$$is\int_{-\frac{\beta}{2}}^{\frac{\beta}{2}} d\tau\,\dot{\phi}(\tau) = is[\phi(\beta/2) - \phi(-\beta/2) + 2\pi N], \tag{2.65}$$

where N is a winding number, that is the number of times $\phi(\tau)$ winds around the north pole of $\mathscr{S}^2$ as τ progresses from $-\beta/2$ to $\beta/2$. This term is insensitive to any continuous deformation of the field on $\mathscr{S}^2$; thus it is topological. Its effect on the transition amplitude will be studied in the subsequent chapters. The transition amplitude, Eqn.(2.51) in the coordinate dependent form can be written as

$$\langle\theta_f,\phi_f|e^{-\beta\hat{H}}|\theta_i,\phi_i\rangle = \int \mathcal{D}\phi\mathcal{D}(\cos\theta)\,e^{-S_E}, \tag{2.66}$$

which defines the transition from an initial state $|\theta_i,\phi_i\rangle$ at $\tau = -\beta/2$ to a final state $|\theta_f,\phi_f\rangle$ at $\tau = \beta/2$, subject to the boundary conditions $(\phi(-\beta/2),\theta(-\beta/2)) = (\phi_i,\theta_i)$ and $(\phi(\beta/2),\theta(\beta/2)) = (\phi_f,\theta_f)$. In most cases of physical interest, either $\phi_i = \phi_f$ or $\theta_i = \theta_f$. The classical equations of motion are easily derived:

$$is\dot{\theta}\sin\theta = \frac{\partial U}{\partial\phi}, \tag{2.67}$$

$$is\dot{\phi}\sin\theta = -\frac{\partial U}{\partial\theta}. \tag{2.68}$$

These equations are obtained from the least-action principle, whose solution gives the classical path for which the action, Eqn.(2.63) is stationary $\delta S_E = 0$. Although one is usually interested in a real, physical trajectory, these equations are in fact, incompatible, unless one variable (either θ or ϕ) becomes imaginary. The energy along the trajectory has to vanish, since it is conserved by the dynamics, and normalized to zero at the starting point. The conservation of energy is easily discerned by multiplying Eqn.(2.67) by $\dot{\phi}$ and

Eqn.(2.68) by $\dot{\theta}$ and substracting the resulting equations; this yields

$$\frac{\partial U}{\partial \phi}\dot{\phi} + \frac{\partial U}{\partial \theta}\dot{\theta} = 0 \quad \Rightarrow \quad U(\theta, \phi) = \text{const.} = 0. \tag{2.69}$$

2.4 Conclusion and Discussion

We have reviewed two formalisms of path integral that will be indispensable in this thesis. We derived the position state path integral from first principle; we further studied its application to tunneling in double well potential via analytical continuation to imaginary time. For $SU(2)$ spin systems, the position state path integral formalism is inadequate; this is resolved by the use of spin coherent states. We derived the coordinate dependent and independent forms of the spin coherent path integral formalism, which are applicable to $SU(2)$ spin systems. The effective potential mapping of spin systems will lead to systems in which the position state path integral method will be indispensable; this will be implemented in Chapter (6) for molecular magnets. In Chapter (3) and Chapter (7) we will implement the two equivalent forms of spin coherent state path integral.

CHAPTER 3

QUANTUM TUNNELING OF LARGE SPIN SYSTEMS

Know how to solve every problem
that has been solved.

Richard Feynman

3.1 Introduction

The study of macroscopic quantum tunneling is endowed with many fascinating phenomena. It has a wide range of applications in many molecular magnets, as well as in superconducting quantum interference devices (SQUID). For spin systems, the integer and the half-odd integer spins have remarkably different tunneling behaviours. Integer spins can tunnel, while tunneling for half-odd integer spins are suppressed at zero magnetic field. The suppression of tunneling for half-odd integer spins is a consequence of the WZ term, which is imaginary and first-order in time derivative. This term produces a phase in the transition amplitude, which leads to destructive quantum interference between different tunneling paths for half-odd integer spins, while it is constructive for integer spins. In this chapter we will present this serendipitous discovery of suppression of tunneling in macroscopic quantum spin systems. The derivations outlined in Sec.(2.3.2) will be fully implemented.

The format of this chapter is as follows: we will review the work of Loss *et al*[86], Henley and Delft [56] in Sec.(3.2.1). We will explicitly show how quantum phase interference (suppression of tunneling) arises in quantum spin systems. Its experimental observation will be presented. In Sec.(3.2.2), we will present the results obtained by Garg [1], that in the presence of a hard-axis magnetic field, neither integer spin nor half-odd integer spin is suppressed; rather, the tunneling splitting oscillates with the magnetic

field, only vanishes at a certain critical value of the field. The experimental observation of this theoretical prediction will be presented in Sec.(3.2.3). For a spin model with z easy-axis anisotropy at zero magnetic field, there is a subtlety in obtaining the quantum phase interference. This is because the WZ term, which is responsible for this effect seems to vanish for this particular model. This problem was reconciled by Owerre and Paranjape [104], it will be presented in Sec.(3.2.4), and our article will be included in Sec.(3.6). In Sec.(3.3), we will generalize our analysis of macroscopic quantum tunneling to antiferromagnetic exchange-coupled dimer. We will show that for this system, the quantum phase interference appears in the guise of changing the nature of the ground state energies for integer and half-odd integer spins. These results were obtained by Paranjape and the author of this thesis[103]. Our article on this analysis will be included in Sec.(3.7). Sec.(3.4) deals with coordinate independent formalism. In this section we will corroborate the result of quantum phase interference by coordinate independent analysis. This analysis will be solely based on two articles of Paranjape and the author of this thesis [104, 108], which will be included in Sec.(3.6) and Sec.(6.7). Finally, we will present a concluding remark.

3.2 Quantum tunneling in biaxial ferromagnetic spin models

3.2.1 Biaxial ferromagnetic spin model with y-easy axis

We begin this section with the consideration of a biaxial spin model in the absence of an external magnetic field. The Hamiltonian of this system is given by [24, 86, 87]

$$\hat{H} = D\hat{S}_z^2 + E\hat{S}_x^2; \quad D > E > 0. \tag{3.1}$$

Classically, this model possesses an XOY-easy-plane anisotropy with an easy-axis along the y-direction, hard-axis along the z-direction, and medium axis along the x-direction. Quantum mechanically, the easy axis corresponds to the quantization axis,

because the Casmir operator $\hat{\mathbf{S}}^2 = \hat{S}_x^2 + \hat{S}_y^2 + \hat{S}_z^2 = s(s+1)$, transforms Eqn.(3.1) into a different form, given by

$$\hat{H} = -E\hat{S}_y^2 + (D-E)\hat{S}_z^2 + \text{const.}, \tag{3.2}$$

where first term is the unperturbed term, and the second term is the transverse or splitting term; the transverse term does not commute with the unperturbed term. Thus, the minimum energy of this Hamiltonian requires a representation in which $\hat{S}_y$ is diagonal. Evidently, different representations of a biaxial spin Hamiltonian in the absence of an external magnetic field [1] can be related to each other by redefining the anisotropy constants. For instance, Eqn.(3.1) is related to $\hat{H} = -A\hat{S}_x^2 + B\hat{S}_z^2$ [87] by $E = A$; $D = A + B$. Thus, it suffices to consider just Eqn.(3.1). Semiclassically, the corresponding classical energy is

$$U(\theta, \phi) = Ds^2 \cos^2\theta + Es^2 \sin^2\theta \cos^2\phi. \tag{3.3}$$

The minimum energy corresponds to $(\phi, \theta) = (\pm\pi/2, \pi/2)$; these minima are located at $\pm\hat{\mathbf{y}}$ as shown in Fig.(3.1), and the maximum is located at $(\phi, \theta) = (0, \pi/2)$. From energy conservation, Eqn.(2.69) one obtains

$$\cos\theta = \pm i \frac{\sqrt{\lambda}\cos\phi}{\sqrt{1 - \lambda\cos^2\phi}}; \quad \lambda = E/D. \tag{3.4}$$

This expression eliminates the θ variable from Eqn.(2.68); integrating the resulting equation yields[2] [24, 87, 154]

$$\sin\phi(\tau) = \frac{\sqrt{1-\lambda}\tanh(\omega\tau)}{\sqrt{1 - \lambda\tanh^2(\omega\tau)}}; \quad \omega = 2s\sqrt{DE}. \tag{3.5}$$

[1] In the presence of a magnetic field, different representations of a biaxial spin model can also be related by the anisotropy constants or rotation of axes

[2] Alternatively, θ can be eliminated by integrating out $\cos\theta$ in Eqn.(2.66). The resulting action has a quadratic first order derivative term, a coordinate (ϕ) dependent mass and a potential [25, 87, 154].

which corresponds to the tunneling of the spin from $\phi = -\pi/2$ at $\tau = -\infty$ to $\phi = \pi/2$ at $\tau = \infty$. The instanton action for this trajectory is

$$S_c = is \int_{-\frac{\pi}{2}}^{\frac{\pi}{2}} d\phi + B, \tag{3.6}$$

where B is given by

$$B = s\sqrt{\lambda} \int_{-\frac{\pi}{2}}^{\frac{\pi}{2}} d\phi \, \frac{\cos\phi}{\sqrt{1 - \lambda\cos^2\phi}} = \ln\left(\frac{1+\sqrt{\lambda}}{1-\sqrt{\lambda}}\right)^s. \tag{3.7}$$

Consider for example the path $(\phi(\tau),\, \theta(\tau))$ connecting the two anisotropy minima at $(\phi, \theta) = (\pm\pi/2, \pi/2)$, then owing to the symmetry of the action S_0 in Eqn.(2.64) (*i.e.*, excluding the total derivative term), the path $(-\phi(\tau),\, \pi - \theta(\tau))$ will also solve the classical equations of motion and B will be the same for both paths, but the total derivative term will be reversed, *i.e.*, $is\int_{\mp\frac{\pi}{2}}^{\pm\frac{\pi}{2}} d\phi = \pm is\pi$. Since the path integral in Eqn.(2.66) contains all paths, in the semiclassical (small $\hbar$) approximation [33, 34, 139], the contributions of these two paths combine to give

$$e^{i\pi s}e^{-B} + e^{-i\pi s}e^{-B} = 2\cos(\pi s)e^{-B}. \tag{3.8}$$

More appropriately, to obtain the tunneling rate one has to use the dilute-instanton gas approximation, that is by summing over a sequences of one instanton followed by any number of anti-instanton/instanton pairs, with an odd number of instantons and anti-instantons as was done in Sec.(2.2.2). The transition amplitude becomes [56, 86]

$$\langle\frac{\pi}{2}|e^{-\beta\hat{H}}|-\frac{\pi}{2}\rangle = \mathcal{N}\sinh\left[2\mathscr{D}\beta\cos(\pi s)e^{-B}\right]. \tag{3.9}$$

where $\mathscr{D}$ is the fluctuation determinant [32–34]. The computation of $\mathscr{D}$ can be done explicitly. $\mathcal{N}$ is a normalization constant, and B is the action for the instanton. The

tunneling rate (energy splitting) from Eqn.(3.9) gives [86]

$$\Delta = 4\mathscr{D}|\cos(\pi s)|e^{-B}. \tag{3.10}$$

The factor $\cos(\pi s)$ is responsible for interference effect and it has markedly different consequences for integer and half-odd integer spins. For integer spin s (bosons), the interference is constructive, $\cos(\pi s) = (-1)^s$, and the tunneling rate is non-zero, however, for half-odd-integer spin s (fermions), the interference is destructive, $\cos(\pi s) = 0$ and the tunneling rate vanishes. Because of the time reversal invariance of Eqn.(3.1), this suppression of tunneling for half-odd integer spins can be inferred from Kramers' degeneracy [72, 95]. This directly implies that the ground state is at least two-fold degeneracy in the semi-classical picture. This semiclassical degeneracy sometimes implies that the two degenerate quantum ground states of the unperturbed term, $|\uparrow\rangle$ and $|\downarrow\rangle$ are exact ground states of the quantum Hamiltonian for half-odd integer spin [56].

3.2.2 Biaxial spin model with an external magnetic field

The analysis of the quenching of tunneling splitting for half-odd integer spins in preceding section is a zero magnetic field effect. In the presence of a magnetic field, another serendipitous observation was made — the complete destructive interference for half-odd integer spins does not occur, instead oscillation occurs [1–3]. Consider a biaxial spin model with an external magnetic field applied along the hard-axis [1–3]

$$\hat{H} = D\hat{S}_z^2 + E\hat{S}_x^2 - h_z\hat{S}_z, \tag{3.11}$$

where $h_z = g\mu_B h$, h is the magnitude of applied field and g is the spin g-factor and μ_B is the Bohr magneton. This Hamiltonian breaks time reversal invariance due the presence of the magnetic field, so Kramers' theorem is inapplicable. Semiclassically, the

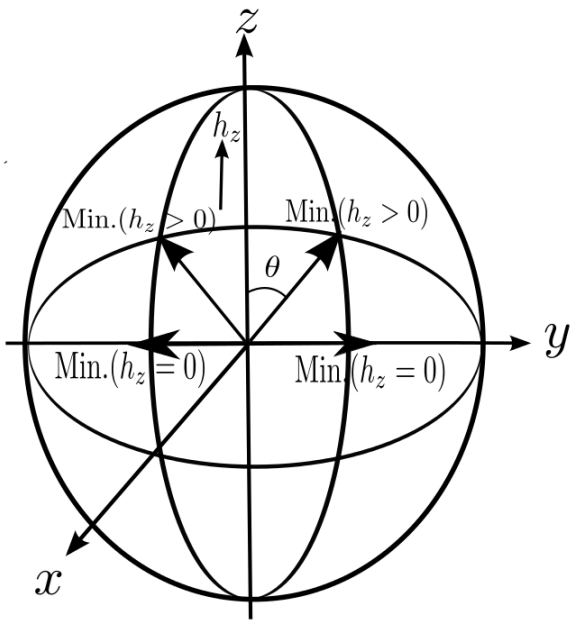

Figure 3.1: The description of a classical spin (thick arrows) on a two-sphere with two classical ground states. For $h_z = 0$, $\theta = \pm\pi/2$, the two classical ground states lie in the $\pm y$ directions which are joined by two tunneling paths in the equator. For $h_z > 0$, $\theta = \pm \arccos\alpha$, the two classical ground states lie in the yz and xz planes.

energy up to an additional constant is

$$U(\theta, \phi) = Ds^2(\cos\theta - \alpha)^2 + Es^2 \sin^2\theta \cos^2\phi, \tag{3.12}$$

with $\alpha = h_z/h_c$; $h_c = 2Ds$, being the coercive field. There are two classical degenerate minima located at $\cos\theta = \alpha$, $\phi = -\pi/2$ and $\cos\theta = \alpha$, $\phi = \pi/2$, provided $h_z < h_c$. These ground states lie in the xz and yz planes at an angle $\theta = \pm \arccos\alpha$; see Fig.(3.1). From energy conservation , Eqn.(2.69) the expression for $\cos\theta$ in terms of ϕ yields

$$\cos\theta = \frac{\alpha + i\lambda^{1/2}\cos\phi(1 - \alpha^2 - \lambda\cos^2\phi)^{1/2}}{1 - \lambda\cos^2\phi}. \tag{3.13}$$

We have chosen the positive solution in Eqn.(3.13) for convenience. Using this equation

and Eqn.(2.68), one obtains the instanton solution

$$\sin\phi(\tau) = \frac{\sqrt{1-\lambda_\alpha}\tanh(\omega_\alpha\tau)}{\sqrt{1-\lambda_\alpha\tanh^2(\omega_\alpha\tau)}}, \tag{3.14}$$

where $\omega_\alpha = 2s\sqrt{DE(1-\alpha^2)}$ and $\lambda_\alpha = \lambda/(1-\alpha^2)$. The classical action for this instanton path is

$$S_c = i\pi\xi + B, \tag{3.15}$$

where

$$\xi = \frac{s}{2\pi}\left(\mathscr{C}_+ - \mathscr{C}_-\right), \tag{3.16}$$

and $\mathscr{C}_+ - \mathscr{C}_-$ is the area enclosed by the two tunneling paths on a 2-sphere as shown in Fig.(3.1), which is given by

$$\mathscr{C}_\pm = \int_{\mp\frac{\pi}{2}}^{\pm\frac{\pi}{2}} d\phi\left(1 - \frac{\alpha}{1-\lambda\cos^2\phi}\right) = \pm\pi\left(1 - \frac{\alpha}{\sqrt{1-\lambda}}\right). \tag{3.17}$$

The instanton action is given by

$$B = s\ln\left(\frac{\sqrt{1-\alpha^2}+\sqrt{\lambda}}{\sqrt{1-\alpha^2}-\sqrt{\lambda}}\right) - \frac{2s\alpha}{\sqrt{1-\lambda}}\ln\left(\frac{\sqrt{(1-\alpha^2)(1-\lambda)}+\alpha\sqrt{\lambda}}{\sqrt{(1-\alpha^2)(1-\lambda)}-\alpha\sqrt{\lambda}}\right). \tag{3.18}$$

In this model, the imaginary path of the instanton action, Eqn.(3.15) has acquired an additional term due to the presence of the magnetic field. In the dilute instanton gas approximation, one obtains that the tunneling rate is then given by

$$\Delta = \Delta_0|\cos(\pi\xi)|; \quad \Delta_0 = 4\mathscr{D}e^{-B}. \tag{3.19}$$

Indeed, Eqn.(3.19) reduces to Eqn.(3.10) in the limit of zero magnetic field. Evidently, the tunneling splitting is no longer suppressed for half-odd integer spin, but rather it

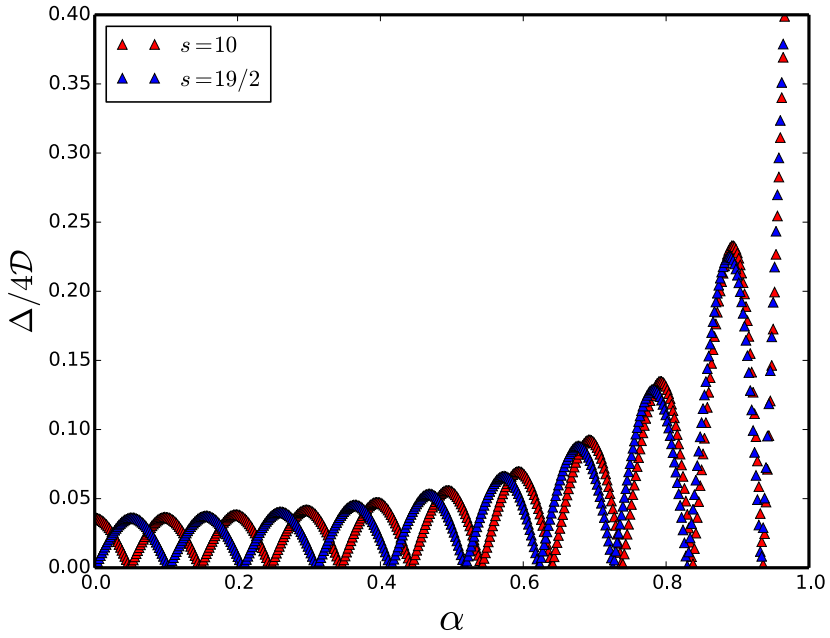

Figure 3.2: Oscillation of the tunneling splitting as a function of the magnetic field parameter α, with $\lambda = 0.03$. Reproduced from [1]

oscillates with the magnetic field; see Fig.(3.2). The splitting vanishes at a critical value of the field, given by

$$\xi = n + \frac{1}{2} \quad \text{or} \quad \alpha = \frac{\sqrt{1-\lambda}}{s}\left(s - n - \frac{1}{2}\right), \tag{3.20}$$

where n is an integer. The period of oscillation is given by

$$\Delta h = \frac{2D\sqrt{1-\lambda}}{g\mu_B}. \tag{3.21}$$

This quenching of tunneling at a critical field only occurs for biaxial spin system with a magnetic applied along the hard anisotropy axis.

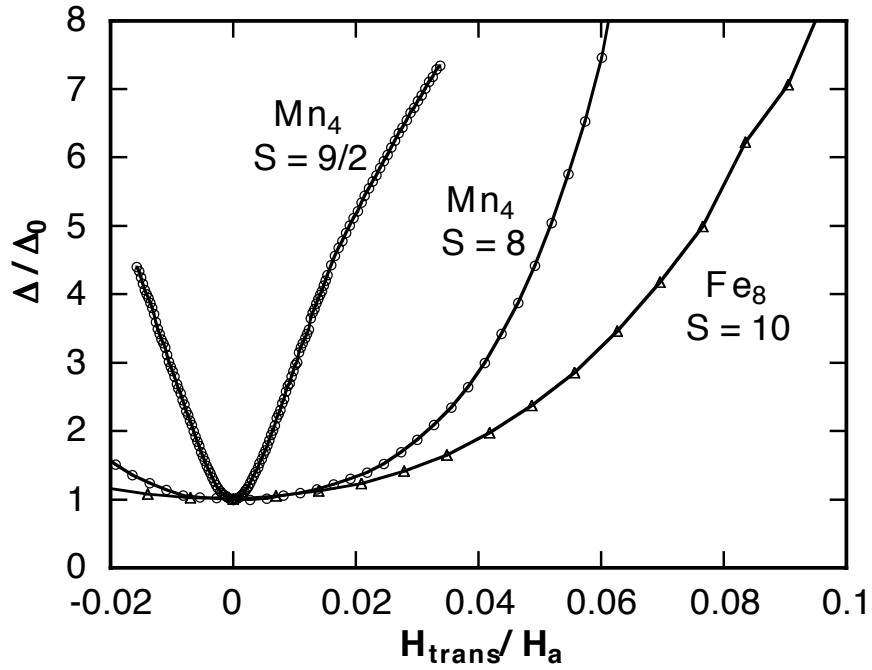

Figure 3.3: Measured tunnel splittings obtained by the Landau-Zener method as a function of transverse field for all three SMMs. The tunnel splitting increases gradually for an integer spin, whereas it increases rapidly for a half-integer spin. Adapted with permission from Wernsdorfer *et. al*[143].

3.2.3 Experimental observations

The experimental confirmation of this spin-parity effect (suppression of tunneling for half-odd integer spin) in spin systems was reported by Wernsdorfer *et. al*[143]. They studied three SMMs in the presence of a transverse field. Landau-Zener method [74, 151] was used to measure the tunnel splitting as a function of the transverse magnetic field. The tunneling probability from the Landau-Zener formula is given by [74, 140, 151]

$$\mathcal{P} = 1 - \exp\left[-\frac{\pi|\Delta|^2}{4s\hbar g\mu_B \frac{dH}{dt}}\right], \tag{3.22}$$

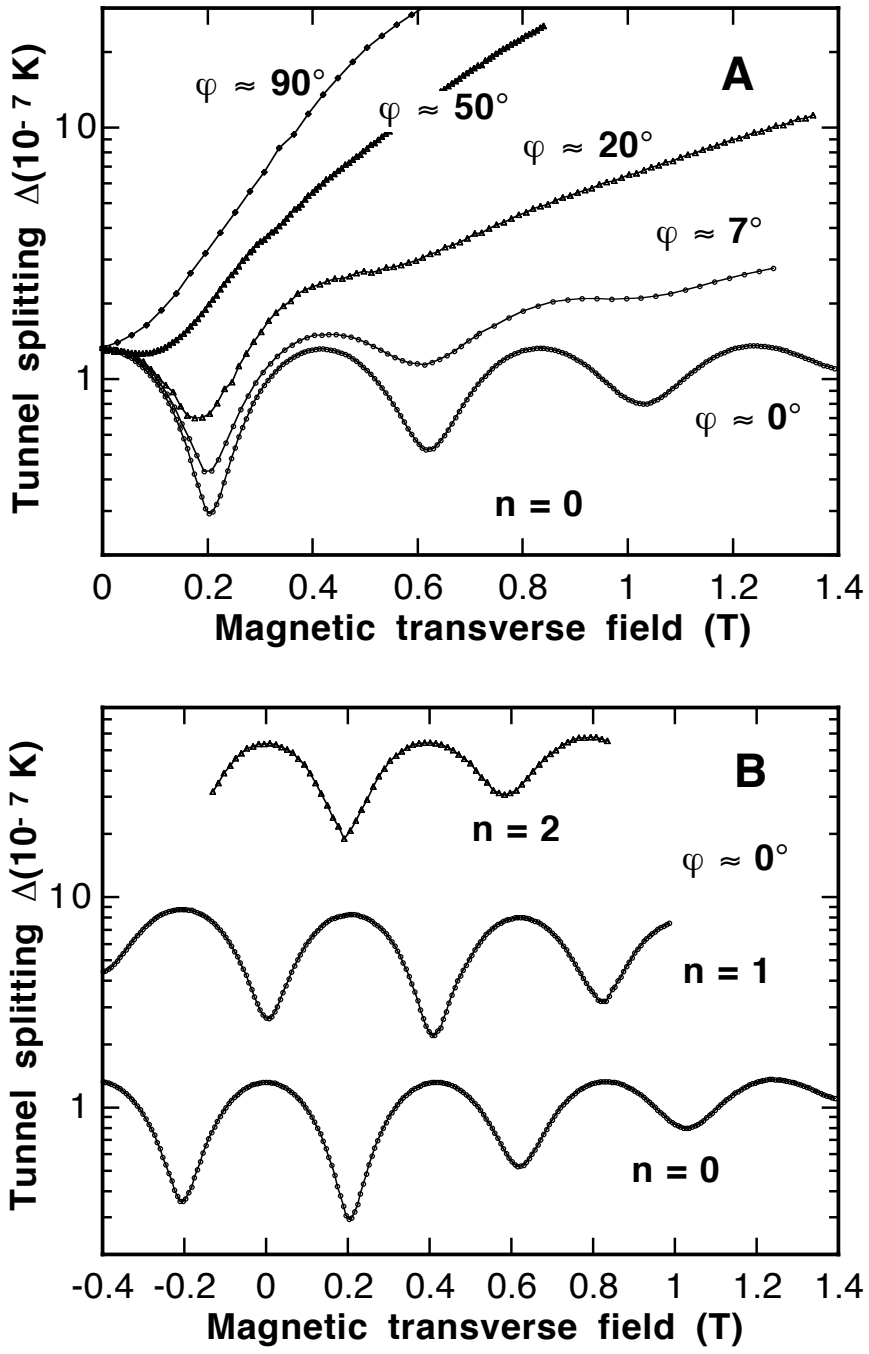

Figure 3.4: Measured tunneling splitting as a function of the applied field for the Hamiltonian $\hat{H} = -AS_z^2 + B(S_x^2 - S_y^2) - g\mu_B H_\perp (S_x \cos\varphi + S_y \sin\varphi)$. Top figure $(\mathbf{A})$ is the quantum transition between $m = \pm 10$ and several values of the azimuth angles φ. Bottom figure $(\mathbf{B})$ is for $\varphi \approx 0^\circ$ and quantum transition between $m = -10$ and $m = 10 - n$, where $n = 0, 1, 2, \cdots$, $m = -s, \cdots, s$, and $s = 10$. $A = 0.275K$, $B = 0.046K$ for Fe_8 molecular cluster. This Hamiltonian is related to that of Eqn.(3.11) by $D = A + B$ and $E = A - B$. Adapted with permission from Wernsdorfer and Sessoli [140].

where $\frac{dH}{dt}$ is the constant field sweeping rate and $g \approx 2$. They established the spin-parity effect by comparing the dependence of the tunneling splitting on the transverse field for integer and half-odd integer spin systems. Observation showed that an integer spin system is insensitive to small transverse fields, whereas half-odd integer spin system is much more sensitive, as shown in Fig.(3.3). These observations are analogous to vanishing tunneling splitting for half-odd integer spins. In the presence of a magnetic field along the hard anisotropy axis, the theoretical prediction of the oscillation of the tunneling splitting was observed experimentally in Fe_8 molecular cluster and Mn_{12} SMMs [140, 142, 145]. In Fig.(3.4), we have shown the experimental confirmation of this theoretical prediction. This experimental result is also confirmed by Landau-Zener method [74, 140, 142, 145, 151]. The value of the period of oscillation in Eqn.(3.21) using the anisotropy parameters for Fe_8 molecular cluster in Fig.(3.4), with $D = A + B$ and $E = A - B$ is $\Delta h = 0.26T$. The value is very small compare to its experimental measured value $0.41T$. In order to fix this discrepancy, an additional fourth order anisotropy of the form $C(S_+^4 + S_-^4)$ is required in Eqn.(3.11) [140, 142]. The inclusion of this term involves tedious theoretical analysis. There is no exact instanton solution, but some approximate schemes have been developed to tackle this problem [42, 52, 110].

3.2.4 Biaxial ferromagnetic spin model with z-easy axis

The biaxial model we reviewed in Sec.(3.2.1) has an easy axis along the y-axis and the corresponding instanton trajectory is in the ϕ coordinate. Thus, the quantum phase interference appeared naturally from the topological term in the action, Eqn.(2.65). If we had considered the z-easy axis model such as [104]

$$\hat{H} = -k_z \hat{S}_z^2 + k_y \hat{S}_y^2; \quad k_z, k_y > 0; \tag{3.23}$$

then the situation would have been different as the instanton trajectory will be in the θ variable. This Hamiltonian is however related to Eqn.(3.1) by $k_z = E$, $k_y = D - E$ or

by the rotation of axis $\hat{S}_z \leftrightarrow \hat{S}_y$. Suppose we wish to solve Eqn.(3.23) as it is, then the corresponding classical energy is

$$U(\theta, \phi) = (k_z + k_y \sin^2 \phi) s^2 \sin^2 \theta. \tag{3.24}$$

Since $\sin^2 \theta \neq 0$, the energy conservation yields

$$\sin \phi = \pm i \sqrt{\frac{k_z}{k_y}}. \tag{3.25}$$

Therefore, ϕ is imaginary and constant. Let $\phi = \phi_R + i\phi_I$, then $\sin \phi = \sin \phi_R \cosh \phi_I + i \cos \phi_R \sinh \phi_I$. We must take $\phi_R = n\pi$ as the RHS of Eqn.(3.25) is imaginary. Hence

$$(-1)^n \sinh \phi_I = \pm \sqrt{\frac{k_z}{k_y}}. \tag{3.26}$$

There are four solutions of this equation, $n = 0$, $\phi = i\phi_I$; $n = 1$,$\phi = \pi - i\phi_I$, for the positive sign and $n = 0$, $\phi = -i\phi_I$; $n = 1$, $\phi = \pi + i\phi_I$, for the negative sign. The classical equation of motion, Eqn.(2.67) simplifies to

$$is \frac{\dot{\theta}}{\sin \theta} = k_y \sin 2\phi = i k_y \sinh 2\phi_I. \tag{3.27}$$

The solution is easily found as

$$\cos \theta (\tau) = -\tanh \omega(\tau - \tau_0), \tag{3.28}$$

where $\omega = 2s\sqrt{k_z(k_y + k_z)}$, and $\theta(\tau) \to 0, \pi$ as $\tau \to \mp\infty$. This corresponds to the tunneling of the state $|\uparrow\rangle$ from $\theta(\tau) = 0$ at $\tau = -\infty$ to the state $|\downarrow\rangle$, $\theta(\tau) = \pi$ at $\tau = \infty$ as shown in Fig.(3.5). The two solutions $\phi = i\phi_I$ and $\phi = \pi + i\phi_I$ in the upper half plane correspond to the instanton, ($\dot{\theta} > 0$), while the solutions $\phi = -i\phi_I$ and $\phi = \pi - i\phi_I$ in the lower half plane correspond to the anti-instanton, ($\dot{\theta} < 0$). Since the

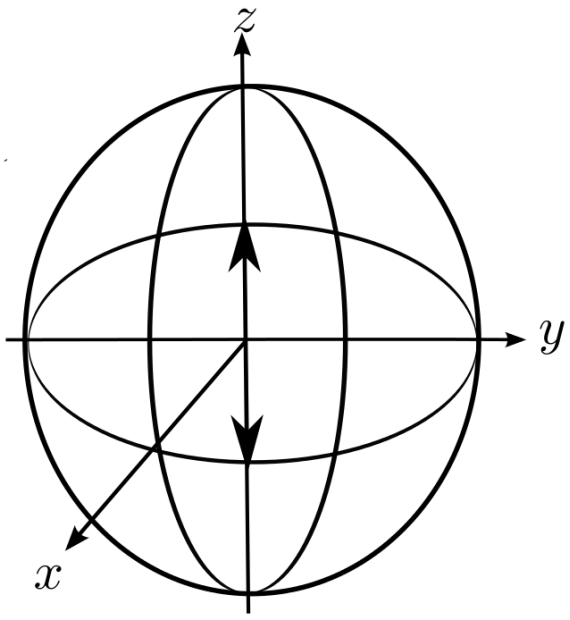

Figure 3.5: The description of a classical spin (thick arrows) on a two-sphere $\mathscr{S}^2$ with two classical ground states pointing along the $\pm\hat{z}$ directions. Tunneling corresponds to the rotation of the spins in the reverse direction.

energy, $U(\theta, \phi)$ in the action always remains zero along this trajectory, the action for this path is determined only by the Wess-Zumino term which is given by

$$S_E = S_{WZ} = is \int_{-\infty}^{\infty} d\tau \, \dot{\phi}(1 - \cos\theta). \tag{3.29}$$

Indeed, if we had the real instanton trajectory in ϕ, as in the previous model, which interpolates between $\phi(\tau) = 0$ at $\tau = -\infty$ and $\phi(\tau) = \pi$ at $\tau = \infty$, it is obvious that the total derivative term is imaginary then one can easily derive the quantum phase interference effect for which half-odd integer is suppressed. In the present analysis, the instanton is not in ϕ but in θ, so care must be taken when computing the action. Since $\phi(\tau)$, although imaginary, is just a constant, this simply implies that the topological term in Eqn.(2.65), which is responsible for the phase interference vanishes. This problem can be rescued by using the technique that we recently employed [103, 104]. We can obtain a non-vanishing action by the translation of ϕ from $\phi = 0$ to $\phi = n\pi + i\phi_I$

before the instanton can occur and then back to $\phi = 0$ after the instanton has occurred. In the present problem, we have two solutions for ϕ, *i.e.*, $\phi = i\phi_I$ and $\phi = \pi + i\phi_I$, corresponding to two instanton paths, call them I and II. The full action is then

$$S_E^I = is \int_0^{\pi + i\phi_I} d\phi (1 - \cos\theta)|_{\theta=0} + is \int_{\pi + i\phi_I}^0 d\phi (1 - \cos\theta)|_{\theta=\pi} = -2\pi is + B, \tag{3.30}$$

where $B = 2s\phi_I$, and

$$S_E^{II} = is \int_0^{i\phi_I} d\phi (1 - \cos\theta)|_{\theta=0} + is \int_{i\phi_I}^0 d\phi (1 - \cos\theta)|_{\theta=\pi} = B. \tag{3.31}$$

Evidently, the total derivative term contributes nothing as the two contributions cancel in the round trip, while the $d\phi \cos\theta$ gives all the answer, since $\cos\theta = 1$ before the instanton has occurred, while $\cos\theta = -1$ after, and B simplifies in two limiting cases:

$$B = \begin{cases} s \ln\left(\frac{4k_z}{k_y}\right), & \text{if } k_y \ll k_z, \\ 2s\left(k_z/k_y\right)^{1/2}, & \text{if } k_y \gg k_z. \end{cases} \tag{3.32}$$

The amplitude for the transition from $\theta = 0$ to $\theta = \pi$ is obtained by summing over a sequence of one instanton, followed by an anti-instanton, with an odd total number of instantons and anti-instantons, but we must add the two exponentials of the actions S_E^I and S_E^{II} for both instanton and anti-instanton, we get that the expression for the amplitude is given by

$$\langle \pi | e^{-\beta \hat{H}} | 0 \rangle = \sinh\left(2\mathscr{D}\beta(1 + \cos(2\pi s))e^{-B}\right). \tag{3.33}$$

The energy splitting can be read off from this expression

$$\Delta = 2\mathscr{D}(1 + \cos(2\pi s))e^{-B}. \tag{3.34}$$

For half-odd integer spin the splitting vanishes, while for integer spin in the perturbative limit $k_y \ll k_z$, we have

$$\Delta = 4\mathscr{D}\left(\frac{k_y}{4k_z}\right)^s. \tag{3.35}$$

This result agrees with the result found by perturbation theory [46].

3.3 Macroscopic quantum tunneling in antiferromagnetic dimer model

So far we have considered only the tunneling phenomenon in noninteracting single molecule magnets (SMMs) . In many cases of physical interest, interactions between two SMMs are taken into account. These interactions can be either ferromagnetic, which aligns the neighbouring spins or antiferromagnetic, which anti-aligns the neighbouring spins. For antiferromagnets, such interactions can be found in some physical systems such as the dimerized molecular magnet $[Mn_4]_2$, which comprises two Mn_4 SMMs of equal spins $s_1 = s_2 = 9/2$ coupled antiferromagnetically. The phenomenon of quantum tunneling of spins in this system has been studied both numerically and experimentally [121, 134]. Cobalt(II) ions are also modelled with two coupled dimer antiferromagnets, with $s_1 = s_2 = 3/2$. In this section we will study antiferromagnetic dimer system with large spins in the absence of a magnetic field.

3.3.1 Model Hamiltonian

The simplest form of the Hamiltonian of an antiferromagnetic dimer in the absence of an external magnetic field can be written as

$$\hat{H} = -D(\hat{S}_{1,z}^2 + \hat{S}_{2,z}^2) + J\hat{\mathbf{S}}_1 \cdot \hat{\mathbf{S}}_2, \tag{3.36}$$

where $J > 0$ is the antiferromagnetic exchange coupling, and $D > 0$ is the easy-axis anisotropy constant; $S_{i,z}, i = 1, 2$ is the projection of the component of the spin along

the z easy-axis. The full Hamiltonian can be alternatively written as

$$H = -D(S_{1z}^2 + S_{2z}^2) + J\left(S_{1z}S_{2z} + \frac{1}{2}(S_1^+S_2^- + S_1^-S_2^+)\right), \tag{3.37}$$

where $S_\nu^\pm = S_{\nu x} \pm iS_{\nu y}$ is the raising and lowering operators; $\nu = 1, 2$. The total z-component of the spins $\hat{S}_z^T = \hat{S}_{1,z} + \hat{S}_{2,z}$ is conserved $[\hat{S}_z^T, \hat{H}] = 0$. However, the individual z-component spins $\hat{S}_{1,z}, \hat{S}_{2,z}$ and the staggered configuration $\hat{S}_z^{st} = \hat{S}_{1,z} - \hat{S}_{2,z}$ are not conserved, $[\hat{S}_{1,2}^z, \hat{H}] \neq 0 \Rightarrow [\hat{S}_z^{st}, \hat{H}] \neq 0$. In this model the exchange term acts as a field bias on its neighbour. In Sec.(3.3.2) we will report on the analysis of this model by Owerre and Paranjape [103], however, the nature of the ground states was first proposed in [11], and perturbation theory analysis is given in [26, 28, 53]. Using density-functional, Park *et al*[113] demonstrated that this simple model can replicate the experimental results in $[Mn_4]_2$ dimer, with $D = 0.58K$ and $J = 0.27K$. This model also plays a crucial role in quantum CNOT gates and SWAP gates for spin-$\frac{1}{2}$ [85]. The Hilbert space of this system is the tensor product of the two spaces, $\mathscr{H} = \mathscr{H}_1 \otimes \mathscr{H}_2$, with dim($\mathscr{H}$)= $(2s_1 + 1) \otimes (2s_2 + 1)$. An expedient basis in this product space, in $\hat{S}_{iz}$ representation can be written as $|s_1, m_1\rangle \otimes |s_2, m_2\rangle \equiv |m_1, m_2\rangle$. We will specialize to the case of equal spins, $s_1 = s_2 = s$.

3.3.2 Spin coherent state path integral analysis

From our model Hamiltonian, it is evident that the two states $|\uparrow, \uparrow\rangle$ and $|\downarrow, \downarrow\rangle$, where $\uparrow \equiv s$, etc., are exact eigenstates of $\hat{S}_{i,z}$, but they are annihilated by the operators $S_i^\pm$. Thus, these two states are indeed exact eigenstates of the quantum Hamiltonian with eigenvalue $(-2D + J)s^2$; hence, they cannot tunnel to each other. However, the antiferromagnetic states $|\uparrow, \downarrow\rangle$ and $|\downarrow, \uparrow\rangle$ are not exact eigenstates of the quantum Hamiltonian; hence we expect resonance quantum tunneling between them. We will show that indeed the two antiferromagnetic states $|\uparrow, \downarrow\rangle$ and $|\downarrow, \uparrow\rangle$ can tunnel to each other. We will obtain the ground state and the energy splitting in the perturbative ($J \ll D$) and the

non-perturbative ($J \gg D$) limits, using the instanton technique via spin coherent state path integral formalism. In this formalism, the Euclidean Lagrangian of this system has the form:

$$L_E = is\dot{\phi}_1(1-\cos\theta_1) + is\dot{\phi}_2(1-\cos\theta_2) + U(\theta_1,\phi_1;\theta_2,\phi_2), \tag{3.38}$$

where[3]

$$U = Ds^2(\sin^2\theta_1 + \sin^2\theta_2) + Js^2\left(\sin\theta_1\sin\theta_2\cos(\phi_1-\phi_2) + \cos\theta_1\cos\theta_2 + 1\right). \tag{3.39}$$

3.3.2.1 Instanton trajectory

The instanton trajectory is obtained from the solution of the classical equations of motion. We now present this solution. There are four degrees of freedom, which yields four classical equations of motion. The first two equations of motion come from the variation of the Lagrangian with respect to $\phi_{1,2}$:

$$i\frac{d}{d\tau}(1-\cos\theta_1) + Js\sin\theta_1\sin\theta_2\sin(\phi_1-\phi_2) = 0, \tag{3.40}$$

$$i\frac{d}{d\tau}(1-\cos\theta_2) - Js\sin\theta_1\sin\theta_2\sin(\phi_1-\phi_2) = 0. \tag{3.41}$$

The other two equations of motion come from the variation with respect to $\theta_{1,2}$:

$$i\dot{\phi}_1\sin\theta_1 + Ds\sin 2\theta_1 + Js[\cos\theta_1\sin\theta_2\cos(\phi_1-\phi_2) - \sin\theta_1\cos\theta_2] = 0, \tag{3.42}$$

$$i\dot{\phi}_2\sin\theta_2 + Ds\sin 2\theta_2 + Js[\cos\theta_2\sin\theta_1\cos(\phi_1-\phi_2) - \sin\theta_2\cos\theta_1] = 0. \tag{3.43}$$

[3]A constant of the form Js^2 has been added to U in order to make the potential zero at the minima $(\theta_1,\phi_1) = (0,0)$ and $(\theta_2,\phi_2) = (\pi,0)$; $(\theta_1,\phi_1) = (\pi,0)$ and $(\theta_2,\phi_2) = (0,0)$.

Adding Eqns (3.40) and (3.41) we obtain the conservation of total spin z-components :

$$\frac{d}{d\tau}\left(\cos\theta_1+\cos\theta_2\right)=0;\ \text{thus},\ \cos\theta_1+\cos\theta_2=\text{const.}=0, \tag{3.44}$$

where the constant is chosen to be zero using the initial condition $\theta_1=0,\theta_2=\pi$; hence, $\theta_2=\pi-\theta_1$. With this constraint, θ_2 can be eliminated from the equations of motion. Noticing that $\sin(\pi-\theta_1)=\sin\theta_1$ and $\cos(\pi-\theta_1)=-\cos\theta_1$, Eqns (3.40) and (3.41) yield the same equation:

$$i\dot{\theta}_1\sin\theta_1+Js\sin^2\theta_1\sin\left(\phi_1-\phi_2\right)=0. \tag{3.45}$$

The $\theta_{1,2}$ variations in Eqns (3.42) and (3.43) can be subtracted, yielding

$$i(\dot{\phi}_1-\dot{\phi}_2)\sin\theta_1+s[2D+J(\cos\left(\phi_1-\phi_2\right)+1)]\sin 2\theta_1=0. \tag{3.46}$$

Introducing the reduced coordinates: $\theta=\theta_1$, $\phi=\phi_1-\phi_2$, Eqn.(3.45) and Eqn.(3.46) can now be derived from the effective Lagrangian:

$$L_E^{\text{eff}}=is\dot{\phi}(1-\cos\theta)+U_{\text{eff}}(\theta,\phi), \tag{3.47}$$

where the effective potential energy is given by

$$U_{\text{eff}}\left(\theta,\phi\right)=s^2(2D+J\left(\cos\phi+1\right))\sin^2\theta. \tag{3.48}$$

Thus, we have reduced the two-body problem to that of a single spin. The equations of motion follow directly from Eqn.(2.67) and Eqn.(2.68), which obviously yield Eqn.(3.45) and Eqn.(3.46). The energy conservation in Eqn.(2.69) gives

$$U_{\text{eff}}\left(\theta,\phi\right)=s^2(2D+J\left(\cos\phi+1\right))\sin^2\theta=0, \tag{3.49}$$

implying $(2D + J(\cos\phi + 1)) = 0$, since $\sin^2\theta \neq 0$, is required for a non-trivial solution. Thus

$$\cos\phi = -\left(1 + \frac{2D}{J}\right), \tag{3.50}$$

and we see that ϕ must be a constant and complex, since $\cos\phi < -1$, for $J \gg D$, and for $J \ll D$, which of course has no solution for real ϕ. We take $\phi = \pi + i\phi_I$, which gives

$$\cosh\phi_I = 1 + \frac{2D}{J}, \tag{3.51}$$

Then, Eqn. (3.45) simplifies:

$$i\frac{\dot{\theta}}{\sin\theta} = -Js\sin\phi = iJs\sinh\phi_I = i\omega_0; \quad \omega_0 = 2Ds\sqrt{1+\kappa}; \quad \kappa = J/D. \tag{3.52}$$

This equation is trivially integrated with solution:

$$\cos\theta(\tau) = -\tanh\omega_0(\tau - \tau_0), \tag{3.53}$$

where $\tau = \tau_0$ is the time at $\theta = \pi/2$. Thus, $\theta(\tau)$ interpolates from 0 to π as $\tau = -\infty \to \infty$.

3.3.2.2 Energy splitting and low-lying states

The energy splitting can be found by calculating the action associated with instanton trajectory. We now show how this is done. If we naively use the fact that $\dot{\phi} = 0$ and Eqn.(3.49), we see that the action for this instanton trajectory simply vanishes, *i.e.*, $S_0 = \int_{-\infty}^{\infty} d\tau\dot{\phi}(1 - \cos\theta) = 0$. This is because we have not taken into account the fact that ϕ must be translated from $\phi = 0$ (any initial point will do, as long as it is consistently used to compute the full amplitude) to $\phi = \pi + i\phi_I$ before the instanton can occur and then back to $\phi = 0$ after the instanton has occurred. Normally such a translation has no effect, either the change at the beginning cancels that at the end, or if the action is second order

in time derivative, moving adiabatically gives no contribution. But in the present case, before the instanton occurs, $\theta = 0$, but after it has occurred, $\theta = \pi$. As $\dot{\phi}$ is multiplied by $\cos\theta$ in the action, the two contributions actually add, there is a net contribution to the action. Indeed the change of the full action for the combination of the instanton and the changes in ϕ is given by

$$S_c = \int_0^{\pi+i\phi_I} -isd\phi\cos\theta|_{\theta=0} + S_0 + \int_{\pi+i\phi_I}^{0} -isd\phi\cos\theta|_{\theta_1=\pi} = -2is\pi + 2s\phi_I, \tag{3.54}$$

where $\phi_I = \operatorname{arccosh}(1 + 2D/J)$. The energy splitting is found from Eqn.(2.37):

$$\Delta = 2\mathscr{D}e^{-S_c} = \begin{cases} 2\mathscr{D}\left(\frac{J}{4D}\right)^{2s}\cos(2\pi s) & \text{if } J \ll D \\ 2\mathscr{D}\exp(-4s\,(D/J)^{1/2})\cos(2\pi s) & \text{if } J \gg D. \end{cases} \tag{3.55}$$

Figure (3.6) shows the behaviour of the energy splitting as a function of the interaction

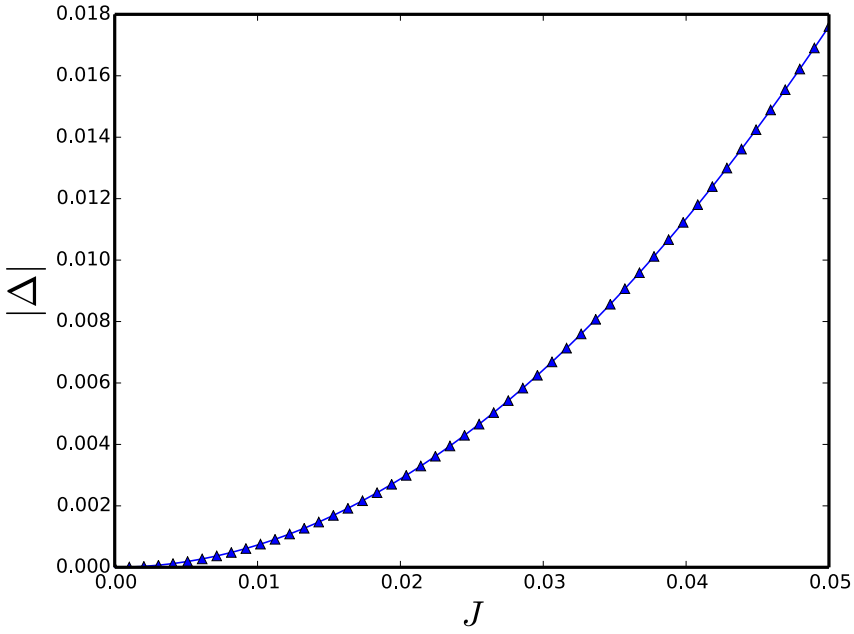

Figure 3.6: The plot of the ground state energy splitting against J obtained from exact diagonalization for $D = 1$ and $s_1 = s_2 = s = 13/2$.

constant for small spins such as $s_1 = s_2 = s = 13/2$. For $J \ll D$, the factor J^{2s} signifies the order of perturbation theory; while $J \gg D$, is non-perturbative. Thus, the exchange interaction plays the same role as the splitting terms in the biaxial model considered previously. This is completely comprehensible, since tunneling requires a term that does not commute with the quantization axis. However, in this model it is evident that both integer and half-odd integer spins can tunnel[4], but their ground and first excited states are different, as we will now show. Following the procedure outlined in Sec.(2.2.2), it evident that for integer spins $s \in \mathbb{Z}$, we have $\cos(2\pi s) = 1$ and $\Delta > 0$; thus, the low energy eigenstates are given by

$$|\mathcal{E}_0\rangle = \frac{1}{\sqrt{2}}(|\downarrow,\uparrow\rangle + |\uparrow,\downarrow\rangle); \quad |\mathcal{E}_1\rangle = \frac{1}{\sqrt{2}}(|\downarrow,\uparrow\rangle - |\uparrow,\downarrow\rangle). \tag{3.56}$$

For half-odd integer spins $s \in \mathbb{Z} + \frac{1}{2}$, we get $\cos(2\pi s) = -1$ and $\Delta < 0$; thus, the low energy eigenstates are given by

$$|\mathcal{E}_0\rangle = \frac{1}{\sqrt{2}}(|\downarrow,\uparrow\rangle - |\uparrow,\downarrow\rangle); \quad |\mathcal{E}_1\rangle = \frac{1}{\sqrt{2}}(|\downarrow,\uparrow\rangle + |\uparrow,\downarrow\rangle). \tag{3.57}$$

In the classical limit $s \to \infty$, we have

$$\lim_{s\to\infty} \Delta = 0 \tag{3.58}$$

Thus, the two Néel states $|\downarrow,\uparrow\rangle$ and $|\uparrow,\downarrow\rangle$ become the classical degenerate ground states as one expects.

3.4 Coordinate independent formalism

The coordinate dependent formalism we presented in Sec.(3.1) — (3.3) is prevalent in most condensed matter literatures, but not much seems to be written about the solutions of these models in a coordinate independent form. The solution of a physical

[4]The Kramers' degeneracy only applies to a system with an odd total number of half-odd integer spins.

problem should be independent of the coordinate system. Having solutions only in a coordinate dependent form leaves a slight but persistent, irritating doubt that somehow the results may have some coordinate dependent artefacts, which of course should not be there. In Sec.(2.3.1) we derived the classical action for spin systems without the use of coordinates. In this section, we will show that one can solve the spin systems we have considered so far in totally coordinate independent way and also recover the quantum phase interference exactly as before.

3.4.1 Classical equations of motion in coordinate independent form

First and foremost, in order to solve the spin models in a coordinate independent form, we first need to know the classical path that minimizes the coordinate independent action

$$S_E[\hat{\mathbf{n}}] = isS_{WZ} + \int d\tau U(\hat{\mathbf{n}}(\tau)); \quad U(\hat{\mathbf{n}}(\tau)) = \langle \hat{\mathbf{n}}|\hat{H}|\hat{\mathbf{n}}\rangle \,. \tag{3.59}$$

The variation of coordinate independent WZ term, Eqn.(2.54) due to small variation of $\hat{\mathbf{n}}$ gives

$$\delta S_{WZ} = \int d\tau \int d\xi \, \partial_\tau[\hat{\mathbf{n}} \cdot (\delta\hat{\mathbf{n}} \times \partial_\xi \hat{\mathbf{n}})] + \int d\tau \int d\xi \, \partial_\xi[\hat{\mathbf{n}} \cdot (\partial_\tau \hat{\mathbf{n}} \times \delta\hat{\mathbf{n}})]. \tag{3.60}$$

To obtain this variation we must remember that $0 = \delta(\hat{\mathbf{n}} \cdot \hat{\mathbf{n}}) = 2\hat{\mathbf{n}} \cdot \delta\hat{\mathbf{n}}$, and $0 = \partial_{\tau,\xi}(\hat{\mathbf{n}} \cdot \hat{\mathbf{n}}) = 2\hat{\mathbf{n}} \cdot \partial_{\tau,\xi}\hat{\mathbf{n}}$ since $\hat{\mathbf{n}}$ is a unit vector. Consequently, the volume defined by the parallelepiped traced out by the three vectors, the variation and the two derivatives, must vanish, $\delta\hat{\mathbf{n}} \cdot (\partial_\tau \hat{\mathbf{n}} \times \partial_\xi \hat{\mathbf{n}}) = 0$ since any three vectors orthogonal to a given vector $\hat{\mathbf{n}}$, lie in the same plane. The first term in Eqn.(3.60) vanishes by virtue of the boundary conditions Eqn.(2.55) and the second term yields

$$\delta S_{WZ} = -\int d\tau \, \delta\hat{\mathbf{n}}(\tau) \cdot [\hat{\mathbf{n}}(\tau) \times \partial_\tau \hat{\mathbf{n}}(\tau)]. \tag{3.61}$$

As $\delta\hat{\mathbf{n}}(\tau)$ is still a constrained variation, necessarily orthogonal to $\hat{\mathbf{n}}$, we may not conclude that the Wess-Zumino term contributes $[\hat{\mathbf{n}}(\tau) \times \partial_\tau \hat{\mathbf{n}}(\tau)]$ to the equation of motion. What we may conclude is that the part which is orthogonal to $\hat{\mathbf{n}}$ must contribute to the equation of motion. The way to implement this, is to take the vector product with $\hat{\mathbf{n}}$, which projects to the orthogonal subspace. Then, using the fact that $\hat{\mathbf{n}}(\tau) \times [\hat{\mathbf{n}}(\tau) \times \partial_\tau \hat{\mathbf{n}}(\tau)] = -\partial_\tau \hat{\mathbf{n}}(\tau)$, the variation of the total action gives the equation of motion

$$is\partial_\tau \hat{\mathbf{n}}(\tau) = -\hat{\mathbf{n}}(\tau) \times \frac{\partial U(\hat{\mathbf{n}}(\tau))}{\partial \hat{\mathbf{n}}(\tau)}. \tag{3.62}$$

This is the imaginary-time equation for Larmor precession in the effective magnetic field $\delta U(\hat{\mathbf{n}}(\tau))/\delta\hat{\mathbf{n}}(\tau)$, often called the Landau-Lifshitz equation [75, 77]. Taking the cross product of Eqn.(3.62) with $\partial_\tau \hat{\mathbf{n}}(\tau)$, and subsequently the dot product with $\hat{\mathbf{n}}(\tau)$, one finds the equation of energy conservation:

$$U(\hat{\mathbf{n}}(\tau)) = \text{constant}. \tag{3.63}$$

3.4.2 Wess Zumino term in coordinate independent form

Having obtained the equation of motion as a function of the trajectory $\hat{\mathbf{n}}(\tau)$, we will need to write the WZ action, Eqn.(2.54) as a function of τ alone in order to compute the instanton action for the trajectory $\hat{\mathbf{n}}(\tau)$. This can only be achieved if the integration over ξ can be done leaving us with the integration over τ in terms of the unit vector $\hat{\mathbf{n}}(\tau)$. This integration can indeed be done. Let us express the unit vector $\hat{\mathbf{n}}(\tau, \xi)$ as

$$\hat{\mathbf{n}}(\tau, \xi) = f(\tau, \xi) n_z(\tau) \hat{\mathbf{z}} + g(\tau, \xi)[n_x(\tau)\hat{\mathbf{x}} + n_y(\tau)\hat{\mathbf{y}}], \tag{3.64}$$

with the boundary conditions given in Eqn.(2.55). From Eqn.(3.64) and $\hat{\mathbf{n}} \cdot \hat{\mathbf{n}} = 1$, one immediately obtains

$$g^2 = \frac{1 - f^2 n_z^2}{1 - n_z^2}. \tag{3.65}$$

Owing to the boundary conditions in Eqn.(2.55), these functions must obey

$$\begin{aligned} &f(\tau, \xi = 0) = 1; f(\tau, \xi = 1) = \frac{1}{n_z(\tau)}; \\ &g(\tau, \xi = 0) = 1; \quad g(\tau, \xi = 1) = 0. \end{aligned} \tag{3.66}$$

Differentiating Eqn.(3.64) with respect to ξ and τ we have

$$\partial_\xi \hat{\mathbf{n}}(\tau, \xi) = n_z \hat{\mathbf{z}} \partial_\xi f + (n_x \hat{\mathbf{x}} + n_y \hat{\mathbf{y}}) \partial_\xi g, \tag{3.67}$$

$$\partial_\tau \hat{\mathbf{n}}(\tau, \xi) = \hat{\mathbf{z}}(n_z \partial_\tau f + f \partial_\tau n_z) + (n_x \hat{\mathbf{x}} + n_y \hat{\mathbf{y}}) \partial_\tau g + g(\partial_\tau n_x \hat{\mathbf{x}} + \partial_\tau n_y \hat{\mathbf{y}}). \tag{3.68}$$

It follows directly that[5]

$$\begin{aligned} \partial_\tau \hat{\mathbf{n}} \times \partial_\xi \hat{\mathbf{n}} = {} & \partial_\tau g (n_z \partial_\tau f + f \partial_\tau n_z)(n_x \hat{\mathbf{y}} - n_y \hat{\mathbf{x}}) + n_z (n_y \hat{\mathbf{x}} - n_x \hat{\mathbf{y}}) \partial_\tau g \partial_\xi f \\ & + n_z (\partial_\tau n_y \hat{\mathbf{x}} - \partial_\tau n_x \hat{\mathbf{y}}) g \partial_\xi f + n_z \hat{\mathbf{z}} (n_y \partial_\tau n_x - n_x \partial_\tau n_y) g \partial_\xi g. \end{aligned} \tag{3.69}$$

Dotting Eqn.(3.69) with Eqn.(3.64), yields

$$\hat{\mathbf{n}} \cdot (\partial_\tau \hat{\mathbf{n}} \times \partial_\xi \hat{\mathbf{n}}) = n_z (g^2 \partial_\xi f - f g \partial_\xi g)(n_x \partial_\tau n_y - n_y \partial_\tau n_x). \tag{3.70}$$

From Eqn.(3.65) we have

$$g \partial_\xi g = -\frac{1}{1 - n_z^2} n_z^2 f \partial_\xi f. \tag{3.71}$$

[5]The cross product of the unit vectors are given by $\hat{\mathbf{z}} \times \hat{\mathbf{x}} = \hat{\mathbf{y}}$, $\hat{\mathbf{x}} \times \hat{\mathbf{y}} = \hat{\mathbf{z}}$, $\hat{\mathbf{y}} \times \hat{\mathbf{z}} = \hat{\mathbf{x}}$.

Thus

$$\hat{\mathbf{n}} \cdot (\partial_\tau \hat{\mathbf{n}} \times \partial_\xi \hat{\mathbf{n}}) = \frac{n_z \partial_\xi f}{1 - n_z^2}(n_x \partial_\tau n_y - n_y \partial_\tau n_x). \tag{3.72}$$

Using these expressions, the WZ can be integrated as

$$\begin{aligned}\int_0^1 d\xi [\hat{\mathbf{n}} \cdot (\partial_\tau \hat{\mathbf{n}} \times \partial_\xi \hat{\mathbf{n}})] &= \int_1^{\frac{1}{n_z}} df \frac{n_z}{1 - n_z^2}(n_x \partial_\tau n_y - n_y \partial_\tau n_x), \\ &= \frac{1 - n_z}{1 - n_z^2}(n_x \partial_\tau n_y - n_y \partial_\tau n_x). \end{aligned} \tag{3.73}$$

The coordinate independent form of WZ action as a function of time alone becomes[6][104]

$$S_{WZ} = is \int d\tau \frac{1}{1 + n_z}(n_x \partial_\tau n_y - n_y \partial_\tau n_x). \tag{3.74}$$

The coordinate dependent action can be easily recovered using the spherical parameterization $n_x = \sin\theta(\tau)\cos\phi(\tau)$; $n_y = \sin\theta(\tau)\sin\phi(\tau)$; $n_z = \cos\theta(\tau)$. Further simplification of Eq. (3.74) yields

$$S_{WZ} = is \int \frac{d(n_y/n_x)}{1 + (n_y/n_x)^2}(1 - n_z) = is \int d[\arctan(n_y/n_x)](1 - n_z). \tag{3.75}$$

3.4.3 Coordinate independent biaxial spin system

In Sec.(3.2.1) and (3.2.4) , we derived the suppression of tunneling for half-odd integer spin for a biaxial single molecule magnet in a particular choice of coordinate. In this section, we will show that these results can be recovered in terms of the unit vector $\hat{\mathbf{n}}(\tau)$. Thus, the suppression of tunneling for half-odd integer spin is independent of the choice of coordinate. Let us begin by considering the biaxial model in Sec.(3.2.1), in the coordinate independent form; the classical energy of the Hamiltonian in Eqn.(3.1) can

[6] A similar expression is given in [4, 15, 71, 128]

be written as

$$U = Ds^2(\hat{\mathbf{n}}\cdot\hat{\mathbf{z}})^2 + Es^2(\hat{\mathbf{n}}\cdot\hat{\mathbf{x}})^2. \tag{3.76}$$

The classical equation of motion, Eqn.(3.62) yields

$$is\partial_\tau\hat{\mathbf{n}} + 2Ds^2(\hat{\mathbf{n}}\cdot\hat{\mathbf{z}})(\hat{\mathbf{n}}\times\hat{\mathbf{z}}) + 2Es^2(\hat{\mathbf{n}}\cdot\hat{\mathbf{x}})(\hat{\mathbf{n}}\times\hat{\mathbf{x}}) = 0. \tag{3.77}$$

Using the energy conservation and $\hat{\mathbf{n}}\cdot\hat{\mathbf{n}} = 1$, it follows that

$$\begin{aligned}
\hat{\mathbf{n}}\cdot\hat{\mathbf{z}} &= \pm i\sqrt{\frac{E}{D}}\hat{\mathbf{n}}\cdot\hat{\mathbf{x}} = \pm i\sqrt{\frac{E}{D-E}(1-(\hat{\mathbf{n}}\cdot\hat{\mathbf{y}})^2)}, \\
\hat{\mathbf{n}}\cdot\hat{\mathbf{x}} &= \pm\sqrt{\frac{D}{D-E}(1-(\hat{\mathbf{n}}\cdot\hat{\mathbf{y}})^2)}.
\end{aligned} \tag{3.78}$$

Then

$$\frac{\hat{\mathbf{n}}\cdot\hat{\mathbf{y}}}{\hat{\mathbf{n}}\cdot\hat{\mathbf{x}}} = \pm\frac{\hat{\mathbf{n}}\cdot\hat{\mathbf{y}}}{\sqrt{\frac{D}{D-E}(1-(\hat{\mathbf{n}}\cdot\hat{\mathbf{y}})^2)}} = \tan\chi. \tag{3.79}$$

Taking the scalar product of Eq. (3.77) with $\hat{\mathbf{y}}$ and using Eqn.(3.78) yields

$$i\partial_\tau(\hat{\mathbf{n}}\cdot\hat{\mathbf{y}}) - 2is\sqrt{DE}(1-(\hat{\mathbf{n}}\cdot\hat{\mathbf{y}})^2) = 0. \tag{3.80}$$

Upon integration we obtain the instanton

$$\hat{\mathbf{n}}\cdot\hat{\mathbf{y}} = n_y = \tanh\omega(\tau-\tau_0), \tag{3.81}$$

where $\omega = 2s\sqrt{DE}$. The instanton interpolates from $n_y = 1$ to $n_y = -1$ as $\tau\to\pm\infty$. Thus, $\arctan(\hat{\mathbf{n}}\cdot\hat{\mathbf{y}}/\hat{\mathbf{n}}\cdot\hat{\mathbf{x}}) \to \pm\pi/2$ as $\tau\to\pm\infty$. Since the energy remains constant

along the instanton trajectory, the action is determined only from the WZ term

$$S_c = is \int_{-\frac{\pi}{2}}^{\frac{\pi}{2}} d[\arctan(n_y/n_x)](1-n_z). \tag{3.82}$$

From Eqn.(3.78) and Eqn.(3.79) we find

$$\hat{\mathbf{n}} \cdot \hat{\mathbf{z}} = n_z = \pm \frac{i\sqrt{\lambda}}{\sqrt{1-\lambda+\left(\frac{n_y}{n_x}\right)^2}}; \quad \lambda = E/D. \tag{3.83}$$

Thus, we recover the action in Eqn.(3.6)

$$S_c = is\pi + B; \quad B = \ln\left(\frac{1+\sqrt{\lambda}}{1-\sqrt{\lambda}}\right)^s. \tag{3.84}$$

The calculation of the energy splitting follows directly from Sec.(3.2.1). Thus, one recovers the quantum phase interference effect in a coordinate independent manner. We conclude that the spin-parity effect is independent of the choice of coordinate. Needless to say, the same analysis can also be done for the z-easy-axis model in Sec.(3.2.4).

3.5 Conclusion and Discussion

We have explicitly investigated quantum tunneling in large spin systems. Using the spin coherent state path integral formalism, we obtained two serendipitous theoretical predictions, that for biaxial ferromagnetic spin systems without a magnetic field, the tunneling rate vanishes for half-odd integer spins, whereas tunneling is allowed for integer spin systems; in the presence of a hard-axis magnetic field, however, the tunneling rate oscillates with the field, and only vanishes at a certain critical value of the field for both integer and half-odd integer spins. For spin systems with z easy-axis anisotropy, we noticed that the WZ term, which is responsible for the quenching of tunneling for half-odd integer spins, vanishes. In order to recover the destructive quantum phase in-

terference for half-odd integer spins, we showed that an adiabatic translation of the ϕ coordinate is needed, and we recovered the quantum phase interference by two tunneling paths whose contributions to the quantum amplitude add up, giving rise to the suppression of tunneling for half-odd integer spins. We presented the experimental observations of these theoretical predictions. Furthermore, we recovered these results (quantum phase interferences) using the coordinate independent formalism.

We further extended our analysis to two interacting spin systems, with a dominant easy axis anisotropy and a weak antiferromagnetic exchange interaction. For this system, we lucidly showed that the WZ action appeared in the guise of changing the ground states for integer and half-odd integer spins. Indeed, we found that the ground and the first excited states are the antisymmetric and symmetric linear, coherent, superposition of the two Néel states for half-odd integer spins, whereas for integer spins the role of these states are interchanged. Macroscopic quantum tunneling of spins is still an active research area, with numerous applications to other interdisciplinary areas. In recent years, researchers have focused on the effect of decoherence due to environmental influence.

3.6 Article for coordinate independent analysis

The coordinate independent article below is currently under review in Physica B. My contributions to this research work are commensurate with my supervisor's (co-author) contributions, which includes originality, problem formulation, methodology, and results.

Coordinate (in)dependence and quantum inteference in quantum spin tunnelling

Solomon Akaraka Owerre and M. B. Paranjape
Groupe de physique des particules, Département de physique, Université de Montréal, C.P. 6128, succursale centre-ville, Montréal, Québec, Canada, H3C 3J7

Abstract

It appears that many authors have systematically avoided the analysis of ferromagnetic (anti-ferromagnetic) spin models with an easy-axis chosen to align along the z axis. However the formulation of physical spin systems with an easy-axis is the simplest when the axis is taken along the z-direction. For such systems which admit tunnelling, the corresponding coordinate in spin coherent state path integral is θ, the instanton is in this variable, while ϕ is always, necessarily, complex and is often just a constant. Since the energy is necessarily also constant and then can be normalized to vanish along the instanton trajectory, the action for the instanton is determined entirely by the Wess-Zumino (WZ) term $S_{WZ} = is\int d\tau\,\dot{\phi}(1-\cos\theta)$. Then, it is hard to conceive of how the instanton can give a non-vanishing result for the tunnelling amplitude when ϕ is a constant. This affords an explanation of why a z easy axis coordinate system seems to be systematically avoided, one does not know how to do the calculation. Aligning the coordinate system so that one has a x or y easy-axis model, the instanton trajectory is in ϕ which then is real and θ is necessarily complex and often constant. The tunnelling amplitude comes from the calculation of the first term of the WZ term which then is real. Furthermore it is obvious in this case, that the total derivative term remains imaginary and therefore generates any quantum phase interference, (such as, for example, the suppression of energy splitting for half-odd integer spin demonstrated by D. Loss, D. P. Di Vincenzo, G. Grinstein, Phys. Rev. Lett. **69**, 3232 (1992) and by J. von Delft, C. Henley, Phys. Rev. Lett. **69**, 3236(1992)[1,2]). This circumstance, when a physical result is obtained on the basis of a total derivative term in the action, leaves one with an uneasy feeling as a total derivative term does not affect the equations of motion and could presumably be thrown away. For the choice of coordinates with a z easy-axis, the WZ action is either real (as ϕ is imaginary) or zero (as $\dot{\phi}=0$), so it is not obvious where the quantum phase interference comes from. In principle the choice of the coordinate system is made to simplify a problem, however, the physical amplitude must not depend on this choice. Here we show, by studying a specific model, that in order to recover the quantum interference when the easy axis is aligned with the z axis, ϕ must be translated from $\phi=0$ to $\phi=\phi_R+i\phi_I$ at first, before the instanton can mediate $\theta: 0\to\pi$, and then $\phi=\phi_R+i\phi_I$ must be translated back to $\phi=0$ after the instanton has occurred. The contribution from the total derivative term in the WZ action for this round trip is exactly zero, but from the $\dot{\phi}\cos\theta$ we obtain the quantum interference. We recover the results found in the references cited above. We end with an exposition of the totally coordinate independent formulation. We are able to solve the equations of motion for the instanton path, and recover the quantum phase interference by evaluating the Wess-Zumino term explictly.

PACS numbers: 75.45.+j, 75.10.Jm, 75.30.Gw, 03.65.Sq

I. INTRODUCTION

In recent years single ferromagnetic spin systems have become a subject of interest due to the fact that they exhibit first- or second-order phase transition between quantum and classical regimes for the escape rate[3–7]. They also allow the possibility of studying macroscopic quantum coherence (MQC) and macroscopic quantum tunnelling (MQT)[8–10]. The term "macroscopic" means that the system involves very large spin, therefore it can be described using a semi-classical approach. Both MQC and MQT usually involve two states separated by a barrier. In MQC, tunnelling between neighbouring degenerate vacua is dominated by the instanton configuration with nonzero topological charge leading to an energy level splitting. Hence, the degeneracy is lifted, and the true ground state is then the coherent superposition of the two degenerate vacua. In MQT, however, tunnelling is dominated by the bounce configuration[11] with zero topological charge leading to the decay of the metastable states. The quantum tunnelling effect in spin systems occur both in ferromagnetic and anti-ferromagnetic spin system[11–15]. In ferromagnetic systems, the macroscopic variables satisfy the well known Landau-Lifshitz differential equation.

The tunnelling rate (energy splitting) is often calculated semi-classically using the instanton method. This method has been studied extensively in one dimension using the imaginary time path integral[16]. For spin systems, however, the imaginary time path integral (the spin coherent-state path integral) contains an additional phase that contributes to the transition amplitude. The phase appears because the overlap of two different coherent states is not unity. The Euclidean (imaginary time) action from this method contains two terms, one term is the spin (magnetic) energy which is real. This term is re-

sponsible for the energy barrier between two states, and the other term (the Wess-Zumino or Berry phase term) is imaginary, first-order in time derivative, and contains a topological (total derivative) term. For a single spin model, the action is usually parametrized by two coordinates θ and ϕ. Since the action is complex, one of these variables has to be complex for the equation of motion to be consistent. It was shown in a specific model[1], that when the real tunnelling coordinate is ϕ (θ is complex), the topological term (which is imaginary) causes destructive interference leading to the vanishing of tunnelling splitting when the total spin of a ferromagnet[1,2] (or the excess spin of an antiferromagnet[1,15,17]) is a half-odd integer. For systems with z-easy-axis[18,19], the real tunnelling coordinate is θ, and ϕ is complex, and to obtain the quantum phase interference for half-odd integer spin is a bit subtle as in this case the topological term is real or zero. In this report, we show by a unique and elegant approach that the well known result, suppression of tunnelling for half-odd integer spin, can be recovered for the z-easy-axis models.

II. MODEL AND METHOD

We will study the simple, single ferromagnetic spin Hamiltonian

$$H = -K_z S_z^2 + K_y S_y^2, \quad K_z \gg K_y > 0 \tag{2.1}$$

using spin coherent state path integral. The above Hamiltonian possesses an easy-axis in the z-direction and hard-axis along the y-direction, so we expect the real tunnelling variable to be θ which parametrizes the rotation in z-axis. The Hamiltonian has been studied in a magnetic field by many authors[8,12] . However, the quantum phase interference for this model has not been reported in any literature, we believe, due the subtlety involved in computing the action for the instanton.

The Hamiltonian studied by M Enz and R Schilling[14]

$$H = -AS_x^2 + BS_z^2, \quad (h = 0) \tag{2.2}$$

possesses an easy x-axis and a hard-axis along the z- axis. This model in the conventional spherical parametrization $\mathbf{S} = (\sin\theta\cos\phi, \sin\theta\sin\phi, \cos\theta)$ is exactly our Hamiltonian Eq.(2.1) in the unconventional spherical parametrization $\mathbf{S} = (\sin\theta\sin\phi, \cos\theta, \sin\theta\cos\phi)$. In order to demonstrate our technique for investigating the quantum phase interference in z easy-axis model, we will stick to the conventional spherical parametrization. It was shown[20] that perturbation theory in the K_y term for integer spin leads to an energy splitting proportional to $(K_y)^s$ while for half-odd integer spin, the splitting vanishes in accordance with Kramers' theorem. We will recover this result using spin coherent state path integral.

The transition amplitude in spin coherent state path integral is given by[21]

$$\langle\theta_f, \phi_f|e^{-\beta H}|\theta_i, \phi_i\rangle = \int \mathcal{D}\left[\cos\theta\right]\mathcal{D}\left[\phi\right] e^{-S_E/\hbar} \tag{2.3}$$

where the Euclidean action is

$$S_E = \int d\tau \left[is\dot{\phi}(1-\cos\theta) + E(\theta,\phi)\right] \tag{2.4}$$

and the classical anisotropy energy Eq.(2.1) is

$$E(\theta,\phi) = (K_z + K_y \sin^2\phi)\sin^2\theta. \tag{2.5}$$

The classical degenerate ground states correspond to $\phi = 0$, $\theta = 0, \pi$, that is the spin is pointing in the north or south pole of the two-sphere. The classical equations of motion obtain by varying the action with respect to θ and ϕ respectively are

$$is\dot{\phi}\sin\theta = -\frac{\partial E(\theta,\phi)}{\partial\theta} \tag{2.6}$$

$$is\dot{\theta}\sin\theta = \frac{\partial E(\theta,\phi)}{\partial\phi} \tag{2.7}$$

It is evident from these two equations, because of the explicit i, that one variable has to be imaginary in order for the equations to be consistent. The only appropriate choice is to take real θ and imaginary ϕ, since the real tunnelling coordinate (z-easy-axis) is θ. This comes out naturally from the conservation of energy, which follows by multiplying Eqn. (2.7) with $\dot{\phi}$ and Eqn. (2.6) by $\dot{\theta}$ and subtracting the two:

$$\frac{dE(\theta,\phi)}{d\tau} = 0 \quad \text{i.e,} \quad E(\theta,\phi) = \text{const.} = 0 \tag{2.8}$$

Thus,

$$E(\theta,\phi) = (K_z + K_y\sin^2\phi)\sin^2\theta = 0 \tag{2.9}$$

Since $\sin^2\theta \neq 0$, it follows that,

$$\sin\phi = \pm i\sqrt{\frac{K_z}{K_y}}, \tag{2.10}$$

Therefore ϕ is imaginary and constant. Let $\phi = \phi_R + i\phi_I$, then $\sin\phi = \sin\phi_R\cosh\phi_I + i\cos\phi_R\sinh\phi_I$. We must take $\phi_R = n\pi$ as the RHS of (2.10) is imaginary. Hence

$$(-1)^n\sinh\phi_I = \pm\sqrt{\frac{K_z}{K_y}}, \tag{2.11}$$

There are four solutions of this equation: $n = 0$, $\phi = i\phi_I$ and $n = 1$,$\phi = \pi - i\phi_I$ for the positive sign and $n = 0$, $\phi = -i\phi_I$ and $n = 1$, $\phi = \pi + i\phi_I$ for the negative sign. Taking into account that $K_z \gg K_y$, we have $\phi_I = \text{arcsinh}\left(\sqrt{\frac{K_z}{K_y}}\right) \approx \frac{1}{2}\ln\left(\frac{4K_z}{K_y}\right)$. The classical equation of motion (2.7) simplifies to

$$is\frac{\dot{\theta}}{\sin\theta} = K_y\sin 2\phi = iK_y\sinh 2\phi_I \tag{2.12}$$

The solution is easily found as

$$\theta(\tau) = 2\arctan[\exp(\omega(\tau - \tau_0))], \tag{2.13}$$

where $\omega = \frac{K_y}{s}\sinh 2\phi_I$. This corresponds to the tunnelling of the state $|\uparrow\rangle$ from $\theta(\tau) = 0$ at $\tau = -\infty$ to the state $|\downarrow\rangle$, $\theta(\tau) = \pi$ at $\tau = \infty$. The two solutions $\phi = i\phi_I$ and $\phi = \pi + i\phi_I$ in the upper half plane correspond to the instanton, $(\dot{\theta} > 0)$ while the solutions $\phi = -i\phi_I$ and $\phi = \pi - i\phi_I$ in the lower half plane correspond to the anti-instanton, $(\dot{\theta} < 0)$.

Since the energy, $E(\theta, \phi)$ in the action Eqn. (2.4) always remains zero along this trajectory the action for this path is determined only by the Wess-Zumino term which is given by

$$S_E = S_{WZ} = is\int_{-\infty}^{\infty} d\tau\, \dot{\phi}(1-\cos\theta) \tag{2.14}$$

We reiterate, if we had the real instanton trajectory in ϕ, as would be the case for x or y easy-axis, which interpolates between $\phi(\tau) = 0$ at $\tau = -\infty$ and $\phi(\tau) = \pi$ at $\tau = \infty$, it is obvious that the total derivative term is imaginary then one can easily derive the quantum phase interference effect for which half-odd integer is suppressed[1,2]. In the present analysis the instanton is not in ϕ but in θ, so care must be taken when computing the action. Naively, one can use the fact that ϕ is constant and hence $\dot{\phi} = 0$ which gives $S_{WZ} = 0$.

This fails to give a non-vanishing action. The problem can be rescued by using the technique that we recently employed[22]. A non-vanishing action can only be obtained by taking into account that ϕ must be translated from $\phi = 0$ to $\phi = n\pi + i\phi_I$ before the instanton can occur and then back to $\phi = 0$ after the instanton has occurred. In the present problem, we have two solutions for ϕ, i.e $\phi = i\phi_I$ and $\phi = \pi + i\phi_I$ corresponding to two instanton paths, call them I and II. The full action is then

$$\begin{aligned} S_E^I &= is\int_0^{\pi+i\phi_I} d\phi(1-\cos\theta)|_{\theta=0} + is\int_{\pi+i\phi_I}^{0} d\phi(1-\cos\theta)|_{\theta=\pi} \\ &= -2\pi is + 2s\phi_I \end{aligned} \tag{2.15}$$

and

$$\begin{aligned} S_E^{II} &= is\int_0^{i\phi_I} d\phi(1-\cos\theta)|_{\theta=0} \\ &+ is\int_{i\phi_I}^{0} d\phi(1-\cos\theta)|_{\theta=\pi} = 2s\phi_I \end{aligned} \tag{2.16}$$

where it is clear that the total derivative term contributes nothing as the two contributions cancel in the round trip, while the $d\phi\cos\theta$ gives all the answer, since $\cos\theta = 1$ before the instanton has occurred, while $\cos\theta = -1$ after. The amplitude for the transition from $\theta = 0$ to $\theta = \pi$ can be calculated by summing over a sequence of one instanton followed by an anti-instanton with an odd total number of instantons and anti-instantons[16], but we must add the two exponentials of the actions S_E^I and S_E^{II} for both instanton and anti-instanton, we get that the expression for the amplitude is given by

$$\langle\pi|e^{-\beta\hat{H}}|0\rangle = \sinh\left(2\kappa\beta(1+\cos(2\pi s))e^{-2s\phi_I}\right) \tag{2.17}$$

where κ is the ratio of the square root of the determinant of the operator governing the second order fluctuations, without the zero mode. The energy splitting can be read off from this expression

$$\Delta E = 2\kappa(1+\cos(2\pi s))e^{-2s\phi_I} \tag{2.18}$$

For half-odd integer spin the splitting vanishes while for integer spin we have

$$\Delta E = 4\kappa\left(\frac{K_y}{4K_z}\right)^s \tag{2.19}$$

which agrees with the result found by perturbation theory[20].

III. COORDINATE INDEPENDENT FORMALISM

In the coordinate independent formalism, the spin is represented by a unit vector $\hat{n}(\tau)$ but no parametrization of the unit vector is assumed. Then the action for the Hamiltonian in Eqn.(2.1) can be written as

$$\begin{aligned} S_E = \int d\tau\mathcal{L}_E = \int d\tau\left[-K_z(\hat{n}\cdot\hat{z})^2 + K_y(\hat{n}\cdot\hat{y})^2\right] \\ + is\int d\tau d\xi\left[\hat{n}\cdot(\partial_\tau\hat{n}\times\partial_\xi\hat{n})\right]. \end{aligned} \tag{3.1}$$

The first term is the anisotropy energy while the second term is the Wess-Zumino term written in the its native, coordinate independent form. The Wess-Zumino term is integrated over a two manifold whose boundary is physical, Euclidean time τ. Thus the configuration in τ is extended into a second dimension with coordinate ξ. The equations of motion arise from variation with respect to $\hat{n}$. However, $\hat{n}$ is a unit vector, hence its variation is not arbitrary, indeed, $\hat{n}\cdot\delta\hat{n} = 0$. Thus to obtain the equations of motion, we vary $\hat{n}$ as if it is not constrained, but then we must project onto the transverse part of the variation:

$$\delta_{\hat{n}}S_E = 0 \;\Rightarrow\; \int d\tau(\delta_{\hat{n}}\mathcal{L}_E)\cdot\delta\hat{n} = 0 \;\Rightarrow\; \hat{n}\times(\delta_{\hat{n}}\mathcal{L}_E) = 0 \tag{3.2}$$

Taking the cross product of the resulting equation one more time with $\hat{n}$ does no harm, and this process yields the equations of motion

$$is\partial_\tau\hat{n} - 2K_z(\hat{n}\cdot\hat{z})(\hat{n}\times\hat{z}) + 2K_y(\hat{n}\cdot\hat{y})(\hat{n}\times\hat{y}) = 0 \tag{3.3}$$

Taking the cross product of the equation with $\partial_\tau\hat{n}$, the first term vanishes as the vectors are parallel yielding

$$-2K_z(\hat{n}\cdot\hat{z})\partial_\tau\hat{n}\times(\hat{n}\times\hat{z}) + 2K_y(\hat{n}\cdot\hat{y})\partial_\tau\hat{n}\times(\hat{n}\times\hat{y}) = 0. \tag{3.4}$$

Simplifying the triple vector product and using $\partial_\tau\hat{n}\cdot\hat{n} = 0$, and taking the scalar product of the subsequent equation with $\hat{n}$ gives

$$\partial_\tau\left(-K_z(\hat{n}\cdot\hat{z})^2 + K_y(\hat{n}\cdot\hat{y})^2\right) = 0 \tag{3.5}$$

which is the conservation of energy. From this equation and that $\hat{n}$ is a unit vector we find

$$\begin{aligned}\hat{n}\cdot\hat{y} &= \pm\sqrt{\frac{K_z}{K_y}((\hat{n}\cdot\hat{z})^2-1)} = \pm i\sqrt{\frac{K_z}{K_y}(1-(\hat{n}\cdot\hat{z})^2)}\\ \hat{n}\cdot\hat{x} &= \pm\sqrt{\frac{K_y+K_z}{K_y}(1-(\hat{n}\cdot\hat{z})^2)}\end{aligned} \tag{3.6}$$

where the $\pm$ signs are not correlated. Then

$$\frac{\hat{n}\cdot\hat{y}}{\hat{n}\cdot\hat{x}} = \pm i\sqrt{\frac{K_z}{K_y+K_z}} = \tan\phi \tag{3.7}$$

hence we recover the result immediately that ϕ is an complex constant, just as before. Taking the scalar product of Eqn. (3.3) yields

$$is\partial_\tau(\hat{n}\cdot\hat{z}) + 2K_y(\hat{n}\cdot\hat{y})(\hat{n}\cdot\hat{x}) = 0 \tag{3.8}$$

and replacing from Eqn. (3.6) gives

$$is\partial_\tau(\hat{n}\cdot\hat{z}) \pm 2i\sqrt{K_z(K_y+K_z)}(1-(\hat{n}\cdot\hat{z})^2) = 0 \tag{3.9}$$

Notice that the i's neatly cancel leaving a trivial, real differential equation for $\hat{n}\cdot\hat{z}$, which we can write as

$$\frac{\partial_\tau(\hat{n}\cdot\hat{z})}{1-(\hat{n}\cdot\hat{z})} + \frac{\partial_\tau(\hat{n}\cdot\hat{z})}{1+(\hat{n}\cdot\hat{z})} = \pm\frac{4}{s}\sqrt{K_z(K_y+K_z)}. \tag{3.10}$$

This integrates as

$$\ln\frac{1+(\hat{n}\cdot\hat{z})}{1-(\hat{n}\cdot\hat{z})} = \pm\frac{4}{s}\sqrt{K_z(K_y+K_z)}(\tau-\tau_0). \tag{3.11}$$

Exponentiating and solving for $\hat{n}\cdot\hat{z}$ gives

$$\hat{n}\cdot\hat{z} = \pm\tanh\left(\frac{2}{s}\sqrt{K_z(K_y+K_z)}(\tau-\tau_0)\right) \tag{3.12}$$

which is exactly the same as the solution found for θ in Eqn. (2.13). The instanton (upper sign) interpolates from $n_z = 1$ to $n_z = -1$ as $\tau \to \pm\infty$.

Thus it is important to know that the equations of motion can be solved without recourse to a specific choice for the coordinates. We will now evaluate the tunnelling amplitude and the quantum interference directly in terms of the coordinate independent variables. Since the energy remains constant along the instanton trajectory, the action is determined entirely from the WZ term

$$S_{WZ} = is\int d\tau\int_0^1 d\xi\,[\hat{n}\cdot(\partial_\tau\hat{n}\times\partial_\xi\hat{n})] \tag{3.13}$$

The integration over ξ can be done explicitly by writing the unit vector as

$$\hat{n}(\tau,\xi) = f(\tau,\xi)n_z(\tau)\hat{z} + g(\tau,\xi)[n_x(\tau)\hat{x} + n_y(\tau)\hat{y}] \tag{3.14}$$

with the boundary conditions $\hat{n}(\tau,\xi=0) = \hat{n}(\tau)$ and $\hat{n}(\tau,\xi=1) = \hat{z}$. Using the expression in Eq.(3.14) and the condition that $\hat{n}\cdot\hat{n} = 1$ one obtains

$$g^2 = \frac{1-f^2n_z^2}{1-n_z^2} \tag{3.15}$$

These functions obey the boundary conditions

$$\begin{aligned}&f(\tau,\xi=0) = 1, f(\tau,\xi=1) = \frac{1}{n_z(\tau)},\\ &g(\tau,\xi=0) = 1, g(\tau,\xi=1) = 0\end{aligned} \tag{3.16}$$

The integrand of Eq.(3.13) can now be written in terms of the functions defined in Eq.(3.14). After a long calculation we obtain

$$\begin{aligned}\hat{n}\cdot(\partial_\tau\hat{n}\times\partial_\xi\hat{n}) &= n_z(g^2f' - fgg')(n_x\dot{n}_y - n_y\dot{n}_x)\\ &= \frac{n_zf'}{1-n_z}(n_x\dot{n}_y - n_y\dot{n}_x)\end{aligned} \tag{3.17}$$

where $f' \equiv \partial_\xi f$, $\dot{n}_{x,y} \equiv \partial_\tau n_{x,y}$. The second equality follows from Eq.(3.15). Replacing Eq.(3.17) into the WZ term, the ξ integration in Eqn. (3.13) can be done explicitly which yields

$$S_{WZ} = is\int d\tau\frac{(n_x\dot{n}_y - n_y\dot{n}_x)}{1+n_z} \tag{3.18}$$

This expression defines the WZ term in the coordinate independent form as a function of time alone. We can always make recourse to any specific coordinates, taking the z easy-axis system, with the spherical parameterization one recovers the usual form of the WZ term use in condensed matter physics i.e Eq. (2.14). Multiplying the top and the bottom of the integrand in Eq.(3.18) by $(1-n_z)$, the resulting integrand simplifies to

$$\begin{aligned}S_{WZ} &= is\int\frac{d(n_y/n_x)}{1+(n_y/n_x)^2}(1-n_z)\\ &= is\int d[\arctan(n_y/n_x)](1-n_z)\\ &= is\int d\phi(1-n_z)\end{aligned} \tag{3.19}$$

It is noted from Eq.(3.7) that ϕ has to be imaginary. In order to recover the quantum phase interference in the coordinate independent formalism, ϕ must to translated from the initial point say $\phi = 0$ to the final point $\phi = n\pi + i\phi_I$, $n = 0, 1$ before and after the instanton occurs[22]. The two contributions to the action from these paths are given by

$$\begin{aligned}S^I_{WZ} &= is\int_0^{\pi+i\phi_I} d\phi(1-n_z)|_{n_z=1} + is\int_{\pi+i\phi_I}^0 d\phi(1-n_z)|_{n_z=-1}\\ &= -2\pi is + 2s\phi_I\end{aligned} \tag{3.20}$$

and

$$\begin{aligned}S^{II}_{WZ} &= is\int_0^{i\phi_I} d\phi(1-n_z)|_{n_z=1}\\ &+ is\int_{i\phi_I}^0 d\phi(1-n_z)|_{n_z=-1} = 2s\phi_I\end{aligned} \tag{3.21}$$

which are the exact expressions as before. Then the previous evaluation quantum interference goes through unchanged.

IV. CONCLUSION

We investigated a biaxial ferromagnetic spin model with z-easy axis. For this model, we found that the real instanton trajectory is in θ while ϕ is imaginary. Since the action for the trajectory is completely determined by the Wess-Zumino term, which in the present problem is either real or zero, it is not clear where the suppression of tunneling for half-odd integer spin comes from. We showed that for this model there are four complex solutions for ϕ of which two correspond to an instanton and the other two correspond to an anti-instanton, therefore there are two instanton and anti-instanton paths. The quantum phase interference is obtained by translating ϕ from zero to these complex solution and back to zero, the exponentials of the two actions add and give rise to a factor of $(1+\cos(2\pi s))$ in the energy splitting, which obviously vanish for half-odd integer. We explicitly solved for the instanton and its corresponding action in the coordinate independent fashion. The quantum phase interference was recovered exactly as before.

V. ACKNOWLEDGMENTS

We thank NSERC of Canada and the Direction des relations internationales de l'Université de Montréal for financial support. We also thank Yassine Hassouni of the Départment de physique, Facult des Seciences, Université Mohammed V Agdal, Rabat, Morocco, for hospitality, where this work was done.

[1] D. Loss, D. P. Di Vincenzo, G. Grinstein, Phys. Rev. Lett. **69**, 3232 (1992)
[2] J. von Delft, C. Henley, Phys. Rev. Lett. **69**, 3236(1992)
[3] E.M. Chudnovsky and D.A. Garanin, Phys. Rev. Lett. **79**, 4469 (1997).
[4] Gwang-Hee Kim, Phys. Rev. B **59**, 11847, (1999); J. Appl. Phys. 86, 1062 (1999)
[5] J.-Q. Liang, H. J. W. Müller-Kirsten, Y.-B. Zhang, Jian-Ge Zhou, F. Zimmerschied and F.-C. Pu , Phys. Rev. B **57**, 529 (1998)
[6] Y.-B. Zhang, J.-Q. Liang, H.J.W. Müller-Kirsten, S.-P. Kou, z.-B. Wang and F.-C. Pu Phys. Rev. B **60**, 12886 (1999)
[7] D. A. Garanin, X. Martìnez Hidalgo, and E. M. Chudnovsky Phys. Rev. B **57**, 13639 (1998)
[8] E.M. Chudnovsky and L. Gunther, Phys. Rev. Lett. **60**, 661(1988); Phys. Rev. B **37**, 9455 (1988).
[9] E. M. Chudnovsky and J. Tejada, Macroscopic Quantum Tunnelling of Magnetic Moment, Cambridge university press (1998)
[10] E. M. Chudnovsky, and B. Barbara, and P. C .E Stamp Int. J. Mod. Phys. B**6**,1355 (1992)
[11] E.M. Chudnovsky and B. Barbara, Phys. lett. A **145**, 205 (1990).
[12] Anupam Garg and Gwang-Hee Kim, Phys. Rev. B **45**, 12921 (1990)
[13] A. Garg, EuroPhys. Lett. **22**, 205 (1993)
[14] Enz M and Schilling R (1986) J. Phys. C: Solid State Phys. 19 L711-5;1765-70
[15] Eugene M. Chudnovsky Journal of Magnetism and Magnetic Material **140**,1821 (1995)
[16] Sidney Coleman, Aspects of symmetry, Cambridge university press (1985)
[17] Yi-Hang Nie, Yan-Hong Jin, J-Q Liang, H J W Müller-Kirsten, D K Park, F-C Pu, J. Phys.: Condens. Matter **12** (2000) L87-L91
[18] Florian Meier and Daniel Loss Phys. Rev. Lett. **86**, 5373 (2001)
[19] O. Waldmann, C. Dobe, H. U. Güdel, and H. Mutka Phys. Rev. B **74**, 054429 (2006)
[20] D A Garanin (1991) J. Phys. A: Math. Gen. 24 L61
[21] John R. Klauder Phys. Rev. D 19, 2349 (1978)
[22] Solomon Akaraka Owerre and M.B. Paranjape, Phys. Rev. B **88**, 220403(R) (2013)

3.7 Article for the two interacting dimer model

The article below on macroscopic quantum tunneling with two interacting spins is published in Physics Review B, Rapid Communications. Reprinted with permission from Ref.[103]. Copyright (2013) by the American Physical Society. My contributions to this research work are commensurate with my supervisor's (co-author) contributions, which includes the following: originality, problem formulation, methodology, and results.

UdeM-GPP-TH-13-222
arXiv:1304.3734

Macroscopic quantum spin tunnelling with two interacting spins.

Solomon A. Owerre and M. B. Paranjape
Groupe de physique des particules, Département de physique, Université de Montréal, C.P. 6128, succ. centre-ville, Montréal, Québec, Canada, H3C 3J7

ABSTRACT

We study the simple Hamiltonian, $H = -K(S_{1z}^2 + S_{2z}^2) + \lambda \vec{S}_1 \cdot \vec{S}_2$, of two, large, coupled spins which are taken equal, each of total spin s with λ the exchange coupling constant. The exact ground state of this simple Hamiltonian is not known for an antiferromagnetic coupling corresponding to the $\lambda > 0$. In the absence of the exchange interaction, the ground state is four fold degenerate, corresponding to the states where the individual spins are in their highest weight or lowest weight states, $|\uparrow,\uparrow\rangle, |\downarrow,\downarrow\rangle, |\uparrow,\downarrow\rangle, |\downarrow,\uparrow\rangle$, in obvious notation. The first two remain exact eigenstates of the full Hamiltonian. However, we show the that the two states $|\uparrow,\downarrow\rangle, |\downarrow,\uparrow\rangle$ organize themselves into the combinations $|\pm\rangle = \frac{1}{\sqrt{2}}(|\uparrow,\downarrow\rangle \pm |\downarrow\uparrow\rangle)$, up to perturbative corrections. For the anti-ferromagnetic case, we show that the ground state is non-degenerate, and we find the interesting result that for integer spins the ground state is $|+\rangle$, and the first excited state is the anti-symmetric combination $|-\rangle$ while for half odd integer spin, these roles are exactly reversed. The energy splitting however, is proportional to λ^{2s}, as expected by perturbation theory to the $2s^{\text{th}}$ order. We obtain these results through the spin coherent state path integral.

PACS numbers: 73.40.Gk,75.45.+j,75.50.Ee,75.50.Gg,75.50.Xx,75.75.Jn

Introduction- We study the case of two large, coupled, quantum spins in the presence of a large, simple, easy axis anisotropy, interacting with each other through a standard spin-spin exchange coupling, corresponding to the Hamiltonian

$$H = -K(S_{1z}^2 + S_{2z}^2) + \lambda \vec{S}_1 \cdot \vec{S}_2. \tag{1}$$

We will consider $K > 0$ and specialize to the case of equal spins $\vec{S}_1 = \vec{S}_2 = \vec{S}$. $\lambda > 0$ gives an anti-ferromagnetic coupling while $\lambda < 0$ sign corresponds to ferromagnetic coupling. The spins $\vec{S}_i$ could correspond to quantum spins of macroscopic multi-atomic molecules [1–3], or the quantum spins a macroscopic ferromagnetic grains [4], or the average spin of each of the two staggered Neél sublattices in a quantum anti-ferromagnet [2, 5].

The non-interacting system is defined by $\lambda = 0$, here the spin eigenstates of S_{iz}, notationally $|s, s_{1z}\rangle \otimes |s, s_{2z}\rangle \equiv |s_{1z}, s_{2z}\rangle$, are obviously exact eigenstates. The ground state is four-fold degenerate, corresponding to the states $|s, s\rangle$, $|-s, -s\rangle$, $|s, -s\rangle$ and $|-s, s\rangle$, which we will write as $|\uparrow,\uparrow\rangle, |\downarrow,\downarrow\rangle, |\uparrow,\downarrow\rangle, |\downarrow,\uparrow\rangle$, each with energy $E = -2Ks^2$. The first excited state, which is 8 fold degenerate, is split from the ground state by energy $\Delta E = K(2s-1)$.

In the weak coupling limit, $\lambda/K \to 0$, it is an interesting question to ask what is the ground state and the first few excited states of the system for large spin $\vec{S}$. Surprisingly, this is yet, in general, an unsolved problem. For spin 1/2, the exact eigenstates are trivially found, for spin 1, the problem is a 9×9 matrix, which again can be diagonalized, but soon the problem becomes intractable. In principle we must diagonalize a $(2s+1)^2 \times (2s+1)^2$ matrix, that though is rather sparse, is not amenable to an exact diagonalization. For weak coupling the anisotropic potential continues to align or anti-align the spins along the z axis in the ground state.

As the non-interacting ground state is four fold degenerate, in first order degenerate perturbation theory, we should diagonalize the exchange interaction in the degenerate subspace. However, it turns out to be already diagonal in that subspace. The full Hamiltonian can be alternatively written as

$$H = -K(S_{1z}^2 + S_{2z}^2) + \lambda \left(S_{1z}S_{2z} + \frac{1}{2}(S_1^+ S_2^- + S_1^- S_2^+) \right), \tag{2}$$

where $S_i^{\pm} = S_{ix} \pm iS_{iy}$ for $i = 1, 2$. $S_i^{\pm}$ act as raising and lowering operators for S_{iz}, and hence they must annihilate the states $|\uparrow,\uparrow\rangle, |\downarrow,\downarrow\rangle$. Thus the two states $|\uparrow,\uparrow\rangle, |\downarrow,\downarrow\rangle$ are actually exact eigenstates of the full Hamiltonian with exact energy eigenvalue $(-2K + \lambda)s^2$. These two states do not mix with the two states $|\uparrow,\downarrow\rangle, |\downarrow,\uparrow\rangle$ as the eigenvalue of $S_{1z} + S_{2z}$, which is conserved, is respectively $+2s$, $-2s$ and 0. The perturbation, apart from the diagonal term $\lambda S_{1z}S_{2z}$, acting on the two states $|\uparrow,\downarrow\rangle, |\downarrow,\uparrow\rangle$ takes them out of the degenerate subspace, thus this part does not give any correction to the energy. The action of the diagonal term on either of these states is equal to $-\lambda s^2$. Thus the perturbation corresponds to the identity matrix within the degenerate subspace of the two states $|\uparrow,\uparrow\rangle, |\downarrow,\downarrow\rangle$, with eigenvalue $-\lambda s^2$. This yields, in first order degenerate perturbation theory, the perturbed energy eigenvalue of $(-2K - \lambda)s^2$ for the two states $|\uparrow,\downarrow\rangle, |\downarrow,\uparrow\rangle$. Thus the following picture emerges of the first four levels in first order degenerate perturbation theory. For the $\lambda < 0$ (ferromagnetic coupling), the states $|\uparrow,\uparrow\rangle, |\downarrow,\downarrow\rangle$ are the exact, degenerate ground states of the theory, with energy eigenvalue

$(-2K+\lambda)s^2 = (-2K-|\lambda|)s^2$. The first excited states are also degenerate, but only within first order degenerate perturbation theory. They are given by $|\uparrow,\downarrow\rangle, |\downarrow,\uparrow\rangle$, with energy eigenvalue $(-2K-\lambda)s^2 = (-2K+|\lambda|)s^2$. For the $\lambda > 0$ (anti-ferromagnetic coupling), the roles are exactly reversed. The states $|\uparrow,\downarrow\rangle, |\downarrow,\uparrow\rangle$ give the degenerate ground state with energy $(-2K-\lambda)s^2$ in first order degenerate perturbation, while the states $|\uparrow,\uparrow\rangle, |\downarrow,\downarrow\rangle$ give the exact, first (doubly degenerate) excited level with energy $(-2K+\lambda)s^2$.

In this communication, we will show that in fact, the states $|\pm\rangle = \frac{1}{\sqrt{2}}(|\uparrow,\downarrow\rangle \pm |\downarrow\uparrow\rangle)$ are the appropriate linear combinations implied by the degenerate perturbation theory, for the ground state in the anti-ferromagnetic case, and they are the second and third excited states in the ferromagnetic case. We will also show that the states $|\pm\rangle$ are no longer degenerate. The perturbing Hamiltonian links the state $|\pm s, \mp s\rangle$ only to the state $|\pm s \mp 1, \mp s \pm 1\rangle$. To reach the state $|\mp s, \pm s\rangle$ from the state $|\pm s, \mp s\rangle$ requires one to go to $2s^{\text{th}}$ order in perturbation, and s is assumed to be large. Indeed, we find our results via macroscopic quantum tunnelling using the spin coherent state path integral. Using the path integral to determine large orders in perturbation theory has already been studied in field theory [6].

Spin coherent state path integral - The quantum (large) spin systems can be described by the spin coherent state path integral [7–9].

$$\langle\chi|e^{-\beta H}|\psi\rangle = \mathcal{N}\int_{\psi}^{\chi}\mathcal{D}\theta_i\mathcal{D}\phi_i\; e^{-S_E}. \tag{3}$$

S_E is the Euclidean action which corresponding to dynamics of particles moving on a two sphere, and which contains first order kinetic term, the Wess-Zumino-Novikov-Witten (WZNW) term for the spin degree of freedom [10]. The WZNW term for a spin degree of freedom can be written in a parametrisation independent fashion by extending the time dimension by an additional spatial dimension denoted by x. Then the WZNW term corresponds to the integral

$$S_{WZNW} = \sigma\int dt\int_0^1 dx\hat{S}(t,x)\cdot(\partial_x\hat{S}(t,x)\times\partial_t\hat{S}(t,x)). \tag{4}$$

where $\hat{S}(t,x)$ is a 3-vector of unit norm, which satisfies at $x=0$ the boundary condition $\hat{S}(t,0) = \hat{S}(t)$, and at $x=1$ that the spin configuration is constant, which we can take $\hat{S}(t,1) = \hat{z}$. It does not actually matter how the spin configuration is extended into the extra dimension, as long as the boundary conditions are respected, the integral Eq.(4) changes only by an integer multiple of 4π. Thus taking $\sigma = N/2$ where N is an integer, means that this discrete ambiguity is unobservable in the functional integral (3), and nicely gives us the quantization of the spin. We refer the reader to [10] for all the details. If we parametrize the configuration explicitly as $\hat{S}(t,x) = (\sin((1-x)\theta(t))\cos\phi(t), \sin((1-x)\theta(t))\sin\phi(t), \cos((1-x)\theta(t)))$ which satisfies the boundary conditions at $x=0$ and $x=1$, then after an easy calculation of the integrand we find that the x integration can be explicitly done giving

$$\begin{aligned} S_{WZNW} &= \int dt\int_0^1 dx - \sigma\dot{\phi}(t)\sin((1-x)\theta(t)) \\ &= \int dt\; -\sigma\dot{\phi}(t)\cos((1-x)\theta(t))\Big|_0^1 \\ &= \int dt - \sigma\dot{\phi}(t)(1-\cos(\theta(t))). \end{aligned} \tag{5}$$

Hence we recover the familiar expression in condensed matter physics for the the Wess-Zumino-Novikov-Witten term.

Our two spin system, in real time, is governed by an action $S = \int dt\mathcal{L}$ where,

$$\begin{aligned} \mathcal{L} = \int dx\,\sigma_1\hat{S}_1\cdot(\partial_x\hat{S}_1\times\partial_t\hat{S}_1) - V_1(\hat{S}_1) + \\ + \int dx\,\sigma_2\hat{S}_2\cdot(\partial_x\hat{S}_2\times\partial_t\hat{S}_2) - V_2(\hat{S}_2) - \lambda\hat{S}_1\cdot\hat{S}_2 \end{aligned} \tag{6}$$

where now $\hat{S}_i = (\sin\theta_i\cos\phi_i, \sin\theta_i\sin\phi_i, \cos\theta_i)\,, i = 1,2$ are two different 3-vectors of unit norm, representing semi-classically the quantum spin [4] and σ_i are the values of each spin. In terms of spherical coordinates the Lagrangian takes the form

$$\begin{aligned} \mathcal{L} &= -\sigma_1\dot{\phi_1}(1-\cos\theta_1) - V_1(\theta_1,\phi_1) \\ &- \sigma_2\dot{\phi_2}(1-\cos\theta_2) - V_2(\theta_2,\phi_2) \\ &- \lambda\left(\sin\theta_1\sin\theta_2\cos(\phi_1-\phi_2) + \cos\theta_1\cos\theta_2\right). \end{aligned} \tag{7}$$

We consider the special case of equal spins, with $\sigma_1 = \sigma_2 = s$. Our analysis is valid if we restrict our attention to any external potential with easy-axis, azimuthal symmetry, with a reflection symmetry (along the azimuthal axis), as in [11], $V_i(\theta_i,\phi_i) \equiv V(\theta_i) = V(\pi-\theta_i), i = 1,2$. The potential is further assumed to have a minimum at the north pole and the south pole, at $\theta_i = 0$, and π. In our case the potential is explicitly

$$V(\hat{S}_i) \equiv V(\theta_i,\phi_i) = K\sin^2\theta_i. \tag{8}$$

It was shown in Ref. [11], for uncoupled spins, that quantum tunnelling between the spin up and down states of each spin separately is actually absent because of conservation of the z component of each spin. With the exchange interaction only the total z component is conserved allowing transitions $|\uparrow,\downarrow\rangle \longleftrightarrow |\downarrow,\uparrow\rangle$. In general tunnelling exists if there is an equipotential path that links the beginning and end points. We will see that such an equipotential path exists, but through complex values of the phase space variables.

We must find the critical points of the Euclidean action with $t \to -i\tau$, see Ref. [12], which gives

$$\mathcal{L}_E = is\dot{\phi_1}(1-\cos\theta_1) + V(\theta_1) + is\dot{\phi_2}(1-\cos\theta_2) + V(\theta_2) + \lambda\left(\sin\theta_1\sin\theta_2\cos(\phi_1-\phi_2) + \cos\theta_1\cos\theta_2\right). \quad (9)$$

The solutions must start at $(\theta_1, \phi_1) = (0, 0)$ and $(\theta_2, \phi_2) = (\pi, 0)$, say, and evolve to $(\theta_1, \phi_1) = (\pi, 0)$ and $(\theta_2, \phi_2) = (0, 0)$. In Euclidean time, the WZNW term has become imaginary and the equations of motion in general only have solutions for complexified field configurations. Varying with respect to ϕ_i gives equations that correspond to the conservation of angular momentum:

$$is\frac{d}{d\tau}(1-\cos\theta_1) + \lambda\sin\theta_1\sin\theta_2\sin(\phi_1-\phi_2) = 0 \quad (10)$$

$$is\frac{d}{d\tau}(1-\cos\theta_2) - \lambda\sin\theta_1\sin\theta_2\sin(\phi_1-\phi_2) = 0 \quad (11)$$

Varying with respect to θ_i gives the equations:

$$\frac{\partial\mathcal{L}_E}{\partial\theta_1} = 0 = \frac{\partial\mathcal{L}_E}{\partial\theta_2} \quad (12)$$

Adding Eqn's (10) and (11) we simply get

$$\frac{d}{d\tau}(\cos\theta_1 + \cos\theta_2) = 0. \quad (13)$$

Hence $\cos\theta_1 + \cos\theta_2 = l = 0 \quad \Longrightarrow \theta_2 = \pi - \theta_1$, where the constant l is chosen to be zero using the initial condition $\theta_1 = 0, \theta_2 = \pi$. We can now eliminate θ_2 from the equations of motion and writing $\theta = \theta_1$, $\phi = \phi_1 - \phi_2$ and $\Phi = \phi_1 + \phi_2$ and taking $V_i(\theta_i) = V(\theta_i) = V(\pi - \theta_i)$ we get the effective Lagrangian:

$$\mathcal{L} = is\dot{\Phi} - is\dot{\phi}\cos\theta + U(\theta, \phi) \quad (14)$$

where $U(\theta,\phi) = 2V(\theta) + \lambda\left(\sin^2\theta\cos\phi - \cos^2\theta\right) + \lambda$ is the effective potential energy. We have added a constant λ so that the potential is normalized to zero at $\theta = 0$. The first term in the Lagrangian is a total derivative and drops out. The equations of motion become:

$$is\dot{\phi}\sin\theta = -\frac{\partial U(\theta,\phi)}{\partial\theta} \quad (15)$$

$$is\dot{\theta}\sin\theta = \frac{\partial U(\theta,\phi)}{\partial\phi} \quad (16)$$

These equations have no solutions on the space of real functions $\theta(\tau), \phi(\tau)$ due to the explicit i on the left hand side. The analog of conservation of energy follows immediately from these equations, this is easily derived by multiplying (15) by $\dot{\theta}$ and (16) by $\dot{\phi}$ and subtracting, giving:

$$\frac{dU(\theta,\phi)}{d\tau} = 0 \quad \text{i.e,} \quad U(\theta,\phi) = const. = 0 \quad (17)$$

The constant has been set to 0 using the initial condition $\theta = 0$. Thus we have, specializing to our case Eqn. (8)

$$U(\theta,\phi) = (2K + \lambda(\cos\phi + 1))\sin^2\theta = 0 \quad (18)$$

implying $(2K + \lambda(\cos\phi + 1)) = 0$ since $\sin^2\theta \neq 0$, is required for a non-trivial solution. Thus

$$\cos\phi = -\left(\frac{2K}{\lambda} + 1\right) \quad (19)$$

and we see that ϕ must be a constant. This is not valid in general, it is due to the specific choice of the external potential Eqn. (8). Since $K > |\lambda|$ we get $|\cos\phi| > 1$, which of course has no solution for real ϕ. We take $\phi = \phi_R + i\phi_I$ which gives $\cos\phi = \cos\phi_R\cosh\phi_I - i\sin\phi_R\sinh\phi_I$. As the RHS of Eqn. (19) is real, we must have either $\phi_I = 0$ or $\phi_R = n\pi$ or both. Clearly the $\phi_I = 0$ cannot yield a solution for Eqn. (19), hence we must have $\phi_R = n\pi$. As we must impose 2π periodicity on ϕ_R only $n = 0$ or 1 exist. Then we get

$$\cos\phi = (-1)^n\cosh\phi_I = \begin{cases} -\left(\frac{2K}{\lambda} + 1\right) & \text{if } \lambda > 0 \\ +\left(\frac{2K}{|\lambda|} - 1\right) & \text{if } \lambda < 0 \end{cases} \quad (20)$$

Thus $n = 1$ for $\lambda > 0$ and $n = 0$ for $\lambda < 0$ allowing for the unified expression

$$\cosh\phi_I = \frac{2K + \lambda}{|\lambda|}. \quad (21)$$

Eqn. (16) simplifies to

$$is\frac{\dot{\theta}}{\sin\theta} = -\lambda\sin\phi = -i\lambda(-1)^n\sinh\phi_I = i|\lambda|\sinh\phi_I \quad (22)$$

as $\lambda(-1)^n = -|\lambda|$. Eqn. (21) has two solutions positive ϕ_I corresponds to the instanton, $(\dot{\theta} > 0)$, and negative ϕ_I corresponds to the anti-instanton, $(\dot{\theta} < 0)$. The equation is trivially integrated with solution

$$\theta(\tau) = 2\arctan\left(e^{\omega(\tau-\tau_0)}\right) \quad (23)$$

where $\omega = (|\lambda|/s)\sinh\phi_I$ and at $\tau = \tau_0$ we have $\theta(\tau) = \pi/2$. Thus $\theta(\tau)$ interpolates from 0 to π as $\tau = -\infty \to \infty$ for the instanton and from π to 0 for an anti-instanton.

Using $\dot{\phi} = 0$ and (17) we see that the action for this instanton trajectory, let us call it S_0, simply vanishes $S_0 = \int_{-\infty}^{\infty} d\tau\mathcal{L} = 0$. So where could the amplitude come from? We have not taken into account the fact that ϕ must be translated from $\phi = 0$ (any initial point will do, as long as it is consistently used to compute the full amplitude) to $\phi = n\pi + i\phi_I$ before the instanton can occur and then back to $\phi = 0$ after the instanton has occurred. Normally such a translation has no effect, either the change at the beginning cancels that at the end, or if the action is second order in time derivative, moving adiabatically gives no contribution. But in the present

case, before the instanton occurs, $\theta = 0$, but after it has occurred, $\theta = \pi$. As $\dot{\phi}$ is multiplied by $\cos\theta$ in the action, the two contributions actually add, there is a net contribution to the action. Indeed the change of the full action for the combination of the instanton and the changes in ϕ is given by

$$\begin{aligned}\Delta S &= \int_0^{n\pi+i\phi_I} -is d\phi \cos\theta|_{\theta=0} + S_0 + \int_{n\pi+i\phi_I}^0 -is d\phi \cos\theta|_{\theta=\pi} \\ &= -is2n\pi + 2s\phi_I. \end{aligned} \tag{24}$$

We will use this information to compute the following matrix element, using the spin coherent states $|\theta,\phi\rangle$ and the lowest two energy eigenstates $|E_0\rangle$ and $|E_1\rangle$:

$$\begin{aligned}\langle\theta_f,\phi_f|e^{-\beta H}|\theta_i,\phi_i\rangle &= e^{-\beta E_0}\langle\theta_f,\phi_f|E_0\rangle\langle E_0|\theta_i,\phi_i\rangle \\ &+e^{-\beta E_1}\langle\theta_f,\phi_f|E_1\rangle\langle E_1|\theta_i,\phi_i\rangle + \cdots \end{aligned} \tag{25}$$

On the other hand, the matrix element is given by the spin coherent state path integral

$$\langle\theta_f,\phi_f|e^{-\beta H}|\theta_i,\phi_i\rangle = \mathcal{N}\int_{\theta_i,\phi_i}^{\theta_f,\phi_f}\mathcal{D}\theta\mathcal{D}\phi\; e^{-S_E}. \tag{26}$$

The integration is done in the saddle point approximation. With $(\theta_i,\phi_i) = (0,0)$ corresponding to the state $|\uparrow,\downarrow\rangle$ and $(\theta_f,\phi_f) = (\pi,0)$ corresponding to the state $|\downarrow,\uparrow\rangle$we get, with a mild abuse of notation

$$\langle\downarrow,\uparrow|e^{-\beta H}|\uparrow,\downarrow\rangle = \mathcal{N}e^{-\Delta S}\kappa\beta(1+\cdots) \tag{27}$$

where κ is the ratio of the square root of the determinant of the operator governing the second order fluctuations about the instanton excluding the time translation zero mode, and that of the free determinant. It can in principle be calculated, but we have not done this. The zero mode is taken into account by integrating over the position of the occurrence of the instanton giving rise to the factor of β. $\mathcal{N}$ is the overall normalisation including the square root of the free determinant which is given by $Ne^{-E_0\beta}$ where E_0 is the unperturbed ground state energy and N is a constant from the ground state wave function. The result exponentiates, but since we must sum over all sequences of one instanton followed by any number of anti-instanton/instanton pairs, the total number of instantons and anti-instantons is odd, and we get

$$e^{-\Delta S}\kappa\beta \to \sinh\left(e^{-\Delta S}\kappa\beta\right) \tag{28}$$

Given $\Delta S = -is2n\pi + 2s\phi_I$ and solving Eqn. (21) for ϕ_I for $K \gg |\lambda|$

$$\phi_I = \operatorname{arccosh}\left(\frac{2K+\lambda}{|\lambda|}\right) \approx \ln\left(\frac{4K}{|\lambda|}\right) \tag{29}$$

gives [13]:

$$e^{-\Delta S} = \begin{cases} e^{is2\pi - 2s\phi_I} & \text{if } \lambda > 0 = \begin{cases}\left(\frac{|\lambda|}{4K}\right)^{2s} & \text{if } s \in \mathbf{Z} \\ -\left(\frac{|\lambda|}{4K}\right)^{2s} & \text{if } s \in \mathbf{Z}+1/2\end{cases} \\ \left(\frac{|\lambda|}{4K}\right)^{2s} & \text{if } \lambda < 0 \end{cases} \tag{30}$$

Then we get

$$\langle\downarrow,\uparrow|e^{-\beta H}|\uparrow,\downarrow\rangle = \pm\left(\frac{1}{2}e^{\left(\frac{|\lambda|}{4K}\right)^{2s}\kappa\beta} - \frac{1}{2}e^{-\left(\frac{|\lambda|}{4K}\right)^{2s}\kappa\beta}\right)Ne^{-\beta E_0} \tag{31}$$

where the $-$ sign only applies for the case of anti-ferromagnetic coupling with half odd integer spin, $\lambda > 0, s = \mathbf{Z} + 1/2$. An essentially identical analysis yields

$$\begin{aligned}\langle\downarrow,\uparrow|e^{-\beta H}|\downarrow,\uparrow\rangle &= \langle\uparrow,\downarrow|e^{-\beta H}|\uparrow,\downarrow\rangle \\ &= \left(\frac{1}{2}e^{\left(\frac{|\lambda|}{4K}\right)^{2s}\kappa\beta} + \frac{1}{2}e^{-\left(\frac{|\lambda|}{4K}\right)^{2s}\kappa\beta}\right)Ne^{-\beta E_0}. \end{aligned} \tag{32}$$

These calculated matrix elements should now be compared with what is expected for the exact theory:

$$\begin{aligned}\langle\downarrow,\uparrow|e^{-\beta H}|\uparrow,\downarrow\rangle &= e^{-\beta(E_0-\frac{1}{2}\Delta E)}\langle\downarrow,\uparrow|E_0\rangle\langle E_0|\uparrow,\downarrow\rangle \\ &+ e^{-\beta(E_0+\frac{1}{2}\Delta E)}\langle\downarrow,\uparrow|E_1\rangle\langle E_1|\uparrow,\downarrow\rangle \end{aligned} \tag{33}$$

and say

$$\begin{aligned}\langle\downarrow,\uparrow|e^{-\beta H}|\downarrow,\uparrow\rangle &= e^{-\beta(E_0-\frac{1}{2}\Delta E)}\langle\downarrow,\uparrow|E_0\rangle\langle E_0|\downarrow,\uparrow\rangle \\ &+ e^{-\beta(E_0+\frac{1}{2}\Delta E)}\langle\downarrow,\uparrow|E_1\rangle\langle E_1|\downarrow,\uparrow\rangle \end{aligned} \tag{34}$$

The energy splitting can be read off from this result

$$\Delta E = E_1 - E_2 = 2\left(\frac{|\lambda|}{4K}\right)^{2s}\kappa \tag{35}$$

and our main result follows, the low energy eigenstates are given by

$$|E_0\rangle = \frac{1}{\sqrt{2}}(|\downarrow,\uparrow\rangle + |\uparrow,\downarrow\rangle) \qquad |E_1\rangle = \frac{1}{\sqrt{2}}(|\downarrow,\uparrow\rangle - |\uparrow,\downarrow\rangle) \tag{36}$$

for $\lambda < 0$ (although here the energy eigenstates should be $|E_3\rangle$ and $|E_4\rangle$) and $\lambda > 0$ for $s \in \mathbf{Z}$, while for the anti-ferromagnetic $\lambda > 0$ case with $s \in \mathbf{Z} + 1/2$ we get

$$|E_0\rangle = \frac{1}{\sqrt{2}}(|\downarrow,\uparrow\rangle - |\uparrow,\downarrow\rangle) \qquad |E_1\rangle = \frac{1}{\sqrt{2}}(|\downarrow,\uparrow\rangle + |\uparrow,\downarrow\rangle). \tag{37}$$

This understanding of the ground state in the anti-ferromagnetic case is our main result. This difference in the ground states for integer and half odd integer spins is understood in terms of the Berry phase [7] (computed by

the change in the Wess-Zumino term) for the evolution corresponding to the instanton. It can also be understood by looking at perturbation theory to order $2s$, the details cannot be given here. Briefly, one finds that the effective 2×2 Hamiltonian for the degenerate subspace is proportional to the identity plus off diagonal terms that are symmetric. For the integer spin case the off diagonal terms are negative and for the half odd integer case they are positive. Diagonalizing this 2×2 matrix gives the solutions for the ground states, exactly as we have found.

Conclusions- We have found the low energy eigenvalues and the corresponding eigenstates for the Hamiltonian of two equal, large, spins interacting with an easy axis anisotropy and a standard exchange interaction, the latter which is considered as a perturbation. We find that the two states $|\downarrow,\uparrow\rangle, |\uparrow,\downarrow\rangle$ reorganize into the symmetric and the anti-symmetric superposition because of quantum tunnelling transitions. These transitions correspond to the $2s^{\rm th}$ order effects in perturbation theory. The symmetric combination is the lower energy state for integer spin while the anti-symmetric state is the the lower energy state for half odd integer spins. These states are respectively the ground states for an anti-ferromagnetic coupling.

Acknowledgments- We thank Ian Affleck, Sung-Sik Lee and Cliff Burgess for useful discussions and we thank NSERC of Canada for financial support.

[1] J. Ummethum, J. Nehrkorn, S. Mukherjee, N. B. Ivanov1, S. Stuiber, Th. Strässle, P. L. W. Tregenna-Piggott, H. Mutka, G. Christou, O. Waldmann, and J. Schnack Phys. Rev. B **86**, 104403 (2012)

[2] O. Waldmann, C. Dobe, H. U. Güdel, and H. Mutka Phys. Rev. B **74**, 054429 (2006)

[3] Florian Meier, Jeremy Levy and Daniel Loss, Phys. Rev. B **68**, 134417 (2003)

[4] E.M. Chudnovsky and L. Gunther, Phys. Rev. Lett. **60**, 661(1988); Phys. Rev. B **37**, 9455 (1988).

[5] Florian Meier and Daniel Loss Phys. Rev. Lett. **86**, 5373 (2001); Phys. Rev. B **64**, 224411 (2001)

[6] J. C. Collins and D. E. Soper, Annals Phys. **112**, 209 (1978); J. Zinn-Justin, Physics Reports **70**, 109 (1981)

[7] D.Loss, D. P. Di Vincenzo, G. Grinstein, Phys. Rev. Lett. **69**, 3232 (1992); J. von Delft, C. Henley, Phys. Rev. Lett. **69**, 3236(1992)

[8] John R. Klauder Phys. Rev. D **19**, 2349 (1978)

[9] Alexander Altland and Ben Simons, Condensed Matter Field Theory, Cambridge University Press, New York, (2010); Hagen Kleinert, Path Integrals in Quantum Mechanics, Statistics, Polymer Physics and Financial Markets, World scientific publishing Co. Pte. Ltd (2009)

[10] J. Wess, B. Zumino, Phys. Lett. B **37**:95,1971; S.P. Novikov, Usp.Mat.Nauk, 37N5:3-49,1982; E. Witten, Nucl. Phys., B**160**:57,1979.

[11] Avinash Khare, M.B Paranjape, Phys. Rev. B **83**, 172401 (2011) [arXiv:hep-th/0806.4692].

[12] Sidney Coleman Phys. Rev. D **15**, 10 (1977); Anupam Garg, Evgueny Kochetov, Kee-Su Park and Michael Stone, Journal of mathematical physics, **44**, 48 (2003)

[13] We thank Sung-Sik Lee for a discussion at this point which led to the understanding of the (expected to him) following result.

CHAPTER 4

ROTATING ENTANGLED STATES OF AN EXCHANGE-COUPLED DIMER

> If you can't explain it simply, you don't understand it well enough.
>
> Albert Einstein

4.1 Introduction

Quite recently, the problem of a molecular magnet which is free to rotate about an easy axis direction has been the focus of interest in macroscopic quantum phenomenon. The conservation of the total angular momentum plays a decisive role in these studies, because the rotating nanomagnet couples to its mechanical motion in an equal and opposite directions. This problem has been studied experimentally for free magnetic clusters and magnetic microresonators [36]. For a biaxial ferromagnetic spin system which can rotate about the easy-axis direction, an extensive theoretical study has also been investigated [29, 30]; it shows that the coupling of mechanical motion, together with the spin renormalizes the magnetic anisotropy and increases the tunneling splitting.

In this chapter we will investigate the rotation of an antiferromagnetic exchange-coupled dimer about the easy axis direction. This chapter is solely based on the published article of the present author of this thesis [102] and the article will be included at end of this chapter. In the perturbative limit, we showed in Sec.(3.3), that the energy splitting between the ground state and the first-excited state of this system arises from $2s^{\text{th}}$ in degenerate perturbation theory. Thus, the Hamiltonian at this order is simply a 2×2 matrix; it can be written as

$$\hat{H}\psi_{\pm} = \mathcal{E}_{\pm}\psi_{\pm}; \quad \Delta = \mathcal{E}_{+} - \mathcal{E}_{-} \sim \left(\frac{|\mathcal{J}|}{4\mathcal{D}}\right)^{2s}; \tag{4.1}$$

where

$$\psi_- = \frac{1}{\sqrt{2}} \left(|\uparrow, \downarrow\rangle - |\downarrow, \uparrow\rangle \right), \tag{4.2}$$

$$\psi_+ = \frac{1}{\sqrt{2}} \left(|\uparrow, \downarrow\rangle + |\downarrow, \uparrow\rangle \right). \tag{4.3}$$

This 2×2 matrix is similar to that of a two-level system. Thus, there exits a one-to-one correspondence between this system and that of a two-level entangled pseudospin $\frac{1}{2}$ particles. The arrangement of this chapter is as follows: In Sec.(4.2), we will present the mapping of this exchange coupled-dimer model to a pseudospin $\frac{1}{2}$ two-level system. Sec.(4.3) deals with the effects of a staggered magnetic field on the resulting two-level system of this exchange coupled-dimer. In Sec.(4.4), we will study the effects of an environmental coupling to this system. The case of independent boson model will be studied in detail. In Sec.(4.5), we will consider the effects of rotation on two-level system. We will derive the exact low-energy eigenstates and eigenvalues of this rotating dimer model. We will also discuss the effect of a dissipative environment on this rotating two-level system. The final section gives a concluding remark.

4.2 Mapping to a pseudospin one-half particles

The ground state, Eqn.(4.2) corresponds to the maximally entangled antisymmetric combination, whereas the first excited state, Eqn.(4.3) corresponds to the maximally entangled symmetric combination for half-odd integer spins. For integer spins, these roles are reversed. In quantum computing terminology, these energy eigenstates are entangled states for spin $\frac{1}{2}$ particles; they play a decisive role in quantum information processes, such as quantum teleportation and quantum register. There are equal probabilities of measuring either $|\downarrow, \uparrow\rangle$ or $|\uparrow, \downarrow\rangle$, that is $\frac{1}{2}$. The eigenvalue equation, Eqn.(4.1) is effectively similar to that of a two-level system; thus, this system can be mapped to an entangled pseudospin $\frac{1}{2}$ particles, whose motion is restricted to the subspace of the to-

tal Hilbert space. The most expedient way of doing this mapping is by constructing an equivalent pseudospin $\frac{1}{2}$ matrices using the two-qubit states $|\downarrow,\uparrow\rangle$ and $|\uparrow,\downarrow\rangle$. These matrices can be constructed as follows:

$$\hat{\alpha}_x = \psi_+\psi_+^\dagger - \psi_-\psi_-^\dagger = |\uparrow,\downarrow\rangle\langle\downarrow,\uparrow| + |\downarrow,\uparrow\rangle\langle\uparrow,\downarrow|, \tag{4.4}$$

$$\hat{\alpha}_y = i[\psi_+\psi_-^\dagger - \psi_-\psi_+^\dagger] = -i\,|\uparrow,\downarrow\rangle\langle\downarrow,\uparrow| + i\,|\downarrow,\uparrow\rangle\langle\uparrow,\downarrow|, \tag{4.5}$$

$$\hat{\alpha}_z = \psi_+\psi_-^\dagger + \psi_-\psi_+^\dagger = |\uparrow,\downarrow\rangle\langle\uparrow,\downarrow| - |\downarrow,\uparrow\rangle\langle\downarrow,\uparrow|, \tag{4.6}$$

$$\hat{I} = \psi_+\psi_+^\dagger + \psi_-\psi_-^\dagger = |\uparrow,\downarrow\rangle\langle\uparrow,\downarrow| + |\downarrow,\uparrow\rangle\langle\downarrow,\uparrow|. \tag{4.7}$$

Indeed, these matrices are entangled, since they cannot be separated as $\hat{\alpha}_{1,x} \otimes \hat{\alpha}_{2,x}$, etc.; it is noted that in the two-qubit form, they satisfy the usual commutation and anti-commutation relations $[\hat{\alpha}_k, \hat{\alpha}_j] = 2i\epsilon_{ijk}\hat{\alpha}_k$ and $\{\hat{\alpha}_k, \hat{\alpha}_j\} = 2\delta_{ij}$. In the matrix representation, they are 4×4 sparse matrices, which are not Pauli matrices but their subspace contains the usual 2×2 Pauli matrices. The Hamiltonian $\hat{H}$ can now be projected unto the two qubit states $|\downarrow,\uparrow\rangle$ and $|\uparrow,\downarrow\rangle$; the projected Hamiltonian is given by

$$\hat{H}_\alpha = \sum_{m,n=\pm s} |m,-m\rangle\,\hat{H}_{mn}\,\langle n,-n|, \tag{4.8}$$

where $\hat{H}_{mn} = \langle m,-m|\hat{H}|n,-n\rangle$.

Adding and subtracting the two equations in Eqn.(4.1) we obtain

$$\hat{H}\,|\uparrow,\downarrow\rangle = \frac{\sqrt{2}}{2}(\mathcal{E}_+\psi_+ + \mathcal{E}_-\psi_-), \tag{4.9}$$

$$\hat{H}\,|\downarrow,\uparrow\rangle = \frac{\sqrt{2}}{2}(\mathcal{E}_+\psi_+ - \mathcal{E}_-\psi_-). \tag{4.10}$$

Acting on the left hand side with either $\langle\uparrow,\downarrow|$ or $\langle\downarrow,\uparrow|$ we obtain the following matrix

elements

$$\langle\downarrow,\uparrow|\hat{H}|\downarrow,\uparrow\rangle = \langle\uparrow,\downarrow|\hat{H}|\uparrow,\downarrow\rangle = \frac{1}{2}(\mathcal{E}_+ + \mathcal{E}_-) = 0,$$
$$\langle\downarrow,\uparrow|\hat{H}|\uparrow,\downarrow\rangle = \langle\uparrow,\downarrow|\hat{H}|\downarrow,\uparrow\rangle = \frac{1}{2}(\mathcal{E}_+ - \mathcal{E}_-) = \frac{\Delta}{2}. \tag{4.11}$$

Consequently, the projected Hamiltonian, Eqn.(4.8) becomes

$$\hat{H}_\alpha = \frac{\Delta}{2}\hat{\alpha}_x, \tag{4.12}$$

with its eigenvalues given by $\{-\Delta/2, \Delta/2\}$. Thus, we have successfully mapped the antiferromagnetic exchange-coupled dimer to a pseudospin $\frac{1}{2}$ two-level system.

4.3 Effects of a staggered magnetic field

Let us consider applying a time varying staggered magnetic field along the easy z axis on the exchange-coupled dimer model. The additional Zeeman Hamiltonian is of the form

$$\hat{H}_Z = -h(t)(\hat{S}_{1,z} - \hat{S}_{2,z}) = -g\mu_B h(\hat{S}_{1,z} - \hat{S}_{2,z})\cos\omega t. \tag{4.13}$$

The projection of this Hamiltonian unto the two-qubit states is straightforward. The matrix element are simply given by

$$\langle\uparrow,\downarrow|\hat{H}_Z|\uparrow,\downarrow\rangle = -2sg\mu_B h\cos\omega t; \quad \langle\downarrow,\uparrow|\hat{H}_Z|\downarrow,\uparrow\rangle = 2sg\mu_B h\cos\omega t;$$
$$\langle\downarrow,\uparrow|\hat{H}_Z|\uparrow,\downarrow\rangle = \langle\uparrow,\downarrow|\hat{H}_Z|\downarrow,\uparrow\rangle = 0. \tag{4.14}$$

Thus, Eqn.(4.12) acquires an additional diagonal term, and the resulting equation

becomes

$$\hat{H}_\alpha = \frac{\Delta}{2}\hat{\alpha}_x - 2sg\mu_B h\hat{\alpha}_z \cos\omega t. \tag{4.15}$$

If we perform a unitary transformation along the y-axis using the operator

$$\hat{U}(\phi) = \exp(-i\phi\hat{\alpha}_y/2); \quad \phi = -\pi/2. \tag{4.16}$$

It is evident that the resulting Hamiltonian in this reference frame is given by

$$\hat{H}_\alpha \to \hat{U}^{-1}(\phi)\hat{H}_\alpha\hat{U}(\phi) = -\frac{\Delta}{2}\hat{\alpha}_z - sg\mu_B h\hat{\alpha}_x \cos\omega t. \tag{4.17}$$

The corresponding wave function of this system is given by

$$|\psi(t)\rangle = \mathcal{C}_{\uparrow,\downarrow}(t)e^{-i\mathcal{E}_+ t}\,|\uparrow,\downarrow\rangle + \mathcal{C}_{\downarrow,\uparrow}(t)e^{-i\mathcal{E}_- t}\,|\downarrow,\uparrow\rangle\,, \tag{4.18}$$

with $|\mathcal{C}_{\uparrow,\downarrow}(t)|^2 + |\mathcal{C}_{\downarrow,\uparrow}(t)|^2 = 1$ and $\mathcal{E}_\pm = \pm\Delta/2$. In the rotating wave approximation[118, 124], the coefficients are found to be

$$\begin{aligned}
\mathcal{C}_{\uparrow,\downarrow}(t) &= e^{-i\Delta' t/2}\left[\cos\left(\frac{\Omega t}{2}\right) + i\frac{\Delta'}{\Omega}\sin\left(\frac{\Omega t}{2}\right)\right], \\
\mathcal{C}_{\downarrow,\uparrow}(t) &= ie^{i\Delta' t/2}\frac{\Omega_R}{\Omega}\sin\left(\frac{\Omega t}{2}\right),
\end{aligned} \tag{4.19}$$

where

$$\Delta' = \Delta - \omega; \quad \Omega = \sqrt{\Omega_R^2 + \Delta'^2}; \quad \Omega_R = sg\mu_B h. \tag{4.20}$$

The expectation values of the observables are easily found using these results. They are

as follow:

$$\langle\hat{\alpha}_x\rangle_t = \frac{\Omega_R\Delta'}{\Omega^2}(1-\cos(\Omega t)), \tag{4.21}$$

$$\langle\hat{\alpha}_y\rangle_t = -\frac{\Omega_R}{\Omega}\sin(\Omega t), \tag{4.22}$$

$$\langle\hat{\alpha}_z\rangle_t = \frac{\Delta'^2}{\Omega^2} + \frac{\Omega_R^2}{\Omega^2}\cos(\Omega t). \tag{4.23}$$

4.4 The effects of an environmental coupling

In many cases of physical interest, the spin interacts with its environment. The environmental effect is customarily modelled as a bath of harmonic oscillators (bosons). The environmental effect on the Hamiltonian, Eqn.(4.12) can be written in the customary form[82]:

$$\hat{H} = \frac{\Delta}{2}\hat{\alpha}_x + \hat{I}\sum_k \epsilon_k \hat{b}_k^\dagger \hat{b}_k + \chi S_z = \hat{H}_\alpha + \hat{H}_B + H_{int}, \tag{4.24}$$

where $\hat{H}_\alpha = \Delta\hat{\alpha}_x/2$; $\hat{H}_B = \sum_k \epsilon_k \hat{b}_k^\dagger \hat{b}_k$; $H_{int} = \hat{\chi}\hat{S}_z$; $\hat{\chi} = \sum_k \gamma_k(\hat{b}_k + \hat{b}_k^\dagger)$; $\hat{S}_z = \hat{\alpha}_z/2$; $\hat{b}_k^\dagger(\hat{b}_k)$ are the creation (annihilation) operators of phonons with the wave number k. In terms of the basis states, this Hamiltonian can be written as

$$\hat{H} = (|\uparrow,\downarrow\rangle\frac{\Delta}{2}\langle\downarrow,\uparrow| + \text{h.c}) + |\downarrow,\uparrow\rangle\hat{K}_-\langle\downarrow,\uparrow| + |\uparrow,\downarrow\rangle\hat{K}_+\langle\uparrow,\downarrow|, \tag{4.25}$$

where $\hat{K}_\pm = \sum_k \epsilon_k \hat{b}_k^\dagger \hat{b}_k \pm \hat{\chi}$. In the interaction picture, we can solve for the time-evolution of $\hat{\alpha}_z(t)$ using the Heisenberg equation of motion with respect to $\hat{H}_\alpha$. The resulting expression is given by

$$\hat{\alpha}_z(t) = \hat{\alpha}_z\cos(\Delta t) + \hat{\alpha}_y\sin(\Delta t). \tag{4.26}$$

The coefficients of the trigonometric functions are determined from the initial con-

ditions at $t = 0$. The indispensable operator from which all other observables can be calculated is the reduced density matrix. It is given by

$$\hat{\rho}(t) = Tr_B \left(e^{-i\hat{H}t} \hat{\rho}(0) e^{i\hat{H}t} \right), \tag{4.27}$$

where $\hat{\rho}(0) = \hat{\rho}_\alpha \otimes \hat{\rho}_B$; $\hat{\rho}_\alpha$ acts on the spin space and $\hat{\rho}_B = e^{-\beta \hat{H}_B}/Z_B$ is the density matrix of a free boson. This system is exactly soluble in the limit $\Delta \to 0$ (independent boson model). In this limit, the bosonic bath can be traced out in Eqn.(4.27). The object of interest in this model is usually the average values of the time evolution of the observables $\hat{\alpha}_i$, $i = x, y, z$. Using the interacting picture formulation of quantum mechanics, we have

$$\langle \hat{S}_+(t) \rangle = Tr_\alpha \left(\hat{U}'(t,0) \rho(0) \hat{U}'(0,t) S_+(0) \right), \tag{4.28}$$

where $\hat{S}_+ = \hat{S}_x + i\hat{S}_y$; $\hat{U}'(t,0) = \mathcal{T} e^{-i \int_0^t dt \hat{H}'(t)}$; $\hat{H}'(t) = e^{i\hat{H}_B t} \hat{H}_{int} e^{-i\hat{H}_B t}$. A straightforward calculation of the trace yields

$$\langle \hat{S}_+(t) \rangle = C(t) \langle \hat{S}_+(0) \rangle, \tag{4.29}$$

$C(t) = \langle \mathcal{T} e^{-i \int_0^t \hat{\chi}'(t) dt} \rangle_0$ being the coherence factor between the states $|\downarrow, \uparrow\rangle$ and $|\uparrow, \downarrow\rangle$. By symmetry consideration we have $\langle \hat{S}_-(t) \rangle = C(t) \langle \hat{S}_-(0) \rangle$, hence

$$\langle \hat{\alpha}_x(t) \rangle = C(t) \langle \hat{\alpha}_x(0) \rangle. \tag{4.30}$$

The evaluation of the equilibrium expectation value with the use of Wicks theorem[90] gives

$$C(t) = e^{-\mathcal{W}(t)}; \quad |C(t)| = e^{-Re[\mathcal{W}(t)]}. \tag{4.31}$$

$$\mathcal{W}(t) = \sum_k \frac{\gamma_k^2}{\epsilon_k^2}[(1+n_B)(1-e^{-i\epsilon_k t}) + n_B(1-e^{-i\epsilon_k t}) - i\epsilon_k t], \quad n_B = (e^{\beta\epsilon_k}-1)^{-1}. \tag{4.32}$$

In the continuum limit we have

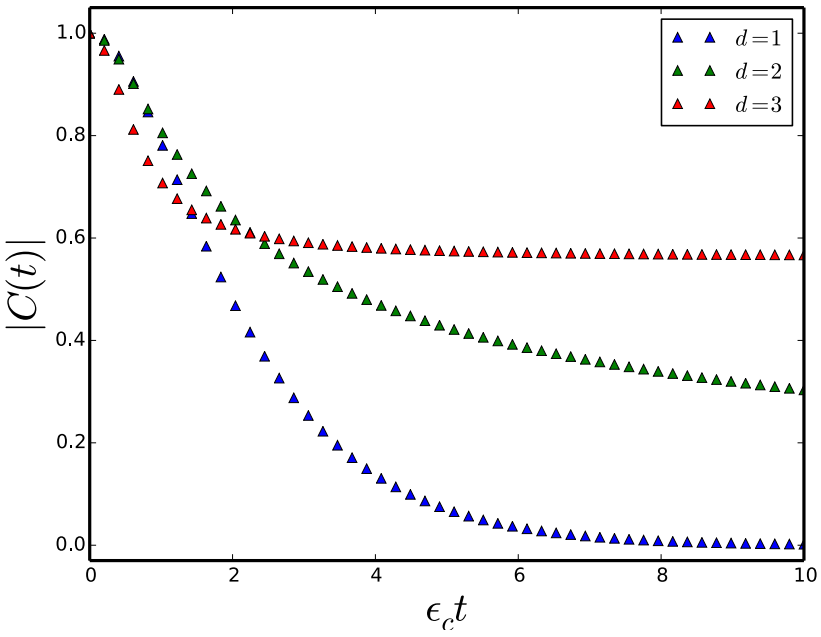

Figure 4.1: The plot of $|C(t)|$ against time for ohmic $d = 1$ and super-Ohmic $d = 2, 3$ dissipations. The function reaches a maximum of one and decays to zero at long times for the ohmic dissipation but it is never decays to zero for the super-ohmic dissipation.

$$Re[\mathcal{W}(t)] = 2\int_0^\infty d\epsilon \frac{J(\epsilon)}{\epsilon^2} \sin^2\left(\frac{\epsilon t}{2}\right) \cot\left(\frac{\beta\epsilon}{2}\right), \tag{4.33}$$

where the spectral density function $J(\epsilon) = N_d(\epsilon)\gamma(\epsilon)^2 = \mathcal{O}_d\gamma_0^2\epsilon^d e^{-\epsilon/\epsilon_c}$; $N_d(\epsilon)$ is the d-dimensional density of phonon modes and $\mathcal{O}_d$ is the d-dimensional volume. For $d = 1, 2, 3$ we have $\mathcal{O}_1 = L/\pi c_s$; $\mathcal{O}_2 = A/2\pi c_s^2$; $\mathcal{O}_3 = V/2\pi^2 c_s^3$; where L, A, V are the length, area and volume of the system respectively; c_s is the speed of sound. In Fig.(4.1), we have shown the plot of $|C(t)|$ for $d = 1, 2, 3$, with $\beta\epsilon_c = 1$. In the super-ohmic

dissipation, $d = 2, 3$, the coherence factor never decays to zero, whereas for the ohmic dissipation $d = 1$, the coherence factor completely decays to zero for large times $\epsilon_c t \gg 1$; this is quite evident from Eqn.(4.33). For $\Delta \neq 0$, several techniques have been developed to study this model. The most lucid exposition of functional integral analysis can be found in [82].

4.5 Rotation, Interaction and Environment

Rotation of a nanomagnet about the easy-axis by a certain angle introduces an additional coupling to the spin Hamiltonian; this is due to the mechanical motion of the system about the axis of rotation[29, 30]. This additional coupling involves the angular momentum vectors of the rotating molecules. In this section, we will study the effect of rotating our model Hamiltonian about its easy-axis. In our simple dimer model, the ground state has a total spin of $S_z = S_{1,z} + S_{2,z} = 0$. Thus, the total z-component of the two SMMS is a conserved quantity, which directly implies that the Hamiltonian is invariant about this axis. Indeed, the Hamiltonian possesses a continuous symmetry about this axis. We must seek for a direction on the easy-axis that does not commute with the Hamiltonian. A nontrivial rotation of Eqn.(3.36) about the easy z-axis can be achieved by

$$\hat{\tilde{H}} = e^{-i(S_{1,z}-S_{2,z})\phi} \hat{H} e^{i(S_{1,z}-S_{2,z})\phi}, \tag{4.34}$$

where $\phi = \phi_1 - \phi_2$ is the relative angle on this axis and $S_{i,z} |\downarrow, \uparrow\rangle \cong (-1)^i s |\downarrow, \uparrow\rangle$. This transformation can be physically realized in a spin-torque nano-oscillator with a two-level macroscopic spin (nanomagnet), which is free to rotate about its staggered easy-axis. A good example is that of a spin-torque nano-oscillator based on a synthetic antiferromagnetic free layer, which has been studied numerically[41].

Generalizing the procedure of the previous section, the projection of Eqn.(4.34) unto

the two-qubit spin basis gives

$$\hat{\tilde{H}}_\alpha = \sum_{m,n=\pm s} |-m, m\rangle \, \hat{\tilde{H}}_{mn} \, \langle n, -n| = \frac{\Delta}{2}[\hat{\alpha}_x \cos(4s\phi) + \hat{\alpha}_y \sin(4s\phi)]. \tag{4.35}$$

The argument of the trigonometric functions can be related to the tunneling of the spins in which $S_{1,z}$ changes by $2s$ and $S_{2,z}$ changes by $-2s$, yielding a total spin of zero. The complete Hamiltonian of the rotated system must include its mechanical motion about that axis. Thus, the complete Hamiltonian is given by

$$\hat{H} = \frac{\hbar^2(L_{1,z} - L_{2,z})^2}{2I} + \frac{\Delta}{2}[\hat{\alpha}_x \cos(4s\phi) + \hat{\alpha}_y \sin(4s\phi)], \tag{4.36}$$

where the orbital angular momenta are $L_{i,z} = -i(d/d\phi_i)$, and $I = I_{1,z} - I_{2,z}$ is the relative moment of inertia of the system about the axis of rotation. Under a unitary transformation with the operator $\hat{U}(\phi) = \exp(-2is\phi\hat{\alpha}_z)$, Eqn.(4.36) becomes

$$\hat{H} \to \hat{U}^{-1}(\phi)\hat{H}\hat{U}(\phi) = \frac{\hbar^2(L_{1,z} - L_{2,z})^2}{2I} + \frac{\Delta}{2}\hat{\alpha}_x. \tag{4.37}$$

The first term is as a consequence of mechanical motion of the system which is being rotated. The total angular momenta $\mathcal{J}_{i,z} = L_{i,z} + S_{i,z}$ is a conserved quantity. It is crucial to note that in the original problem, *i.e.*, Eq(3.36), the individual components of the spins $S_{1,z}$ and $S_{2,z}$ are not conserved. This leads to an avoided level crossing Δ, thus allowing for the conservation of the individual total angular momenta $\mathcal{J}_{1,z}$ and $\mathcal{J}_{2,z}$. If one had included the orbital angular momenta in Eqn.(3.36), then the problem is no longer a reduced problem and the total angular momenta $\mathcal{J}_{1,z}$ and $\mathcal{J}_{2,z}$ won't be conserved. It will be interesting to investigate the effect of this inclusion on the energy splitting for large spins. In terms of $\mathcal{J}$, Eqn.(4.37) can be written as

$$\hat{H} = \frac{\hbar^2[(\mathcal{J}_{1,z} - \mathcal{J}_{2,z})^2 + (2s\hat{\alpha}_z)^2]}{2I} + \frac{\Delta}{2}\hat{\alpha}_x - \frac{\hbar^2 4s(\mathcal{J}_{1,z} - \mathcal{J}_{2,z})\hat{\alpha}_z}{2I}. \tag{4.38}$$

The simultaneous eigenstate of this system is given by

$$|\Psi_{j_1 j_2}\rangle = \frac{1}{\sqrt{2}} |j_1, j_2\rangle_{l_1,l_2} \otimes (\mathcal{C}_{\uparrow,\downarrow} |\uparrow,\downarrow\rangle + \mathcal{C}_{\downarrow,\uparrow} |\downarrow,\uparrow\rangle), \tag{4.39}$$

where $\mathcal{J}_{i,z} |j_1, j_2\rangle = j_i |j_1, j_2\rangle$. Diagonalization of this Hamiltonian yields the corresponding eigenvalues

$$\mathcal{E}_{j_1 j_2} = \frac{\Delta}{2}\left[\frac{\beta}{2}\left(1 + \frac{(j_1 - j_2)^2}{(2s)^2}\right) \pm \sqrt{1 + \frac{(j_1 - j_2)^2}{(2s)^2}\beta^2}\right], \tag{4.40}$$

with $\beta = 2(2\hbar s)^2/(I\Delta)$. It is noted that the energy levels are degenerate with the sign of $j_1 - j_2$ for $j_1, j_2 \neq 0$. The coefficients of the wave function are found to be

$$\begin{aligned} \mathcal{C}_{\uparrow,\downarrow} &= \sqrt{1 + \beta(j_1 - j_2)/\sqrt{(2s)^2 + (\beta(j_1 - j_2))^2}}, \\ \mathcal{C}_{\downarrow,\uparrow} &= \sqrt{1 - \beta(j_1 - j_2)/\sqrt{(2s)^2 + (\beta(j_1 - j_2))^2}}. \end{aligned} \tag{4.41}$$

Having obtained the wave function and its coefficients, we will proceed to the evaluation of the expectation values of the observables $\hat{\alpha}_i$. They are found to be

$$\langle\hat{\alpha}_x\rangle = \frac{1}{2}\left(\mathcal{C}_{\uparrow,\downarrow}\mathcal{C}^{\dagger}_{\downarrow,\uparrow} + \mathcal{C}_{\downarrow,\uparrow}\mathcal{C}^{\dagger}_{\uparrow,\downarrow}\right) = \sqrt{1 - \frac{(\beta(j_1 - j_2))^2}{(2s)^2 + (\beta(j_1 - j_2))^2}}, \tag{4.42}$$

$$\langle\hat{\alpha}_y\rangle = \frac{i}{2}\left(\mathcal{C}_{\downarrow,\uparrow}\mathcal{C}^{\dagger}_{\uparrow,\downarrow} - \mathcal{C}_{\uparrow,\downarrow}\mathcal{C}^{\dagger}_{\downarrow,\uparrow}\right) = 0, \tag{4.43}$$

$$\langle\hat{\alpha}_z\rangle = \frac{1}{2}\left(\mathcal{C}_{\uparrow,\downarrow}\mathcal{C}^{\dagger}_{\uparrow,\downarrow} + \mathcal{C}_{\downarrow,\uparrow}\mathcal{C}^{\dagger}_{\downarrow,\uparrow}\right) = \frac{\beta(j_1 - j_2)}{\sqrt{(2s)^2 + (\beta(j_1 - j_2))^2}}. \tag{4.44}$$

In Fig.(4.2), we have shown the plot of the average values of the spins $\langle\hat{\alpha}_x\rangle$ and $\langle\hat{\alpha}_z\rangle$ as a function of the parameter β. The average value $\langle\hat{\alpha}_x\rangle$ decays with increasing values of $j_1 - j_2$, only becomes zero at sufficiently large values of $j_1 - j_2$. The coherence factor in Fig.(4.1) and the plot of the average $\langle\hat{\alpha}_x\rangle$ in Fig.(4.2) have a similar trend. In the absence of an external magnetic field, the two spins are aligned in an equal and opposite

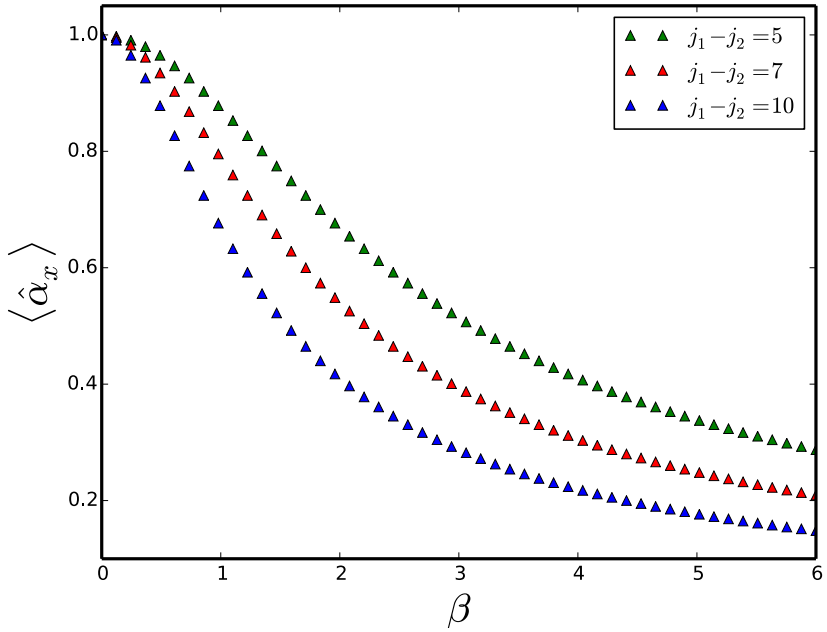

(a)

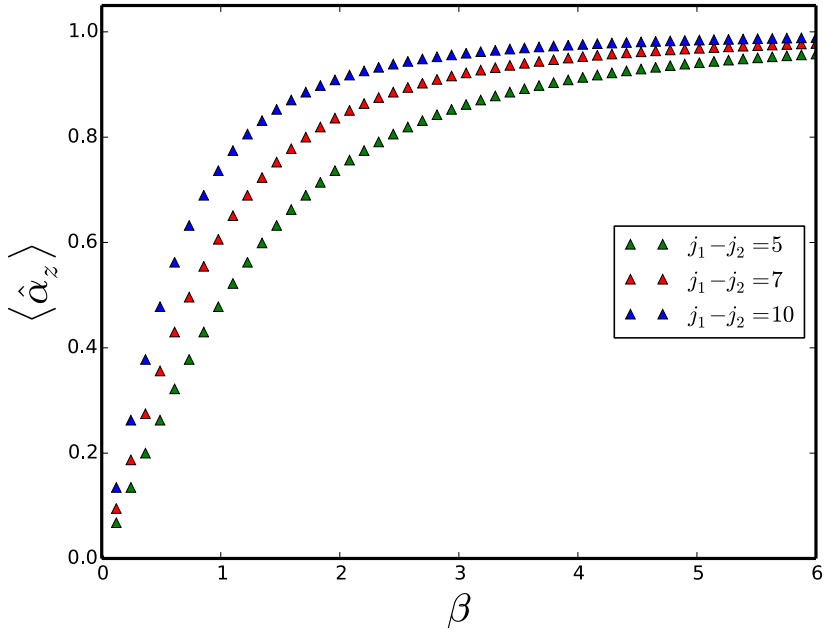

(b)

Figure 4.2: The expectation values of $\langle \hat{\alpha}_x \rangle$ and $\langle \hat{\alpha}_z \rangle$ plotted against the parameter β with $s = 9/2$.

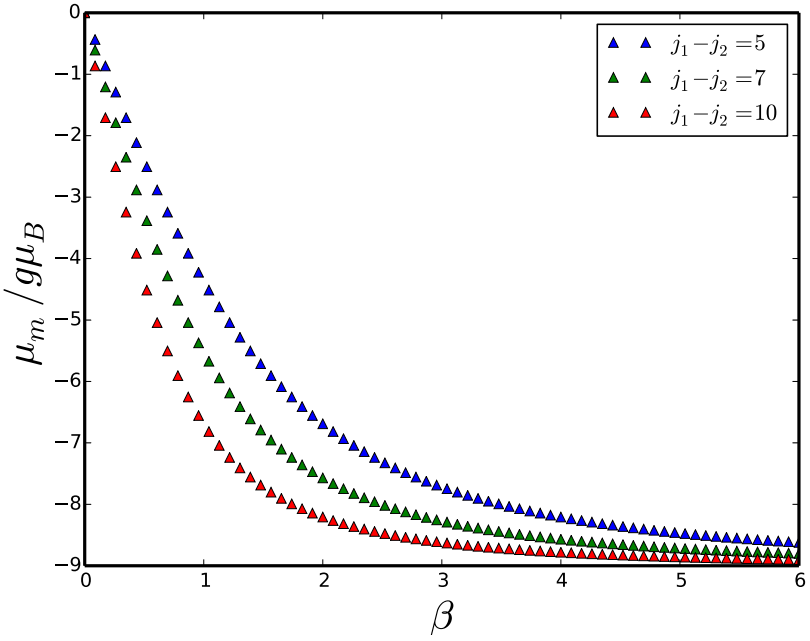

Figure 4.3: The plot of staggered magnetic moment against β with $s = 9/2$.

directions so that the total magnetization vanishes; however, the staggered magnetic moment does not vanish. It is computed as

$$\mu_m = g\mu_B \sum_{i=1}^{2} (-1)^i \langle S_{i,z} \rangle = -\frac{2s\beta g\mu_B (j_1 - j_2)}{\sqrt{(2s)^2 + (\beta(j_1 - j_2))^2}}, \tag{4.45}$$

where g is the electrons g-factor and μ_B is the Bohr magneton. Fig.(4.3) shows the behaviour of this magnetic moment as a function of β. In terms of the rotation angle ϕ_i, Eqn.(4.37) can be written as

$$\hat{H} = \frac{2\hbar^2}{I}\frac{d^2}{d\phi^2} + \frac{\Delta}{2}\hat{\alpha}_x. \tag{4.46}$$

In this form, we can solve for the wave function in terms of ϕ. Applying the unitary transformation in Eqn.(4.16), the second term in Eqn.(4.46) transforms to a term propor-

tional to $\hat{\alpha}_z$; the wave function of the resulting Hamiltonian can be written as

$$\Phi^{\pm}(\phi) = Ae^{im_l\phi} + Be^{-im_l\phi}; \quad \mathcal{E}^{\pm}_{m_l} = \frac{2m_l^2\hbar^2}{I} \mp \frac{\Delta}{2}, \tag{4.47}$$

with the boundary condition $\Phi(\phi + 2\pi) = \Phi(\phi)$, where $m_l = 0, \pm 1, \pm 2 \cdots$, is the relative quantum numbers.

In the presence of a dissipative environment, it will be of interest to know how a dissipative environment couples to a rotating molecular dimeric nanomagnet. This problem has not yet been reported in any literature. Since we already know that the rotation about the easy-axis leaves this axis unchanged. In a straightforward manner, we can generalize the previous analysis. Without any loss of generality, the full Hamiltonian can be written as

$$\begin{aligned}\hat{H} = &\frac{\hbar^2[(\mathcal{J}_{1,z} - \mathcal{J}_{2,z})^2 + (2s\hat{\alpha}_z)^2]}{2I} + \frac{\Delta}{2}\hat{\alpha}_x + \sum_k \epsilon_k b_k b_k^{\dagger} - \hbar^2 4s(\mathcal{J}_{1,z} - \mathcal{J}_{2,z})\hat{\alpha}_z/2I \\ &+ \frac{\hat{\alpha}_z}{2}\sum_k \gamma_k(b_k + b_k^{\dagger}).\end{aligned} \tag{4.48}$$

This system now involves the interaction of the total angular momenta with the spins, and the spins with the environment. The first step in solving this problem is to find an equivalent density matrix operator of Eqn.(4.27), from which other observables can be calculated. In principle, this analysis can actually be done.

4.6 Conclusion and Discussion

In conclusion, we have obtained the two-level system of an antiferromgnetically exchange-coupled dimer, which possesses a macroscopic quantum tunneling phenomenon. We obtained the exact eigenstates and eigenvalues of this dimer in a rotating frame. In the presence of an environment, we derived the corresponding Hamiltonian, which will be of interest to study. This Hamiltonian contains two interactions, namely, angular

momentum and spin; spin and bosonic environment. These results can be applied in quantum computation and spintronics using molecular nanomagnets.

4.7 Article for rotating entangled states of an antiferromagnetic dimer model.

The article that appears below on rotating entangled states of an antiferromagnetic dimer model is published in Journal of Applied Physics. Reproduced with permission from Ref.[102]. Copyright 2014, AIP Publishing LLC.

Rotating Entangled States of an Exchange-Coupled Dimer of Single-Molecule Magnets.

S. A Owerre
Groupe de physique des particules, Département de physique, Université de Montréal, C.P. 6128, succ. centre-ville, Montréal, Québec, Canada, H3C 3J7

Abstract

An antiferromagnetically exchange-coupled dimer of single molecule magnets which possesses a large spin tunneling has been investigated. For this system the ground and first excited states are entangled states and the Hamiltonian is effectively similar to that of a two-state system at $2s^{\text{th}}$ order in perturbation theory, thus this system can be mapped to an entangled pseudospin 1/2 particles. We study the effects of interaction and rotation of this system about its staggered easy-axis direction . The corresponding Hamiltonian of a rotated two-state entangled spin system is derived with its exact low-energy eigenstates and eigenvalues. We briefly discuss the effect of a dissipative environment on this rotated two-state system.

PACS numbers: 75.45.+j, 75.50.Xx, 33.20.Sn, 85.65.+h

Introduction- Macroscopic quantum tunneling and coherence of a single, molecular, magnetic large spin system (such as Mn_{12} and Fe_8) have been the subject of interest for decades[1,2]. These systems are composed of several molecular magnetic ions, whose spins are coupled by intermolecular interactions giving rise to an effective single large spin. Their tunneling behaviour as well as quenching of tunneling have been studied extensively by spin coherent state path integral formalism[1–5] and experimental method[6]. In its simplest form, the Hamiltonian is comprised of two terms, one term $\hat{H}_{\parallel}$, which commutes with the z-component of the spin and the other term $\hat{H}_{\perp}$, which does not commute with the z-component of the spin is responsible for the tunneling splitting between the two degenerate ground states $\mid \pm s\rangle$ of $\hat{H}_{\parallel}$. Due to tunneling, the ground and the first-exited states become the symmetric and antisymmetric linear superpositions of $\mid \pm s\rangle$. In recent years, the problem of a molecular magnet which is free to rotate about the easy axis has attracted considerable attention. This problem involves the conservation of the total angular momentum due the fact that the rotating nanomagnet couples to its mechanical motion in an equal and opposite directions. It has been studied experimentally for free magnetic clusters[7,8] and magnetic microresonators[9,10]. A theoretical study has also been investigated[11,13], which shows that the coupling of the mechanical motion and the spin renormalizes the magnetic anisotropy and increases the tunneling splitting.

The tunneling phenomenon of nanomagnet is not restricted to single molecule magnets (SMMs). In many cases of physical interest, interactions between two large spins are taken into account. These interactions can be either ferromagnetic, which aligns the neighbouring spins or antiferromagnetic, which anti-aligns the neighbouring spins. One physical system in which these interactions occur is the dimerized molecular magnet $[Mn_4]_2$. This system comprises two Mn_4 SMMs of equal spins $s_1 = s_2 = 9/2$, which are coupled antiferromagnetically. The phenomenon of quantum tunneling of spins in this system has been be studied both numerically and experimentally[14,15]. A theoretical study via spin coherent state path integral formalism has been reported recently[18] and perturbation theory has also been investigated[16,17]. In this case the situation is quite different from that of SMMs in that quantum tunneling is achieved via entangled antiferromagnetic states. For a free antiferromagnetically exchange-coupled dimer, it is interesting to ask how does the spins couple with the mechanical motion of the system, what is the effective two-state system and what is the effect of a dissipative environment on such rotating particles. These questions are yet an unsolved problem. We will try to address them in this paper.

Tunneling of antiferromagnetically exchange-coupled dimer, two-state system and dissipative environment - In this section we will briefly review the model of antiferromagnetically exchange-coupled dimer of SMMs with large equal spins, and its tunneling effect. For this system, the simplest form of the Hamiltonian in the absence of an external magnetic field can be written as

$$\hat{H} = -\mathcal{D}(\hat{\mathcal{S}}^2_{1,z} + \hat{\mathcal{S}}^2_{2,z}) + \mathcal{J}\hat{\boldsymbol{S}}_1 \cdot \hat{\boldsymbol{S}}_2 = \hat{H}_0 + \hat{H}_{int} \qquad (1)$$

where $\mathcal{J} > 0$ is the antiferromagnetic exchange coupling, $\mathcal{J} < 0$ is the ferromagnetic exchange coupling and $\mathcal{D} \gg \mathcal{J} > 0$ is the easy-axis anisotropy constant, $\mathcal{S}_{i,z}, i = 1, 2$ is the projection of the component of the spin along the z easy-axis. It has been demonstrated by density-functional theory[21] that this simple model can reproduce experimental results in $[Mn_4]_2$ dimer with $\mathcal{D} = 0.58K$ and $\mathcal{J} = 0.27K$. For spin 1/2, this model can be used to model a two-qubit of quantum dots interacting via a tunneling junction. It also plays a crucial role in quantum CNOT gates and SWAP gates[19]. The total z-component of the spins $\mathcal{S}_z = \mathcal{S}_{1,z} + \mathcal{S}_{2,z}$ is a conserved quantity, thus the Hamiltonian is invariant under

rotation about this direction. However, the individual z-component spins $\mathcal{S}_{1,z}, \mathcal{S}_{2,z}$ and the staggered configuration $\mathcal{S}_{1,z} - \mathcal{S}_{2,z}$ are not conserved. In the absence of $\hat{H}_{int}$, the Hamiltonian is four-fold degenerate corresponding to the states where the individual spins are in their highest weight or lowest weight states, $|\uparrow,\uparrow\rangle, |\downarrow,\downarrow\rangle, |\uparrow,\downarrow\rangle, |\downarrow,\uparrow\rangle$, where $|\uparrow,\downarrow\rangle = |\uparrow\rangle \otimes |\downarrow\rangle \equiv |s,-s\rangle$ etc, with the exchange interaction term $\mathcal{J}$, the two ferromagnetic states $|\uparrow,\uparrow\rangle$ and $|\downarrow,\downarrow\rangle$ are still degenerate but the antiferromagnetic states $|\uparrow,\downarrow\rangle$ and $|\downarrow,\uparrow\rangle$ are not. Perturbation theory[16,17], spin coherent state path integral formalism and effective potential mapping[18] showed that these two antiferromagnetic states are linked to each other at $2s^{\text{th}}$ order in $\hat{H}_{int}$, that is $\mathcal{J}^{2s}$. Thus, these two states reorganize into symmetric and antisymmetric linear superposition. The quantum spin Hamiltonian at $2s^{\text{th}}$ order can then be written effectively as

$$\hat{H}\psi_{\pm} = \mathcal{E}_{\pm}\psi_{\pm}, \quad \Delta = \mathcal{E}_{+} - \mathcal{E}_{-} \sim \left(\frac{|\mathcal{J}|}{4\mathcal{D}}\right)^{2s} \tag{2}$$

where

$$\psi_{-} = \frac{1}{\sqrt{2}}\left(|\uparrow,\downarrow\rangle - |\downarrow,\uparrow\rangle\right), \tag{3}$$
$$\psi_{+} = \frac{1}{\sqrt{2}}\left(|\uparrow,\downarrow\rangle + |\downarrow,\uparrow\rangle\right),$$

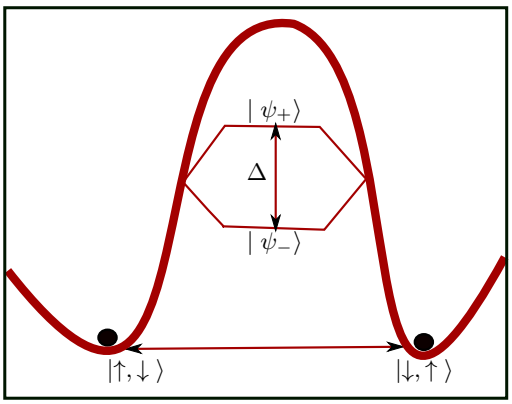

FIG. 1: Sketch of the potential energy with a barrier. The two antiferromagnetic states $|\uparrow,\downarrow\rangle$ and $|\downarrow,\uparrow\rangle$ are localized at the left and the right minimum of the potential, due to tunneling these states reorganize into antisymmteric and symmetric combination with an energy splitting separating them.

The ground state corresponds to the maximally entangled antisymmetric combination while the first excited state corresponds to the maximally entangled symmetric combination for half-odd integer spins. For integer spins these roles are reversed. In quantum computing terminology for spin 1/2 particles, these energy eigenstates are entangled states which play a decisive role in quantum information processes, such as quantum teleportation and quantum register. There are equal probabilities of measuring either $|\downarrow,\uparrow\rangle$ or $|\uparrow,\downarrow\rangle$, that is 1/2. The eigenvalue equation, Eq.(2) is effectively similar to that of a two-state system, thus this system can be mapped to an entangled pseudospin 1/2 particles whose motion is restricted to the subspace of the total Hilbert space. A convenient way of doing this mapping is by constructing the components of a matrix operator with the two-qubit states $|\downarrow,\uparrow\rangle$ and $|\uparrow,\downarrow\rangle$ as

$$\begin{aligned}
\hat{\alpha}_x &= |\uparrow,\downarrow\rangle\langle\downarrow,\uparrow| + |\downarrow,\uparrow\rangle\langle\uparrow,\downarrow| \\
\hat{\alpha}_y &= -i\,|\uparrow,\downarrow\rangle\langle\downarrow,\uparrow| + i\,|\downarrow,\uparrow\rangle\langle\uparrow,\downarrow| \\
\hat{\alpha}_z &= |\uparrow,\downarrow\rangle\langle\uparrow,\downarrow| - |\downarrow,\uparrow\rangle\langle\downarrow,\uparrow| \\
\hat{I} &= |\uparrow,\downarrow\rangle\langle\uparrow,\downarrow| + |\downarrow,\uparrow\rangle\langle\downarrow,\uparrow|
\end{aligned} \tag{4}$$

These matrices are entangled since they cannot be separated as $\hat{\alpha}_{1,x} \otimes \hat{\alpha}_{2,x}$, etc. It is noted that in the two-qubit form they satisfy the usual commutation and anti-commutation relations $[\hat{\alpha}_k, \hat{\alpha}_j] = 2i\epsilon_{ijk}\hat{\alpha}_k$ and $\{\hat{\alpha}_k, \hat{\alpha}_j\} = 2\delta_{ij}$. In the matrix representation they are 4×4 sparse matrices which are not Pauli matrices but their subspace contains the usual 2×2 Pauli matrices. The Hamiltonian $\hat{H}$ can now be projected unto the two qubit states $|\downarrow,\uparrow\rangle$ and $|\uparrow,\downarrow\rangle$:

$$\hat{H}_{\alpha} = \sum_{m,n=\pm s} |\, m,-m\rangle \hat{H}_{mn} \langle n,-n\,| \tag{5}$$

where $\hat{H}_{mn} = \langle m,-m|\hat{H}|n,-n\rangle$. Using Eqns.(2) and (3), the matrix elements are found to be

$$\begin{aligned}
\langle\downarrow,\uparrow|\hat{H}|\downarrow,\uparrow\rangle &= \langle\uparrow,\downarrow|\hat{H}|\uparrow,\downarrow\rangle = 0 \\
\langle\downarrow,\uparrow|\hat{H}|\uparrow,\downarrow\rangle &= \langle\uparrow,\downarrow|\hat{H}|\downarrow,\uparrow\rangle = \Delta/2
\end{aligned} \tag{6}$$

Thus the projected Hamiltonian becomes

$$\hat{H}_{\alpha} = \frac{\Delta}{2}\hat{\alpha}_x \tag{7}$$

with its eigenvalues given by $\{-\Delta/2, \Delta/2\}$. In many cases of physical interest, the spin interacts with its environment which is usually modeled as a bath of bosons. The environmental effect on the Hamiltonian, Eq.(7) is written in the usual form[20].

$$\hat{H} = \frac{\Delta}{2}\hat{\alpha}_x + I\sum_k \epsilon_k \hat{b}_k^{\dagger}\hat{b}_k + \chi S_z = \hat{H}_{\alpha} + \hat{H}_B + H_{int} \tag{8}$$

where $\hat{H}_{\alpha} = \Delta\hat{\alpha}_x/2$, $\hat{H}_B = \sum_k \epsilon_k \hat{b}_k^{\dagger}\hat{b}_k$, $H_{int} = \hat{\chi}\hat{S}_z$, $\hat{\chi} = \sum_k \gamma_k(\hat{b}_k + \hat{b}_k^{\dagger})$, $\hat{S}_z = \hat{\alpha}_z/2$ and $\hat{b}_k^{\dagger}, \hat{b}_k$ are the annihilation and creation operators of phonons with the wave number k. In terms of the basis states, this Hamiltonian can be written as

$$\hat{H} = (|\uparrow,\downarrow\rangle\frac{\Delta}{2}\langle\downarrow,\uparrow| + h.c) + |\downarrow,\uparrow\rangle\hat{K}_{-}\langle\downarrow,\uparrow| + |\uparrow,\downarrow\rangle\hat{K}_{+}\langle\uparrow,\downarrow| \tag{9}$$

where $\hat{K}_{\pm} = \sum_k \epsilon_k \hat{b}_k^{\dagger}\hat{b}_k \pm \hat{\chi}$. In the interaction picture we can solve for the time-evolution of $\hat{\alpha}_z(t)$ using the

Heisenberg equation of motion with respect to $\hat{H}_\alpha$. The resulting expression is given by

$$\hat{\alpha}_z(t) = \hat{\alpha}_z \cos(\Delta t) + \hat{\alpha}_y \sin(\Delta t) \tag{10}$$

The coefficients of the trigonometric function are determined from the initial conditions at $t = 0$. The operator from which all other observables can be calculated is the reduced density operator. It is given by

$$\hat{\rho}(t) = Tr_B \left(e^{-i\hat{H}t} \hat{\rho}(0) e^{i\hat{H}t} \right) \tag{11}$$

where $\hat{\rho}(0) = \hat{\rho}_\alpha \otimes \hat{\rho}_B$, where $\hat{\rho}_\alpha$ acts on the spin space and $\hat{\rho}_B = e^{-\beta \hat{H}_B}/Z_B$ is the density matrix of a free boson. This system is exactly solvable in the limit $\Delta \to 0$ (independent boson model). In this limit the bosonic bath can be traced out in Eq.(11). The object of interest in this model is usually the average values of the time evolution of the observables $\hat{\alpha}_i$, $i = x, y, z$. Using the interacting picture formulation of quantum mechanics, we have

$$\langle \hat{S}_+(t) \rangle = Tr_\alpha \left(\hat{U}'(t,0) \rho(0) \hat{U}'(0,t) S_+(0) \right) \tag{12}$$

where $\hat{S}_+ = \hat{S}_x + i\hat{S}_y$, $\hat{U}'(t,0) = Te^{-i\int_0^t dt \hat{H}'(t)}$ and $\hat{H}'(t) = e^{i\hat{H}_B t} \hat{H}_{int} e^{-i\hat{H}_B t}$. A straight forward calculation of the trace yields

$$\langle \hat{S}_+(t) \rangle = C(t) \langle \hat{S}_+(0) \rangle , \tag{13}$$

with $C(t) = \langle T e^{-i\int_0^t \hat{\chi}'(t) dt} \rangle_0$ is the coherence factor between the states $|\downarrow, \uparrow\rangle$ and $|\uparrow, \downarrow\rangle$. By symmetry consideration we have $\langle \hat{S}_-(t) \rangle = C(t) \langle \hat{S}_- \rangle (0)$, hence

$$\langle \hat{\alpha}_x(t) \rangle = C(t) \langle \hat{\alpha}_x(0) \rangle \tag{14}$$

The evaluation of the equilibrium expectation value with the use of Wicks theorem[22] gives

$$C(t) = e^{-\mathcal{D}(t)}, \quad \text{and } |C(t)| = e^{-Re[\mathcal{D}(t)]} \tag{15}$$

$$\mathcal{D}(t) = \sum_k \frac{\gamma_k^2}{\epsilon_k^2} [(1+n_B)(1-e^{-i\epsilon_k t}) + n_B(1-e^{-i\epsilon_k t}) - i\epsilon_k t], \quad n_B = (e^{\beta\epsilon_k} - 1)^{-1} \tag{16}$$

In the continuum limit we have

$$Re[\mathcal{D}(t)] = 2\int_0^\infty d\epsilon \frac{J(\epsilon)}{\epsilon^2} \sin^2\left(\frac{\epsilon t}{2}\right) \cot\left(\frac{\beta\epsilon}{2}\right) \tag{17}$$

where the spectral density function $J(\epsilon) = N_d(\epsilon)\gamma(\epsilon)^2 = \mathcal{K}_d \gamma_0^2 \epsilon^d e^{-\epsilon/\epsilon_c}$ and $N_d(\epsilon)$ is the d-dimensional density of phonon modes. For $d = 1, 2, 3$ we have $\mathcal{K}_1 = L/\pi c_s$, $\mathcal{K}_2 = A/2\pi c_s^2$ and $\mathcal{K}_3 = V/2\pi^2 c_s^3$, where L, A, V are the length, area and volume of the system respectively, c_s is the speed of sound. In Fig.(2) we have plotted $|C(t)|$ for $d = 1, 2, 3$, with $\beta\epsilon_c = 1$. In the super-ohmic dissipation, $d = 2, 3$, the coherence factor never decays to zero while for the ohmic dissipation $d = 1$, the coherence factor completely decays to zero for large times $\epsilon_c t \gg 1$, this is quite obvious from Eq.(17). For $\Delta \neq 0$, several techniques have been developed to study this model. The most elaborate functional integral analysis can be found in Ref.[20].

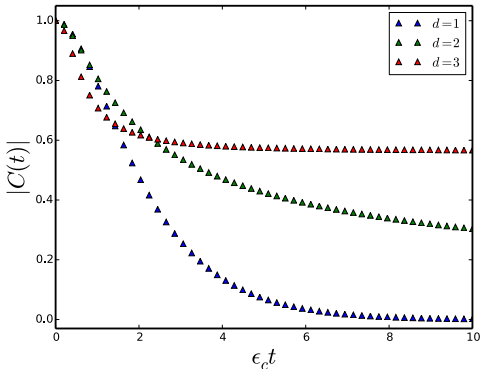

FIG. 2: The plot of $|C(t)|$ against time for ohmic $d = 1$ and super-hhimc $d = 2, 3$ dissipations. The function reaches a maximum of one and decays to zero at long times for the ohmic dissipation but it is never decays zero for the super-ohmic dissipation.

Suppose we apply a time varying staggered magnetic field along the easy z axis on the exchange-coupled dimer model, the Zeeman Hamiltonian is of the form $\hat{H}_Z = -h(t)(\hat{\mathcal{S}}_{1,z} - \hat{\mathcal{S}}_{2,z}) = -g\mu_B h(\hat{\mathcal{S}}_{1,z} - \hat{\mathcal{S}}_{2,z}) \cos\omega t$, then projecting unto the two-qubit states, Eq.(7) becomes

$$\hat{H}_\alpha = \frac{\Delta}{2}\hat{\alpha}_x - 2sg\mu_B h \hat{\alpha}_z \cos\omega t \tag{18}$$

Transforming along the y-axis with the unitary operator

$$\hat{U}(\phi) = \exp(-i\phi\hat{\alpha}_y/2), \quad \phi = -\pi/2 \tag{19}$$

one obtains

$$\hat{H}_\alpha \to \hat{U}^{-1}(\phi)\hat{H}_\alpha \hat{U}(\phi) = -\frac{\Delta}{2}\hat{\alpha}_z - sg\mu_B h \hat{\alpha}_x \cos\omega t \tag{20}$$

The corresponding wave function of this system is given by

$$|\psi(t)\rangle = \mathcal{C}_{\uparrow,\downarrow}(t) e^{-i\mathcal{E}_+ t} |\uparrow, \downarrow\rangle + \mathcal{C}_{\downarrow,\uparrow}(t) e^{-i\mathcal{E}_- t} |\downarrow, \uparrow\rangle \tag{21}$$

with $|\mathcal{C}_{\uparrow,\downarrow}(t)|^2 + |\mathcal{C}_{\downarrow,\uparrow}(t)|^2 = 1$ and $\mathcal{E}_\pm = \pm\Delta/2$. In the rotating wave approximation[23,25], the coefficients are given by

$$\mathcal{C}_{\uparrow,\downarrow}(t) = e^{-i\Delta' t/2}\left[\cos\left(\frac{\Omega t}{2}\right) + i\frac{\Delta'}{\Omega}\sin\left(\frac{\Omega t}{2}\right)\right]$$
$$\mathcal{C}_{\downarrow,\uparrow}(t) = ie^{i\Delta' t/2}\frac{\Omega_R}{\Omega}\sin\left(\frac{\Omega t}{2}\right) \tag{22}$$

where

$$\Delta' = \Delta - \omega, \quad \Omega = \sqrt{\Omega_R^2 + \Delta'^2} \quad \text{and} \quad \Omega_R = sg\mu_B h \tag{23}$$

Using these results the expectation values of the observables α_i are

$$\langle\hat{\alpha}_x\rangle_t = \frac{\Omega_R\Delta'}{\Omega^2}(1-\cos(\Omega t)) \tag{24}$$

$$\langle\hat{\alpha}_y\rangle_t = -\frac{\Omega_R}{\Omega}\sin(\Omega t) \tag{25}$$

$$\langle\hat{\alpha}_z\rangle_t = \frac{\Delta'^2}{\Omega^2} + \frac{\Omega_R^2}{\Omega^2}\cos(\Omega t) \tag{26}$$

Rotation, interaction and environment- Rotation of a nanomagnet about the easy-axis by an angle introduces an additional coupling to the spin Hamiltonian due the the mechanical motion of the system about the axis of rotation[11–13]. This coupling involves the angular momentum vectors of the rotating molecules[24]. In this section, we will study the effect of rotating our model Hamiltonian about its easy-axis. In our simple dimer model, the ground state has a total spin of $\mathcal{S}_z = \mathcal{S}_{1,z} + \mathcal{S}_{2,z} = 0$. Thus, the total z-component of the two SMMS is a conserved quantity, which directly implies that any rotation about this axis will leave the Hamiltonian invariant. We must seek for a direction on the easy-axis that does not commute with the Hamiltonian. A nontrivial rotation of Eq.(1) about the easy z-axis can be achieved by

$$\hat{\tilde{H}} = e^{-i(\mathcal{S}_{1,z}-\mathcal{S}_{2,z})\phi}\hat{H}e^{i(\mathcal{S}_{1,z}-\mathcal{S}_{2,z})\phi} \tag{27}$$

where $\phi = \phi_1 - \phi_2$ is the relative angle on this axis and $\mathcal{S}_{i,z}\mid\downarrow,\uparrow\rangle \cong (-1)^i s\mid\downarrow,\uparrow\rangle$. This transformation can be physically realized in a spin-torque nano-oscillator with a two-state macroscopic spin (nanomagnet) which is free to rotate about its staggered easy-axis. A good example is that of a spin-torque nano-oscillator based on a synthetic antiferromagnet free layer which has been studied numerically[26]. Generalizing the procedure of the previous section, the projection of Eq.(27) unto the two-qubit spin basis gives

$$\begin{aligned}\hat{\tilde{H}}_\alpha &= \sum_{m,n=\pm s}\mid -m,m\rangle\hat{\tilde{H}}_{mn}\langle n,-n\mid \\ &= \frac{\Delta}{2}[\hat{\alpha}_x\cos(4s\phi) + \hat{\alpha}_y\sin(4s\phi)]\end{aligned} \tag{28}$$

In this case the argument of the trigonometric functions can be related to the tunneling of the spins in which $\mathcal{S}_{1,z}$ changes by $2s$ and $\mathcal{S}_{2,z}$ changes by $-2s$. The complete Hamiltonian of the rotated system must include its mechanical motion about that axis. Thus we have

$$\hat{H} = \frac{\hbar^2(L_{1,z}-L_{2,z})^2}{2I} + \frac{\Delta}{2}[\hat{\alpha}_x\cos(4s\phi) + \hat{\alpha}_y\sin(4s\phi)] \tag{29}$$

where the orbital angular momenta are $L_{i,z} = -i(d/d\phi_i)$, and $I = I_{1,z} - I_{2,z}$ is the relative moment of inertia of the system about the axis of rotation. Under a unitary transformation with the operator $\hat{U}(\phi) = \exp(-2is\phi\hat{\alpha}_z)$, Eq.(29) becomes

$$\hat{H} \to \hat{U}^{-1}(\phi)\hat{H}\hat{U}(\phi) = \frac{\hbar^2(L_{1,z}-L_{2,z})^2}{2I} + \frac{\Delta}{2}\hat{\alpha}_x \tag{30}$$

The first term is as a consequence of mechanical motion of the system which is being rotated. The total angular momenta $J_{i,z} = L_{i,z} + \mathcal{S}_{i,z}$ is a conserved quantity. It is crucial to note that in the original problem i.e Eq(1), the individual components of the spins $\mathcal{S}_{1,z}$ and $\mathcal{S}_{2,z}$ are not conserved. This leads to an energy splitting Δ, thus allowing for the conservation of the individual total angular momenta $\mathcal{J}_{1,z}$ and $\mathcal{J}_{2,z}$. If one had included the orbital angular momenta in Eq.(1), then the problem is no longer a reduced problem and the total angular momenta $\mathcal{J}_{1,z}$ and $\mathcal{J}_{2,z}$ won't be conserved. It will be interesting to investigate the effect of this inclusion on the energy splitting for large spins. In terms of J, Eq.(30) can be written as

$$\begin{aligned}\hat{H} = &\frac{\hbar^2[(J_{1,z}-J_{2,z})^2 + (2s\hat{\alpha}_z)^2]}{2I} + \frac{\Delta}{2}\hat{\alpha}_x \\ &- \hbar^2 4s(J_{1,z}-J_{2,z})\hat{\alpha}_z/2I\end{aligned} \tag{31}$$

The simultaneous eigenstate of this system is given by

$$\mid\Psi_{j_1j_2}\rangle = \frac{1}{\sqrt{2}}\mid j_1,j_2\rangle_{l_1,l_2}\otimes(\mathcal{C}_{\uparrow,\downarrow}\mid\uparrow,\downarrow\rangle + \mathcal{C}_{\downarrow,\uparrow}\mid\downarrow,\uparrow\rangle) \tag{32}$$

where $J_{i,z}\mid j_1,j_2\rangle = j_i\mid j_1,j_2\rangle$. Diagonalization of this Hamiltonian yields the corresponding eigenvalues

$$\mathcal{E}_{j_1j_2} = \frac{\Delta}{2}\left[\frac{\beta}{2}\left(1+\frac{(j_1-j_2)^2}{(2s)^2}\right) \pm \sqrt{1+\frac{(j_1-j_2)^2}{(2s)^2}\beta^2}\right] \tag{33}$$

with $\beta = 2(2\hbar s)^2/(I\Delta)$. It is noted that the energy levels are degenerate with the sign of $j_1 - j_2$ for $j_1, j_2 \neq 0$. The coefficients of the wave function are found to be

$$\begin{aligned}\mathcal{C}_{\uparrow,\downarrow} &= \sqrt{1+\beta(j_1-j_2)/\sqrt{(2s)^2+(\beta(j_1-j_2))^2}} \\ \mathcal{C}_{\downarrow,\uparrow} &= \sqrt{1-\beta(j_1-j_2)/\sqrt{(2s)^2+(\beta(j_1-j_2))^2}}\end{aligned} \tag{34}$$

Now that we have obtained the wave function and its coefficients, the expectation values of the observables $\hat{\alpha}_i$ can be easily evaluated. They are given by

$$\langle\hat{\alpha}_x\rangle = \sqrt{1-\frac{(\beta(j_1-j_2))^2}{(2s)^2+(\beta(j_1-j_2))^2}} \tag{35}$$

$$\langle\hat{\alpha}_y\rangle = 0 \tag{36}$$

$$\langle\hat{\alpha}_z\rangle = \frac{\beta(j_1-j_2)}{\sqrt{(2s)^2+(\beta(j_1-j_2))^2}} \tag{37}$$

In Fig.(3) we have shown the plot of the average values of the spins $\langle\hat{\alpha}_x\rangle$ and $\langle\hat{\alpha}_z\rangle$ as a function of the parameter β. The average value $\langle\hat{\alpha}_x\rangle$ decays with increasing values of $j_1 - j_2$, only becomes zero at sufficiently large values of $j_1 - j_2$. Notice a similar trend between the coherence factor in Fig.(2) and the average $\langle\hat{\alpha}_x\rangle$.

In the absence of an external magnetic field, the two spins are aligned in an equal and opposite directions so

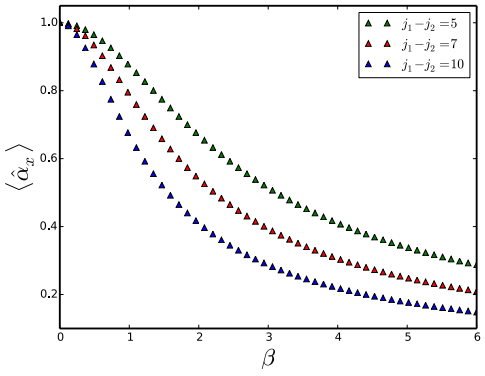

(a)

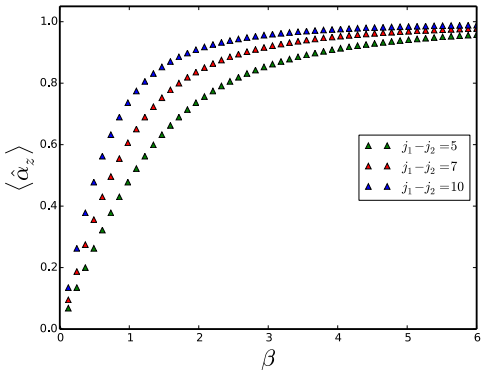

(b)

FIG. 3: The expectation values of $\langle\hat{\alpha}_x\rangle$ and $\langle\hat{\alpha}_z\rangle$ plotted against the parameter β. Line are labelled with the values of $j_1 - j_2$.

that the total magnetization vanishes, however the staggered magnetic moment does not vanish, which can be computed as

$$\mu_s = g\mu_B \sum_i (-1)^i \langle \mathcal{S}_{i,z}\rangle = -\frac{2s\beta g\mu_B(j_1-j_2)}{\sqrt{(2s)^2+(\beta(j_1-j_2))^2}} \tag{38}$$

where g is the electrons g-factor and μ_B is the Bohr magneton. In terms of the rotation angle ϕ_i, Eq.(30) can be written as

$$\hat{H} = \frac{2\hbar^2}{I}\frac{d^2}{d\phi^2} + \frac{\Delta}{2}\hat{\alpha}_x \tag{39}$$

This form of the Hamiltonian allows one to solve for the wave function in terms of ϕ. By applying the unitary transformation in Eq.(19), the wave function can be written as

$$\Phi^{\pm}(\phi) = Ae^{im_l\phi} + Be^{-im_l\phi}, \quad \mathcal{E}^{\pm}_{m_l} = \frac{2m_l^2\hbar^2}{I} \mp \frac{\Delta}{2} \tag{40}$$

with the boundary condition $\Phi(\phi + 2\pi) = \Phi(\phi)$, where $m_l = 0, \pm1, \pm2\cdots$, is the relative quantum numbers. Let us briefly address the question we raised in the introduction. How does a dissipative environment couple to a rotating molecular dimeric nanomagnet? We reiterate the fact that this question is yet an unsolved problem, however, since the rotation about the easy-axis leaves this axis unchanged, a straight forward generalization of the previous analysis gives

$$\hat{H} = \frac{\hbar^2[(J_{1,z}-J_{2,z})^2 + (2s\hat{\alpha}_z)^2]}{2I} + \frac{\Delta}{2}\hat{\alpha}_x + \sum_k \epsilon_k b_k b_k^\dagger - \hbar^2 4s(J_{1,z}-J_{2,z})\hat{\alpha}_z/2I + \frac{\hat{\alpha}_z}{2}\sum_k \gamma_k(b_k + b_k^\dagger) \tag{41}$$

This system involves the interaction of the total angular momenta with the spins, and the spins with the environment. The first step in solving this problem is to find an equivalent density matrix operator of Eq.(11) from which other observables can be calculated. This analysis can be done in principle.

Conclusions- In conclusion, we have investigated an antiferromagnetically exchange-coupled dimer of single molecule magnet which possesses a large spin tunneling. Perturbation theory to $2s^{\text{th}}$ order transforms the system into an effective two-state system with the ground and the first excited states being an entangled state of the degenerate eigenstates of the free Hamiltonian with an energy splitting between them. The nature of this Hamiltonian allows us to map the system onto an entangled pseudospin 1/2 two-state system. For an antiferromagnetically exchange-coupled dimer which is free to rotate about the staggered easy-axis, we obtained the eigenstate and eigenvalues of this system. The average values of the system observables were calculated and plotted with the parameter of the system. Finally, we briefly discussed the environmental influence on a rotating exchange-coupled dimer. These results can be applied to a free magnetic dimer clusters in a cavity. It is also useful in quantum computation using entangled two-qubit states.

Acknowledgments- The author would like to thank NSERC of Canada for financial support with the grant no. R0003315. Also the author acknowledges useful discussions with Joachim Nsofini and Manu Paranjape .

[1] E.M. Chudnovsky and L. Gunther, Phys. Rev. Lett. **60**, 661 (1988)

[2] E.M. Chudnovsky, J. Tejada, Macroscopic Quantum Tunneling of the Magnetic Moment, Cambridge University Press, Cambridge, UK, 1998.

[3] D.Loss, D. P. Di Vincenzo, G. Grinstein, Phys. Rev. Lett.

69, 3232 (1992)
[4] J. von Delft, C. Henley, Phys. Rev. Lett. **69**, 3236(1992)
[5] John R. Klauder Phys. Rev. D **19**, 2349 (1978)
[6] W. Wernsdorfer and R. Sessoli, Science **284**, 133, (1999)
[7] I.M.L. Billas, A. Châtelain, W.A. de Heer, Science 265, 1682, (1994) .
[8] X.S. Xu, S. Yin, W.A. de Heer,Phys. Rev. Lett. **95** 237209, (2005).
[9] T.M. Wallis, J. Moreland, P. Kabos, App. Phys. Lett. **89** 122502, (2006) .
[10] J.P. Davis, D. Vick, D.C. Fortin, J.A.J. Burgess, W.K. Hiebert, M.R. Freeman, App. Phys. Lett. **96** 072513, (2010).
[11] E.M. Chudnovsky and D.A. Garanin, Phys. Rev. B **81**, 214423 (2010)
[12] E.M. Chudnovsky in Molecular Magnets Physics and Applications, Springer (2014), p.61
[13] Michael F. O' Keeffe and Eugene M. Chudnovsky, Phys. Rev. B **83**, 092402 (2011)
[14] R. Tiron, W. Wernsdorfer, D. Foguet-Albiol, N. Aliaga-Alcalde, and G. Christou, Phys. Rev. Lett. **91**, 227203 (2003)
[15] S. Hill, R. S. Edwards, N. Aliaga-Alcalde, G. Christou, science **302**, 1015 (2003)
[16] E. M. Chudnovsky and Javier Tejada, Rinton Press, Princeton, NJ, (2006); E. M. Chudnovsky , Javier Tejada , Carlos Calero and Ferran Macia, Rinton Press, Princeton, NJ, (2006)
[17] Kim Gwang-Hee, Phys. Rev. B **67**, 024421 (2003); ibid **68**, 144423 (2003)
[18] S. A. Owerre and M.B Paranjape, Phys. Rev. B **88**, 220403(R), (2013), Phys. Lett. A 378, 1407 (2014)
[19] D. Loss and D. DiVincenzo, Phys. Rev. A **57**, 120, (1998).
[20] A. J. Leggett, S. Chakravarty, A. T. Dorsey , Matthew P. A. Fisher, Anupam Garg , and W. Zwerger, Phys. Rev. Mod. **59**, 1 (1987)
[21] Park K., Mark R. Pederson, Steven L. Richardson, Nuria Aliaga-Alcalde, and George Christou, Phys. Rev. B **68**, 020405 (2003)
[22] Gerald D. Mahan, Many- Particle Physics, 3rd Edition, Kluwer Academic/Plenum Pulishers, New york, (2000).
[23] M. O. Scully and M. S. Zubairy, Quantum Optics (University Press, Cambridge, 1997).
[24] J. H. Van Vleck, Rev. Mod. Phys. **23**, 213 (1951)
[25] I. I. Rabi, Phys. Rev. **51**, 652 (1937)
[26] I. Firastrau, L. D. Buda-Prejbeanu, B. Dieny and U. Ebels, J. Appl. Phys. **113**, 113908 (2013)

CHAPTER 5

EFFECTIVE POTENTIAL METHOD AND ESCAPE RATE

> Every word or concept, clear as it may seem to be, has only a limited range of applicability.
>
> Werner Heisenberg

5.1 Introduction

In the main introduction of this thesis, we emphasized that the spin coherent state path integral formalism is valid in the large s (semiclassical) limit. In other words, if one imposes a commutator relation on the spherical coordinates, $[\phi, p] = i\hbar$, where $p = s\cos\theta$, then the spin commutator relation $[\hat{S}_i, \hat{S}_j] = i\epsilon_{ijk}\hat{S}_k$ is only recovered in the large s limit[1]. On the other hand, the effective potential method maps a spin Hamiltonian directly to a particle Hamiltonian, with an effective potential [123, 148, 150]. This method is exact, and uses no classical references. In this method, one introduces the spin wave function using the $\hat{S}_z$ eigenstates, then the resulting eigenvalue equation $\hat{H}\,|\psi\rangle = \mathcal{E}\,|\psi\rangle$ is transformed to a differential equation, which is further reduced to a Schrödinger equation with an effective potential and a constant or coordinate dependent mass. The energy spectrum of the spin system coincides with the $2s+1$ energy levels for the particle moving in a potential field. This method, however, is not general in the sense that it does not apply to any form of Hamiltonian. The two major disadvantages of this method are as follows:

1). The particle Hamiltonian resulting from the effective potential mapping does not have a WZ term (Berry phase); thus, it seems that the quantum phase interference

[1]The proof of this statement can be found in the Appendix A of Müller *et al* [99]

effect disappears. However, the wavefunction resulting from this mapping contains all the necessary information that captures the spin parity effect.

2). The effective potential mapping is ineffective to spin systems with quartic anisotropies, such as $\hat{H} = -D\hat{S}_z^2 - B\hat{S}_z^4 + C(\hat{S}_+^4 + \hat{S}_-^4) - H_x\hat{S}_x$ and $\hat{H} = D\hat{S}_z^2 + E\hat{S}_x^2 + C(\hat{S}_+^4 + \hat{S}_-^4)$.

Thus, the effective potential (EP) method is only efficient for spin systems that are quadratic in the spin operators. The format of this chapter is as follows: we will review the EP method of a uniaxial spin model with a transverse magnetic field in Sec.(5.2.1); this was first derived in Ref. [123, 148, 150]. In Sec.(5.2.2), we will review the effective potential method of the biaxial ferromagnetic spin model in Sec.(3.2.1). This method will be the basis for investigating the quantum-classical phase transitions of the escape rate in large spin systems, which we be presented in Chapter (6). In Sec.(5.3), we will present different methods for studying quantum-classical phase transitions of the escape rate. Sec.(5.4) deals with concluding remarks and discussions.

5.2 From spin Hamiltonian to particle Hamiltonian

5.2.1 Effective potential method for a uniaxial spin model

We commence by considering the effective potential method of a uniaxial spin system in a magnetic field. This system is described by the Hamiltonian

$$\hat{H} = -D\hat{S}_z^2 - H_x\hat{S}_x. \tag{5.1}$$

where $H_x = g\mu_B h$. It is believed that this Hamiltonian describes Mn_{12} acetate molecular magnet with a ground state of $s = 10$ [21, 27, 45, 114]. An experimental review of this molecular magnet can be found in [61]. Scharf *et al* [123] considered the problem of finding the exact eigenstates of this Hamiltonian. The eigenvalue equation is given by

$$\hat{H}\left|\psi\right\rangle = \mathcal{E}\left|\psi\right\rangle. \tag{5.2}$$

The spin wave function in the $\hat{S}_z$ representation is of the form [123]

$$|\psi\rangle = \sum_{\sigma=-s}^{s} \binom{2s}{s+\sigma}^{-1/2} c_\sigma |s,\sigma\rangle . \tag{5.3}$$

Noticing that $\hat{S}_x = \frac{1}{2}(\hat{S}_+ + \hat{S}_-)$ and

$$\hat{S}_\pm |s,\sigma\rangle = \sqrt{(s \mp \sigma)(s \pm \sigma + 1)}\, |s,\sigma \pm 1\rangle , \tag{5.4}$$

$$\hat{S}_z |s,\sigma\rangle = \sigma |s,\sigma\rangle . \tag{5.5}$$

The combination of Eqn.(5.1)–(5.5) gives the eigenvalue equation

$$-(D\sigma^2 + \mathcal{E})c_\sigma - \frac{1}{2}H_x[(s-\sigma+1)c_{\sigma-1} + (s+\sigma+1)c_{\sigma+1}] = 0, \tag{5.6}$$

where $\sigma = -s, -s+1, \cdots, s$ and $c_\sigma = 0$ for $|\sigma| > s$. This equation is a tridiagonal

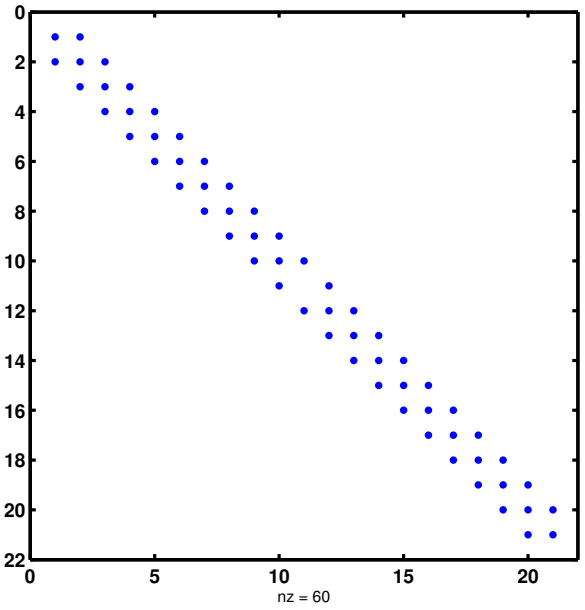

Figure 5.1: The tridiagonal sparse matrix representation of 21×21 matrix for $s = 10$, with 60 nonzero values.

$(2s+1) \times (2s+1)$ matrix which can be exactly diagonalized for $s = \frac{1}{2}$ to $s = 10$, with the exact eigenvalues completely determined; see Figs.(5.1) and (5.2) . However, for very large spins, Eqn.(5.6) is too cumbersome to solve in a quantum mechanical way. The mapping onto a particle problem becomes crucial. This mapping, which is called

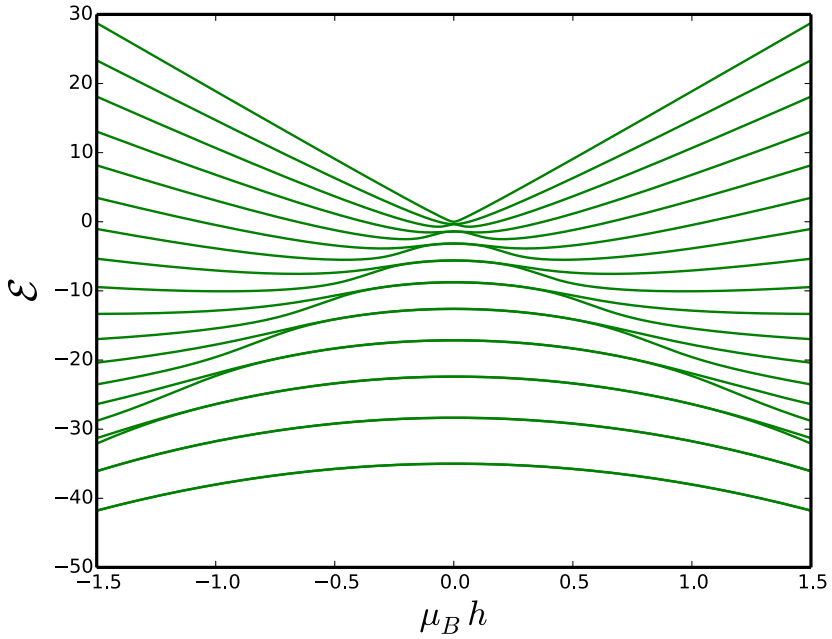

Figure 5.2: The exact diagonalization of Eqn.(5.6) for $s = 10$ and $D = 0.35$. At $h = 0$, the states are labeled by $\sigma = \pm 10, \pm 9, \cdots, 0$. There are 21 energy level which are split by the magnetic field. The splitting in the perturbative limit $h \ll D$ is $\sim (h/D)^{2s}$, which evidently is very small to be observed in the diagram.

the effective potential method, lies on the proper choice of a generating function that converts Eqn.(5.6) into a differential equation:

$$\mathcal{G}(x) = \sum_{\sigma=-s}^{s} c_\sigma e^{\sigma x}. \tag{5.7}$$

Substituting into Eqn.(5.6), the differential equation in $\mathcal{G}(x)$ becomes

$$-D\frac{d^2\mathcal{G}}{d^2x} + H_x \sinh x \frac{d\mathcal{G}}{dx} - (H_x s \cosh x + \mathcal{E})\mathcal{G} = 0. \tag{5.8}$$

A quick glance at Eqn.(5.8) shows that any transformation that eliminates the first derivative term, transforms Eqn.(5.8) to a Schrödinger equation. Indeed, such a transformation can be found; it is given by

$$\Psi(x) = e^{-y(x)}\mathcal{G}(x), \tag{5.9}$$

where $y(x)$ is determined by demanding that the coefficient of the first derivative in Ψ vanishes[2] upon substituting Eqn.(5.9) into Eqn.(5.8). This condition yields

$$y(x) = \tilde{s}h_x \cosh(x), \tag{5.10}$$

where $h_x = H_x/2D\tilde{s} < 1$ and $\tilde{s} = (s + \frac{1}{2})$ is a quantum renormalization. The transformation in Eqn.(5.9) can be regarded as the coordinate or particle wave function since $\Psi(x) \to 0$ as $x \to \pm\infty$. Thus, the resulting differential equation in $\Psi(x)$ is reminiscent of a Schödinger equation, which describes a particle in an effective potential [123, 148, 150]:

$$H\Psi(x) = \mathcal{E}\Psi(x); \quad H = \frac{\hat{p}^2}{2m} + U(x); \quad \hat{p} = -i\frac{d}{dx}. \tag{5.11}$$

The mass and the effective potential are given by

$$U(x) = D\tilde{s}^2(h_x \cosh x - 1)^2; \quad m = \frac{1}{2D} \tag{5.12}$$

where a constant has been added to normalize the potential to zero at the minima $x_{\text{min}} = \pm \operatorname{arccosh}\left(\frac{1}{h_x}\right)$. The maximum is at $x_{\text{max}} = 0$, with the height of the barrier given by

$$\Delta U = U_{\text{max}} - U_{\text{min}} = D\tilde{s}^2(1 - h_x)^2. \tag{5.13}$$

These two minima correspond to the localization of the states $|\uparrow\rangle$ and $|\downarrow\rangle$. This po-

[2] An elaborate calculation will be given in Sec.(6.3.2) for the case of dimer model.

tential is of the form of a double well, which was studied in Sec.(2.2.2), with $\pm a = \pm \operatorname{arccosh}\left(\frac{1}{h_x}\right)$. We presented a lucid calculation of the instanton solution of this problem in Sec.(2.2.2). The Euclidean Lagrangian corresponds to Eqn.(2.23), with the mass and the potential are given by Eqn.(5.12). The solution of the Euclidean classical equation of motion, Eqn.(2.27) yields the instanton trajectory [148, 150]

$$x(\tau) = \pm 2 \operatorname{arctanh}\left[\sqrt{\frac{1-h_x}{1+h_x}} \tanh(\omega_0 \tau)\right], \tag{5.14}$$

where $\omega_0 = D\tilde{s}\sqrt{1-h_x^2}$ is the frequency of oscillation at the wells of the potential. The corresponding action for this trajectory is

$$B = \int_{-\infty}^{\infty} d\tau \, m\dot{x}^2 = 2\tilde{s}\left[\frac{1}{2}\ln\left(\frac{1+\sqrt{1-h_x^2}}{h_x}\right) - \sqrt{1-h_x^2}\right]. \tag{5.15}$$

The computation of the ground state energy splitting including the prefactor yields [27, 148]

$$\Delta = \frac{8D\tilde{s}^{3/2}(1-h_x^2)^{5/2}}{\pi^{1/2}} \left(\frac{e^{\sqrt{1-h_x^2}}}{1+\sqrt{1-h_x^2}}\right)^{2\tilde{s}} h_x^{2s}. \tag{5.16}$$

The factor h_x^{2s} signifies that the energy splitting arises from $2s^{\text{th}}$ order in degenerate perturbation theory in h_x. In the presence of a longitudinal magnetic field, *i.e.*, along z-axis, the two degenerate minima of the potential become non-degenerate — one with lower energy and the other with higher energy. The problem becomes that of a quantum decay of a metastable state [149]. The nature of the Hamiltonian determines the form of the generating function. In Eqn.(5.7), the generating function contains a real exponential function. In most cases, it is expedient to use an imaginary exponential function to avoid some technical issues, as we will see in the next section. For this particular problem, however, it is possible to analytically solve the Schrödinger equation and find the energy levels of the particle in the potential Eqn.(5.12), such solution has been reported [120].

5.2.2 Effective potential method for the XOY-easy-plane model

In Sec.(3.2.1), we present a lucid calculation of tunneling in biaxial spin model via spin coherent state path integral formalism. We will now show how the particle mapping recovers this result. The Hamiltonian of this system has the usual form

$$\hat{H} = D_1 \hat{S}_z^2 + D_2 \hat{S}_x^2. \tag{5.17}$$

This system can be mapped to a particle problem with the same procedure as in the previous section. However, due to the nature of this Hamiltonian, there exist another convenient approach to map this system to a particle Hamiltonian. This is done by introducing a non-normalized spin coherent state[3] of the form [4, 66, 115, 119]

$$|z\rangle = e^{zS^-} |s,s\rangle = \sum_{\sigma=-s}^{s} \binom{2s}{s+\sigma}^{1/2} z^{s-\sigma} |s,\sigma\rangle = e^{is\phi} \sum_{\sigma=-s}^{s} \binom{2s}{s+\sigma}^{1/2} e^{-i\sigma\phi} |s,\sigma\rangle \,, \tag{5.18}$$

where the last equality sign follows by restricting the complex variable z on a unit circle, *i.e.*, $z = e^{i\phi}$. Acting from the left by $\langle\psi|$ and subsequently taking the complex conjugate we obtain

$$e^{is\phi} \langle z|\psi\rangle = \sum_{\sigma=-s}^{s} \binom{2s}{s+\sigma}^{1/2} c_\sigma e^{i\sigma\phi} \equiv \Phi(\phi), \tag{5.19}$$

where $c_\sigma = \langle s,\sigma|\psi\rangle$, and $\Phi(\phi)$ is the generating function[4] with periodic boundary condition $\Phi(\phi + 2\pi)$= $e^{2i\pi s}\Phi(\phi)$. From Eqn.(5.18) we have

$$e^{is\phi} \langle z|\hat{S}_z|\psi\rangle = \sum_{\sigma=-s}^{s} \binom{2s}{s+\sigma}^{1/2} \sigma c_\sigma e^{i\sigma\phi} = -i\frac{d\Phi(\phi)}{d\phi}. \tag{5.20}$$

[3]This non-normalized spin coherent state can be thought of as the spin wave function in this case.

[4]It is convenient to use this generating function for models with x or y easy axis, while Eqn.(5.7) is convenient for z easy axis models. This avoids the problem of a negative mass particle.

Thus, we have

$$\sum_{\sigma=-s}^{s} \binom{2s}{s+\sigma}^{1/2} \langle s,\sigma|\hat{S}_z|\psi\rangle\, e^{i\sigma\phi} = -i\frac{d\Phi(\phi)}{d\phi}. \tag{5.21}$$

Similar expressions can be derived for $\langle z|\hat{S}_x|\psi\rangle$ and $\langle z|\hat{S}_y|\psi\rangle$. Consequently, the action of the spin operators on this function yields the following expressions [148, 150]

$$\hat{S}_z = -i\frac{d}{d\phi};\ \hat{S}_x = s\cos\phi - \sin\phi\frac{d}{d\phi};\ \hat{S}_y = s\sin\phi + \cos\phi\frac{d}{d\phi}. \tag{5.22}$$

The eigenvalue equation becomes

$$\hat{H}\Phi(\phi) = \mathcal{E}\Phi(\phi). \tag{5.23}$$

Using Eqn.(5.17) and Eqn.(5.22), Eqn.(5.23) becomes a differential equation of the form [99, 148]

$$-D_1(1-\kappa\sin^2\phi)\frac{d^2\Phi}{d\phi^2} - D_2(s-\frac{1}{2})\sin 2\phi\frac{d\Phi}{d\phi} + D_2(s^2\cos^2\phi + s\sin^2\phi)\Phi = \mathcal{E}\Phi, \tag{5.24}$$

where $\kappa = D_2/D_1$. A convenient way to obtain a Schrödinger equation with a constant mass is by introducing an incomplete elliptic integral of the first kind [5, 18]

$$x = F(\phi,\lambda) = \int_0^{\phi} d\varphi \frac{1}{\sqrt{1-\lambda^2\sin^2\varphi}}, \tag{5.25}$$

with amplitude ϕ and modulus $\lambda^2 = \kappa$. The trigonometric functions are related to the Jacobi elliptic functions by $\mathrm{sn}(x,\lambda) = \sin\phi$, $\mathrm{cn}(x,\lambda) = \cos\phi$ and $\mathrm{dn}(x,\lambda) =$

$\sqrt{1-\lambda^2\,\mathrm{sn}^2(x,\lambda)}$. In this new variable the differential equation becomes

$$P_1\frac{d^2\Phi}{dx^2}+P_2\frac{d\Phi}{dx}+P_3\Phi=\mathcal{E}\Phi, \tag{5.26}$$

where

$$P_1=-D_1;\ P_2=-2D_2 s\frac{\mathrm{sn}(x,\lambda)\,\mathrm{cn}(x,\lambda)}{\mathrm{dn}(x,\lambda)};\ P_3=s^2\,\mathrm{cn}^2(x,\lambda)+s\,\mathrm{sn}^2(x,\lambda). \tag{5.27}$$

Let us introduce a transformation of the form

$$\Psi(x)=e^{-y(x)}\Phi(\phi(x)). \tag{5.28}$$

Plugging Eqn.(5.28) into Eqn.(5.26), and demanding that the coefficient of the first derivative of Ψ vanishes we obtain the expression for $y(x)$ as

$$y(x)=s\log[\mathrm{dn}(x,\lambda)]. \tag{5.29}$$

Thus, Eqn.(5.26) transforms into a Schrödinger equation $H\Psi(x)=\mathcal{E}\Psi(x)$ with

$$H=-\frac{1}{2m}\frac{d^2}{dx^2}+U(x);\quad m=\frac{1}{2D_1}. \tag{5.30}$$

The effective potential is given by

$$U(x)=D_2 s(s+1)\frac{\mathrm{cn}^2(x,\lambda)}{\mathrm{dn}^2(x,\lambda)}. \tag{5.31}$$

The exact instanton trajectory can be found in the usual way; it is given by

$$\mathrm{sn}[x(\tau),\lambda]=\tanh(\omega_0\tau);\quad \omega_0^2=4s(s+1)D_1D_2. \tag{5.32}$$

This solution interpolates from $x_i = -\mathcal{K}(\kappa)$ ($\phi = -\pi/2$) at $\tau = -\infty$ to $x_f = \mathcal{K}(\kappa)$ ($\phi = \pi/2$) at $\tau = \infty$, where $x = \pm\mathcal{K}(\kappa)$ corresponds to one of the two minima of Eqn.(5.31). The action for this trajectory is found to be [24, 98, 99],

$$B = \sqrt{s(s+1)}\ln\left(\frac{1+\sqrt{\kappa}}{1-\sqrt{\kappa}}\right), \tag{5.33}$$

which coincides with the result of the spin coherent state path integral formalism in Eqn.(3.7), except for the quantum renormalization $s(s+1)$. For large spin systems $s \gg 1$, this coefficient $s(s+1)$ can be approximated as s^2. Thus, the two actions become the same.

5.3 Methods for studying quantum-classical phase transitions of the escape rate

Thus far, we have studied macroscopic quantum tunneling of spins at zero temperature, which is dominated by vacuum instanton trajectory. As we mentioned in chapter (1), transition at finite temperature can be either first- or second-order. In this section, we will present a lucid exposition of quantum-classical phase transitions of the escape rate, and different methods of studying these transitions at finite temperature. In order to begin our discussion, we will need to define the escape rate at finite temperature. In the semiclassical approximation, the escape rate of a particle through a potential barrier is obtained by taking the Boltzmann average over tunneling probabilities [6, 27]:

$$\Gamma = \int_{U_{\rm min}}^{U_{\rm max}} d\mathcal{E}\mathcal{P}(\mathcal{E})e^{-\beta(\mathcal{E}-U_{\rm min})}, \tag{5.34}$$

where $\beta^{-1} = T$ is the temperature, which is assumed to be less than the height of the potential barrier. This defines the temperature assisted tunneling rate; $\mathcal{P}(\mathcal{E})$ is an imaginary time transition amplitude from excited states at an energy $\mathcal{E}$, and $U_{\rm min}$ is the

bottom of the potential energy. The transition amplitude is defined as

$$\mathcal{P}(\mathcal{E}) = \mathcal{A}e^{-S(\mathcal{E})}, \tag{5.35}$$

where $\mathcal{A}$ is a prefactor independent of $\mathcal{E}$. The Euclidean action is of the form

$$S(\mathcal{E}) = 2\int_{x_1(\mathcal{E})}^{x_2(\mathcal{E})} dx\sqrt{2m(x)}\sqrt{U(x)-\mathcal{E}}, \tag{5.36}$$

where $x_{1,2}(\mathcal{E})$ are the roots of the integrand in Eqn.(5.36), which are the classical turning points ($U(x_{1,2}) = \mathcal{E}$) of a particle with energy $-\mathcal{E}$ in the inverted potential $-U(x)$ as depicted in Fig.(1.1). We have taken the mass, $m(x)$ to be coordinate dependent for a general consideration. The factor of 2 in Eqn.(5.36) corresponds to the back and forth oscillatory motion of the particle in the inverted potential (see Fig.1.1). In other words, the particle crosses the barrier twice.

5.3.1 Phase transition with thermon action

Absorbing the transition amplitude in Eqn.(5.35) into the definition of the escape rate in Eqn.(5.34), we obtain

$$\Gamma = \mathcal{A}\int_{U_{\text{min}}}^{U_{\text{max}}} d\mathcal{E}e^{-\mathcal{S}_p}, \tag{5.37}$$

where

$$\mathcal{S}_p = S(\mathcal{E}) + \beta(\mathcal{E} - U_{\text{min}}), \tag{5.38}$$

is the thermon action or the periodic instanton action [20]. In the method of steepest decent (for $T < \hbar\omega_0$), one can introduce fluctuations around the classical path that minimizes this thermon action, *i.e.*, $\frac{d\mathcal{S}_p}{d\mathcal{E}} = 0$. The escape rate, Eqn.(5.37) in this method is thus written as [21]

$$\Gamma \sim e^{-\mathcal{S}_{\text{min}}(\mathcal{E})}, \tag{5.39}$$

where $\mathcal{S}_{\text{min}}(\mathcal{E})$ is the minimum of the thermon action in Eqn.(5.38) with respect to energy. In many cases of physical interest, when the energy is in the range $U_{\text{min}} < \mathcal{E} < U_{\text{max}}$, the Euclidean action $S(\mathcal{E})$ can be computed in the whole range of energy for any given potential in terms of complete elliptic integrals and hence the thermon action $\mathcal{S}_p$. This corresponds to the action of the periodic instanton[63] or thermon. At the bottom of the potential, $\mathcal{E} = U_{\text{min}}$; the minimum thermon action becomes the vacuum instanton action, that is

$$\mathcal{S}_{\text{min}}(U_{\text{min}}) = S(U_{\text{min}}). \tag{5.40}$$

Thus, the vacuum instanton action of the previous sections becomes, $B = S(U_{\text{min}})/2$, since it corresponds to half of the period of oscillation. Eqn.(5.39) becomes the transition amplitude formula for a pure quantum tunneling. However, at the top of the barrier $\mathcal{E} = U_{\text{max}}$, the Euclidean action vanishes, $S(U_{\text{max}}) = 0$; the minimum thermon action becomes

$$\mathcal{S}_{\text{min}}(U_{\text{max}}) = \mathcal{S}_0 = \beta\Delta U. \tag{5.41}$$

This defines the classical or thermodynamic action; it corresponds to the action of a constant trajectory, $x(\tau) = x_b$ at the top of the potential barrier [20]. The escape rate Eqn.(5.39) becomes the Boltzmann formula for a pure classical (thermal) activation.

Indeed, if we compare the plot of the thermon action in Eqn.(5.38) and that of the thermodynamic action in Eqn.(5.41) against temperature, there exist a critical temperature T^c at which the thermodynamic action crosses the thermon action. If this intersection is *sharp*, the critical temperature T^c can be thought of as a first-order crossover ("phase transition") temperature from classical (thermal) to quantum regimes. This leads to the crossover temperature defined in Eq(1.1), $T^c = T_0^{(1)}$. At this temperature $T_0^{(1)}$, there is discontinuity in the first-derivative of the action $\mathcal{S}_p$. However, if this intersection is *smooth*, the critical temperature is said to be of second-order, which is exactly the tem-

perature defined in Eqn.(1.2), $T^c = T_0^{(2)}$. The second derivative of the thermon action in this case has a jump at $T_0^{(2)}$. This is the basic understanding of the quantum-classical phase transitions of the escape rate.

5.3.2 Phase transition with thermon period of oscillation

Quantum-classical phase transitions of the escape rate can indeed be studied from the behaviour of the period of oscillation $\beta(\mathcal{E})$ as a function of energy $\mathcal{E}$. The period of oscillation is found from the dominant term in Eqn.(5.37), which comes from the minimum of the thermon action Eqn.(5.38)

$$\beta(\mathcal{E}) = \frac{1}{T} = -\frac{dS(\mathcal{E})}{d\mathcal{E}} = \int_{x_1(\mathcal{E})}^{x_2(\mathcal{E})} dx \sqrt{\frac{2m(x)}{U(x) - \mathcal{E}}}. \tag{5.42}$$

This expression defines the period of oscillation of a particle with energy $-\mathcal{E}$ in the inverted potential $-U(x)$. At the bottom of the potential $\mathcal{E} = U_{\text{min}}$, we get $\beta(\mathcal{E}) = \infty$, *i.e.*, $T = 0$. Thus, transition is dominated by quantum tunneling, which is mediated by vacuum instanton trajectories (see Sec.(5.2.1) and (5.2.2)), whereas at the top of the barrier $\mathcal{E} = U_{\text{max}}$, $\beta(\mathcal{E}) \to \beta_0^{(2)} = 2\pi/\omega_b$ [6], which explicitly depends on the frequency of oscillation at the bottom of the inverted potential. The behaviour of the period of oscillation as a function energy is of two kinds:

1). If $\beta(\mathcal{E})$ is a non-montonic function of energy, in other words, if $\beta(\mathcal{E})$ has a minimum at some point $\mathcal{E}_0 < U_{\text{max}}$, $\beta_{\text{min}} = \beta(\mathcal{E}_0)$ and then rises again, then first-order phase transition occurs [20]. At a certain energy within the range $U_{\text{min}} < \mathcal{E}_1 < \mathcal{E}_0$, the thermon action sharply intercepts with the thermodynamic action, yielding the actual crossover temperature $\frac{1}{\beta_0^{(1)}} = \frac{1}{\beta(\mathcal{E}_1)}$.

2). A monotonic decrease of $\beta(\mathcal{E})$ with increasing $\mathcal{E}$ from the bottom to the top of the barrier indicates the presence of second-order phase transition[20, 21, 27]. In this case the thermon action $\mathcal{S}_p$ smoothly intercepts with the thermodynamic action $\mathcal{S}_0$,

yielding the crossover temperature $\frac{1}{\beta_0^{(2)}}$ [20, 50], which is exactly Eqn.(1.2).

5.3.3 Phase transition with free energy

The escape rate, Eqn.(5.39) can also be written in a slightly different form [21]:

$$\Gamma \sim e^{-\beta F_{\min}}, \tag{5.43}$$

where $F_{\min} = \beta^{-1}\mathcal{S}_{\min}(\mathcal{E})$ is the minimum of the effective free energy

$$F = \beta^{-1}\mathcal{S}_p = \mathcal{E} + \beta^{-1}S(\mathcal{E}) - U_{\min}, \tag{5.44}$$

with respect to $\mathcal{E}$. The crossover from thermal to quantum regimes (first-order phase transition) occurs when two minima in the F vs. $\mathcal{E}$ curve have the same free energy. All the interesting physics of phase transition in spin systems can also be captured when the energy is very close (but not equal) to the top of the potential barrier, $\mathcal{E} \to U_{\max}$. In this case the free energy characterizes first- and second-order phase transitions in analogy with Landau's theory of phase transition, if one knows the exact expression of the action $S(\mathcal{E})$ for any given mass and potential. In most models with a magnetic field the action $S(\mathcal{E})$ cannot be obtained exactly, one has to study the free energy numerically.

5.3.4 Phase transition with criterion formula

An alternative method for determining the quantum-classical phase transitions of the escape rate, as well as the phase boundary was considered by Müller *et al* [97]. They studied the Euclidean action near the top of the potential barrier, which had been considered earlier by Gorokhov and Blatter [50]. For the general case of a particle that possesses a coordinate dependent mass, they found that near the top of the potential

barrier, the expression that determines any sort of phase transition is given by [97]

$$\mathcal{I} = \left[U'''(x_b)\left(g_1 + \frac{g_2}{2}\right) + \frac{1}{8}U''''(x_b) + \omega^2 m'(x_b)g_2 + \omega^2 m'(x_b)\left(g_1 + \frac{g_2}{2}\right) + \frac{1}{4}\omega^2 m''(x_b)\right]_{\omega=\omega_b}, \tag{5.45}$$

where

$$g_1 = -\frac{\omega^2 m'(x_b) + U'''(x_b)}{4U''(x_b)}; \tag{5.46}$$

$$g_2 = -\frac{3m'(x_b)\omega^2 + U'''(x_b)}{4\left[4m(x_b)\omega^2 + U''(x_b)\right]}; \tag{5.47}$$

$$\omega_b^2 = -\frac{U''(x_b)}{m(x_b)}; \quad \text{where} \quad m' \equiv \frac{dm(x)}{dx}; \quad \text{etc.}; \tag{5.48}$$

x_b represents the position of the sphaleron[5] at the bottom of the well of the inverted potential as shown in Fig.(1.1). The criterion for first-order phase transition is determined from the condition that $\mathcal{I} < 0$; $\mathcal{I} > 0$ determines the second-order transition; the phase boundary between the first- and the second-order phase transitions is determined by $\mathcal{I} = 0$. The criterion formula in Eqn.(5.45) is quite general. It can be simplified in two special cases

i). If the mass of the particle is a constant and the potential energy is an even function, Eqn.(5.45) reduces to

$$\mathcal{I} = \frac{1}{8}U''''(x_b). \tag{5.49}$$

Thus, the coefficient of the fourth-order term in the expansion of the potential around x_b quickly determines the first- and the second-order phase transitions, as well as the phase boundary [21].

[5]Sphalerons are static, unstable, finite-energy solutions of the classical equations of motion.

ii). If mass is still a constant but the potential is an odd function, Eqn.(5.45) reduces to

$$\mathcal{I} = -\frac{5}{24}\frac{[U'''(x_b)]^2}{U''(x_b)} + \frac{1}{8}U''''(x_b). \tag{5.50}$$

5.4 Conclusion and Discussion

We have reviewed the effective potential method, which enables one to map a spin system unto a particle problem. For the case of a uniaxial spin model in the presence of a magnetic field, we obtained the corresponding effective potential, the instanton trajectory and its action. For a biaxial spin model, we showed that the effective potential method reproduces the result of the spin coherent state path integral up to a quantum renormalization. However, not all soluble spin models possess an exact instanton solution. Two exceptional cases will be studied in Chapter (6). We also present a lucid explanation of quantum-classical phase transitions of the escape rate in spin systems or in any system that has a potential energy function with a potential barrier; different methods for studying these transitions were outlined. In Chapter (6), we will implement these methods for some interesting spin systems.

CHAPTER 6

QUANTUM-CLASSICAL PHASE TRANSITIONS OF THE ESCAPE RATE IN LARGE SPIN SYSTEMS

> There is a great satisfaction in building good tools for other people to use.
>
> Freeman Dyson

6.1 Introduction

The phase transition of the escape rate in spin systems was first studied by Chudnovsky and Garanin [21, 27] for a uniaxial spin model in a magnetic field; the Hamhiltonian for this system is given by

$$\hat{H} = -k_z \hat{S}_z^2 - h_x \hat{S}_x. \tag{6.1}$$

This model is a good approximation for $Mn_{12}Ac$ molecular nanomagnet, with a ground state of $s = 10$, and 21 energy levels. Transition between these states can occur either by quantum tunneling (QT) or thermally assisted tunneling (TAT). Using the effective potential method, Chudnovsky and Garanin [21, 27] computed the exact free energy function defined in Eqn.(5.44). Near the top of the barrier, they showed that the phase transition can be understood in analogy of Landau's theory of phase transition, whose free energy function has the form $F = a\psi^2 + b\psi^4 + c\psi^6$; $a = 0$ determines the quantum-classical transition; $b = 0$ determines the boundary between the first- and the second-order phase transitions.

The quantum-classical phase transitions in the biaxial spin systems follow a similar trend to that of uniaxial spin model in a magnetic field. Liang *et. al* [63] studied the

model:

$$\hat{H} = k_z \hat{S}_z^2 + k_y \hat{S}_y^2, \tag{6.2}$$

by spin coherent state path integral. They obtained the exact periodic instanton trajectory and its corresponding action; indeed, they showed that the dimensionless anisotropy constant $\lambda = \frac{k_y}{k_z} < 1$ plays the same role as the magnetic field in the uniaxial model. For a biaxial spin model with an external magnetic field, other interesting features arise. In this case there are two dimensionless parameters, thus one can study how the crossover temperatures vary with the magnetic field at the phase boundary. Many biaxial spin systems in the presence of an external magnetic field, with different easy axes directions have been studied by different approaches, although these systems are related by their anisotropy constants. Chudnovsky and Garanin [22, 23] studied two different biaxial spin models of the form

$$\hat{H} = -k_z \hat{S}_z^2 + k_x \hat{S}_x^2 - h_x \hat{S}_x, \tag{6.3}$$

$$\hat{H} = -k_z \hat{S}_z^2 + k_x \hat{S}_x^2 - h_z \hat{S}_z, \tag{6.4}$$

by direct numerical method and perturbation theory with respect to k_x respectively. These two models possess z-easy axis, x-hard axis, and y- medium axis respectively, with the magnetic field applied along the hard and easy axes respectively. The first model, *i.e.*, Eqn.(6.3) is related to the model Eqn.(3.11) in Sec.(3.2.2) by rescaling the anisotropy constants. It is realized in Fe_8 molecular cluster with $s = 10$, $k_z = 0.229K$, and $k_x = 0.092K$. The second model, Eqn.(6.4), has a magnetic field along the easy axis, which creates a bias potential minima. For this model the effect of the external magnetic field on the crossover temperatures was explicitly demonstrated by perturbation theory. Based on the results obtained in these models, Kim [51] considered the

effective potential method of the model:

$$\hat{H} = -k_z \hat{S}_z^2 + k_y \hat{S}_y^2 - h_x \hat{S}_x - h_z \hat{S}_z. \tag{6.5}$$

This model is exactly the model in Eqn.(6.4) for $h_x = 0$; for $h_z = 0$, the magnetic field h_x is along the medium axis, it is related to Eqn.(6.3) only by the rotation of axis $\hat{S}_y \to \hat{S}_x$. Kim [51] obtained the effective potential of this model, but with a coordinate dependent mass; he further demonstrated that the order of the phase transitions agrees with the results of numerical analysis and perturbation theory. Using an unconventional generating function, a constant mass was obtained in Ref.[111, 112]. The effect on the order of phase transitions are identical.

In this chapter we will present two models, different from those mentioned above. This chapter is organized as follows: we will present the effective potential method of a biaxial model with a medium axis magnetic field in Sec.(6.2). Our paper on this analysis will be included in Sec.(6.5). In Sec.(6.3) we will investigate the effective potential method of an antiferromagnetic exchange-coupled dimer model in the presence of a staggered magnetic field. The quantum-classical phase transitions of the escape rate of these models will be lucidly studied. Our paper on this analysis will be included in Sec.(6.6). Finally, in Sec.(6.4) we will conclude our analysis and comment on their significance.

6.2 Phase transition in a biaxial model with a medium axis magnetic field

6.2.1 Model Hamiltonian

The model we will consider is that of a biaxial ferromagnetic spin in an external magnetic field [105, 108]:

$$\hat{H} = D_1 \hat{S}_z^2 + D_2 \hat{S}_x^2 - h_x \hat{S}_x, \tag{6.6}$$

where $D_1 \gg D_2 > 0$, and $\hat{S}_i, i = x, y, z$ is the components of the spin. This model possesses an easy XOY plane with an easy-axis along the y-direction and an external magnetic field along the x-axis. At zero magnetic field, there are two classical degenerate ground states corresponding to the minima of the energy located at $\pm y$, these ground states remain degenerate for $h_x \neq 0$ in the easy XY plane. The phase transition of this model has been studied in [96] by spin coherent state path integral formalism. However, the crossover temperatures were not obtained and the vacuum instanton action was obtained in a tedious mathematical formula using elliptic integrals. In this thesis, we will show the power of the effective potential method by deriving the exact vacuum instanton trajectory and its corresponding action in a simplified way.

6.2.2 Particle mapping

The effective potential method for this model follows exactly the same procedure in Sec.(5.2.2). From Eqn.(5.19) and Eqn.(5.22), the differential equation is given by

$$\begin{aligned} &- D_1(1 - \kappa \sin^2\phi)\frac{d^2\Phi}{d\phi^2} - (D_2(s - \frac{1}{2})\sin 2\phi - h_x \sin\phi)\frac{d\Phi}{d\phi} \\ &+ (D_2 s^2 \cos^2\phi + D_2 s \sin^2\phi - h_x s \cos\phi)\Phi = \mathcal{E}\Phi. \end{aligned} \tag{6.7}$$

Using the incomplete elliptic integral of first kind in Eqn.(5.25) and repeating the same analysis in Sec.(5.2.2), the particle Hamiltonian gives

$$H = \frac{p^2}{2m} + U(x); \quad p = -i\frac{d}{dx}; \tag{6.8}$$

where the effective potential, the mass and the wave function are given by [105]

$$U(x) = \frac{D_2 \tilde{s}^2[\mathrm{cn}(x,\lambda) - \alpha_x]^2}{\mathrm{dn}^2(x,\lambda)}; \quad m = \frac{1}{2D_1}; \tag{6.9}$$

$$\Psi(x) = \frac{\Phi(\phi(x))}{[\mathrm{dn}(x,\lambda)]^s} \exp\left[- \tilde{s}\alpha_x \sqrt{\frac{\kappa}{(1-\kappa)}}\, \mathrm{arccot}\left(\sqrt{\frac{\kappa}{(1-\kappa)}}\, \mathrm{cn}(x,\lambda)\right)\right]; \tag{6.10}$$

where $\tilde{s} = (s + \frac{1}{2})$, $\lambda^2 = \kappa = D_2/D_1$ and $\alpha_x = h_x/2D_2\tilde{s}$. In order to arrive at this potential we have used the approximation $s(s+1) \sim \tilde{s}^2$ and shifted the minimum energy to zero by adding a constant of the form $D_2\tilde{s}^2\alpha_x^2$. The potential, Eqn.(6.9) has minima at $x_0 = 4n\mathcal{K}(\lambda) \pm \mathrm{cn}^{-1}(\alpha_x, \lambda)$ and maxima at $x_{sb} = \pm 4n\mathcal{K}(\lambda)$ for small barrier and at $x_{lb} = \pm 2(2n+1)\mathcal{K}(\lambda)$ for large barrier as shown in Fig.(6.1). The heights of the potential for small and large barriers are given by [96, 105]

$$\begin{aligned} \Delta U_{sb} &= D_2\tilde{s}^2(1-\alpha_x)^2, \\ \Delta U_{lb} &= D_2\tilde{s}^2(1+\alpha_x)^2. \end{aligned} \tag{6.11}$$

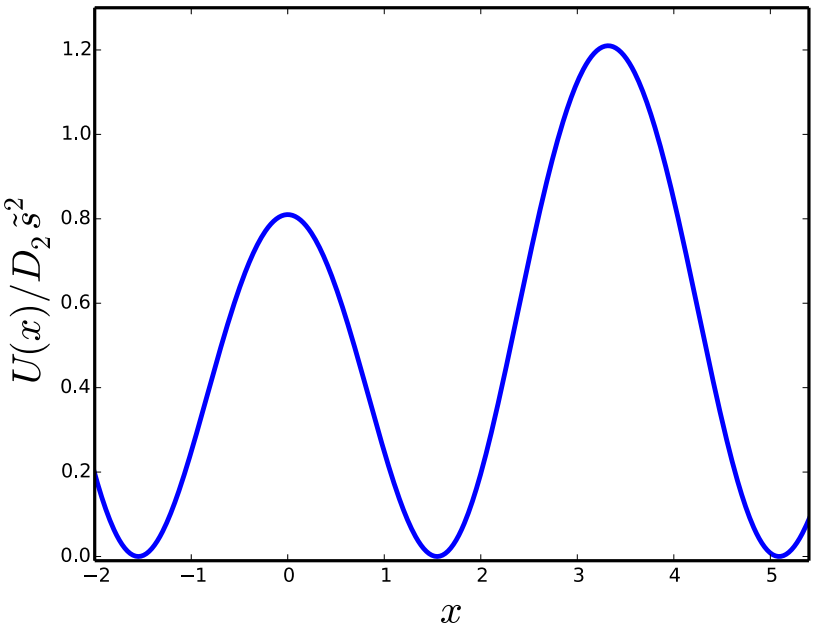

Figure 6.1: The plot of the effective potential, Eqn.(6.9) for $\alpha_x = 0.1$, $\lambda = 0.2$. For this potential $x_{sb} = 0$ and $x_{lb} = 2\mathcal{K}(0.2)$.

6.2.3 Vacuum instanton trajectory

The Euclidean Lagrangian corresponding to the particle Hamiltonian is given by

$$L_E = \frac{1}{2}m\dot{x}^2 + U(x). \tag{6.12}$$

The Euler-Lagrange equation of motion gives

$$m\ddot{x} - \frac{dU}{dx} = 0 \Rightarrow \frac{1}{2}m\dot{x}^2 - U(x) = -\mathcal{E}. \tag{6.13}$$

The vacuum instanton corresponds to trajectory with zero energy $\mathcal{E} = 0$. Using the mass and the potential energy, a straightforward calculation gives the classical trajectory [105]

$$\tau = \int_0^{\bar{x}} dx \sqrt{\frac{m}{2U(x)}}, \tag{6.14}$$

$$\mathrm{sn}[\bar{x}(\tau), \lambda] = \frac{2\sqrt{\frac{1-\alpha_x}{1+\alpha_x}}\tanh(\omega_0\tau)}{1 + \frac{1-\alpha_x}{1+\alpha_x}\tanh^2(\omega_0\tau)}, \tag{6.15}$$

where $\omega_0 = D_1\tilde{s}\sqrt{\kappa(1-\alpha_x^2)}$ is the frequency at the bottom of the potential. The instanton (upper sign) interpolates from the left minimum $\bar{x}(\tau) = -\,\mathrm{sn}^{-1}(\sqrt{1-\alpha_x^2}, \lambda)$ at $\tau = -\infty$ to the center of the barrier $\bar{x}(\tau) = 0$ at $\tau = 0$ and reaches the right minimum $\bar{x}(\tau) = \mathrm{sn}^{-1}(\sqrt{1-\alpha_x^2}, \lambda)$ at $\tau = \infty$. The corresponding action is [105, 148]

$$B = \int_{-\mathrm{sn}^{-1}\left(\sqrt{1-\alpha_x^2}\right)}^{\mathrm{sn}^{-1}\left(\sqrt{1-\alpha_x^2}\right)} \sqrt{2mU(x)}, \tag{6.16}$$

$$= \tilde{s}\left[\ln\left(\frac{1+\sqrt{\kappa(1-\alpha_x^2)}}{1-\sqrt{\kappa(1-\alpha_x^2)}}\right) \pm 2\alpha_x\sqrt{\frac{\kappa}{1-\kappa}}\arctan\left(\frac{\sqrt{(1-\kappa)(1-\alpha_x^2)}}{\alpha_x}\right)\right], \tag{6.17}$$

where the upper and lower signs are for tunneling in large and small barriers respectively. The tunneling splitting can be found in the usual way by summing over instanton and anti-instanton configurations. When $\alpha_x = \pm 1$, there is no large and small barriers, the trajectory and its action reduce to $\bar{x}(\tau) = 0 = B$, hence there is no tunnelling. Notice that all the results in this section reduce to the results obtained in Sec.(5.2.2) in the limit $\alpha = 0$.

6.2.4 Phase boundary and crossover temperatures

The phase transition of the escape rate in this model has been studied by Müller *et. al* [96] using spin coherent state path integral. In this thesis we will consider it in the effective potential method. Having obtained the potential and the mass, the phase transition of the escape rate can be analyzed using any of the methods outlined in Sec.(5.3.1) — (5.3.4). In this section we will apply that of Sec.(5.3.4). Since the potential is an even function and the mass is a constant, only the fourth derivative term in Eqn.(5.45) gives a nonzero value. Expanding the potential in Eqn.(6.9) near the maximum points x_{sb} and x_{lb} yields

$$U(x) = a - b(x - x_{sb})^2 + c(x - x_{sb})^4 + O(x^6), \tag{6.18}$$

$$U(x) = e - f(x - x_{lb})^2 + g(x - x_{lb})^4 + O(x^6), \tag{6.19}$$

where the constants are given by

$$a = (1 - \alpha_x)^2; \quad b = (1 - \alpha_x)(1 - \kappa(1 - \alpha_x)); \tag{6.20}$$

$$c = \frac{1}{12}[4 - \alpha_x - 4\kappa(3 - \alpha_x)(1 - \alpha) + 8\kappa^2(1 - \alpha_x)^2]; \tag{6.21}$$

$$e = (1 + \alpha_x)^2; \quad f = (1 + \alpha_x)(1 - \kappa(1 + \alpha_x)); \tag{6.22}$$

$$g = \frac{1}{12}[4 + \alpha_x - 4\kappa(3 + \alpha_x)(1 + \alpha) + 8\kappa^2(1 + \alpha_x)^2]. \tag{6.23}$$

The coefficients c and g are the same as $\mathcal{I}$ in Eqn.(5.49). At the phase boundary between the first and second-order transitions $\mathcal{I} = 0 = c = g$. Thus, we obtain [105]

$$\kappa_{sb}^{\pm}(\alpha_x) = \frac{3 - 4\alpha_x + \alpha_x^2 \pm (1-\alpha_x)\sqrt{1 - 4\alpha_x + \alpha_x^2}}{4(1-\alpha_x)^2}, \tag{6.24}$$

$$\kappa_{lb}^{\pm}(\alpha_x) = \frac{3 + 4\alpha_x + \alpha_x^2 \pm (1+\alpha_x)\sqrt{1 + 4\alpha_x + \alpha_x^2}}{4(1+\alpha_x)^2}, \tag{6.25}$$

The phase diagrams of Eqns.(6.24) and (6.25) are shown in Fig.(6.2), with the value of κ^- increasing with increasing magnetic field for small barrier while it decreases with increasing magnetic field for large barrier. In both cases, the first-order phase transition occurs in the regime $\kappa_{sb/lb}^{-} > 1/2$. For small barrier, Eqn.(6.24) is consistent with the results obtained in [51, 111, 112]. The crossover temperature for the first-order transition is estimated from Eqn.(1.1), that is

$$T_0^{(1)} = \frac{\Delta U}{2B}. \tag{6.26}$$

This temperature can be obtained directly from Eqns.(6.11) and (6.17). In Fig.(6.3(b)) we have shown the plot of first-order crossover temperature at the phase boundary using Eqns.(6.24) and (6.25). For $\alpha_x \ll 1$, we obtain

$$T_0^{(c)} \approx \frac{D_2\tilde{s}}{\ln[(3+2\sqrt{2})e^{\pm\frac{3\alpha_x}{\sqrt{2}}}]}, \tag{6.27}$$

where the upper and the lower signs correspond to small and large barriers respectively. Both small and large barrier temperatures coincide at $\alpha_x = 0$ or $\kappa = \frac{1}{2}$ with $T_0^{(c)} = D_2\tilde{s}/\ln(3+2\sqrt{2})$. For the case of second-order transition, the crossover temperature is given by Eqn.(1.2) with ω_b given by Eqn.(5.48). The second order transition temperature

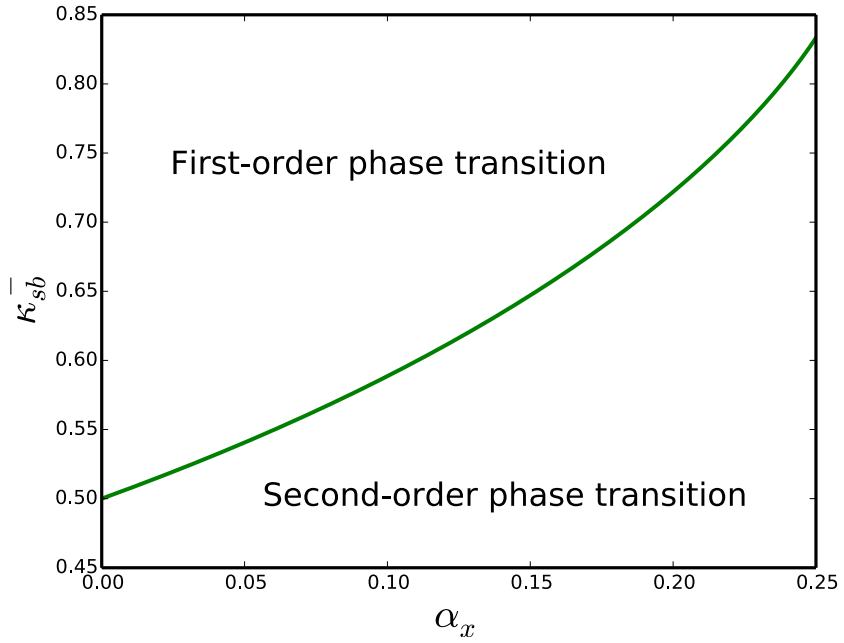

(a)

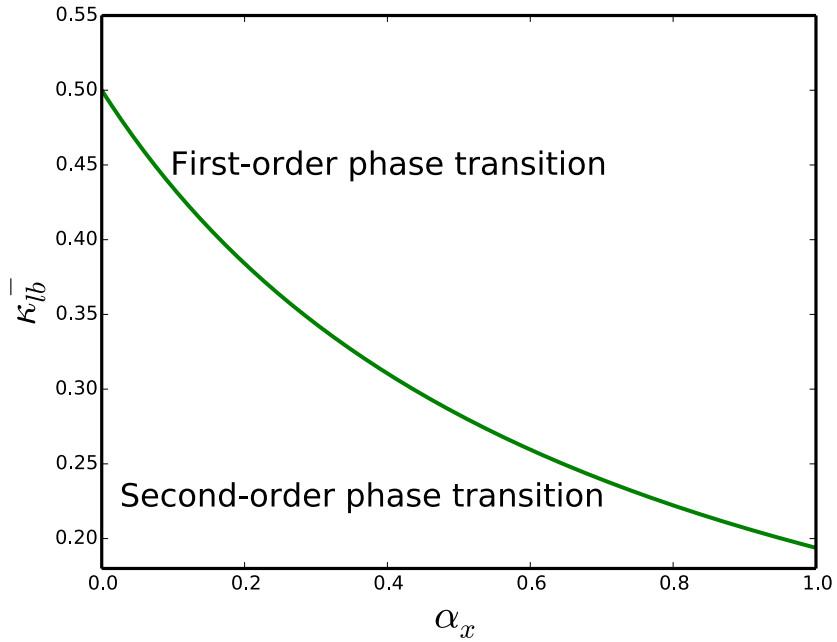

(b)

Figure 6.2: The phase diagram κ^- vs α_x at the phase boundary (a): Small barrier. (b): Large barrier.

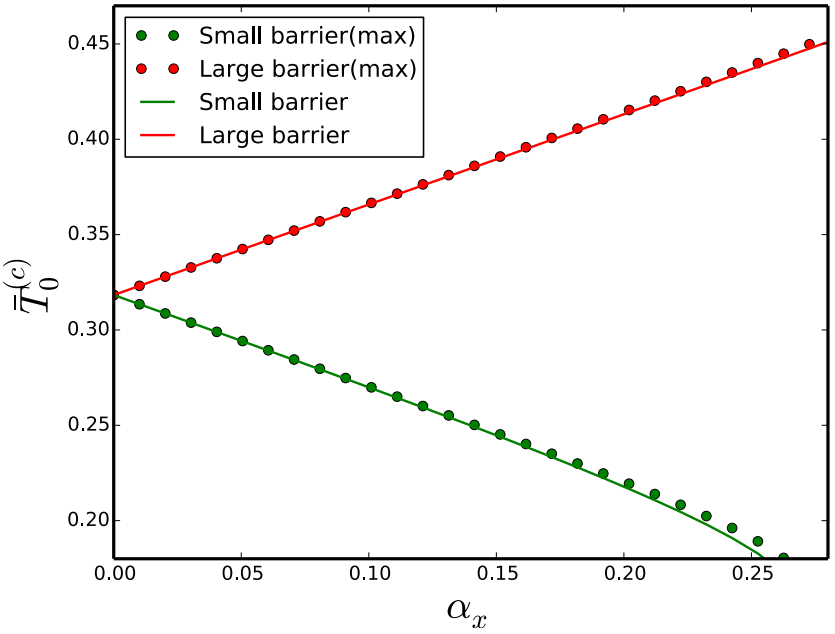

(a)

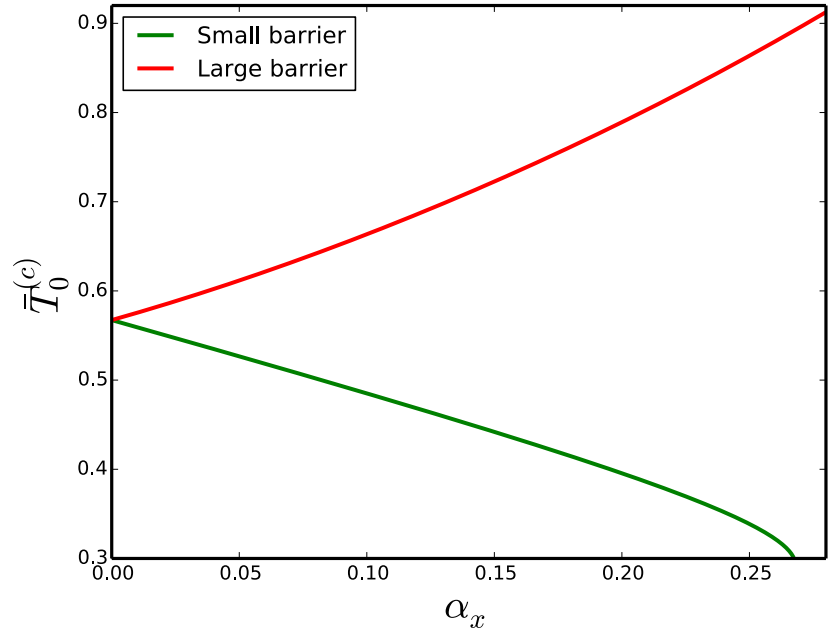

(b)

Figure 6.3: Colour online: Dependence of the crossover temperatures on the magnetic field at the phase boundary: (a) Second-order and its maximum for the small and large barrier, (b) First-order for the small and the large barrier. These graphs are plotted with $T_0^{(c)} = T_0^{(c)}/D_2\tilde{s}$.

and its maximum are found to be

$$T_0^{(2)} = \frac{\omega_b}{2\pi} = \frac{D_2\tilde{s}\sqrt{(1\pm\alpha_x)}}{\pi}\left(\frac{1-(1\pm\alpha_x)\,\kappa}{\kappa}\right)^{1/2}, \tag{6.28}$$

$$T_0^{(\max)} = \frac{D_2\tilde{s}}{2\pi\kappa}, \tag{6.29}$$

where the upper and lower signs correspond to the large and small barriers respectively. Fig.(6.3(a)) shows the crossover temperatures at the phase boundary. For $\alpha_x \ll 1$ we find

$$T_0^{(c)} \approx \frac{D_2\tilde{s}\left(1\pm\frac{3}{2}\alpha_x\right)}{\pi}. \tag{6.30}$$

which coincides at $\alpha_x = 0$ or $\kappa = \frac{1}{2}$.

6.2.5 Free energy with a magnetic field

In this section we will study the phase transition of this model using the free energy method in section(5.3.3). The analysis of this model using free energy has been studied in the absence of a magnetic field [155]. The crossover temperature from classical to quantum regime occurs when two minima in the F vs. $\mathcal{E}$ curve have the same free energy . For the case of zero magnetic field (only small barrier exist), it was shown that the phase transition from classical to quantum regime occurred at the crossover temperature $T_0^{(1)} = 1.122T_0^{(2)}$ for $\kappa = 0.8$ [155]. We want to see the influence of the magnetic field on this crossover temperature[1]. In order to obtain the free energy we first need to obtain the periodic instanton action (action with finite energy $\mathcal{E}$). However, in the presence of a magnetic field, this action cannot be obtained exactly [96]. Thus, we will study the free energy numerically. The thermon action is given by

$$\mathcal{S}_p(\mathcal{E}) = 2\sqrt{2m}\int_{x_1}^{x_2} dx\sqrt{U(x)-\mathcal{E}} + \beta(\mathcal{E}-U_{\min}). \tag{6.31}$$

[1]Basically, we would like to see if the magnetic field increases or decreases this crossover temperature

We will write this action in terms of a dimensionless energy quantity

$$Q = \frac{U_{\max} - \mathcal{E}}{U_{\max} - U_{\min}}. \tag{6.32}$$

Evidently, $Q \to 0$ near the top of the barrier and $Q \to 1$ near the bottom of the barrier[2].

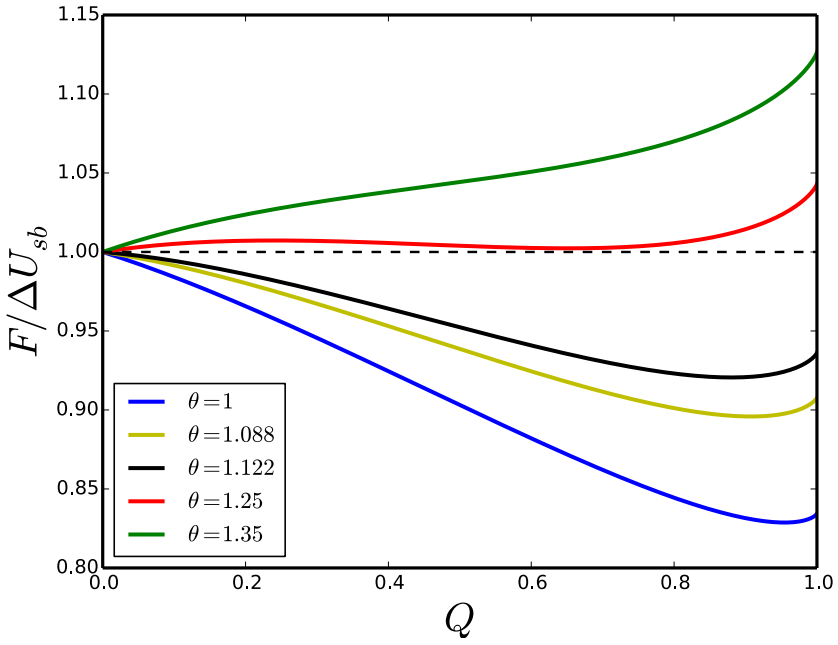

Figure 6.4: The numerical plot of the free energy for $\kappa = 0.8$ and $\alpha = 0.05$.

Setting $y = \mathrm{sn}(x, \lambda)$ and using Eqn.(6.9) we have

$$\mathcal{S}_p(Q) = 2\tilde{s}\sqrt{\kappa}\tilde{S}(Q) + \beta\Delta U_{sb}(1 - Q), \tag{6.33}$$

$$\tilde{S}(Q) = \int_{y_1}^{y_2} dy \frac{1}{(1-\kappa y^2)} \left[\frac{\left(\sqrt{1-y^2} - \alpha\right)^2 - (1-\alpha)^2(1-Q)(1-\kappa y^2)}{1-y^2} \right]^{\frac{1}{2}}, \tag{6.34}$$

[2]The dimensionless energy quantity Q lies in the range $Q \in [0, 1]$

where the turning points y_1 and y_2 are determined by setting the numerator in the square bracket to zero. The free energy Eqn.(5.44) can then be written as

$$\frac{F(Q)}{\Delta U_{sb}} = 1 - Q + \frac{2\theta\sqrt{1-\kappa(1-\alpha)}}{\pi\left(1-\alpha\right)^{3/2}}\tilde{S}(Q), \tag{6.35}$$

where $\theta = T/T_0^{(2)}$, and $T_0^{(2)}$ is given in Eqn.(6.28).

In Fig.(6.4) we have shown the numerical plot of the free energy with some of the temperature parameters in [155], and the same dimensionless anisotropy constant $\kappa = 0.8$, but in the presence of a small magnetic field $\alpha = 0.05$. We noticed that the phase transition from classical to quantum regime (where two minima of a curve have the same free energy) has been shifted to $\theta = 1.25$ or $T_0^{(1)} = 1.25T_0^{(2)}$, which is larger than the zero magnetic field value $T_0^{(1)} = 1.122T_0^{(2)}$ [155]. Thus, the magnetic field increases the crossover temperatures. It is tempting to conclude that this is always the case in the presence of a magnetic field. In Sec.(6.3), we will study a different model and show that the magnetic field plays an opposite role.

6.3 Phase transition in antiferromagnetic dimer model

6.3.1 Model Hamiltonian

Thus far we have studied quantum-classical phase transitions of the escape rate in ferromagnetic spin systems. This chapter devoted to the study of antiferromagnetic exchange-coupled dimer model, in the presence of a staggered magnetic field, applied along an easy z-axis. The Hamiltonian of this system is given by

$$\hat{H} = J\hat{\mathbf{S}}_A \cdot \hat{\mathbf{S}}_B - D(\hat{S}_{A,z}^2 + \hat{S}_{B,z}^2) + h_z(\hat{S}_{A,z} - \hat{S}_{B,z}), \tag{6.36}$$

which is reminiscent of the model in Sec.(3.3), except for the staggered magnetic field. As usual, $J > 0$ is the antiferromagnetic exchange coupling, $D > 0$ is the easy z-axis

anisotropy, $h_z = g\mu_B h$ is the external magnetic field, μ_B is the Bohr magneton, and $g = 2$ is the spin g-factor. In terms of the raising and lowering operators we have

$$\hat{H} = J[\hat{S}_{A,z}\hat{S}_{B,z} + \frac{1}{2}(\hat{S}_A^-\hat{S}_B^+ + \hat{S}_A^+\hat{S}_B^-)] - D(\hat{S}_{A,z}^2 + \hat{S}_{B,z}^2) + h_z(\hat{S}_{A,z} - \hat{S}_{B,z}). \quad (6.37)$$

The Hilbert space $\mathscr{H}$ of this system is the tensor product of the two spaces $\mathscr{H} = \mathscr{H}_A \otimes \mathscr{H}_B$, with dim($\mathscr{H}$)= $(2s_A + 1) \otimes (2s_B + 1)$. In this product space, a convenient basis can be written as

$$|s_A, \sigma_A\rangle \otimes |s_B, \sigma_B\rangle \equiv |\sigma_A, \sigma_B\rangle \,. \quad (6.38)$$

where $\sigma_A = -s_A, -s_A + 1, \cdots, s_A$ and $\sigma_B = -s_B, -s_B + 1, \cdots, s_B$. The action of the spin operators on this state is given by

$$\hat{S}_A^{\pm} |\sigma_A, \sigma_B\rangle = \sqrt{(s_A \mp \sigma_A)(s_A \pm \sigma_A + 1)}\, |\sigma_A \pm 1, \sigma_B\rangle \,, \quad (6.39)$$

$$\hat{S}_{A,z} |\sigma_A, \sigma_B\rangle = \sigma_A |\sigma_A, \sigma_B\rangle \,. \quad (6.40)$$

Similar relations hold for $\hat{S}_B^{\pm}$ and $\hat{S}_{B,z}$ with the replacement $\sigma_A \leftrightarrow \sigma_B$.

As we pointed out in Sec.(3.3), for $D > J$, this model has been used to investigate the dimerized molecular magnet $[Mn_4]_2$, which comprises two Mn_4 SMMs of equal spins $s_A = s_B = s = 9/2$ coupled antiferromagnetically. There are $(2s + 1)^2 \times (2s + 1)^2 = 100 \times 100$ matrices, which are sparsely populated giving rise to an exact numerical diagonalization of 100 non-zero energy states [88, 121, 133, 134, 144]. The values of the anisotropy parameters which were used to fit the experimental data for this dimer are $J = 0.13$ Kelvin and $D = 0.77$ Kelvin[121, 134]. The hysteresis loops in Fig.(6.5) shows the tunneling transitions through plateaus as was obtained from experimental measurement. The step heights are temperature independent below 400mK, which indicates quantum tunneling between the ground energy states.

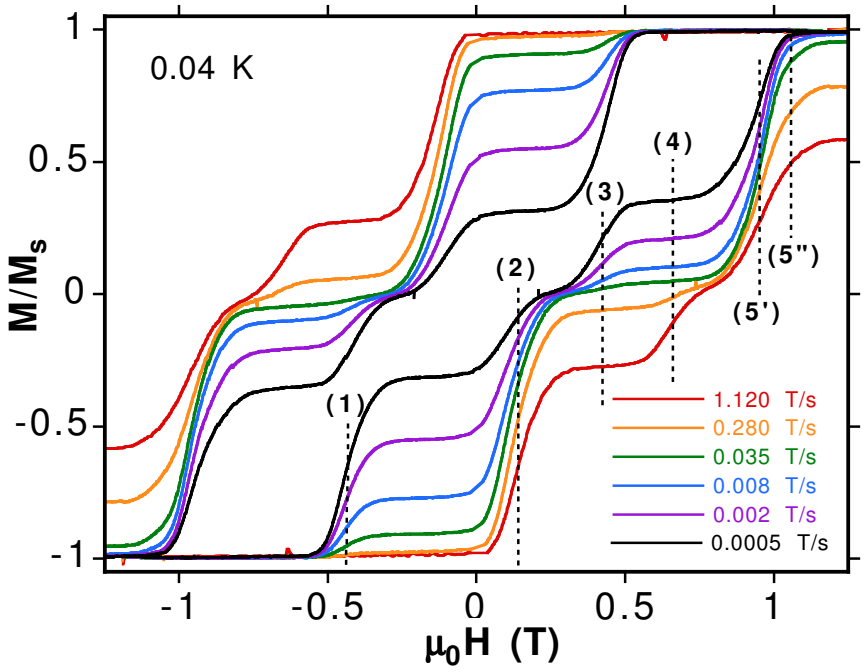

Figure 6.5: Hysteresis loops for the $[Mn_4]_2$ dimer at several field sweep rates and 40 mK. The tunnel transitions are labeled from 1 to 5 corresponding to the plateaus. Adapted with permission from Tiron *et. al* [134]

6.3.2 Effective potential of the model Hamiltonian

We now give a comprehensive derivation of the effective potential for the dimer model in Eqn.(6.36), based on the work of Paranjape and the present author of this thesis [106]. As we know by now, the first step is to introduce a spin wave function of the system. In a more general form, the spin wave function of this system can be written as a tensor product of two subspaces:

$$\psi = \psi_A \otimes \psi_B = \sum_{\substack{\sigma_A=-s_A \\ \sigma_B=-s_B}}^{s_A,s_B} \mathcal{C}_{\sigma_A,-\sigma_B}\mathcal{M}_{\sigma_A,-\sigma_B}, \tag{6.41}$$

where

$$\mathcal{M}_{\sigma_A,-\sigma_B} = \binom{2s_A}{s_A+\sigma_A}^{-1/2}\binom{2s_B}{s_B-\sigma_B}^{-1/2}|\sigma_A,-\sigma_B\rangle\,. \tag{6.42}$$

This is the appropriate composite spin wave function in the Hilbert space $\mathscr{H}$. The second step is to find the eigenvalue equation using this spin wave function. The eigenvalue equation is given by $\hat{H}\psi = \mathcal{E}\psi$; using Eqn.(6.39) and Eqn.(6.40), the action of the spin Hamiltonian Eqn.(6.37) on the spin wave function Eqn.(6.41) yields

$$\sum_{\substack{\sigma_A=-s_A \\ \sigma_B=-s_B}}^{s_A,s_B} \mathcal{C}_{\sigma_A,-\sigma_B}\Bigg[[-J\sigma_A\sigma_B + h_z(\sigma_A+\sigma_B) - D(\sigma_A^2+\sigma_B^2) - \mathcal{E}]\mathcal{M}_{\sigma_A,-\sigma_B} + \frac{J(s_A-\sigma_A)(s_B-\sigma_B)}{2}\mathcal{M}_{\sigma_A+1,-\sigma_B-1} + \frac{J(s_A+\sigma_A)(s_B+\sigma_B)}{2}\mathcal{M}_{\sigma_A-1,-\sigma_B+1}\Bigg] = 0. \tag{6.43}$$

This equation can be written compactly as

$$\begin{aligned}&\left[-J\sigma_A\sigma_B - D(\sigma_A^2+\sigma_B^2) + h_z(\sigma_A+\sigma_B) - \mathcal{E}\right]\mathcal{C}_{\sigma_A,-\sigma_B} \\ &+ \frac{J(s_A-\sigma_A+1)(s_B-\sigma_B+1)}{2}\mathcal{C}_{\sigma_A-1,-\sigma_B+1} \\ &+ \frac{J(s_A+\sigma_A+1)(s_B+\sigma_B+1)}{2}\mathcal{C}_{\sigma_A+1,-\sigma_B-1} = 0,\end{aligned} \tag{6.44}$$

where the $\mathcal{C}'s$ above the highest weight state and below the lowest weight state are all

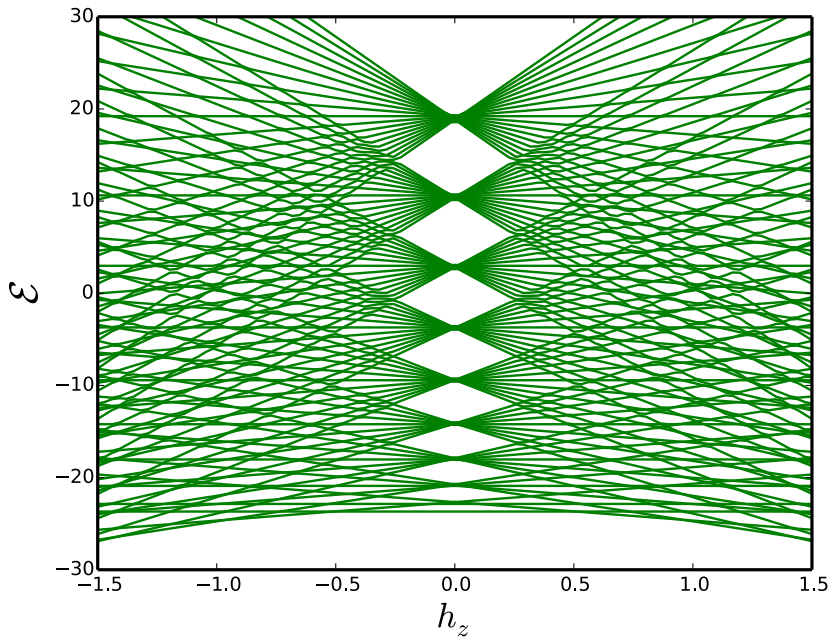

Figure 6.6: Plot of energy vs. staggered magnetic field of Eqn.(6.44) for $s_A = s_B = 9/2$, $J = 0.95$, and $D = 0.01$.

zero, *i.e.*, $\mathcal{C}_{-s_i-1} = 0 = \mathcal{C}_{s_i+1}$, etc., $i = A, B$. This eigenvalue equation is a sparse $(2s_A + 1)^2 \times (2s_B + 1)^2$ matrix which can be exactly diagonalized for $s_A = s_B = 9/2$[134, 144]. The diagonal elements are all degenerate and given by[3]

$$\mathcal{E}\left(\sigma_A, \sigma_B\right) = -J\sigma_A\sigma_B - D(\sigma_A^2 + \sigma_B^2) + h_z(\sigma_A + \sigma_B) \tag{6.45}$$

The energy levels between the states σ_A, σ_B and $\bar{\sigma}_A, \bar{\sigma}_B$ cross each other when $\mathcal{E}\left(\sigma_A, \sigma_B\right) = \mathcal{E}\left(\bar{\sigma}_A, \bar{\sigma}_B\right)$, which yields

[3]For ferromagnetic coupling $\sigma_B \rightarrow -\sigma_B$, this eigenvalue is the exact ground state energy of the quantum Hamiltonian, Eqn.(6.36), with $\sigma_A = \pm s_A$ and $\sigma_B = \pm s_B$, and the eigenstates are $|\sigma_A = s_A, \sigma_B = s_B\rangle$ and $|\sigma_A = -s_A, \sigma_B = -s_B\rangle$, these two states are degenerate for $h_z = 0$ or $s_A = s_B = s$, and there is no tunneling between them.

$$h_z = \frac{D\left(\sigma_A^2 + \sigma_B^2 - \bar{\sigma}_A^2 - \bar{\sigma}_B^2\right) + J\left(\bar{\sigma}_A\bar{\sigma}_B - \sigma_A\sigma_B\right)}{\bar{\sigma}_A + \bar{\sigma}_B - \sigma_A - \sigma_B} \tag{6.46}$$

An addition of small off-diagonal terms avoids these crossings as shown in Fig.(6.6) for $s_A = s_B = 9/2$ with 100 eigenvalues. These avoided energy crossings can only be visualized by zooming Fig.(6.6). However, for very large spin systems such as nanoparticles, nanomagnets and magnetic grains, the problem of finding the eigenvalues is completely analytically through the effective potential method. In this method we seek for a convenient transformation that converts this expression , *i.e.*, Eqn.(6.44) into a differential equation. As we have shown in the preceding chapter, this technique involves the introduction of a generating function[148, 150]. For this two-body problem, the generating function is of the form:

$$\mathcal{G}(x_1, x_2) = \sum_{\substack{\sigma_A = -s_A \\ \sigma_B = -s_B}}^{s_A, s_B} \mathcal{C}_{\sigma_A, -\sigma_B} e^{\sigma_A x_1} e^{-\sigma_B x_2}. \tag{6.47}$$

With this generating function, Eqn.(6.44) transforms into a differential equation for $\mathcal{G}$:

$$\begin{aligned} &- D\left(\frac{d^2\mathcal{G}}{dx_1^2} + \frac{d^2\mathcal{G}}{dx_2^2}\right) - J\cosh\left(x_1 - x_2\right)\frac{d}{dx_1}\left(\frac{d\mathcal{G}}{dx_2}\right) + J\frac{d}{dx_1}\left(\frac{d\mathcal{G}}{dx_2}\right) \\ &- \left(h_z - Js_A\sinh(x_1 - x_2)\right)\frac{d\mathcal{G}}{dx_2} + \left(h_z - Js_B\sinh(x_1 - x_2)\right)\frac{d\mathcal{G}}{dx_1} \\ &+ \left(Js_As_B\cosh(x_1 - x_2) - \mathcal{E}\right)\mathcal{G} = 0. \end{aligned} \tag{6.48}$$

As one should anticipate, the hyperbolic functions in Eqn.(6.48) emerge as functions of the relative coordinate. This is usually the case for two interacting particles. Thus, we can reduce Eqn.(6.48) to functions of the relative and the center of mass coordinates,

defined by

$$r = x_1 - x_2; \quad q = \frac{x_1 + x_2}{2}. \tag{6.49}$$

In terms of these two coordinates, Eqn.(6.48) reduces to a second-order differential equation with variable coefficients:

$$\mathcal{J}_1(r)\frac{d^2\mathcal{G}}{dr^2} + \mathcal{J}_2(r)\frac{d^2\mathcal{G}}{dq^2} + \mathcal{J}_3(r)\frac{d\mathcal{G}}{dr} + \mathcal{J}_4(r)\frac{d\mathcal{G}}{dq} + \mathcal{J}_5(r)\mathcal{G} = \mathcal{E}\mathcal{G}, \tag{6.50}$$

where the $\mathcal{J}_i(r)$ functions are given by[4]

$$\begin{aligned}
&\mathcal{J}_1(r) = -2\left(D + \frac{J}{2} + \frac{J}{2}\cosh r\right); \quad \mathcal{J}_2(r) = -\frac{1}{2}\left(D - \frac{J}{2} - \frac{J}{2}\cosh r\right); \\
&\mathcal{J}_3(r) = (2h_z + J(s_A + s_B)\sinh r); \quad \mathcal{J}_4(r) = -\frac{J(s_A - s_B)}{2}\sinh r; \\
&\mathcal{J}_5(r) = -Js_As_B\cosh r;
\end{aligned} \tag{6.51}$$

and the generating function $\mathcal{G}(r, q)$ is now given by

$$\mathcal{G}(r, q) = \sum_{\substack{\sigma_A = -s_A \\ \sigma_B = -s_B}}^{s_A, s_B} \mathcal{C}_{\sigma_A, -\sigma_B} e^{\frac{(\sigma_A + \sigma_B)r}{2}} e^{(\sigma_A - \sigma_B)q}. \tag{6.52}$$

The differential equation, Eqn.(6.50), is the general form with $s_A \neq s_B$; however, the exact solution is unknown[5]. But in most cases of physical interest such as molecular magnets and molecular wheels [92, 129, 134, 144], the two spins are equal. Thus, it is reasonable to consider a special case of equal spins $s_A = s_B = s$. Evidently, in this special case the expression for $\mathcal{J}_4(r)$ vanishes, which enables us to write the generating function $\mathcal{G}(r, q)$ as a product of two terms $\mathcal{G}(r, q) = \mathcal{G}_1(r)\mathcal{G}_2(q)$. Therefore, Eqn.(6.50) reduces to two, separate, independent equations which are satisfied when they are equal to constants $\mathscr{C}$ and $-\mathscr{C}$ respectively:

[4] We have used the transformation $r \to r + i\pi$ for technicality.

[5] By exact solution we mean the corresponding particle Hamiltonian for $s_A \neq s_B$.

$$\frac{d^2\mathcal{G}_2(q)}{dq^2} = \mathscr{C}\mathcal{G}_2(q), \tag{6.53}$$

$$\mathcal{J}_1(r)\frac{d^2\mathcal{G}_1(r)}{dr^2} + \mathcal{J}_3(r)\frac{d\mathcal{G}_1(r)}{dr} + (\mathcal{J}_5(r) - \mathcal{E})\,\mathcal{G}_1(r) = -\mathscr{C}\mathcal{J}_2(r)\mathcal{G}_1(r). \tag{6.54}$$

The first equation obviously does not contain sufficient information about the system, thus we will focus on the second equation. We then seek for a transformation that eliminates the first derivative term in Eqn.(6.54); such a transformation is of the form:

$$\Psi(r) = e^{-y(r)}\mathcal{G}_1(r), \tag{6.55}$$

where $y(r)$ is to be determined. Substituting into Eqn.(6.54) we obtain

$$\mathcal{J}_1\Psi'' + (2\mathcal{J}_1 y' + \mathcal{J}_3)\,\Psi' + [\mathcal{J}_3 y' + \mathcal{J}_5 + \mathscr{C}\mathcal{J}_2 + \mathcal{J}_1\left(y'' + y'^2\right)]\Psi = \mathcal{E}\Psi, \tag{6.56}$$

where prime denotes derivative with respect to r. It is evident that the elimination of the first derivative term in Eqn.(6.54) demands that the coefficient of the first derivative of Ψ vanishes. Thus, we must have

$$2\mathcal{J}_1 y' + \mathcal{J}_3 = 0. \tag{6.57}$$

This gives the expression for $y(r)$ as

$$y(r) = s\ln(2 + \kappa + \kappa\cosh r) + \frac{2s\alpha}{\sqrt{1+\kappa}}\operatorname{arctanh}\left(\frac{\tanh\left(\frac{r}{2}\right)}{\sqrt{1+\kappa}}\right), \tag{6.58}$$

where $\kappa = J/D$ and $\alpha = h_z/2Ds$. Simplifying Eqn.(6.56) using Eqn.(6.58), we arrive at the Schrödinger equation [106][6]:

[6]Since $\Psi(r) \to 0$ as $r \to \pm\infty$, it makes sense to call $\Psi(r)$ a particle wave function.

$$H\Psi(r) = \mathcal{E}\Psi(r); \quad H = \frac{\hat{p}^2}{2\mu(r)} + U(r); \quad \hat{p} = -i\frac{d}{dr}; \tag{6.59}$$

which describes a particle in a potential.

The coordinate dependent reduced mass $\mu(r)$ is given by

$$\mu(r) = \frac{1}{2D\left(2 + \kappa + \kappa\cosh r\right)}, \tag{6.60}$$

and the effective potential is given by[7]

$$U(r) = 2D\tilde{s}^2 u(r) : u(r) = \frac{2\alpha^2 + \kappa(1-\cosh r) + 2\alpha\kappa\sinh r}{(2 + \kappa + \kappa\cosh r)} + O\left(\tilde{s}^{-2}\right). \tag{6.61}$$

In this potential, we have used the large s limit $s \sim s+1 \sim \tilde{s} = (s + \frac{1}{2})$, thus terms of order $\tilde{s}^{-2}$ can be dropped. It is apparent that the magnetic field term in Eqn.(6.61) breaks inversion or time-reversal symmetry $r \to -r$. Thus, the minima of the potential are non-degenerate.

6.3.3 Analysis with zero staggered magnetic field

The derivations in the previous section employed several transformations, approximations, and rigorous mathematical analysis. It is indeed required that we test the correctness of these derivations. This can be done by computing the quantities that we already know their exact expressions at zero magnetic field from Sec.(3.3). These quantities include: the vacuum instanton action, the energy splitting, etc.; thus, if the effective potential method is correct, it must reproduce the result of spin coherent state path integral at zero magnetic field. We will commence by setting the magnetic field parameter in Eqn.(6.61) to zero. The resulting exact effective potential is now of the form

$$U(r) = 2Ds(s+1)u(r), \quad u(r) = \frac{\kappa(1-\cosh r)}{(2 + \kappa + \kappa\cosh r)}. \tag{6.62}$$

[7] A constant of the form $J\tilde{s}^2 = D\kappa\tilde{s}^2$ has been added to the potential for convenience.

Since we are considering large spin systems, the coefficient $s(s+1)$ will be approximated as s^2. The potential is now symmetric with degenerate minima, and hence the turning points are $\pm r(\mathcal{E})$. The minimum energy is $u_{\text{min}} = -1$, and the maximum is $u_{\text{max}} = 0$; thus, $\Delta U = U_{\text{max}} - U_{\text{min}} = 2Ds^2$. The maximum of the barrier height is located at $r_b = 0$ as shown in Fig.(6.7).

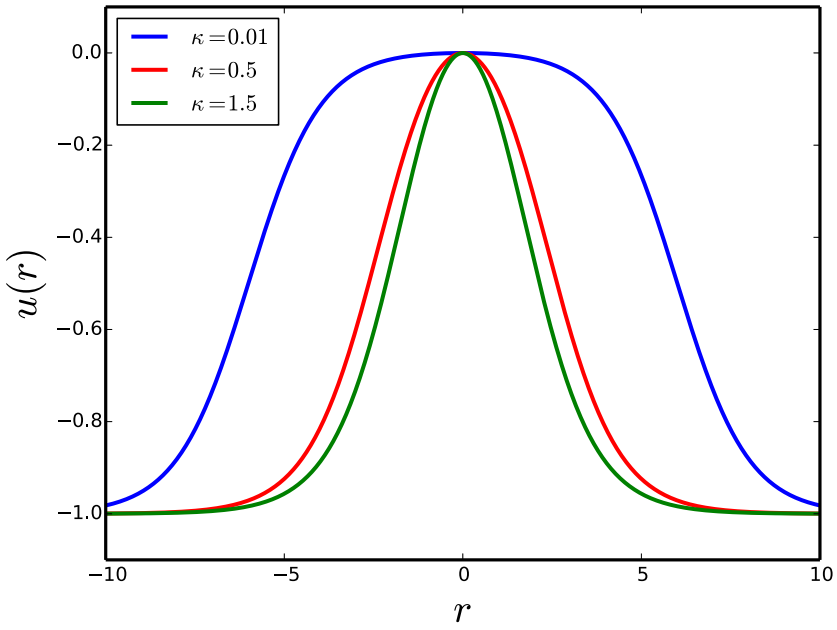

Figure 6.7: The plot of the potential for several values of κ with $D = 1$.

6.3.3.1 Periodic instanton method at zero magnetic field

The periodic instanton action is an indispensable quantity to compute when considering quantum-classical phase transitions of the escape rate. From this quantity, it is easy to derive the vacuum instanton action. In most cases, this quantity cannot be obtained exactly; in the present problem we can indeed find the exact expression of the quantity. We will begin from the Euclidean Lagrangian corresponding to the Hamiltonian in

Eqn.(6.59); it is given by

$$L_E = \frac{1}{2}\mu(r)\dot{r}^2 + U(r). \tag{6.63}$$

The Euler-Lagrange equation of motion gives

$$\mu(\bar{r}_p)\ddot{\bar{r}}_p + \frac{1}{2}\frac{d\mu(\bar{r}_p)}{d\bar{r}_p}\dot{\bar{r}}_p^2 - \frac{dU}{d\bar{r}_p} = 0. \tag{6.64}$$

Integrating once, we obtain

$$\frac{1}{2}\mu(\bar{r}_p)\dot{\bar{r}}_p^2 - U(\bar{r}_p) = -\mathcal{E}, \tag{6.65}$$

where $\mathcal{E}$ is the integration constant. Thus, the periodic instaton trajectory can be found from the solution of Eqn(6.65):

$$\tau = \int_0^{\bar{r}_p} dr \sqrt{\frac{\mu(r)}{2(U(r)-\mathcal{E})}}, \tag{6.66}$$

$$= \frac{1}{\sqrt{2}\omega_b}\int_0^{\bar{r}_p} dr \frac{1}{\sqrt{a+b-2b\cosh^2\left(\frac{r}{2}\right)}}, \tag{6.67}$$

where $\omega_b = 2Ds\sqrt{\kappa}$ is the frequency of oscillation at the well of the inverted potential of Fig.(6.7), $a = 1-(2+\kappa)\mathcal{E}'$, $b = 1+\kappa\mathcal{E}'$, and $\mathcal{E}' = \mathcal{E}/2Ds^2\kappa$. In terms of a new variable $y = \cosh\left(\frac{r}{2}\right)$, we have

$$\omega_b\tau = \frac{1}{\sqrt{b}}\int_1^{\bar{y}_p} dy \frac{1}{\sqrt{(y^2-1)(\frac{a+b}{2b}-y^2)}}, \tag{6.68}$$

where $\bar{y}_p = \cosh\left(\frac{\bar{r}_p}{2}\right)$. Introducing another change of variable:

$$x^2 = \frac{y^2-1}{\lambda^2 y^2}; \quad \lambda^2 = \frac{a-b}{a+b}. \tag{6.69}$$

The integral in Eqn.(6.68) becomes

$$\omega_b \tau = \sqrt{\frac{2}{a+b}} \int_0^{\bar{x}_p} dx \frac{1}{\sqrt{(1-x^2)(1-\lambda^2 x^2)}}, \tag{6.70}$$

where

$$\bar{x}_p = \sqrt{\frac{\bar{y}_p^2 - 1}{\lambda^2 \bar{y}_p^2}} = \frac{1}{\lambda} \tanh\left(\frac{\bar{r}_p}{2}\right). \tag{6.71}$$

If we set $x = \sin\theta$, we have

$$\omega_b \tau = \sqrt{\frac{2}{a+b}} \int_0^{\bar{\theta}_p} d\theta \frac{1}{\sqrt{1-\lambda^2 \sin^2\theta}}, \tag{6.72}$$

$$= \sqrt{\frac{2}{a+b}} F(\bar{\theta}_p, \lambda) = \sqrt{\frac{2}{a+b}} \, \mathrm{sn}^{-1}(\sin\bar{\theta}_p, \lambda), \tag{6.73}$$

where $F(\bar{\theta}_p, \lambda)$ is an incomplete elliptic integral of the first kind [18] with modulus λ, the amplitude $\bar{\theta}_p$ is given by

$$\sin\bar{\theta}_p = \frac{1}{\lambda} \tanh\left(\frac{\bar{r}_p}{2}\right). \tag{6.74}$$

Substituting Eqn.(6.74) into Eqn.(6.73), and solving for $\bar{r}_b$ we obtain the periodic instanton

$$\bar{r}_p(\tau) = 2 \, \mathrm{arctanh}[\lambda \, \mathrm{sn}(\omega_p \tau, \lambda)]; \quad \omega_p = \omega_b \sqrt{\frac{a+b}{2}}. \tag{6.75}$$

It is required that as $\tau \to \pm\frac{\beta}{2}$, the periodic instanton trajectory must tend to the classical turning points. In other words, $\bar{r}_p \to \pm r(\mathcal{E}) = \pm \, \mathrm{arccosh}\left(\frac{a}{b}\right)$ as $\tau \to \pm\frac{\beta}{2}$; see Fig.(6.8). This condition demands that $\mathrm{sn}(\omega_p\tau, \lambda) \to \pm 1$ as $\tau \to \pm\frac{\beta}{2}$. Using the fact that $\mu(\bar{r}_p)$

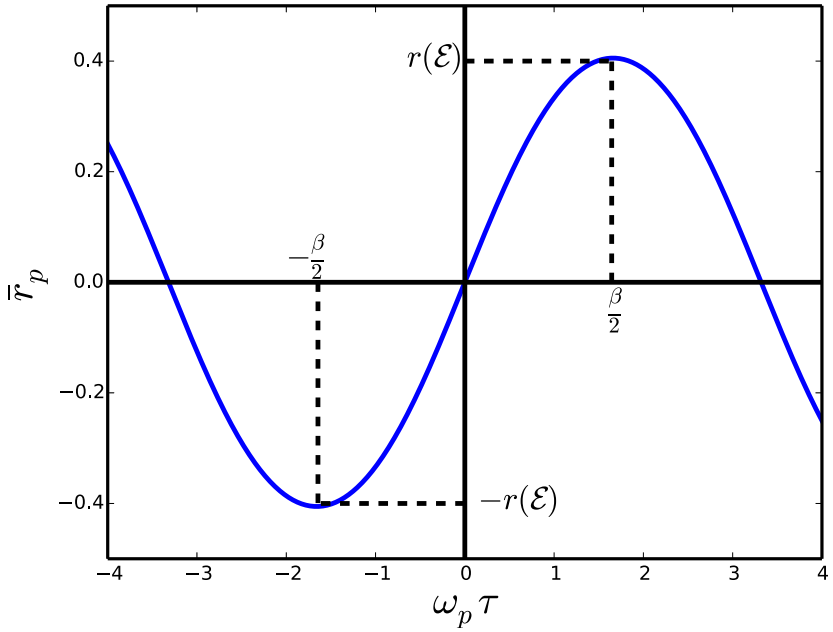

Figure 6.8: The periodic instanton trajectory with $\lambda = 0.2$.

and $\dot{\bar{r}}_p^2$ are given by

$$\mu(\bar{r}_p) = \frac{\mathrm{dn}^2(\omega_p\tau, \lambda)}{4D[1 + \kappa - \lambda^2\,\mathrm{sn}^2(\omega_p\tau, \lambda)]}; \quad \dot{\bar{r}}_p^2 = (2\lambda\omega_p)^2 \frac{\mathrm{cn}^2(\omega_p\tau, \lambda)}{\mathrm{dn}^2(\omega_p\tau, \lambda)}; \tag{6.76}$$

and making the transformation $x = \mathrm{sn}(\omega_p\tau, \lambda)$, the action for the periodic instanton path can be computed as

$$\tilde{\mathcal{S}}_p = \int_{-\frac{\beta}{2}}^{\frac{\beta}{2}} d\tau \mu(\bar{r}_p)\dot{\bar{r}}_p^2 + \beta(\mathcal{E} - U_{\text{min}}) = \bar{\mathcal{S}}_p + \beta(\mathcal{E} - U_{\text{min}}), \tag{6.77}$$

where

$$\bar{\mathcal{S}}_p = 2s\sqrt{2(a+b)\kappa} \int_0^1 dx \frac{(1-\gamma^2x^2) - (1-\gamma^2)}{(1-\gamma^2x^2)\sqrt{(1-x^2)(1-\lambda^2x^2)}}, \tag{6.78}$$

$$= 2s\sqrt{2(a+b)\kappa}[\mathcal{K}(\lambda) - (1-\gamma^2)\Pi(\gamma^2, \lambda)], \tag{6.79}$$

where $\gamma^2 = \lambda^2(1+\kappa)^{-1}$. The functions $\mathcal{K}(\lambda)$ and $\Pi(\gamma^2, \lambda)$ are known as the complete elliptic integral of the first and the third kinds respectively [5, 18], which are given by the two integrals in Eqn.(6.78).

6.3.3.2 Vacuum instanton at zero magnetic field

In this section we will consider one of the results obtained from spin coherent state path integral, *i.e.*, the vacuum instanton action. Since vacuum instanton invariably occurs at zero temperature $T \to 0$, which implies that $\beta \to \infty$, the energy of the particle must be close to the minima of the potential, yielding tunneling between degenerate ground states. Near the bottom of the barrier[8] $\mathcal{E} \to U_{\text{min}} = -2Ds^2$, $a \to 2(1+\kappa)/\kappa$, and $b \to 0$; thus, $\lambda \to 1$, we get $\mathrm{sn}(v, 1) \to \tanh v$. The periodic instanton trajectory, Eqn.(6.75) reduces to a vacuum instanton:

$$\bar{r}_p(\tau) \to \bar{r}_0 = 2\omega_0\tau; \quad \omega_p \to \omega_0 = 2Ds\sqrt{1+\kappa}. \tag{6.80}$$

As $\tau \to \pm\infty$, we have $\bar{r}_0 \to \pm\infty$, which corresponds to the minima of the zero magnetic field potential. Apparently, the frequency of oscillation at the bottom of the potential[9], ω_0, is the same as that of the spin coherent state path integral counterpart in Eqn.(3.52); however, the vacuum instanton trajectories are different. Indeed, we will show that Eqn.(6.80) is the correct vacuum instanton that will reproduce the correct energy splitting. A particle sitting at the minima of this potential is massless, $\mu(\bar{r}_0 \to \pm\infty) = 0$, but the vacuum instanton mass is nonzero. It is given by

$$\mu(\bar{r}_0) = [2D(2 + \kappa + \kappa\cosh(2\omega_0\tau))]^{-1}. \tag{6.81}$$

[8]Thus far, we have studied vacuum instanton with zero energy, because the minimum energy can always be normalized to zero by adding a constant, but in this case it is not normalized to zero.

[9]The frequency is given by $\omega_0^2 = \left.\frac{|U''(r)|}{\mu(r)}\right|_{r\to\pm\infty}$

Near the top of the barrier $\mathcal{E} \to U_{\max} = 0$, $a \to 1$, and $b \to 1$, thus $\lambda \to 0$, the periodic instanton reduces to a sphaleron at the top of the barrier

$$\bar{r}_p(\tau) \to r_b = 0; \quad \omega_p \to \omega_b = 2Ds\sqrt{\kappa}. \tag{6.82}$$

The mass of the sphaleron is given by

$$\mu(r_b) = [4D(1+\kappa)]^{-1}, \tag{6.83}$$

and the corresponding action from Eqn.(6.79) is

$$\tilde{\mathcal{S}}_p \to \mathcal{S}_0 = \beta\Delta U. \tag{6.84}$$

The action associated with the vacuum instanton trajectory can be obtained either by expanding the elliptic integrals in Eqn.(6.79) near the bottom of the potential $\lambda \to 1$, or simply by computing the action associated with the vacuum instanton path in Eqn.(6.80). The latter gives[10]

$$\tilde{\mathcal{S}}_p \to B = \int_{-\infty}^{\infty} d\tau \mu(\bar{r}_0)\dot{\bar{r}}_0^2 = 4s \operatorname{arctanh}\left(\frac{1}{\sqrt{1+\kappa}}\right), \tag{6.85}$$

$$= 2s \ln\left(\frac{\sqrt{1+\kappa}+1}{\sqrt{1+\kappa}-1}\right). \tag{6.86}$$

This is the exact vacuum instanton action. In the perturbative and the non-perturbative limits, Eqn.(6.86) simplifies to

$$B = \begin{cases} 2s \ln\left(\frac{J}{4D}\right); & \text{if } J \ll D; \\ 4s\left(D/J\right)^{1/2}; & \text{if } J \gg D. \end{cases} \tag{6.87}$$

[10]We have used Eqn.(6.81) and the fact that $\dot{\bar{r}}_0^2$ is given by $\dot{\bar{r}}_0^2 = (2\omega_0)^2$

which is the same action we derived in Sec.(3.3.2) by spin coherent state path integral, but the imaginary term, which is responsible for different ground state behaviour of integer and half-odd integer spins has does not appear in this action. It has been encoded in the particle wavefunction. The energy splitting follows from Eqn.(2.37). We conclude that the effective potential method of Sec.(6.3.2) is correct.

6.3.3.3 Zero magnetic field thermon action

We will now investigate the quantum-classical phase transitions of the escape rate using the method of Sec.(5.3.1). The thermon action only differs from the periodic instanton in Eqn.(6.77) by a factor of 2. It is given by

$$\mathcal{S}_p = 2\int_{-\frac{\beta}{2}}^{\frac{\beta}{2}} d\tau \mu(\bar{r}_p)\dot{\bar{r}}_p^2 + \beta(\mathcal{E} - U_{\min}) = 2\bar{\mathcal{S}}_p + \beta(\mathcal{E} - U_{\min}), \tag{6.88}$$

where $\bar{\mathcal{S}}_p$ is given by Eqn.(6.79). In terms of the dimensionless energy quantity Q in Eqn.(6.32) we have

$$\mathcal{S}_p = \mathcal{S}_0(1-Q) + 8s\sqrt{(\kappa+Q)}[\mathcal{K}(\lambda) - (1-\gamma^2)\Pi(\gamma^2,\lambda)], \tag{6.89}$$

where $\mathcal{S}_0$ is the thermodynamic action:[11]

$$\mathcal{S}_0 = \mathcal{S}_p(Q=0) = \beta\Delta U = \frac{2Ds^2}{T}. \tag{6.90}$$

The crossover temperature from temperature assisted quantum tunneling to classical thermal activation (which can be either first- or second-order) can be analyzed from the plot of these two actions as a function of temperature [12]. The first- and the second-order phase transitions occur where the two curves sharply intersect and smoothly join

[11] This is the thermon action for a constant trajectory $\bar{r}_p(\tau) = r_b = 0$ at the top of the barrier.

[12] In order to generate these figures one has to use the fact that $T = \frac{1}{\beta(\mathcal{E})}$ in Eqn.(6.96).

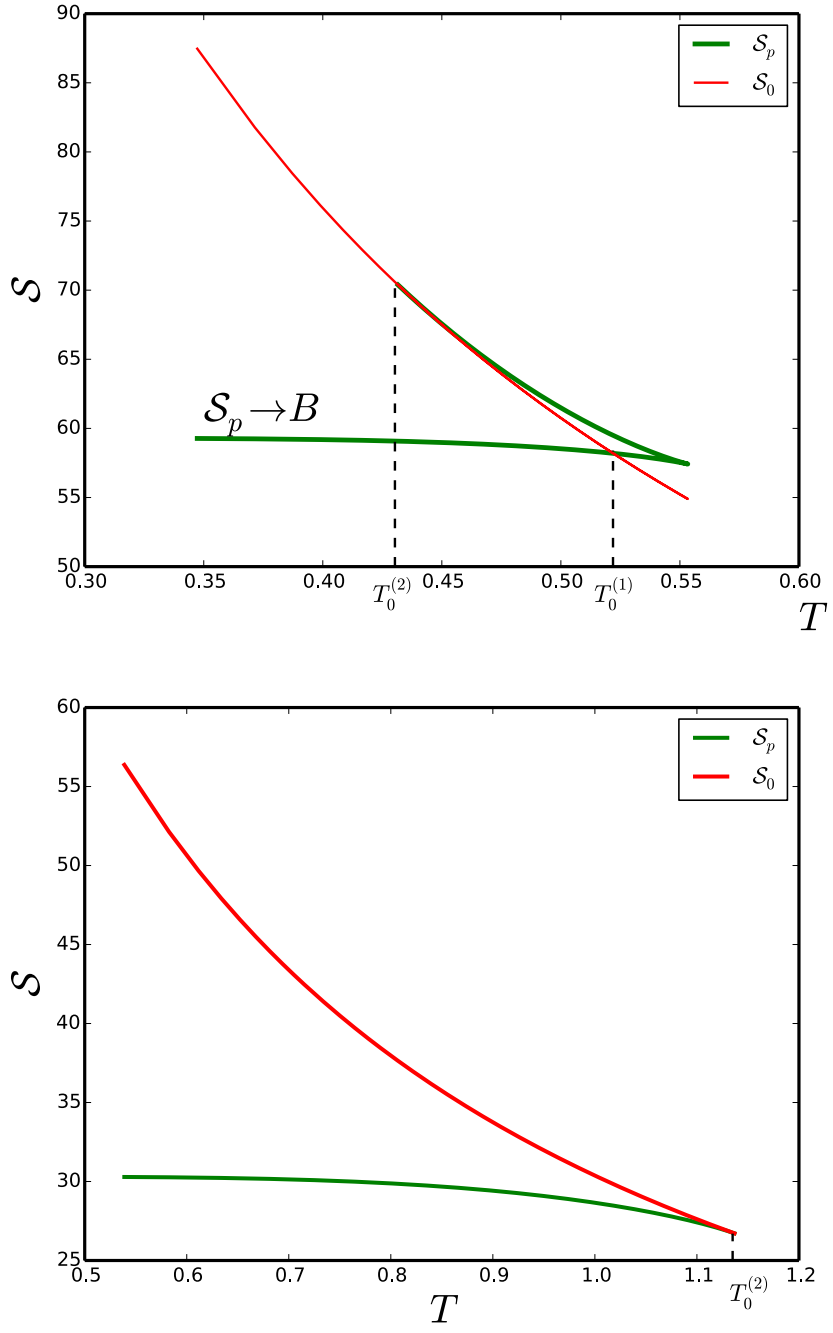

Figure 6.9: Dependence of the actions on temperature. The top figure is for first-order phase transition with the experimental parameters[121, 134]: $s = 9/2$; $D = 0.75$; $\kappa = 0.16$. The bottom figure is for second- order phase transition with; $s = 9/2$; $D = 0.75$; $\kappa = 1.12$.

at lowest action respectively. As depicted in Fig.(6.9), we observe the sharp and smooth intersections of the two actions corresponding to the first- and the second-order phase transitions respectively. In this system the physical understanding of a sharp first-order

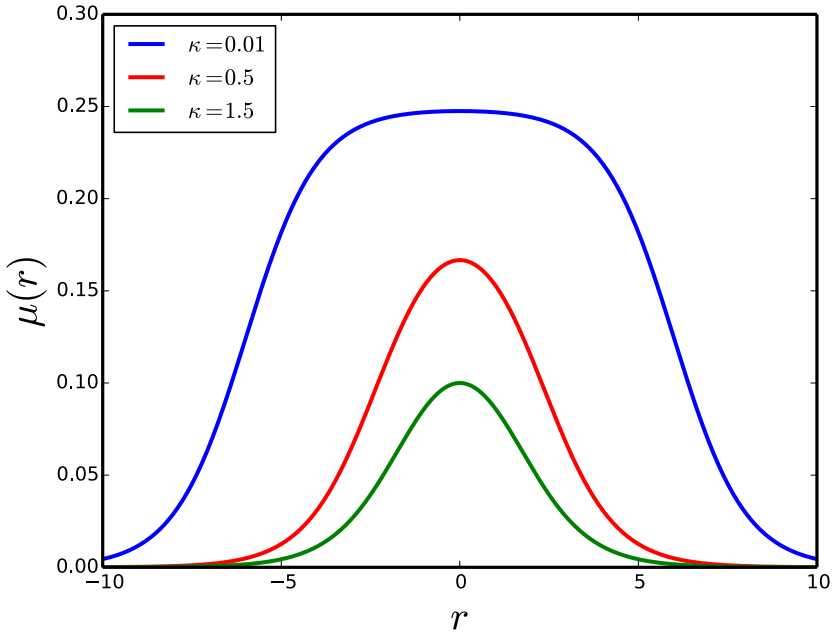

Figure 6.10: The plot of the position dependent mass in Eqn.(6.60) for several values of κ with $D = 1$.

phase transition is as follows: the mass at the top of the barrier $\mu(r_b)$ in Eqn.(6.83) is heavier than that at the bottom of the barrier $\mu(\pm\infty) = 0$. For small κ, the mass in Eqn.(6.60) and the potential in Eqn.(6.62) have a flat and wider barrier top due the heaviness of the mass at the top of the barrier as shown in Fig.(6.7) and Fig.(6.10). This makes tunneling from excited states inauspicious; thus, ground state tunneling competes with thermal classical activation, consequently, a sharp first-order quantum-classical phase transition occurs.

6.3.3.4 Zero magnetic field free energy

As an alternative method, the quantum-classical phase transitions of the escape rate can also be investigated using the method of Sec.(5.3.3), as we now show. From the thermon action, the free energy can be constructed:

$$F = \beta^{-1}\mathcal{S}_p, \tag{6.91}$$

where $\mathcal{S}_p$ is given by Eqn.(6.89); thus the free energy can be written exactly:

$$F(Q) = \Delta U\left(1 - Q + \frac{4}{\pi}\theta\sqrt{\kappa(\kappa+Q)}[\mathcal{K}(\lambda) - (1-\gamma^2)\Pi(\gamma^2,\lambda)]\right), \tag{6.92}$$

where $\theta = \beta^{-1}/T_0^{(2)} = T/T_0^{(2)}$ is a dimensionless temperature quantity, and $T_0^{(2)}$ is given in Eqn.(6.102). The modulus of the complete elliptic integrals λ and the elliptic characteristic γ are related to Q by

$$\lambda^2 = \frac{(1+\kappa)Q}{\kappa+Q}; \quad \gamma^2 = \frac{Q}{\kappa+Q}. \tag{6.93}$$

As shown in Fig.(6.11), the top two curves have only one minimum at the top of the barrier, $Q = 0$. For $\theta = 1.054$ or $T_0^{(1)} = 1.054T_0^{(2)}$, two minima have the same free energy. This corresponds to the crossover temperature (first-order transition) from classical to quantum regimes. As the temperature decreases from this crossover temperature, a new minimum of the free energy is formed; this new minimum becomes lower than the one at $Q = 0$.

As we mentioned before, phase transition occurs near the top of the potential barrier, so it is required that we expand this free energy close to the barrier top. Near the top of the barrier $Q \to 0$, the complete elliptic integrals can be expanded up to order Q^3. The corresponding series expansions are given in Appendix(I). The full simplification

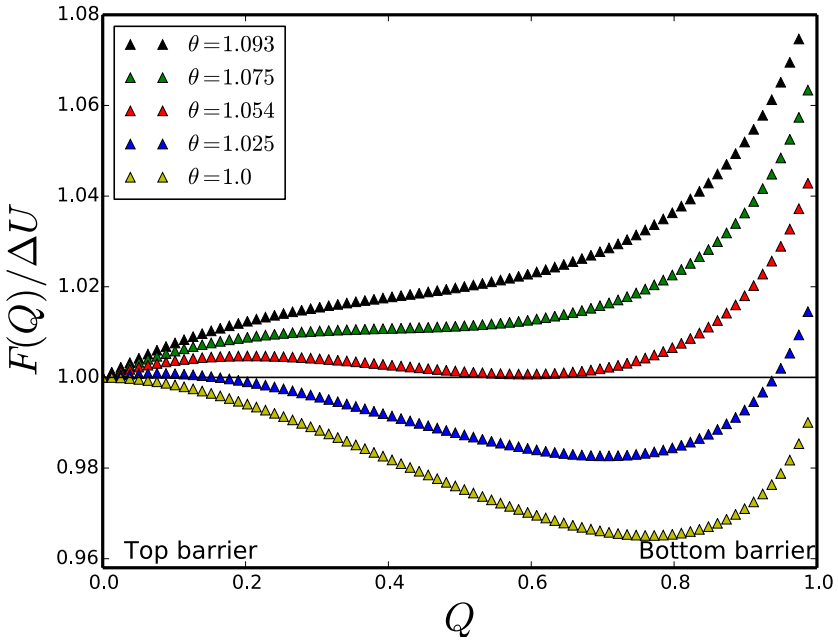

Figure 6.11: The effective free energy of the escape rate vs. Q for $\kappa = 0.4$ and several values of $\theta = T/T_0^{(2)}$, first-order transition.

of Eqn.(6.92) yields

$$F = \Delta U[1 + (\theta - 1)Q + \frac{\theta}{8\kappa}(\kappa - 1)Q^2 + \frac{\theta}{64\kappa^2}(3\kappa^2 - 2\kappa + 3)Q^3]. \tag{6.94}$$

The above expression is reminiscent of the free energy obtained in ferromagnetic spin system [21, 27]; it has the form of Landau's free energy:

$$F = F_0 + a\psi^2 + b\psi^4 + c\psi^6. \tag{6.95}$$

Serendipitously, the coefficient of Q in Eqn.(6.94) is equivalent to the coefficient a in the Landau's free energy; whereas the coefficient of Q^2 is equivalent to b in the Landau free energy; $b < 0$ corresponds to the regime of first-order transition; $b > 0$ corresponds to the regime of second-order transition; of course, $b = 0$ corresponds to the phase boundary.

Thus, $\kappa < 1$ indicates the regime of first-order phase transition; $\kappa > 1$ indicates the regime of second-order phase; evidently, $\kappa = 1$ indicates the phase boundary. These conditions can also be corroborated from the criterion formula in Eqn.(5.45) with $x_b = r_b = 0$, which corresponds to the top of the potential barrier.

6.3.3.5 Thermon period of oscillation

As a second alternative method, we will study the phase transition of the escape rate using the method of Sec.(5.3.2). The thermon period of oscillation $\beta(\mathcal{E})$ is given by [13]

$$\beta(\mathcal{E}) = -\frac{dS(\mathcal{E})}{d\mathcal{E}} = \frac{1}{T} = \int_{-r(\mathcal{E})}^{r(\mathcal{E})} dr \sqrt{\frac{2\mu(r)}{U(r) - \mathcal{E}}}. \tag{6.96}$$

Differentiating with respect to $\mathcal{E}$ gives

$$\frac{d\beta(\mathcal{E})}{d\mathcal{E}} = -\frac{d^2S(\mathcal{E})}{d\mathcal{E}^2} = -\frac{1}{T}\frac{d^2F}{d\mathcal{E}^2}. \tag{6.97}$$

This relation is equivalent to the requirement that the thermon period of oscillation monotonically increases with decreasing energy, which indicates a second-order phase transition. The period of oscillation can be obtained exactly:

$$\beta(\mathcal{E}) = \frac{1}{T} = \frac{2\sqrt{2}}{\omega_b} \int_0^{r(\mathcal{E})} dr \frac{1}{\sqrt{a - b\cosh r}}, \tag{6.98}$$

where

$$r(\mathcal{E}) = \cosh^{-1}\left(\frac{a}{b}\right), \tag{6.99}$$

a, b and ω_b are given in Eqn.(6.67) and Eqn.(6.82) respectively. The integral in Eqn.(6.98) is in fact standard, it is given by the complete elliptic integral of the first kind [18] (

[13] Notice that Eqn.(6.96) is the addition of the two limits $\tau \to \pm\frac{\beta}{2}$ in Eqn.(6.66).

$\bar{\theta}_p = \pi/2$ in Eqn.(6.74)). Thus we obtain

$$\beta(\mathcal{E}) = \frac{4}{\omega_p}\mathcal{K}(\lambda) = \frac{2}{Ds\sqrt{\kappa + Q}}\mathcal{K}(\lambda), \tag{6.100}$$

where ω_p is given in Eqn.(6.75) and the relation between λ and Q is given by Eqn.(6.93).

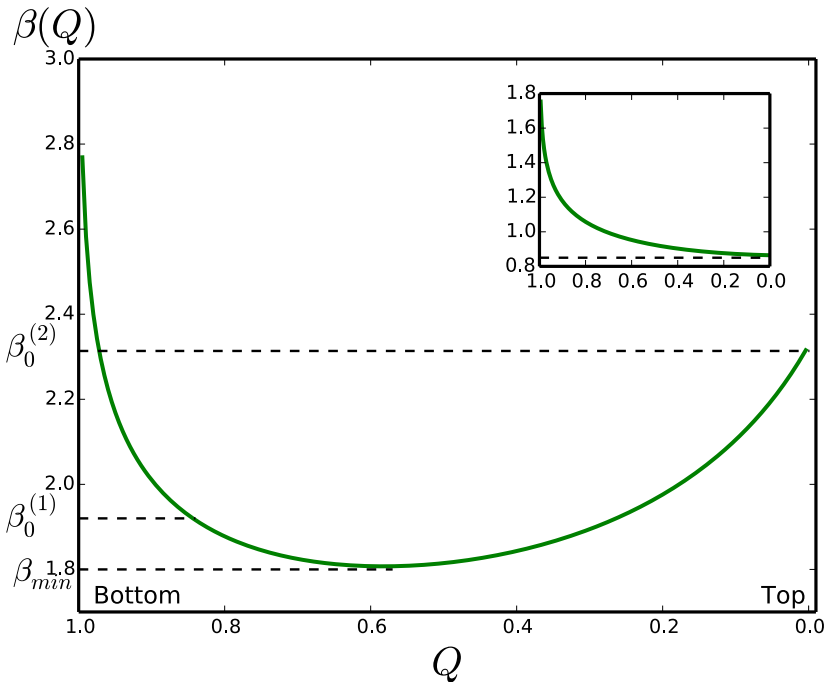

Figure 6.12: The period of oscillation vs. Q, using the experimental parameters in [121, 134]: $s = 9/2$; $D = 0.75K$; $J = 0.12K \Rightarrow \kappa = 0.16$ (first-order transition). Inset $\kappa = 1.16$ (second-order transition). $\beta_0^{(1)}$ and $\beta_0^{(2)}$ are the actual crossover temperatures for first- and second-order phase transitions respectively.

At the top of the barrier $Q = 0$, $\lambda = 0$, $\mathcal{K}(\lambda) = \pi/2$ and $\beta(U_{\max}) = \beta_0^{(2)} = 2\pi/\omega_b$. While at the bottom of the barrier $Q = 1$, $\lambda = 1$, $\mathcal{K}(\lambda) = \infty$ and $\beta(U_{\min}) = \infty$, which corresponds to tunneling mediated by vacuum instanton. Fig.(6.12) shows the plot of $\beta(\mathcal{E})$ vs. Q with $\kappa = 0.16$, $s = 9/2$, and $D = 0.75K$, which are the experimental parameters in Ref.[121, 134] . Indeed, for $\kappa < 1$, the period is a nonmonotonic function of energy indicating the existence of first-order phase transition, while for $\kappa > 1$, the period decreases with increasing energy from the bottom to the top of the barrier, which

indicates a second-order transition.

6.3.3.6 Zero magnetic field crossover temperatures

Having obtained the action at the bottom of the potential, which corresponds to the instanton action in Eqn.(6.86), the first-order crossover temperature is given by

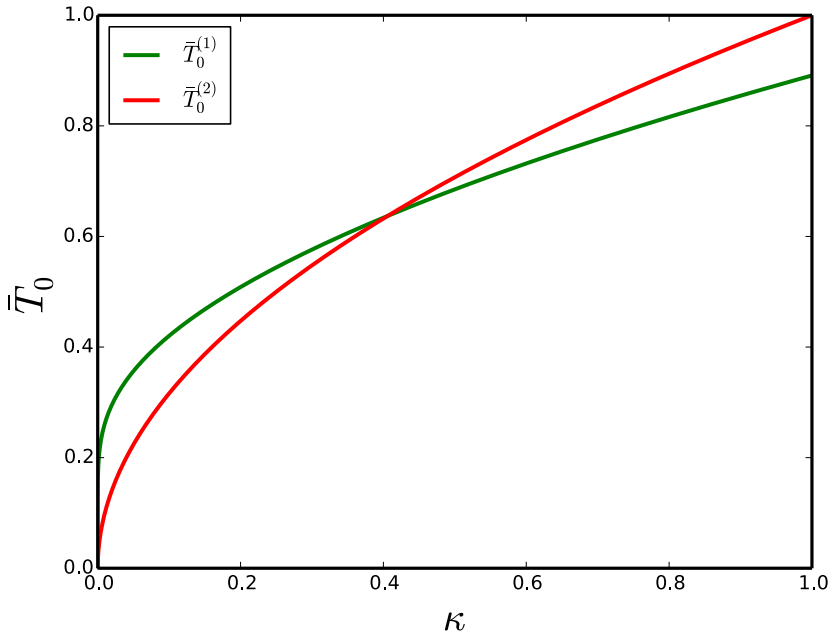

Figure 6.13: Zero magnetic field crossover temperatures plotted against κ. The functions increase rapidly as κ varies between 0 and 1. $\bar{T}_0 = \pi T_0^{(1,2)}/Ds$

$$T_0^{(1)} = \frac{\Delta U}{S(U_{\text{min}})} = \frac{\Delta U}{2B} = \frac{Ds}{4\,\text{arctanh}\left(\frac{1}{\sqrt{1+\kappa}}\right)}. \tag{6.101}$$

For the case of second-order transition, we have

$$T_0^{(2)} = \frac{1}{\beta_0^{(2)}} = \frac{Ds\sqrt{\kappa}}{\pi}. \tag{6.102}$$

Fig.(6.13) shows the plot of $T_0^{(1)}$ and $T_0^{(2)}$ against κ. The functions increase rapidly with an increase in κ and coincide at $\kappa = 0$ and $\kappa = 0.4$. At $\kappa = 0.4$, we obtain $T_0^{(1)} = 1.002T_0^{(2)}$, which is 95.1% of the crossover temperature obtained from the free energy. Thus, Eqn.(6.101) and Eqn.(6.102) underestimate the crossover temperature found in Fig.(6.11) by 4.9% . In the limit of very small κ, however, this value becomes accurate. With the use of experimental parameters[121, 134]: $s = 9/2$; $D = 0.75K$; $J = 0.12K$; $\kappa = 0.16$; we obtain $T_0^{(1)} = 0.51K$ and $T_0^{(2)} = 0.43K$. These temperatures are indicated in Fig.(6.12) and Fig.(6.9).

6.3.4 Analysis with a staggered magnetic field

In the preceding sections we lucidly studied the phase transition of the interacting dimer model at zero magnetic field. We will now consider the full Hamiltonian derived in Sec.(6.3.2). More interesting phenomena will be studied in this section. We will study the influence of the staggered magnetic field on the phase boundary, the crossover temperatures , and the free energy. These analyses will be based on the potential and the position dependent mass in Eqn.(6.61) and Eqn.(6.60). In Fig.(6.14) we have shown the plot of this potential for some values of the parameters. The potential has a maximum at

$$r_b = \ln\left(\frac{1+\alpha}{1-\alpha}\right), \tag{6.103}$$

and the height of the potential barrier is given by

$$\Delta U = U_{\text{max}} - U_{\text{min}} = 2D\tilde{s}^2\left(1-\alpha\right)^2. \tag{6.104}$$

6.3.4.1 Phase boundary with magnetic field

We will begin the analysis of this model by obtaining the criterion formula for the first-order phase transition using Eqn.(5.45). The derivatives in Eqn.(5.45) can be computed by using Eqn.(6.61), Eqn.(6.60) and Eqn.(6.103). The corresponding expres-

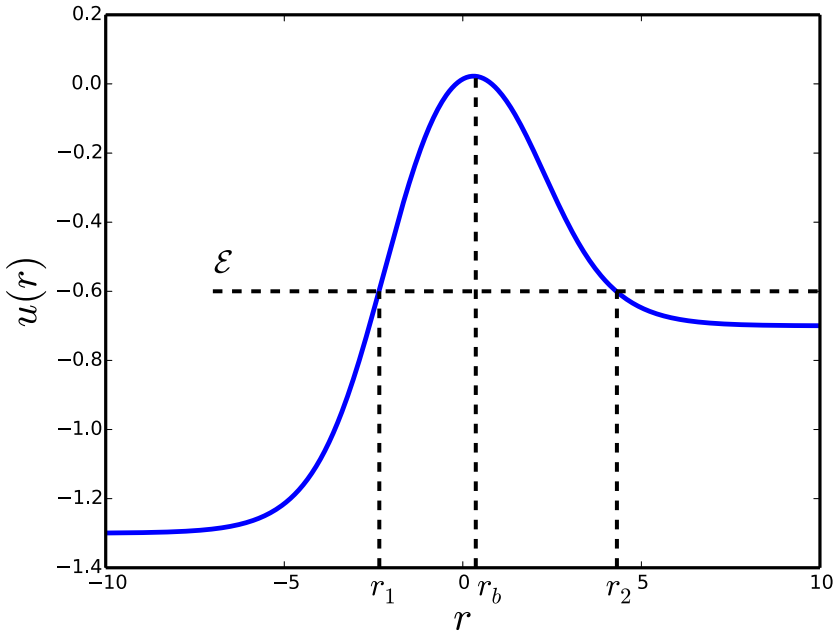

Figure 6.14: The plot of the effective potential and its inverse as a function of r for $\kappa = 0.6$ and $\alpha = 0.15$.

sions for the derivatives are given in Appendix(I). Substituting these expressions into Eqn.(5.45) we obtain

$$\mathcal{I} = \frac{\Delta U \kappa (1+\alpha)^2 [\kappa - 1 + \alpha^2 (1+2\kappa)]}{16(1-\alpha^2+\kappa)^2}. \tag{6.105}$$

Evidently, $\mathcal{I}$ is similar to the coefficient of Q^2 in Eqn.(6.94) for $\alpha = 0$. Consequently, the condition for the first-order phase transition is determined by $\mathcal{I} < 0$. The boundary between the first- and the second-order transitions requires $\mathcal{I} = 0$. The resulting expression at the phase boundary yields

$$\kappa_c = \frac{1-\alpha_c^2}{1+2\alpha_c^2}, \tag{6.106}$$

where the subscript represents the critical value at the phase boundary. At zero staggered magnetic field, the critical value at the phase boundary is $\kappa_c = 1$ and the first-

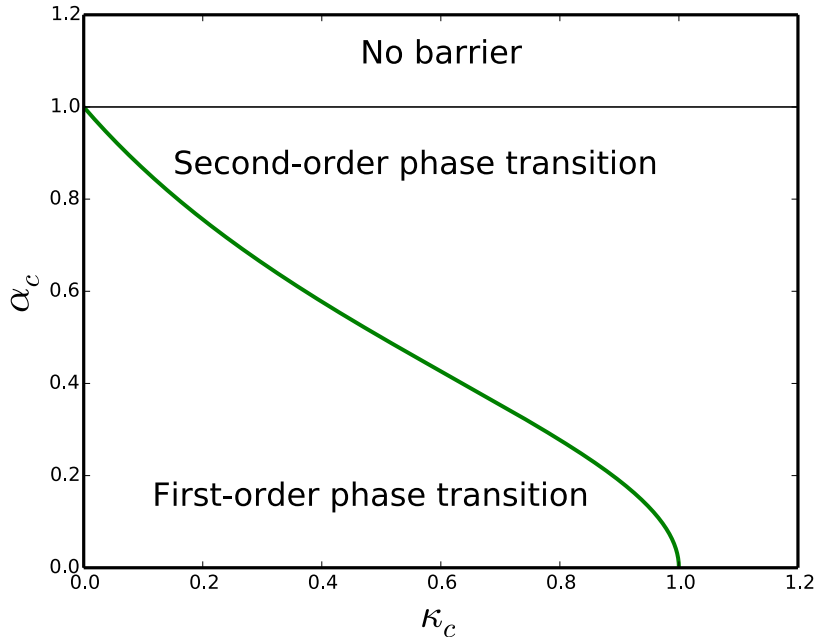

Figure 6.15: Colour online: The phase diagram of α_c vs. κ_c. In the regime of first-order phase transition, $\mathcal{I} < 0$; in the regime of second-order transition, $\mathcal{I} > 0$; of course, $\mathcal{I} = 0$ at the phase boundary, indicated by the green line.

order phase transition occurs in the regime $\kappa < 1$, which is consistent with the result of Sec.(6.3.3.4). In Fig.(6.15) we have shown the plot of α_c against κ_c; Indeed, α_c decreases as κ_c increases; at $\kappa_c = 0$ we have $\alpha_c = 1$, which gives no tunnelling since the individual z-components of the spins commute with the Hamiltonian. Physically, at this point, the potential energy becomes infinitely thick and the spins cannot tunnel.

6.3.4.2 Free energy with a magnetic field and Landau analogy

In the presence of a magnetic field, the periodic (thermon) instanton action is given by

$$\mathcal{S}_p = 2\int_{r_1}^{r_2} dr\sqrt{2\mu(r)\left(U(r)-\mathcal{E}\right)} + \beta(\mathcal{E}-U_{\text{min}}), \tag{6.107}$$

where r_1 and r_2 are the turning points in Fig.(6.14). In terms of the dimensionless energy quantity Q, this action together with Eqn.(6.61) and Eqn.(6.60) is given by

$$\mathcal{S}_p(Q) = 2\tilde{s}\sqrt{2}\int_{r_1}^{r_2} dr \frac{\sqrt{a - b\cosh r + c\sinh r}}{2 + \kappa(1 + \cosh r)} + \beta\Delta U(1 - Q), \tag{6.108}$$

where

$$a = 2\alpha^2 + \kappa - (2 + \kappa)(\alpha^2 - Q(1 - \alpha)^2); \tag{6.109}$$

$$b = \kappa(1 + \alpha^2 - Q(1 - \alpha)^2); \quad c = 2\kappa\alpha. \tag{6.110}$$

The turning points are determined from the solution of the equation:

$$a - b\cosh r + c\sinh r = 0, \tag{6.111}$$

which yields four turning points corresponding to the roots of the hyperbolic functions:

$$r_1 = -\operatorname{arccosh}\left(\frac{ab - c\sqrt{a^2 - b^2 + c^2}}{b^2 - c^2}\right), \tag{6.112}$$

$$r_2 = \operatorname{arccosh}\left(\frac{ab + c\sqrt{a^2 - b^2 + c^2}}{b^2 - c^2}\right), \tag{6.113}$$

$$r_3 = -\operatorname{arccosh}\left(\frac{ab + c\sqrt{a^2 - b^2 + c^2}}{b^2 - c^2}\right), \tag{6.114}$$

$$r_4 = \operatorname{arccosh}\left(\frac{ab - c\sqrt{a^2 - b^2 + c^2}}{b^2 - c^2}\right). \tag{6.115}$$

However, only the two turning points r_1 and r_2 labeled in Fig.(6.14) are relevant in the tunneling regime. At zero magnetic field $c = 0$, the potential becomes symmetric hence $r_1 = -r_2$. This action, however, cannot be integrated exactly either by periodic instanton method or otherwise. Thus, we have to resort to numerical analysis. The exact

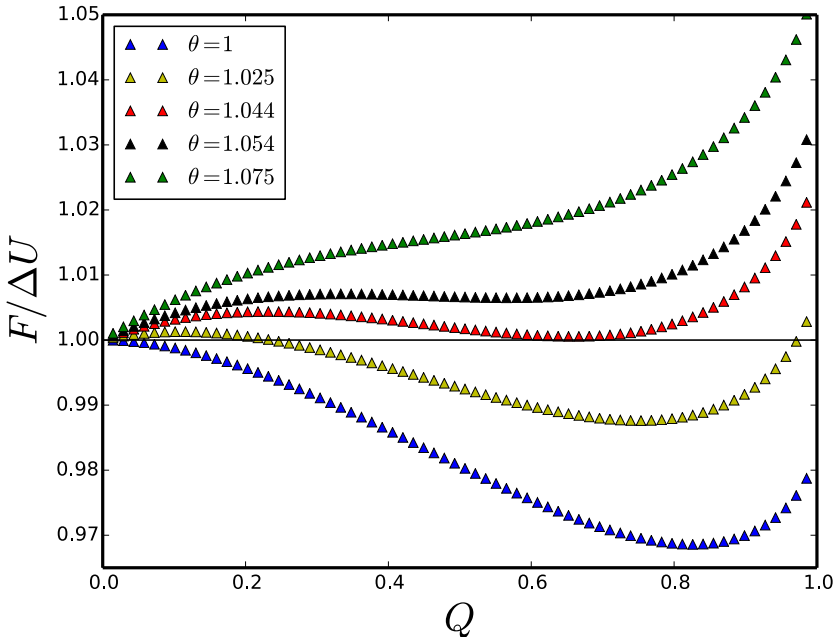

Figure 6.16: Colour online: The numerical plot of the free energy with $\kappa = 0.4$ and $\alpha = 0.15$. The phase transition from thermal to quantum regimes occurs at $\theta = 1.044$, which is smaller than that of zero magnetic field, $\theta = 1.054$.

free energy can then be written as

$$\frac{F}{\Delta U} = 1 - Q + \frac{\theta}{\pi(1-\alpha)^2}\sqrt{2\kappa(1-\alpha^2)}\int_{r_1}^{r_2} dr \frac{\sqrt{a - b\cosh r + c\sinh r}}{2 + \kappa(1+\cosh r)}, \quad (6.116)$$

where the barrier height ΔU is given in Eqn.(6.104), $\theta = \beta^{-1}/T_0^{(2)} = T/T_0^{(2)}$, and $T_0^{(2)}$ is given in Eqn.(6.122). Fig.(6.16) shows the numerical plot of this free energy with $\kappa = 0.4$ and $\alpha = 0.15$. The minimum of the free energy remains at ΔU for the top three curves, however, the quantum-classical phase transition (where two minima of a curve have the same free energy) has been shifted down to $T_0^{(1)} = 1.044T_0^{(2)}$ due the presence of a small magnetic field. Thus, the presence of a staggered magnetic field in this model decreases the crossover temperatures. This can also be confirmed from the plot of the period of oscillation in Fig.(6.17) and the actions in Fig.(6.18). The phase transition can also be investigated by analogy with Landau's theory of phase transition

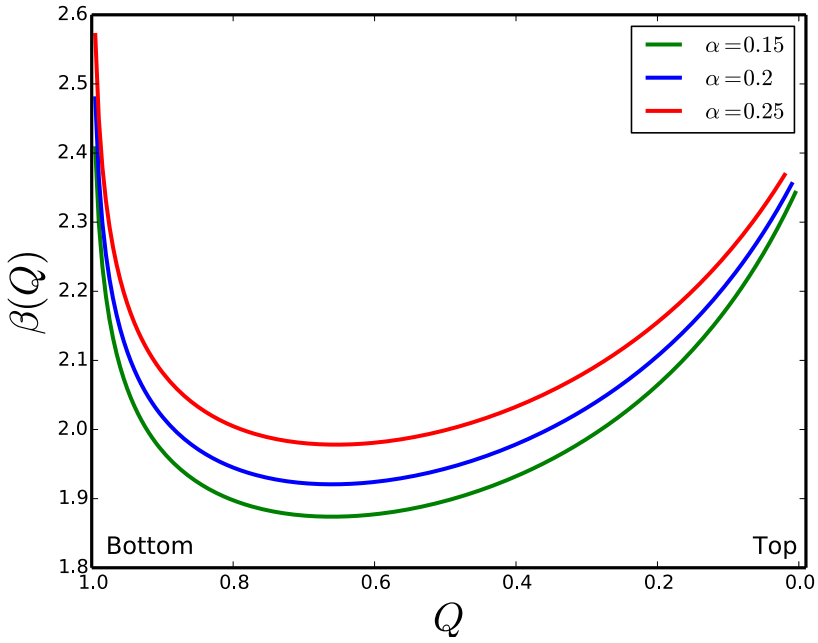

Figure 6.17: Colour online: The period of oscillation vs. Q with; $s = 9/2$; $D = 0.75$; $\kappa = 0.16$ (first-order transition) and different values of α.

as we did in the case of zero magnetic field. Since the expression for the action cannot be obtained exactly in the whole range of energy as we did previously, we need some sort of approximation such as series expansion with a small quantity. Indeed such a small quantity exist — that is the dimensionless energy quantity Q. The general expansion of the action near the top of the barrier r_b, with $Q \ll 1$, is given by [51]

$$\mathcal{S}_p(Q) = \pi\sqrt{\frac{2\mu(r_b)}{U''(r_b)}}\Delta U[Q + bQ^2 + O(Q^3)] + \beta\Delta U(1-Q), \tag{6.117}$$

where b is given by

$$b = \frac{\Delta U}{16UU''}\left[\frac{12U''''U'' + 15(U''')^2}{2(U'')^2} + 3\left(\frac{\mu'}{\mu}\right)\left(\frac{U'''}{U''}\right) + \left(\frac{\mu''}{\mu}\right) - \frac{1}{2}\left(\frac{\mu'}{\mu}\right)^2\right]_{r=r_b}, \tag{6.118}$$

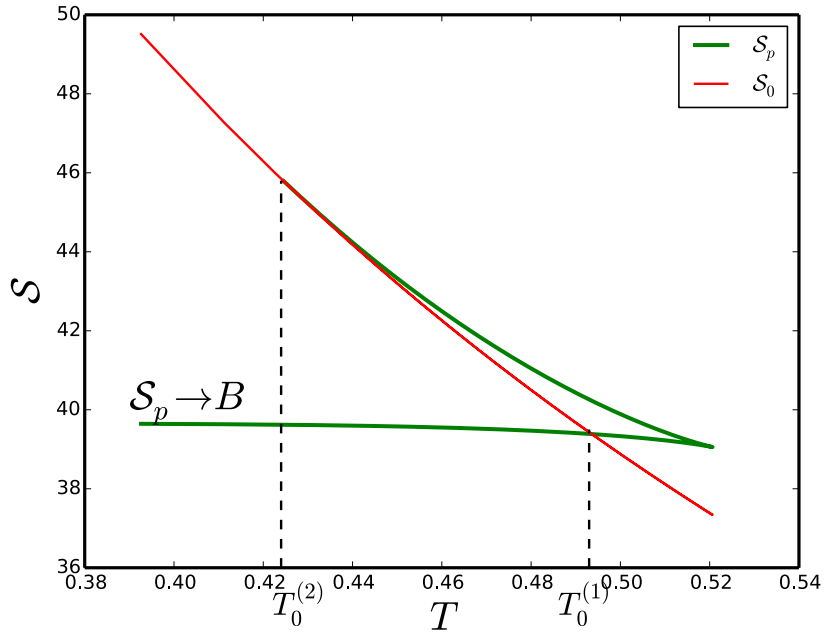

Figure 6.18: Dependence of the thermon and thermodynanmic actions on temperature, with the experimental paramters[121, 134]: $s = 9/2$; $D = 0.75$; $\kappa = 0.16$; $\alpha = 0.2$ (first-order transition).

and $U''(r_b) = -D\tilde{s}^2 u''(r_b)/2!$; $U'''(r_b) = D\tilde{s}^2 u'''(r_b)/3!$; $U''''(r_b) = D\tilde{s}^2 u''''(r_b)/4!$. We can now write down the expression for the free energy as a series in Q:

$$F = \Delta U(1 + (\theta - 1)Q + b\theta Q^2 + \cdots). \tag{6.119}$$

We are mostly interested in the coefficient of Q^2. The expression for b is found to be:

$$b = \frac{\kappa - 1 + \alpha^2(1 + 2\kappa)}{8\kappa(1 + \alpha)^2}. \tag{6.120}$$

At the phase boundary $b = 0$, which recovers Eqn.(6.106) and the exact coefficient of Q^2 in Eqn.(6.94) when $\alpha = 0$.

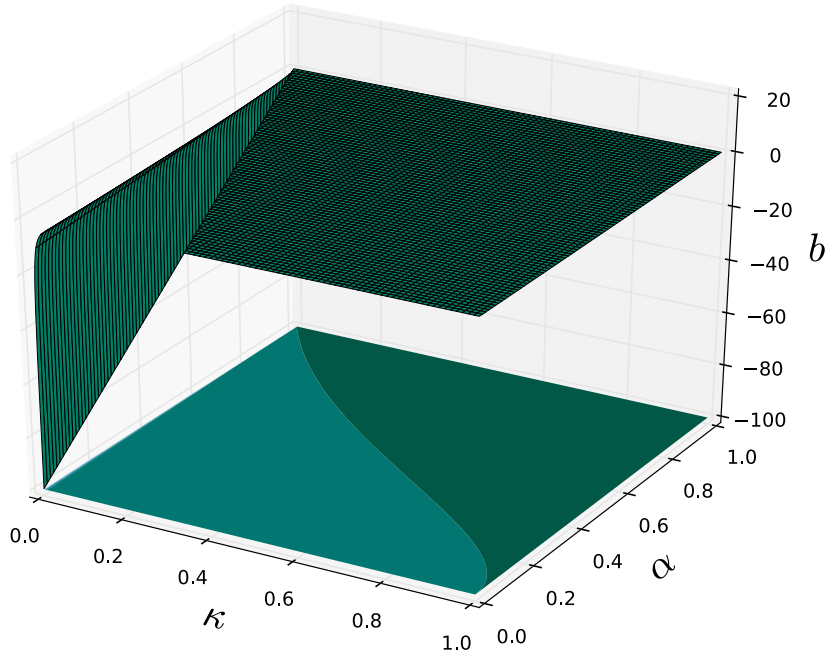

Figure 6.19: Three dimensional plot of the Landau coefficient b. Region of first-order phase transition $b < 0$. Second-order transition $b > 0$. The phase boundary $b = 0$ is placed on the bottom plane for proper view of the top plane.

6.3.4.3 Crossover temperatures in the presence of a magnetic field

The first-order crossover temperature can be estimated numerically from Eqn.(6.104) and Eqn.(6.108), with $Q \to 1$:

$$T_0^{(1)} = \frac{\Delta U}{S(Q \to 1)} = \frac{D\tilde{s}(1-\alpha^2)}{\sqrt{2}\int_{r_1}^{r_2} dr \frac{\sqrt{a-b\cosh r + c\sinh r}}{2+\kappa(1+\cosh r)}}. \tag{6.121}$$

In the case of second-order transition the crossover temperature can be estimated exactly from Eqn.(1.2):

$$T_0^{(2)} = \frac{\omega_b}{2\pi} = \frac{D\tilde{s}}{\pi}\sqrt{\kappa(1-\alpha^2)}. \tag{6.122}$$

Numerically, we find that $T_0^{(1)}/T_0^{(2)} \approx 0.989$ at $\kappa = 0.4$ and $\alpha = 0.15$, which is 94.7% of the value we obtained from the free energy. Thus, Eqn.(6.121) and Eqn.(6.122) underestimate the crossover temperatures by 5.3%. Plugging Eqn.(6.106) into Eqn.(6.122) we obtain the second-order crossover temperature at the phase boundary:

$$T_0^{(c)} = \frac{D\tilde{s}}{\pi}\frac{(1-\alpha_c^2)}{\sqrt{1+2\alpha_c^2}} = \frac{D\tilde{s}\kappa_c}{\pi}\left(\frac{3}{1+2\kappa_c}\right)^{\frac{1}{2}}. \tag{6.123}$$

The plot of $T_0^{(c)}$ vs. α_c is shown in Fig.(6.20) for the first- and the second-order

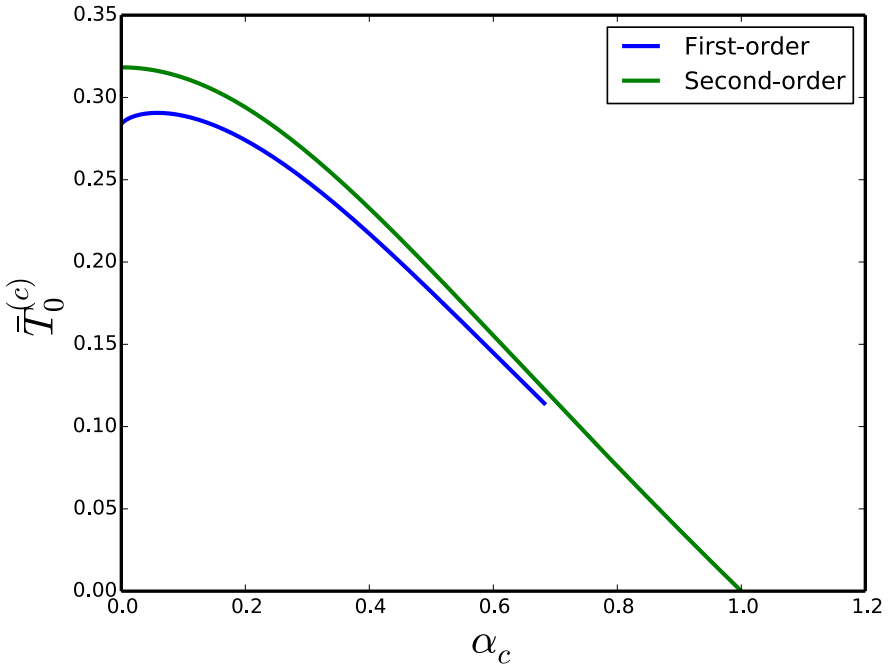

Figure 6.20: The crossover temperatures at the phase boundary between first- and second-order transitions plotted against α_c, where $\bar{T}_0^{(c)} = T_0^{(c)}/D\tilde{s}$.

phase transitions. For $[Mn_4]_2$ dimer, the parameters are: $s = 9/2$, $D = 0.75K$, and $J = 0.12K$[121, 134], which implies that $\kappa = 0.16$, yielding $\alpha_c = 0.80$ at the phase boundary. Clearly this value is not in the regime of first-order phase transition as shown in Fig.(6.20). One finds that the value of the second-order crossover temperature at the

phase boundary is $\bar{T}_0^{(c)} = 0.076 \Rightarrow T_0^{(c)} = 0.29K$, which is within the closed curve in Fig.(6.20), and much smaller than that of Fe_8 molecular cluster. Wernsdorfer *et al*[144] have experimentally obtained the Arrhenius plot of $[Mn_4]_2$ dimer. They showed that the relaxation rate is temperature-dependent above $0.3K$ with $\tau_0 = 3.8 \times 10^{-6}s$ and $\Delta U = 10.7K$ and below $0.3K$, the relaxation rate is temperature-independent with a relaxation rate of $8 \times 10^5 s$, indicating the quantum tunneling of the spins between the ground states .

6.4 Conclusion and Discussion

We have lucidly studied of the phase transition of the escape rate in large spin systems. For a biaxial ferromagnetic model with a magnetic field applied along the spin medium axis, we explicitly obtained the vacuum instanton trajectory and the corresponding vacuum instanton action. The crossover temperatures were obtained and we showed that the magnetic field has a great influence on the phase boundary between the first- and the second-order phase transitions. We explicitly showed via the free energy method that the magnetic field increases the crossover temperature from its zero magnetic field value. In the case of an antiferromagnetic exchange-coupled dimer in the presence of a staggered magnetic field, we derived the exact effective potential method of this model. The result of spin coherent state path integral at zero magnetic field for this dimer was shown to be consistent with the effective potential method. We obtained the exact thermon action, as well as the exact free energy at zero magnetic field. We lucidly presented the order of the phase transitions. For nonzero staggered magnetic field, we numerically solved for the thermon action, the free energy, and the crossover temperatures, and analyzed the order of phase transitions. These new results can be corroborated experimentally; we hope that this will be done as soon as possible.

6.5 Article for quantum-classical phase transition in ferromagnetic spin systems

The article below on quantum-classical phase transition in ferromagnetic spin systems is published in Journal of Magnetism and Magnetic materials. Reprinted from Ref.[105], copyright (2014), with permission from Elsevier. I conceived the idea of this paper. My supervisor (co-author) gave some indispensable technical advice. The originality, problem formulation, methodology, and results were obtained predominately by me and partly by my co-author.

UdeM-GPP-TH-13-229

Quantum-classical transition of the escape rate of a biaxial ferromagnetic spin with an external magnetic field.

S. A. Owerre and M. B. Paranjape
Groupe de physique des particules, Département de physique, Université de Montréal, C.P. 6128, succ. centre-ville, Montréal, Québec, Canada, H3C 3J7

Abstract

We study the model of a biaxial single ferromagnetic spin Hamiltonian with an external magnetic field applied along the medium axis. The phase transition of the escape rate is investigated. Two different but equivalent methods are implemented. Firstly, we derive the semi-classical description of the model which yields a potential and a coordinate dependent mass. Secondly, we employ the method of spin-particle mapping which yields a similar potential to that of semi-classical description but with a constant mass. The exact instanton trajectory and its corresponding action, which have not been reported in any literature is being derived. Also, the analytical expressions for the first- and second-order crossover temperatures at the phase boundary are derived. We show that the boundary between the first-and the second-order phase transitions is greatly influenced by the magnetic field.

PACS numbers: 75.45.+j, 75.10.Jm, 75.30.Gw, 03.65.Sq

Introduction- In recent years, the study of single ferromagnetic spin systems has been of considerable interest to condensed matter physicists. These systems have been pointed out[1,3] to be a good candidate for investigating first- and second-order phase transition of the quantum-classical escape rate. The quantum-classical escape rate transition takes place in the presence of a potential barrier. At very low temperature (close to zero), transitions occur by quantum tunnelling through the barrier and the rate is governed by $\Gamma \sim e^{-B}$, where B is the instanton (imaginary time solution of the classical equation of motion) action. At high temperatures, the particle has the possibility of hopping over the barrier (classical thermal activation), in this case transition is governed by $\Gamma \sim e^{-\frac{\Delta V}{T}}$, where ΔV is the energy barrier. At the critical point when these two transition rates are equal, there exits a crossover temperature (first-order transition) $T_0^{(1)}$ from quantum to thermal regime, it is estimated as $T_0^{(1)} = \Delta V/B$. In principle these transitions are greatly influenced by the anisotropy constants and the external magnetic fields. The second-order phase transition occurs for particles in a cubic or quartic parabolic potential, it take place at the temperature $T_0^{(2)}$, below $T_0^{(2)}$ one has the phenomenon of thermally assisted tunnelling and above $T_0^{(2)}$ transition occur due to thermal activation to the top of the potential barrier[1,3]. The order of these transitions can also be determined from the period of oscillation $\tau(E)$ near the bottom of the inverted potential. Monotonically increasing $\tau(E)$ with the amplitude of oscillation gives a second-order transition while nonmonotonic behaviour of $\tau(E)$ (that is a mininmum in the $\tau(E)$ vs E curve, E being the energy of the particle) gives a first-order transition[1].

The model of a uniaxial single ferromagnetic spin with a transverse magnetic field, which is believed to describe the molecualr magnet $MnAc_{12}$ was considered by Garanin and Chudnovsky[1], the Hamiltonian is of the form $\hat{H} = -D\hat{\mathcal{S}}_z^2 - h_x\hat{\mathcal{S}}_x$, using the spin-particle mapping version of this Hamiltonian[5–7], they showed that the transition from thermal to quantum regime is of first-order in the regime $h_x < sD/2$ and of second-order in the regime $sD/2 < h_x < 2sD$. For other single-molecule magnets such as Fe_8, a biaxial ferromagnetic spin model is a good approximation. In this case, Lee *et al*[13] considered the model $\hat{H} = K(\hat{\mathcal{S}}_z^2 + \lambda\hat{\mathcal{S}}_y^2) - 2\mu_B h_y\hat{\mathcal{S}}_y$, using spin coherent state path integral, they obtained a potential and a coordinate dependent mass from which they showed that the boundary between the first and the second-order transitions sets in at $\lambda = 0.5$ for $h_y = 0$ while the order of the transitions is greatly influenced by the magnetic field and the anisotropy constants for $h_y \neq 0$. Zhang *et al*[14] studied the model $\hat{H} = K_1\hat{\mathcal{S}}_z^2 + K_2\hat{\mathcal{S}}_y^2$ using spin-particle mapping and periodic instanton method. The phase boundary between the first- and the second-order transitions was shown to occur at $K_2 = 0.5K_1$. The model with z-easy axis in an applied field has been also studied by numerical and perturbative methods[2]. In this paper, we study a biaxial spin system with an external magnetic field applied along the medium axis using spin-coherent state path integral and the formalism of spin-particle mapping. Unlike other models with an external magnetic field[4,12,14], the spin-particle mapping yields a simplified potential and a constant mass which allows us to solve for the exact instanton trajectory and its corresponding action in the presence of a magnetic field. We also present the analytical results of the crossover temperatures for the first- and the second-order transitions at the phase boundary.

Spin model and spin coherent state path integral- Consider the Hamiltonian of a biaxial ferromagnetic spin (single-molecule magnet) in an external magnetic field

$$\hat{H} = \mathcal{D}\hat{\mathcal{S}}_z^2 + \mathcal{E}\hat{\mathcal{S}}_x^2 - h_x\hat{\mathcal{S}}_x \tag{1}$$

where $\mathcal{D} \gg \mathcal{E} > 0$, and $\mathcal{S}_i, i = x, y, z$ is the components of the spin. This model possesses an easy XOY plane with an easy-axis along the y-direction and an external magnetic field along the x-axis. At zero magnetic field, there are two classical degenerate ground states corresponding to the minima of the energy located at $\pm y$, these ground states remain degenerate for $h_x \neq 0$ in the easy XY plane. The semi-classical form of the quantum Hamiltonian can be derived using spin coherent state path integral. In the coordinate dependent form, the spin-coherent-state is defined by[15,16]

$$\mid \hat{\mathbf{n}}\rangle = \left(\cos\frac{1}{2}\theta\right)^{2s} \exp\left\{\tan\left(\frac{1}{2}\theta\right) e^{i\phi}\hat{\mathcal{S}}^{-}\right\} \mid s, s\rangle \quad (2)$$

where $\hat{\mathbf{n}} = s(\sin\theta\cos\phi, \sin\theta\sin\phi, \cos\theta)$ is the unit vector parametrizing the spin on a two-sphere S^2. The overlap between two coherent states is found to be

$$\langle\hat{\mathbf{n}}'|\hat{\mathbf{n}}\rangle = \left[\cos\frac{1}{2}\theta\cos\frac{1}{2}\theta' + \sin\frac{1}{2}\theta\sin\frac{1}{2}\theta' e^{-i\Delta\phi}\right]^{2s} \quad (3)$$

where $\Delta\phi = \phi' - \phi$. The expectation value of the spin operator in the large s limit is approximated as $\langle\hat{\mathbf{n}}'|\hat{\boldsymbol{S}}|\hat{\mathbf{n}}\rangle \approx s\left[\hat{\mathbf{n}} + O\left(\sqrt{s}\right)\right]\langle\hat{\mathbf{n}}'|\hat{\mathbf{n}}\rangle$. For infinitesimal separated angle, $\Delta\theta = \theta' - \theta$, Eq.(3) reduces to

$$\langle\hat{\mathbf{n}}'|\hat{\mathbf{n}}\rangle \approx 1 - is\Delta\phi(1 - \cos\theta). \quad (4)$$

These states satisfy the overcompletness relation (resolution of identity)

$$\mathcal{N}\int d\phi\, d(\cos\theta) \mid \hat{\mathbf{n}}\rangle\langle\hat{\mathbf{n}} \mid = \hat{I}. \quad (5)$$

Using these equations, the transition amplitude is easily obtained as

$$\langle\hat{\mathbf{n}}_f|e^{-\beta\hat{H}}|\hat{\mathbf{n}}_i\rangle = \int \mathscr{D}\phi\mathscr{D}(\cos\theta)e^{-S} \quad (6)$$

The Euclidean action ($t \to -i\tau$) is given by $S = \int_{-\beta/2}^{\beta/2} d\tau\, \mathcal{L}$, with

$$\mathcal{L} = is\dot{\phi}(1 - \cos\theta) + V(\theta, \phi) \quad (7)$$

$$V(\theta, \phi) = \mathcal{D}s^2\cos^2\theta + \mathcal{E}s^2\sin^2\theta\cos^2\phi - sh_x\sin\theta\cos\phi \quad (8)$$

These two equations (7) and (8) describe the semi-classical dynamics of the spin on S^2. Two degenerate minima exit for $h_x < h_c = 2\mathcal{E}s$, which are located at $\theta = \pi/2$: $\phi = 2\pi n \pm \arccos\alpha_x$, where $\alpha_x = h_x/h_c$, $n \in \mathbb{Z}$, and the of the maximum is at $\theta = \pi/2$: $\phi = n\pi$ with the height of the barrier ($n = 0$) given by

$$\Delta V = \mathcal{E}s^2(1 - \alpha_x)^2 \quad (9)$$

Taking into consideration the fact that $\mathcal{D} \gg \mathcal{E}$, the deviation away from the easy plane is very small, thus one can expand $\theta = \pi/2 - \eta$, where $\eta \ll 1$. Integration over the fluctuation η in Eq.(6) yields an effective theory describe by

$$\mathcal{L}_{\text{eff}} = is\dot{\phi} + \frac{1}{2}m(\phi)\dot{\phi}^2 + V(\phi) \quad (10)$$

where

$$V(\phi) = \mathcal{E}s^2(\cos\phi - \alpha_x)^2 \quad (11)$$

and

$$m(\phi) = \frac{1}{2\mathcal{D}(1 - \kappa\cos^2\phi + 2\alpha_x\kappa\cos\phi)} \quad (12)$$

with $\kappa = \mathcal{E}/\mathcal{D}$. An additional constant of the form $\mathcal{E}s^2\alpha_x^2$ has been added to the potential for convenience. The first term in the effective Lagrangian is a total derivative which does not contribute to the classical equation of motion, however, it has a significant effect in the quantum transition amplitude, producing a quantum phase interference in spin systems[10,11]. The two classical degenerate minima which corresponds to $\phi = 2\pi n \pm \arccos\alpha_x$ are separated by a small barrier at $\phi = 0$ and a large barrier at $\phi = \pi$. The phase transition of the escape rate of this model can be investigated using the potential Eq.(11) and the mass Eq.(12)[13], in this paper, however, we will study this transition via the method of mapping a spin system onto a quantum mechanical particle in a potential field. A classical trajectory (instanton) exits for zero magnetic field, in this case the classical equation of motion

$$m(\bar{\phi})\ddot{\bar{\phi}} + \frac{1}{2}m(\bar{\phi})'\dot{\bar{\phi}}^2 = \frac{dV}{d\bar{\phi}} \quad (13)$$

integrates to

$$\sin\bar{\phi} = \pm\frac{\sqrt{(1-\kappa)}\tanh(\omega\tau)}{\sqrt{1 - \kappa\tanh^2(\omega\tau)}} \quad (14)$$

where $\omega = 2s\sqrt{\mathcal{E}\mathcal{D}}$ and the upper and lower signs are for instanton and anti-instanton respectively. The corresponding action for this trajectory yields[10,17] $S_0 = B \pm is\pi$,

$$B = s\ln\left(\frac{1 + \sqrt{\kappa}}{1 - \sqrt{\kappa}}\right) \quad (15)$$

For small anisotropy parameters, $\kappa \ll 1$, the coordinate dependent mass can be approximated as $m \approx 1/2\mathcal{D}$, the approximate instanton trajectory in this limit yields

$$\sin\bar{\phi} = \pm\frac{2\sqrt{\frac{1-\alpha_x}{1+\alpha_x}}\tanh(\omega\tau)}{[1 + \frac{1-\alpha_x}{1+\alpha_x}\tanh^2(\omega\tau)]} \quad (16)$$

where $\omega = s\sqrt{\mathcal{E}\mathcal{D}(1-\alpha_x^2)}$ and the corresponding action is

$$B = 2s\sqrt{\kappa}[\sqrt{1-\alpha_x^2} \pm \alpha_x \arcsin(\sqrt{1-\alpha_x^2})] \tag{17}$$

The upper and the lower signs in the action correspond to the large and small barriers respectively while that in the trajectory is for instanton and anti-instanton. At zero magnetic field, the instanton interpolates between the classical degenerate minima $\bar{\phi} = \pm\pi/2$ at $\tau = \pm\infty$. For coordinate dependent mass the classical trajectory can be integrated in terms of the Jacobi elliptic functions. This solution will be presented in the next section using a simpler method.

Particle mapping - In this section, we will consider the formalism of mapping a spin system to a quantum-mechanical particle in a potential field[5]. In this formalism one introduces a nonnormalized spin coherent state, the action of the spin operators on this state yields the following expressions[6,7]

$$\hat{\mathcal{S}}_x = s\cos\phi - \sin\phi\frac{d}{d\phi},\ \hat{\mathcal{S}}_y = s\sin\phi + \cos\phi\frac{d}{d\phi}$$
$$\hat{\mathcal{S}}_z = -i\frac{d}{d\phi} \tag{18}$$

The Shrödinger equation can be written as

$$\hat{H}\Phi(\phi) = E\Phi(\phi) \tag{19}$$

where the generating function is defined as

$$\Phi(\phi) = \sum_{m=-s}^{s} \frac{\mathcal{C}_m}{\sqrt{(s-m)!(s+m)!}} e^{im\phi} \tag{20}$$

with periodic boundary condition $\Phi(\phi+2\pi) = e^{2i\pi s}\Phi(\phi)$. Using Eqns.(1), (18) and (19), the differential equation for $\Phi(\phi)$ yields

$$-\mathcal{D}(1+\kappa\sin^2\phi)\frac{d^2\Phi}{d\phi} - (\mathcal{E}(s-\frac{1}{2})\sin 2\phi - h_x\sin\phi)\frac{d\Phi}{d\phi}$$
$$+ (\mathcal{E}s^2\cos^2\phi + \mathcal{E}s\sin^2\phi - h_x s\cos\phi)\Phi = E\Phi \tag{21}$$

Now let's introduce the incomplete elliptic integral of first kind

$$x = F(\phi,\lambda) = \int_0^{\phi} d\varphi \frac{1}{\sqrt{1-\lambda^2\sin^2\varphi}} \tag{22}$$

with amplitude ϕ and modulus $\lambda^2 = \kappa$. The trigonometric functions are related to the Jacobi elliptic functions by $\mathrm{sn}(x,\lambda) = \sin\phi$, $\mathrm{cn}(x,\lambda) = \cos\phi$ and $\mathrm{dn}(x,\lambda) = \sqrt{1-\lambda^2\,\mathrm{sn}^2(x,\lambda)}$. In this new variable, Eq.(21) transforms into a Schrödinger equation $H\Psi(x) = E\Psi(x)$ with

$$H = -\frac{1}{2m}\frac{d^2}{dx^2} + V(x), \quad m = \frac{1}{2\mathcal{D}} \tag{23}$$

The effective potential is given by

$$V(x) = \frac{\mathcal{E}\tilde{s}^2[\mathrm{cn}(x,\lambda) - \alpha_x]^2}{\mathrm{dn}^2(x,\lambda)} \tag{24}$$

$$\Psi(x) = \frac{\Phi(\phi(x))}{[\mathrm{dn}(x,\lambda)]^s}\exp\Bigg[-\tilde{s}\alpha_x\sqrt{\frac{\kappa}{(1-\kappa)}}$$
$$\mathrm{arccot}\left(\sqrt{\frac{\kappa}{(1-\kappa)}}\,\mathrm{cn}(x,\lambda)\right)\Bigg] \tag{25}$$

where $\tilde{s} = (s+\frac{1}{2})$ and $\alpha_x = h_x/2\mathcal{E}\tilde{s}$. In order to arrive at this potential we have used the large s limit $s(s+1) \sim \tilde{s}^2$ and shifted the minimum energy to zero by adding a constant of the form $\mathcal{E}\tilde{s}^2\alpha_x^2$. Unlike the spin coherent state version, the mass of the particle is constant in this case which appears to be the approximate form of Eq.(12) in the limit of small anisotropy parameters, but the potentials Eq.(11) and Eq.(24) are of similar form, infact they are equal when $\lambda \to 0$ except for the quantum renormalization $\tilde{s}$. At zero magnetic field the potential Eq.(24) reduces to a well-known potential studied by periodic instanton method[14]. In many models with an external magnetic field[4,12,14], the resulting effective potential from spin-particle mapping is always too complicated for one to solve for the instanton trajectory, however in this case the effective potential is in a compact form, allowing us to find the exact classical trajectory (see the next section).

Phase transition and instanton solution- We will now study the phase transition of the escape rate of this model and the instanton solution in the presence of a magnetic field. The potential Eq.(24) has minima at $x_0 = 4n\mathcal{K}(\lambda) \pm \mathrm{cn}^{-1}(\alpha_x)$ and maxima at $x_{sb} = \pm 4n\mathcal{K}(\lambda)$ for small barrier and at $x_{lb} = \pm 2(2n+1)\mathcal{K}(\lambda)$ for large barrier, where $\mathcal{K}(\lambda)$ is the complete elliptic function of first kind i.e $F(\frac{\pi}{2},\lambda)$. The heights of the potential for small and large barriers are given by

$$\Delta V_{sb} = \mathcal{E}\tilde{s}^2(1-\alpha_x)^2$$
$$\Delta V_{lb} = \mathcal{E}\tilde{s}^2(1+\alpha_x)^2 \tag{26}$$

The Euclidean Lagrangian corresponding to the particle Hamiltonian is

$$\mathcal{L} = \frac{1}{2}m\dot{x}^2 + V(x) \tag{27}$$

It follows that the classical equation of motion is

$$m\ddot{\bar{x}} = \frac{dV}{d\bar{x}} \tag{28}$$

which corresponds to the motion of the particle in the inverted potential $-V(x)$. Upon integration, Eq.(28) gives the instanton solution

$$\mathrm{sn}(\bar{x},\lambda) = \pm\frac{2\sqrt{\frac{1-\alpha_x}{1+\alpha_x}}\tanh(\omega\tau)}{[1+\frac{1-\alpha_x}{1+\alpha_x}\tanh^2(\omega\tau)]} \tag{29}$$

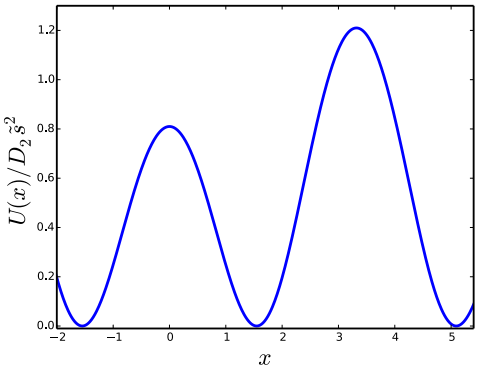

FIG. 1: The plot of the effective potential, Eq.(24) for $\alpha_x = 0.1$, $\kappa = 0.2$, where $v(x) = V(x)/\mathcal{E}\tilde{s}^2$.

where $\omega = \tilde{s}\sqrt{\mathcal{E}\mathcal{D}(1-\alpha_x^2)}$. This trajectory has not been reported in any literature. It is the exact classical trajectory in the presence of an external magnetic field. The instanton (upper sign) interpolates from the left minimum $\bar{x}(\tau) = -\,\mathrm{sn}^{-1}(\sqrt{1-\alpha_x^2})$ at $\tau = -\infty$ to the center of the barrier $\bar{x}(\tau) = 0$ at $\tau = 0$ and reaches the right minimum $\bar{x}(\tau) = \mathrm{sn}^{-1}(\sqrt{1-\alpha_x^2})$ at $\tau = \infty$. At zero magnetic field, Eq.(29) is equivalent to the well-known instanton solution[8], which is equivalent to Eq.(14). It is noted that this trajectory is the same as Eqn.(16) except that the trigonometric sine function is being replaced by the Jacobi elliptic sine function and $s \to \tilde{s}$, however, in the limit $\lambda \to 0$, both solutions are the same, since the potentials Eqns.(11) and (24) and the masses Eqn.(12) and Eqn.(23) are the same in this limit (the Jacobi elliptic functions becomes the trigonometric functions). The action for the trajectory, Eq.(29) yields

$$B = \tilde{s}\Bigg[\ln\left(\frac{1+\sqrt{\kappa(1-\alpha_x^2)}}{1-\sqrt{\kappa(1-\alpha_x^2)}}\right) \pm 2\alpha_x\sqrt{\frac{\kappa}{1-\kappa}}\arctan\left(\frac{\sqrt{(1-\kappa)(1-\alpha_x^2)}}{\alpha_x}\right)\Bigg] \tag{30}$$

When $\alpha_x = \pm 1$, there is no large and small barriers, the trajectory and its action reduce to $\bar{x}(\tau) = 0 = B$, hence there is no tunnelling. It is noted that this action reduces to Eq.(17) in the limit $\kappa \ll 1$ and to Eq.(15) when $\alpha_x = 0$ except that s is being replaced by $\tilde{s}$. At nonzero energy (finite temperature), the particle has the possibility of hopping over the potential barrier (thermal activation), the escape rate (transition amplitude) of the particle can be either first- or second-order depending on the shape of the potential. In order to investigate the analogy of this transition to Landau's theory of phase transition, consider the the escape rate of a particle at finite temperature through a potential barrier in the quasiclassical approximation[3,10]

$$\Gamma \sim \int dE\, \mathcal{W}(E) e^{-(E-E_{\min})/T} \tag{31}$$

where $\mathcal{W}(E)$ is the tunnelling probability of a particle at an energy E, and $E_{\min}$ is the energy at bottom of the potential. The tunnelling probability in imaginary time is given as $\mathcal{W}(E) \sim e^{-S(E)}$, therefore we have

$$\Gamma \sim e^{-F_{\min}/T} \tag{32}$$

where $F_{\min}$ is the minimum of the free energy $F \equiv E + TS(E) - E_{\min}$ with respect to E. The imaginary time action is expressed as

$$S(E) = 2\sqrt{2m}\int_{-x(E)}^{x(E)} dx\sqrt{V(x)-E} \tag{33}$$

where $\pm x(E)$ are the turning point for the particle with energy $-E$ in an inverted potential. Introducing a dimensionless quantity $Q = (V_{\max} - E)/(V_{\max} - V_{\min})$ where $V_{\max}(V_{\min})$ corresponds to the top (bottom) of the potential, the expansion of the imaginary time action around x_b gives[4]

$$S(E) = \frac{2\pi\Delta V}{\omega_0}[Q^2 + bQ^2 + O(Q^3)] \tag{34}$$

where

$$b = \frac{\Delta V}{48(V''(x))^3}[5(V'''(x))^2 - 3V''''(x)V''(x)]_{x=x_b}$$

and $\omega_0^2 = -V''(x_b)/m > 0$ is the frequency of oscillation at the bottom of the inverted potential, x_b corresponds to the maximum of the potential.

By the analogy with the Landau theory of phase transition, the phase boundary between the first- and second-order transition (see Fig.(1)) is obtained by setting the coefficient of Q^2 to zero i.e $b = 0$. Using the maximum of the small and large barriers of the potential Eq.(24) at x_{sb} and x_{lb} we obtain

$$b_{sb} = (\kappa - \kappa_{sb}^{+}(\alpha_x))(\kappa - \kappa_{sb}^{-}(\alpha_x)) \tag{35}$$

$$b_{lb} = (\kappa - \kappa_{lb}^{+}(\alpha_x))(\kappa - \kappa_{lb}^{-}(\alpha_x)) \tag{36}$$

where

$$\kappa_{sb}^{\pm}(\alpha_x) = \frac{3 - 4\alpha_x + \alpha_x^2 \pm (1-\alpha_x)\sqrt{1-4\alpha_x+\alpha_x^2}}{4(1-2\alpha_x+\alpha_x^2)} \tag{37}$$

$$\kappa_{lb}^{\pm}(\alpha_x) = \frac{3 + 4\alpha_x + \alpha_x^2 \pm (1+\alpha_x)\sqrt{1+4\alpha_x+\alpha_x^2}}{4(1+2\alpha_x+\alpha_x^2)} \tag{38}$$

Thus by setting $b = 0$ we obtain the four solution in Eqns.(37) and(38). At $\alpha_x = 0$, the critical values at the phase boundary are $\kappa_c = 1$ or $\frac{1}{2}$ for the plus or the minus signs respectively[4,9,14]. Expanding for small field $\alpha_x \ll 1$, we obtain $\kappa_{sb/lb}^{+} \approx 1 \pm \frac{\alpha_x}{4}$ and $\kappa_{sb/lb}^{-} \approx \frac{1}{2}(1 \pm \frac{3}{2}\alpha_x)$, where the plus and minus signs correspond to the small and large barriers respectively. The phase diagrams of Eqns.(37) and(38) are shown in

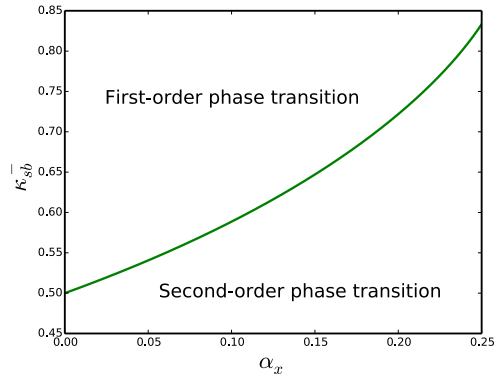

(a)

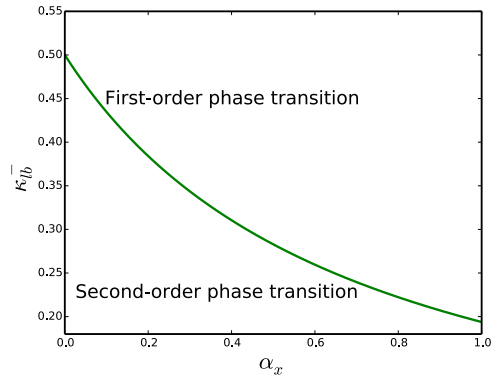

(b)

FIG. 2: The phase diagram κ^{-} vs α_x at the phase boundary for small barrier (a) and large barrier (b).

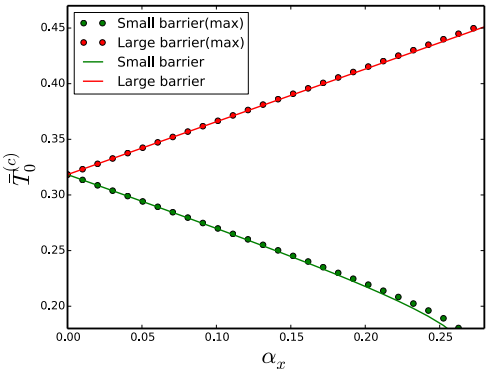

(a)

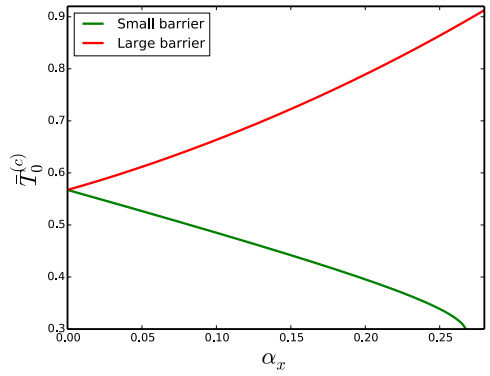

(b)

FIG. 3: Colour online: Dependence of the crossover temperatures on the magnetic field at the phase boundary: (a) Second-order (solid line) and its maximum (dashed line) for the small and large barrier, (b) First-order for the small and the large barrier. These graphs are plotted with $T_0^{(c)} = T_0^{(c)}/\mathcal{E}\tilde{s}$.

Fig.(2), with the value κ^{-} increasing with increasing magnetic field for small barrier while it decreases with increasing magnetic field for large barrier, the first-order phase transition occurs in the regime $\kappa^{-}_{sb/lb} > 1/2$ in both cases. The crossover temperature for the first-order transition is estimated as $T_0^{(1)} = \Delta V/B$ which is easily obtained from Eqns.(26) and (30). Expanding for $\alpha_x \ll 1$ at the phase boundary (with the expressions for $\kappa^{-}_{sb/lb}(\alpha_x)$), we obtain the crossover temperatures as $T_0^{(c)} \approx \mathcal{E}\tilde{s}/(\ln[(3+2\sqrt{2})e^{\pm\frac{3\alpha_x}{\sqrt{2}}}])$, where the upper and lower signs correspond to small and large barrier respectively. Both temperatures coincide at $\alpha_x = 0 \Rightarrow \kappa^{-}_{sb/lb} = 1/2$ with $T_0^{(c)} = \mathcal{E}\tilde{s}/\ln(3+2\sqrt{2})$ as shown in Fig.(3(b)). In the case of second-order transition the crossover temperature is estimated as $T_0^{(2)} = \omega_0/2\pi$. This is easily obtained as

$$T_0^{(2)} = \frac{\mathcal{E}\tilde{s}\sqrt{(1\pm\alpha_x)}}{\pi}\left(\frac{1-(1\pm\alpha_x)\,\kappa}{\kappa}\right)^{1/2} \tag{39}$$

The maximum of this function occurs at $\alpha_x = \pm(1-2\kappa)/2\kappa$, with

$$T_0^{(\max)} = \frac{\mathcal{E}\tilde{s}}{2\pi\kappa} \tag{40}$$

where the upper and lower signs correspond to the large and small barriers respectively. Substituting the expressions for $\kappa^{-}_{sb/lb}(\alpha_x)$ into Eqns. (39) and (40) we obtain the temperatures at the phase boundary as shown in Fig.(3(a)). The critical temperature at the phase boundary decreases with increasing magnetic field for small barrier while for large barrier it increases with increasing magnetic field. In the regime of small field $\alpha_x \ll 1$, it behaves linearly as $T_0^{(c)} \approx \mathcal{E}\tilde{s}(1\pm\frac{3}{2}\alpha_x)/\pi$. Both barriers coincide at $\alpha_x = 0 \Rightarrow \kappa^{-}_{sb/lb} = 1/2$, with $T_0^{(c)} = \mathcal{E}\tilde{s}/\pi$ which is smaller than that of first-order.

Conclusions- In conclusion, we have investigated an effective particle Hamiltonian which corresponds exactly to a biaxial spin model. Using this Hamiltonian we studied the phase transition of the escape rate of a particle

at zero and nonzero temperatures. The analytical expressions for the instanton trajectories and the crossover temperatures were obtained. We showed that the boundary between the first-and second-order phase transition is greatly influenced by the magnetic field.

Acknowledgments- The authors would like to thank NSERC of Canada for financial support.

[1] E.M. Chudnovsky and D.A. Garanin, Phys. Rev. Lett. **79**, 4469 (1997).
[2] E.M. Chudnovsky and D.A. Garanin, Phys. Rev. B **59**, 3671 (1999); Phys. Rev. B **63**, 024418 (2000)
[3] D. A. Garanin, X. Martìnez Hidalgo, and E. M. Chudnovsky Phys. Rev. B **57**, 13639 (1998)
[4] Gwang-Hee Kim, Phys. Rev. B **59**, 11847, (1999); J. Appl. Phys. 86, 1062 (1999)
[5] G Scharf, W F Wreszinski and -J L van Hemmen, J. Phys. A: Math. Gen **20**, 4309 (1987)
[6] O.B. Zaslavskii, Phys. Lett. A **145**, 471 (1990)
[7] V.V. Ulyanov, O.B. Zaslavskii, Phys. Rep. **214**, 179 (1992)
[8] J.-Q. Liang, H. J. W. Müller-Kirsten, D. K. Park and F.-C. Pu , Phys. Rev. B **61**, 8856 (2000)
[9] Our model for $h_x = 0$ is equivalent to that of Ref. [14] if we set $K_1 = \mathcal{D}$ and $K_2 = \mathcal{E}$ and it is equivalent to that of Ref. [4] if we set $K_\perp = \mathcal{D} - \mathcal{E}$ and $K_{||} = \mathcal{E}$.
[10] Daniel Loss, David P. DiVincenzo, and G. Grinstein, Phys. Rev. Lett. **69**, 3232 (1992)
[11] J. von Delft, C. Henley, Phys. Rev. Lett. **69**, 3236(1992)
[12] Chang-Soo Park, Sahng-Kyoon Yoo and Dal-Ho Yoon Phys. Rev. B **61**, 11618, (2000)
[13] S.-Y. Lee, H. J. W. Müller-Kirsten, D. K. Park, and F. Zimmerschied ; Phys. Rev. B **58**, 5554 (1998).
[14] Y.-B. Zhang, J.-Q. Liang, H.J.W. Muller-Kirsten, S.-P. Kou, X.-B. Wang and F.-C. Pu Phys. Rev. B **60**, 12886 (1999)
[15] J. M. Radcliffe, J. Phys. A: Gen. Phys **4** (1971), 313.
[16] John R. Klauder, Phys. Rev. D **19**, 2349 (1979).
[17] E. M. Chudnovsky and L. Gunther, Phys. Rev. Lett. **60**, 661 (1988)

6.6 Article for quantum-classical phase transition in anti-ferromagnetic dimer model

The article below on quantum-classical phase transition in dimeric molecular magnets is published in Physics Letters A. Reprinted from Ref.[106], copyright (2014), with permission from Elsevier. I conceived the idea of this paper based on our previous published article in Physics Review B. My supervisor (co-author) gave some indispensable technical advice. The originality, problem formulation, methodology, and results were obtained predominately by me and partly by my co-author.

UdeM-GPP-TH-13-227

Phase transition between quantum and classical regimes for the escape rate of dimeric molecular nanomagnets in a staggered magnetic field

S. A. Owerre and M. B. Paranjape
Groupe de physique des particules, Département de physique, Université de Montréal, C.P. 6128, succ. centre-ville, Montréal, Québec, Canada, H3C 3J7

Abstract

We study the phase transition of the escape rate of exchange-coupled dimer of single-molecule magnets which are coupled either ferromagnetically or antiferromagnetically in a staggered magnetic field and an easy z-axis anisotropy. The Hamiltonian for this system has been used to study dimeric molecular nanomagnet $[Mn_4]_2$ which is comprised of two single molecule magnets coupled antiferromagnetically. We generalize the method of mapping a single-molecule magnetic spin problem onto a quantum-mechanical particle to dimeric molecular nanomagnets. The problem is mapped to a single particle quantum-mechanical Hamiltonian in terms of the relative coordinate and a coordinate dependent reduced mass. It is shown that the presence of the external staggered magnetic field creates a phase boundary separating the first- from the second-order transition. With the set of parameters used by R. Tiron, *et al* , Phys. Rev. Lett. **91**, 227203 (2003), and S. Hill, *et al* science **302**, 1015 (2003) to fit experimental data for $[Mn_4]_2$ dimer we find that the critical temperature at the phase boundary is $T_0^{(c)} = 0.29K$. Therefore, thermally activated transitions should occur for temperatures greater than $T_0^{(c)}$.

PACS numbers: 75.45.+j, 75.10.Jm, 75.30.Gw, 03.65.Sq

I. INTRODUCTION

The study of single-molecule magnets (SMMs) has been the subject of experimental and theoretical interest in recent years. These systems have been pointed out[7,8] to be a good candidate for investigating first- and second-order phase transition of the quantum-classical escape rate. The quantum-classical escape rate transition takes place in the presence of a potential barrier, it is mainly in two categories− classical thermal activation over the barrier and quantum tunnelling through the barrier. At high temperatures, transition occurs by classical thermal activation over the barrier while at low-temperatures, transition occurs by quantum tunnelling between two degenerate classical minima. In principle these transitions are greatly influenced by the anisotropy constants and the external magnetic fields. There exits a crossover temperature (first-order transition) $T_0^{(1)}$ from quantum to thermal regime, it is estimated as $T_0^{(1)} = \Delta U/B$, ΔU is the energy barrier and B is the instanton action responsible for quantum tunnelling. The second-order phase transition occurs for particles in a cubic or quartic parabolic potential, it takes place at the temperature $T_0^{(2)}$, below $T_0^{(2)}$ one has the phenomenon of thermally assisted tunnelling and above $T_0^{(2)}$ transition occur due to thermal activation to the top of the potential barrier[7,8,13].

Garanin and Chudnovsky[7] have studied the model of a uniaxial single ferromagnetic spin with a transverse magnetic field, which is believed to describe the molecular magnet Mn_{12}Ac with a total spin of $s = 10$. They showed by using the method of spin-particle mapping[1–3], that the phase transition can be understood in analogy of Landau's theory of phase transition, with the free energy expressed as $F = a\psi^2 + b\psi^4 + c\psi^6$, where $a = 0$ determines the quantum-classical transition and $b = 0$ determines the boundary between the first- and second-order phase transition. Many authors[4,13,17,18] have searched for the possibility of these transitions in the biaxial single ferromagnet spin systems. To the best of our knowledge, the possibility of these transitions for exchange-coupled dimer spin systems has not been reported in any literature. In many cases of physical interest, the spins in a physical system, in principle interact with each other either ferromagnetically or antiferromagnetically. One physical example in which these interactions occur is the molecular wheels such as Mn_{12}[19,29,30], and the molecular dimer $[Mn_4]_2$[21,26], which comprises two Mn_4 SMMs of equal spins $s_A = s_B = 9/2$, which are coupled antiferromagnetically. These systems are usually modelled with two interacting giant sublattice spins. Additional terms such as easy axis anisotropy, transverse anisotropy and an external magnetic field are usually added to the model Hamiltonian. Therefore, the thermodynamic and low-energy properties of these systems can be studied effectively by two interacting large spin Hamiltonian. Due to recent experiment on molecular Mn_{12} wheel[29,30] and $[Mn_4]_2$ dimer[21,26–28] , such effective Hamiltonian has attracted so much attention. In this paper we will study one form of this effective Hamiltonian.

II. MODEL HAMILTONIAN

Consider the effective Hamiltonian of an exchange-coupled dimer of SMMs such as $[Mn_4]_2$ in a staggered

magnetic field with an easy z-axis anisotropy

$$\hat{H} = J\hat{\mathbf{S}}_A \cdot \hat{\mathbf{S}}_B - D(\hat{S}^2_{A,z} + \hat{S}^2_{B,z}) + g\mu_B h(\hat{S}_{A,z} - \hat{S}_{B,z}) \tag{2.1}$$

where J is the isotropic Heisenberg exchange interaction, and $J > 0 (J < 0)$ are antiferromagnetic (ferromagnetic) exchange coupling respectively and $D > |J| > 0$ is the easy z-axis anisotropy, h is the external magnetic field, μ_B is the Bohr magneton and $g = 2$ is the electron g-factor. The last term indicates that there are staggered magnetic fields $-h$ and h applied to the two sublattices A and B respectively. For the antiferromagnetic coupling, the spins are aligned (classically speaking) antiparallel along the z-axis. The anisotropy and the magnetic field terms in the Hamiltonian create two classical minima located at $\pm z$-axis, these minima (one being metastable) are separated by an energy barrier, and any spin configuration can escape from one minimum to the other either by thermal activation over the barrier or by quantum tunnelling through the barrier. We have omitted a fourth order anisotropy term which is very small compare to the easy-axis term. The spin operators obey the usual commutator relation: $\left[\hat{S}_{j\alpha}, \hat{S}_{k\beta}\right] = i\epsilon_{\alpha\beta\gamma}\delta_{jk}\hat{S}_{k\gamma}$ $(j,k = A,B;\, \alpha,\beta,\gamma = x,y,z)$. The Hilbert space of this system is the tensor product of the two spaces $\mathscr{H} = \mathscr{H}_A \otimes \mathscr{H}_B$ with $\dim(\mathscr{H}) = (2s_A + 1) \otimes (2s_B + 1)$. The basis of S^z_j in this product space is given by $\mid s_A, m_A\rangle \otimes \mid s_B, m_B\rangle \equiv \mid m_A, m_B\rangle$. The eigenvalue of the diagonal term of the Hamiltonian is simply given by

$$\mathcal{E}_d = Jm_Am_B - D(m^2_A + m^2_B) + g\mu_B h(m_A - m_B) \tag{2.2}$$

Note that for antiferromagnetic coupling, either m_A or m_B should be replaced with $-m_A$ or $-m_B$, while for ferromagnetic coupling, Eq.(2.2) is the exact ground state energy of the quantum Hamiltonian, Eq.(2.1), with the eigenstates $\mid m_A = s_A, m_B = s_B\rangle$ and $\mid m_A = -s_A, m_B = -s_B\rangle$, these two states are degenerate for $h = 0$ or $s_A = s_B = s$. In principle the spectrum of the Hamiltonian Eq.(2.1) for antiferromagnetic spin configuration can be found by exact numerical diagonalization for some compounds[26,30]. Similar models of this form have been extensively studied by different methods[6,19,23,24]. Since the individual z-components of the spins do not commute with the Hamiltonian (only the total z-component of the spins $\hat{S}_z = \hat{S}_{A,z} + \hat{S}_{B,z}$ commutes), the two antiferromagnetic classical ground states $|\downarrow,\uparrow\rangle$, and $|\uparrow,\downarrow\rangle$, where $|\downarrow,\uparrow\rangle \equiv \mid m_A = -s, m_B = s\rangle$ etc, are not exact eigenstates of Eq.(2.1), in principle there should be an energy splitting between these two states due to tunnelling. We showed[16] via spin coherent state path integral, for $h = 0$ that the degeneracy of the two states $|\uparrow,\downarrow\rangle$ and $|\downarrow,\uparrow\rangle$ are lifted by the transverse exchange interaction $J \neq 0$ and the energy splitting is proportional to $|J|^{2s}$ corresponding to $2s^{\text{th}}$ order in perturbation theory in the J term. This result had been obtained by perturbation theory[10,11,14]. Thus, the ground and the first excited states become the anti-symmetric and symmetric linear coherent superpositions of these two antiferromagnetic classical ground states[9]. The form of the Hamiltonian Eq.(2.1) has been used to investigate $[Mn_4]_2$ dimer[20,21,26] for which $s_A = s_B = s = 9/2$, thus there are $(2s+1)^2 \times (2s+1)^2 = 100 \times 100$ matrices which are sparsely populated giving rise to an exact numerical digonalization of 100 non-zero energy states. The parameters use to fit experimental data for this dimer are $J = 0.12K$, $D = 0.75K$. At zero magnetic field, it has been demonstrated by density-functional theory that this simple model can reproduce experimental results in $[Mn_4]_2$ dimer with $D = 0.58K$ and $J = 0.27K$[28]. This model also plays a role in quantum computation for investigating controlled-NOT quantum logic gates[22]. The purpose of this paper is to map this model to a quantum mechanical particle in an effective potential and investigate the influence of the staggered magnetic field on the first- and second-order phase transition between quantum and classical regimes for the escape rate. We will show that the result of spin coherent state path integral can be recovered from this effective potential mapping. We will focus on the case of antiferromagnetic coupling since the form of Hamiltonian we choose does not possess any ground state tunnelling for the ferromagnetic case.

III. METHODOLOGY

In the spin-particle formalism, one introduces the spin wave function using the $S_{iz}, i = 1,2$ eigenstates[1–3], and the resulting eigenvalue equation is then transformed to a differential equation, which is further reduced to a Schrödinger equation with an effective potential and a constant or coordinate dependent mass. In the present problem the spin wave function can be written in a more general form as

$$\psi = \psi_A \otimes \psi_B = \sum_{\substack{m_A=-s_A \\ m_B=-s_B}}^{s_A,s_B} \mathcal{C}_{m_A,m_B}\mathcal{G}_{m_A,m_B} \tag{3.1}$$

where

$$\mathcal{G}_{m_A,m_B} = \binom{2s_A}{s_A + m_A}^{-1/2} \binom{2s_B}{s_B + m_B}^{-1/2} \mid m_A, m_B\rangle \tag{3.2}$$

It is noted that either $m_A \to -m_A$ or $m_B \to -m_B$ since we are interested in the case of antiferromagnetic spin configuration, however, as we will see later, one can check that this replacement does not alter the resulting differential equation. The action of the spin Hamiltonian Eq.(2.1) on the spin wave function Eq.(3.1) yields

an eigenvalue equation

$$\hat{H}\psi = \sum_{\substack{m_A=-s_A \\ m_B=-s_B}}^{s_A,s_B} \mathcal{C}_{m_A,m_B}\Bigg[\frac{J(s_A-m_A)(s_B+m_B)}{2}\mathcal{G}_{m_A+1,m_B-1} + \frac{J(s_A+m_A)(s_B-m_B)}{2}\mathcal{G}_{m_A-1,m_B+1} + \Big(Jm_Am_B + g\mu_B h(m_A-m_B) - D(m_A^2+m_B^2)\Big) \times \mathcal{G}_{m_A,m_B}\Bigg] = \mathcal{E}\psi \tag{3.3}$$

which can be written in a more compact form as

$$\mathcal{E}\mathcal{C}_{m_A,m_B} = \left[Jm_Am_B - D(m_A^2+m_B^2) + g\mu_B h(m_A-m_B)\right]\mathcal{C}_{m_A,m_B} + \frac{J(s_A-m_A+1)(s_B+m_B+1)}{2}\mathcal{C}_{m_A-1,m_B+1} + \frac{J(s_A+m_A+1)(s_B-m_B+1)}{2}\mathcal{C}_{m_A+1,m_B-1} \tag{3.4}$$

where $\mathcal{C}_{-s_i-1} = 0 = \mathcal{C}_{s_i+1}$, etc, $i = A, B$. In order to transform this expression, Eq.(3.4) into a differential equation , we introduce the characteristic function[1,2] for the two particles

$$\mathcal{F}(x_1,x_2) = \sum_{\substack{m_A=-s_A \\ m_B=-s_B}}^{s_A,s_B} \mathcal{C}_{m_A,m_B}e^{m_Ax_1}e^{m_Bx_2} \tag{3.5}$$

It is well-known that when the magnetic field is applied along the hard-axis a topological phase (oscillation of tunnelling splitting) is generated due to an imaginary term arising from the Euclidean action[4–6] . In the present problem the magnetic field is along the easy-axis, so we do not expect such effect in this model. In our representation the characteristic function Eq.(3.5) is not periodic, but by complexifying the variables x_1 and x_2 one can see that the function satisfies $\mathcal{F}(x_1+2\pi i, x_2+2\pi i) = e^{2\pi i(s_A+s_B)}\mathcal{F}(x_1,x_2)$. The differential equation for $\mathcal{F}$ yields

$$-D\left(\frac{d^2\mathcal{F}}{dx_1^2}+\frac{d^2\mathcal{F}}{dx_2^2}\right) - J\cosh(x_1-x_2)\frac{d}{dx_1}\left(\frac{d\mathcal{F}}{dx_2}\right) + J\frac{d}{dx_1}\left(\frac{d\mathcal{F}}{dx_2}\right) - (g\mu_Bh - Js_A\sinh(x_1-x_2))\frac{d\mathcal{F}}{dx_2} + (g\mu_Bh - Js_B\sinh(x_1-x_2))\frac{d\mathcal{F}}{dx_1} + (Js_As_B\cosh(x_1-x_2)-\mathcal{E})\mathcal{F} = 0 \tag{3.6}$$

As one expects from two interacting particles, the hyperbolic functions in Eq.(3.6) emerge as functions of the relative coordinate. Proceeding in a similar way to that of classical theory, we introduce the relative and center of mass coordinates as

$$r = x_1 - x_2, \quad q = \frac{x_1+x_2}{2} \tag{3.7}$$

then Eq.(3.6) reduces to a second-order differential equation with variable coefficients in terms of the relative and center of mass coordinates

$$\mathcal{P}_1(r)\frac{d^2\mathcal{F}}{dr^2} + \mathcal{P}_2(r)\frac{d^2\mathcal{F}}{dq^2} + \mathcal{P}_3(r)\frac{d\mathcal{F}}{dr} + \mathcal{P}_4(r)\frac{d\mathcal{F}}{dq} + (\mathcal{P}_5(r)-\mathcal{E})\mathcal{F} = 0 \tag{3.8}$$

where the $\mathcal{P}_i(r)$ functions are given by

$$\begin{aligned}
\mathcal{P}_1(r) &= -2\left[D + \frac{J}{2} - \frac{J}{2}\cosh r\right] \\
\mathcal{P}_2(r) &= -\frac{1}{2}\left[D - \frac{J}{2} + \frac{J}{2}\cosh r\right], \\
\mathcal{P}_3(r) &= (2g\mu_Bh - J(s_A+s_B)\sinh r), \\
\mathcal{P}_4(r) &= \frac{J(s_A-s_B)}{2}\sinh r,\ \mathcal{P}_5(r) = Js_As_B\cosh r
\end{aligned} \tag{3.9}$$

$\mathcal{F} = \mathcal{F}(r,q)$ and $r \to r+i\pi$ has been used for convenience.

In general, for $s_A \neq s_B$ the exact solution of Eq.(3.8) is unknown. But in most cases of physical interest such as molecular magnets and molecular wheels[27], the two spins are equal. Thus, it is reasonable to consider a special case of equal spins $s_A = s_B = s$. In this case the expression for $\mathcal{P}_4(r)$ vanishes and the rest of Eq.(3.8) can then be simplified by separation of variable, $\mathcal{F}(r,q) = \mathcal{F}_1(r)\mathcal{F}_2(q)$. Therefore, Eqn.(3.6) reduces to two, separate, independent equations which are satisfied when they are equal to constants $\mathscr{C}$ and $-\mathscr{C}$ respectively:

$$\frac{d^2\mathcal{F}_2(q)}{dq^2} = \mathscr{C}\mathcal{F}_2(q), \tag{3.10}$$

$$\mathcal{P}_1(r)\frac{d^2\mathcal{F}_1(r)}{dr^2} + \mathcal{P}_3(r)\frac{d\mathcal{F}_1(r)}{dr} + (\mathcal{P}_5(r)-\mathcal{E})\,\mathcal{F}_1(r) = -\mathscr{C}\mathcal{P}_2(r)\mathcal{F}_1(\tag{3.11}$$

The first equation obviously does not contain sufficient information about the system, thus we will focus on the second equation. We then seek for a transformation that eliminates the first derivative term in Eqn.(3.11); such a transformation is of the form:

$$\Psi(r) = e^{-y(r)}\mathcal{F}_1(r), \tag{3.12}$$

where $y(r)$ is to be determined. Substituting into Eqn.(3.11) we obtain

$$\mathcal{P}_1\Psi'' + (2\mathcal{P}_1y' + \mathcal{P}_3)\Psi' + [\mathcal{P}_3y' + \mathcal{P}_5 + \mathscr{C}\mathcal{P}_2 + \mathcal{P}_1\left(y'' + y'^2\right)]\Psi = \mathcal{E}\Psi, \tag{3.13}$$

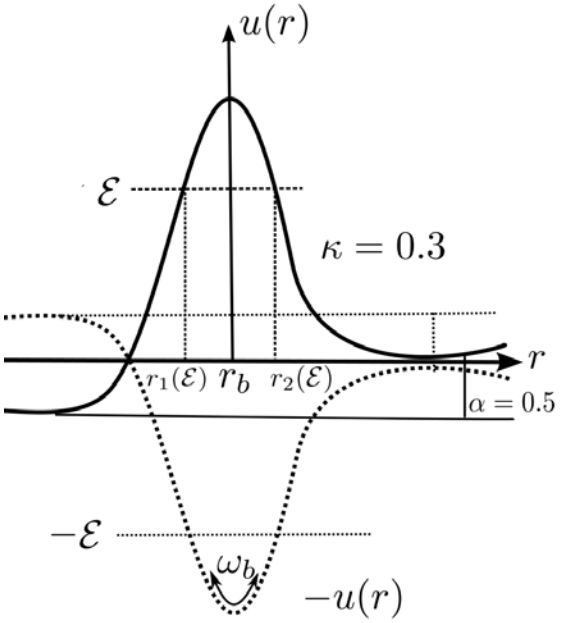

FIG. 1: The effective potential and its inverse vs. r for $\kappa = 0.3$ and $\alpha = 0.5$

where prime denotes derivative with respect to r. It is evident that the elimination of the first derivative term in Eqn.(3.11) demands that the coefficient of the first derivative of Ψ vanishes. Thus, we must have

$$2\mathcal{P}_1 y' + \mathcal{P}_3 = 0. \tag{3.14}$$

This gives the expression for $y(r)$ as

$$y(r) = s\ln(2+\kappa+\kappa\cosh r) + \frac{2s\alpha}{\sqrt{1+\kappa}}\operatorname{arctanh}\left(\frac{\tanh\left(\frac{r}{2}\right)}{\sqrt{1+\kappa}}\right), \tag{3.15}$$

where $\kappa = J/D$ and $\alpha = h_z/2Ds$. Simplifying Eqn.(3.13) using Eqn.(3.15), we arrive at the Schrödinger equation:

$$H\Psi(r) = \mathcal{E}\Psi(r) \tag{3.16}$$

with

$$H = -\frac{\nabla^2}{2\mu(r)} + U(r), \quad \nabla = \frac{d}{dr} \tag{3.17}$$

The effective potential $U(r) = 2D\tilde{s}^2 u(r)$ and the coordinate dependent reduced mass $\mu(r)$ are given by

$$u(r) = \frac{2\alpha^2 + \kappa(1-\cosh r) + 2\alpha\kappa\sinh r}{(2+\kappa+\kappa\cosh r)} \tag{3.18}$$

$$\mu(r) = \frac{1}{2D\,(2+\kappa+\kappa\cosh r)} \tag{3.19}$$

We have used the large s limit[13,17] $s \sim s+1 \sim \tilde{s} = (s+\frac{1}{2})$, hence terms independent of $\tilde{s}$ drop out in Eq.(3.18), also an additional constant has been added to the potential for convenience. It is noted that the presence of the sine hyperbolic creates a metastable minimum, however, in the absence of the magnetic field the potential becomes even with two degenerate minima as shown in Fig.(1).

IV. PHASE TRANSITION OF THE ESCAPE RATE

In this section we study the phase transition of our system in the absence of a staggered magnetic field $\alpha = 0$, as well as the phase diagram in the presence of a staggered magnetic field $\alpha \neq 0$. For a coordinate dependent massive particle, the existence of first-order phase transition has been shown[18,25] to be determined from the condition

$$\Big[U'''(r_b)\left(g_1 + \frac{g_2}{2}\right) + \frac{1}{8}U''''(r_b) + \omega^2\mu'(r_b)g_2 + \omega^2\mu'(r_b)\left(g_1+\frac{g_2}{2}\right) + \frac{1}{4}\omega^2\mu''(r_b)\Big]_{\omega=\omega_b} < 0 \tag{4.1}$$

where

$$g_1 = -\frac{\omega^2\mu'(r_b) + U'''(r_b)}{4U''(r_b)} \tag{4.2}$$

$$g_2 = -\frac{3\mu'(r_b)\omega^2 + U'''(r_b)}{4\left[4\mu(r_b)\omega^2 + U''(r_b)\right]}$$

$$\omega_b^2 = -\frac{U''(r_b)}{\mu(r_b)}$$

and $'$ represents derivatives with respect to r. The subscript b represents the coordinate of the sphaleron at the bottom of the well of the inverted potential, and ω_b is the frequency of oscillation at the bottom of the well of the inverted potential. By setting the first derivative of the potential to zero, we obtain that the sphaleron position is located at $r_b = \ln\left(\frac{1+\alpha}{1-\alpha}\right)$, and the height of the potential barrier is given by

$$\Delta U = 2D\tilde{s}^2\,(1-\alpha)^2 \tag{4.3}$$

Alternatively, in terms of the free energy of the system, we have that the escape rate of a particle through a potential barrier in the semiclassical approximation is obtained by taking the Boltzmann average over tunneling probabilities[15]

$$\Gamma \propto \int_{U_{\min}}^{U_{\max}} d\mathcal{E}\mathcal{P}(\mathcal{E})e^{-\beta(\mathcal{E}-U_{\min})}, \quad \beta^{-1} = T \tag{4.4}$$

where $\mathcal{P}(\mathcal{E})$ is an imaginary time transition amplitude at an energy $\mathcal{E}$, and $U_{\min}$ is the bottom of the potential energy. The transition amplitude is defined as

$$\mathcal{P}(\mathcal{E}) \sim e^{-S(\mathcal{E})} \tag{4.5}$$

and the Euclidean action is given by

$$S(\mathcal{E}) = 2\int_{-r(\mathcal{E})}^{r(\mathcal{E})} dr\sqrt{2\mu(r)\left(U(r)-\mathcal{E}\right)} \tag{4.6}$$

where $\pm r(\mathcal{E})$ are the turning points ($U(\pm r(\mathcal{E})) = \mathcal{E}$) at zero magnetic field for the particle with energy $-\mathcal{E}$ in an inverted potential $-U(r)$. The factor of 2 in Eq.(4.6) corresponds to the back and forth oscillation of the period in the inverted potential. In many cases of physical interest, this integral can be computed in the whole range of energy for any given potential in terms of complete elliptic integrals. In the limit $\mathcal{E} \to U_{\min}$, its value corresponds to an instanton or bounce action. All the interesting physics of phase transition in spin systems occur when the energy is very close to the top of the potential barrier, $\mathcal{E} \to U_{\max}$. In the method of steepest decent, for small temperatures $T < \hbar\omega_0$, where ω_0 is the frequency of oscillation at the minimum of the potential, Eq.(4.4) is dominated by a stationary point

$$\beta = \tau(\mathcal{E}) = -\frac{dS(\mathcal{E})}{d\mathcal{E}} = \int_{-r(\mathcal{E})}^{r(\mathcal{E}} dr\sqrt{\frac{2\mu(r)}{U(r)-\mathcal{E}}} \tag{4.7}$$

which is the period of oscillation of a particle with energy $-\mathcal{E}$ in the inverted potential $-U(x)$. In the limit $\mathcal{E} \to U_{\min}$, the period $\tau(\mathcal{E}) \to \infty$, that is $T \to 0$ which corresponds to an instanton while for $\mathcal{E} \to U_{\max}$, $\tau(\mathcal{E}) \to 2\pi/\omega_b$[15]. The escape rate, Eq.(4.4) in the method of steepest decent can also be written as[7,8]

$$\Gamma \sim e^{-\beta F_{\min}} \tag{4.8}$$

and $F_{\min}$ is the minimum of the effective free energy

$$F = \mathcal{E} + \beta^{-1}S(\mathcal{E}) - U_{\min} \tag{4.9}$$

with respect to $\mathcal{E}$.

This free energy can be used to characterize first- and second-order phase transitions in analogy with Landau's theory of phase transition, only if one can find the expression of the action $S(\mathcal{E})$ for a given mass and potential.

A. Analyses with zero staggered magnetic field

At zero staggered magnetic field, it is well-known that the ground state energy splitting of the quantum spin Hamiltonian is proportional to J^{2s} which has been obtained by different methods[10,11,14,16]. In this section we will show how this result can be recovered from the present formalism. At zero staggered magnetic field the effective potential, Eq.(3.18) is of the form

$$U(r) = \frac{2D\kappa s(s+1)(1-\cosh r)}{(2+\kappa+\kappa\cosh r)} \tag{4.10}$$

Since $s \gg 1$, we can approximate $s(s+1)$ as s^2. In this case one can obtain the exact expression for the action, Eq.(4.6) in the whole range of energy by making the substitution $y = \cosh\left(\frac{r}{2}\right)$. The action becomes

$$S(\mathcal{E}) = 4s\sqrt{2(a+b)\kappa}\int_1^{1/\lambda} dy\frac{1}{(1+\kappa y^2)}\sqrt{\frac{1-\lambda^2y^2}{y^2-1}} \tag{4.11}$$

where $\lambda^2 = \frac{2b}{a+b}$, $a = 1-(2+\kappa)\mathcal{E}'$, $b = 1+\kappa\mathcal{E}'$, and $\mathcal{E}' = \mathcal{E}/2Ds^2\kappa$.

Introducing the variable

$$x^2 = \frac{1-1/y^2}{\lambda'^2}, \quad \lambda'^2 = 1-\lambda^2 = \frac{a-b}{a+b} \tag{4.12}$$

Eq.(4.11) becomes

$$S(\mathcal{E}) = 4s\sqrt{2(a+b)\kappa}[\mathcal{K}(\lambda') - (1-\gamma^2)\Pi(\gamma^2,\lambda')] \tag{4.13}$$

where $\gamma^2 = \lambda'^2/(1+\kappa)$. $\mathcal{K}(\lambda')$ and $\Pi(\gamma^2,\lambda')$ are the complete elliptic integral of first and third kinds. Near the bottom of the potential the action is

$$S(\mathcal{E}) \approx S(U_{\min}) = 8s\,\mathrm{arctanh}(\gamma) = 4s\ln\left(\frac{\sqrt{1+\kappa}+1}{\sqrt{1+\kappa}-1}\right) \tag{4.14}$$

In the perturbative limit $\kappa \ll 1$, Eq.(4.14) simplifies to

$$S(U_{\min}) \approx 4s\ln\left(\frac{4}{\kappa}\right) = 4s\ln\left(\frac{4D}{J}\right) \tag{4.15}$$

The ground state energy splitting in the perturbative limit is obtained as

$$\Delta\mathcal{E}_0 = 2\mathscr{D}\exp\left(-\frac{S(U_{\min})}{2}\right) = 2\mathscr{D}\left(\frac{J}{4D}\right)^{2s} \tag{4.16}$$

where $\mathscr{D}$ is a prefactor which is not crucial in the present analysis. The factor J^{2s} indicates that the two classical antiferromagnetic ground state configurations are linked to each other in the $2s^{\text{th}}$ order in perturbation theory. Thus the zero magnetic field quantum spin Hamiltonian at $2s^{\text{th}}$ order can be written effectively as

$$\hat{H}\psi_\pm = \mathcal{E}_\pm\psi_\pm \tag{4.17}$$

where

$$\psi_\pm = \frac{1}{\sqrt{2}}\left(|\uparrow,\downarrow\rangle \pm |\downarrow,\uparrow\rangle\right), \quad \Delta\mathcal{E}_0 = \mathcal{E}_+ - \mathcal{E}_- \tag{4.18}$$

Thus, the ground and the first excited states are entangled states. The antisymmetric and symmetric linear superpositions are the ground and the first excited states respectively for half-odd integer spins[9,16] while the roles are reversed for integer spins. It is noted that Kramers degeneracy does not apply in this model since we have an even number of spins.

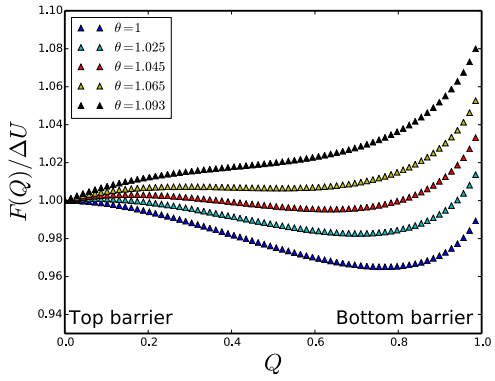

(a)

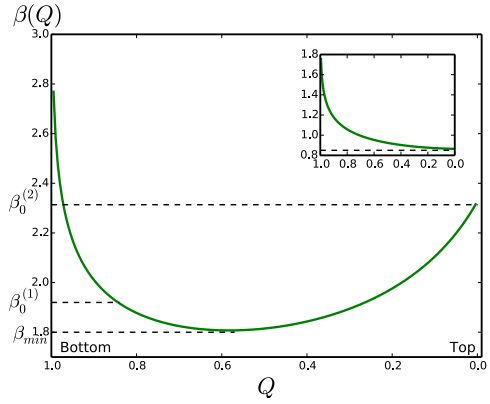

(b)

FIG. 2: (a): The effective free energy of the escape rate vs Q for $\kappa = 0.1$ and several values of $\theta = T/T_0^{(2)}$. (b) : The period of oscillation vs Q for several values of κ, first-order transition.

Having obtained the action for all possible values of the energy, that is Eq.(4.13), the free energy Eq.(4.9) can now be written down exactly. In terms of the dimensionless energy quantity $Q = (U_{\max} - \mathcal{E})/(U_{\max} - U_{\min})$ where $U_{\max}(U_{\min})$ correspond to the top (bottom) of the potential, $Q \to 0(1)$ at the top (bottom) of the potential respectively. The free energy can then be written as

$$F/\Delta U = 1 - Q + \frac{4}{\pi}\theta\sqrt{\kappa(\kappa+Q)}[\mathcal{K}(\lambda') - (1-\gamma^2)\Pi(\gamma^2,\lambda')] \tag{4.19}$$

where $\theta = T/T_0^{(2)}$ is a dimensionless temperature quantity, and $T_0^{(2)} = \omega_b/2\pi$. The modulus of the complete elliptic integrals λ' and the elliptic characteristic γ are related to Q by

$$\lambda'^2 = \frac{(1+\kappa)Q}{\kappa+Q}, \quad \gamma^2 = \frac{Q}{\kappa+Q} \tag{4.20}$$

We have already known that the phase transition occurs near the top of the potential barrier, so it is required that we expand this free energy close to the barrier top.

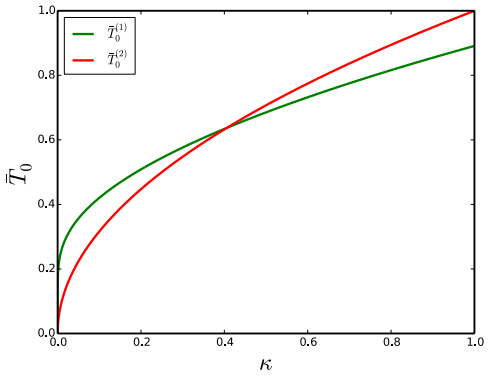

FIG. 3: Zero magnetic field crossover temperatures plotted against κ. The functions increase rapidly as κ varies between 0 and 1. $\mathcal{T}_0 = \pi T_0^{(1,2)}/Ds$

Thus, near the top of the barrier $Q \to 0$, the expansion of the complete elliptic integrals up to order Q^3 are given by

$$\mathcal{K}(\lambda') = \frac{\pi}{2}\left[1 + \frac{(1+\kappa)}{4\kappa}Q + \frac{(1+\kappa)(9\kappa-7)}{64\kappa^2}Q^2 + \frac{(1+\kappa)(17+\kappa(25\kappa-22))}{256\kappa^3}Q^3\right] \tag{4.21}$$

$$\Pi(\gamma^2,\lambda') = \frac{\pi}{2}\left[1 + \frac{(3+\kappa)}{4\kappa}Q + \frac{\kappa(14+9\kappa)-3}{64\kappa^2}Q^2 + \frac{7-\kappa(1-\kappa(25\kappa-33))}{256\kappa^3}Q^3\right] \tag{4.22}$$

The full simplification of Eq.(4.19) yields

$$F/\Delta U = 1 + (\theta-1)Q + \frac{\theta}{8\kappa}(\kappa-1)Q^2 + \frac{\theta}{64\kappa^2}(3\kappa^2-2\kappa+3)Q^3 \tag{4.23}$$

This free energy looks more like the Landau's free energy, which suggests that we should compare the two free energies. The Landau's free energy has the form

$$F = a\psi^2 + b\psi^4 + c\psi^6 \tag{4.24}$$

Surprisingly, the coefficient of Q in Eq.(4.23) is equivalent to the coefficient a in Landau's free energy. It changes sign at the phase temperature $T = T_0^{(2)}$. The phase boundary between the first- and the second-order phase transitions depends on the coefficient of Q^2, it is equivalent to the coefficient b in Eq.(4.24). It changes sign at $\kappa = 1$. Thus $\kappa < 1$ indicates the regime of first-order phase transition. These conditions for the phase boundary and the first-order phase transition can also be obtained from the criterion given in Eq.(4.1) with $x_s = r_b = 0$, which corresponds to the top of the potential barrier when the magnetic field $\alpha = 0$.

In Fig.(2(a)) we have shown the plot of the free energy against Q for $\kappa = 0.4$ (first-order transition). In the top

two curves, the minimum of the free energy is at $Q = 0$. As the temperature is lowered, a new minimum of the free energy is formed. For $\theta = 1.055$ or $T_0^{(1)} = 1.055T_0^{(2)}$, this new minimum becomes the same as the one at $Q = 0$. This corresponds to the crossover temperature from classical to quantum regimes.

The calculation of the period of oscillation $\tau(\mathcal{E})$ yields

$$\tau(\mathcal{E}) = -\frac{dS(\mathcal{E})}{d\mathcal{E}} = \int_{-r(\mathcal{E})}^{r(\mathcal{E})} dr \sqrt{\frac{2\mu(r)}{U(r) - \mathcal{E}}} = \frac{2\sqrt{2}}{Ds\sqrt{(a+b)\kappa}}\mathcal{K}(\lambda') = \frac{2}{Ds\sqrt{(\kappa+Q)}}\mathcal{K}(\lambda') \tag{4.25}$$

The plot of $\tau(\mathcal{E})$ vs Q is shown in Fig.(2(b)) for several values of κ. The period lies in the interval $2\pi/\omega_b \leq \tau(\mathcal{E}) \leq \infty$ for $0 \leq Q \leq 1$. The order of phase transition can be characterized by the behaviour of the period of oscillation as a function of energy. For first-order phase transition, the period of oscillation $\tau(\mathcal{E})$ is nonmonotonic function of $\mathcal{E}$ in other words $\tau(\mathcal{E})$ has a minimum at some point $\mathcal{E}_1 < \Delta U$ and then rises again, while for second-order phase transition $\tau(\mathcal{E})$ is monotonically increasing with decreasing energy[7,12]. Indeed for $\kappa < 1$, the period is a nonmonotonic function of energy indicating the existence of first-order phase transition. For $\kappa > 1$, the period is increasing with decreasing energy which indicates a second-order phase transition. The action at the bottom of the potential, which corresponds to the instanton action i.e Eq.(4.14) can now be used to estimate the first-order crossover temperature:

$$T_0^{(1)} = \frac{\Delta U}{S(U_{\min})} = \frac{Ds}{4\,\mathrm{arctanh}(\gamma)}, \quad \gamma \approx \frac{1}{1+\kappa} \tag{4.26}$$

For the case of second-order transition, we have

$$T_0^{(2)} = \frac{\omega_b}{2\pi} = \frac{Ds\sqrt{\kappa}}{\pi} \tag{4.27}$$

In Fig.(3) we have shown the plot of $T_0^{(1)}$ and $T_0^{(2)}$ against κ. The functions increase rapidly with an increase in κ and coincide at $\kappa = 0$ and $\kappa = 0.4$. At $\kappa = 0.4$, we obtain $T_0^{(1)} = 1.002T_0^{(2)}$. Thus, Eq.(4.26) underestimates the crossover temperature found in Fig.(2(a)). As in the uniaxial ferromagnetic spin model[7], one expects that both temperatures coincide for very small values of κ. With the use of experimental parameters: $s = 9/2$, $D = 0.75K$, and $J = 0.12K$ we obtain $T_0^{(1)} = 0.51K$ and $T_0^{(2)} = 0.43K$.

B. Analyses with a staggered magnetic field

In the presence of a staggered field, we would like to obtain the free energy in the whole range of energy, but this calculation is too cumbersome. So we will first use the criterion in Eq.(4.1). After a tedious but straightforward calculation of the derivatives in Eqs.(4.1) and (4.2), we obtain the condition for the first-order phase transition as

$$\frac{D\kappa\tilde{s}^2(1-\alpha^2)(-1+\kappa+\alpha^2(1+2\kappa))}{8(1-\alpha^2+\kappa)^2} < 0 \tag{4.28}$$

Setting this expression to zero, we obtain the phase boundary between the first- and second-order transitions as

$$\alpha_c = \pm\sqrt{\frac{1-\kappa_c}{1+2\kappa_c}} \tag{4.29}$$

where the subscript c represents the critical value of the parameters at the phase boundary. We will take only the positive sign in this expression. At zero staggered magnetic field, we obviously recover the results of the previous section. In Fig.(4) we have shown the plot of the function κ_c against α_c. The plot shows a decreasing function with increasing α_c, at $\kappa_c = 0$ we have $\alpha_c = 1$ which gives no tunnelling since the individual z-components of the spins commute with the Hamiltonian, thus Eq.(3.1) is an exact eigenstate which leads to a constant potential. The shaded and unshaded regions correspond to the two regions of first- and the second-order transitions respectively, separated by a phase boundary. Using the set of parameters in a realistic model of $[Mn_4]_2$ dimer[21,26] $J = 0.12K$, $D = 0.75K \Rightarrow \kappa_c = 0.16$, we obtain $\alpha_c = 0.80$. In the present analysis these values obviously fall in the regime of the first-order phase transition.

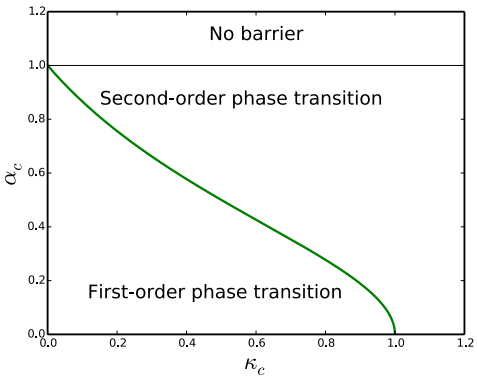

FIG. 4: Colour online: The phase diagram of κ_c vs α_c. There is no tunnelling at $\kappa_c = 0$ since the individual spins $\hat{S}_{A,z}$ and $\hat{S}_{B,z}$ commute with the Hamiltonian leading to a constant potential.

In order to show the analogy of these transitions to Landau's theory of phase transition as we did in the previous section, let us consider an alternative method for deriving the critical condition Eq.(4.29). Since we cannot compute the imaginary time action in Eq.(4.6) exactly, we will expand it near the top of the barrier, that is $Q \to 0$.

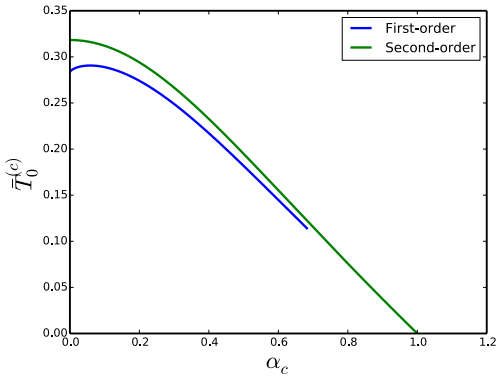

FIG. 5: The crossover temperature at the phase boundary between first- and second-order transitions plotted against α_c. $T_0^{(c)}$ has been rescaled as $T_0^{(c)}/D\tilde{s}$.

The expansion of the imaginary time action around r_b gives[13]

$$S(\mathcal{E}) = \pi\sqrt{\frac{2\mu(r_b)}{U''(r_b)}}\Delta U[Q + \mathcal{G}Q^2 + O(Q^3)] \quad (4.30)$$

where

$$\mathcal{G} = \frac{\Delta U}{16U''}\left[\frac{12U''''U'' + 15(U''')^2}{2(U'')^2} + 3\left(\frac{\mu'}{\mu}\right)\left(\frac{U'''}{U''}\right)\right. \quad (4.31)$$
$$\left. + \left(\frac{\mu''}{\mu}\right) - \frac{1}{2}\left(\frac{\mu'}{\mu}\right)^2\right]_{r=r_b}$$

$U''(r_b) = -D\tilde{s}^2u''(r_b)/2!$, $U'''(r_b) = D\tilde{s}^2u'''(r_b)/3!$, and $U''''(r_b) = D\tilde{s}^2u''''(r_b)/4!$.

By the analogy with the Landau theory of phase transition, the phase boundary between the first- and second-order transition (see Fig.(1)) is obtained by setting the coefficient of Q^2 to zero i.e $b = \mathcal{G} = 0$. Using Eqns.(3.18) and (3.19) we obtain that this condition yields

$$\frac{(-1 + \kappa + \alpha^2(1 + 2\kappa))}{8\kappa(1 + \alpha)^2} = 0 \quad (4.32)$$

which again recovers Eq.(4.29) and the exact coefficient of Q^2 in Eq.(4.23) at $\alpha = 0$. In the case of second-order transition the crossover temperature is estimated as $T_0^{(2)} = \omega_b/2\pi$. Using this expression and Eq.(4.29) we obtain the crossover temperature at the phase boundary as

$$T_0^{(c)} = \frac{D\tilde{s}}{\pi}\frac{(1 - \alpha_c^2)}{\sqrt{1 + 2\alpha_c^2}} = \frac{D\tilde{s}\kappa_c}{\pi}\left(\frac{3}{1 + 2\kappa_c}\right)^{\frac{1}{2}} \quad (4.33)$$

The plot of $T_0^{(c)}$ vs α_c(using Eq.(4.29)) is shown in Fig.(2), with the parameters for the experimental data in $[Mn_4]_2$ dimer[21,26], $s = 9/2$, $D = 0.75K$, $\kappa_c = 0.16 \Rightarrow \alpha_c = 0.80$, we find $T_0^{(c)} = 0.29K$. This crossover temperature is completely accessible as it has been experimentally demonstrated that there exist a crossover temperature below which quantum tunnelling is dominant[27].

V. CONCLUSIONS

In conclusion, we have investigated an effective Hamiltonian of a dimeric molecular nanomagnet which interacts ferromagnetically or antiferromagnetically. Using the method of mapping a spin system to a particle in an effective potential, we showed that this model can be mapped to a relative coordinate dependent massive particle in a potential field. We showed that the boundary between the first-and second-order phase transitions is greatly influenced by the staggered magnetic field. The parameter values for molecular $[Mn_4]_2$ dimer in recent experiments was shown to fall in the regime of first-order phase transition. The results obtained here are experimentally accessible.

VI. ACKNOWLEDGMENTS

We thank NSERC of Canada for financial support.

[1] G Scharf, W F Wreszinski and -J L van Hemmen, J. Phys. A: Math. Gen **20**, 4309 (1987)
[2] O.B. Zaslavskii, Phys. Lett. A **145**, 471 (1990)
[3] V.V. Ulyanov, O.B. Zaslavskii, Phys. Rep. **214**, 179 (1992)
[4] J.-Q. Liang, H. J. W. Müller-Kirsten, D. K. Park and F.-C. Pu , Phys. Rev. B **61**, 8856 (2000)
[5] Anupam Garg, Europhys. Lett. **22**, 205 (1993)
[6] Yi-Hang Nie, Yan-Hong Jin, J-Q Liang, H.J. W. Müller-Kirsten, D K Park, F-C Pu, J. Phys.: Condens. Matter, **12**, L87-L91 (2000)
[7] E.M. Chudnovsky and D.A. Garanin, Phys. Rev. Lett. **79**, 4469 (1997).
[8] D. A. Garanin, X. Martìnez Hidalgo, and E. M. Chudnovsky Phys. Rev. B **57**, 13639 (1998)
[9] E. M. Chudnovsky and Bernard Barbara, Phys. Lett. A, 145 (1990) 205.
[10] E. M. Chudnovsky and Javier Tejada, Lectures on Magnetism with 128 problems. Rinton Press, Princeton, NJ, (2006)
[11] E. M. Chudnovsky , Javier Tejada , Carlos Calero and Ferran Macia, Problem Solutions to Lectures on Magnetism, Rinton Press, Princeton, NJ, (2007)

[12] E.M. Chudnovsky Phys. Rev. A **46**, 8011 (1992);
[13] Gwang-Hee Kim, Phys. Rev. B **59**, 11847, (1999); J. Appl. Phys. 86, 1062 (1999)
[14] Gwang-Hee Kim, Phys. Rev. B **67**, 024421 (2003); ibid **68**, 144423 (2003)
[15] Affleck. I Phys. Rev. Lett. **46**, 388 (1981)
[16] S. A Owerre and M.B Paranjape, Phys. Rev. B **88**, 220403(R), (2013).
[17] Chang-Soo Park, Sahng-Kyoon Yoo and Dal-Ho Yoon Phys. Rev. B **61**, 11618, (2000)
[18] Y.-B. Zhang, J.-Q. Liang, H.J.W. Muller-Kirsten, S.-P. Kou, X.-B. Wang and F.-C. Pu Phys. Rev. B **60**, 12886 (1999)
[19] O. Waldmann, C. Dobe, H. U. Güdel, and H. Mutka Phys. Rev. B **74**, 054429 (2006)
[20] S. Hill and A. Wilson, J. Low Temp. Phys. **142**, 267, (2008)
[21] S. Hill, R. S. Edwards, N. Aliaga-Alcalde, G. Christou, science **302**, 1015 (2003)
[22] Jing-Min Hou, Li-Jun Tian, Mo-lin Ge, Chin. Phys. Lett., **22**, 2147(2005)
[23] Florian Meier, Jeremy Levy, and Daniel Loss, Phys. Rev. B **68**, 134417, (2003)
[24] Ji-Min Duan and Anupam Garg, Physica B. **194**, 323 (1994)
[25] H.J.W. Müeller-Kirsten, D.K.Park and J.M.S. Rana Phys. Rev. B **60**, 6662 (1999)
[26] R. Tiron, W. Wernsdorfer, D. Foguet-Albiol, N. Aliaga-Alcalde, and G. Christou, Phys. Rev. Lett. **91**, 227203 (2003)
[27] Wernsdorfer W., R. Tiron D.N. Hendrickson, N. Aliaga-Alcalde, and G. Christou, Journal of Magnetism and Magnetic Materials **272**, 1037 (2004)
[28] Park K., Mark R. Pederson, Steven L. Richardson, Nuria Aliaga-Alcalde, and George Christou, Phys. Rev. B **68**, 020405 (2003)
[29] W. Wernsdorfer, T. C. Stamatatos, and G. Christou, Phys. Rev. Lett. **101**, 237204 (2008)
[30] Christopher M. Ramsey, Enrique del Barco, Stephen Hill, Sonali J. Shah, Christopher C. Beedle and David N. Hendrickson, Nature Physics **4**, 277 (2008)

6.7 Review article to appear in Physics Reports

The article below is a review article on macroscopic quantum tunneling and quantum-classical phase transitions of the escape rate in large spin systems; set to be published in Physics Reports. Reprinted from Ref.[108], copyright (2014), with permission from Elsevier. This article is a summary of the preceding chapters. I conceived the idea, my supervisor (co-author) support it. I wrote the article including, problem formulation, methodology, and results. My co-author edited it.

Macroscopic quantum tunneling and quantum-classical phase transitions of the escape rate in large spin systems

S. A. Owerre and M. B. Paranjape

Groupe de physique des particules, Département de physique, Université de Montréal, C.P. 6128, succ. centre-ville, Montréal, Québec, Canada, H3C 3J7

This article presents a review on the theoretical and the experimental developments on macroscopic quantum tunneling and quantum-classical phase transitions of the escape rate in large spin systems. A substantial amount of research work has been done in this area of research over the years, so this article does not cover all the research areas that have been studied, for instance the effect of dissipation is not discussed and can be found in other review articles. We present the basic ideas with simplified calculations so that it is readable to both specialists and nonspecialists in this area of research. A brief derivation of the path integral formulation of quantum mechanics in its original form using the orthonormal position and momentum basis is reviewed. For tunneling of a particle into the classically forbidden region, the imaginary time (Euclidean) formulation of path integral is useful, we review this formulation and apply it to the problem of tunneling in a double well potential. For spin systems such as single molecule magnets, the formulation of path integral requires the use of non-orthonormal spin coherent states in $(2s+1)$ dimensional Hilbert space, the coordinate independent and the coordinate dependent form of the spin coherent state path integral are derived. These two (equivalent) forms of spin coherent state path integral are applied to the tunneling of single molecule magnets through a magnetic anisotropy barrier. Most experimental and numerical results are presented. The suppression of tunneling for half-odd integer spin (spin-parity effect) at zero magnetic field is derived using both forms of spin coherent state path integral, which shows that this result (spin-parity effect) is independent of the choice of coordinate. At nonzero magnetic field we present both the experimental and the theoretical results of the oscillation of tunneling splitting as a function of the applied magnetic field applied along the spin hard anisotropy axis direction. The experimental and the theoretical results of the tunneling in antiferromagnetic exchange coupled dimer model are also reviewed. As the spin coherent state path integral formalism is a semi-classical method, an alternative exact mapping of a spin Hamiltonian to a particle Hamiltonian with a potential field (effective potential method) is derived. This effective potential method allows for the investigation of quantum-classical phase transitions of the escape rate in large spin systems. We present different methods for investigating quantum-classical phase transitions of the escape rate in large spin systems. These methods are applied to different spin models.

PACS numbers: 75.45.+j, 75.50.Tt, 75.30.Gw, 03.65.Sq,75.10.Jm, 75.60.Ej, 61.46.+w

Contents

I. INTRODUCTION

One of the remarkable manifestations of quantum mechanics is the concept of quantum tunneling. This involves the presence of a potential barrier, that is the region where the potential energy is greater than the energy of the particle. In classical mechanics, the tunneling of a particle through this barrier is prohibited as it requires the particle to have a negative kinetic energy, however, in quantum mechanics we find a nonzero probability for finding the particle in the classically forbidden region. Thus, a quantum particle can tunnel through the barrier. In one dimensional systems, the tunneling amplitude (whose modulus squared gives the probability) is usually computed using two fundamental methods, namely, the Wentzel- s-Brillouin (WKB) method (Landau and Lifshitz, 1977) and the "instanton" method(Coleman, 1977, 1985; Dashen, Hasslacher and Neveu, 1974; Gervais and Sakita, 1975; Gervais, Jevicki and Sakita, 1975; Jackiw and Rebbi, 1976; Langer, 1967; Polyakov, 1977) via the Feynman path integral formulation(Feynman and Hibbs, 1965) of quantum mechanics. The term "instanton" refers to classical solutions of the equations of motion when the time coordinate has been continued to Euclidean time, $t \to -i\tau$. For particle in a double well potential with two degenerate minima, the basic understanding is that in the absence of tunneling the classical ground states of the system, which correspond to the minima of the potential, remain degenerate. Tunneling lifts this degeneracy and the true ground state and the first excited state become the symmetric and antisymmetric linear superposition of the classical ground states with an energy splitting between them(Coleman, 1985; Landau and Lifshitz, 1977). In some cases the two minima of the potential are not degenerate. The state with lower energy is the true vacuum, while the state with higher energy is the false vacuum, which is then rendered unstable due to quantum tunneling. In this case one looks for the decay rate of the false vacuum(Coleman, 1977; Callan and Coleman, 1977). Such a scenario plays a vital role in cosmology, especially in the theory of early universe and inflation. Additionally,

in some quantum systems, tunneling does not involve the splitting of the classical ground states or the decay of the false vacuum, but rather a dynamic oscillation of the (phase) difference between two macroscopic order parameters (Cooper, 1956), which are separated by a thin normal layer, through tunneling of the microscopic effective excitations, such as Cooper pairs as in Josephson effect(Esposito et al, *et al.*, 2007; Josephson, 1986).

In the last few decades, the tunneling phenomenon has been extended to other branches of physics. Tunneling has been predicted in single, molecular, large magnetic spin systems such as $MnAc_{12}$, Mn_{12} and Fe_8(Chudnovsky and Gunther, 1988; Enz and Schilling, 1986; Van Hemmen and Sütö, 1986; Wernsdorfer and Sessoli, 1999). These single molecule magnets (SMMs) are composed of several molecular magnetic ions, whose spins are coupled by intermolecular interactions giving rise to an effective single giant spin, which can tunnel through its magnetic anisotropy barrier, hence the name "macroscopic quantum spin tunneling[1]". Van Hemmen and Sütö (1986) first studied the tunneling in a uniaxial ferromagnetic spin model with an applied magnetic field using the WKB method. Enz and Schilling (1986) considered a biaxial model with a magnetic field using instanton technique, subsequently, Chudnovsky and Gunther (1988) studied a more general biaxial spin model by solving the instanton trajectory of the Landau Lifshitz equation. These studies were based on a semi-classical description, that is by representing the spin operator as a unit vector parameterized by spherical coordinates. In this description, the spin is represented by a particle on a two-dimensional sphere $\mathcal{S}^2$, however, in the presence of a topological term, called the Berry's phase term or Wess-Zumino action (Berry, 1984; Wess and Zumino, 1971; Witten , 1979), which effectively corresponds to the magnetic field of a magnetic monopole at the centre of the two sphere. Based on this semi-classical description, it was predicted that for integer spins tunneling is allowed, while for half-odd integer spin tunneling is completely suppressed at zero (external) magnetic field (Henley and Delft, 1992; Loss, DiVincenzo and Grinstein, 1992). The vanishing of tunneling for half-odd integer spins is understood as a consequence of destructive interference between tunneling paths, which is directly related to Kramers degeneracy(Kramers, 1930; Messiah, 1962) due to the time reversal invariance of the Hamiltonian. In the presence of a magnetic field applied along the spin hard axis, Garg (1993) showed that the tunneling splitting does not vanish for half-odd integer spins, but rather oscillates with the field and only vanishes at a certain critical value of the field, which was later observed experimentally in Fe_8 molecular cluster (Sessoli *et al.*, 2000; Wernsdorfer and Sessoli, 1999; Wernsdorfer *et al.*, 2000). In this case tunneling suppression is not related to Kramers degeneracy due to the presence of a magnetic field.

An exact mapping of spin system was considered by Scharf, Wreszinski and Hemmen (1987) and Zaslavskii (1990a); Zaslavskii and Ulyanov (1992). They studied the exact mapping of a spin system unto a particle in a potential field in contrast to the semi-classical approach. This method, which is called the effective potential method, deals with an exact correspondence between a spin Hamiltonian and a particle in a potential field. It gives the possibility for investigating spin tunneling just like a particle in a one-dimensional double well potential. In recent years spin tunneling effect has been observed in many small ferromagnetic spin particles such as Fe_8 (Sangregorio, *et al.*, 1997), $Mn_{12}Ac$ (Friedman *et al.*, 1996; Thomas, *et al.*, 1996; Zhang, *et al.*, 1996), in ferrimagnetic nanoparticles (Wernsdorfer *et al.*, 1997) and also in antiferromagnetic particles (Awshalom, *et al.*, 1992; Gider, *et al.*, 1995; Tejada, *et al.*, 1997),antiferromagnetic exchange coupled dimer $[Mn_4]_2$ (Hill, *et al.*, 2003; Tiron, *et al.*, 2003a) and antiferromagnetic ring clusters with even number of spins (Meier and Loss, 2001; Meier, *et al.*, 2003; Taft, *et al.*, 1994). These molecular magnets also play a decisive role in quantum computing (Leuenberger and Loss, 2001; Tejada, *et al.*, 2001). An extensive review on the experimental analysis of SMMs can be found in (Gatteschi and Sessoli, 2003).

The possibility of quantum tunneling, which is mediated by a vacuum instanton trajectory, requires a very low temperature $T \to 0$. For pure quantum tunneling, the transition amplitude in the stationary phase approximation is $\Gamma = \mathscr{A}e^{-B}$, where B is the vacuum instanton action and $\mathscr{A}$ is a pre-factor. At nonzero temperature, quantum tunneling becomes inconsequential, then the particle has the possibility of crossing over the barrier, a process called classical thermal activation (see Fig.(1)). The study of thermal activation dates back to the work of Kramers (1940) for the diffusion of a particle over the barrier. A review of this subject for both particle and spin system can be found in the existing literature(Coffey, Kalmykov and Waldron, 1996; Hänggi, Talkner and Borkovec, 1990; Stamp, Chudnovsky and Barbara, 1992). In this case the transition is governed by the Van't Hoff-Arrhenius Law (Hänggi, Talkner and Borkovec, 1990) $\Gamma = \mathscr{B}e^{-\beta\Delta U}$, where ΔU is the height of the potential barrier , β is the inverse temperature and $\mathscr{B}$ is a pre-factor.

The basic understanding of quantum-classical phase transitions of the escape rate is as follows: for a particle in a metastable cubic potential or double well quartic parabolic potential $U(x)$, with no environmental influence (dissipation), transition at finite temperature is dominated by thermon (periodic) instanton trajectory[2], whose action

---

[1] In most literature, macroscopic quantum tunneling refers to tunneling in a bias (metastable) potential while macroscopic quantum coherence refers to tunneling in a potential with degenerate minima (Leggett, 1995). We will use the former to refer to both systems.

[2] This is simply the solution of the imaginary time classical equation of motion with an energy $\mathcal{E}$.

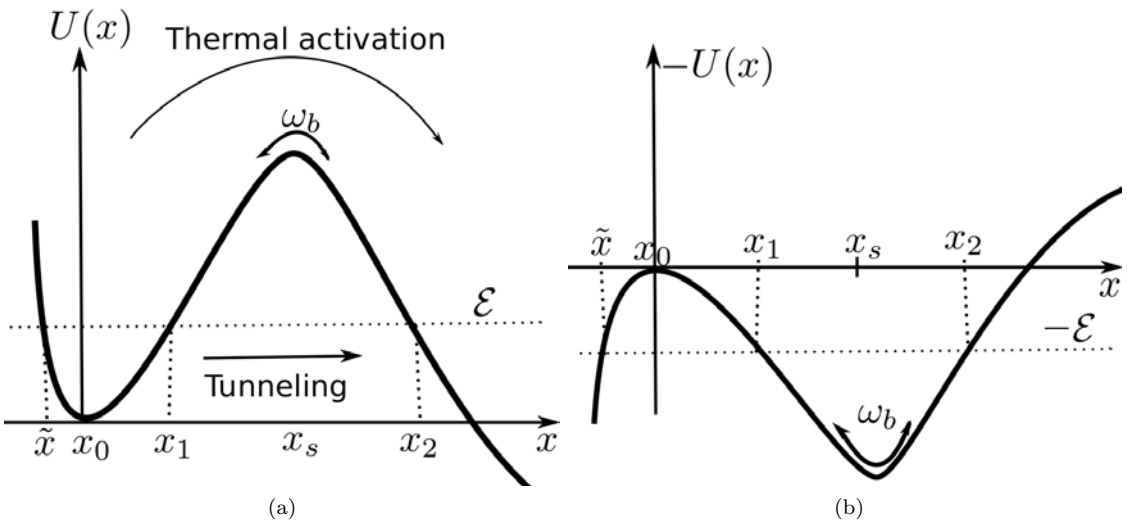

FIG. 1 (a): A sketch of a metastable potential showing the regions of quantum tunneling at low temperature and classical thermal activation at high temperature. (b): The inverted potential. The coordinates x_1 and x_2 are the classical turning points.

is given by $\mathcal{S}_p(\mathcal{E})$ (Chudnovsky, 1992), where $\mathcal{E}$ is the energy of the particle in the inverted potential $-U(x)$. The escape rate is defined by taking the Boltzmann average over tunneling probabilities at finite energy(Affleck, 1981). At the bottom of the barrier we have $\mathcal{S}_p(\mathcal{E}) \to S(U_{\min})$, where $S(U_{\min})$ is the action at the bottom of the barrier, while at the top of the barrier $\mathcal{S}_p(\mathcal{E}) \to \mathcal{S}_0 = \beta\Delta U$, which is the action of a constant trajectory at the top of the barrier.

Now, if we compare the plot of the thermon action $\mathcal{S}_p$ and that of the thermodynamic action $\mathcal{S}_0$ against temperature(Chudnovsky, 1992), there exist a critical temperature T^c at which the thermodynamic action crosses the thermon action. If this intersection is *sharp*, the critical temperature T^c can be thought of as a first-order "phase transition" (crossover) temperature from classical (thermal) to quantum regimes. At this temperature $T^c = T_0^{(1)}$, there is a discontinuity in the first-derivative of the action $\mathcal{S}_p$(Gorokhov and Blatter, 1997). The approximate form of this crossover temperature can be estimated by comparing the quantum action $S(U_{\min})$ at the bottom of the barrier and that of the classical action at the top of the barrier $\mathcal{S}_0$ (Stamp, Chudnovsky and Barbara, 1992)[3]:

$$T_0^{(1)} = \frac{1}{\beta_0^{(1)}} = \frac{\Delta U}{S(U_{\min})} = \frac{\Delta U}{2B}. \tag{1}$$

For a particle with a constant mass, the physical understanding for a sharp first-order phase transition to occur is that the top of the barrier should be flat(Chudnovsky,*et al.*, 1998). This condition is not widely accepted. It has been argued that the necessary condition for a sharp first-order phase transition to occur is that the top of the barrier should be wider so that tunneling through the barrier from the ground state is more auspicious than that from the excited states(Zhang, *et al.*, 1999). For a particle with a position dependent mass, the necessary condition for a sharp first-order phase transition to occur requires the mass of the particle at the top of the barrier to be heavier than that at the bottom of the barrier. In this case tunneling from higher excited states is inauspicious. Thus, thermal activation competes with ground state tunneling leading to first-order phase transition. Thermally assisted tunneling (TAT), that is tunneling from excited states which reduces to ground state tunneling at $T = 0$ occurs for temperatures below $T_0^{(1)}$. In this case the particle tunnels through the barrier at the most favourable energy $\mathcal{E}(T)$, which goes from the top of the barrier to the bottom of the barrier as the temperature decreases (Chudnovsky,*et al.*, 1998).

However, if the intersection of the thermon action $\mathcal{S}_p$ and that of the thermodynamic action $\mathcal{S}_0$ is *smooth*, the critical temperature is said to be of second-order $T^c = T_0^{(2)}$. The second derivative of the thermon action in this case

[3] Actually, the thermon action is defined over the whole period of oscillation of a particle in the inverted potential. In other words, the particle crosses the barrier twice. Thus, $B = S(U_{\min})/2$ as the vacuum instanton is defined by half of the whole period.

has a jump at $T_0^{(2)}$. This crossover temperature is defined as (Goldanskii, 1959a,b)

$$T_0^{(2)} = \frac{1}{\beta_0^{(2)}} = \frac{\omega_b}{2\pi}, \tag{2}$$

where ω_b is the frequency of oscillation at the bottom of the inverted potential $-U(x)$, that is $\omega_b^2 = -\frac{U''(x_s)}{m}$. This formula follows from equating the Van't Hoff-Arrhenius exponential factor $\beta\Delta U$ at finite nonzero temperature and the approximate form of the WKB exponential factor $2\pi\Delta U/\omega_b$ at zero temperature.

Using functional integral approach, Affleck (1981) and Larkin and Ovchinnikov (1983, 1984) demonstrated that, in the regime $T < T_0^{(2)}$, there is a competing effect between thermal activation and quantum tunneling leading to TAT. For $T \gg T_0^{(2)}$, quantum tunneling is suppressed and assisted thermal activation becomes the dominant factor in the escape rate. For $T \approx T_0^{(2)}$, the two regimes smoothly join with a jump of the second derivative of the escape rate. Thus, $T_0^{(2)}$ corresponds to the crossover temperature from thermal regime to TAT. In term of the potential, for a constant mass particle a smooth second-order crossover is favourable with a potential with a parabolic barrier top. An alternative criterion for the first- and the second-order quantum-classical phase transitions was demonstrated by Chudnovsky (1992) based on the shape of the potential. He showed that for a first-order phase transition, the period of oscillation $\beta(\mathcal{E})$ is nonmonotonic function of $\mathcal{E}$, in other words, $\beta(\mathcal{E})$ has a minimum at some point $\mathcal{E}_0 < \Delta U$ and then rises again, while for second-order phase transition $\beta(\mathcal{E})$ is monotonically increasing with decreasing $\mathcal{E}$. Müller, Park and Rana (1999) derived a general criterion formula for investigating first- and second-order phase transitions, which is similar to the criterion formula derived by Kim (1999).

In this report, we will review the theoretical and the experimental developments on macroscopic quantum tunneling and quantum-classical phase transitions of the escape rate in large spin systems. The article is organized as follows. In section(II.A), we will introduce the basic idea of path integral for a one-dimensional particle from Feynman point of view and review its application to the tunneling of a particle in a double well potential. In section(II.B) we will apply this idea to spin systems using spin coherent states. The path integral for spin systems will be derived in the the coordinate independent form. We will show the steps on how to move from coordinate independent to coordinate dependent form. In section (III) we will then apply this coordinate dependent formalism to tunneling problem of SMMs. The quantum phase interference (quenching of tunneling splitting) will be derived and some experimental results will be presented. Due to lack of solution of these models in coordinate independent form in most of the literature, we will show that both the instanton trajectory and the quantum phase interference can be recovered using the coordinate independent formalism. We will further extend our consideration to tunneling in an exchange coupled dimer model and to an antiferromagnetic spin model in general. Section(IV) deals with the effective potential method, we will review the mapping of a large spin model onto a particle Hamiltonian that consists of a potential energy and a mass. In section(V) we will present different methods for studying the quantum-classical phase transitions of the escape rate. We will also apply these methods to both SMMs and exchange coupled dimer model. Theoretical, numerical and experimental results will be presented. In section(VI) we will summarize our analysis and comment on their significance.

II. PATH INTEGRAL FORMULATION

A. Position state path integral

In this section we start with a brief review of path integral formulation of quantum mechanics. This formulation is an elegant alternative method of quantum mechanics. It reproduces the Schrödinger formulation of quantum mechanics and the principle of least action in classical mechanics. In this method the classical action enters into the calculation of a quantum object, the transition amplitude, thereby allowing for a quantum interpretation of a solution of the classical equations of motion. The basic idea of the path integral is that unlike a classical particle with a unique trajectory or path, a quantum particle follows an infinite set of possible trajectories to go from an initial state say $|x\rangle$ at $t = 0$ to a final state say $|x'\rangle$ at time $t = t'$. The sum over all the possible paths (histories of the particle) appropriately weighted, determines the quantum amplitude of the transition. The weight for each path is exactly the phase corresponding to the exponential of the classical action of the path, multiplied by the imaginary number i. Consider a particle moving in one dimension, the Hamiltonian of this system is of usual form:

$$\hat{H} = \frac{\hat{p}^2}{2m} + U(\hat{x}). \tag{3}$$

Let us introduce the complete, orthonormal eigenstates of the position $\hat{x}$ and the momentum $\hat{p}$ operators:

$$\hat{x}\,|x\rangle = x\,|x\rangle\,, \quad \hat{p}\,|p\rangle = p\,|p\rangle\,, \tag{4}$$

$$\langle x'|x\rangle = \delta(x'-x), \quad \langle p'|p\rangle = \delta(p'-p), \tag{5}$$

with

$$\langle x|p\rangle = e^{ipx/\hbar}. \tag{6}$$

The resolution of identities are

$$\int dx\,|x\rangle\,\langle x| = \hat{\mathbf{I}} = \int \frac{dp}{2\pi\hbar}\,|p\rangle\,\langle p|\,. \tag{7}$$

Expressing the unitary operator $e^{-i\hat{H}t}$ as $[e^{-i\hat{H}t/N}]^N$ and using Eqs.(3)–(7), the transition amplitude in the limit $N \to \infty$ is given by (Feynman and Hibbs, 1965; Feynman, 1948)

$$\mathcal{A}(x',t';x,0) = \langle x'|e^{-i\hat{H}t'/\hbar}|x\rangle = \int \mathcal{D}x(t)\,e^{iS[x(t)]/\hbar}, \tag{8}$$

where $\mathcal{D}x(t)$ is the measure for integration over all possible classical paths $x(t)$ that satisfy the boundary conditions $x(0) = x$ and $x(t') = x'$, where

$$S[x(t)] = \int_0^{t'} dtL, \quad L = \frac{1}{2}m\left(\frac{dx}{dt}\right)^2 - U(x), \tag{9}$$

is the classical action and the Lagrangian of the system. We have written down the path integral for a one-dimensional particle, generalization to higher dimensions is straightforward.

The well-known classical equation of motion can be derived in a very simple way. In the semiclassical limit, *i.e.,* $\hbar \to 0$, the phase $e^{iS[x(t)]/\hbar}$ oscillates very rapidly in such a way that nearly all paths cancel each other. The main contribution to the path integral comes from the paths for which the action is stationary, *i.e.,* $\delta S[x(t)] = 0$, which yields the classical equation of motion.

1. Imaginary time path integral formalism

The main motivation of imaginary time propagator comes from the partition function in statistical mechanics, which is given by

$$Z = Tr(e^{-\beta\hat{H}}), \tag{10}$$

where $\beta = 1/T$ is the inverse temperature of the system. Inserting the position resolution of identity in Eqn.(7) into the RHS of Eqn.(10) gives

$$Z = \int dx\mathcal{A}(x,\beta;x,0), \tag{11}$$

where

$$\mathcal{A}(x,\beta;x,0) = \langle x|e^{-\beta\hat{H}}|x\rangle\,. \tag{12}$$

Suppose we consider the time in Eqn.(8) to be purely imaginary, which can be written as $t' = -i\beta$, where β is real. Then, substituting into Eqn.(8) we obtain the propagator evaluated at imaginary time (MacKenzie, 2000; Polyakov, 1977; Weiss and Walter, 1983):

$$\mathcal{A}_E = \langle x'|e^{-\beta\hat{H}/\hbar}|x\rangle = \int \mathcal{D}x(\tau)\,e^{-S_E[x]/\hbar}, \tag{13}$$

where the action is now given by the appropriate analytical continuation of the action, nominally defined as

$$S_E[x] = \int_0^{-i\beta} dt\left[\frac{1}{2}m\left(\frac{dx}{dt}\right)^2 - U(x)\right]. \tag{14}$$

Then setting $x' = x$ in Eqn.(13) yields the partition function Eqn.(12). Thus, the propagator continued to imaginary time gives the partition function. This method is very useful in finding the ground state of a physical system in statistical physics and condensed matter physics. The analytical continuation is obtained by defining a real variable $\tau = it$, which is called the "imaginary or Euclidean time", we see that τ and t are related as follows: $t : 0 \to -i\beta$, $\tau : 0 \to \beta$. Thus, $S_E[x(\tau)] = -iS[x(t \to -i\tau)]$. Typically, if $S[x(t)] = \int dt(T - V)$, the Euclidean action is given by $S_E[x(\tau)] = \int d\tau(T + V)$, as the kinetic energy changes sign with the continuation to imaginary time. The Euclidean action and the Lagrangian are

$$S_E[x(\tau)] = \int_{-\beta/2}^{\beta/2} d\tau L_E; \quad L_E = \frac{1}{2}m\left(\frac{dx}{d\tau}\right)^2 + U(x), \tag{15}$$

using time translation invariance. The boundary conditions for the imaginary time propagator are $x(-\beta/2) = x$ and $x(\beta/2) = x'$. This analysis of imaginary time propagator plays a decisive role in tunneling problems, such as that of a particle in a one dimensional double well potential, since the period of oscillation or the momentum of the particle is imaginary in the tunneling region $\mathcal{E} < \Delta U$(Landau and Lifshitz, 1977; Weiss and Walter, 1983), which is neatly compensated by the imaginary time. Thus, it is almost always convenient to use imaginary time corresponding to the replacement $t \to -i\tau$ (Polyakov, 1977; Weiss and Walter, 1983) when considering tunnelling problems.

2. Instantons in the double well potential

In many textbooks of quantum mechanics, tunneling (barrier penetration) is usually studied using the WKB method. In the tunneling region, the WKB exponent is imaginary, the wave function in the becomes

$$\psi(x) \propto \frac{1}{\sqrt{|p|}} \exp\left[-\int_{-x_1}^{x_1} \frac{|p|}{\hbar} dx\right], \tag{16}$$

where $p = \sqrt{2m(U(x) - \mathcal{E})}$ is the momentum of the particle, and $\pm x_1$ are the classical tunneling points $U(\pm x_1) = \mathcal{E}$. At the ground state, the energy splitting is given by (Landau and Lifshitz, 1977; Weiss and Walter, 1983)

$$\Delta = \frac{\hbar\omega}{\sqrt{e\pi}} \exp\left[-\int_{-a}^{a} \frac{|p|}{\hbar} dx\right], \tag{17}$$

where $\pm a$ are such that $U(\pm a) = \mathcal{E}_0$. The instanton approach, however, uses the imaginary time formulation of path integral to find this ground state energy splitting. If we consider the classical equation of motion in imaginary time $\delta S_E = 0$ we get:

$$m\ddot{x} = \frac{dU(x)}{dx}, \quad \text{where} \quad \ddot{x} \equiv \frac{d^2x}{d\tau^2}, \tag{18}$$

which is the equation of motion with $-U(x)$. In other words, it describes the motion of a particle in an inverted potential as shown in Fig.(2). Upon integration, one finds that the analog of the total "energy" is conserved:

$$\mathcal{E} = \frac{1}{2}m\left(\frac{dx}{d\tau}\right)^2 - U(x). \tag{19}$$

There are at least three possible solutions of this equation of motion. The first solution corresponds to a particle sitting on the top of the left hill $x = -a$ in Fig.(2) , and the second solution corresponds to a particle sitting on the top of the right hill $x = a$. These are constant solutions which do not give any tunneling. However, there is a third solution in which the particle starts at the left hill at $\tau \to -\infty$ rolls over through the dashed line, and finally arrives at the right hill at $\tau \to \infty$. This solution corresponds exactly to the barrier penetration in the WKB method. Such trajectory mediates tunneling and it is called an instanton. Quantum mechanically, the propagator for this instanton trajectory is given by

$$\mathcal{A}\left(-a, -\frac{\beta}{2}; a, \frac{\beta}{2}\right) = \langle a|e^{-\beta\hat{H}/\hbar}|-a\rangle\,. \tag{20}$$

For instance, the potential could be taken to be

$$U(x) = \frac{\omega_0^2}{4}(x^2 - a^2)^2, \tag{21}$$

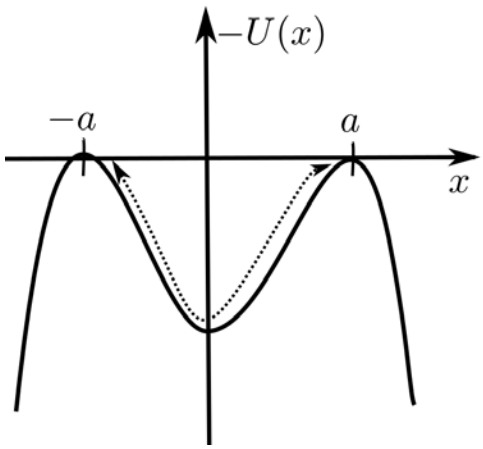

FIG. 2 A sketch of an inverted double well potential with two minima at $\pm a$. There are two trivial solutions corresponding to a fixed motion of the particle at the top of the left or right hill of the potential. Tunneling is achieved by a nontrivial solution in which the particle starts at the top of the left hill at $\tau \to -\infty$ and roll through the dashed line and emerges at the top of the right hill at $\tau \to +\infty$. Such a solution is called an instanton.

but it is actually not necessary to make a specific choice, just the general form pictured in Fig.2 needs to be satisfied. Tunneling between the two minima of $U(x)$ requires the computation of the transition amplitudes:

$$\langle \pm a | e^{-\beta \hat{H}/\hbar} | -a \rangle \, . \tag{22}$$

In order to calculate this amplitude one has to know the solution of the classical equation of motion that obeys the boundary condition of Eqn.(13) as $\beta \to \infty$. There are two trivial solutions corresponding to no motion with the particle fixed at the top of the left or right hill of the potential. Tunneling is achieved by a nontrivial solution in which the particle starts at the top of the left hill at $\tau \to -\infty$, roll through the dashed line in Fig.(2), and emerges at the top of the right hill at $\tau \to +\infty$. This nontrivial solution has zero "energy" $\mathcal{E} = 0$ since initially it starts at the top of the hill at $-a$ where the potential is zero and its kinetic energy is zero. The solution of Eqn.(19) corresponding to the explicit potential Eqn. (21), is given by (MacKenzie, 2000; Polyakov, 1977)

$$x(\tau) = a \tanh[\frac{\omega_0}{2}(\tau - \tau_0)], \quad \omega_0^2 = \gamma a^2/m, \tag{23}$$

where τ_0 is an integration constant which corresponds to the time at which the solution crosses $x = 0$.

The action for the solution is given by

$$\begin{aligned} B &= \int_{-\beta/2}^{\beta/2} d\tau \left[\frac{1}{2} m \left(\frac{dx}{d\tau} \right)^2 + U(x) \right], & (24) \\ &= \int_{-\beta/2}^{\beta/2} d\tau \sqrt{2mU(x)} \frac{dx}{d\tau}, & (25) \\ &= \int_{-a}^{a} dx \sqrt{2mU(x)}, & (26) \\ &= \frac{2\sqrt{2m}}{3} \omega_0 a^2, & (27) \end{aligned}$$

where $\mathcal{E} = 0$ from Eqn.(19) is used in the second line, and only in the last equation is the specific potential Eqn.(21) used. This action is exactly the WKB exponent in Eqn.(17). In the approximation of the method of steepest descent, the path integral, Eqn.(13) is dominated by the path which passes through the configuration for which the action is stationary, *i.e.,* Eqn.(23), and the integral is given by the Gaussian approximation about the stationary point. Then, the one instanton contribution to the transition amplitude is (Coleman, 1977, 1985)

$$\langle a | e^{-\beta \hat{H}/\hbar} | -a \rangle \propto e^{-B/\hbar} [1 + O(\hbar)]. \tag{28}$$

In fact, one must consider other critical points which correspond to a dilute instanton gas. The justification of the dilute instanton gas approximation is beyond the purview of this review, we refer the reader to dedicated expositions of the subject, (Coleman, 1977, 1985). The upshot is that one must sum over all sequences of one instanton followed by any number of anti-instanton/instanton pairs, the total number of instantons and anti-instantons is odd for the transition $-a \leftrightarrow a$ but even for the transition $-a \rightarrow -a$ ($a \rightarrow a$). The result of this summation yields (Coleman, 1985)

$$\langle \pm a|e^{-\beta\hat{H}/\hbar}|-a\rangle = \mathcal{N}\frac{1}{2}[\exp(\mathscr{D}\beta e^{-B/\hbar}) \mp \exp(-\mathscr{D}\beta e^{-B/\hbar})], \tag{29}$$

where $\mathcal{N}$ is the overall normalization including the square root of the free determinant which is given by $Ne^{-\beta\mathcal{E}_0}$ where $\mathcal{E}_0 = \frac{1}{2}\hbar\omega_0$ is the unperturbed ground state energy and N is a constant from the ground state wave function. $\mathscr{D}$ is the ratio of the square root of the determinant of the operator governing the second order fluctuations about the instanton excluding the time translation zero mode, and that of the free determinant. It can in principle be calculated. A zero mode, occurring because of time translation invariance, is not integrated over, and is taken into account by integrating over the Euclidean time position of the occurrence of the instanton giving rise to the factor of β. The left hand side of Eqn.(29) can also be written as

$$\langle \pm a|e^{-\beta\hat{H}/\hbar}|-a\rangle = \sum_n \langle \pm a|n\rangle \langle n|-a\rangle e^{-\beta\mathcal{E}_n}, \tag{30}$$

where $\hat{H}|n\rangle = \mathcal{E}_n|n\rangle$. Taking the upper sign on both sides of Eqs.(29) and (30) and comparing the terms, one finds that the non-perturbative energy splitting between the ground and the first excited states is given by

$$\Delta = \mathcal{E}_1 - \mathcal{E}_0 = 2\hbar\mathscr{D}e^{-B/\hbar}. \tag{31}$$

In a similar manner, by comparing the coefficients one obtains symmetric ground state

$$|\mathcal{E}_0\rangle = \frac{1}{\sqrt{2}}\left(|a\rangle + |-a\rangle\right), \tag{32}$$

and an antisymmetric first excited state

$$|\mathcal{E}_1\rangle = \frac{1}{\sqrt{2}}\left(|a\rangle - |-a\rangle\right). \tag{33}$$

The analysis in the first part of this review will be based on computing the instanton trajectory, its action, and the corresponding energy splitting for any given model that possesses tunneling.

B. Spin coherent state path integral

For a spin system, the basic idea of path integral formulation is retained, however, instead of the orthogonal position $|x\rangle$ and momentum $|p\rangle$ basis, a basis of spin coherent states is used (Klauder, 1979; Lieb, 1973; Perelomov, 1986; Radcliffe, 1971). This basis is defined through the following construction. Let $|s,s\rangle$ be the highest weight vector in a particular representation of the rotation group, taken as its simply connected covering group $SU(2)$. This state is an eigenstate of the operators $\hat{S}_z$ and $\hat{\mathbf{S}}$:

$$\hat{S}_z|s,s\rangle = s|s,s\rangle; \quad \hat{\mathbf{S}}^2|s,s\rangle = s(s+1)|s,s\rangle. \tag{34}$$

The spin operators $\hat{S}_i$, $i = x,y,z$ form an irreducible representation of the Lie algebra of $SU(2)$,

$$[\hat{S}_i, \hat{S}_j] = i\epsilon_{ijk}\hat{S}_k, \tag{35}$$

where ϵ_{ijk} is the totally antisymmetric tensor symbol and summation over repeated indices is implied in Eqn.(35). The coherent state, $|\hat{\mathbf{n}}\rangle$, an element of the $2s+1$ dimensional Hilbert (representation) space for the spin states, is defined as (Eduardo and Stone, 1988; Eduardo, 1991; Klauder, 1979; Lieb, 1973; Perelomov, 1986; Zhang, Feng and Gilmore, 1990)

$$|\hat{\mathbf{n}}\rangle = e^{i\theta\hat{\mathbf{m}}\cdot\hat{\mathbf{S}}}|s,s\rangle = \sum_{m=-s}^{s}\mathcal{M}^s(\hat{\mathbf{n}})_{ms}|s,m\rangle, \tag{36}$$

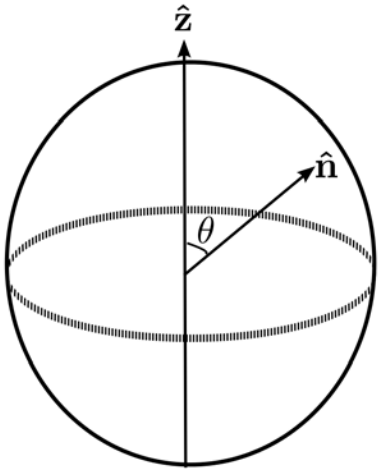

FIG. 3 The directions of the unit vectors $\hat{\mathbf{z}}$ and $\hat{\mathbf{n}}$ on a two-sphere .

where $\hat{\mathbf{n}} = (\cos\phi\sin\theta, \sin\phi\sin\theta, \cos\theta)$ is a unit vector ie. $\hat{\mathbf{n}}^2 = 1$ and $\hat{\mathbf{m}} = (\hat{\mathbf{n}} \times \hat{\mathbf{z}})/|\hat{\mathbf{n}} \times \hat{\mathbf{z}}|$ is a unit vector orthogonal to $\hat{\mathbf{n}}$ and where $\hat{\mathbf{z}}$ is the quantization axis pointing from the origin to the north pole of a unit sphere and $\hat{\mathbf{n}} \cdot \hat{\mathbf{z}} = \cos\theta$ as shown in Fig.(3). Rotating the unit vector $\hat{\mathbf{z}}$ about the $\hat{\mathbf{m}}$ direction by the angle θ brings it exactly to the unit vector $\hat{\mathbf{n}}$. $|\hat{\mathbf{n}}\rangle$ corresponds to a rotation of an eigenstate of $\hat{S}_z$, i.e $|s, s\rangle$, to an eigenstate with a quantization axis along $\hat{\mathbf{n}}$ on a two-dimensional sphere $\mathcal{S}^2 = SU(2)/U(1)$. The matrices $\mathcal{M}^s(\hat{\mathbf{n}})$ satisfy the relation

$$\mathcal{M}^s(\hat{\mathbf{n}}_1)\mathcal{M}^s(\hat{\mathbf{n}}_2) = \mathcal{M}^s(\hat{\mathbf{n}}_3)e^{i\mathcal{G}(\hat{\mathbf{n}}_1,\hat{\mathbf{n}}_2,\hat{\mathbf{n}}_3)\hat{S}_z}, \tag{37}$$

where $\mathcal{G}(\hat{\mathbf{n}}_1, \hat{\mathbf{n}}_2, \hat{\mathbf{n}}_3)$ is the area of a spherical triangle with vertices $\hat{\mathbf{n}}_1, \hat{\mathbf{n}}_2, \hat{\mathbf{n}}_3$. Note that Eqn.(37) is not a group multiplication, thus the matrices $\mathcal{M}^s(\hat{\mathbf{n}})$ do not form a group representation. Unlike the position and momentum eigenstates in Eqn.(5), the inner product of two coherent states is not orthogonal:

$$\langle\hat{\mathbf{n}}|\hat{\mathbf{n}}'\rangle = e^{is\mathcal{G}(\hat{\mathbf{n}},\hat{\mathbf{n}}',\hat{\mathbf{z}})}[\frac{1}{2}(1 + \hat{\mathbf{n}} \cdot \hat{\mathbf{n}}')]^s. \tag{38}$$

It has the following property:

$$\hat{\mathbf{n}} \cdot \hat{\mathbf{S}}\,|\hat{\mathbf{n}}\rangle = s\,|\hat{\mathbf{n}}\rangle \Rightarrow \langle\hat{\mathbf{n}}|\hat{\mathbf{S}}|\hat{\mathbf{n}}\rangle = s\hat{\mathbf{n}}. \tag{39}$$

The resolution of identity is given by

$$\hat{\mathbf{I}} = \frac{2s+1}{4\pi}\int d^3\hat{\mathbf{n}}\delta(\hat{\mathbf{n}}^2 - 1)\,|\hat{\mathbf{n}}\rangle\,\langle\hat{\mathbf{n}}|\,, \tag{40}$$

where $\hat{\mathbf{I}}$ is a $(2s+1) \times (2s+1)$ identity matrix, and the delta function ensures that $\hat{\mathbf{n}}^2 = 1$. The derivation of spin coherent state path integral now follows a similar fashion with Sec.(II.A). Using the expression in Eqn.(38) and Eqn.(40) one can express the imaginary time transition amplitude between $|\hat{\mathbf{n}}_i\rangle$ and $|\hat{\mathbf{n}}_f\rangle$ as a path integral. The analogous form of Eqn.(13) for spin system is given by (Eduardo, 1991; Zhang, Feng and Gilmore, 1990)

$$\langle\hat{\mathbf{n}}_f|e^{-\beta\hat{H}(\hat{\mathbf{S}})}|\hat{\mathbf{n}}_i\rangle = \int \mathcal{D}\hat{\mathbf{n}}\, e^{-S_E[\hat{\mathbf{n}}]}, \tag{41}$$

where

$$S_E[\hat{\mathbf{n}}] = isS_{WZ} + \int d\tau U(\hat{\mathbf{n}}(\tau)), \quad U(\hat{\mathbf{n}}(\tau)) = \langle\hat{\mathbf{n}}|\hat{H}|\hat{\mathbf{n}}\rangle\,, \tag{42}$$

and S_{WZ} arises because of the additional phase $e^{is\mathcal{G}(\hat{\mathbf{n}},\hat{\mathbf{n}}',\hat{\mathbf{z}})}$ in Eqn.(38). We have set $\hbar = 1$ in the path integral. The Wess-Zumino (WZ) action, S_{WZ} is given by[4] (Eduardo and Stone, 1988; Eduardo, 1991; Novikov, 1982; Wess and

[4] An alternative way of deriving this equation can be found in (Blasone and Jizba, 2012).

Zumino, 1971; Witten , 1979)

$$S_{WZ} = \int_{\frac{1}{2}\mathcal{S}^2} d\tau d\xi\, \hat{\mathbf{n}}(\tau,\xi) \cdot [\partial_\tau \hat{\mathbf{n}}(\tau,\xi) \times \partial_\xi \hat{\mathbf{n}}(\tau,\xi)], \tag{43}$$

where $\hat{\mathbf{n}}(\tau)$ has been extended over a topological half-sphere $\frac{1}{2}\mathcal{S}^2$ in the variables τ, ξ. In the topological half-sphere we define $\hat{\mathbf{n}}$ with the boundary conditions

$$\hat{\mathbf{n}}(\tau,0) = \hat{\mathbf{n}}(\tau), \;\; \hat{\mathbf{n}}(\tau,1) = \hat{\mathbf{z}}, \tag{44}$$

so that the original configuration lies at the equator and the point $\xi = 1$ is topologically compactified by the boundary condition. This can be easily obtained by imagining that the original closed loop $\hat{\mathbf{n}}(\tau)$ at $\xi = 0$ is simply pushed up to along the meridians to $\hat{\mathbf{n}}(\tau) = \hat{\mathbf{z}}$ at $\xi = 1$. The Wess-Zumino term originates from the non-orthogonality of spin coherent states in Eqn.(38). Geometrically, it defines the area of the closed loop on the spin space, defined by the nominally periodic, original configuration $\hat{\mathbf{n}}(\tau)$. It crucial to note that there is an ambiguity of modulo 4π, since different ways of pushing the original configuration up can give different values for the area enclosed by the closed loop as one can imagine that the closed loop englobes the whole two sphere any integer number of times, but this ambiguity has no physical significance since $e^{i4N\pi s} = 1$ for integer and half-odd integer s. The action, Eqn.(42) is valid for a semiclassical spin system whose phase space is $\mathcal{S}^2$. It is the starting point for studying macroscopic quantum spin tunneling between the minima of the energy $U(\hat{\mathbf{n}})$.

III. MACROSCOPIC QUANTUM TUNNELING OF LARGE SPIN SYSTEMS

A. Coordinate dependent formalism

Most often a coordinate dependent version of Eqn.(43) is used in the condensed matter literature. It seems that most people find it difficult to study macroscopic quantum spin tunneling in the coordinate independent form. In this section, we will show how one can use any coordinate system of interest. In section (III.B), we will show that the coordinate independent form can reproduce all the known results in quantum spin tunneling. Since the spin particle lives on a two-sphere, the most convenient choice of coordinate are spherical polar coordinates. Parametrizing the unit vector as $\hat{\mathbf{n}}(\tau,\xi) = (\cos\phi(\tau)\sin\theta_\xi(\tau), \sin\phi(\tau)\sin\theta_\xi(\tau), \cos\theta_\xi(\tau))$, with $\theta_\xi(\tau) = (1-\xi)\theta(\tau)$, which satisfies the boundary conditions, Eqn.(44) at $\xi = 0$ and $\xi = 1$. Then

$$\partial_\tau \hat{\mathbf{n}} = \hat{\boldsymbol{\theta}}\dot{\theta}_\xi(\tau) + \hat{\boldsymbol{\phi}} \sin\theta_\xi(\tau)\dot{\phi}(\tau), \tag{45}$$

and

$$\partial_\xi \hat{\mathbf{n}} = \hat{\boldsymbol{\theta}}(-\theta(\tau)), \tag{46}$$

where $\hat{\boldsymbol{\theta}}$ and $\hat{\boldsymbol{\phi}}$ are the usual polar and azimuthal unit vectors which form an orthogonal triad with $\hat{\mathbf{n}}$ such that $\hat{\boldsymbol{\theta}} \times \hat{\boldsymbol{\phi}} = \hat{\mathbf{n}}$ (and cyclic permutations). Thus we find the triple product becomes

$$\hat{\mathbf{n}}(\tau,\xi) \cdot (\partial_\tau \hat{\mathbf{n}}(\tau,\xi) \times \partial_\xi \hat{\mathbf{n}}(\tau,\xi)) = \dot{\phi}(\tau)\theta(\tau)\sin\theta_\xi(\tau). \tag{47}$$

Thus, the WZ term, Eqn.(43) simplifies to (Khare and Paranjape, 2011; Owerre and Paranjape, 2013)

$$S_{WZ} = \int d\tau \int_0^1 d\xi\, \dot{\phi}(\tau)\theta(\tau)\sin\theta_\xi(\tau) = \int d\tau\, \dot{\phi}(\tau)(1-\cos\theta(\tau)). \tag{48}$$

This is the coordinate dependent form of WZ term or Berry phase (Berry, 1984), which is the expression found in most condensed matter literature. It corresponds to the area of the unit two-sphere swept out by $\hat{\mathbf{n}}(\tau)$ as it forms a closed path on $\mathcal{S}^2$. To understand this explicitly, one can think of the integral in Eqn.(48) as a line integral of a gauge field, which only has a ϕ component, integrated over a closed path on the two sphere, parametrized by τ. We denote the closed path as $\mathcal{C}$ and it is the boundary of a region $\mathcal{S}$, with evidently $\mathcal{C} = \partial\mathcal{S}$, then

$$\int d\tau\, \dot{\phi}(\tau)(1-\cos\theta(\tau)) = \oint_{\mathcal{C}} A_\phi d\phi. \tag{49}$$

Then using Stokes theorem, we have

$$\oint_{\mathcal{C}} A_\phi d\phi = \int_{\mathcal{S}} d(A_\phi d\phi), \tag{50}$$

written in the notation of differential forms. However, the gauge field $\vec{A} = A_\phi \hat{\boldsymbol{\phi}} = (1 - \cos\theta)\hat{\boldsymbol{\phi}}$ corresponds exactly to the gauge field of a magnetic monopole located at the centre of the sphere. Such a gauge field was first described by Dirac (Dirac , 1931), and gives rise to a constant radial magnetic field, apart from a string singularity located at the south pole, which is an unobservable gauge artefact if the magnetic charge is appropriately quantized. The non observability of this string singularity in quantum mechanics was the seminal observation by Dirac if s, in Eqn.(42), is quantized to be a half integer. Explicitly, the corresponding magnetic field is simply $d(A_\phi d\phi) = \partial_\theta A_\phi d\theta \wedge d\phi = \sin\theta d\theta \wedge d\phi$ which is the area element in spherical polar coordinates on the unit two sphere. Thus $\oint_{\mathcal{C}} A_\phi d\phi = \int_{\mathcal{S}} d(A_\phi d\phi) = \int_{\mathcal{S}} \sin\theta d\theta \wedge d\phi = \text{area}\,(\mathcal{S})$.

The general form of the Euclidean action in coordinate dependent formalism is then

$$S_E = is \int d\tau\, \dot{\phi}(\tau) + S_0, \tag{51}$$

where

$$S_0 = \int d\tau [\, -is\dot{\phi}(\tau)\cos\theta(\tau) + U(\theta(\tau), \phi(\tau))]. \tag{52}$$

The first term in Eqn.(51) is a boundary term, which does not affect the classical equation of motion. It can be integrated out as

$$is \int_{-\frac{\beta}{2}}^{\frac{\beta}{2}} d\tau\, \dot{\phi}(\tau) = is[\phi(\beta/2) - \phi(-\beta/2) + 2\pi N], \tag{53}$$

where N is a winding number, that is the number of times $\phi(\tau)$ winds around the north pole of $\mathcal{S}^2$ as τ progresses from $-\beta/2$ to $\beta/2$. This term is insensitive to any continuous deformation of the field on $\mathcal{S}^2$, thus it is topological. Its effect on the transition amplitude will be studied later.

1. Easy z-axis uniaxial spin model in a magnetic field

Having derived the coordinate dependent action for a spin system, we will now turn to specific models where this formula can be implemented. Consider a uniaxial system with an easy $\hat{\mathbf{z}}$ axis (direction of minimum energy) and a magnetic field along the $\hat{\mathbf{x}}$ axis, the corresponding Hamiltonian is given by (Chudnovsky and Gunther, 1988; Van Hemmen and Sütö, 1986)

$$\hat{H} = -D\hat{S}_z^2 - H_x\hat{S}_x, \tag{54}$$

where $D > 0$ is the easy axis anisotropy and $H_x = g\mu_B h$, h is the magnitude of the field, g is the spin g-factor and μ_B is the Bohr magneton. This model is a special case of the Lipkin-Meshkov-Glick model introduced in nuclear physics (Lipkin, Meshkov and Glick, 1965), which has been recently exactly solved (Ribeiro, Vidal and Mosseri, 2007, 2008). This Hamiltonian is a good approximation for Mn_{12} acetate molecular magnet with a ground state of $s = 10$ (Chudnovsky,*et al.*, 1998; Chudnovsky and Garanin, 1997; Friedman *et al.*, 1996; Novak and Sessoli, 1994; Paulsen and Park, 1994). An experimental review of this molecular magnet can be found in (Gatteschi and Sessoli, 2003). The description of the tunneling of spin in the quantum spin terminology is as follows. For $H_x = 0$, the Hamiltonian has a two fold degenerate ground state corresponding to the two ground states in the $\hat{S}_z$ representation, *i.e,* $|\uparrow\rangle$ and $|\downarrow\rangle$, where $|\uparrow\rangle \equiv |s\rangle$ and $|\downarrow\rangle \equiv |-s\rangle$. For $H_x \neq 0$, these two states are no longer degenerate since $\hat{S}_x = (\hat{S}_+ + \hat{S}_-)/2$ where $\hat{S}_+ |-s\rangle \propto |-s+1\rangle$ and $\hat{S}_- |s\rangle \propto |s-1\rangle$. In the limit of small magnetic field, perturbation theory on the magnetic field term shows that the two degenerate ground states are split with an energy difference which is given by (Garanin , 1991; Zaslavskii and Ulyanov, 1999)

$$\Delta = \frac{4Ds^{3/2}}{\pi^{1/2}} \left(\frac{eh_x}{2}\right)^{2s}, \quad h_x = H_x/2Ds. \tag{55}$$

The factor h_x^{2s} signifies that the splitting arises from $2s^{\text{th}}$ order in degenerate perturbation theory. This implies that the two quantum states $|\uparrow\rangle$ and $|\downarrow\rangle$ can tunnel to each other through a magnetic energy barrier, a process called

quantum spin tunneling [5]. Thus, the ground and the first excited states become the symmetric and antisymmetric linear superposition of the degenerate states:

$$|g\rangle = \frac{1}{\sqrt{2}}(|\uparrow\rangle + |\downarrow\rangle); \quad |e\rangle = \frac{1}{\sqrt{2}}(|\uparrow\rangle - |\downarrow\rangle). \tag{56}$$

In the absence of the perturbative or splitting term, the energy splitting in Eqn.(55) vanishes, which directly implies that tunneling is only allowed when the Hamiltonian does not commute with the quantization axis, in this case $\hat{S}_z$. In the semi-classical analysis, the spin operator becomes a vector parametrized by spherical coordinate of length:

$$S_x^2 + S_y^2 + S_z^2 = s^2. \tag{57}$$

The corresponding classical energy of Eqn.(54) is given by

$$U(\theta, \phi) = Ds^2 \sin^2\theta - H_x s \sin\theta\cos\phi + H_x^2/4D, \tag{58}$$

where an additional constants have been added to normalize the minimum of the potential to zero. The minimum energy requires

$$\left.\frac{\partial U}{\partial \theta}\right|_{\phi=0} = 0 \quad \text{and} \quad \left.\frac{\partial^2 U}{\partial \theta^2}\right|_{\phi=0} > 0, \tag{59}$$

which yields two classical degenerate minima at $(\phi, \theta) = (0, \theta_0)$ and $(\phi, \theta) = (0, \pi - \theta_0)$ with $\sin\theta_0 = h_x = H_x/H_c$, provided $H_x < H_c = 2Ds$. The maximum energy corresponds to $(\phi, \theta) = (0, \pi/2)$.

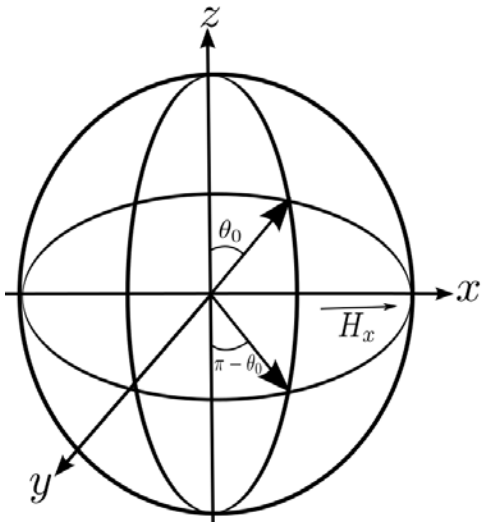

FIG. 4 The description of a classical spin (thick arrows) on a two-sphere with two classical ground states at $\phi = 0$. The magnetic field is applied parallel to the x-axis. The x-axis has been rotated on the right hand side for proper view.

These two classical minima correspond to the spin pointing in $\pm zx$ plane (see Fig.(4)), which are analogous to the two quantum states $|\uparrow\rangle$ and $|\downarrow\rangle$. The barrier height is

$$\Delta U = U_{\max} - U_{\min} = Ds^2(1 - h_x)^2. \tag{60}$$

Due to tunneling the degeneracy of these ground states will be lifted and one finds that the true ground state is the linear superposition of the two unperturbed ground states. This tunneling is mediated by an instanton which is

---

[5] In the semi-classical description, tunneling means the rotation of the two equivalent directions of the spin on a two-sphere as shown in Fig.(4)

a solution of the classical equations of motion:

$$is\dot{\theta}\sin\theta = \frac{\partial U}{\partial \phi}, \tag{61}$$

$$is\dot{\phi}\sin\theta = -\frac{\partial U}{\partial \theta}. \tag{62}$$

These equations are obtained from the least-action principle, whose solution gives the classical path for which the action, Eqn.(51) is stationary $\delta S_E = 0$. Although one is usually interested in a real, physical trajectory, these equations are in fact, incompatible, unless one variable (either θ or ϕ) becomes imaginary. The energy along the trajectory has to vanish, since it is conserved by the dynamics, and normalized to zero at the starting point. This can be seen by multiplying Eqn.(61) by $\dot{\phi}$ and Eqn.(62) by $\dot{\theta}$ and subtracting the resulting equations which yields

$$\frac{\partial U}{\partial \phi}\dot{\phi} + \frac{\partial U}{\partial \theta}\dot{\theta} = 0 \quad \Rightarrow \quad U(\theta,\phi) = \text{const.} = 0. \tag{63}$$

The transition amplitude, Eqn.(41), in the coordinate dependent form can be written as

$$\langle \theta_f, \phi_f | e^{-\beta \hat{H}} | \theta_i, \phi_i \rangle = \int \mathcal{D}\phi \mathcal{D}(\cos\theta)\, e^{-S_E}, \tag{64}$$

which defines the transition from an initial state $|\theta_i, \phi_i\rangle$ at $\tau = -\beta/2$ to a final state $|\theta_f, \phi_f\rangle$ at $\tau = \beta/2$, subject to the boundary conditions $(\phi(-\beta/2), \theta(-\beta/2)) = (\phi_i, \theta_i)$ and $(\phi(\beta/2), \theta(\beta/2)) = (\phi_f, \theta_f)$. In most cases of physical interest, either $\phi_i = \phi_f$ or $\theta_i = \theta_f$. In the present problem $\phi_i = \phi_f = 0$ while $\theta_i = \theta_0$ and $\theta_f = \pi - \theta_0$. Similar to the double well problem in Fig.(2), the boundary conditions require that the real tunneling trajectory (either θ or ϕ not both) approaches the two minima of U at $\tau = \pm\infty$. Using Eqn.(58) one obtains from Eqn.(63)

$$\sin(\phi/2) = \pm i(\sin\theta - \sin\theta_0)/2\sqrt{\sin\theta \sin\theta_0}. \tag{65}$$

From Eqs.(58), (61) and (65), the classical trajectory (instanton) is found to be (Chudnovsky and Gunther, 1988; Garg and Kim, 1992)

$$\cos\theta(\tau) = -\cos\theta_0 \tanh(\omega_h \tau), \quad \omega_h = Ds\cos\theta_0, \tag{66}$$

which interpolates from $\theta(\tau) = \theta_0$ at $\tau = -\infty$ to $\theta(\tau) = \pi - \theta_0$ at $\tau = \infty$. Since the energy remains constant (which is normalized to zero) along the instanton trajectory, the action for this trajectory is determined only by the WZ term in Eqn.(51). It is found to be (Garg and Kim, 1992)

$$B = 2s\left[\frac{1}{2}\ln\left(\frac{1+\cos\theta_0}{1-\cos\theta_0}\right) - \cos\theta_0\right]. \tag{67}$$

Absence of tunneling when $h_x = 0$ corresponds to $B = \infty$. The energy splitting in the dilute instanton gas approximation is given by (Garg and Kim, 1992; Garg, 2000)

$$\Delta = \frac{8Ds^{3/2}\cos^{5/2}\theta_0}{\pi^{1/2}\sin\theta_0}\left(\frac{1-\cos\theta_0}{1+\cos\theta_0}\right)^{s+\frac{1}{2}} e^{2s\cos\theta_0}. \tag{68}$$

In the perturbative limit, that is for a very small magnetic field, $\theta_0 \to 0$, the splitting, Eqn.(68) reduces to

$$\Delta = \frac{8Ds^{3/2}(1-h_x^2/2)^{5/2}e^{2s(1-h_x^2/2)}}{\pi^{1/2}(4-h_x^2)^{s+\frac{1}{2}}} h_x^{2s}. \tag{69}$$

The factor h_x^{2s} reproduces the correct order of perturbation theory result as given in Eqn.(55).

2. Biaxial spin model and quantum phase inteference

Let us consider the biaxial spin model in the absence of an external magnetic field (Chudnovsky and Gunther, 1988; Enz and Schilling, 1986; Loss, DiVincenzo and Grinstein, 1992)

$$\hat{H} = D_1 \hat{S}_z^2 + D_2 \hat{S}_x^2; \quad D_1 > D_2 > 0. \tag{70}$$

In the classical terminology, this model possesses an XOY-easy-plane anisotropy with an easy-axis along the y-direction, hard-axis along the z-direction and medium axis along the x-direction. Quantum mechanically, the easy axis corresponds to the quantization axis, since the Casimir operator $\hat{\mathbf{S}}^2 = \hat{S}_x^2 + \hat{S}_y^2 + \hat{S}_z^2 = s(s+1)$, can be used to rewrite Eqn.(70) as

$$\hat{H} = -D_2 \hat{S}_y^2 + (D_1 - D_2)\hat{S}_z^2 + \text{const.} \tag{71}$$

The first term is the unperturbed term while the second term is the transverse or splitting term which does not commute with the unperturbed term. Thus, the minimum energy of this Hamiltonian requires a representation in which $\hat{S}_y$ is diagonal. This means that different representations of a biaxial spin Hamiltonian in the absence of an external magnetic field [6] can be related to each other by redefining the anisotropy constants. For instance Eqn.(70) is related to $\hat{H} = -A\hat{S}_x^2 + B\hat{S}_z^2$ (Enz and Schilling, 1986) by $D_2 = A$, $D_1 = A + B$. Thus, it suffices to consider just Eqn.(70). Semiclassically, the corresponding classical energy is

$$U(\theta, \phi) = D_1 s^2 \cos^2\theta + D_2 s^2 \sin^2\theta \cos^2\phi. \tag{72}$$

The minimum energy corresponds to $(\phi, \theta) = (\pm\pi/2, \pi/2)$, which are located at $\pm\hat{\mathbf{y}}$ as shown in Fig.(6), and the maximum is located at $(\phi, \theta) = (0, \pi/2)$. From the conservation of energy Eqn.(63) one obtains

$$\cos\theta = \pm i \frac{\sqrt{\lambda}\cos\phi}{\sqrt{1 - \lambda\cos^2\phi}}, \quad \lambda = D_2/D_1. \tag{73}$$

Taking into account that the deviation of the spin away from the easy plane is very small, an alternative method to eliminate θ from the equation of motion is to integrate out $\cos\theta$ in Eqn.(64)(Chudnovsky and Martinez, 2000; Enz and Schilling, 1986; Zhang, *et al.*, 1998). In this case the resulting action has a quadratic first order derivative term, a coordinate (ϕ) dependent mass and a potential . Integration of the classical equation of motion Eqn.(62) yields (Chudnovsky and Gunther, 1988; Enz and Schilling, 1986; Zhang, *et al.*, 1998)

$$\sin\phi(\tau) = \frac{\sqrt{1-\lambda}\tanh(\omega\tau)}{\sqrt{1 - \lambda\tanh^2(\omega\tau)}}, \quad \omega = 2s\sqrt{D_1 D_2}, \tag{74}$$

which corresponds to the tunneling of the spin from $\phi = \pi/2$ at $\tau = \infty$ to $\phi = -\pi/2$ at $\tau = -\infty$. The instanton action for this trajectory is

$$S_c = is\int_{-\frac{\pi}{2}}^{\frac{\pi}{2}} d\phi + B, \tag{75}$$

where B is given by

$$B = s\sqrt{\lambda}\int_{-\frac{\pi}{2}}^{\frac{\pi}{2}} d\phi \, \frac{\cos\phi}{\sqrt{1 - \lambda\cos^2\phi}} = \ln\left(\frac{1+\sqrt{\lambda}}{1-\sqrt{\lambda}}\right)^s. \tag{76}$$

Now, consider for example the path $(\phi(\tau), \theta(\tau))$ connecting the two anisotropy minima at $(\phi, \theta) = (\pm\pi/2, \pi/2)$, then owing to the symmetry of the action S_0, Eqn.(52) (that is excluding the total derivative term), the path $(-\phi(\tau), \pi - \theta(\tau))$ will also solve the classical equations of motion and B will be the same for both paths but the total derivative term will be reversed: $is\int_{\mp\frac{\pi}{2}}^{\pm\frac{\pi}{2}} d\phi = \pm is\pi$. Since the path integral in Eqn.(64) contains all paths, in the semiclassical (small $\hbar$) approximation (Coleman, 1977, 1985; Weiss and Walter, 1983), the contributions of these two paths can be combined to give

$$e^{i\pi s}e^{-B} + e^{-i\pi s}e^{-B} = 2\cos(\pi s)e^{-B}. \tag{77}$$

More appropriately, to obtain the tunneling rate one has to use the dilute-instanton gas approximation that is by summing over a sequences of one instanton followed by any number of anti-instanton/instanton pairs, with an odd

---

[6] In the presence of a magnetic field, different representation of a biaxial spin models can also be related by the anisotropy constants or rotation of axes

number of instantons and anti-instantons (see Sec.(II.A.2)). The transition amplitude becomes (Henley and Delft, 1992; Loss, DiVincenzo and Grinstein, 1992)

$$\langle \frac{\pi}{2}|e^{-\beta\hat{H}}|-\frac{\pi}{2}\rangle = \mathcal{N}\sinh\left[2\mathscr{D}\beta\cos(\pi s)e^{-B}\right], \tag{78}$$

where $\mathscr{D}$ is the fluctuation determinant (Coleman, 1977; Callan and Coleman, 1977; Coleman, 1985). The computation of $\mathscr{D}$ can be done explicitly. $\mathcal{N}$ is a normalization constant and B is the action for the instanton. The tunneling rate (energy splitting) from Eqn.(78) gives (Loss, DiVincenzo and Grinstein, 1992)

$$\Delta = 4\mathscr{D}|\cos(\pi s)|e^{-B}, \tag{79}$$

The factor $\cos(\pi s)$ is responsible for interference effect and it has markedly different consequences for integer and half-odd integer spins. For integer spins (bosons), the interference is constructive $\cos(\pi s) = (-1)^s$, and the tunneling rate is non-zero, however, for half-odd-integer spins (fermions), the interference is destructive $\cos(\pi s) = 0$ and the tunneling rate vanishes. This suppression of tunneling for half-odd-integer spins in this model can be related to Kramers degeneracy (Kramers, 1930; Messiah, 1962) due to the time reversal invariance of Eqn.(70). This directly implies that the ground state is at least two-fold degeneracy in the semi-classical picture. This semi-classical degeneracy sometimes implies that the two degenerate quantum ground states of the unperturbed term, $|\uparrow\rangle$ and $|\downarrow\rangle$ are exact ground states of the quantum Hamiltonian for half-odd integer spin (Henley and Delft, 1992).

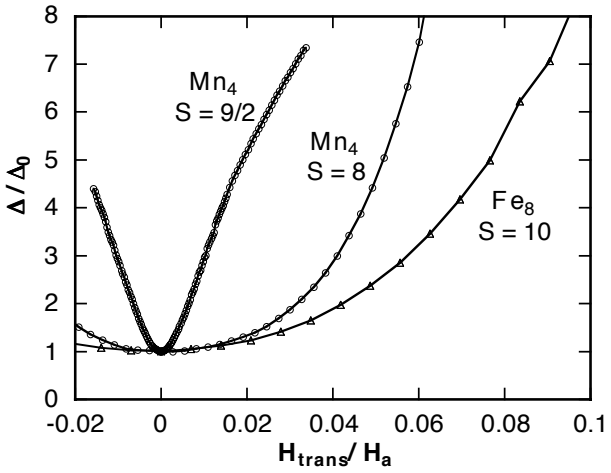

FIG. 5 Measured tunnel splittings obtained by the Landau-Zener method as a function of transverse field for all three SMMs. The tunnel splitting increases gradually for an integer spin, whereas it increases rapidly for a half-integer spin. Adapted with permission from Wernsdorfer *et al.*, 2002

In this biaxial model we have just reviewed, the quantum phase interference appeared naturally from the topological term in the action, Eqn.(53) since the instanton trajectory is in the ϕ variable. If we had considered the z-easy axis model such as

$$\hat{H} = -k_z\hat{S}_z^2 + k_y\hat{S}_y^2, \quad k_z, k_y > 0, \tag{80}$$

then the situation would have been different. This Hamiltonian is related to Eqn.(70) by $k_z = D_2$, $k_y = D_1 - D_2$ or by rotation of axis $\hat{S}_z \leftrightarrow \hat{S}_y$. Suppose we wish to solve Eqn.(80) as it is, then the corresponding classical energy is

$$U(\theta,\phi) = (k_z + k_y\sin^2\phi)s^2\sin^2\theta, \tag{81}$$

One finds from the conservation of energy that $\phi(\tau)$ is an imaginary constant and $\theta(\tau)$ is the real tunneling trajectory which is given by (Owerre and Paranjape, 2014a)

$$\theta(\tau) = 2\arctan[\exp(\omega(\tau-\tau_0))], \tag{82}$$

where $\omega = 2s\sqrt{k_z(k_y+k_z)}$, and $\theta(\tau) \to 0, \pi$ as $\tau \to \mp\infty$. The fact that $\phi(\tau)$, although imaginary, is just a constant simply implies that the topological term in Eqn.(53) which is responsible for the phase interference vanishes. The

transition amplitude arises from the necessity to translate ϕ from some fiducial value, taken without loss of generality to be zero, to the complex constant value before the instanton trajectory in θ and then followed by the translation of ϕ back to its fiducial value after the instanton trajectory. It was explicitly shown, that translation of ϕ in the complex plane yields the transition amplitude and the corresponding energy splitting is of the form: (Owerre and Paranjape, 2014a, 2013)

$$\Delta = 2\mathscr{D}(1+\cos(2\pi s))e^{-B}, \tag{83}$$

where

$$B = \begin{cases} s\ln\left(\frac{4k_z}{k_y}\right) & \text{if } k_y \ll k_z, \\ 2s\left(k_z/k_y\right)^{1/2} & \text{if } k_y \gg k_z. \end{cases} \tag{84}$$

The fluctuation determinant is calculated to be $\mathscr{D} = 8\sqrt{2}k_z s^{3/2}/\pi^{1/2}$ for $k_y \ll k_z$ and $\mathscr{D} = 8(sk_zk_y)^{3/2}/\pi^{1/2}$ for $k_y \ll k_z$(Garg and Kim, 1992). Thus, we recover that tunneling is restricted for half-odd integer spins. For integer spin and the semiclassical limit $s \gg 1$, simple operatorial quantum mechanical perturbation theory in the splitting term for $k_y \ll k_z$ gives (Garanin , 1991)

$$\Delta = \frac{8k_z s^{3/2}}{\pi^{1/2}}\left(\frac{k_y}{4k_z}\right)^s, \tag{85}$$

which is consistent with Eqn.(83) for integer spin s. The experimental confirmation of this spin-parity effect (i.e suppression of tunneling for half-odd integer spin) in spin systems was reported by Wernsdorfer *et al.* (2002). They studied three SMMs in the presence of a transverse field using Landau-Zener method to measure the tunnel splitting as a function of transverse field. They established the spin-parity effect by comparing the dependence of the tunneling splitting on the transverse field for integer and half-odd integer spin systems. Observation showed that an integer spin system is insensitive to small transverse fields whereas a half-odd integer spin system is much more sensitive as shown in Fig.(5). This observation is analogous to the fact that half-odd integer spin does not tunnel.

3. Biaxial spin model with an external magnetic field

The quantum phase interference (quenching of tunneling splitting) we saw in the previous section is a zero magnetic field effect. In the presence of a magnetic field complete destructive interference for half-odd integer spins does not occur instead oscillation occurs. Consider the biaxial spin model with an external magnetic field applied along the hard-axis (Garg, 1993, 1999, 2001)

$$\hat{H} = D_1\hat{S}_z^2 + D_2\hat{S}_x^2 - h_z\hat{S}_z, \tag{86}$$

where $h_z = g\mu_B h$, h is the magnitude of applied field and g is the spin g-factor and μ_B is the Bohr magneton. This Hamiltonian can also be written as

$$\hat{H} = -D_2\hat{S}_y^2 + (D_1 - D_2)\hat{S}_z^2 - h_z\hat{S}_z + \text{const.} \tag{87}$$

Thus, we see explicitly that the easy (quantization) axis is along the y-direction. Unlike the previous model this Hamiltonian is no longer time reversal invariant due the presence of the magnetic field, so Kramers theorem is no longer applicable. This Hamiltonian has been studied experimentally for Fe_8 molecular cluster (Sangregorio, *et al.*, 1997; Sessoli *et al.*, 2000; Wernsdorfer and Sessoli, 1999). There are $2s+1$ energy level spectra where $s = 10$ and a quantum number $m = -10, -9, \cdots, 10$. At very low temperature ($T < 0.36K$) only the lowest states $m = \pm 10$ are occupied which can tunnel macroscopically. In the semi-classical analysis, the classical energy up to an additional constant is

$$U(\theta,\phi) = D_1 s^2(\cos\theta - \alpha)^2 + D_2 s^2\sin^2\theta\cos^2\phi, \tag{88}$$

with $\alpha = h_z/h_c$, $h_c = 2D_1 s$ being the coercive field.

There are two classical degenerate minima located at $\cos\theta = \alpha$, $\phi = -\pi/2$ and $\cos\theta = \alpha$, $\phi = \pi/2$ provided $h_z < h_c$. These ground states lie in the xz and yz planes at an angle $\theta = \pm\arccos\alpha$ as shown in Fig.(6). From energy conservation , Eqn.(63) the expression for $\cos\theta$ in terms of ϕ yields

$$\cos\theta = \frac{\alpha + i\lambda^{1/2}\cos\phi(1-\alpha^2-\lambda\cos^2\phi)^{1/2}}{1-\lambda\cos^2\phi}, \tag{89}$$

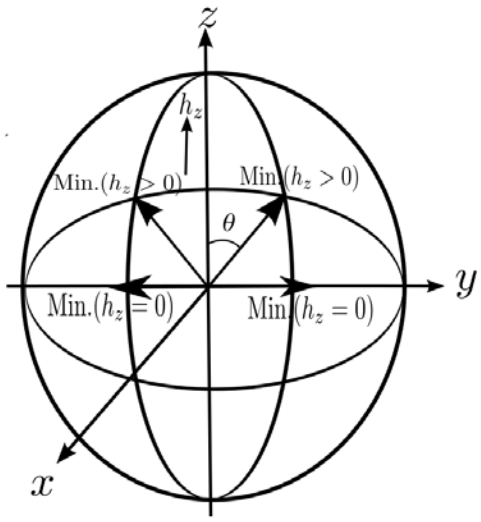

FIG. 6 The description of a classical spin (thick arrows) on a two-sphere with two classical ground states. For $h_z = 0$, $\theta = \pm\pi/2$, the two classical ground states lie in the $\pm y$ directions which are joined by two tunneling paths in the equator. For $h_z > 0$, $\theta = \pm \arccos\alpha$, the two classical ground states lie in the yz plane. Reproduced from Schilling (1995)

We have chosen the positive solution in Eqn.(89) for convenience. Using this equation and Eqn.(62), one obtains the instanton solution:

$$\sin\phi(\tau) = \frac{\sqrt{1-\lambda_H}\tanh(\omega_H\tau)}{\sqrt{1-\lambda_H\tanh^2(\omega_H\tau)}}, \tag{90}$$

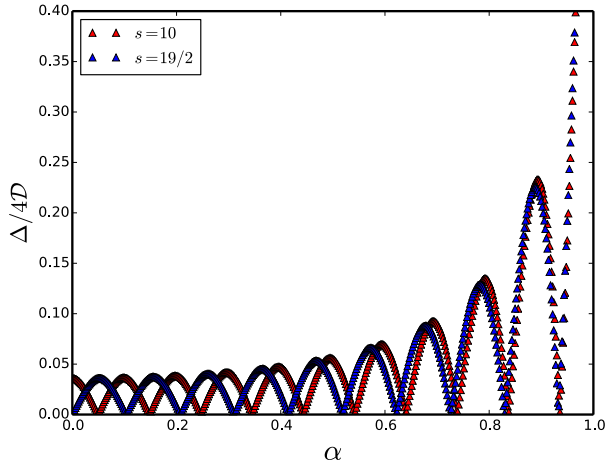

FIG. 7 Color online: Oscillation of the tunneling splitting as a function of the magnetic field parameter α. Solid line is for interger spins while dotted line is for half-odd integer spins.

where $\omega_H = 2s\sqrt{D_1 D_2(1-\alpha^2)}$ and $\lambda_H = \lambda/(1-\alpha^2)$. The classical action for this instanton path is

$$S_c = i\pi\Theta + B, \tag{91}$$

where

$$\Theta = \frac{s}{2\pi}\left(\mathscr{S}_+ - \mathscr{S}_-\right), \tag{92}$$

and $\mathscr{S}_+ - \mathscr{S}_-$ is the area enclosed by the two tunneling paths on a 2-sphere as shown in Fig.(6), which is given by

$$\mathscr{S}_\pm = \int_{\mp\frac{\pi}{2}}^{\pm\frac{\pi}{2}} d\phi \left(1 - \frac{\alpha}{1-\lambda\cos^2\phi}\right) = \pm\pi\left(1 - \frac{\alpha}{\sqrt{1-\lambda}}\right). \tag{93}$$

The instanton action is given by

$$B = s\ln\left(\frac{\sqrt{1-\alpha^2}+\sqrt{\lambda}}{\sqrt{1-\alpha^2}-\sqrt{\lambda}}\right) - \frac{2s\alpha}{\sqrt{1-\lambda}}\ln\left(\frac{\sqrt{(1-\alpha^2)(1-\lambda)}+\alpha\sqrt{\lambda}}{\sqrt{(1-\alpha^2)(1-\lambda)}-\alpha\sqrt{\lambda}}\right). \tag{94}$$

In this problem the imaginary path of the instanton action, Eqn.(91) has acquired an additional term due to the presence of the magnetic field. In the dilute instanton gas approximation, one obtains that the tunneling rate is then given by

$$\Delta = \Delta_0|\cos(\pi\Theta)|, \quad \Delta_0 = 4\mathscr{D}e^{-B}, \tag{95}$$

which clearly reduces to Eqn.(79) in the limit of zero magnetic field. Now, the tunneling splitting is no longer suppressed for half-odd integer spin but rather oscillates with the magnetic field (see Fig.(7)) with a period of oscillation of

$$\Delta h = \frac{2D\sqrt{1-\lambda}}{g\mu_B}, \tag{96}$$

only vanishes at

$$\Theta = (n+1/2) \quad \text{or} \quad \alpha = \sqrt{1-\lambda}\,(s-n-1/2)/s, \tag{97}$$

where n is an integer. It is crucial to note that the quenching of tunneling at a critical field only occurs for biaxial spin system with a magnetic applied along the hard anisotropy axis.

4. Landau Zener effect

The uniaxial and the biaxial models we have studied so far can be mapped to a two-level pseudospin $\frac{1}{2}$ particle system (Chudnovsky and Garanin , 2010; Chudnovsky, 2014; Owerre, 2014). Let us consider a two-level system which is described by an unperturbed Hamiltonian $\hat{H}_0(\eta)$ that depends explicitly on a parameter η. Suppose that the eigenstates of this Hamiltonian are $|m\rangle$ and $|m'\rangle$, then the eigenvalue equation yields

$$\hat{H}_0(\eta)\,|m\rangle = \zeta_1(\eta)\,|m\rangle\,, \tag{98}$$

$$\hat{H}_0(\eta)\,|m'\rangle = \zeta_2(\eta)\,|m'\rangle\,, \tag{99}$$

where $\zeta_{1,2}(\eta)$ are the corresponding eigenenergies. It is assumed that the eigenstates $|m\rangle$ and $|m'\rangle$ are independent of the parameter η, and that at some value of η, $\hat{H}_0(\eta)$ possesses a symmetry which allows level crossing (degeneracy) of the two eigenvalues $\zeta_{1,2}(\eta)$. The parameter η could be an applied magnetic field(Wernsdorfer, *et al.*, 2005). In the presence of a perturbative term $\hat{V}$, the total Hamiltonian can be written as

$$\hat{H} = \hat{H}_0 + \hat{V}. \tag{100}$$

The Hamiltonian can be diagonalized in the basis $\{\,|m\rangle\,, |m'\rangle\,\}$, the corresponding matrix is given by

$$\hat{H}(\eta) = \begin{pmatrix} \varepsilon_1(\eta) & \Delta \\ \Delta^* & \varepsilon_2(\eta) \end{pmatrix}, \tag{101}$$

where

$$\varepsilon_1 = \zeta_1(\eta) + \langle m|\hat{V}|m\rangle\,, \tag{102}$$

$$\varepsilon_2 = \zeta_2(\eta) + \langle m'|\hat{V}|m'\rangle\,, \tag{103}$$

$$\Delta = 2|\,\langle m|\hat{V}|m'\rangle\,| \Rightarrow \langle m|\hat{V}|m'\rangle = \frac{1}{2}\Delta e^{-i\phi}. \tag{104}$$

Diagonalizing Eqn.(101), one obtains the eigenvalues:

$$\varepsilon_+ = \frac{1}{2}\big[(\varepsilon_1+\varepsilon_2) + \big(\varepsilon(\eta)^2 + 4|\Delta|\big)^{1/2}\big], \tag{105}$$

$$\varepsilon_- = \frac{1}{2}\big[(\varepsilon_1+\varepsilon_2) - \big(\varepsilon(\eta)^2 + 4|\Delta|\big)^{1/2}\big], \tag{106}$$

where $\varepsilon(\eta) = \varepsilon_1 - \varepsilon_2$. If both the unperturbed energies are degenerate at some critical value η_c where $\varepsilon(\eta_c) = 0$, we see that the two levels $\varepsilon_\pm$ never cross each other unless the avoided crossing term Δ vanishes. Let us consider the time-dependent Schrödinger equation:

$$\hat{H}\,|\psi(t)\rangle = i\frac{\partial\,|\psi(t)\rangle}{\partial t}. \tag{107}$$

The wave function can be taken as a linear combination of the unperturbed states:

$$|\psi(t)\rangle = C_1(t)e^{-i\int \varepsilon_1 dt}\,|m\rangle + C_2(t)e^{-i\int \varepsilon_2 dt}\,|m'\rangle\,. \tag{108}$$

Using Eqn.(102)–(104), the time-dependent Schrödinger equation can be written as

$$i\dot{C}_1 = \Delta e^{-i\int_0^t \varepsilon(t')dt'}C_2, \tag{109}$$

$$i\dot{C}_2 = \Delta^* e^{i\int_0^t \varepsilon(t')dt'}C_1. \tag{110}$$

These two differential equations must be solved with the boundary conditions:

$$C_1(-\infty) = 0, \quad |C_2(-\infty)| = 1. \tag{111}$$

Using the fact that Δ is time-independent, differentiating Eqn.(109) and substituting Eqn.(110) into the resulting equation yields

$$\ddot{C}_1 - i\varepsilon(t)\dot{C}_1 + |\Delta|^2 C_1 = 0. \tag{112}$$

Writing $\varepsilon(t) = \alpha t$, $f = \Delta e^{i\phi}$ and

$$C_1 = y e^{i\frac{1}{2}\int_0^t \varepsilon(t')dt'}. \tag{113}$$

Eqn.(112) transforms into the form:

$$\ddot{y} + \left(f^2 + i\frac{\alpha}{2} + \frac{\alpha^2}{4}t^2\right)y = 0, \tag{114}$$

which transforms into the Weber equation:(Whittaker, 1902) by setting $n = -if^2/\alpha$ and $z = \sqrt{\alpha}e^{i\pi/4}t$:

$$\frac{d^2y}{dz^2} + \left(n + \frac{1}{2} - \frac{1}{4}z^2\right)y. \tag{115}$$

The solutions of this differential equation are parabolic cylinder functions. The general solution of Eqn.(112) has the form(Zener, 1932)

$$C_1(t) = \left[aD_{-\nu-1}(-i\sqrt{\alpha}e^{i\pi/4}t) + bD_\nu(\sqrt{\alpha}e^{i\pi/4}t)\right]e^{i\varepsilon(t)/4}, \tag{116}$$

where a and b are constants determined by the initial conditions. In the limit $t \to \infty$, the asymptotic form of the excitation probability is found to be(Jan, *et al.*, 1981; Landau, 1932; Landau and Lifshitz, 1977; Zener, 1932)

$$\mathcal{P} = 1 - |C_1(\infty)|^2 = 1 - \exp\left[-\frac{2\pi|\Delta|^2}{\frac{d\varepsilon}{dt}}\right], \tag{117}$$

which is the famous Landau-Zener formula. The theoretical prediction of the oscillation of tunneling splitting of the model in Sec.(III.A.3) has been observed experimentally in Fe_8 molecular cluster and Mn_{12} SMMs using this

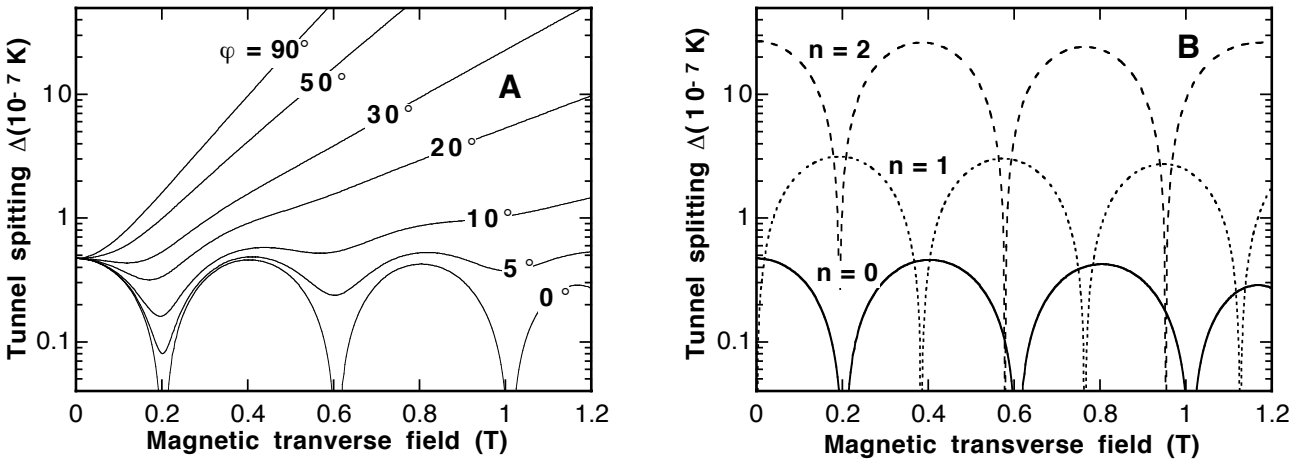

FIG. 8 Calculated tunneling splitting as a function of the applied field using Landau-Zener method for the Hamiltonian $\hat{H} = -AS_z^2 + B(S_x^2 - S_y^2) + C(S_+^4 + S_-^4) - g\mu_B h S_x$. For $C = 0$, it is related to that of Eqn.(86) by $D_1 = A + B$ and $D_2 = A - B$. (**A**) is the quantum transition between $m = \pm 10$ for several values of the azimuth angles ϕ. (**B**) is the quantum transition between $m = -10$ and $m = 10 - n$ at $\phi = 0$, where $n = 0, 1, 2, \cdots$, $m = -s, \cdots, s$, and $s = 10$ $A = 0.275K$, $B = 0.046K$ and $C = -2.9 \times 10^{-5}K$ for Fe_8 molecular cluster. Adapted with permission from Wernsdorfer and Sessoli, 1999

Landau Zener technique (Wernsdorfer and Sessoli, 1999; Wernsdorfer *et al.*, 2000; Wernsdorfer, Chakov and Christou, 2005). In Fig.(8) we have shown the experimental confirmation of this theoretical prediction. It explicitly shows the oscillations of the tunnel splittings as a function of the magnetic field applied along the hard anisotropy axis. This field is responsible for the periodic change in the avoided level crossing Δ, which we found from the semiclassical analysis as a destructive or constructive quantum interference, with the period of oscillation given in Eqn.(96). The tunneling probability from the Landau Zener formula is given by (Wernsdorfer and Sessoli, 1999)

$$\mathcal{P} = 1 - \exp\left[- \frac{\pi |\Delta|^2}{4s\hbar g \mu_B \frac{dH}{dt}} \right], \tag{118}$$

where $\frac{dH}{dt}$ is the constant field sweeping rate and $g \approx 2$.

The value of the period of oscillation, Eqn.(96) using the anisotropy parameters for Fe_8 molecular cluster in Fig.(8) with $D_1 = A + B$ and $D_2 = A - B$ is $\Delta h = 0.26T$. The value is very small compare to its experimental measured value $0.41T$. In order to fix this discrepancy an additional fourth order anisotropy of the form $C(S_+^4 + S_-^4)$ is required in Eqn.(86) (Wernsdorfer and Sessoli, 1999; Wernsdorfer *et al.*, 2000). The inclusion of this term involves a tedious theoretical analysis. There is no exact instanton solution but some approximate schemes have been developed to tackle this problem (Chang and Garg, 2002; Foss and Friedman, 2009; Kim, 2002).

5. Antiferromagnetic exchange coupled dimer model

We have considered only the tunneling phenomenon of single molecule magnets (SMMs) . In many cases of physical interest, interactions between two large spins are taken into account. These interactions can be either ferromagnetic, which aligns the neighbouring spins or antiferromagnetic, which anti-aligns the neighbouring spins. One physical system in which these interactions occur is the dimerized molecular magnet $[Mn_4]_2$. It comprises two Mn_4 SMMs of equal spins $s_1 = s_2 = 9/2$, which are coupled antiferromagnetically. The phenomenon of quantum tunneling of spins in this system has been be studied both numerically and experimentally (Hill, *et al.*, 2003; Tiron, *et al.*, 2003a). For this system, the simplest form of the Hamiltonian in the absence of an external magnetic field can be written as

$$\hat{H} = -D(\hat{S}_{1,z}^2 + \hat{S}_{2,z}^2) + J\hat{\mathbf{S}}_1 \cdot \hat{\mathbf{S}}_2, \tag{119}$$

where $J > 0$ is the antiferromagnetic exchange coupling. and $D \gg J > 0$ is the easy-axis anisotropy constant, $S_{i,z}, i = 1, 2$ is the projection of the component of the spin along the z easy-axis. In this model the exchange term acts as a field bias on its neighbour. We will report here on the analysis of this model by (Owerre and Paranjape, 2013), however the nature of the ground states was first proposed by (Barbara and Chudnovsky, 1990) and the energy splitting was obtained by (Kim, 2003) and the quantum operator perturbation theoretical analysis is given in

(Chudnovsky and Tejada, 2006; Chudnovsky et al , 2007). Park, *et al.* (2003) demonstrated using density-functional theory that this simple model can reproduce experimental results in $[Mn_4]_2$ dimer with $D = 0.58K$ and $J = 0.27K$. It also plays a crucial role in quantum CNOT gates and SWAP gates for spin 1/2 (Loss and DiVincenzo, 1998).

The total z-component of the spins $\hat{S}_z = \hat{S}_{1,z} + \hat{S}_{2,z}$ is a conserved quantity. However, the individual z-component spins $\hat{S}_{1,z}, \hat{S}_{2,z}$ and the staggered configuration $\hat{S}_{1,z} - \hat{S}_{2,z}$ are not conserved. The Hilbert space of this system is the tensor product of the two spaces $\mathscr{H} = \mathscr{H}_1 \otimes \mathscr{H}_2$ with $\dim(\mathscr{H}) = (2s_1 + 1) \otimes (2s_2 + 1)$. The basis of S_j^z in this product space is given by $|s_1, \sigma_1\rangle \otimes |s_2, \sigma_2\rangle \equiv |\sigma_1, \sigma_2\rangle$. We immediately specialize to the case $s_1 = s_2 = s$. In the absence of the exchange interaction, the ground state of the Hamiltonian is four-fold degenerate corresponding to the states where the individual spins are in their highest weight or lowest weight states, $|\uparrow,\uparrow\rangle, |\downarrow,\downarrow\rangle, |\uparrow,\downarrow\rangle, |\downarrow,\uparrow\rangle$, where $|\uparrow,\downarrow\rangle = |\uparrow\rangle \otimes |\downarrow\rangle \equiv |s, -s\rangle$ etc, with the exchange interaction term J, the two ferromagnetic states $|\uparrow,\uparrow\rangle$ and $|\downarrow,\downarrow\rangle$ are still degenerate, exact eigenstate of the Hamiltonian, but the antiferromagnetic states $|\uparrow,\downarrow\rangle$ and $|\downarrow,\uparrow\rangle$ are not. These two antiferromagnetic states link with each other at $2s^{\text{th}}$ order in degenerate perturbation theory in the exchange transverse term, that is at order J^{2s} (Kim, 2003; Owerre and Paranjape, 2013). Thus, the exchange interaction plays the same role as the splitting terms in the uniaxial and biaxial models considered previously. This is completely understandable since tunneling requires a term that does not commute with the quantization axis. However, in this model we will see that both integer and half-odd integer spins can tunnel[7] but their ground and first excited states are different. Up to an additional constant, the classical energy corresponds to

$$U = Js^2 \left(\sin\theta_1 \sin\theta_2 \cos(\phi_1 - \phi_2) + \cos\theta_1 \cos\theta_2 + 1\right) + Ds^2(\sin^2\theta_1 + \sin^2\theta_2). \tag{120}$$

The minimum energy corresponds to $\phi_1 - \phi_2 = \pi$: $\theta_1 = 0$, $\theta_2 = \pi$, $\phi_1 - \phi_2 = \pi$: $\theta_1 = \pi$, $\theta_2 = 0$ and the maximum at $\phi_1 - \phi_2 = \pi$: $\theta_1 = \pi/2$, $\theta_2 = \pi/2$. There are four classical equations of motion but we already have the constraint that the total z-component spins is conserved, that is $\cos\theta_1 + \cos\theta_2 = 0 \Rightarrow \theta_2 = \pi - \theta_1 = \pi - \theta$. Introducing the variables $\phi = \phi_1 - \phi_2$ and $\Phi = \phi_1 + \phi_2$ (which is cyclic), one finds that the two spin problem reduces to an effective single spin problem which is described by the Lagrangian:

$$\mathcal{L}_E = is\dot{\phi}(1 - \cos\theta) + U(\theta, \phi), \tag{121}$$

where the effective energy is

$$U(\theta, \phi) = 2Ds^2 \sin^2\theta \left(1 + \frac{\lambda}{2}(1 + \cos\phi)\right), \tag{122}$$

and $\lambda = J/D \ll 1$. Since $\sin^2\theta \neq 0$ as θ varies as the tunneling progresses, energy conservation requires

$$\cos\phi = -\left(\frac{2}{\lambda} + 1\right). \tag{123}$$

Thus, $|\cos\phi| > 1$ as $\lambda \ll 1$. Therefore there is no real solution for ϕ as expected. It was shown that the proper choice of ϕ for antiferromagnetic coupling is $\phi = \pi + i\phi_I$, where ϕ_I is real (Owerre and Paranjape, 2013). Plugging this into Eqn.(123) we obtain $\phi_I \approx \ln(4/\lambda)$.

From the classical equation of motion Eqn.(61) one finds that the classical trajectory has the form

$$\theta(\tau) = 2\arctan\left(e^{\omega(\tau - \tau_0)}\right), \tag{124}$$

where $\omega = Js\sinh\phi_I = 2Ds\sqrt{1+\kappa}$, $\kappa = J/D$ and at $\tau = \tau_0$ we have $\theta(\tau) = \pi/2$. Thus $\theta(\tau)$ interpolates from 0 to π as $\tau = -\infty \to \infty$ for the instanton and from π to 0 for an anti-instanton. The action for this trajectory is found to be

$$S_0 = -i2s\pi + 2s\phi_I. \tag{125}$$

The energy splitting between the ground and the first excited states is given by (Kim, 2003; Owerre and Paranjape, 2013)

$$\Delta = 2\mathscr{D}\left(\frac{J}{4D}\right)^{2s} \cos(2\pi s). \tag{126}$$

---

[7] It is crucial to note that Kramers degeneracy only applies to a system with an odd total number of half-odd integer spin.

For half-odd integer spin $\Delta < 0$ the ground $|g\rangle$ and the first excited $|e\rangle$ states are

$$|g\rangle = \frac{1}{\sqrt{2}}(|\downarrow,\uparrow\rangle - |\uparrow,\downarrow\rangle); \qquad |e\rangle = \frac{1}{\sqrt{2}}(|\downarrow,\uparrow\rangle + |\uparrow,\downarrow\rangle); \tag{127}$$

while for integer spins $\Delta > 0$ we have

$$|g\rangle = \frac{1}{\sqrt{2}}(|\downarrow,\uparrow\rangle + |\uparrow,\downarrow\rangle); \qquad |e\rangle = \frac{1}{\sqrt{2}}(|\downarrow,\uparrow\rangle - |\uparrow,\downarrow\rangle). \tag{128}$$

In this case there is no suppression of tunneling even at zero field, the phase term that arises from the imaginary term in Eqn.(125) switches the ground state from odd to even for half-odd integer and integer spins respectively. This shows that for half-odd integer spins, the ground state is the state with $s = 0$. This result has been experimentally shown that $[Mn_4]_2$ represents an unequivocal and unprecedented example of quantum tunneling in a monodisperse antiferromagnet with no uncompensated spin ($s = 0$) in the ground state (Wernsdorfer, *et al.*, 2004). In the presence of an external magnetic field applied along the easy axis, there are $(2s+1)^2 \times (2s+1)^2 = 100 \times 100$ matrices which are sparsely populated giving rise to an exact numerical diagonalization of 100 non-zero energy states as shown in Fig.(9) , (Hu, Chen and Shen, 2003; Hill, *et al.*, 2003; Tiron, *et al.*, 2003a,b; Wernsdorfer, *et al.*, 2004). The values of the anisotropy parameters that were used to fit experimental data for this dimer are $J = 0.13K$, $D = 0.77K$(Hill, *et al.*, 2003; Tiron, *et al.*, 2003a). An analogous two spin problem is that of a biaxial antiferromagnetic particle of two

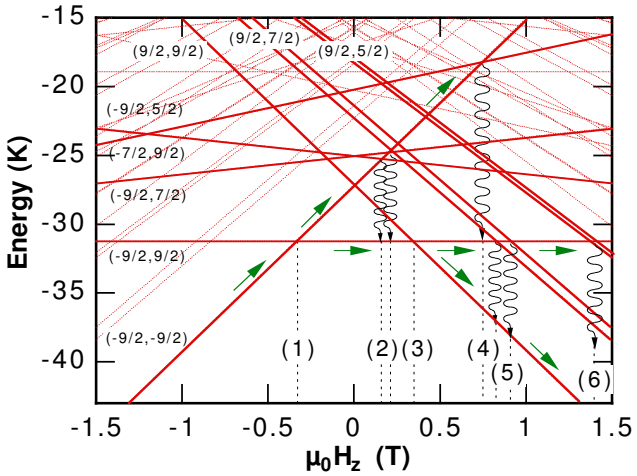

FIG. 9 Color online: The so-called exact numerical diagonalization of the dimer model plotted as a function of applied magnetic field with the parameters $D = 0.77K$, $J = 0.13K$. Each state is labeled by $|m_1, m_2\rangle$. Dotted lines, labeled 1 to 5, indicate the strongest tunnel resonances: 1: (-9/2,9/2) to (-9/2 ,9/2); 2: (-9/2,9/2) to (-9/2 ,7/2), followed by relaxation to (-9/2,9/2); 3: (-9/2,9/2) to (9/2 ,9/2); 4: (-9/2,-9/2) to (-9/2 ,5/2), followed by re- laxation to (-9/2,9/2); 5: (-9/2,9/2) to (7/2 ,9/2), followed by relaxation to (9/2,9/2). In order to get most of these transitions theoretical one needs to add term like $J(S_1^+ S_2^+ + S_1^- S_2^-)$ in Eqn.(119). Adapted with permission from Tiron, *et al.*, 2003a

collinear ferromagnetic sublattices with a small non-compensation $s = s_1 - s_2 \neq 0$. The corresponding Hamiltonian (Chudnovsky , 1995; Garg and Duan, 1994; Liang, *et al.*, 2000) is

$$\hat{H} = \sum_{a=1,2} (k_1 \hat{S}_a^{z2} + k_2 \hat{S}_a^{y2} - h\hat{S}_a^z) + J\hat{\mathbf{S}}_1 \cdot \hat{\mathbf{S}}_2, \tag{129}$$

where $k_1 \gg k_2 > 0$ are the anisotropy constants. It possesses an easy x-axis and xy easy plane, and the magnetic field h is applied along the hard z-axis. The two spins are unequal unlike the dimer model considered above so one is interested in the sublattice rotation of the Néel vector (Barbara and Chudnovsky, 1990). The classical energy is of the form:

$$U = Js_1 s_2 \left(\sin\theta_1 \sin\theta_2 \cos(\phi_1 - \phi_2) + \cos\theta_1 \cos\theta_2\right) + \sum_{a=1,2} (k_1 s_a^2 \cos^2\theta_a + k_2 s_a^2 \sin^2\theta_a \sin^2\phi_a - h s_a \cos\theta_a) \tag{130}$$

The full action contains two WZ terms thus, there are four equations of motion in general. There is no operator that commutes with this Hamiltonian therefore there is no constraint. In order to get an effective single spin problem,

several approximations have to be made. Firstly, we have to assume that the two spins s_1 and s_2 are almost antiparallel. Therefore, one can replace θ_2 and ϕ_2 by $\theta_2 = \pi - \theta_1 - \epsilon_\theta$ and $\phi_2 = \pi + \phi_1 + \epsilon_\phi$ where $\epsilon_\theta, \epsilon_\phi \ll 1$ are small fluctuations. Replacing θ_2 and ϕ_2 in the action and setting $s_1 = s_2 = s_0$ except for the terms containing $s_1 - s_2 = s$, and integrating out the fluctuations $\epsilon_\theta, \epsilon_\phi$ from the path integral one obtains an effective single spin model, which can then be solved using the procedures outline above. However, unlike the dimer model, one finds in this case that in the absence of the magnetic field, tunneling of hampered when s is half-odd integer (Chudnovsky , 1995) while in the presence of the magnetic field, tunneling splitting oscillates with the field only vanishes at a certain critical value (Liang, *et al.*, 2000)

B. Coordinate independent formalism

1. Equation of motion and Wess-Zumino action

The coordinate dependent formalism we have just reviewed in the previous section is widely used in most condensed matter literature, but not much seems to be written about the solutions of these models in a coordinate independent form. The solution of a physical problem should be independent of the coordinate system. Having solutions only in a coordinate dependent form leaves a slight but persistent, irritating doubt that somehow the results may have some coordinate dependent artefacts, which of course should not be there. In section (II.A) we derived the classical action for the spin system without the use of coordinates. In this section we will show that one can solve the spin models we have considered so far in totally coordinate independent way and also recover the quantum phase interference exactly as before. First of all, we need to know the classical path that minimizes the coordinate independent action Eqn.(42):

$$S_E[\hat{\mathbf{n}}] = isS_{WZ} + \int d\tau U(\hat{\mathbf{n}}(\tau)), \quad U(\hat{\mathbf{n}}(\tau)) = \langle \hat{\mathbf{n}}|\hat{H}|\hat{\mathbf{n}}\rangle \,. \tag{131}$$

The variation of coordinate independent WZ term, Eqn.(43) due to small variation of $\hat{\mathbf{n}}$ gives

$$\delta S_{WZ} = \int d\tau \int d\xi \, \partial_\tau [\hat{\mathbf{n}} \cdot (\delta\hat{\mathbf{n}} \times \partial_\xi \hat{\mathbf{n}})] + \int d\tau \int d\xi \, \partial_\xi [\hat{\mathbf{n}} \cdot (\partial_\tau \hat{\mathbf{n}} \times \delta\hat{\mathbf{n}})]. \tag{132}$$

To obtain this variation we must remember that $0 = \delta(\hat{\mathbf{n}} \cdot \hat{\mathbf{n}}) = 2\hat{\mathbf{n}} \cdot \delta\hat{\mathbf{n}}$, and $0 = \partial_{\tau,\xi}(\hat{\mathbf{n}} \cdot \hat{\mathbf{n}}) = 2\hat{\mathbf{n}} \cdot \partial_{\tau,\xi}\hat{\mathbf{n}}$, since $\hat{\mathbf{n}}$ is a unit vector. Consequently, the volume defined by the parallelepiped traced out by the three vectors, the variation and the two derivatives, must vanish, $\delta\hat{\mathbf{n}} \cdot (\partial_\tau \hat{\mathbf{n}} \times \partial_\xi \hat{\mathbf{n}}) = 0$ since any three vectors orthogonal to a given vector $\hat{\mathbf{n}}$, lie in the same plane. The first term in Eqn.(132) vanishes by virtue of the boundary conditions Eqn.(44) and the second term yields

$$\delta S_{WZ} = -\int d\tau \, \delta\hat{\mathbf{n}}(\tau) \cdot [\hat{\mathbf{n}}(\tau) \times \partial_\tau \hat{\mathbf{n}}(\tau)]. \tag{133}$$

As $\delta\hat{\mathbf{n}}(\tau)$ is still a constrained variation, necessarily orthogonal to $\hat{\mathbf{n}}$, therefore

$$\frac{\delta S_{WZ}}{\delta\hat{\mathbf{n}}(\tau)} \neq [\hat{\mathbf{n}}(\tau) \times \partial_\tau \hat{\mathbf{n}}(\tau)]. \tag{134}$$

What we may conclude is that the part of $[\hat{\mathbf{n}}(\tau) \times \partial_\tau \hat{\mathbf{n}}(\tau)]$ which is orthogonal to $\hat{\mathbf{n}}$ will contribute to the equation of motion. The way to implement this, is to take the vector product with $\hat{\mathbf{n}}$, which implements the projection to the appropriate orthogonal directions. Then, using the fact that $\hat{\mathbf{n}}(\tau) \times [\hat{\mathbf{n}}(\tau) \times \partial_\tau \hat{\mathbf{n}}(\tau)] = -\partial_\tau \hat{\mathbf{n}}(\tau)$, the variation of the total action gives the equation of motion:

$$is\partial_\tau \hat{\mathbf{n}}(\tau) = -\hat{\mathbf{n}}(\tau) \times \frac{\partial U(\hat{\mathbf{n}}(\tau))}{\partial\hat{\mathbf{n}}(\tau)}. \tag{135}$$

This is the imaginary-time equivalent for the equation for Larmor precession in the effective magnetic field $\delta U(\hat{\mathbf{n}}(\tau))/\delta\hat{\mathbf{n}}(\tau)$, often called the Landau-Lifshitz equation (Landau and Lifshitz, 1935, 1991). Taking the cross product of Eqn.(135) with $\partial_\tau \hat{\mathbf{n}}(\tau)$, and subsequently the dot product with $\hat{\mathbf{n}}(\tau)$, one finds immediately the equation of energy conservation:

$$U(\hat{\mathbf{n}}(\tau)) = \text{const.} \tag{136}$$

Having obtained the equation of motion as a function of the trajectory $\hat{\mathbf{n}}(\tau)$, we wish need to write the WZ action, Eqn.(43) as a function of τ alone, as done in the coordinate dependent formulation as in Eqn.(48), in order to compute

the instanton action for the trajectory $\hat{\mathbf{n}}(\tau)$. This can only be achieved if the integration over ξ can be done leaving us with the integration over τ in terms of the unit vector $\hat{\mathbf{n}}(\tau)$. This integration can indeed be done. Let us express the unit vector $\hat{\mathbf{n}}(\tau,\xi)$ as

$$\hat{\mathbf{n}}(\tau,\xi) = f(\tau,\xi)n_z(\tau)\hat{\mathbf{z}} + g(\tau,\xi)[n_x(\tau)\hat{\mathbf{x}} + n_y(\tau)\hat{\mathbf{y}}], \tag{137}$$

with the boundary conditions given in Eqn.(44). From Eqn.(137) and $\hat{\mathbf{n}}\cdot\hat{\mathbf{n}} = 1$ one obtains immediately

$$g^2 = \frac{1 - f^2 n_z^2}{1 - n_z^2}. \tag{138}$$

Owing to the boundary conditions in Eqn.(44), these functions must obey

$$f(\tau,\xi=0) = 1; \quad f(\tau,\xi=1) = \frac{1}{n_z(\tau)}; \quad g(\tau,\xi=0) = 1; \quad g(\tau,\xi=1) = 0. \tag{139}$$

A long but straightforward calculation (Owerre and Paranjape, 2014a) shows that

$$\hat{\mathbf{n}}(\tau,\xi)\cdot(\partial_\tau\hat{\mathbf{n}}(\tau,\xi)\times\partial_\xi\hat{\mathbf{n}}(\tau,\xi)) = \frac{n_z\partial_\xi f}{1-n_z}(n_x\dot{n}_y - n_y\dot{n}_x). \tag{140}$$

The WZ term becomes[8](Owerre and Paranjape, 2014a)

$$S_{WZ} = is\int d\tau\frac{(n_x\dot{n}_y - n_y\dot{n}_x)}{1+n_z}. \tag{141}$$

This expression defines the WZ term in the coordinate independent form as a function of time alone. By spherical parameterization one can easily recover the coordinate dependent form given by Eqn. (48). Further simplification of Eqn. (141) yields

$$S_{WZ} = is\int\frac{d(n_y/n_x)}{1+(n_y/n_x)^2}(1-n_z) = is\int d[\arctan(n_y/n_x)](1-n_z). \tag{142}$$

2. Coordinate independent uniaxial spin model in a magnetic field

Now let us consider the uniaxial model in section(III.A.1). The corresponding classical energy in coordinate independent form is

$$U(\hat{\mathbf{n}}) = -Ds^2(\hat{\mathbf{n}}\cdot\hat{\mathbf{z}})^2 - H_x s\hat{\mathbf{n}}\cdot\hat{\mathbf{x}}. \tag{143}$$

From Eqn.(135) we obtain the equation of motion

$$is\partial_\tau\hat{\mathbf{n}} - 2Ds^2(\hat{\mathbf{n}}\cdot\hat{\mathbf{z}})(\hat{\mathbf{n}}\times\hat{\mathbf{z}}) - H_x s(\hat{\mathbf{n}}\times\hat{\mathbf{x}}) = 0. \tag{144}$$

Taking the cross product of this equation with $\partial_\tau\hat{\mathbf{n}}$ and using the fact that $\hat{\mathbf{n}}(\tau)\cdot\partial_\tau\hat{\mathbf{n}}(\tau) = 0$ we obtain the conservation of energy

$$Ds^2((\hat{\mathbf{n}}\cdot\hat{\mathbf{z}})^2 - 1) + H_x s\hat{\mathbf{n}}\cdot\hat{\mathbf{x}} - H_x^2/4D = 0, \tag{145}$$

where an additional constants have been added for convenience. Using this expression together with the constraint $\hat{\mathbf{n}}\cdot\hat{\mathbf{n}} = 1$ we find the relations

$$\hat{\mathbf{n}}\cdot\hat{\mathbf{x}} = \frac{1}{2h_x}(1 + h_x^2 - (\hat{\mathbf{n}}\cdot\hat{\mathbf{z}})^2); \quad \hat{\mathbf{n}}\cdot\hat{\mathbf{y}} = \pm\frac{i}{2h_x}(1 - h_x^2 - (\hat{\mathbf{n}}\cdot\hat{\mathbf{z}})^2). \tag{146}$$

The ratio of these two expressions give

$$\frac{\hat{\mathbf{n}}\cdot\hat{\mathbf{y}}}{\hat{\mathbf{n}}\cdot\hat{\mathbf{x}}} = \pm i\frac{1 - h_x^2 - (\hat{\mathbf{n}}\cdot\hat{\mathbf{z}})^2}{1 + h_x^2 - (\hat{\mathbf{n}}\cdot\hat{\mathbf{z}})^2} = \tan\chi, \tag{147}$$

---

[8] A similar expression is given in (Blasone and Jizba, 2012; Garg , *et al.*, 2003; Klauder, 1979; Stone, Park and Garg, 2000)

which is imaginary. Taking the scalar product of Eqn. (144) with $\hat{\mathbf{z}}$ and using Eqn.(146) we obtain

$$is\partial_\tau(\hat{\mathbf{n}}\cdot\hat{\mathbf{z}}) \pm iDs^2(1-h_x^2-(\hat{\mathbf{n}}\cdot\hat{\mathbf{z}})^2)=0. \tag{148}$$

The above equation integrates as

$$\hat{\mathbf{n}}\cdot\hat{\mathbf{z}} = \pm\sqrt{1-h_x^2}\tanh(\omega_h\tau), \quad \omega_h = Ds\sqrt{1-h_x^2}, \tag{149}$$

which is the same as Eqn.(66). To determine the action for this trajectory we use Eqn.(142), that is

$$B = is\int \frac{d(n_y/n_x)}{1+(n_y/n_x)^2}(1-n_z). \tag{150}$$

From Eqn.(147) we find:

$$B = \pm s\int_{\mp\sqrt{1-h_x^2}}^{\pm\sqrt{1-h_x^2}} \frac{n_z dn_z}{1-n_z^2}(1-n_z) = 2s\left[\frac{1}{2}\ln\left(\frac{1+\sqrt{1-h_x^2}}{1-\sqrt{1-h_x^2}}\right)-\sqrt{1-h_x^2}\right], \tag{151}$$

which is exactly the coordinate dependent result in Eqn.(67).

3. Coordinate independent biaxial model and suppression of tunneling

In section(III.A.2), we reviewed the suppression of tunneling for half-odd integer spin for a biaxial single molecule magnet a particular choice of coordinate. In this section we will show that these results can be recovered in terms of the unit vector $\hat{\mathbf{n}}(\tau)$. Thus, the suppression of tunneling for half-odd integer spin is independent of the choice of coordinate. In the coordinate independent form, the classical energy of the Hamiltonian, Eqn.(70) can be written as

$$U = D_1 s^2(\hat{\mathbf{n}}\cdot\hat{\mathbf{z}})^2 + D_2 s^2(\hat{\mathbf{n}}\cdot\hat{\mathbf{x}})^2, \tag{152}$$

The classical equation of motion, Eqn.(135) yields

$$is\partial_\tau\hat{\mathbf{n}} + 2D_1 s^2(\hat{\mathbf{n}}\cdot\hat{\mathbf{z}})(\hat{\mathbf{n}}\times\hat{\mathbf{z}}) + 2D_2 s^2(\hat{\mathbf{n}}\cdot\hat{\mathbf{x}})(\hat{\mathbf{n}}\times\hat{\mathbf{x}}) = 0. \tag{153}$$

From the conservation of energy and the fact that $\hat{\mathbf{n}}\cdot\hat{\mathbf{n}}=1$, it follows that

$$\hat{\mathbf{n}}\cdot\hat{\mathbf{z}} = \pm i\sqrt{\frac{D_2}{D_1}}\hat{\mathbf{n}}\cdot\hat{\mathbf{x}} = \pm i\sqrt{\frac{D_2}{D_1-D_2}(1-(\hat{\mathbf{n}}\cdot\hat{\mathbf{y}})^2)}; \quad \hat{\mathbf{n}}\cdot\hat{\mathbf{x}} = \pm\sqrt{\frac{D_1}{D_1-D_2}(1-(\hat{\mathbf{n}}\cdot\hat{\mathbf{y}})^2)}. \tag{154}$$

Then

$$\frac{\hat{\mathbf{n}}\cdot\hat{\mathbf{y}}}{\hat{\mathbf{n}}\cdot\hat{\mathbf{x}}} = \pm\frac{\hat{\mathbf{n}}\cdot\hat{\mathbf{y}}}{\sqrt{\frac{D_1}{D_1-D_2}(1-(\hat{\mathbf{n}}\cdot\hat{\mathbf{y}})^2)}} = \tan\chi. \tag{155}$$

Taking the scalar product of Eqn. (153) with $\hat{\mathbf{x}}$ and using Eqn.(154) yields

$$is\partial_\tau(\hat{\mathbf{n}}\cdot\hat{\mathbf{y}}) - i2s^2\sqrt{D_1D_2}(1-(\hat{\mathbf{n}}\cdot\hat{\mathbf{y}})^2)=0. \tag{156}$$

Upon integration we obtain the instanton:

$$\hat{\mathbf{n}}\cdot\hat{\mathbf{y}} = n_y = \tanh\left(\omega(\tau-\tau_0)\right), \tag{157}$$

where $\omega = 2s\sqrt{D_1D_2}$. The instanton interpolates from $n_y=1$ to $n_y=-1$ as $\tau\to\pm\infty$. Thus, $\arctan(\hat{\mathbf{n}}\cdot\hat{\mathbf{y}}/\hat{\mathbf{n}}\cdot\hat{\mathbf{y}})\to\pm\pi/2$ as $\tau\to\pm\infty$. Since the energy remains constant along the instanton trajectory, the action is determined only from the WZ term:

$$S_c = is\int_{-\frac{\pi}{2}}^{\frac{\pi}{2}} d[\arctan(n_y/n_x)](1-n_z). \tag{158}$$

From Eqn.(154) and Eqn.(155) we find

$$\hat{\mathbf{n}}\cdot\hat{\mathbf{z}} = n_z = \pm\frac{i\sqrt{\lambda}}{\sqrt{1-\lambda+\left(\frac{n_y}{n_x}\right)^2}}, \quad \lambda = D_2/D_1. \tag{159}$$

Thus, we recover the action in Eqn.(75)

$$S_c = is\pi + \ln\left(\frac{1+\sqrt{\lambda}}{1-\sqrt{\lambda}}\right)^s. \tag{160}$$

The calculation of the energy splitting follows directly from section(III.A.2). Thus, one recovers the spin-parity effect in a coordinate independent manner. This simply means that the spin-parity effect is independent of the choice of coordinate.

IV. EFFECTIVE POTENTIAL (EP) METHOD

As we mentioned earlier, the spin coherent state path integral formalism is valid in the large s limit, in other words if one imposes the commutator relation $[\phi, p] = i\hbar$, where $p = s\cos\theta$, then the spin commutator relation $[\hat{S}_i, \hat{S}_j] = i\epsilon_{ijk}\hat{S}_k$ is only recovered in the large s limit[9]. On the other hand, the effective potential method uses an exact mapping (Scharf, Wreszinski and Hemmen , 1987; Zaslavskii, 1990a; Zaslavskii and Ulyanov, 1992). In this method, one introduces the spin wave function using the $\hat{S}_z$ eigenstates, and the resulting eigenvalue equation $\hat{H}\left|\psi\right\rangle = \mathcal{E}\left|\psi\right\rangle$ is then transformed to a differential equation, which is further reduced to a Schrödinger equation with an effective potential and a constant or coordinate dependent mass. The energy spectrum of the spin system now coincides with the $2s+1$ energy levels for the particle moving in a potential field. The limitations of the method are as follow:

1). In the effective potential method, the WZ term (Berry phase) does not appear in the corresponding particle action, the quantum phase interference effect seems to disappear, however, in some special cases with a magnetic field one can recover the quenching of tunneling at the critical field from the periodicity of the particle wave function.

2). The effective potential method of higher order anisotropy spin models such as $\hat{H} = -D\hat{S}_z^2 - B\hat{S}_z^4 + C(\hat{S}_+^4 + \hat{S}_-^4) - H_x\hat{S}_x$ and $\hat{H} = D_1\hat{S}_z^2 + D_2\hat{S}_x^2 + C(\hat{S}_+^4 + \hat{S}_-^4)$ are very cumbersome to map onto a particle problem. In fact there is no effective potential method for such systems. Therefore the effective potential method is only efficient for large spin systems that are quadratic in the spin operators.

A. Effective method for a uniaxial spin model with a transverse magnetic field

In this section we will consider the effective potential method of the uniaxial model we studied in section(III.A.1). The Hamiltonian of this system is given by

$$\hat{H} = -D\hat{S}_z^2 - H_x\hat{S}_x. \tag{161}$$

Consider the the problem of finding the exact eigenstates of this Hamiltonian. The eigenvalue equation is

$$\hat{H}\left|\psi\right\rangle = \mathcal{E}\left|\psi\right\rangle, \tag{162}$$

where the spin wave function in the $\hat{S}_z$ representation is given by (Scharf, Wreszinski and Hemmen , 1987)

$$\left|\psi\right\rangle = \sum_{\sigma=-s}^{s}\binom{2s}{s+\sigma}^{-1/2} c_\sigma\left|s,\sigma\right\rangle. \tag{163}$$

---

[9] The proof of this is given in (Müller, *et al.*, 2000), Appendix A

Using the fact that $\hat{S}_x = \frac{1}{2}\left(\hat{S}_+ + \hat{S}_-\right)$ and

$$\hat{S}_\pm \left|s,\sigma\right\rangle = \sqrt{(s\mp\sigma)(s\pm\sigma+1)}\left|s,\sigma\pm1\right\rangle. \tag{164}$$

A straightforward calculation using Eqns.(161),(164), and (163) in Eqn.(162) gives:

$$-D\sigma^2 c_\sigma - \frac{1}{2}H_x[(s-\sigma+1)c_{\sigma-1} + (s+\sigma+1)c_{\sigma+1}] = \mathcal{E}c_\sigma, \tag{165}$$

where $\sigma = -s, -s+1, \cdots, s$, and $c_\sigma = 0$ for $|\sigma| > s$. Introducing a generating function of the form:

$$\mathcal{G}(x) = \sum_{\sigma=-s}^{s} c_\sigma e^{\sigma x}, \tag{166}$$

the eigenvalue equation, that is Eqn.(165) transforms to a second-order differential equation of the form:

$$b_1\frac{d^2\mathcal{G}}{d^2x} + b_2\frac{d\mathcal{G}}{dx} - b_3\mathcal{G} = \mathcal{E}\mathcal{G}, \tag{167}$$

where

$$b_1 = -D; \quad b_2 = H_x\sinh x; \quad b_3 = H_x s\cosh x. \tag{168}$$

The spin-particle correspondence follows from a special transformation of the form[10]

$$\Psi(x) = e^{-y(x)}\mathcal{G}(x), \tag{169}$$

where $y(x) = \tilde{s}h_x\cosh(x)$, $h_x = H_x/2D\tilde{s} < 1$, and $\tilde{s} = (s+\frac{1}{2})$ is a quantum renormalization. This transformation in Eqn.(169) is regarded as the coordinate or particle wave function since $\Psi(x) \to 0$ as $x \to \pm\infty$. Plugging this transformation into Eqn.(167) removes the first derivative term yielding the Schrödinger equation(Scharf, Wreszinski and Hemmen , 1987; Zaslavskii, 1990a; Zaslavskii and Ulyanov, 1992):

$$\hat{H}\Psi(x) = \mathcal{E}\Psi(x); \quad \hat{H} = -\frac{1}{2m}\frac{d^2}{dx^2} + U(x), \tag{170}$$

where

$$U(x) = D\tilde{s}^2(h_x\cosh x - 1)^2; \quad m = \frac{1}{2D}. \tag{171}$$

As before we have added a constant to normalize the potential to zero at the minimum $\cosh x = 1/h_x$. In Eqn.(169), the generating function contains a real exponential function. This choice is usually a matter of convenience. In most cases it is convenient to use an imaginary exponential function to avoid some technical issues, as we will see in the next section. The minimum of the potential is now at $x_{\rm mim} = \pm\,\mathrm{arccosh}(1/h_x)$ and the maximum is at $x_{\max} = 0$ with the height of the barrier given by

$$\Delta U = D\tilde{s}^2(1-h_x)^2. \tag{172}$$

It is possible to analytically solve the Schrödinger equation and find the energy levels of the particle in the potential Eqn.(171), such solution has been reported (Razavy, 1980). This potential is of the form of a double well we saw in Sec.(II.A) with $\pm a = \pm\,\mathrm{arccosh}(1/h_x)$. The instanton solution of such a problem follows the same approach (Coleman, 1985). The Euclidean Lagrangian corresponds to Eqn.(15) with the mass and the potential given by Eqn.(171). The solution of the Euclidean classical equation of motion, Eqn.(19) yields the instanton trajectory (Zaslavskii, 1990a; Zaslavskii and Ulyanov, 1992)

$$x(\tau) = \pm 2\,\mathrm{arctanh}\left[\sqrt{\frac{1-h_x}{1+h_x}}\tanh(\omega\tau)\right], \tag{173}$$

---

[10] Substituting Eqn.(169) into Eqn.(167) gives $b_1\Psi'' + (2b_1y' + b_2)\Psi' + [b_2y' + b_3 + b_1\left(y'' + y'^2\right)]\Psi = \mathcal{E}\Psi$. The function $y(x)$ is determined by demanding the coefficient of Ψ' vanishes.

where $\omega = D\tilde{s}\sqrt{1-h_x^2}$. This nontrivial solution corresponds to the motion of the spin particle at the top of the left hill at $\tau \to -\infty$, $x(\tau) \to -a$ and roll through the dashed line in Fig.(2) and emerges at the top of the right hill at $\tau \to \infty$, $x(\tau) \to a$. The corresponding action for this trajectory is

$$B = 2\tilde{s}\left[\frac{1}{2}\ln\left(\frac{1+\sqrt{1-h_x^2}}{h_x}\right) - \sqrt{1-h_x^2}\right]. \tag{174}$$

The computation of the ground state energy splitting yields (Chudnovsky,*et al.*, 1998; Zaslavskii, 1990a)

$$\Delta = \frac{8D\tilde{s}^{3/2}(1-h_x^2)^{5/2}}{\pi^{1/2}}\left(\frac{e^{\sqrt{1-h_x^2}}}{1+\sqrt{1-h_x^2}}\right)^{2\tilde{s}} h_x^{2s}, \tag{175}$$

which recovers the factor h_x^{2s} we saw previously in the spin coherent state path integral formalism. In the presence of a longitudinal magnetic field i.e along z-axis, the two degenerate minima of the potential become biased, one with lower energy and the other with higher energy. The problem becomes that of a quantum decay of a metastable state (Zaslavskii, 1990b).

B. Effective method for biaxial spin models

1. Biaxial ferromagnetic spin with hard axis magnetic field

The biaxial spin model also possesses a particle mapping via the EP method. Consider the biaxial system studied in sec.(III.A.3)

$$\hat{H} = D_1\hat{S}_z^2 + D_2\hat{S}_x^2 - h_z\hat{S}_z. \tag{176}$$

A convenient way to map this system to particle Hamiltonian is by introducing a non-normalized spin coherent state (Ersin and Garg, 2003; Garg , *et al.*, 2003; Perelomov, 1986; Radcliffe, 1971):

$$|z\rangle = e^{zS^-}|s,s\rangle = \sum_{\sigma=-s}^{s}\binom{2s}{s+\sigma}^{1/2} z^{s-\sigma}|s,\sigma\rangle = e^{is\phi}\sum_{\sigma=-s}^{s}\binom{2s}{s+\sigma}^{1/2} e^{-i\sigma\phi}|s,\sigma\rangle\,. \tag{177}$$

The last equality sign follows by restricting the complex variable on a unit circle, i.e $z = e^{i\phi}$. Acting from the left by $e^{-is\phi}\langle\psi|$ and subsequently taking the complex conjugate we obtain

$$\langle z|\psi\rangle = e^{is\phi}\sum_{\sigma=-s}^{s}\binom{2s}{s+\sigma}^{1/2} c_\sigma e^{i\sigma\phi} \equiv e^{is\phi}\Phi(\phi), \tag{178}$$

where $c_\sigma = \langle s,\sigma|\psi\rangle$ and $\Phi(\phi)$ is the generating function[11], with periodic boundary condition $\Phi(\phi+2\pi) = e^{2i\pi s}\Phi(\phi)$. From Eqn.(177) we have

$$\langle z|\hat{S}_z|\psi\rangle = e^{is\phi}\sum_{\sigma=-s}^{s}\binom{2s}{s+\sigma}^{1/2}\sigma c_\sigma e^{i\sigma\phi} = -ie^{is\phi}\frac{d\Phi(\phi)}{d\phi}. \tag{179}$$

Similar expressions can be derived for $\langle z|\hat{S}_x|\psi\rangle$ and $\langle z|\hat{S}_y|\psi\rangle$. Thus, the action of the spin operators on this function yields the following expressions (Zaslavskii, 1990a; Zaslavskii and Ulyanov, 1992):

$$\hat{S}_z = -i\frac{d}{d\phi}; \quad \hat{S}_x = s\cos\phi - \sin\phi\frac{d}{d\phi}; \quad \hat{S}_y = s\sin\phi + \cos\phi\frac{d}{d\phi}. \tag{180}$$

---

[11] It is convenient to use the generating function for x or y easy axis models while Eqn.(166) is convenient for z easy axis model. In that way one avoids the problem of a negative mass particle.

The Schrödinger equation can then be written as

$$\hat{H}\Phi(\phi) = \mathcal{E}\Phi(\phi). \tag{181}$$

From Eqn.(176) and Eqn.(180) one obtains the differential (Müller, *et al.*, 2000; Zaslavskii, 1990a):

$$-D_1(1-\lambda\sin^2\phi)\frac{d^2\Phi}{d\phi} - D_2(s-\frac{1}{2})\sin 2\phi\frac{d\Phi}{d\phi} + ih_z\frac{d\Phi}{d\phi} + (D_2 s^2\cos^2\phi + D_2 s\sin^2\phi)\Phi = \mathcal{E}\Phi. \tag{182}$$

A convenient way to obtain a Schrödinger equation with a constant is by introducing an incomplete elliptic integral of first kind (Abramowitz and Stegun, 1972; Byrd and Friedman, 1979) and the particle wave function:

$$x = F(\phi,\kappa) = \int_0^\phi d\varphi\frac{1}{\sqrt{1-\kappa^2\sin^2\varphi}}; \quad \Psi(x) = e^{-iu(x)}[\mathrm{dn}(x)]^{-s}\Phi(\phi(x)), \tag{183}$$

with amplitude ϕ and modulus $\kappa^2 = \lambda$. The trigonometric functions are related to the Jacobi elliptic functions by $\mathrm{sn}(x) = \sin\phi$, $\mathrm{cn}(x) = \cos\phi$ and $\mathrm{dn}(x) = \sqrt{1-\kappa^2\,\mathrm{sn}^2(x)}$. The function $u(x)$ is defined by

$$\frac{du}{dx} = \frac{\alpha s}{\mathrm{dn}(x)}, \quad \alpha = h_z/2D_2 s. \tag{184}$$

The imaginary phase is a topological shift in the wave function which is related to Aharonov Bohm effect (Aharonov and Bohm, 1959). In this new variable, Eqn.(182) transforms into a Schrödinger equation with

$$H = \frac{1}{2m}\Big[-i\frac{d}{dx} + A(x)\Big] + U(x); \quad m = \frac{1}{2D_1}. \tag{185}$$

The effective potential and the gauge field are given by

$$U(x) = \eta\,\mathrm{cd}(x)^2; \quad \mathrm{cd}(x) = \frac{\mathrm{cn}(x)}{\mathrm{dn}(x)}; \tag{186}$$

$$A(x) = -\frac{(2s+1)\alpha}{\mathrm{dn}(x)}; \tag{187}$$

where $\eta = D_2 s(s+1) + \frac{\lambda\alpha^2}{4(1-\lambda)}$. The potential has a period of $2\mathcal{K}(\kappa)$, where $\mathcal{K}(\kappa)$ is the complete elliptic function of first kind that is $\phi = \pi/2$ in the upper limit of Eqn.(183). Using Eqn.(184) one finds that the wave function obeys the periodic boundary condition(Müller, *et al.*, 1999; Sahng, *et al.*, 2000)

$$\Psi(x + 4\mathcal{K}(\kappa)) = e^{i2\pi s(1-\alpha/\sqrt{1-\lambda})}\Psi(x). \tag{188}$$

The corresponding Euclidean Lagrangian of this particle Hamiltonian is

$$L_E = \frac{1}{2}m\dot{x}^2 + iA(x)\dot{x} + U(x). \tag{189}$$

The second term of this equation drops out from the classical equation of motion, however, it is responsible for the suppression of tunneling splitting just like the WZ term (Berry phase) in the spin coherent state path integral formalism. Thus one finds that the exact instanton solution is

$$\mathrm{sn}[x(\tau)] = \tanh(\omega\tau), \quad \omega^2 = 4s(s+1)D_1 D_2, \tag{190}$$

which interpolates from $x_i = -\mathcal{K}(\kappa)$ ($\phi = -\pi/2$) at $\tau = -\infty$ to $x_f = \mathcal{K}(\kappa)$ ($\phi = \pi/2$) at $\tau = \infty$. The action for this trajectory is found to be

$$S_c = -i(2s+1)b + B, \tag{191}$$

where $b = \pi\alpha/\sqrt{1-\lambda}$ and B is given by

$$B = \sqrt{\frac{\eta}{D_2}}\ln\left(\frac{1+\sqrt{\lambda}}{1-\sqrt{\lambda}}\right). \tag{192}$$

By summing over instantons and anti-instantons configurations, it was shown that the energy splitting is given by(Müller, *et al.*, 2000)

$$\Delta = \Delta_0 |\cos(s\pi + b)|, \quad \Delta_0 = 4\mathscr{D}e^{-B}. \tag{193}$$

Thus one recovers the suppression of tunneling as before.

As an alternative approach of recovering the quenching of tunneling splitting, consider the transition from $x = 0$ to $x = 2\mathcal{K}(\kappa)$ and $x = 0$ to $x = -2\mathcal{K}(\kappa)$. The former is counterclockwise transition while the latter is clockwise transition, thus the total transition amplitude vanishes:

$$\mathcal{A}(2\mathcal{K}(\kappa), t; 0, 0) + \mathcal{A}(-2\mathcal{K}(\kappa), t; 0, 0) = 0, \tag{194}$$

where $\mathcal{A}$ represent the Feynman propagator given in Eqn.(8). In terms of the wave function the propagator can be written as(Coleman, 1977; Callan and Coleman, 1977; Coleman, 1985; Feynman and Hibbs, 1965)

$$\mathcal{A}(x_f, t; x_i, 0) = \sum_l \Psi_l(x_f)\Psi_l^*(x_i)e^{-i\mathcal{E}_l t}. \tag{195}$$

Then from Eqs.(194) and (195) one obtains the relation

$$\Psi_l(2\mathcal{K}(\kappa)) = -\Psi_l(-2\mathcal{K}(\kappa)), \tag{196}$$

which yields from Eqn.(188)

$$e^{i2\pi s(1-\alpha/\sqrt{1-\lambda})} = -1, \tag{197}$$

for any quantum number l. From this equation one obtains the condition for suppression of tunneling (Sahng, *et al.*, 2000)

$$\alpha = \sqrt{1-\lambda}\,(s - n - 1/2)\,/s, \tag{198}$$

just as Eqn.(97).

2. Biaxial ferromagnetic spin with medium axis magnetic field

Suppose we apply a magnetic field in the medium x-axis corresponding to the Hamiltonian:

$$\hat{H} = D_1\hat{S}_z^2 + D_2\hat{S}_x^2 - H_x\hat{S}_x. \tag{199}$$

As we pointed out in sec.(III.A.3), the quenching of tunneling at the critical field is only seen with biaxial spin models with magnetic field along the hard-axis, thus this model does not possess such effect. At zero magnetic field, there are two classical degenerate ground states corresponding to the minima of the energy located at $\pm\hat{\mathbf{y}}$, these ground states remain degenerate for $h_x \neq 0$ in the easy XY plane. The particle Hamiltonian is

$$H = -\frac{1}{2m}\frac{d^2}{dx^2} + U(x), \quad m = \frac{1}{2D_1}, \tag{200}$$

with the effective potential and the wave function given by (Owerre and Paranjape, 2014b)

$$U(x) = \frac{D_2\tilde{s}^2[\mathrm{cn}(x) - \alpha_x]^2}{\mathrm{dn}^2(x)}; \quad \Psi(x) = \frac{\Phi(\phi(x))}{[\mathrm{dn}(x)]^s}\exp\left[-\mathrm{arccot}\left(\sqrt{\frac{\lambda}{(1-\lambda)}}\,\mathrm{cn}(x)\right)\right], \tag{201}$$

where $\tilde{s} = (s+\frac{1}{2})$ and $\alpha_x = H_x/2D_2\tilde{s}$. In order to arrive at this potential we have used the approximation $s(s+1) \sim \tilde{s}^2$ and shifted the minimum energy to zero by adding a constant of the form $D_2\tilde{s}^2\alpha_x^2$. The potential, Eqn.(201) has minima at $x_0 = 4n\mathcal{K}(\kappa) \pm \mathrm{cn}^{-1}(\alpha_x)$ and maxima at $x_{sb} = \pm 4n\mathcal{K}(\kappa)$ for small barrier and at $x_{lb} = \pm 2(2n+1)\mathcal{K}(\kappa)$ for large barrier. The heights of the potential for small and large barriers are given by (Müller, *et al.*, 1998; Owerre and Paranjape, 2014b)

$$\Delta U_{sb} = D_2\tilde{s}^2(1-\alpha_x)^2; \quad \Delta U_{lb} = D_2\tilde{s}^2(1+\alpha_x)^2, \tag{202}$$

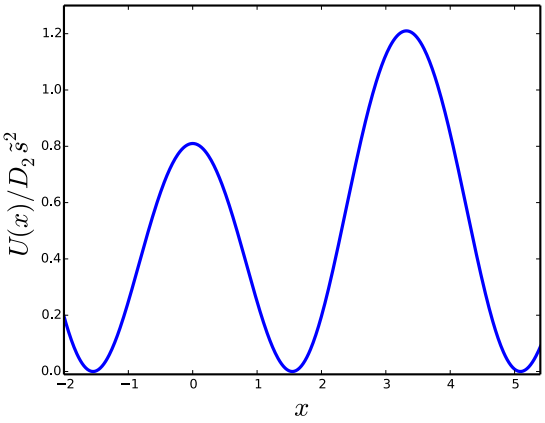

FIG. 10 Color online: The plot of the effective potential in Eqn.(201) for $\alpha_x = 0.1$, $\kappa = 0.2$.

The classical trajectory yields

$$\mathrm{sn}[x(\tau)] = \pm\frac{2\sqrt{\frac{1-\alpha_x}{1+\alpha_x}}\tanh(\omega\tau)}{[1+\frac{1-\alpha_x}{1+\alpha_x}\tanh^2(\omega\tau)]}, \tag{203}$$

and the corresponding action is (Owerre and Paranjape, 2014b; Zaslavskii, 1990a)

$$B = \tilde{s}\Bigg[\ln\left(\frac{1+\sqrt{\lambda(1-\alpha_x^2)}}{1-\sqrt{\lambda(1-\alpha_x^2)}}\right) \pm 2\alpha_x\sqrt{\frac{\lambda}{1-\lambda}}\arctan\left(\frac{\sqrt{(1-\lambda)(1-\alpha_x^2)}}{\alpha_x}\right)\Bigg], \tag{204}$$

where the upper and lower signs are for tunneling in large and small barriers respectively. The tunneling splitting can be found in the usual way by summing over instanton and anti-instanton configurations. During our discussion of phase transition in the next section, we will return to this concept of large and small barriers in detail. In this section we have specifically chosen biaxial spin models that possess an exact instanton solution. The transformations in Eqns.(180)—(178) are derived by restricting the analysis on a unit circle parameterize by the angle ϕ. In these two models, the variable ϕ and then x correspond exactly to the azimuthal angle ϕ in the spin coherent state path integral. In other representations of a biaxial spin system, this is not true and the EP method gives a very complicated effective potential, one can neither find the exact instanton solution nor the suppression of tunneling. However, without computing the explicit instanton trajectory, the action at the bottom of the potential well can be found in some cases by another elegant approach as we will see in the next section.

V. QUANTUM-CLASSICAL PHASE TRANSITIONS OF THE ESCAPE RATE IN LARGE SPIN SYSTEMS

A. Methods for studying quantum-classical phase transitions of the escape rate

In the preceding sections, we have reviewed quantum tunneling in spin systems which is dominated by instanton trajectory at zero temperature. As we mentioned in Section(I), transitions at finite temperature can be either first or second-order. In this section we will now discuss the phase transition of the escape rate from thermal to quantum regime at nonzero temperature. The escape rate of a particle through a potential barrier in the semiclassical approximation is obtained by taking the Boltzmann average over tunneling probabilities (Affleck, 1981; Chudnovsky,*et al.*, 1998):

$$\Gamma = \int_{U_{\min}}^{U_{\max}} d\mathcal{E}\,\mathscr{P}(\mathcal{E})e^{-\beta(\mathcal{E}-U_{\min})}, \tag{205}$$

where $\beta^{-1} = T$ is the temperature of the system, which is much less than the height of the potential barrier. This defines the temperature assisted tunneling rate, and $\mathscr{P}(\mathcal{E})$ is an imaginary time transition amplitude from excited

states at an energy $\mathcal{E}$. The integration limits $U_{\max}$ and $U_{\min}$ are the top and bottom of the potential energy respectively. The transition amplitude is defined as

$$\mathscr{P}(\mathcal{E}) = \mathscr{A} e^{-S(\mathcal{E})}, \tag{206}$$

where $\mathscr{A}$ is a prefactor independent of $\mathcal{E}$. The Euclidean action is of the form:

$$S(\mathcal{E}) = 2\int_{x_1(\mathcal{E})}^{x_2(\mathcal{E})} dx\sqrt{2m(x)(U(x)-\mathcal{E})}, \tag{207}$$

where $x_{1,2}(\mathcal{E})$ are the roots of the integrand in Eqn.(207), which are the classical turning points ($U(x_{1,2}) = \mathcal{E}$) of a particle with energy $-\mathcal{E}$ in the inverted potential $-U(x)$ as depicted in Fig.(1). The mass $m(x)$ is coordinate dependent in general. The factor of 2 in Eqn.(207) corresponds to the back and forth oscillatory motion of the particle in the inverted potential (see Fig.1). In other words, the particle crosses the barrier twice.

1. Phase transition with thermon action

The escape rate can as well be written as

$$\Gamma = \mathscr{A}\int_{U_{\min}}^{U_{\max}} d\mathcal{E} e^{-\mathcal{S}_p}, \tag{208}$$

where

$$\mathcal{S}_p = S(\mathcal{E}) + \beta(\mathcal{E} - U_{\min}), \tag{209}$$

is the thermon action (Chudnovsky, 1992). In the method of steepest decent (for small temperatures $T < \hbar\omega_0$, ω_0 is the frequency at the bottom of the potential), one can introduce fluctuations around the classical path that minimizes this thermon action, i.e $\frac{d\mathcal{S}_p}{d\mathcal{E}} = 0$. The escape rate, Eqn.(208) in this method is thus written as (Chudnovsky and Garanin, 1997)

$$\Gamma \sim e^{-\mathcal{S}_{\min}(\mathcal{E})}, \tag{210}$$

and $\mathcal{S}_{\min}(\mathcal{E})$ is the minimum of the thermon action in Eqn.(209) with respect to energy.

In many cases of physical interest, when the energy is in the range $U_{\min} < \mathcal{E} < U_{\max}$, the Euclidean action $S(\mathcal{E})$ can be computed exactly or numerically in the whole range of energy for any given potential in terms of complete elliptic integrals and hence the thermon action $\mathcal{S}_p$. This corresponds to the action of the periodic instanton(Liang, *et al.*, 2000) or thermon. At the bottom of the potential $\mathcal{E} = U_{\min}$, the minimum thermon action becomes the vacuum instanton action, that is

$$\mathcal{S}_{\min}(U_{\min}) = S(U_{\min}). \tag{211}$$

Thus, the vacuum instanton action of the previous sections becomes $B = S(U_{\min})/2$, since it corresponds to half of the period of oscillation. Eqn.(210) becomes the transition amplitude formula for a pure quantum tunneling. However, at the top of the barrier $\mathcal{E} = U_{\max}$, the Euclidean action vanishes, $S(U_{\max}) = 0$, the minimum thermon action (thermodynamic action) becomes

$$\mathcal{S}_{\min}(U_{\max}) = \mathcal{S}_0 = \beta\Delta U. \tag{212}$$

This corresponds to the action of a constant trajectory $x(\tau) = x_s$ at the bottom of the inverted potential (Chudnovsky, 1992). The escape rate Eqn.(210) becomes the Boltzmann formula for a pure thermal activation. As we showed in section(I), the crossover temperature from thermal to quantum regimes ("first-order phase transition") occurs when the escape rate Eqn.(210) with $\mathcal{S}_{\min}(U_{\min})$ is equal to that with $\mathcal{S}_{\min}(U_{\max})$, which yields Eqn.(1). At this temperature the thermon action $\mathcal{S}_p$ sharply intersects with the thermodynamic action $\mathcal{S}_0$ leading to a discontinuity in the first-derivative of the action $\mathcal{S}_p$ at $\beta_0^{(1)}$. For second-order phase transition the thermon action $\mathcal{S}_p$ smoothly joins the thermodynamic action $\mathcal{S}_0$ at $\beta = \beta_0^{(2)}$.

2. Phase transition with thermon period of oscillation

The dominant term in Eqn.(208) comes from the minimum of the thermon action Eqn.(209), which is given by

$$\beta(\mathcal{E}) = -\frac{dS(\mathcal{E})}{d\mathcal{E}} = \int_{x_1(\mathcal{E})}^{x_2(\mathcal{E})} dx \sqrt{\frac{2m(x)}{U(x)-\mathcal{E}}} \equiv \tau(\mathcal{E}). \tag{213}$$

This is the period of oscillation of a particle with energy $-\mathcal{E}$ in the inverted potential $-U(x)$. At the bottom of the potential $\mathcal{E} = U_{\min}$, the period $\beta(\mathcal{E}) = \infty$ i.e $T = 0$ which corresponds to the vacuum instanton of section(IV), while at the top of the barrier $\mathcal{E} = U_{\max}$, $\beta(\mathcal{E}) \to \beta_0^{(2)} = 2\pi/\omega_b$ (Affleck, 1981). The first and second-order transitions can be studied from the behaviour of $\beta(\mathcal{E})$ as a function of $\mathcal{E}$.

1). If $\beta(\mathcal{E})$ has a minimum at some point $\mathcal{E}_0 < U_{\max}$, $\beta_{\min} = \beta(\mathcal{E}_0)$ and then rises again, i.e non-monotonic, then first-order phase transition occurs (Chudnovsky, 1992). At a certain energy within the range $U_{\min} < \mathcal{E}_1 < \mathcal{E}_0$, the thermon action sharply intersects with the thermodynamic action, yielding the actual crossover temperature $\beta_0^{(1)} = \beta(\mathcal{E}_1)$.

2). A monotonic decrease of $\beta(\mathcal{E})$ with increasing $\mathcal{E}$ from the bottom to the top of the barrier indicates the presence of second-order phase transition(Chudnovsky,*et al.*, 1998; Chudnovsky and Garanin, 1997; Chudnovsky, 1992). In this case the thermon action $\mathcal{S}_p$ smoothly intersects with the thermodynamic action $\mathcal{S}_0$, yielding the crossover temperature $\beta_0^{(2)}$ (Chudnovsky, 1992; Gorokhov and Blatter, 1997), which is exactly Eqn.(2).

3. Phase transition with free energy

The semiclassical escape rate Eqn.(210) can be written in a slightly different form:

$$\Gamma \sim e^{-\beta F_{\min}}, \tag{214}$$

where $F_{\min} = \beta^{-1}\mathcal{S}_{\min}(\mathcal{E})$ is the minimum of the effective free energy

$$F = \beta^{-1}\mathcal{S}_p = \mathcal{E} + \beta^{-1}S(\mathcal{E}) - U_{\min}, \tag{215}$$

with respect to $\mathcal{E}$. The crossover from thermal to quantum regimes (first-order phase transition) occurs when two minima in the F vs. $\mathcal{E}$ curve have the same free energy. All the interesting physics of phase transition in spin systems can also be captured when the energy is very close (but not equal) to the top of the potential barrier, $\mathcal{E} \to U_{\max}$. In this case the free energy can then be used to characterize first- and second-order phase transitions in analogy with Landau's theory of phase transition if one knows the exact expression of the action $S(\mathcal{E})$ for any given mass and potential. In most models with a magnetic field the action $S(\mathcal{E})$ cannot be obtained exactly, one has to study the free energy numerically.

4. Phase transition with criterion formula

An alternative method for determining the phase transition of the escape rate, as well as the phase boundary was considered by Müller, Park and Rana (1999). They studied the Euclidean action near the top of the potential barrier, which had been considered earlier by Gorokhov and Blatter (1997). For the general case of a particle that possesses a coordinate dependent mass, they found that near the top of the potential barrier the expression that depends on the potential, which determines the type of phase transition is given by (Müller, Park and Rana, 1999)

$$\mathscr{C} = \left[U'''(x_s)\left(g_1 + \frac{g_2}{2}\right) + \frac{1}{8}U''''(x_s) + \omega^2 m'(x_s)g_2 + \omega^2 m'(x_s)\left(g_1 + \frac{g_2}{2}\right) + \frac{1}{4}\omega^2 m''(x_s)\right]_{\omega=\omega_b}, \tag{216}$$

where

$$g_1 = -\frac{\omega^2 m'(x_s) + U'''(x_s)}{4U''(x_s)}, \tag{217}$$

$$g_2 = -\frac{3m'(x_s)\omega^2 + U'''(x_s)}{4\left[4m(x_s)\omega^2 + U''(x_s)\right]}, \tag{218}$$

$$\omega_b^2 = -\frac{U''(x_s)}{m(x_s)}; \quad m' \equiv \frac{dm(x)}{dx}\,, \text{etc.} \tag{219}$$

The coordinate x_s represents the position of the sphaleron[12] at the bottom of the inverted potential as shown in Fig.(1). The criterion for first-order phase transition requires $\mathscr{C} < 0$, while $\mathscr{C} > 0$ implies a second-order transition, and the phase boundary between the first- and the second-order phase transitions is of course $\mathscr{C} = 0$. The criterion formula in Eq.(216) is quite general. It can be simplified in two special cases:

1). If the mass of the particle is a constant and the potential energy is an even function, Eq.(216) reduces to

$$\mathscr{C} = \frac{1}{8}U''''(x_s). \tag{220}$$

Thus, expanding the potential around x_s, the coefficient of the fourth-order term quickly determines the first- and the second-order phase transitions, as well as the phase boundary (Chudnovsky and Garanin, 1997).

2). If mass is still a constant but the potential is an odd function, Eq.(216) reduces to

$$\mathscr{C} = -\frac{5}{24}\frac{[U'''(x_s)]^2}{U''(x_s)} + \frac{1}{8}U''''(x_s). \tag{221}$$

B. Phase transition in uniaxial spin model in a magnetic field

1. Spin model Hamiltonian

We have written down all the necessary formulae for studying the phase transition of the escape rate for a uniaxial spin model in an applied field. An extensive analysis of this model can be found in (Chudnovsky,*et al.*, 1998; Chudnovsky and Tejada, 1998). In this section we will briefly review the theoretical analysis and recent experimental development. For this system we saw that the spin Hamiltonian is given by

$$\hat{H} = -D\hat{S}_z^2 - H_x\hat{S}_x. \tag{222}$$

As we mentioned before this system is a good approximation for $Mn_{12}Ac$, with a ground state of $s = 10$ and 21 energy levels. Transition between these states can occur either by quantum tunneling (QT) or thermally assisted tunneling (TAT) as depicted in Fig.(16).

2. Particle Hamiltonian

As we explicitly showed in Sec.(IV.A), the spin Hamiltonian in Eqn.(222) corresponds to the particle potential and the mass:

$$U(x) = D\tilde{s}^2(h_x\cosh x - 1)^2, \quad m = \frac{1}{2D}. \tag{223}$$

Since the potential is an even function and the mass is constant, the quickest way to determine the regime where the first-order transition sets in, is by considering where the coefficient of the fourth order term changes sign near $x_s = 0$. Expanding the potential around x_s we have

$$U(x) \approx U(0) + D\tilde{s}^2[-h_x(1-h_x)x^2 + \frac{h_x}{3}\left(h_x - \frac{1}{4}\right)x^4 + O(x^6)]. \tag{224}$$

---

[12] Sphalerons are static, unstable, finite-energy solutions of the classical equations of motion.

The coefficient of x^2 in Eqn.(224) is negative for $h_x < 1$, which corresponds to nonvanishing of the potential barrier, Eqn.(172). The coefficient of x^4 is similar to $\mathscr{C}$ in Eq.(220), it is given by(Müller, Park and Rana, 1999)

$$\mathscr{C} = D\tilde{s}^2 h_x \left(h_x - \frac{1}{4}\right). \tag{225}$$

Clearly, $\mathscr{C}$ changes sign for $h_x < \frac{1}{4}$, which corresponds to the regime of the first-order transition from thermal

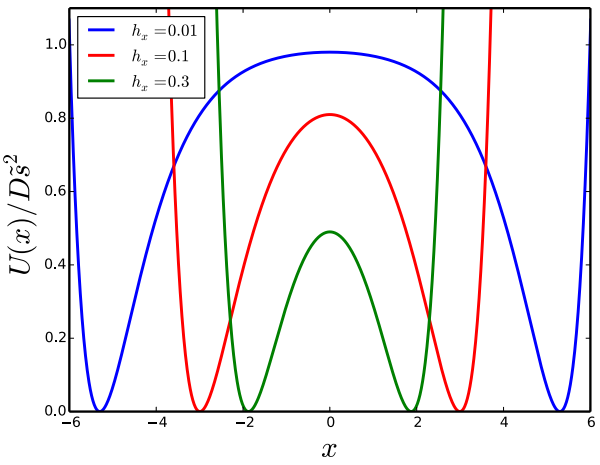

FIG. 11 Color online: The plot of the potential in Eq.(223) for several values of h_x.

activation to quantum tunneling. It is positive for $h_x > \frac{1}{4}$, which is the regime of second-order phase transition, and of course vanishes at the phase boundary $h_{cx} = \frac{1}{4}$.

3. Thermon or periodic instanton action

An alternative approach to investigate quantum-classical phase transitions of the escape rate is by computing the thermon action:

$$\mathcal{S}_p = 2\sqrt{2m}\int_{-x_1}^{x_1} dx\sqrt{U(x)-\mathcal{E}} + \beta(\mathcal{E} - U_{\min}), \tag{226}$$

where $\pm x_1$ are the roots of the integrand which are the classical turning points. This action corresponds to the action of the periodic instanton trajectory[13] of Eq.(223). That is the solution of the classical equation of motion:

$$\frac{1}{2}m\dot{x}^2 - U(x) = -\mathcal{E}. \tag{227}$$

Integrating this equation using Eq.(223) one finds that the periodic instanton trajectory is given by (Zhang, *et al.*, 1999)

$$x_p = \pm 2\tanh^{-1}\left[\xi_p \,\mathrm{sn}\left(\omega_p\tau, k\right)\right], \tag{228}$$

where

$$k^2 = \frac{1-\left(\sqrt{\tilde{\mathcal{E}}}+h_x\right)^2}{1-\left(\sqrt{\tilde{\mathcal{E}}}-h_x\right)^2}, \quad \xi_p^2 = \frac{1-h_x\pm\sqrt{\tilde{\mathcal{E}}}}{1+h_x\pm\sqrt{\tilde{\mathcal{E}}}}, \tag{229}$$

$$\omega_p^2 = (D\tilde{s})^2\left[1-(\sqrt{\tilde{\mathcal{E}}}-h_x)^2\right], \quad \tilde{\mathcal{E}} = \mathcal{E}/D\tilde{s}^2. \tag{230}$$

---

[13] The thermon action in Eq.(226) only differs from the periodic instanton action by a factor of 2 in Eq.(226). So we will use the two names interchangeably.

It is required that as $\tau \to \pm\frac{\beta}{2}$, this trajectory must tend to the classical turning points $x_p \to \pm x_1$ as depicted in Fig(12). Let us define dimensionless energy quantity(Chudnovsky,*et al.*, 1998; Chudnovsky and Garanin, 1997):

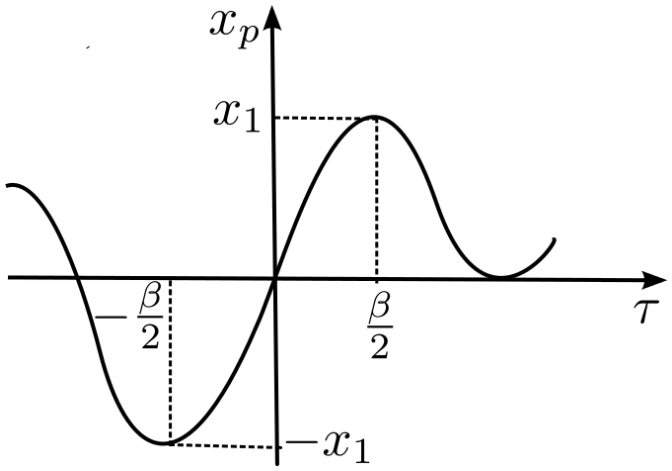

FIG. 12 The plot of the periodic trajectory in Eq.(228).

$$P = \frac{U_{\max} - \mathcal{E}}{U_{\max} - U_{\min}}. \tag{231}$$

Clearly $P \to 0$ at the top of the barrier $\mathcal{E} \to U_{\max}$, and $P \to 1$ at the bottom of the barrier $\mathcal{E} \to U_{\min}$. By making a change of variable $y = \cosh x$, Eq.(226) can be reduced to complete elliptic integrals (Abramowitz and Stegun, 1972; Byrd and Friedman, 1979) in the whole range of energy. It is found to be of the form (Chudnovsky,*et al.*, 1998):

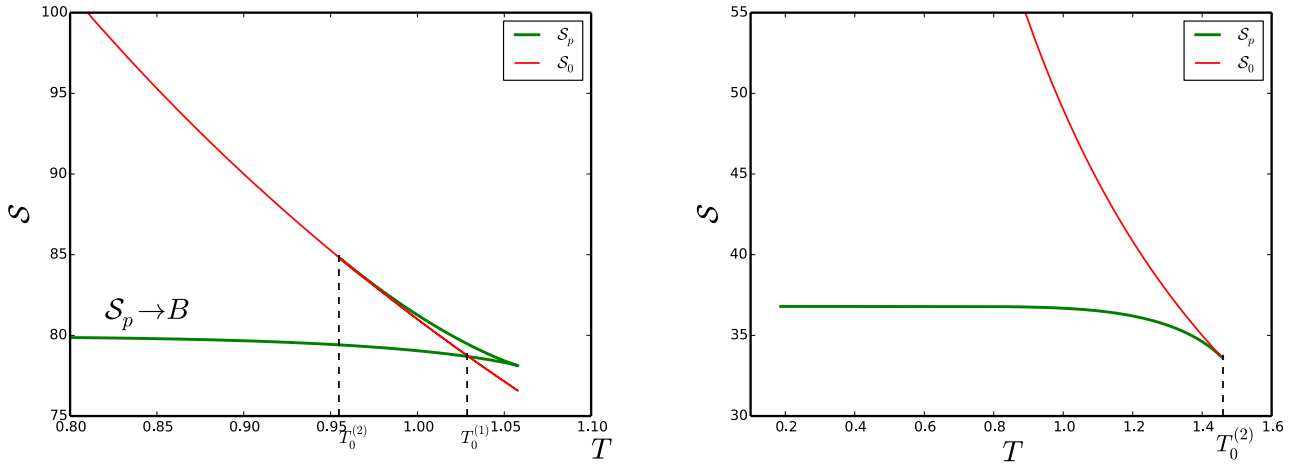

FIG. 13 Color online: The plot of the thermon action Eqn.(209) and thermodynamic action Eqn.(212) against temperature. Left: $s = 10$, $D = 1$ $h_x = 0.1$ (first-order transition), where B is the vacuum instanton action. Right: $s = 10$, $D = 1$, $h_x = 0.3$ (second-order transition).

$$\mathcal{S}_p = 4\tilde{s}\sqrt{(1-h_x)g_+}\mathcal{I}(\alpha^2, k) + \beta\Delta U(1-P), \tag{232}$$

where

$$g_\pm = P + h_x\left(1 \pm \sqrt{1-P}\right)^2, \tag{233}$$

$$\mathcal{I}(\alpha^2, k) = (1+\alpha^2)\mathcal{K}(k) - E(k) + (\alpha^2 - k^2/\alpha^2)(\Pi(\alpha^2, k) - \mathcal{K}(k)); \quad \alpha^2 = (1-h_x)P/g_+; \quad k^2 = g_-/g_+; \tag{234}$$

where $\mathcal{K}(k)$, $E(k)$ and $\Pi(\alpha^2, k)$ are the complete elliptic integral of the first, the second and the third kinds respectively. In Fig.(13) we have shown the plot of the actions Eqn.(232) and Eqn.(212) as a function of temperature. Indeed one observes the sharp and smooth intersections corresponding to the first- and the second-order phase transitions temperatures respectively.

4. Free energy function

The free energy can also be used to study the quantum-classical phase transitions in this systems. It can be written down exactly from Eqn.(232). It is given by

$$\frac{F}{\Delta U} = 1 - P + \frac{4\theta\sqrt{h_x g_+}}{\pi\left(1-h_x\right)^{3/2}}\mathcal{I}(\alpha^2, k), \tag{235}$$

where $\theta = T/T_0^{(2)}$, and $T_0^{(2)}$ is given by Eq.(238). Near the top of the barrier $P \ll 1$, the free energy of this spin model yields (Chudnovsky,*et al.*, 1998; Chudnovsky and Garanin, 1997)

$$F(P)/\Delta U = 1 + (\theta - 1)P + \frac{\theta}{8}\left(1 - \frac{1}{4h_x}\right)P^2 + \frac{3\theta}{64}\left(1 - \frac{1}{3h_x} + \frac{1}{64h_x^3}\right)P^3 + O(P^4). \tag{236}$$

This free energy should be compared with the Landau's free energy function:

$$F = F_0 + a\psi^2 + b\psi^4 + c\psi^6. \tag{237}$$

The analogy between these two free energies comes from identifying the coefficient of P^2 as the Landau coefficient b,

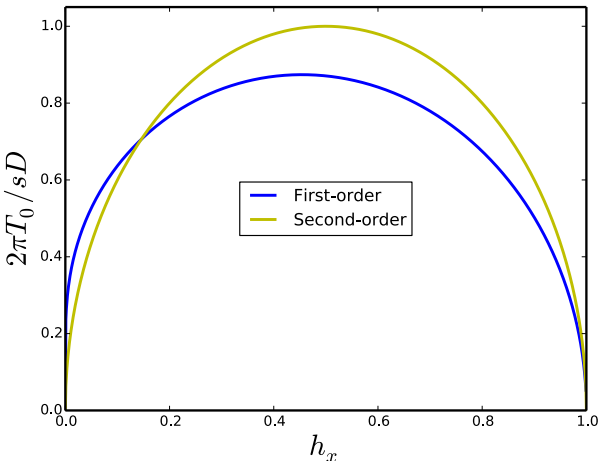

FIG. 14 Color online: The plot of the of the first-and second-order cross over temperatures against h_x. Reproduced with permission from Chudnovsky,*et al.*, 1998.

which determines the regime of first-order phase transition $b < 0$, and that of second-order phase transition $b > 0$. The boundary between the first- and the second-order phase transition corresponds $b = 0$. We see that these conditions recover the results in Sec.(V.B.2). The plot of the free energy in the whole range of energy is shown in Fig.(15). The actual crossover temperature from thermal to quantum regimes is determined when two minima of a curve have the free energy. For $h_x = 0.1$, it is found to be at $T_0^{(1)} = 1.076T_0^{(2)}$. This crossover temperature is approximately given by $T_0^{(1)} = \Delta U/S(\mathcal{E} \to 0)$, which can be obtained easily from Eqn.(172) and Eqn.(174). For the second order transition one finds that at $x_s = x_{\max} = 0$

$$T_0^{(2)} = \frac{1}{\beta_0^{(2)}} = \frac{D\tilde{s}}{\pi}\sqrt{h_x(1-h_x)}. \tag{238}$$

In the limit $h_x \to 1$ one finds $T_0^{(1)}/T_0^{(2)} \approx 0.833$. The plot of these temperatures are shown in Fig.(14). It is crucial

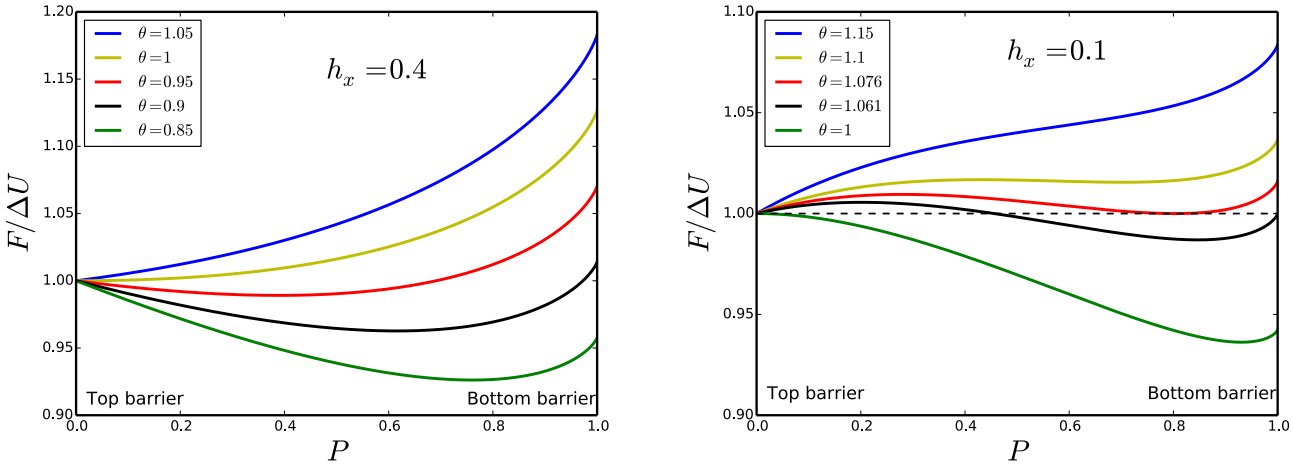

FIG. 15 Color online: The plot of the of the free energy as a function of P for $h_x = 0.4$ second-order transition and $h_x = 0.1$ first-order transition. Reproduced with permission from Chudnovsky and Garanin, 1997.

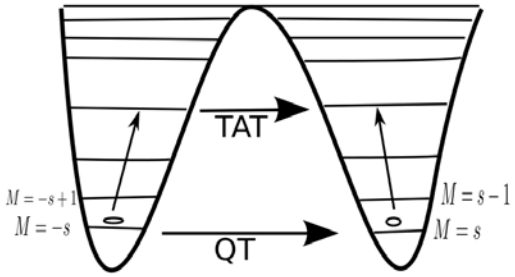

FIG. 16 A sketch of quantum tunneling(QT) and thermally assisted resonant tunneling (TAT) in $Mn_{12}Ac$ molecular magnet.

to note that the magnetic field plays a decisive role on the crossover temperatures for the first-and the second-order phase transitions. It is the main parameter that drives tunneling in this system. Physically, the sharp first-order phase transition in this model occurs due to the flatness or wideness of the barrier top in the small magnetic field limit as shown in Fig.(11). In the strong magnetic field limit, the top of the barrier is of the parabolic form (see Fig.(11)) which leads to suppression of first-order phase transition. In the limit of zero magnetic field the Hamiltonian Eq.(222) commutes with the z-component of the spin, thus $\hat{S}_z$ is a constant of motion and the potential in Eq.(223) becomes a constant. Hence, there is no dynamics (tunneling) and no quantum-classical phase transitions[14].

5. Experimental results

Recently, experiments have been conducted to measure these crossover temperatures. Experimental result for $Mn_{12}Ac$ molecular magnet with the model in Eqn.(239) has confirmed the existence of an abrupt and gradual crossover temperature ($T \sim 1.1K$) between thermally assisted and pure quantum tunneling (Bokacheva, Kent and Marc, 2000; Garanin and Chudnovsky, 2000; Kent, *et al.*, 2000; Leuenberger and , 2000) as shown in Fig.(17). Below the crossover temperature the magnetization relaxation becomes temperature independent, which indicates that transition occur by QT between the $m_{esc} = \pm s$ states. Above the crossover temperature transition favours the excited states with $m_{esc} < s$ (TAT). Quite recently, a similar result was observed in Mn_{12}-tBuAc molecular nanomagnet with a spin ground state of $s = 10$. This molecular nanomagnet has the same magnetic anisotropy as $Mn_{12}Ac$ but the molecules are very isolated and the crystals have less disorder and a higher symmetry(Wernsdorfer, Murugesu, and Christou,

[14] The basic understanding is that in the zero magnetic field limit, the barrier becomes infinitely thick and tunneling cannot occur.

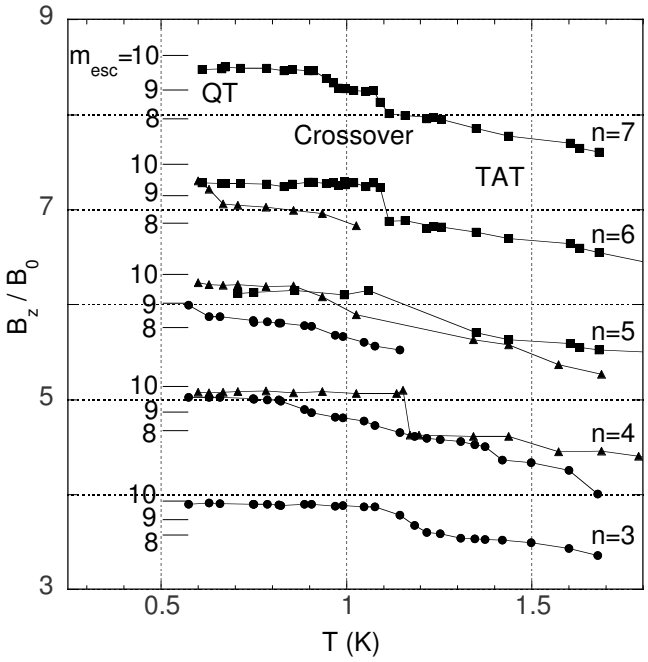

FIG. 17 Peak positions of the first derivative of the magnetization plotted against the temperature in $Mn_{12}Ac$ molecular magnet. At the ground state $M = s = 10$, the peak is independent of temperature (QT) while for excited states $M < s$ transition occurs by TAT. Adapted with permission from Bokacheva, Kent and Marc, 2000

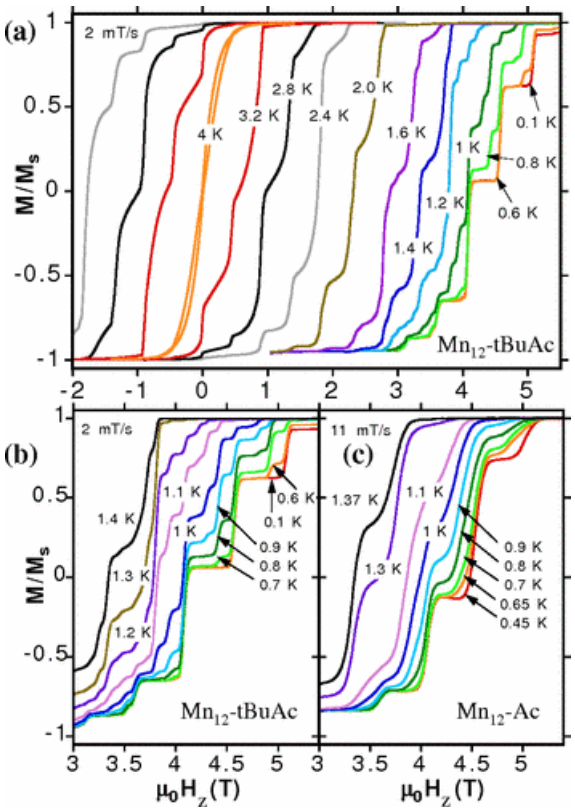

FIG. 18 Color online: Temperature dependence of hysteresis loops of (b) Mn_{12}-tBuAc and (c) $Mn_{12}Ac$ SMMs at different temperatures and a constant field sweep rate as indicated in the figure. With decreasing temperature , the hysteresis increases due to a decrease in the transition rate of thermal assisted tunneling. Adapted with permission from Wernsdorfer, Murugesu, and Christou, 2006

2006). The Hamiltonian for this system has the form:

$$\hat{H} = -D\hat{S}_z^2 - B\hat{S}_z^4 - h_z\hat{S}_z + \hat{H}_\perp, \tag{239}$$

where $h_z = g_z\mu_0\mu_B H_z$ and $\hat{H}_\perp$ is the splitting term which is comprised of $\hat{S}_x$ and $\hat{S}_y$. In the absence of $\hat{H}_\perp$, the 21 energy levels of Eqn.(239) can be found by the so-called exact numerical diagonalization in the $\hat{S}_z$ representation. The inclusion of a small perturbation $\hat{H}_\perp$ leads to an avoided level crossings in the degenerate energy subspace. The crossover temperature for the compound occurs at $T \sim 0.6K$. The hysteresis loops in Fig.(18) show a temperature independent quantum tunneling at the lowest energy levels below $0.6K$, while the temperature dependent thermal assisted tunneling at the excited states occurs above $0.6K$.

C. Phase transition in biaxial spin model

1. Model Hamiltonian and spin coherent state path integral

The phase transition in biaxial spin systems follow a similar trend to that of uniaxial spin model in a magnetic field. The first work on this system was begun by Liang, *et al.* (1998). They studied the model:

$$\hat{H} = K_1\hat{S}_z^2 + K_2\hat{S}_y^2, \quad K_2/K_1 = \lambda < 1, \tag{240}$$

by spin coherent state path integral and periodic instanton method. This Hamiltonian is related to that of Eqn.(70) and Eqn.(72) by $K_1 = D_1$, $K_2 = D_2$ and $\phi \to \pi/2 - \phi$. It can also be related to any biaxial spin model in the absence of a magnetic field. The effective Lagrangian of this system can be obtained by integrating out $\cos\theta$ from the spin coherent state path integral, Eqn.(64), one finds that the effective classical Euclidean Lagrangian is

$$L_E = is\dot{\phi} + \frac{1}{2}m(\phi)\dot{\phi}^2 + U(\phi), \tag{241}$$

where

$$m(\phi) = \frac{1}{2K_1(1 - \lambda\sin^2\phi)}, \quad U(\phi) = K_2 s^2 \sin^2\phi. \tag{242}$$

The potential barrier height is located at $\phi_s = \frac{\pi}{2}$, and the minimum energy is located at $\phi = 0$.

2. Periodic instanton

The periodic instanton trajectory of this model can be computed from the classical equation of motion:

$$m(\phi_p)\ddot{\phi}_p + \frac{1}{2}\frac{dm(\phi_p)}{d\phi_p}\dot{\phi}_p^2 - \frac{dU}{d\phi_p} = 0. \tag{243}$$

Integrating once we obtain:

$$\frac{1}{2}m(\phi_p)\dot{\phi}_p^2 - U(\phi_p) = -\mathcal{E}, \tag{244}$$

where $\mathcal{E}$ is the integration constant. The corresponding periodic instanton solution of this equation yields

$$\phi_p = \arcsin\left[\frac{1 - k^2\,\mathrm{sn}^2(\omega_p\tau, k)}{1 - \lambda^2 k^2\,\mathrm{sn}^2(\omega_p\tau, k)}\right]^{\frac{1}{2}}, \tag{245}$$

where

$$k^2 = \frac{n^2 - 1}{n^2 - \lambda}, \quad n^2 = \frac{K_2 s^2}{\mathcal{E}}; \quad \omega_p^2 = \omega_0^2(1 - \frac{\lambda}{n^2}); \quad \omega_0^2 = 4K_1K_2s^2. \tag{246}$$

The classical action for this trajectory is found to be

$$\mathcal{S}_p = \frac{4\omega}{\lambda K_1}\mathcal{I}(k^2\lambda, k) + \beta(\mathcal{E} - U_{\min}), \tag{247}$$

$$\mathcal{I}(k^2\lambda, k) = [\mathcal{K}(k) - (1 - k^2\lambda)\Pi(k^2\lambda, k)], \tag{248}$$

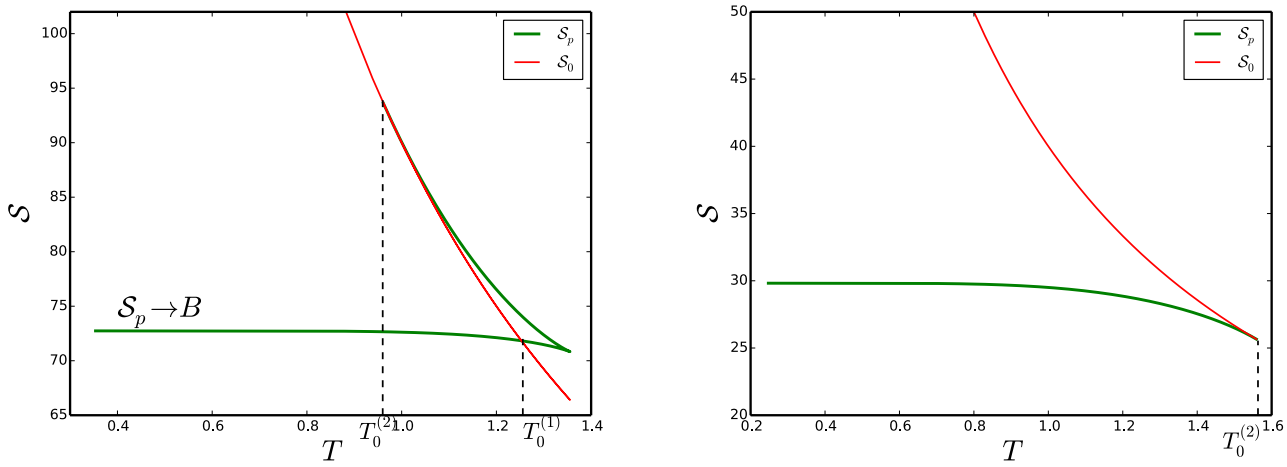

FIG. 19 Color online: The plot of the thermon action Eqn.(247) and thermodynamic action Eqn.(212) against temperature for the biaxial model. Left: $s = 10$, $K_1 = 1$, $\lambda = 0.9$ (first-order transition), where B is the vacuum instanton action. Right: $s = 10$, $K_1 = 1$, $\lambda = 0.4$ (second-order transition). Reproduced with permission from (Liang, *et al.*, 1998).

where $\mathcal{K}$ and Π are the complete elliptic integrals of the first and the third kinds respectively, and the period of oscillation is given by

$$\beta(\mathcal{E}) = \frac{2}{\sqrt{K_1}\sqrt{K_2 s^2 - \mathcal{E}\lambda}}\mathcal{K}(k). \tag{249}$$

Near the top of the barrier $\mathcal{E} \to U_{\max} = K_2 s^2$ and $\beta(\mathcal{E}) \to \beta_0^{(2)} = 2\pi/\omega_b$, with ω_b defined by Eqn.(219) and near the bottom of the barrier $\mathcal{E} \to U_{\min} = 0$ and $\beta(\mathcal{E}) \to \infty$, then $\mathcal{S}_p$ reduces to the usual vacuum ($T = 0$) instanton solution, Eqn.(76). Fig.(19) shows the thermon and the thermodynamic actions with the crossover temperatures indicated, which is of similar trend to that of Fig.(13) .

3. Free energy and crossover temperatures

The ground state crossover temperature is determined from $T_0^{(1)} = \Delta U/\mathcal{S}_p(\mathcal{E} \to U_{\min}) = K_2 s^2/\mathcal{S}_p(\mathcal{E} \to U_{\min})$. For the second order phase transition we have $T_0^{(2)} = \omega_b/2\pi$. In the limit $\lambda \to 0$, one finds that $T_0^{(1)}/T_0^{(2)} = \pi/4 \approx 0.785$. The exact free energy follows from Eqn.(247):

$$\frac{F}{\Delta U} = 1 - P + \frac{4\theta\sqrt{(1-\lambda)[1-\lambda(1-P)]}}{\pi\lambda}\mathcal{I}(k^2\lambda, k), \tag{250}$$

where $\theta = T/T_0^{(2)}$, and $T_0^{(2)} = sK_1\sqrt{\lambda(1-\lambda)}/\pi$. Near the top of the barrier $P \ll 1$, the free energy reduces to (Zhang, *et al.*, 1999)

$$F/\Delta U \cong 1 + (\theta - 1)\,P + \frac{\theta}{4\,(1-\lambda)}\left(\frac{1}{2} - \lambda\right)P^2 + \frac{\theta}{8\,(1-\lambda)^2}\left(\lambda^2 - \lambda + \frac{3}{8}\right)P^3 + O(P^4). \tag{251}$$

The coefficient of the P^2 changes sign when $\lambda > \frac{1}{2}$, which corresponds to the regime of first-order phase transition. In this analysis, the mass is coordinate dependent, therefore the coefficient of ϕ^4 in the series expansion near $\phi_s = \frac{\pi}{2}$ cannot determine the condition for any type of quantum-classical phase transitions, thus Eqn.(216) becomes indispensable. Using Eqn.(216) with $x_s = \phi_{\max} = \frac{\pi}{2}$ one obtains (Müller, Park and Rana, 1999)

$$\mathscr{C} = K_2 s^2 \frac{1-2\lambda}{1-\lambda}, \tag{252}$$

where $\mathscr{C}$ is equivalent to the coefficient of the P^2 in Eq.(251). It is evident that $\mathscr{C} < 0$ for $\lambda > \frac{1}{2}$, corresponding to the regime of first-order phase transition. At the phase boundary $\mathscr{C} = 0$, which yields the critical value $\lambda_c = \frac{1}{2}$.

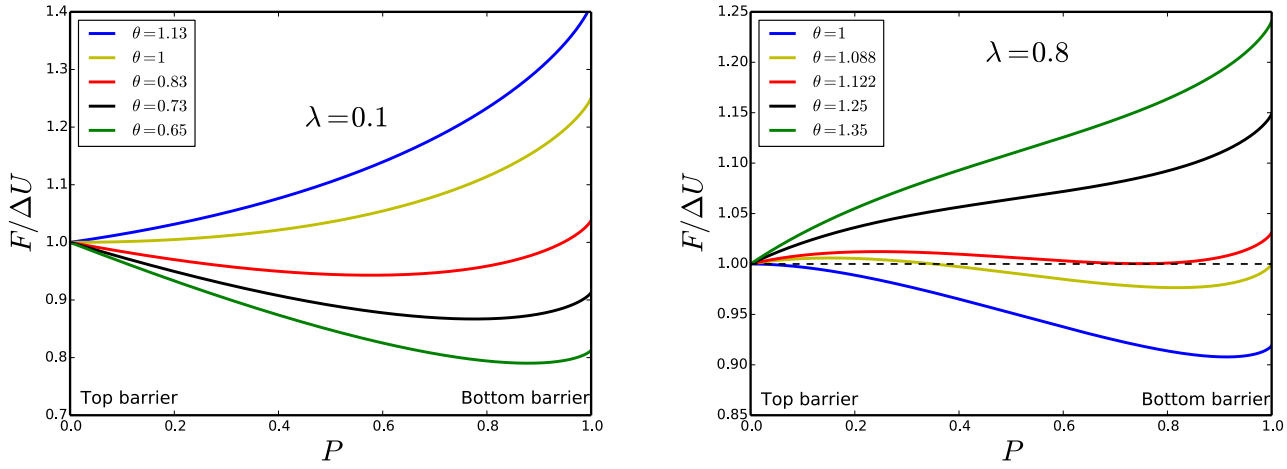

FIG. 20 Color online. The effective free energy of the escape rate vs P. Left: for $\lambda = 0.1$, second-order transition. Right: for $\lambda = 0.8$, first-order transition.

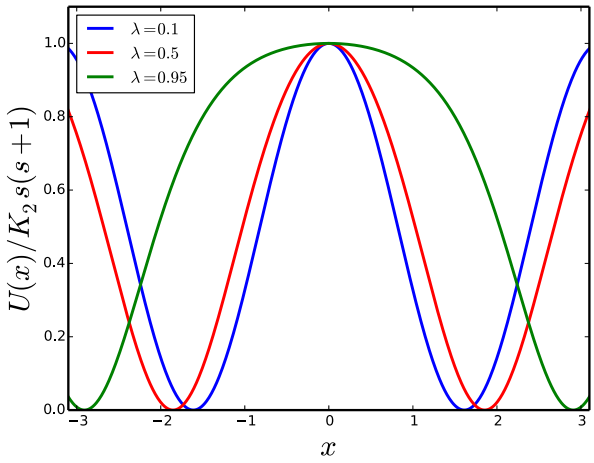

FIG. 21 Color online: The plot of the potential in Eq.(253) for several values of λ.

The plot of Eqn.(250) in the whole range of energy is shown in Fig.(20). For $\lambda = 0.8$, that is first-order transition, the actual crossover from thermal to quantum regime is estimated as $T_0^{(1)} = 1.122T_0^{(2)}$ corresponding to the point where two minima have the same free energy. At $\lambda = 0.1$, there is only one minimum of T for all $T > T_0^{(2)}$, i.e $\theta > 1$ at the top of the barrier. For $\theta < 1$, the minimum continuously shifts to the bottom of the barrier with lowering temperatures. This corresponds to a second-order phase transition. The ratio of the anisotropy constants λ in this model plays a similar role as h_x in the uniaxial model. In general, the splitting term in the Hamiltonian is responsible for the dynamics of the system, and leads to the phase transition in large spin systems. However, the sharp first-order phase transition in this model is not as result of the flatness of the barrier top as in the case of the uniaxial model. It should be noted that the mass of the particle at the top of the barrier $m\left(\frac{\pi}{2}\right) = [2K_1(1-\lambda)]^{-1}$ is heavier than that of the bottom of the barrier $m(0) = [2K_1]^{-1}$. The former is responsible for the sharp first-order crossover. A constant mass in this model can be achieved through the effective potential method. The spin Hamiltonian corresponds to the effective potential and the mass (Müller, *et al.*, 1999):

$$U(x) = K_2 s(s+1)\frac{\mathrm{cn}^2(x,\lambda)}{\mathrm{dn}^2(x,\lambda)}; \quad m = \frac{1}{2K_1}; \tag{253}$$

where $x_s = x_{\max} = 0$. It is now trivial to check that Eq.(253) yields the same result in the large spin limit $s(s+1) \sim s^2$.

Since the mass is now a constant, the flatness of the barrier as $\lambda \to 1$ leads to a sharp first-order phase transition (see Fig.(21)).

D. Phase transition in easy z-axis biaxial spin model with a magnetic field

1. Introduction

In the presence of a magnetic field, other interesting features arise. In this case one can study how the crossover temperatures vary with the magnetic field at the phase boundary. Many biaxial spin models in the presence of

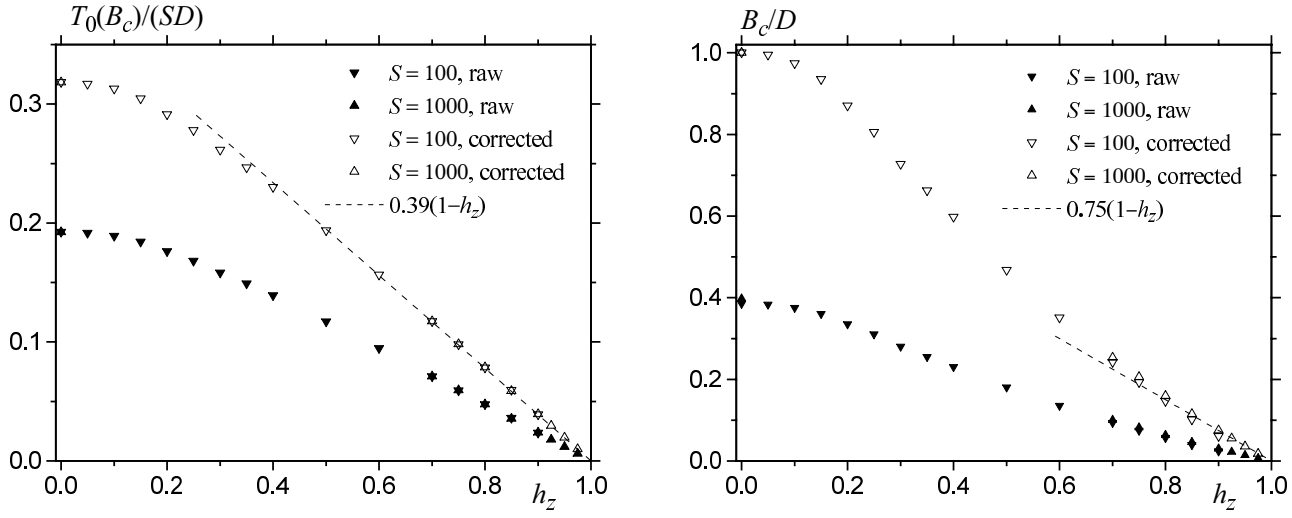

FIG. 22 Left: The crossover temperature $T_0^{(c)}$ at the phase boundary between first- and second-order transitions for the model $\hat{H} = -D\hat{S}_z^2 + B\hat{S}_x^2 - H_z\hat{S}_z$. Right: The phase boundary between the first- and the second-order phase transitions for the same model using perturbation theory, where $h_z = H_z/2Ds$. Adapted with permission from Chudnovsky and Garanin, 1999

an external magnetic with different easy axes directions have been studied by different approaches, although these systems are related by their anisotropy constants. The early work on these models began with Müller, *et al.* (1998). They studied a Hamiltonian of the form:

$$\hat{H} = K(\hat{S}_z^2 + \lambda\hat{S}_y^2) - 2\mu_B h_y \hat{S}_y, \quad \lambda < 1, \tag{254}$$

by spin coherent state path integral formalism. This Hamiltonian possesses an easy x-axis, y-medium axis and z hard axis. They explicitly demonstrated numerically the influence of the magnetic field on the crossover temperatures, and the period of oscillation. This analysis is however valid only in the regime $\lambda < 1$. In the case of a field parallel to the z-axis, their approach will break down, since such magnetic field pushes the spin away from the x-y plane. Chudnovsky and Garanin (1999, 2000) have studied two biaxial spin models of the form

$$\hat{H} = -D\hat{S}_z^2 + B\hat{S}_x^2 - H_x\hat{S}_x, \tag{255}$$

by direct numerical method and

$$\hat{H} = -D\hat{S}_z^2 + B\hat{S}_x^2 - H_z\hat{S}_z, \tag{256}$$

by perturbation theory with respect to B. However, the perturbative approach is less justified in the large B limit. These two models have an easy z axis, x hard axis and y medium axis with the magnetic field applied along the hard and easy axes respectively. The first model, i.e Eqn.(255) is related to the model in Eqn.(86) sec(III.A.3) by rescaling the anisotropy constants[4]. It is realized in Fe_8 molecular cluster with $s = 10$, $D = 0.229K$ and $B = 0.092K$. The second model, Eqn.(256) has a magnetic field along the easy axis which creates a bias potential minima. For this model the effect of the external magnetic field on the crossover temperatures was explicitly demonstrated by perturbation theory. In Fig.(22) we show the phase boundary and its crossover temperature $T_0^{(c)}$ obtained via perturbation theory for the model in Eqn.(256).

2. Effective potential method

Based on the results obtained from perturbation theory and numerical methods, Kim (1999) considered the effective potential method of the model:

$$\hat{H} = -K_{\parallel}\hat{S}_z^2 + K_{\perp}\hat{S}_y^2 - H_x\hat{S}_x - H_z\hat{S}_z. \tag{257}$$

For $H_x = 0$, this model is exactly the model in Eqn.(256), and for $H_z = 0$ the magnetic field H_x is along the medium axis. It is related to Eqn.(255) only by the rotation of axis $\hat{S}_y \to \hat{S}_x$. If one introduces the spin wave function in Eqn.(163), then using the generating function

$$\Phi(x) = \sum_{m=-s}^{s} \frac{c_m e^{mx}}{\sqrt{(s-m)!(s+m)!}}, \tag{258}$$

and the particle wave function function

$$\Psi(x) = e^{-y(x)}\Phi(x), \tag{259}$$

where $y(x)$ is determined in the usual way[10]. The corresponding effective potential and the coordinate dependent mass are given by

$$u(x) = \frac{1}{1+k\cosh 2x}[(1-k)(h_x \sinh x - h_z)^2 - 2h_x(1+k)\cosh x - 2h_z k \sinh 2x + k(1-\cosh 2x)], \tag{260}$$

$$m(x) = \frac{1}{K_{\parallel}(2+k_t)(1+k\cosh 2x)}, \tag{261}$$

where $U(x) = \tilde{s}^2 K_{\parallel} u(x)$, $k = k_t/(2+k_t)$ and $k_t = K_{\perp}/K_{\parallel}$, $h_{x,z} = H_{x,z}/2K_{\parallel}\tilde{s}$. The large s limit, *i.e.,* $s \gg 1$ has been used, thus terms independent of s drop out in the potential.

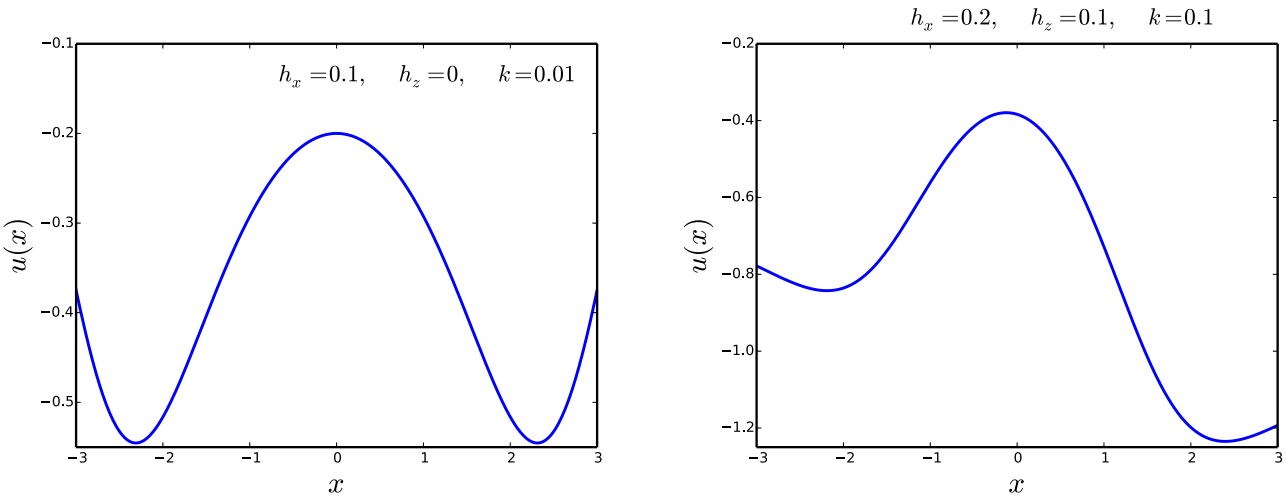

FIG. 23 Color online: The plot of the effective potential in Eqn.(260) with different parameters.

3. Phase boundary and crossover temperatures

We consider two cases $h_z = 0$, $h_x \neq 0$, and $h_x = 0$, $h_z \neq 0$. Let us consider the first case $h_z = 0$ and $h_x \neq 0$, in this case the potential reduces to

$$u(x) = \frac{(1+k)(h_x \cosh x - 1)^2}{1+k\cosh 2x}, \tag{262}$$

where a constant of the form $(1+h_x^2)$ has been added to normalize the potential to zero at the minimum $x_{\min} = \pm \operatorname{arccosh}\left(\frac{1}{h_x}\right)$. This potential is now an even function with a maximum at $x_s = x_{\max} = 0$. The barrier height is $\Delta U = K_{\|}\tilde{s}^2(1-h_x)^2$ (see Fig.(23)). In the limit $k_t \to 0$, Eqn.(261) and (262) reduce to that of the uniaxial model studied in Sec.(V.B). The thermon action is given by

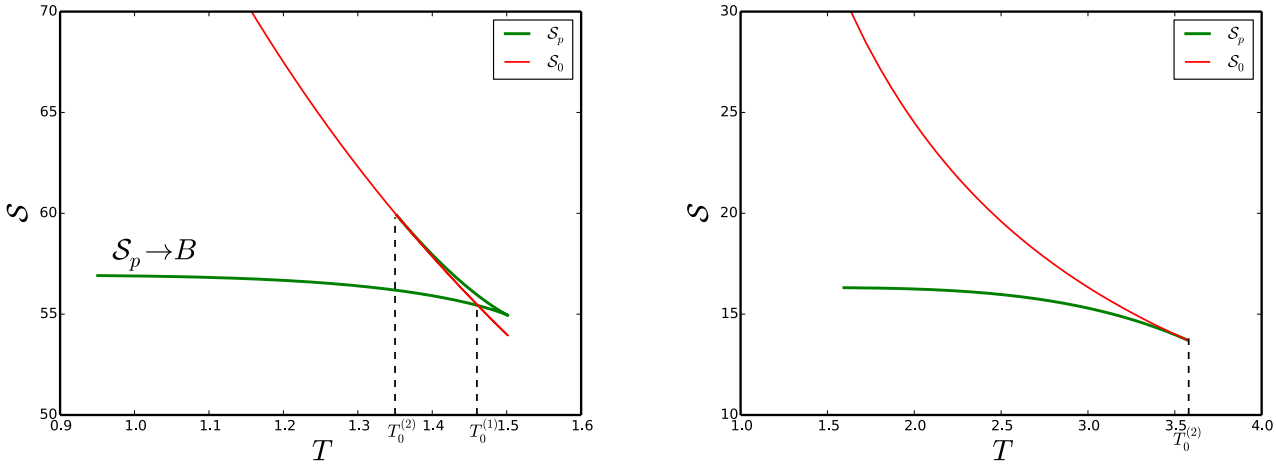

FIG. 24 Color online: The plot of the thermon action Eqn.(263) and thermodynamic action Eqn.(212) against temperature for the biaxial model with magnetic field h_x. Left: $s = 10$, $K_{||} = 1$, $k_t = 0.1$, $h_x = 0.1$ (first-order transition), where B is the vacuum instanton action. Right: $s = 10$, $K_{||} = 1$, $k_t = 1.5$, $h_x = 0.3$ (second-order transition).

$$\mathcal{S}_p = 2\tilde{s}\sqrt{\frac{2}{2+k_t}}\int_{-x_1}^{x_1} dx \frac{\sqrt{c_1\cosh^2 x - c_2\cosh x + c_3}}{1+k-2k\cosh^2 x} + \beta\Delta U(1-P), \tag{263}$$

where

$$c_1 = (1+k)h_x^2 - 2k(1-h_x)(1-P); \quad c_2 = 2h_x(1+k); \quad c_3 = 1+k-(1-k)(1-h_x)^2(1-P). \tag{264}$$

The turning points $\pm x_1$ are found by setting the term in the square root to zero. Integrating the classical equation of motion one finds that the denominator in Eqn.(262) cancels the mass in Eqn.(261). Thus, this action Eqn.(263) corresponds to the action of the periodic instanton trajectory in Eqn.(228) but with $\tilde{\mathcal{E}} = \mathcal{E}/K_{||}\tilde{s}^2(1+k)$ and $\omega^2 = (K_{||}\tilde{s})^2(1+k)(1+k_t)(1-(h_x-\sqrt{\tilde{\mathcal{E}}}))^2/2$. Mathematically, the integral in Eqn.(263) can be evaluated exactly in terms of complete elliptic integrals(Abramowitz and Stegun, 1972; Byrd and Friedman, 1979). At the bottom of the barrier $P \to 1$, the exact vacuum instanton action is given by (Kim, 1999)

$$S(U_{\min}) = 2B = 2\tilde{s}\left[\ln\left(\frac{\sqrt{1+k_t}+\sqrt{(1-h_x^2)}}{\sqrt{1+k_t}-\sqrt{(1-h_x^2)}}\right) - \frac{2h_x}{\sqrt{k_t}}\arctan\left(\frac{\sqrt{k_t(1-h_x^2)}}{(1+k_t)h_x^2}\right)\right]. \tag{265}$$

This expression is consistent with the small barrier action in Eqn.(204), if one uses the relation of the anisotropy constants. In Fig.(24) we have shown the plot of this action Eqn.(263) and the thermodynamic action Eqn.(212) against temperature. We notice that the plot of these two actions has a similar trend to every other model, which indicates the presence of the quantum-classical phase transitions in each of the models. The free energy can also be obtained from Eqn.(263). Kim (1999) expanded this integral in Eqn.(263) around $x_s = x_{\max}$ in terms of P for a general potential and coordinate dependent mass:

$$\mathcal{S}_p = \pi\sqrt{\frac{2m(x_s)}{U''(x_s)}}\Delta U[P + bP^2 + O(P^3)] + \beta\Delta U(1-P), \tag{266}$$

where

$$b = \frac{\Delta U}{16U''}\left[\frac{12U''''U'' + 15(U''')^2}{2(U'')^2} + 3\left(\frac{m'}{m}\right)\left(\frac{U'''}{U''}\right) + \left(\frac{m''}{m}\right) - \frac{1}{2}\left(\frac{m'}{m}\right)^2\right]_{x=x_s}, \tag{267}$$

$U''(x_s) = -K_\parallel \tilde{s}^2 u''(x_s)/2!$, $U'''(x_s) = K_\parallel \tilde{s}^2 u'''(x_s)/3!$, and $U''''(x_s) = K_\parallel \tilde{s}^2 u''''(x_s)/4!$.

In analogy with Landau's theory of phase transition, b corresponds to the coefficient of ψ^4 in the Landau free energy expression Eqn.(237), and $b < 0$ determines the condition for first-order transition while $b = 0$ determines the boundary between the first- and the second-order transition. One can check that this condition, Eqn.(267) yields exactly the same result as Eqn.(216). Applying the criterion, Eqn.(267) one obtains the phase boundary between first- and second-order:

$$h_x^{\pm} = \frac{1 - 14k_t + k_t^2 \pm (1+k_t)\sqrt{1+34k_t+k_t^2}}{8(1-k_t)}. \tag{268}$$

At $k_t = 0$, corresponding to the uniaxial limit, the phase boundary reduces to $h_x^c = h_x^+ = 1/4$, which is exactly the result obtained before. At $h_x = 0$, one obtains $k_t = 1$ which also corresponds to the result of the biaxial model without magnetic field, since the anisotropy constants are related by $K_\parallel = D_2$ and $K_\perp = D_1 - D_2$. In the small anisotropy limit $k_t \ll 1$, the phase boundary behaves linearly as $h_x^+ \approx (1+3k_t)/4$. The approximate form for the

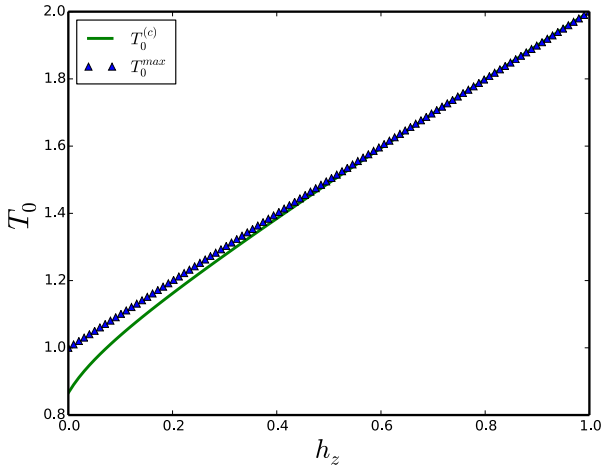

FIG. 25 Color online: The second-order crossover temperature at the phase boundary and its maximum at $h_z = 0$. $T_0 = 2\pi T_0/\tilde{s}K_\parallel$. Reproduced with permission from Kim, 1999

first-order crossover temperature is estimated as $T_0^{(1)} = \Delta U/S(U_{\min})$. Notice that this model does not have a large barrier so the concept of large and small barriers does not apply here. In Sec.(V.E) we will present a complete phase diagram for small and large barriers for the model in Eqn.(199). For the case of second-order transition the crossover temperature and its maximum are given by

$$T_0^{(2)} = \frac{\tilde{s}K_\parallel}{\pi}\sqrt{(k_t+h_x)(1-h_x)}; \quad T_0^{\max} = \frac{\tilde{s}K_\parallel}{2\pi}(1+k_t). \tag{269}$$

Using the value of $h_x = h_x^+$ at the phase boundary, Eqn.(268), one obtains the crossover temperature at the phase boundary $T_0^{(c)}$. As shown in Fig.(25) the difference between these temperatures vanishes at $k_t = 1$ which is the critical value at the phase boundary for $h_x = 0$.

For the second case $h_x = 0$ and $h_z \neq 0$, the potential Eqn.(260) is an odd function with a bias minima, and the barrier height is $\Delta U = K_\parallel \tilde{s}^2(1-h_z)^2$. The maxima is located at $x_s = x_{\max} = \frac{1}{2}\ln\left(\frac{1+h_z}{1-h_z}\right)$. Direct application of Eqn.(267) yields

$$b = K_\parallel \tilde{s}^2 \frac{(2+k_t)}{16k_t(1+h_z)^2}\left(h_z^2(1+2k_t) - (1-k_t)\right), \tag{270}$$

At the phase boundary $b = 0$ which yields

$$k_t^c = \frac{1-h_{cz}^2}{1+2h_{cz}^2}. \tag{271}$$

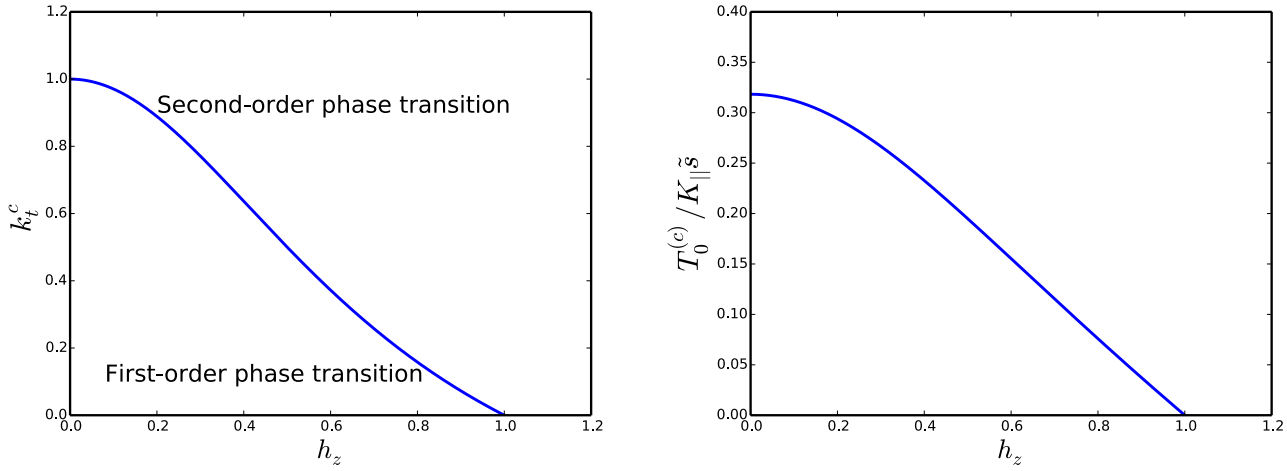

FIG. 26 Color online: Left: The phase boundary between the first- and second-order transitions at $h_x = 0$. Right: The crossover temperature $T_0^{(c)}$at the boundary between first- and second-order transitions. Reproduced with permission from Kim, 1999

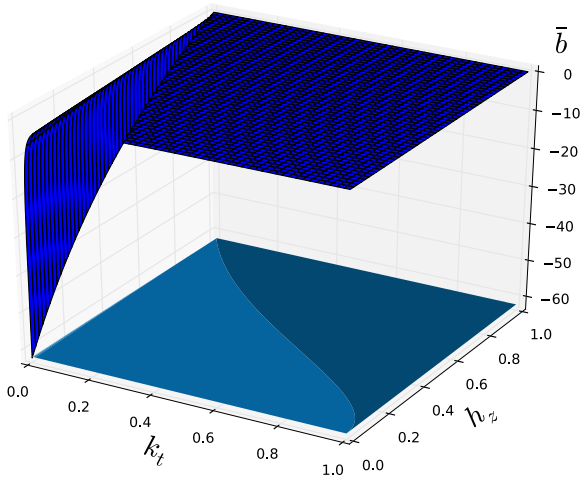

FIG. 27 Color online: Three dimensional plot of the Landau coefficient $\bar{b} = b/K_{||}\tilde{s}^2$. In this figure $\bar{b} < 0$ is for first-order transition, $\bar{b} > 0$ is for second-order transition, and the phase boundary $\bar{b} = 0$ is placed on the lower two dimensional plane for proper view of the upper plane.

The plot of Eq.(270) is shown in Fig.(27), indicating the regions of the phase transitions based on the sign of b. For small field parameter $h_z \ll 1$, the critical value decreases as $k_t^c \approx 1 - 3h_{cz}^2$. One obtains that the second-order crossover at the phase boundary is

$$T_0^{(c)} = \frac{K_\parallel \tilde{s}}{\pi} \frac{1 - h_{cz}^2}{\sqrt{1 + 2h_{cz}^2}}, \tag{272}$$

which has the form $T_0^{(c)}/K_\parallel \tilde{s} \approx (1 - 2h_z^2)/\pi$ for $h_z \ll 1$. The plot of Eqn.(271) and (272) is shown in Fig.(26). It clearly shows the consistency of the result with that of perturbation theory in Fig.(22). At $k_t = 0$, there is no tunneling due to the following: Quantum mechanically, in this limit the Hamiltonian commutes with $\hat{S}_z$, thus there is no splitting term since $\hat{S}_z$ is conserved quantity. In the effective potential method, this implies that the barrier becomes infinitely thick and the spin cannot tunnel.

4. An alternative model

It is sometimes difficult to deal with a particle Hamiltonian with a position dependent mass. It is possible to get a particle with a constant mass from the model in Eqn.(257) using another approach. Let us consider the model[15]

$$\hat{H} = -A\hat{S}_z^2 - C\hat{S}_x^2 - H_x\hat{S}_x - H_z\hat{S}_z. \tag{273}$$

This model is exactly the same as Eqn.(257) if we set $A = K_{\|} + K_{\perp}$ and $C = K_{\perp}$. Introducing an unconventional generating function of the form

$$\mathcal{G}(x) = \sum_{m=-s}^{s} \frac{c_m}{\sqrt{(s-m)!(s+m)!}} \left(\frac{\mathrm{sn}\, x + 1}{\mathrm{cn}\, x}\right)^s, \tag{274}$$

and the particle wave function function

$$\Psi(x) = e^{-y(x)}\mathcal{G}(x). \tag{275}$$

As in the previous analysis, $y(x)$ is determined by the usual procedure[10]. One finds that the corresponding effective potential and the mass are given by (Chang, *et al.*, 2000, 1999), $U(x) = \tilde{s}^2 A u(x)$

$$u(x) = \frac{1}{4\,\mathrm{dn}^2\, x}[(\alpha_x\,\mathrm{sn}\, x - \alpha_z\,\mathrm{cn}\, x)^2 - 4b - 4(b\alpha_z\,\mathrm{sn}\, x + \alpha_x\,\mathrm{cn}\, x)], \quad m = \frac{1}{2A}, \tag{276}$$

where the large s limit $s \sim s+1 \sim (s+\frac{1}{2}) = \tilde{s}$ has been used. $b = C/A$ and $\alpha_{x,z} = H_{x,z}/sA$, the modulus of the elliptic functions is $k^2 = 1-b$. The maximum of the potential is at $x_s = x_{\max} = 0$ for $\alpha_z = 0$.

5. Phase boundary and crossover temperatures

Since the mass is now a constant and the potential is even for $\alpha_z = 0$, the criterion for the first-order transition, Eqn.(216) is determined only by the fourth derivative of the potential at x_s or by considering where the coefficient of the fourth order expansion changes sign near x_s. For $\alpha_z = 0$ we find

$$U(x) \approx U(0) + A\tilde{s}^2[-\frac{1}{4}(2-2b-\alpha_x)(2b+\alpha_x)x^2 + \frac{1}{24}(\alpha_x - \alpha_x^+)(\alpha_x - \alpha_x^-)x^4 + O(x^6)]. \tag{277}$$

The vanishing of the coefficient of x^4 determines the phase boundary

$$\alpha_{cx}^{\pm} = \frac{1 - 16b_c(1-b_c) \pm \sqrt{1 + 32b_c(1-b_c)}}{4(1-b_c)}, \tag{278}$$

which is exactly the result obtained by Chang, *et al.* (2000). Eqn.(278) is consistent with Eqn.(268) by noticing that $b = k_t/(1+k_t)$ and $\alpha_x = 2(1-b)h_x$. The second-order crossover temperature is given by

$$T_0^{(2)} = \frac{A\tilde{s}}{2\pi}\sqrt{(2b+\alpha_x)(2(1-b)-\alpha_x)}. \tag{279}$$

Plugging Eqn.(278) into Eqn.(279) one obtains the crossover temperature at the phase boundary. For $\alpha_x = 0$ in Eqn.(276), the maximum occur at $x_s = \mathrm{sn}^{-1}[-\alpha_z/2(1-b)]$, the potential is no longer an even function, therefore the coefficient of the fourth order expansion near x_s cannot determine the regime of first-order transition. With the help of Eqn.(221) one obtains the phase boundary and the crossover temperature at the phase boundary (Chang, *et al.*, 1999)

$$\alpha_{cz} = 2(1-b_c)\sqrt{\frac{1-2b_c}{1+b_c}}; \quad T_0^c = \frac{2\tilde{s}A\sqrt{3}b_c}{\pi}\sqrt{\frac{1-b_c}{1+b_c}}. \tag{280}$$

---

[15] An alternative choice is $\hat{H} = K_1\hat{S}_z^2 + K_2\hat{S}_y^2 - H_x\hat{S}_x$. Setting $H_x = 0$ in Eqn.(273), these models are related by $K_1 = A$ and $K_2 = A - B$ (Müller, *et al.*, 1999).

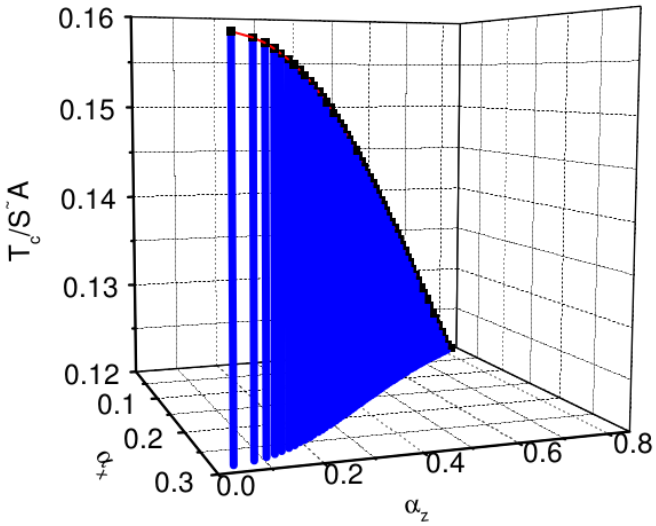

FIG. 28 Color online: 3D numerical plot of the crossover temperature $T_c(\alpha_{cz}, \alpha_{cx})/\tilde{s}A$ at the boundary as a function of field parameters α_{cx} and α_{cz} with $b_c = 0.29$. From Chang, *et al.* (2000)

These expressions are consistent with Eqn.(271) and (272). At $\alpha_{cz} = 0 = \alpha_{cx}^{+}$, one finds that $b_c = 1/2$ which corresponds to the result of Sec.(V.D.3) with the anisotropy constants related by $A = K_1$ and $C = K_1 - K_2$, implying that $\lambda = 1 - b$. In the limit of small anisotropy $b_c \ll 1$, one finds $\alpha_{cz} \approx 2(1 - 5b_c/2)$ and $T_0^c \approx 2\tilde{s}A\sqrt{3}b_c/\pi$. The phase diagram of these expressions are related to Fig.(25) and Fig.(26). For iron cluster Fe_8, $s = 10$, $A = 0.316K$, and $C = 0.092K$(Barra, *et al.*, 1996; Sangregorio, *et al.*, 1997) one finds that $T_0^c = 0.79K$. In Fig.(28) we have shown a 3-dimensional plot of $T^c(\alpha_{cx}, \alpha_{cz})$. It is evident that T^c decreases as α_z increases, while it increases with increasing α_x.

E. Phase transition in easy x-axis biaxial spin model with a medium axis magnetic field

1. Effective potential of medium axis magnetic field model

For the model we considered in Sec.(IV.B.2), that is

$$\hat{H} = D_1\hat{S}_z^2 + D_2\hat{S}_x^2 - H_x\hat{S}_x. \tag{281}$$

The effective potential and the mass were obtained as

$$U(x) = \frac{D_2\tilde{s}^2[\mathrm{cn}(x) - \alpha_x]^2}{\mathrm{dn}^2(x)}, \quad m = \frac{1}{2D_1}. \tag{282}$$

This Hamiltonian is related to Eqn.(257) for $H_z = 0$ if one sets $D_1 = K_\parallel + K_\perp$ and $D_2 = K_\parallel$, it is also related to Eqn.(273) for $H_z = 0$ if one sets $D_1 = A$ and $D_2 = A - B$, but unlike these models, we saw that the potential, Eqn.(282) has large and small barriers (see Fig.(10)) located at $x_{lb} = \pm 2(2n+1)\mathcal{K}(\kappa)$ and $x_{sb} = \pm 4n\mathcal{K}(\kappa)$ respectively, with the barrier heights given by Eqn.(202). The phase transition of the escape rate was studied by Müller, *et al.* (1998) using spin coherent state path integral. In this review we will consider it in the effective potential method.

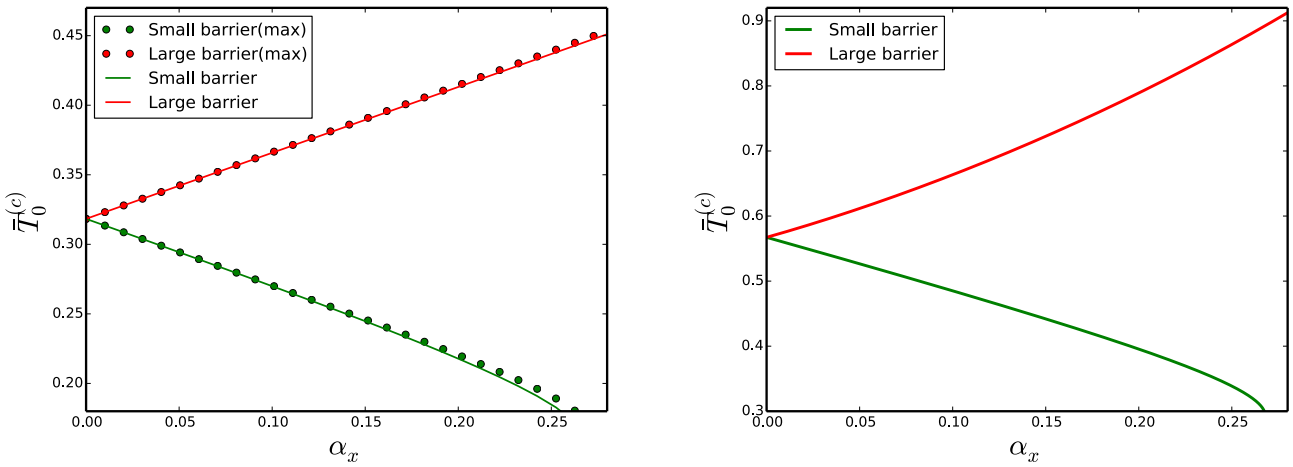

FIG. 29 Colour online: Dependence of the crossover temperatures on the magnetic field at the phase boundary. Left: Second-order (solid line) and its maximum (dashed line) for the small and large barrier. Right: First-order for the small and the large barrier. These graphs are plotted with $T_0^{(c)} = T_0^{(c)}/D_2\tilde{s}$. Adapted with permission from Owerre and Paranjape, 2014b

2. Phase boundary and crossover temperatures

Using Eqn.(216) and the maximum points x_{lb}, x_{sb}, the boundary between the first and second-order transition for small and large barriers are found to be (Owerre and Paranjape, 2014b)

$$\lambda_{sb}^{\pm}(\alpha_x) = \frac{3 - 4\alpha_x + \alpha_x^2 \pm (1-\alpha_x)\sqrt{1 - 4\alpha_x + \alpha_x^2}}{4(1 - 2\alpha_x + \alpha_x^2)}, \tag{283}$$

$$\lambda_{lb}^{\pm}(\alpha_x) = \frac{3 + 4\alpha_x + \alpha_x^2 \pm (1+\alpha_x)\sqrt{1 + 4\alpha_x + \alpha_x^2}}{4(1 + 2\alpha_x + \alpha_x^2)}. \tag{284}$$

For small barrier one can check that Eqn.(283) is consistent with Eqn.(278) and Eqn.(268). The crossover temperature for the first-order transition is estimated as $T_0^{(1)} = \Delta U/2B$, which can be obtained from Eqn.(202) and (204). At the phase boundary we find that $T_0^{(c)} \approx D_2\tilde{s}/(\ln[(3+2\sqrt{2})e^{\pm\frac{3\alpha_x}{\sqrt{2}}}])$ for $\alpha_x \ll 1$, where the upper and lower signs correspond to small and large barrier respectively. Both temperatures coincide at $\alpha_x = 0, \lambda = \frac{1}{2}$ with $T_0^{(c)} = D_2\tilde{s}/\ln(3+2\sqrt{2})$. For the case of second-order transition, the crossover temperature and its maximum are found to be

$$T_0^{(2)} = \frac{D_2\tilde{s}\sqrt{(1\pm\alpha_x)}}{\pi}\left(\frac{1-(1\pm\alpha_x)\lambda}{\lambda}\right)^{1/2}, \tag{285}$$

$$T_0^{(\max)} = \frac{D_2\tilde{s}}{2\pi\lambda}. \tag{286}$$

where the upper and lower signs correspond to the large and small barriers respectively. At the phase boundary one finds that Eqn.(285) behaves as $T_0^{(c)} \approx D_2\tilde{s}(1 \pm \frac{3}{2}\alpha_x)/\pi$ for $\alpha_x \ll 1$, which coincides at $\alpha_x = 0, \lambda = \frac{1}{2}$ as shown in Fig.(29). The evidence of this crossover temperatures has predicted in Fe_8 molecular cluster with $s = 10$. There are 21×21 matrices with $2s+1$ states which can be found by the so-called exact numerical diagonalization. The energy barrier of this system is much smaller than that of $Mn_{12}Ac$. In the low-temperature limit, specifically for $T < 0.4K$, only the two lowest energy level with $M = \pm s$ are occupied and tunneling is possible between these two states. For this system experimentally measured relaxation rate showed a temperature independent rate below 400mK which suggests the evidence of spin tunneling across its anisotropy energy barrier (Sangregorio, *et al.*, 1997) (see Fig.(30)).

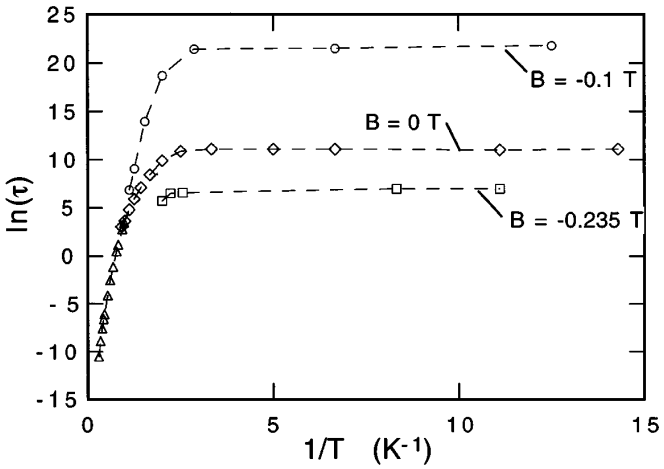

FIG. 30 Temperature dependence on the relaxation time τ. Points below 400 mK show temperature independent quantum tunneling. Adapted with permission from Sangregorio, *et al.*, 1997

3. Free energy

In the presence of a magnetic field, the Euclidean action cannot be obtained exactly or analytically (Müller, *et al.*, 1998), thus it is studied numerically. The periodic instanton action or the thermon action is given by

$$\mathcal{S}_p(\mathcal{E}) = 2\sqrt{2m}\int_{x_1}^{x_2} dx\sqrt{U(x)-\mathcal{E}} + \beta(\mathcal{E}-U_{\min}). \tag{287}$$

Setting $y = \mathrm{sn}(x,\lambda)$ and using Eqn.(201) we have

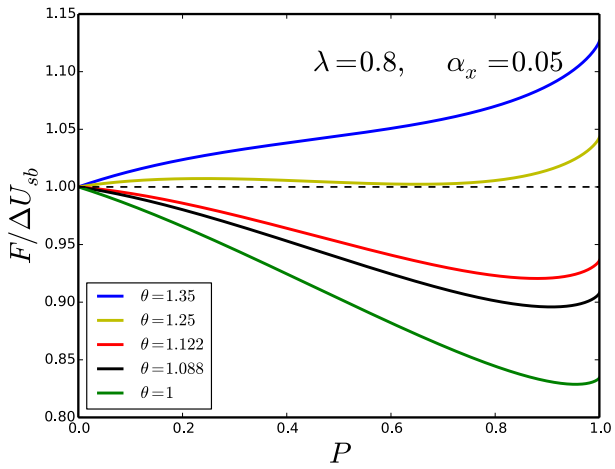

FIG. 31 Color online: The numerical plot of the free energy for $\kappa = 0.8$ and $\alpha = 0.05$.

$$\mathcal{S}_p(P) = 2\tilde{s}\sqrt{\kappa}\tilde{S}(P) + \beta\Delta U(1-P), \tag{288}$$

$$\tilde{S}(P) = \int_{y_1}^{y_2} dy\left[\frac{\left(\sqrt{1-y^2}-\alpha_x\right)^2 - Q(1-\kappa y^2)}{(1-\kappa y^2)^2(1-y^2)}\right]^{\frac{1}{2}}, \tag{289}$$

where $Q=(1-\alpha_x)^2(1-P)$, and the turning points y_1 and y_2 are determined by setting the numerator in the square bracket to zero. The free energy can then be written as

$$\frac{F(P)}{\Delta U_{sb}}=1-P+\frac{2\theta\sqrt{1-\kappa(1-\alpha)}}{\pi\left(1-\alpha\right)^{3/2}}\tilde{S}(P), \tag{290}$$

where $\theta=T/T_0^{(2)}$, $T_0^{(2)}$ is given in Eqn.(285), and ΔU_{sb} is given in Eqn.(202).

In Fig.(31) we have shown the numerical plot of the free energy with some of the temperature parameters in (Zhang, *et al.*, 1999), and the same dimensionless anisotropy constant $\lambda=0.8$, but in the presence of a small magnetic field $\alpha_x=0.05$. We notice that the phase transition from classical to quantum regime (where two minima of a curve have the same free energy) has been shifted to $\theta=1.25$ or $T_0^{(1)}=1.25T_0^{(2)}$, which is larger than the zero magnetic field value $T_0^{(1)}=1.122T_0^{(2)}$ in Fig.(20)(b) (Zhang, *et al.*, 1999). Thus, the magnetic field increases the crossover temperature for this model as we found in the previous model in Sec.(V.D.4). However, for large barrier we expect the crossover temperature to decrease. Thus, the large barrier plays a similar role as the longitudinal field H_z in Sec.(V.D.4).

F. Phase transition in exchange-coupled dimer model

1. Model Hamiltonian

In Sec.(III.A.5), we reviewed the problem of an antiferromagnetic exchange-coupled dimer model via spin coherent state path integral formalism. In this section we will study the effective potential method of the model. In the presence of a staggered magnetic field applied along easy z-axis, the Hamiltonian is given by

$$\hat{H}=J\hat{\mathbf{S}}_A\cdot\hat{\mathbf{S}}_B-D(\hat{S}_{A,z}^2+\hat{S}_{B,z}^2)+g\mu_B h(\hat{S}_{A,z}-\hat{S}_{B,z}), \tag{291}$$

where $J>0$ is antiferromagnetic exchange coupling respectively , $D>J>0$ is the easy z-axis anisotropy, and h is the external magnetic field, μ_B is the Bohr magneton and $g=2$ is the spin g-factor.

2. Effective potential

The spin wave function in this case can be written in a more general form as

$$\psi=\psi_A\otimes\psi_B=\sum_{\substack{\sigma_A=-s_A\\ \sigma_B=-s_B}}^{s_A,s_B}\mathcal{C}_{\sigma_A,-\sigma_B}\mathcal{F}_{\sigma_A,-\sigma_B}, \tag{292}$$

where

$$\mathcal{F}_{\sigma_A,-\sigma_B}=\binom{2s_A}{s_A+\sigma_A}^{-1/2}\binom{2s_B}{s_B-\sigma_B}^{-1/2}|\sigma_A,-\sigma_B\rangle\,. \tag{293}$$

Following the same procedures outlined above, one finds that the effective potential $U(r)$ and the coordinate dependent reduced mass $\mu(r)$ are given by (Owerre and Paranjape, 2014c)

$$U(r)=\frac{2D\tilde{s}^2[2\alpha^2+\kappa(1-\cosh r)+2\alpha\kappa\sinh r]}{(2+\kappa+\kappa\cosh r)}, \tag{294}$$

$$\mu(r)=\frac{1}{2D\left(2+\kappa+\kappa\cosh r\right)}. \tag{295}$$

In order to arrive at these equations we have used the fact that the two giant spins are equal $s_A=s_B=s$ and the approximation $s(s+1)\sim\tilde{s}^2=(s+\frac{1}{2})^2$, where $\kappa=J/D$ and $\alpha=g\mu_B h/2D\tilde{s}$. The variable r denotes the relative coordinate of the particles, the center of mass coordinate does not contain any information about the system.

3. Periodic Instanton at zero magnetic field

In the absence of a magnetic field, the effective potential is now of the form

$$U(r) = 2Ds(s+1)u(r), \quad u(r) = \frac{\kappa(1-\cosh r)}{(2+\kappa+\kappa\cosh r)}. \tag{296}$$

Since we are considering large spin systems, the coefficient $s(s+1)$ will be approximated as s^2. The potential is now symmetric with degenerate minima, and hence the turning points are $\pm r(\mathcal{E})$ with the maximum of the barrier height located at $r_b = 0$ as shown in Fig.(32). The action associated with the thermon action is given by

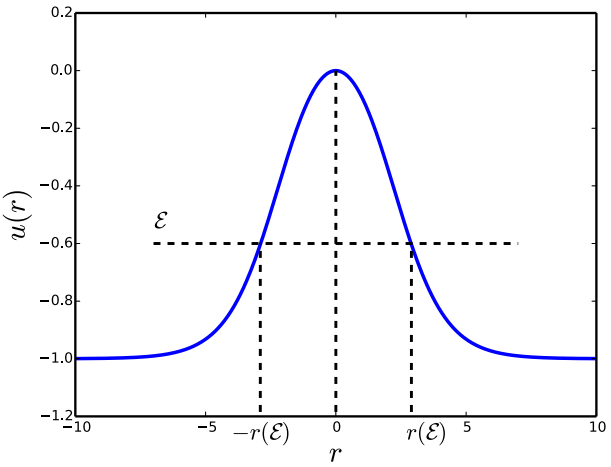

FIG. 32 Color online: The plot of the potential for $\kappa = 0.6$. The minimum energy is $u_{\min} = -1$, and the maximum is $u_{\max} = 0$. Thus, $\Delta U = U_{\max} - U_{\min} = 2Ds^2$.

$$S(\mathcal{E}) = 2\int_{-r(\mathcal{E})}^{r(\mathcal{E})} dr\sqrt{2\mu(r)\,(U(r)-\mathcal{E})}. \tag{297}$$

This action can be integrated exactly for all possible values of the energy without computing the periodic instanton trajectory explicitly (Owerre and Paranjape, 2014c). In this paper, we will obtain this action by first calculating the periodic instanton trajectory corresponding to the action. The Euclidean Lagrangian is given by

$$L_E = \frac{1}{2}\mu(r)\dot{r}^2 + U(r). \tag{298}$$

The Euler-Lagrange equation of motion gives

$$\mu(\bar{r}_p)\ddot{\bar{r}}_p + \frac{1}{2}\frac{d\mu(\bar{r}_p)}{d\bar{r}_p}\dot{\bar{r}}_p^2 - \frac{dU}{d\bar{r}_p} = 0. \tag{299}$$

Integrating once we obtain

$$\frac{1}{2}\mu(\bar{r}_p)\dot{\bar{r}}_p^2 - U(\bar{r}_p) = -\mathcal{E}, \tag{300}$$

where $\mathcal{E}$ is the integration constant. Thus, the periodic instanton trajectory can be found from the solution of this equation:

$$\tau = \int_0^{\bar{r}_p} dr\sqrt{\frac{\mu(r)}{2(U(r)-\mathcal{E})}} = \frac{1}{\sqrt{2}\omega_b}\int_0^{\bar{r}_p} dr\frac{1}{\sqrt{a+b-2b\cosh^2\left(\frac{r}{2}\right)}}, \tag{301}$$

where $\omega_b = 2Ds\sqrt{\kappa}$ is the frequency of oscillation at the well of the inverted potential of Fig.(32), $a = 1-(2+\kappa)\mathcal{E}'$, $b = 1+\kappa\mathcal{E}'$, and $\mathcal{E}' = \mathcal{E}/2Ds^2\kappa$. In terms of a new variable $y = \cosh\left(\frac{r}{2}\right)$, we have

$$\omega_b\tau = \frac{1}{\sqrt{b}}\int_1^{\bar{y}_p} dy \frac{1}{\sqrt{(y^2-1)(\frac{a+b}{2b}-y^2)}}, \tag{302}$$

where $\bar{y}_p = \cosh\left(\frac{\bar{r}_p}{2}\right)$. Introducing another change of variable:

$$x^2 = \frac{y^2-1}{\lambda^2 y^2}, \quad \lambda^2 = \frac{a-b}{a+b}. \tag{303}$$

The integral in Eqn.(302) becomes

$$\omega_b\tau = \sqrt{\frac{2}{a+b}}\int_0^{\bar{x}_p} dx \frac{1}{\sqrt{(1-x^2)(1-\lambda^2x^2)}} = \sqrt{\frac{2}{a+b}}F(\bar{\theta}_p,\lambda) = \sqrt{\frac{2}{a+b}}\,\mathrm{sn}^{-1}(\sin\bar{\theta}_p,\lambda), \tag{304}$$

where

$$\bar{x}_p = \sin\bar{\theta}_p = \sqrt{\frac{\bar{y}_p^2-1}{\lambda^2\bar{y}_p^2}} = \frac{1}{\lambda}\tanh\left(\frac{\bar{r}_p}{2}\right), \tag{305}$$

and $F(\bar{\theta}_p,\lambda)$ is an incomplete elliptic integral of first kind with modulus λ and $\bar{\theta}_p$ Substituting Eqn.(305) into Eqn.(304), and solving for $\bar{r}_b$ we obtain the periodic instanton:

$$\bar{r}_p(\tau) = 2\,\mathrm{arctanh}[\lambda\,\mathrm{sn}(\omega_p\tau,\lambda)], \quad \omega_p = \omega_b\sqrt{\frac{a+b}{2}}. \tag{306}$$

It is required that as $\tau \to \pm\frac{\beta}{2}$, the periodic instanton trajectory must tend to the classical turning points defined in Eqn.(297). In other words, $\bar{r}_p \to \pm r(\mathcal{E}) = \pm\,\mathrm{arccosh}\left(\frac{a}{b}\right)$ as $\tau \to \pm\frac{\beta}{2}$ as depicted in Fig.(33). This demands that $\mathrm{sn}(\omega_p\tau,\lambda) \to \pm 1$ as $\tau \to \pm\frac{\beta}{2}$. Using the fact that $\mu(\bar{r}_p)$ and $\dot{\bar{r}}_p^2$ are given by

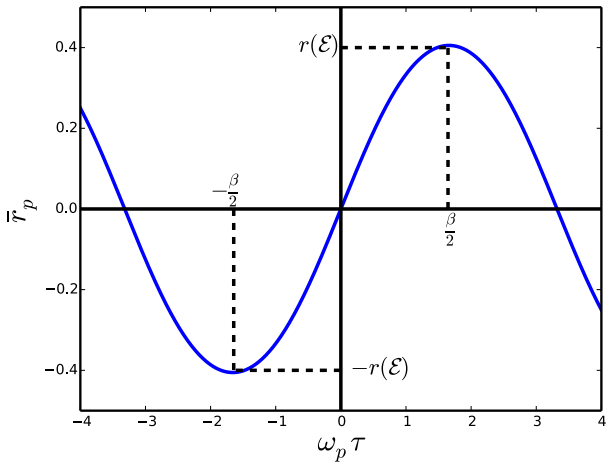

FIG. 33 Color online: The periodic instanton trajectory with $\lambda = 0.2$. The turning points $\pm r(\mathcal{E})$ are shown in Fig.(32).

$$\mu(\bar{r}_p) = \frac{\mathrm{dn}^2(\omega_p\tau,\lambda)}{4D[1+\kappa-\lambda^2\,\mathrm{sn}^2(\omega_p\tau,\lambda)]}; \quad \dot{\bar{r}}_p^2 = (2\lambda\omega_p)^2\frac{\mathrm{cn}^2(\omega_p\tau,\lambda)}{\mathrm{dn}^2(\omega_p\tau,\lambda)}, \tag{307}$$

and making the transformation $x = \mathrm{sn}(\omega_p\tau,\lambda)$, the action for the periodic instanton path can be computed as

$$S_p = \int_{-\frac{\beta}{2}}^{\frac{\beta}{2}} d\tau\mu(\bar{r}_p)\dot{\bar{r}}_p^2 + \beta(\mathcal{E}-U_{\min}) = 2s\sqrt{2(a+b)\kappa}[\mathcal{K}(\lambda)-(1-\gamma^2)\Pi(\gamma^2,\lambda)] + \beta(\mathcal{E}-U_{\min}), \tag{308}$$

where $\gamma^2 = \lambda^2(1+\kappa)^{-1}$. The functions $\mathcal{K}(\lambda)$ and $\Pi(\gamma^2,\lambda)$ are known as the complete elliptic integral of first and third kinds respectively.

4. Vacuum instanton at zero magnetic field

Since vacuum instanton occurs at zero temperature $T \to 0$, which implies that $\beta \to \infty$, the energy of the particle must be close to the minima of potential yielding tunneling between degenerate ground states. Near the bottom of the barrier $\mathcal{E} \to U_{\min} = -2Ds^2$, $a \to 2(1+\kappa)/\kappa$ and $b \to 0$, thus $\lambda \to 1$, we get $\mathrm{sn}(v,1) \to \tanh v$. The periodic instanton trajectory, Eqn.(306) reduces to a vacuum instanton:

$$\bar{r}_p(\tau) \to \bar{r}_0 = 2\omega_0\tau, \quad \omega_p \to \omega_0 = 2Ds\sqrt{1+\kappa}. \tag{309}$$

As $\tau \to \pm\infty$, $\bar{r}_0 \to \pm\infty$, which corresponds to the minima of the zero magnetic field potential. A particle sitting at the minimum of this potential is massless, $\mu(\bar{r}_0 \to \infty) = 0$, but the vacuum instanton mass is not zero. It is given by

$$\mu(\bar{r}_0) = [2D(2+\kappa+\kappa\cosh(2\omega_0\tau))]^{-1}. \tag{310}$$

In Fig.(34), we have shown the dependence of the dimensionless anisotropy constant on the vacuum instanton mass. Near the top of the barrier $\mathcal{E} \to U_{\max} = 0$, $a \to 1$ and $b \to 1$, thus $\lambda \to 0$, the periodic instanton reduces to a sphaleron

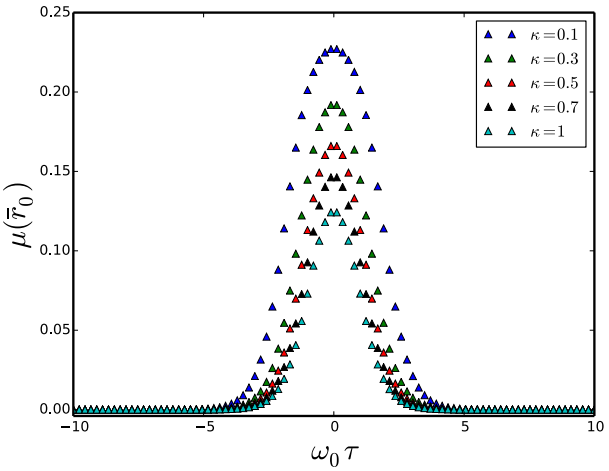

FIG. 34 Color online: Dependence of the dimensionless anisotropy constant on the vacuum instanton mass, with $D = 1$.

(static, unstable, finite-energy solutions of the classical equations of motion) at the top of the barrier:

$$\bar{r}_p(\tau) \to r_b = 0, \quad \omega_p \to \omega_b = 2Ds\sqrt{\kappa}. \tag{311}$$

The mass of the sphaleron is given by

$$\mu(r_b) = [4D(1+\kappa)]^{-1}. \tag{312}$$

In Fig.(35) we have shown the plot of the ratio of the frequencies ω_p/ω_0 and ω_p/ω_b against energy for several values of κ. The action associated with the vacuum instanton trajectory can be obtained by expanding the elliptic integrals in Eqn.(308) near the bottom of the potential $\lambda \to 1$, or simply by computing the action associated with the vacuum instanton path in Eqn.(309). Using Eqn.(310) and the fact that $\dot{\bar{r}}_0^2$ is given by

$$\dot{\bar{r}}_0^2 = (2\omega_0)^2. \tag{313}$$

One can easily confirm by direct integration that the vacuum instanton action is given by

$$B = \int_{-\infty}^{\infty} d\tau \mu(\bar{r}_0)\dot{\bar{r}}_0^2 = 4s\,\mathrm{arctanh}\left(\frac{1}{\sqrt{1+\kappa}}\right) = 2s\ln\left(\frac{\sqrt{1+\kappa}+1}{\sqrt{1+\kappa}-1}\right). \tag{314}$$

This is the exact vacuum instanton action. In the perturbative limit $J \ll D$, which implies that $\kappa \ll 1$, Eqn.(314) reduces to

$$B \approx 2s\ln\left(\frac{4}{\kappa}\right) = 2s\ln\left(\frac{4D}{J}\right). \tag{315}$$

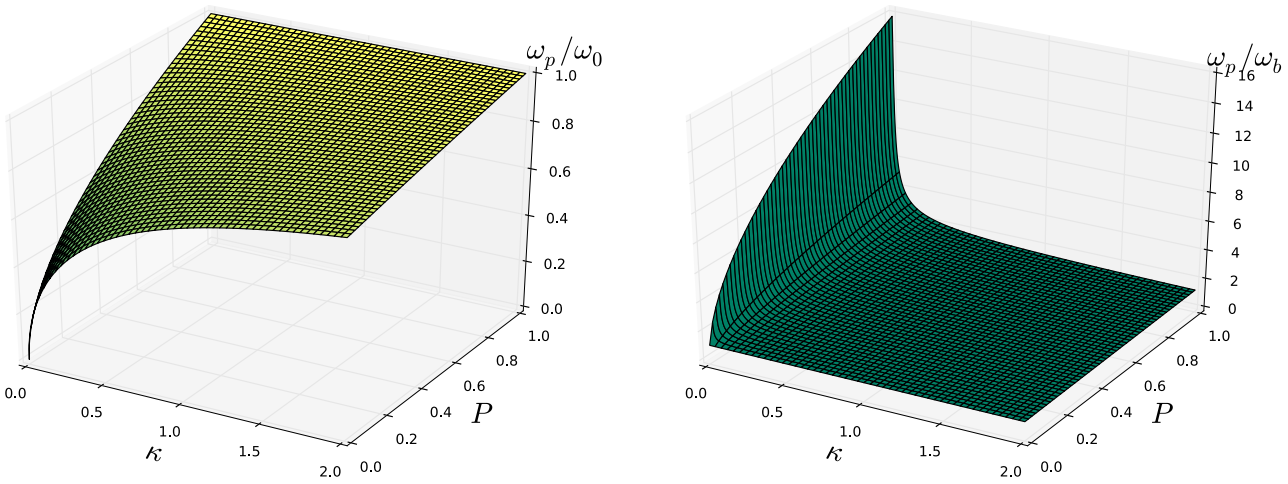

FIG. 35 Color online: The 3-d plot of the ratio of the periodic instanton frequency in Eqn.(306) to that of vacuum instanton in (309), and to that of sphaleron in Eqn.(311). At the bottom of the barrier $\omega_p \to \omega_0$, and at the top of the barrier $\omega_p \to \omega_b$.

This is the same action that was obtained by spin coherent state path integral in Eqn.(125), but the imaginary term in the spin coherent state path integral result, which is responsible for different ground state behaviour of integer and half-odd integer spins has disappeared. This is one of the disadvantages of mapping a spin system to a particle system.

5. Free energy and phase transition at zero magnetic field

We will now investigate the phase transition of the escape rate using the free energy method . Having obtained the periodic instanton action for all possible values of the energy, that is Eqn.(308), the free energy associated with the escape rate can then be written as

$$\frac{F}{\Delta U} = 1 - P + \frac{4}{\pi}\theta\sqrt{\kappa(\kappa+P)}[\mathcal{K}(\lambda) - (1-\gamma^2)\Pi(\gamma^2,\lambda)], \tag{316}$$

where $\theta = T/T_0^{(2)}$ is a dimensionless temperature quantity, and $T_0^{(2)} = Ds\sqrt{\kappa}/\pi$. The modulus of the complete elliptic integrals λ and the elliptic characteristic γ are related to P by

$$\lambda^2 = \frac{(1+\kappa)P}{\kappa+P}, \quad \gamma^2 = \frac{P}{\kappa+P}. \tag{317}$$

In Fig.(36) we have shown the plot of the free energy against P for $\kappa = 0.4$ (first-order transition). In the top three curves, the minimum of the free energy is at the top of the barrier, $P = 0$. For $\theta = 1.054$ or $T_0^{(1)} = 1.054T_0^{(2)}$, two minima have the same free energy. This corresponds to the crossover temperature from classical to quantum regimes. As the temperature decreases from this crossover temperature, a new minimum of the free energy is formed, this new minimum becomes lower than the one at $P = 0$. We have pointed out that phase transition occurs near the top of the potential barrier, so it is required that we expand this free energy close to the barrier top. Thus, near the top of the barrier $P \to 0$, the complete elliptic integrals can be expanded up to order P^3. The full simplification of Eqn.(316) yields

$$\frac{F}{\Delta U} = 1 + (\theta-1)P + \frac{\theta(\kappa-1)}{8\kappa}P^2 + \frac{\theta(3\kappa^2-2\kappa+3)}{64\kappa^2}P^3. \tag{318}$$

Similar to the case of uniaxial spin model in a transverse magnetic field (Chudnovsky,*et al.*, 1998; Chudnovsky and Garanin, 1997), this free energy looks more like the Landau's free energy, which suggests that we should compare the two free energies. The Landau's free energy has the form:

$$F = F_0 + a\psi^2 + b\psi^4 + c\psi^6. \tag{319}$$

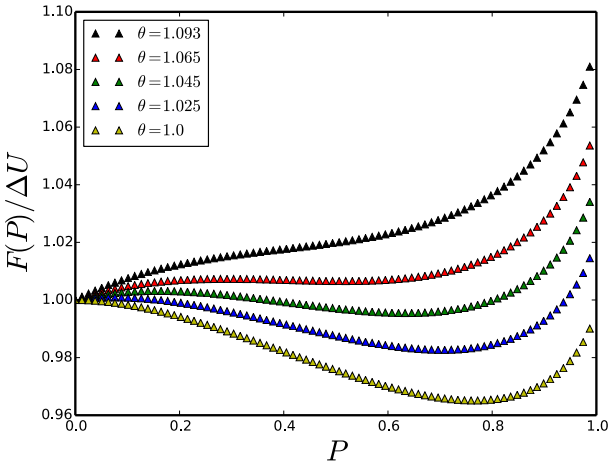

FIG. 36 Color online: The effective free energy of the escape rate vs. P for $\kappa = 0.4$ and several values of $\theta = T/T_0^{(2)}$, first-order transition.

The coefficient of P in Eqn.(318) is equivalent to the coefficient a in Landau's free energy. It changes sign at the phase temperature $T = T_0^{(2)}$. The phase boundary between the first- and the second-order phase transitions depends on the coefficient of P^2, it is equivalent to the coefficient b in Eqn.(319). It changes sign at $\kappa = 1$. Thus $\kappa < 1$ indicates the regime of first-order phase transition. The period of oscillation $\beta(\mathcal{E})$ is found to be

$$\beta(\mathcal{E}) = \frac{2\sqrt{2}}{Ds\sqrt{(a+b)\kappa}}\mathcal{K}(\lambda). \tag{320}$$

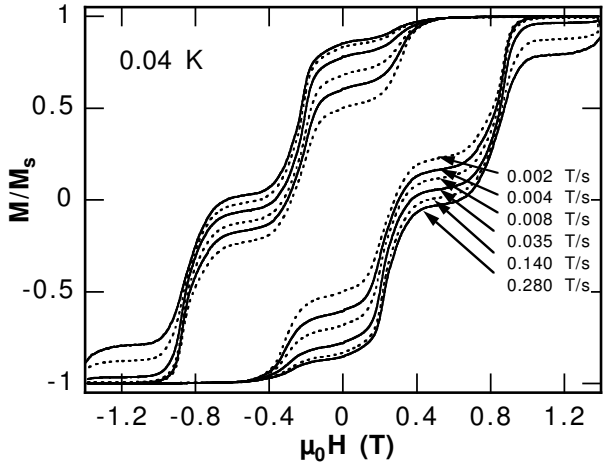

FIG. 37 Hysteresis loops for the $[Mn_4]_2$ dimer at several field sweep rates and 40 mK. The tunnel transitions are labeled from 1 to 5 corresponding to the plateaus. Adapted with permission from Tiron, *et al.*, 2003a

6. Free energy with magnetic field

In the previous section we considered the phase transition of the interacting dimer model at zero magnetic field. In this section we will study the influence of the staggered magnetic field on the phase boundary, the crossover temperatures and the free energy. These analyses will be based on the potential and the position dependent mass in Eqn.(294) and Eqn.(295). In Fig.(38) we have shown the plot of this potential for some values of the parameters.

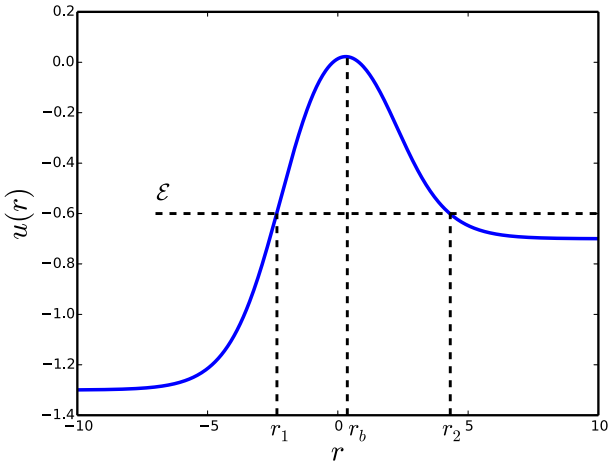

FIG. 38 Color online: The plot of the effective potential and its inverse as a function of r for $\kappa = 0.6$ and $\alpha = 0.15$.

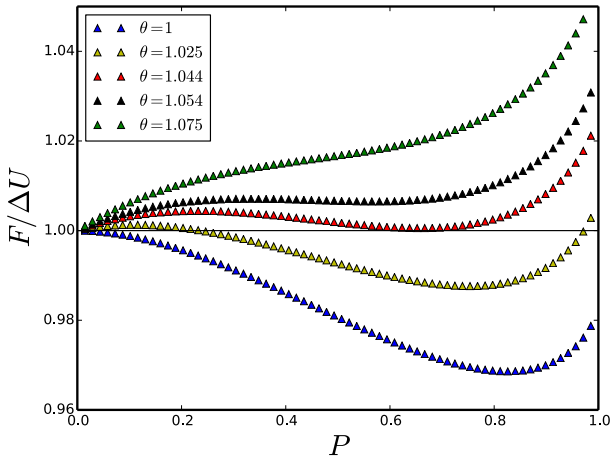

FIG. 39 Color online: The numerical plot of the free energy with $\kappa = 0.4$ and $\alpha = 0.15$. The phase transition from thermal to quantum regimes occurs at $\theta = 1.044$, which is smaller than that of zero magnetic field, $\theta = 1.054$.

The potential has a maximum at

$$r_b = \ln\left(\frac{1+\alpha}{1-\alpha}\right), \tag{321}$$

and the height of the potential barrier is given by

$$\Delta U = U_{\max} - U_{\min} = 2D\tilde{s}^2\,(1-\alpha)^2\,. \tag{322}$$

In the presence of a magnetic field, the periodic instanton action or thermon action is given by

$$\mathcal{S}_p = 2\tilde{s}\sqrt{2}\tilde{S}(P) + \beta(\mathcal{E} - U_{\min}); \quad \tilde{S}(P) = \int_{r_1}^{r_2} dr \frac{\sqrt{a_1 - a_2\cosh r + a_3 \sinh r}}{2 + \kappa(1+\cosh r)}; \tag{323}$$

where

$$a_1 = 2\alpha^2 + \kappa - (2+\kappa)(\alpha^2 - P(1-\alpha)^2); \quad a_2 = \kappa(1 + \alpha^2 - P(1-\alpha)^2); \quad a_3 = 2\kappa\alpha. \tag{324}$$

The turning points are determined from the solution of the equation:

$$a_1 - a_2\cosh r + a_3 \sinh r = 0. \tag{325}$$

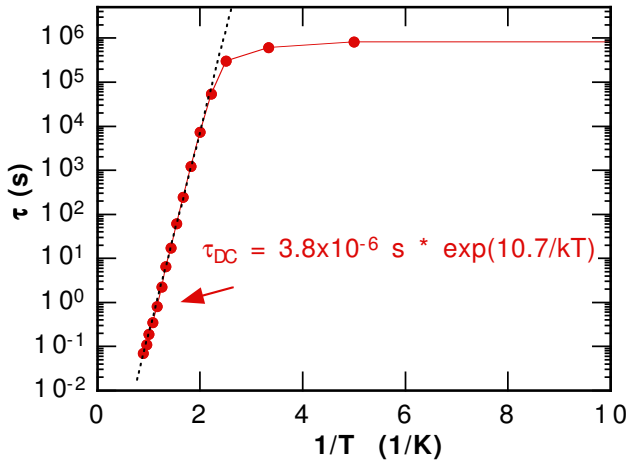

FIG. 40 Color online: Arrhenius plot of the relaxations times τ vs. the inverse temperature for $[Mn_4]_2$ dimer with the model Hamiltonian $\hat{H} = J\hat{\mathbf{S}}_A \cdot \hat{\mathbf{S}}_B - D(\hat{S}^2_{A,z} + \hat{S}^2_{B,z}) + g\mu_B\mu_0 h(\hat{S}_{A,z} + \hat{S}_{B,z})$. Adapted with permission from Wernsdorfer, *et al.*, 2004

At zero magnetic field $a_3 = 0$, the potential becomes symmetric hence $r_1 = -r_2$. This action, however cannot be integrated exactly either by periodic instanton method or otherwise. Thus, we have to resort to numerical analysis. The exact free energy can then be written as

$$\frac{F}{\Delta U} = 1 - P + \frac{\theta}{\pi(1-\alpha)^2}\sqrt{2\kappa(1-\alpha^2)}\tilde{S}(P), \tag{326}$$

where the barrier height ΔU is given in Eqn.(322), $\theta = T/T_0^{(2)}$, and $T_0^{(2)} = \frac{D\tilde{s}}{\pi}\sqrt{\kappa(1-\alpha^2)}$. In Fig.(39) we have shown the numerical plot of this free energy with $\kappa = 0.4$ and $\alpha = 0.15$. In this case, the minimum of the free energy remains at ΔU for the top three curves, however, the quantum-classical phase transition (where two minima of a curve have the same free energy) has been shifted down to $T_0^{(1)} = 1.044T_0^{(2)}$ due the the presence of a small magnetic field. Thus, the presence of a longitudinal staggered magnetic field in this model decreases the crossover temperatures as in the case of biaxial ferromagnetic spin models.

7. Phase boundary and crossover temperatures

The phase boundary with the help of Eqn.(216) yields

$$\alpha_c = \pm\left(\frac{1-\kappa_c}{1+2\kappa_c}\right)^{\frac{1}{2}}. \tag{327}$$

One finds that the second-order transition crossover temperature $T_0^{(2)}$ at the phase boundary yields

$$T_0^{(c)} = \frac{D\tilde{s}\kappa_c}{\pi}\left(\frac{3}{1+2\kappa_c}\right)^{\frac{1}{2}}. \tag{328}$$

For $[Mn_4]_2$ dimer, the parameters are: $s = 9/2$, $D = 0.75K$, and $J = 0.12K$ (Hill, *et al.*, 2003; Tiron, *et al.*, 2003a), one finds that the value of the crossover temperature at the phase boundary is $T_0^{(c)} = 0.29K$, which is much smaller than that of Fe_8 molecular cluster. In Fig.(40), we show the experimental result of the Arrhenius plot of $[Mn_4]_2$ dimer. The plot shows that the relaxation rate is temperature-dependent above ca. $0.3K$ with $\tau_0 = 3.8 \times 10^{-6}s$ and $\Delta U = 10.7K$ and below ca. $0.3K$, the relaxation rate is temperature-independent with a relaxation rate of $8 \times 10^5 s$ indicating the quantum tunneling of the spins between the ground states (Wernsdorfer, *et al.*, 2004). The hysteresis loops in Fig.(37) show the tunneling transitions through plateaus as obtained from experimental measurement. The step heights are temperature independent below 400mK, which indicates quantum tunneling between the ground energy states.

VI. CONCLUSION AND DISCUSSION

In this review we discussed recent theoretical and experimental developments on macroscopic quantum tunneling and phase transitions in spin systems. We reviewed different theoretical approaches to the problem of spin tunneling in single molecule magnets and exchange coupled dimer models. It is now understood that the suppression of tunneling at zero magnetic field for half-odd integer spin system is independent of the coordinate representation but only depends on the WZ or Berry phase term. This is related to Kramers degeneracy, and its experimental confirmation has been reported(Wernsdorfer *et al.*, 2002). Theoretically, it is still an open problem to determine the necessary conditions in which classical degenerate ground state for half-odd integer spin implies degenerate ground states in the pure quantum case. In the presence of a magnetic field along the spin hard anisotropy axis, tunneling is not suppressed for half-odd integer spins but rather oscillates with the field in accordance with the experimental observations.

Experimental and theoretical research on single-molecule magnets have focused on the search for other molecular magnets that exhibit tunneling and crossover temperatures. This research is expanding rapidly, and with the advance in technology, these molecular magnets have been used in the implementation of Grover's algorithm and magnetic qubits in quantum computing (Leuenberger and Loss, 2001; Tejada, *et al.*, 2001). Other interesting areas include tunneling of Neél vector in antiferromagnetic ring clusters with even number of spins (Meier and Loss, 2001; Meier, *et al.*, 2003; Taft, *et al.*, 1994). As far as we know the odd number of antiferromagnetic spin chain has not been reported. The present authors have suggested that this might give rise to solitons due to the spin frustration (Owerre and Paranjape, 2014d). Most experimental research has focused on organizing the SMMs into layers with the possibility of singling out the individual molecules(Leon, *et al.*, 1998, 2001).

Acknowledgments

The authors would like thank NSERC of Canada for financial support. We thank Ian Affleck, Sung Sik Lee and Joachim Nsofini for useful discussions.

References

Affleck. I Phys. Rev. Lett. **46**, 388 (1981)
Aharonov, Y. Bohm, D. , Phys. Rev. **115**, 485 (1959)
Abramowitz M. and Stegun I. A., Handbook of Mathematical Functions (New York: Dover), (1972)
Awshalom D. D., J. F. Smyth, G. Grinstein, D. P. DiVencenzo, and D. Loss, Phys. Rev. Lett. **68**, 3092 (1992)
Berry, M. V., 1984, Proc. R. Soc. Lond. A **392**, 45
Barra A.-L., P. Debrunner, D. Gatteschi, C. E. Schulz, and R. Sessoli, Europhys. Lett. 35, 133 (1996).
Barbara, B and Chudnovsky E. M., Phys. Lett. A, 145 (1990) 205.
Blasone M. and Petr Jizba, J. Phys. A: Math. Theor. **45**, 244009, (2012)
Byrd P. F. and M. D. Friedman, Handbook of Elliptic Integrals for Engineers and Scientists Springer, New York, (1979).
Bokacheva L., Andrew D. Kent and Marc A. Walters Phys. Rev. Lett. **85**, 4803, (2000)
Chang-Soo Park, Sahng-Kyoon Yoo and Dal-Ho Yoon Phys. Rev. B **61**, 11618, (2000)
Chang-Soo Park, Sahng-Kyoon Yoo, D. K. Park and Dal-Ho Yoon Phys. Rev. B **59**, 13581, (1999)
Chang-Soo Park and Anupam Garg, Phys. Rev. B **65**,064411, (2002)
Chudnovsky E. M. and Gunther L. , Phys. Rev. Lett. **60**, 661 (1988)
Chudnovsky E. M., Garanin D. A., and X. Martìnez Hidalgo, Phys. Rev. B **57**, 13639 (1998)
Chudnovsky E.M. and Garanin D.A. , Phys. Rev. Lett. **79**, 4469 (1997).
Chudnovsky E.M. and Garanin D.A., Phys. Rev. B **59**, 3671 (1999)
Chudnovsky E.M. and Garanin D.A., Phys. Rev. B **63**, 024418 (2000)
Chudnovsky E.M. , Journal of Magnetism and Magnetic Materials 1821, **140** (1995)
Chudnovsky E.M. Phys. Rev. A **46**, 8011 (1992);
Chudnovsky E. M. and X. Martinez-Hidalgo, Europhys. Lett. **50**, 395, (2000)
Chudnovsky E. M. and J. Tejada, Macroscopic Tunneling of the Magnetic Moment, (Cambridge University Press, Cambridge, UK, 1998), Chap. 7.
Chudnovsky E. M. and J. Tejada, Lectures on magnetism, Rinton Press, (2006).
Chudnovsky, E. M., Javier Tejada, Carlos Calero, and Ferran Maci, Problem solutions to lectures on magnetism, Rinton Press, (2007).
Chudnovsky E.M. and D.A. Garanin, Phys. Rev. B **81**, 214423 (2010)
Chudnovsky E.M. in Molecular Magnets Physics and Applications, Springer (2014), p.61
Coleman S. , Phys. Rev. D **15**, 2929 (1977)
Callan C. G. and S. Coleman, Phys. Rev. D **16**, 1762 (1977).
Coleman S., Aspects of Symmetry (Cambridge University Press, 1985), Chap. 7.

Cooper L. N. , Phys. Rev. **104**, 1189 (1956).
Coffey W. T., Yu. P. Kalmykov, and J. T. Waldron, The Langevin Equation, (World Scientific, Singapore), (1996).
Dashen R., B. Hasslacher, and A. Neveu, Phys. Rev. D **10**, 4114 (1974); ibid, Phys. Rev. D **10**, 4130 (1974); ibid, Phys. Rev. D **10**, 4138 (1974)
Dirac P., Proc. Roy. Soc. (London) A 133, 60 (1931)
Eduardo Fradkin and Michael Stone, Phys. Rev. B **38**, 7215, (1998).
Eduardo Fradkin, Field Theories of Condensed Matter Systems (Addison-Wesley, Redwood City) (1991)]
Enz M. and R. Schilling, J. Phys. C: Solid State Phys., **19**, 1765 (1986); Ibid **19**, L711 (1986)
Ersin Keçecioğlu and Anupam Garg, Phys. Rev. B **67**, 054406 (2003)
Esposito F. P., L.-P. Guay, R. B. MacKenzie, Paranjape M.B and L. C. R. Wijewardhana, Phys. Rev. Lett. **98**, 241602 (2007)
Feynman R.P. and A.R Hibbs, Quantum Mechanics and Path Integrals (McGraw-Hill, Inc) (1965)
Feynman R.P., Rev. Mod. Phys. **20**, 367 (1948)
Foss-Feig M. S. and Jonathan R. Friedman, Euro. Phys. Lett **86** 27002, 2009.
Friedman J. R., M. P. Sarachik, J. Tejada, and R. Ziolo, Phys. Rev. Lett. **76**, 3830 (1996).
Garanin D. A. (1991) J. Phys. A: Math. Gen. 24 L61
Garanin D.A. and Chudnovsky E.M., Phys. Rev. B **65**, 094423 (2002)
Garg A., Evgueny Kochetov, Kee-Su Park and Michael Stone, J. Math. Phys. **44**, 48 (2003)
Garg A. and Gwang-Hee Kim Phys. Rev. B **45**, 12921 (1992)
Garg A., Europhys. Lett. **22**, 205 (1993)
Garg A. and Ji-Min Duan, J. Phys.: Condens. Matter **7**, 2171 (1995)
Garg A. Phys. Rev. B **60**, 6705 (1999)
Garg A., Am. J. Phys. **68**, 430 (2000)
Garg A. Phys. Rev. B **64**, 094414 (2001); ibid **64**, 094413 (2001)
Gervais J-L. and Sakita B., Phys. Rev. D **11**, 2943 (1975);
Gervais J-L. , Jevicki A. and Sakita B. , Physics Reports 23 (1976), p. 237
Gider S., D. D. Awshalom, T. Douglas, S. Mann, and M. Chaprala, Science **268**, 77 (1995).
Goldanskii V.I. , Dokl. Acad. Nauk SSSR **124**, 1261 (1959a) [Sov. Phys. Dokl. **4**, 74 (1959)]
Goldanskii V.I. , Dokl. Acad. Nauk SSSR **127**, 1037 (1959b)
Gorokhov D. A. and G. Blatter, Phys. Rev. B **56**, 3130 (1997)
Gatteschi D. and Roberta Sessoli, Angew. Chem. Int. Ed., **42** 268, 2003
Hu J. M., Zhi-De Chen, and Shun-Qing Shen, Phys. Rev. B **68**, 104407 (2003)
Henley C. and J. von Delft , Phys. Rev. Lett. **69**, 3236 (1992)
Hänggi P., P. Talkner, and M. Borkovec, Rev. Mod. Phys. **62**, 251 (1990)
Hill S., R. S. Edwards, N. Aliaga-Alcalde, G. Christou, Science **302**, 1015 (2003)
Jackiw R. and Rebbi C.Phys. Rev. Lett. 37,172 (1976)
Josephson, B. D, Phys. Rev. Lett. **1**, 251 (1962).
Jan R. Rubbmark, Michael M. Kash, Michael G. Littman, and Daniel Kleppner, Phys. Rev. B **23**, 3107 (1981)
Khare A. and M. B. Paranjape, Phys. Rev. B **83**, 172401 (2011)
Kim Gwang-Hee, Phys. Rev. B **59**, 11847, (1999); J. Appl. Phys. 86, 1062 (1999)
Kim Gwang-Hee, J. Appl. Phys. 91, 3289 (2002)
Kim Gwang-Hee, Phys. Rev. B **67**, 024421 (2003); ibid **68**, 144423 (2003)
Kent A. D. , Yicheng Zhong, L. Bokacheva1, D. Ruiz, D. N. Hendrickson and M. P. Sarachik, Europhys. Lett. **49** 521, (2000)
Klauder J.R., Phys. Rev. D **19**, 2349 (1979).
Kramers H. A., Proc. Amsterdam Acad. **33**, 959 (1930)
Kramers H. A., Physica Amsterdam **7**, 284 (1940)
Leon M. C., H. Soyer, E. Coronado, C. Mingotaud, C. J. Gomez-Garcia, P. Delhaes, Angew. Chem., **110**, 3053, (1998); Angew. Chem. Int. Ed. , **37**, 2842, (1998)
Leon M. C., E. Coronado, P. Delhaes, C. J. Gomez- Garcia, C. Mingotaud, Adv. Mater., **13**, 574 (2001).
Landau, L.D. and Lifshitz E.M. , Phys. Z. Sowietunion, **8**, 153, (1935)
L. Landau, Phys. Z. Sowjetunion 2, 46 (1932)
Landau, L.D. and Lifshitz E.M. , Quantum mechanics, 3rd ed. (Pergamon, New york), (1977)
Landau L. D. and Lifshitz E. M Statistical Mechanics, Part 1 (Oxford: Pergamon Press), (1991)
J. S. Langer, Annals of Physics, 41, 108, (1967)
Larkin A. I. and Yu. N. Ovchinnikov, Pis'ma Zh. Éksp. Teor. Fiz. **37**, 322 (1983) [JETP Lett. **37**, 382 (1983)]
Larkin A. I. and Yu. N. Ovchinnikov Zh. Éksp. Teor. Fiz. 86, 719 (1984)
Leggett A.J., in Quantum Tunneling of Magnetization-QTM'94(Eds.: L. Gunther, B. Barbara), Kluwer, Dordrecht, 1995, p. 1.
Leuenberger M. N. and Daniel Loss, Phys. Rev. B **61**, 1286 (2000).
Leuenberger M. N. and Daniel Loss, Nature **410**, 789 (2001)
Liang J-Q , Yi-Hang Nie, Yan-Hong Jin, H .J .W. Müller-Kirsten, D K Park, F-C Pu, J. Phys.: Condens. Matter **12** (2000) L87-L91
Liang J.-Q., H. J. W. Müller-Kirsten, D. K. Park, and F. Zimmerschied, Phys. Rev. Lett. **81**, 216 (1998)
Lieb, E. H., Commun. Math. Phys. **31**, 327 (1973)
Lipkin H. J., N. Meshkov and A. J. Glick, Nucl. Phys. **B 62**, 188 (1965)

Loss, D David P. DiVincenzo, and G. Grinstein, Phys. Rev. Lett. **69**, 3232 (1992)
Loss, D and D. DiVincenzo, Phys. Rev. A **57**, 120, (1998).
Meier F. and Daniel Loss, Phys. Rev. Lett. **86**, 5373 (2001).
Meier F., Jeremy Levy and Daniel Loss, Phys. Rev. B **68**, 134417 (2003)
Messiah A. , Quantum Mechanics (Wiley, New York, 1962), Vol. II, p. 675, 750ff
Müller-Kirsten H. J. W., J.-Q. Liang, D. K. Park and F.-C. Pu , Phys. Rev. B **61**, 8856 (2000)
Müller-Kirsten H. J. W., S.-Y. Lee, D. K. Park, and F. Zimmerschied ; Phys. Rev. B **58**, 5554 (1998).
Müller-Kirsten H.J.W., Y.-B. Zhang, J.-Q. Liang, S.-P. Kou, X.-B. Wang and F.-C. Pu Phys. Rev. B **60**, 12886 (1999)
Müller-Kirsten H.J.W., D.K.Park and J.M.S. Rana Phys. Rev. B **60**, 6662 (1999)
MacKenzie R., arXiv:quant-ph/0004090 (2000)
Novikov S.P., Usp.Mat.Nauk, 37N5 3-49, (1982)
Novak M. A. and Sessoli R. , in Quantum Tunneling of the Magnetization -QTM'94 (Eds.: L. Gunther, B. Barbara), Kluwer, Dordrecht, 1995 , p. 171.
Owerre S. A. and Paranjape M.B., arXiv:1309.6615 [cond-mat.str-el] (submitted to Physica B),(2014a)
Owerre S.A. and Paranjape M.B., Journal of Magnetism and Magnetic Materials **93**, 358, (2014b)
Owerre S.A. and Paranjape M.B., Phys. Lett. A 378, 1407 (2014c)
Owerre S. A. and Paranjape M.B., Phys. Lett. A 378, 3066 (2014d)
Owerre S. A. and Paranjape M.B., Phys. Rev. B **88**, 220403(R), (2013). There is a typo in the first term of Eqn.(5) in this article.
Owerre S.A., J. Appl. Phys. 115, 153901 (2014)
Paulsen C. and J.-G. Park, in Quantum Tunneling of the Magnetization -QTM'94 (Eds.: L. Gunther, B. Barbara), Kluwer, Dordrecht, 1995, p. 189.
Perelomov A., Generalized Coherent States and Their Applications, Springer, (1986)
Polyakov A. N., Phys. Lett. B**59**, 82 (1975); Nucl. Phys. B121,429 (1977).
Park K., Mark R. Pederson, Steven L. Richardson, Nuria Aliaga-Alcalde, and George Christou, Phys. Rev. B **68**, 020405 (2003)
Radcliffe J. M., J. Phys. A: Gen. Phys **4** , 313 (1971).
Razavy M., Am. J. Phys. **48** 285 (1980).
Ribeiro P., J. Vidal, and R. Mosseri, Phys. Rev. Lett. **99**, 050402 (2007);
Ribeiro P., J. Vidal, and R. Mosseri, Phys. Rev. E **78**, 021106 (2008)
Scharf G ., W. F Wreszinski and -J. L van Hemmen, J. Phys. A: Math. Gen **20**, 4309 (1987)
Schilling R., in Quantum Tunneling of Magnetization-QTM'94 (Eds.: L. Gunther, B. Barbara), Kluwer, Dordrecht, 1995, p. 59.
Sahng-Kyoon Yoo, Soo-Young Lee, Dal-Ho Yoon and Chang-Soo Park, Phys. Rev. B **62**, 3014 (2000)
Stamp P. C. E., E. M. Chudnovsky, and B. Barbara, Int. J. Mod. Phys. B **6**, 1355 (1992)
Sangregorio C. , T. Ohm, C. Paulsen, R. Sessoli, and D. Gatteschi, Phys. Rev. Lett. , **78**, 4645 (1997).
Sessoli R. , W. Wernsdorfer , A. Caneschi, D. Gatteschi, D. Mailly, and A. Cornia, J. Appl. Phys. **87**, 5481 (2000).
Stone M., Kee-Su Park and Anupam Garg, J. Math. Phys. **41**, 8025 (2000)
Taft K. L., C. D. Delfs, G. C. Papaefthymiou, S. Foner, D. Gatteschi, S. J. Lippard, J. Am. Chem. Soc., **116**, 823, (1994)
Tiron R., W. Wernsdorfer, D. Foguet-Albiol, N. Aliaga-Alcalde, and G. Christou, Phys. Rev. Lett. **91**, 227203 (2003a)
Tiron R., W. Wernsdorfer, N. Aliaga-Alcalde, and G. Christou, Phys. Rev. B **68**, 140407(R) (2003b)
Tejada J., X. X. Zhang, E. del Barco, J. M. Hernández, and E. M. Chudnovsky, Phys. Rev. Lett. **79**, 1754 (1997).
Tejada J., E. del Barco, J. M. Hernández, and E. M. Chudnovsky, T. P. Spiller, Nanotechnology , **12**, 181, (2001)
Thomas L., F. Lionti, R. Ballou, D. Gatteschi, R. Sessoli, and B. Barbara, Nature (London) **383**, 145 (1996)
Van Hemmen J. L. and Sütö A., Physica B, **141**, 37, (1986).
Wess. J, B. Zumino, Phys. Lett. B **37** 95, (1971)
Witten. E, Nucl. Phys., B **160** 57, (1979)
Weiss U. and Walter Haeffner, Phys. Rev. D **27**, 2916 (1983)
Wernsdorfer W. and R. Sessoli, science **284**, 133 (1999)
Wernsdorfer W., R. Sessoli, A. Caneschi, D. Gatteschi, and A. Cornia, Europhys. Lett. **50**, 552 (2000).
Wernsdorfer W., E. Bonet Orozco, K. Hasselback, A. Benoit, D. Mailly, O. Kubo, H. Nakano, and B. Barbara, Phys. Rev. Lett. **79**, 4014 (1997).
Wernsdorfer W., N. E. Chakov, and G. Christou, Phys. Rev. Lett. **95**, 037203 (2005).
Wernsdorfer W., S. Bhaduri, C. Boskovic, G. Christou, and D. N. Hendrickson, Phys. Rev. B **65**, 180403(R) (2002).
Wernsdorfer W., R. Tiron D.N. Hendrickson, N. Aliaga-Alcalde, and G. Christou, Journal of Magnetism and Magnetic Materials **272**, 1037 (2004)
Wernsdorfer W. , M. Murugesu, and G. Christou, Phys. Rev. Lett. **96**, 057208(2006)
W. Wernsdorfer, S. Bhaduri, A. Vinslava, and G. Christou, Phys. Rev. B **72**, 214429(2005)
Whittaker E. T., Proc. London Math. Soc. 35 p.417-427(1902)
Zaslavskii O.B. , Phys. Lett. A **145**, 471 (1990a)
Zaslavskii O.B. , Phys. Rev. B **42**, 992 (1990b)
Zaslavskii O.B. and V.V. Ulyanov, Phys. Rep. **214**, 179 (1992)
Zaslavskii O.B. and V.V. Ulyanov, Phys. Rev. B **60**, 6212 (1999)
Zhang, Y.-B., J.-Q. Liang, H.J.W. Müller-Kirsten, Jian-Ge Zhou, F. Zimmerschied, F.-C. Pu, Phys. Rev. B **57** , 529, (1998)
Zhang Y.-B., Yihang Nie , Supeng Kou , Jiuqing Liang , H.J.W. Müller-Kirsten, Fu-Cho Pu, Phys. Lett. A **253**, 345 (1999)

Zhang X. X., J. M. Hernández, F. Luis, J. Bartolomé, J. Tejada, and R. Ziolo, Europhys. Lett. **35**, 301 (1996).
Zener C., Proc. R. Soc. Lond. A 137, 696 (1932)
Zhang W. M., Da Hsuan Feng and Robert Gilmore, Rev. Mod. Phys. **62**, 867 (1990).

CHAPTER 7

ONE-DIMENSIONAL QUANTUM LARGE SPIN CHAIN

One should always generalize.

Carl Jacob

7.1 Introduction

Quantum spin chain is a captivating research area in condensed matter and particle physics. It is the fundamental concept of strongly correlated systems. The work of Bethe and Hulthén [13, 59], for one-dimensional isotropic Heisenberg spin-$\frac{1}{2}$ antiferromagnetic chain was one of the breakthrough in this research area. Anderson [8] also made an early contribution by computing the ground state energies and the spectrum in one-, two-, and three- dimensional systems, by means of spin wave theory. In recent years, a tremendous work has been done in this area of research. In the chapter we consider a cyclic molecular magnet, modeled as an anisotropic Heisenberg model with N large spins $s \gg 1$ regularly spaced on a ring, with odd and even N:

$$\hat{H} = -D\sum_{l=1}^{N} S_{l,z}^2 + J\sum_{l=1}^{N} \mathbf{S}_l \cdot \mathbf{S}_{l+1}; \quad \mathbf{S}_{N+1} = \mathbf{S}_1; \tag{7.1}$$

where $J > 0$ is the Heisenberg exchange interaction coupling constant and $D > 0$ is the easy-axis anisotropy constant; N is the total number of sites. Our model possesses discrete translational and reflection invariance: $S_l^{x,y,z} \to S_{l+1}^{x,y,z}$ and $S_l^{x,y,z} \to -S_l^{x,y,z}$. The continuous rotational invariance of the interaction term is broken to continuous rotational invariance about the z-axis, that is

$$S_l^{\pm} = e^{\pm i\phi} S_l^{\pm}; \quad S_l^{\pm} = \frac{S_{l,x} + iS_{l,y}}{2}; \tag{7.2}$$

where ϕ is the angle of rotation. From Noether's theorem, a continuous symmetry is associated with a conserved quantity. This is the total z-components of spins, since $\left[\sum_l S_{l,z}, \hat{H}\right] = 0$. For even number of sites, this model is a good description for molecular magnets such as $CsFe_8$, with $N = 8$, $s = 5/2$, $J > D$; $NaFe_6$, with $N = 6$, $s = 5/2$, $J > D$ [58, 92, 93, 138], etc. The two fully anti-aligned Neél states are the classical ground states; they form the basis of spin wave theory and macroscopic quantum tunneling. In principle, macroscopic quantum tunneling is permissible if there is any spin configuration that does not commute with the Hamiltonian. Indeed, the staggered z-components $S_z^{st} = \sum_l^N (-1)^l S_{l,z}$, is not conserved. This suggests that the two Néel states, which are not exact eigenstates of the quantum Hamiltonian can tunnel to each other through a classical energy barrier.

For odd number of sites, the Néel states are frustrated, since it is impossible to satisfy all sites antiferromagnetically. Thus, they must contain at least one defect, which is sometimes called a domain wall or soliton[1] [137]. The soliton state is, of course, the classical ground state; however, it is highly degenerate as the soliton can be placed anywhere along the cyclic chain. In the perturbative limit $J \ll D$, we expect quantum fluctuations stemming from the interaction term to lift these degenerate states; this results in delocalization of the soliton, which exterminates antiferromagnetic long-range order with a formation of an energy band. In this respect, Villain [137] has studied the one-dimensional spin-$\frac{1}{2}$ XXZ antiferromagnetic odd spin chain close to the Ising limit, which is a good description for $CsCoBr_3$ and $CsCoCl_3$ [17, 91]. He pointed out in his article that the model defined in Eqn.(7.1) should be of considerable interest as it applies to Co^{++} with $s = \frac{3}{2}$; however, he never solved it for large spin systems. Frustrated systems are indispensable in condensed matter physics as they lead to exotic phases of matter such as spin liquid [10], spin glasses [14], and topological orders [69]. The model in Eqn.(7.1) also has a wide range of applications ranging from quantum computing [94]

[1] Solitons also appear on the periodic chain with even number of sites as excitation from the Néel states, however, there must be at least two.

to optical physics [126]. Quantum large spin chain was first studied by Haldane [54, 55]. He conjectured that in the large spin limit, $s \gg 1$, the excitation spectrum for integer spins has a mass gap, whereas that of half-odd integer spins is gapless. There have been numerous studies to investigate the Haldane's conjecture [19, 70, 135].

In this chapter we will present a lucid exposition of macroscopic quantum tunneling using Eqn.(7.1). The format of this chapter is as follows: the spin wave theory of the model defined in Eqn.(7.1) will be presented in Sec.(7.2) . In Sec.(7.3) we will investigate this model for the case of even number of sites in the perturbative and the non-perturbative limits, using the spin coherent state path integral formalism, which is the appropriate formalism for large spin systems. The general formula for the energy splitting, valid for any even N will be derived. In Sec.(7.4) we will consider the case of odd number of sites. As the spin coherent state path integral formalism is infeasible in this case, we will resort to perturbation theory. The energy band will be obtained, as well as Kramers' degeneracy. In Sec.(7.5) we will conclude our analysis. This chapter will be solely based on the recent publication of Owerre and Paranjape [107], with some extensions. Our paper on this analysis will be included in Sec.(7.6).

7.2 Spin wave theory

We begin by understanding the excitation spectrum of our model Hamiltonian in Eq.(7.1). In this model we expect the spin waves to have a large gap. This is because a spin wave corresponds to introducing a local deviation of the spins away from their respective highest or lowest values of S_z. This incurs an energy cost proportional to D from the anisotropy term;. Evidently, the classical ground states of our model are locally the fully anti-aligned Neél states; we can introduce small quantum fluctuations in the spirit of Holstein-Primakoff transformation [57, 101]. In the linear spin wave theory, the

fluctuation of the spins pointing up can be written as

$$S_{l,z} = s - a_l^\dagger a_l;\ S_l^+ = \sqrt{2s}a_l;\ S_l^- = (S_l^+)^\dagger; \tag{7.3}$$

while the fluctuation of the spins pointing down can be written as

$$S_{l,z} = -s + b_l^\dagger b_l;\ S_l^+ = \sqrt{2s}b_l^\dagger;\ S_l^+ = (S_l^+)^\dagger; \tag{7.4}$$

where $S_l^\pm = S_{l,x} \pm iS_{l,y}$ are the spin raising and lowering operators; a_l, b_l and $a_l^\dagger, b_l^\dagger$ are the bosonic creation and annihilation operators respectively. A direct substitution of Eqn.(7.3) and Eqn.(7.4) into Eqn.(7.1) transforms the spin Hamiltonian into a bosonic Hamiltonian. The corresponding Hamiltonian is diagonalized in the usual way [101], by transforming to the momentum space and applying a Bogoliubov transformation. Straightforwardly, we obtain that the magnon (spin wave) dispersion is given by [54]

$$\varepsilon_q = \sqrt{\varepsilon_0^2 + \varepsilon_1^2 \sin^2(q)} \overset{q\to 0}{\longrightarrow} \sqrt{\varepsilon_0^2 + \varepsilon_1^2 q^2}; \tag{7.5}$$

where $\varepsilon_0 = 2s\sqrt{D(D+2J)}$, $\varepsilon_1 = 2sJ$, and $-\pi \leq q \leq \pi$. Since $D \neq 0$, the magnon dispersion has a gap; this gap is indeed very large in the perturbative limit $D \gg J$.

7.3 Even number of sites

The study of antiferromagnetic molecular magnets with even number of spins is of considerable interest in both theoretical and experimental studies [92, 94, 129, 138]. In the semiclassical description, the easy-axis anisotropy creates an energy barrier of height DNs^2, with two degenerate minima. The two Néel states, which are the classical ground states, are respectively localized in these energy minima; thus, ground state quantum tunneling is allowed, as the two Néel states are not exact eigenstates of the quantum Hamiltonian. Due to tunneling, the degeneracy of the Neél states is lifted and

the states reorganize into symmetric and antisymmetric linear superpositions with an energy splitting between them. This problem is reminiscent of Sec.(3.3) for the two interacting spins, *i.e.*, $N = 2$ in Eqn.(7.1); however, in this section we will derive the general energy splitting valid for any even N.

7.3.1 Classical trajectory for even number of sites

For large spin systems, it is customarily expedient to use the spin coherent state path integral formalism [7, 71, 103]. In this formalism each spin is represented by a unit vector, and the corresponding (Euclidean) Lagrangian is given by

$$L_E = is\sum_{l=1}^{N}[\dot{\phi}_l(1-\cos\theta_l)] + U(\theta_l,\phi_l), \tag{7.6}$$

where the potential is given by

$$U(\theta_l,\phi_l) = Ds^2\sum_{l=1}^{N}\sin^2\theta_l + Js^2\sum_{l=1}^{N}[\sin\theta_l\sin\theta_{l+1}\cos(\phi_l-\phi_{l+1}) + \cos\theta_l\cos\theta_{l+1}]. \tag{7.7}$$

The first term is the usual Wess-Zumino term [146], which arises from the non-orthogonality of spin coherent states, while the second term comprises the anisotropy energy and the exchange interaction energy respectively. The transition amplitude is computed by first deriving the solutions of the classical equation of motion. There are N degrees of freedom for each of the coordinates ϕ_l and θ_l; hence, there are N classical equations of motion for each coordinate. The classical equation of motion for the ϕ_l coordinate yields

$$i\frac{d(1-\cos\theta_l)}{d\tau} = s[\sin\theta_{l-1}\sin\theta_l\sin(\phi_{l-1}-\phi_l) - \sin\theta_l\sin\theta_{l+1}\sin(\phi_l-\phi_{l+1})]. \tag{7.8}$$

Similarly, the classical equation of motion for the θ_l coordinate is given by

$$\begin{aligned} & i\dot{\phi}_l \sin\theta_l + Ds \sin 2\theta_l + Js[\cos\theta_l \sin\theta_{l+1} \cos(\phi_l - \phi_{l+1}) - \cos\theta_{l+1} \sin\theta_l] \\ & + Js[\cos\theta_l \sin\theta_{l-1} \cos(\phi_l - \phi_{l+1}) - \cos\theta_{l-1} \sin\theta_l] = 0. \end{aligned} \tag{7.9}$$

As the chain has periodic boundary condition, summing both sides of Eqn.(7.8) yields

$$i \sum_{l=1}^{N} \frac{d(1-\cos\theta_l)}{d\tau} = 0 \Rightarrow \sum_{l=1}^{N} \cos\theta_l = \text{const.} = 0. \tag{7.10}$$

This equation is the conservation of z-component of the total spin $S_z = \sum_l S_l^z$, as the full Hamiltonian, Eqn.(7.1), is invariant under rotations about the z-axis. There are many solutions of Eqn.(7.10); a particular solution is of the form:

$$\theta_{2j-1} = \theta; \quad \theta_{2j} = \pi - \theta; \tag{7.11}$$

where $j = 1, 2 \cdots, N/2$. This corresponds to almost anti-aligned spins. Plugging Eqn.(7.11) into Eqns.(7.8) and (7.9), the resulting equations are derivable from the effective Lagrangian:

$$\begin{aligned} L_E^{eff} &= is(1-\cos\theta) \sum_{j=1}^{N/2} (\dot{\phi}_{2j-1} - \dot{\phi}_{2j}) + s^2 \sum_{j=1}^{N} \Big[D + J[1 + \cos(\phi_j - \phi_{j+1})] \Big] \sin^2\theta, \\ &= \frac{isN}{2} \dot{\phi}(1-\cos\theta) + U_{eff}, \end{aligned} \tag{7.12}$$

where

$$U_{eff} = Ns^2[D + J(1+\cos\phi)] \sin^2\theta. \tag{7.13}$$

The last equality in Eqn.(7.12) is obtained by making a further simplifying ansatz, $\phi_j - \phi_{j+1} = (-1)^{j+1}\phi$, which effectively reduces the problem to that of N single spin. As

$\sin\theta(\tau) \neq 0$ along the whole trajectory, from energy conservation, $U_{eff} = 0$, we have

$$\cos\phi = -\left(1 + \frac{D}{J}\right), \tag{7.14}$$

It is evident that $\cos\phi < -1$, for $J \ll D$ and for $J \gg D$. Thus, ϕ is a complex constant, which can be written as $\phi = \pi + i\varphi$, reminiscent of the two-spin case [103]. The classical equation of motion for ϕ gives

$$i\dot{\theta} = -2Js\sin\theta\sin\phi = i2sJ\sin\theta\sinh\varphi, \tag{7.15}$$

where

$$\varphi = \operatorname{arccosh}\left(1 + \frac{D}{J}\right). \tag{7.16}$$

Then, Eqn.(7.15) integrates as

$$\cos\theta = -\tanh\omega_0(\tau - \tau_0); \quad \omega_0 = 2sJ\sinh\varphi = 2Ds\sqrt{1 + 2\left(\frac{J}{D}\right)}. \tag{7.17}$$

Indeed, the classical trajectory (instanton) is independent of the number of sites. Thus, the instanton flips the spin-up to spin-down, while the anti-instanton flips spin-down to spin-up for any number of even spin sites. Hence, $|\uparrow,\downarrow,\cdots,\uparrow,\downarrow\rangle \leftrightarrow |\downarrow,\uparrow,\cdots,\downarrow,\uparrow\rangle$.

7.3.2 Energy splitting and low-lying eigenstates

The energy splitting depends upon the action of the instanton trajectory in the preceding section. As $U_{eff} = 0$ along the trajectory, the only contribution to the instanton action comes from the Wess-Zumino term. The action is simply given by[103]

$$\begin{aligned} S_c &= S_0 - \frac{isN}{2}\int_0^{\pi+i\varphi} d\phi\cos\theta|_{\theta=0} - \frac{isN}{2}\int_{\pi+i\varphi}^{0} d\phi\cos\theta|_{\theta=\pi}, \\ &= 0 - isN\pi + Ns\varphi = -isN\pi + Ns\varphi. \end{aligned} \tag{7.18}$$

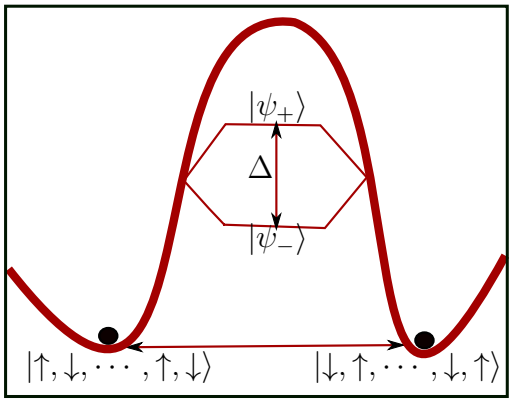

Figure 7.1: A sketch of the classical anisotropy energy, with two degenerate minima. The two degenerate Néel states are localized in each minimum. Due to tunneling between them, they recognize into symmetric and antisymmetric coherent superpositions separated by an energy splitting. In the thermodynamic limit, the splitting vanishes and the two Néel states become the degenerate ground states.

The energy splitting is then

$$\Delta = 2\mathscr{D}e^{-S_c} = \begin{cases} 2\mathscr{D}\left(\frac{J}{2D}\right)^{sN}\cos(sN\pi); & \text{if } J \ll D; \\ 2\mathscr{D}\exp(-sN\,(2D/J)^{1/2})\cos(sN\pi); & \text{if } J \gg D; \end{cases} \tag{7.19}$$

where $\mathscr{D}$ is a determinantal pre-factor. This splitting, Eqn.(7.19), is the general formula for any even sites N, where $N = 2$ replicates the result in Sec.(3.3), with $J \to J/2$, due to the periodicity of Eqn.(7.1). The result for the non-perturbative limit $J \gg D$, is well-known[2] [92, 93, 138]. The two Neél states reorganize into the symmetric and antisymmetric linear superpositions, $|\psi_+\rangle$ and the $|\psi_-\rangle$ as in Ref.[103]; see Fig.(7.1). The factor Ns can be even or odd, depending on the value of the spin. For half-odd

[2]In Ref.[92], the energy splitting in the limit $J \gg D$, was found by integrating out the fluctuations about the staggered Neél state. This method, however, is only valid in the non-perturbative Haldane limit.

integer spin, and for $N = 2(2n+1)$ we find[3] $\Delta < 0$; thus, the ground state is

$$|\psi_-\rangle = \frac{1}{\sqrt{2}}\left(|\uparrow,\downarrow,\cdots\uparrow,\downarrow\rangle - |\downarrow,\uparrow,\cdots\downarrow,\uparrow\rangle\right). \tag{7.20}$$

This states preserves the discrete translational invariance of the Hamiltonian. The first excited state is

$$|\psi_+\rangle = \frac{1}{\sqrt{2}}\left(|\uparrow,\downarrow,\cdots,\uparrow,\downarrow\rangle + |\downarrow,\uparrow,\cdots,\downarrow,\uparrow\rangle\right). \tag{7.21}$$

In all other cases, for any value of the spin s and $N = 2(2n)$ we find $\Delta > 0$, then $|\psi_+\rangle$ is the ground state; $|\psi_-\rangle$ is the first excited state. In the thermodynamic limiit $N \to \infty$, the instanton action becomes infinite, $S_c \to \infty$ and hence the splitting goes to zero, $\Delta \to 0$. Thus, the ground state reduces to the doubly degenerate Néel states $|\uparrow,\downarrow,\cdots,\uparrow,\downarrow\rangle$ and $|\downarrow,\uparrow,\cdots,\downarrow,\uparrow\rangle$. These states spontaneously break the discrete translational invariance of the Hamiltonian; as this is not a continuous symmetry, there is no Goldstone bosons.

7.4 Odd number of sites

7.4.1 Soliton in odd spin chain

For a cyclic chain with an odd number of sites, the formation of a fully anti-aligned Néel state is impossible. This leads to spin frustration; that is, in some domain there exist at least one pair of spins with broken bond. In other words, at least one pair of spins must be aligned instead of anti-aligned. This defect is usually called a soliton or a domain wall. The one-soliton states can be written as

$$|u\rangle = |\uparrow,\downarrow,\cdots,\uparrow,\downarrow,\underbrace{\uparrow,\uparrow}_{u^{th},u+1^{th}},\downarrow,\uparrow\cdots,\uparrow,\downarrow\rangle. \tag{7.22}$$

where $u = 1,\cdots,N$; $\uparrow \equiv s$; $\downarrow \equiv -s$.

[3] There is no Kramers' degeneracy as the total spin of the system is even.

The antiferromagnetic bond between the two aligned spins is broken. The soliton is between the aligned spins at u and $u+1$. Thus, it creates a domain wall between two fully anti-aligned Néel states. These states have a total z component of s; there are another states, which are found by flipping all spins. These states have a total z component of $-s$. In each sector, s or $-s$, the position of the soliton is arbitrary, which leads to N-fold classical degenerate ground states. Since these states are not exact quantum ground states, we shall show that quantum fluctuations stemming from the interaction term lifts these N-fold classical degenerate ground states and recognizes them into a band, thereby exterminates any sort of antiferromagnetic long-range order in the system.

7.4.2 Perturbation theory for odd spin chain

For odd spin chain, spin coherent state path integral formulation is infeasible. There is no instanton trajectory that flips the spins. However, from the even spin chain analysis in Sec.(7.3.2), it is evident that in the perturbative limit $J \ll D$, the energy splitting arises from $2s\left(\frac{N}{2}\right)$ order in degenerate perturbation theory. Thus, it is reasonable to consider perturbation theory as the appropriate formalism for the odd spin chain. The opposite limit $J \gg D$ is, of course, non-perturbative. No solution has been reported in any literature for the odd spin chain. We now give a lucid computation of the energy band in the perturbative limit. It is customary to write Eqn.(7.1) as a sum of two terms:

$$\hat{H} = \hat{H}^0 + \hat{V}, \tag{7.23}$$

where the unperturbed term $\hat{H}^0$ and perturbative term $\hat{V}$ are given by

$$\hat{H}^0 = -D\sum_{l=1}^{N} \hat{S}_{l,z}^2 \tag{7.24}$$

$$\hat{V} = J\sum_{l=1}^{N} \hat{S}_{l,z}\hat{S}_{l+1,z} + \frac{J}{2}\sum_{l=1}^{N}\left(\hat{S}_l^+\hat{S}_{l+1}^- + \hat{S}_l^-\hat{S}_{l+1}^+\right) \tag{7.25}$$

The N-fold classical degenerate ground states are also degenerate ground states of $\hat{H}^0$:

$$\hat{H}^0 \left|u\right\rangle = \mathcal{E}^0 \left|u\right\rangle , \tag{7.26}$$

where $\mathcal{E}^0 = -DNs^2$. At first order in degenerate perturbation theory, we must diagonalize $\hat{V}$ in the degenerate subspace $|u\rangle$:

$$\mathscr{H}^1_{u',u} = \langle u'|\hat{V}|u\rangle \equiv \hat{V}_{u',u}; \quad u', u = 1, 2, \cdots, N. \tag{7.27}$$

The splitting term (second term) in $\hat{V}$ maps $|u\rangle$ to states out of the degenerate subspace; consequently, the inner product of the resulting states and the degenerate states $|u'\rangle$ vanishes. Thus, only the z term in $\hat{V}$ gives a nonzero energy contribution and the eigenvalues are determined by the secular equation:

$$|\hat{V}_{u',u} - \mathcal{E}^1 \delta_{u',u}| = 0. \tag{7.28}$$

Direct computation yields $\hat{V}_{u',u} = Js^2 \left(1 - (N-1)\right) \delta_{u',u}$; hence, the determinant in Eqn.(7.28) is indeed diagonal. Thus, at first-order $\mathcal{E}^u_{\pm} = \mathcal{E}^0 + \mathcal{E}^1 = -DNs^2 - Js^2(N-2)$; which gives a vanishing energy splitting $\Delta = \mathcal{E}^u_+ - \mathcal{E}^u_- = 0$. In each order in perturbation theory less than $2s$, the splitting term in $\hat{V}$ gives a vanishing matrix element. Hence, the energy splitting vanishes and the degeneracy is not lifted. However, at order $2s$, the degenerate subspace is mapped to itself. This gives a nonzero energy splitting and the states reorganize into a band. At order $2s$, we must take $\hat{V}^{2s}$; there are many terms in this power, but we are interested in those terms that map the degenerate subspace to itself. This is called the "one-soliton approximation"; this approximation is crucial if one is interested in the low temperature properties of the system, which is the case here. There are only two terms from the splitting term in $\hat{V}^{2s}$ that map the degenerate subspace to itself, viz. $(S^-_{u+1}S^+_{u+2})^{2s}$ and $(S^+_{u-1}S^-_u)^{2s}$. These two operators can be regarded as quantum fluctuations very close to the position of the soliton. When acting on the state

$|u\rangle$, flip the anti-aligned pair of spins at positions $u+1, u+2$, and at $u-1, u$ respectively, yielding

$$(S^-_{u+1}S^+_{u+2})^{2s}\,|u\rangle \propto |u+2\rangle\,, \tag{7.29}$$

$$(S^+_{u-1}S^-_{u})^{2s}\,|u\rangle \propto |u-2\rangle\,, \tag{7.30}$$

where the states $|u\pm 2\rangle$ are elements of $|u\rangle$ due to periodic boundary condition. It is evident from Eqn.(7.29) that quantum fluctuations from the interaction term translate the soliton over two sites. The second equation, Eqn.(7.30), is simply a Hermitian conjugation, which follows from making the transformation $u \to u+2$ in Eqn.(7.30), reminiscent of the creation and annihilation operators. All other terms in $\hat{V}^{2s}$ such as terms like $(S^+_{u+4}S^-_{u+5})^{2s}$, $(S^+_{u+2}S^-_{u+3})^{2s}$, etc., represent quantum fluctuations away from the position of the soliton. They map to states out of the one-soliton degenerate subspace by inserting soliton-anti-soliton pairs or by changing the value of $S_{l,z}$ to non extremal values[4]. At high temperature, such operators should be taken into consideration.

The one-soliton energy band and the corresponding eigenstates can be computed by generalizing the 2×2 matrix in Ref.[28] to $N\times N$ matrix with components $\mathscr{H}^{2s}_{u',u}$:

$$\mathscr{H}^{2s}_{u',u} = \langle u'|\hat{V}\mathcal{R}^{2s-1}|u\rangle\,, \tag{7.31}$$

where $\mathcal{R}^{2s-1} = \left(\frac{\mathscr{P}}{\mathcal{E}^0-\hat{H}^0}\hat{V}\right)^{2s-1}$; $\mathscr{P} = 1-\sum_{u=1}^{N}|u\rangle\langle u|$.

7.4.3 Energy band

The diagonalization of the $N\times N$ matrix in the preceding section gives the energy band of the system. The components of this matrix can indeed be computed exactly in the one-soliton approxiation. The only terms that survive in Eqn.(7.31) are indeed the

[4] For instance: $(S^+_{u+2}S^-_{u+3})^{2s}|u\rangle \propto |\uparrow,\downarrow,\cdots,\uparrow,\downarrow,\underbrace{\uparrow,\uparrow,\uparrow,\downarrow,\downarrow}_{u,u+1,u+2,u+3,u+4},\uparrow,\downarrow,\cdots,\uparrow,\downarrow\rangle \notin |u\rangle$.

quantum fluctuations close to the soliton, as defined in Eqns.(7.29) and (7.30). Thus,

$$\mathscr{H}^{2s}_{u',u} = \left(\frac{J}{2}\right)^{2s} \Bigg[\langle u'|S^-_{u+1}S^+_{u+2}\left(\frac{\mathscr{P}}{\mathcal{E}^0-\hat{H}^0}S^-_{u+1}S^+_{u+2}\right)^{2s-1}|u\rangle + \langle u'|S^+_{u-1}S^-_{u}\left(\frac{\mathscr{P}}{\mathcal{E}^0-\hat{H}^0}S^+_{u-1}S^-_{u}\right)^{2s-1}|u\rangle \Bigg]. \tag{7.32}$$

The raising and the lowering operators have the following properties:

$$S^+_u|\sigma\rangle = \sqrt{(s-\sigma)(s+\sigma+1)}\,|\sigma+1\rangle\,; \quad u=1,2,\cdots,N; \tag{7.33}$$

$$S^-_u|\sigma\rangle = \sqrt{(s+\sigma)(s-\sigma+1)}\,|\sigma-1\rangle\,; \quad \sigma=-s,-s+1,\cdots s. \tag{7.34}$$

Using Eqn.(7.33) and Eqn.(7.34), and operating $2s$ times on the right hand side of Eqn.(7.32) gives

$$\mathscr{H}^{2s}_{u',u} = \mathscr{C}_J[\langle u'|u+2\rangle + \langle u'|u-2\rangle] \tag{7.35}$$

where $\mathscr{C}_J$ is given by

$$\mathscr{C}_J = \pm\left(\frac{J}{2}\right)^{2s}\prod_{\sigma=1}^{2s}\sigma(2s-\sigma+1)\prod_{\sigma=1}^{2s-1}\frac{1}{2D\sigma(2s-\sigma)}, \tag{7.36}$$

$$= \pm 2D\left(\frac{J}{4D}\right)^{2s}\left[\frac{(2s)!}{(2s-1)!}\right]^2, \tag{7.37}$$

$$= \pm 8Ds^2\left(\frac{J}{4D}\right)^{2s}. \tag{7.38}$$

The first product in Eqn.(7.36) emanates from the two square roots that accompany the action of the raising and lowering operators, and the second product is a consequence of the energy denominators. The plus or minus sign stems from $2s-1$ negative energy denominators in Eqn.(7.32). Thus, if s is integer, $2s-1$ is odd, and we get a minus sign; while for half-odd integer s, $2s-1$ is even, and we get a plus sign. Thus the matrix

$[\mathscr{H}_{u',u}]$, that we must diagonalize is a circulant matrix [60]:

$$[\mathscr{H}^{2s}_{u',u}] = \mathscr{C}_J \begin{bmatrix} 0 & 0 & 1 & 0 & \cdots & 1 & 0 \\ 0 & 0 & 0 & 1 & \cdots & 0 & 1 \\ 1 & 0 & 0 & 0 & 1 & \cdots & 0 \\ \vdots & 1 & 0 & \ddots & \ddots & \ddots & \vdots \\ 0 & 0 & \ddots & \ddots & \ddots & \ddots & 1 \\ 1 & \cdots & \ddots & \ddots & 0 & 0 & 0 \\ 0 & 1 & 0 & \cdots & 1 & 0 & 0 \end{bmatrix}. \tag{7.39}$$

In this matrix each row element is moved one step to the right, periodically, relative to the preceding row. This matrix is indeed a real symmetric matrix. The eigenvalues and eigenvectors are well-known. The j^{th} eigenvalue is given by

$$\varepsilon_j = \mathscr{H}^{2s}_{1,1} + \mathscr{H}^{2s}_{1,2}\tau_j + \mathscr{H}^{2s}_{1,3}\tau_j^2 + \cdots + \mathscr{H}^{2s}_{1,N}\tau_j^{N-1}, \tag{7.40}$$

where $\tau_j = e^{i\frac{2\pi j}{N}}$ is the j^{th} , N^{th} root of unity with corresponding normalized eigenvector $|\frac{2\pi j}{N}\rangle = \frac{1}{\sqrt{N}}(1, \tau_j, \tau_j^2, \cdots, \tau_j^{N-1})^T$; $j = 0, 1, 2, \cdots, N-1$. The only nonzero elements in Eqn.(7.39) are $\mathscr{H}_{1,3}$ and $\mathscr{H}_{1,N-1}$; thus the one-soliton energy band for our model is [107]

$$\begin{aligned} \varepsilon_j &= \mathscr{C}_J(\tau_j^2 + \tau_j^{N-2}) = \mathscr{C}_J(\tau_j^2 + \tau_{-j}^2); \quad \tau_j^N = 1, \\ &= 2\mathscr{C}_J \cos\left(\frac{4\pi j}{N}\right), \end{aligned} \tag{7.41}$$

which is gapless unlike the magnon dispersion in Eqn.(7.5). In terms of the conventional Brillouin zone momentum[5] $q = 2j\pi/aN$, we have $\tau_q = e^{iqa}$, and the energy bands can

[5]For periodic systems, the Fourier transform is customarily given by $c_j = \frac{1}{\sqrt{N}}\sum_q c_q e^{iqaj}$, since periodicity requires $c_{j+N} = c_j$, we must have $q = 2\pi j/aN$.

be written as

$$[\mathscr{H}^{2s}_{u',u}]\,|q\rangle = \varepsilon_q\,|q\rangle\,; \qquad |q\rangle = \frac{1}{\sqrt{N}}(1, \tau_q, \tau_q^2, \cdots, \tau_q^{N-1})^T, \tag{7.42}$$

where[6]

$$\varepsilon_q = \tau_q^2 + \tau_{-q}^2 = \pm 2|\mathscr{C}_J| \cos(2qa)\,. \tag{7.43}$$

The upper sign is for half-odd integer spins, and the lower sign is for integer spins. The

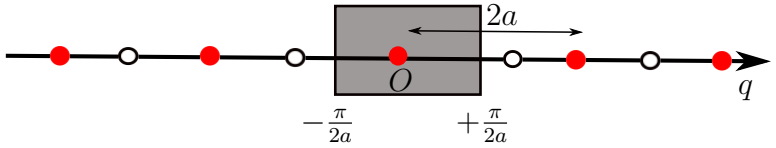

Figure 7.2: The first Brillouin zone of the one-soliton energy band. Due to hopping of the soliton, the lattice spacing has increased by $2a$. Thus, the first Brillouin zone is halved with boundaries $q = \pm\frac{\pi}{2a}$, as indicated by the shaded area.

argument of the cosine function, $2qa$, signifies the total hopping sites of the soliton, that is, the soliton hops over two sites, as a result of quantum fluctuations; see Eqn.(7.35). Thus, the lattice spacing has increased by $2a$; consequently, the first Brillouin zone reduces to a halve, *i.e.,* $-\frac{\pi}{2a} \leq q \leq \frac{\pi}{2a}$; see Fig.(7.2).

Since our model contains odd number of sites and it possesses time-reversal symmetry[7], it is interesting to investigate Kramers' theorem [72, 95], which states that every time-reversal-invariant system comprising an odd number of half-odd integer spins (fermions) is at least doubly degenerate. To investigate this theorem, we restrict our analysis in the first Brillouin zone. In this zone, the states with $q = \pm\frac{\pi}{2a}$ are the degenerate ground states for half-odd integer spins, with $\varepsilon_0 = -2|\mathscr{C}_J|$; they correspond to the Kramers' doublet. For integer spins, however, the state with $q = 0$ and $\varepsilon_0 = -2|\mathscr{C}_J|$ is unique and unpaired. It is the non-degenerate ground state; see Fig.(7.3). Now, let us

[6]For spin-$\frac{1}{2}$ systems, the energy band reduces to $\varepsilon_q = J\cos(2qa)$[16, 137].

[7]Under time-reversal symmetry $\hat{\mathbf{S}} \to -\hat{\mathbf{S}}$; hence, from Eqn.(7.1) $\hat{H} \to \hat{H}$.

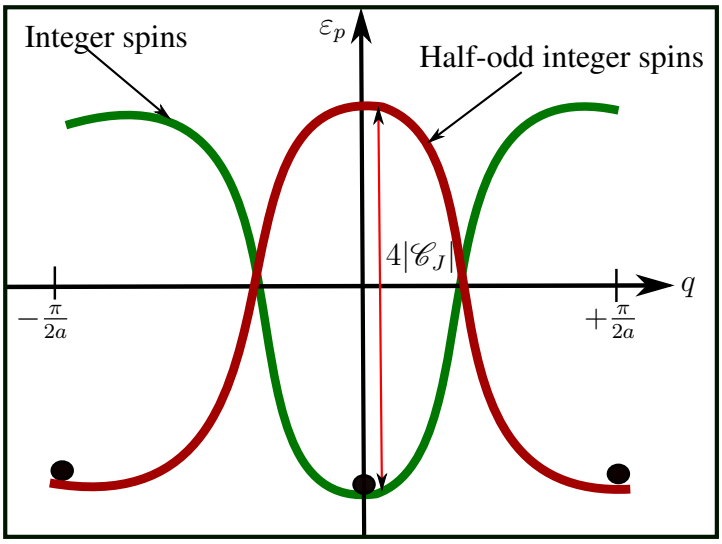

Figure 7.3: Color online: The plot of the one-soliton energy band in the first reduced Brillouin zone. The bandwidth is $4|\mathscr{C}_J|$. For half-odd integer spins, the ground state is doubly degenerate (black spots), with $\varepsilon_0 = -2|\mathscr{C}_J|$; these states can be regarded as the Kramers' doublets [72]. While for integer spins, the ground state (black spot) is non-degenerate, with $\varepsilon_0 = -2|\mathscr{C}_J|$.

expand the cosine function near the bottom of the bands $q = \pm\frac{\pi}{2a}(q = 0)$ for half-odd integer spins (integer spins). We write $q = \pm\frac{\pi}{2a} + k$ for half-odd integer spins, and $q = k$ for integer spins, where $k \ll 1$; then Eqn.(7.43) reduces to

$$\varepsilon_k = \varepsilon_0 + \frac{\hbar^2 k^2}{2m^*}; \quad \text{where} \quad \frac{1}{m^*} = \frac{8a^2|\mathscr{C}_J|}{\hbar^2}, \tag{7.44}$$

which is the familiar non-relativistic energy of free fermions or bosons.

7.4.4 Effect of a transverse magnetic field

We now consider the effect of adding a small magnetic field along the transverse direction. The Hamiltonian becomes

$$\hat{H} = -D\sum_{l=1}^{N} S_{l,z}^2 + J\sum_{l=1}^{N} \mathbf{S}_l \cdot \mathbf{S}_{l+1} + h_x \sum_{l=1}^{N} S_{l,x}; \tag{7.45}$$

where $D \gg J, h_x$. Semiclassically, the spins can be thought of as a classical particle that align along the z-axis, but bend towards the x-axis due to the magnetic field. The perturbative Hamiltonian can be written as

$$\hat{H} = \hat{H}^0 + \hat{V} + \hat{V}_h, \tag{7.46}$$

where $\hat{H}_0$ and $\hat{V}$ are given in Eqns.(7.24) and (7.25). $\hat{V}_h = h_x \sum_{l=1}^{N} S_{l,x}$ is the perturbative (h_x) term. In V_h^{2s}, there are terms like $(S_u^-)^{2s}$ and $(S_{u+1}^-)^{2s}$; acting on the state $|u\rangle$ gives

$$(S_u^-)^{2s}\,|u\rangle \propto |d-1\rangle\,; \quad (S_{u+1}^-)^{2s}\,|u\rangle \propto |d+1\rangle\,; \tag{7.47}$$

where

$$|d\rangle = |\uparrow,\downarrow,\cdots,\uparrow,\underbrace{\downarrow,\downarrow}_{d,d+1},\uparrow,\downarrow\cdots,\uparrow,\downarrow\rangle\,; \quad d = 1,\cdots,N. \tag{7.48}$$

The states $|d \pm 1\rangle$ are elements of $|d\rangle$ due to periodicity . Thus, the magnetic field induces transition between the s sector and the $-s$ sector. The total matrix elements we need to diagonalize can be written as

$$\mathscr{H}^{2s}_{u',u;d',d} = \mathscr{H}^{2s}_{u',u} + \mathscr{H}^{2s}_{d',d} \tag{7.49}$$

where $\mathscr{H}^{2s}_{u',u}$ is given in Eqn.(7.32) and $\mathscr{H}^{2s}_{d',d}$ is given by

$$\mathscr{H}^{2s}_{d',d} = \langle d'|\hat{V}_h \mathcal{R}_h^{2s-1}|u\rangle\,;\, \mathcal{R}_h^{2s-1} = \left(\frac{\mathscr{P}}{\mathcal{E}^0 - \hat{H}^0}\hat{V}_h\right)^{2s-1}\;;\mathscr{P} = 1 - \sum_{d=1}^{N}|d\rangle\,\langle d| \quad (7.50)$$

Thus, the nonzero matrix elements are given by

$$\mathscr{H}^{2s}_{d',d} = \left(\frac{h_x}{2}\right)^{2s}\left[\langle d'|S_u^-\left(\frac{\mathscr{P}}{\mathcal{E}^0-\hat{H}^0}S_u^-\right)^{2s-1}|u\rangle + \langle d'|S_{u+1}^-\left(\frac{\mathscr{P}}{\mathcal{E}^0-\hat{H}^0}S_{u+1}^-\right)^{2s-1}|u\rangle\right], \quad (7.51)$$

$$= \mathscr{C}_{h_x}[\langle d'|d+1\rangle + \langle d'|d-1\rangle]; \quad d' = 1,\cdots,N. \quad (7.52)$$

where $\mathscr{C}_{h_x}$ is given by

$$\mathscr{C}_{h_x} = \pm\left(\frac{h_x}{2}\right)^{2s}\prod_{\sigma=1}^{2s}\sqrt{\sigma(2s-\sigma+1)}\prod_{\sigma=1}^{2s-1}\frac{1}{2D\sigma(2s-\sigma)}, \quad (7.53)$$

$$= \pm\frac{8Ds^2}{(2s)!}\left(\frac{h_x}{4D}\right)^{2s} \approx \pm\frac{4Ds^{3/2}}{\pi^{1/2}}\left(\frac{eh_x}{8Ds}\right)^{2s}. \quad (7.54)$$

The final result in Eqn.(7.54) is obtained by Stirling approximation[8]. The magnetic field term displaces the soliton by one sites. Thus, the matrix $[\mathscr{H}_{\mu,\nu}]$, that we must diagonalize is of the form:

$$[\mathscr{H}^{2s}_{\mu,\nu}] = \begin{bmatrix} 0 & \mathscr{C}_{h_x} & \mathscr{C}_J & 0 & \cdots & \mathscr{C}_J & \mathscr{C}_{h_x} \\ \mathscr{C}_{h_x} & 0 & \mathscr{C}_{h_x} & \mathscr{C}_J & \cdots & 0 & \mathscr{C}_J \\ \mathscr{C}_J & \mathscr{C}_{h_x} & 0 & \mathscr{C}_{h_x} & \mathscr{C}_J & \cdots & 0 \\ \vdots & \mathscr{C}_J & \mathscr{C}_{h_x} & \ddots & \ddots & \ddots & \vdots \\ 0 & 0 & \ddots & \ddots & \ddots & \ddots & \mathscr{C}_J \\ \mathscr{C}_J & \cdots & \ddots & \ddots & \mathscr{C}_{h_x} & 0 & \mathscr{C}_{h_x} \\ \mathscr{C}_{h_x} & \mathscr{C}_J & 0 & \cdots & \mathscr{C}_J & \mathscr{C}_{h_x} & 0 \end{bmatrix}. \quad (7.55)$$

[8]The Stirling approximation is given by $n! \approx \sqrt{2\pi n}\left(\frac{n}{e}\right)^n$

The energy band is given by

$$\varepsilon_j = \mathscr{C}_J(\tau_j^2 + \tau_{-j}^2) + \mathscr{C}_{h_x}(\tau_j + \tau_{-j}) = 2\mathscr{C}_J \cos\left(\frac{4\pi j}{N}\right) + 2\mathscr{C}_{h_x} \cos\left(\frac{2\pi j}{N}\right). \quad (7.56)$$

In terms of the Brillouin zone we have

$$\varepsilon_q = \pm 2|\mathscr{C}_J| \cos(2qa) \pm 2|\mathscr{C}_{h_x}| \cos(qa). \quad (7.57)$$

For a single spin, $J = 0$, then Eqn.(7.45) reduces to $\hat{H} = -DS_z^2 + h_x S_x$, thus Eqn.(7.57) reduces to the exact energy splitting, $2|\mathscr{C}_{h_x}|$ found by Garanin [46].

7.5 Conclusion and Discussion

We have studied the one-dimensional anisotropic Heisenberg spin chain in the perturbative and the non-perturbative limits. We considered two different cases: even number of sites and odd number of sites. For even number of sites, we obtained the exact instanton trajectory and its action, as well as the ground state and the first excited state with the corresponding energy splitting between them. The ground state correspond to the antisymmetric superposition of the two classical degenerate Néel states, while the first excited state corresponds to symmetric combination for half-odd integer spins. In the thermodynamic limit, we found that the energy splitting vanishes and the two Néel states become degenerate, allowing for long range order. These two states break the discrete translational invariance of the system; however, there is no Goldstone bosons as this symmetry is not continuous.

For odd number of sites, we showed that the Néel state contains a broken bond, resulting in a defect which causes a domain wall between two fully anti-aligned states. As this domain wall (soliton) can be placed anywhere along the cyclic chain, the resulting energy is N-fold degenerate in each sector. To obtain the energy band we restricted our consideration to the one-soliton states and we made two assumptions. First, we assume

a strong easy axis anisotropy so that the solitons are well localized, which enables us to use perturbation theory. Second, we assume a small interaction and magnetic field terms, which induces quantum fluctuations around the soliton, thereby giving dynamics to the soliton, causing it to hop. The soliton hops over two sites due to quantum fluctuations stemming from the interaction term, while the fluctuation from the magnetic field causes the soliton to hop over one site. The dynamics of the soliton lifts the degeneracy and the states form a band. For the one-soliton states, we obtained this energy band explicitly using perturbation theory for any spin values. For integer spins, we found that the ground state is unique and non-degenerate, while for half-odd integer spin the ground state is doubly degenerate in accordance with Kramers' theorem. In the non-perturbative limit, that is strong interaction, there is no solution yet for the odd spin chain.

7.6 Article for one-dimensional quantum large spin chain

The article for one-dimensional quantum large spin chain below is published in Physics Letters A. Reprinted from Ref.[107], copyright (2014), with permission from Elsevier. We conceived the idea of this paper. My contributions to the originality, problem formulation, methodology, and results are commensurate with my supervisor's (co-author) contributions.

Haldane-like antiferromagnetic spin chain in the large anisotropy limit

S. A. Owerre and M. B. Paranjape
Groupe de physique des particules, Département de physique, Université de Montréal, C.P. 6128, succ. centre-ville, Montréal, Québec, Canada, H3C 3J7

ABSTRACT

We consider the one dimensional, periodic spin chain with N sites, similar to the one studied by Haldane [1], however in the opposite limit of very large anisotropy and small nearest neighbour, anti-ferromagnetic exchange coupling between the spins, which are of large magnitude s. For a chain with an even number of sites we show that actually the ground state is non degenerate and given by a superposition of the two Neél states, due to quantum spin tunnelling. With an odd number of sites, the Neél state must necessarily contain a soliton. The position of the soliton is arbitrary thus the ground state is N-fold degenerate. This set of states reorganizes into a band. We show that this occurs at order $2s$ in perturbation theory. The ground state is non-degenerate for integer spin, but degenerate for half-odd integer spin as is required by Kramer's theorem [18].

Introduction- The study of quantum spin chains has attracted considerable attention in condensed matter and particle physics over the years. They play a decisive role in the study of strongly correlated quantum systems. In both experimental and theoretical physics, models of quantum spin chain are one of the most fundamental systems endowed with interesting phenomenon. The breakthrough in this subject was begun by the work of Bethe and Hulthén [2, 3] for one-dimensional ($D = 1$), isotropic Heisenberg spin-$\frac{1}{2}$ antiferromagnetic chain. They computed the exact antiferromagnetic ground state and its energy for an infinite chain. Anderson [4] had worked out the ground state energies and the spectrum for $D = 1, 2, 3$ by means of spin wave theory. The inclusion of an anisotropy term introduces much interesting physics ranging from quantum computing [5] to optical physics [6]. The resulting Hamiltonian now possesses two coupling constants which can compete against each other:

$$\hat{H} = -K\sum_{i=1}^{N} S_{i,z}^2 + \lambda\sum_{i=1}^{N} \vec{S}_i \cdot \vec{S}_{i+1} \tag{1}$$

Each spin has magnitude $|\vec{S}_i| = s$ and we will consider the large s limit. The two limiting cases are weak anisotropy $\lambda \gg K$ and weak exchange coupling $\lambda \ll K$, where λ is the Heisenberg exchange interaction coupling constant and K is the anisotropy coupling constant. The limit of weak anisotropy was studied by Haldane [1] in a closely related model. He demonstrated that in the large spin limit, $s \gg 1$, the system can be mapped to a non-linear sigma model in field theory with distinguishing effects between integer and half-odd integer spins. The full rotational symmetry of the interaction term is broken to rotational symmetry about the z-axis with the total z-component $S_{i,z} = \sum_i S_{i,z}$ conserved. The Hamiltonian also possesses a discrete symmetry about the z-axis $S_{i,z} \to -S_{i,z}$. In this letter we will also study the large spin limit, but take the opposite limit of strong anisotropy.

With $\lambda = 0$, the ground state is 2^N fold degenerate, corresponding to each spin in the state $S_z = \pm s$. For an even number of sites, the model is bi-partite, and the two fully anti-aligned Neél states are good starting points to investigate the ground state. For an odd number of sites, the Neél states are frustrated, they must contain at least one defect, which are sometimes called domain wall solitons [7]. There is a high level of degeneracy as the soliton can be placed anywhere along the cyclic chain and this degenerate system is the starting point to investigate the ground state for the case of an odd number of sites. Frustrated systems are of great importance in condensed matter physics as they lead to exotic phases of matter such as spin liquid[8], spin glasses[9] and topological orders [10]. Solitons will also occur on the periodic chain with even number of sites, but they must occur in soliton anti-soliton pairs. Villain [7] has studied the one-dimensional XXZ antiferromagnetic spin chain, however for spin-$\frac{1}{2}$ close to the Ising limit, where our analyses are quite parallel.

Many physical magnetic systems such as $CsNiF_3$ and Co^{++} have been modelled with Hamiltonians of the form of Eq.(1). Models of this form have been of research interest over the years since the work of Haldane[1]. To mention but a few, quite recently, the ground state phase diagrams of the spin-2 XXZ anisotropic Heisenberg chain has been carefully investigated by the infinite system density-matrix-renormalization group (iDMRG) algorithm[22] and other numerical methods[21]. For spin-1 XXZ anisotropic Heisenberg chain, the numerical exact diagonalization has been extensively investigated for finite size systems [19]. For an arbitrary spin, the phase diagrams and correlation exponents of an XXZ anisotropic Heisenberg chain has also been studied by representing the spins as a product of $2s$ spin $\frac{1}{2}$ operators[20]. These research works have been focused on ground state phase diagrams and the existence of Haldane phase (conjecture). In this letter, we will study the spin chain with Hamiltonian given by the simple

form given in Eq.(1) with periodic boundary condition $\vec{S}_{N+1} = \vec{S}_1$, and we consider $K \gg \lambda > 0$, *i.e.* strong easy-axis anisotropy and perturbative Heisenberg antiferromagnetic coupling. In the first part of this letter we will concentrate on the existence of macroscopic quantum tunneling of the Hamiltonian defined in Eq.(1) for the case of even spin chain. This analysis will be based on spin coherent state path integral formalism, which is appropriate for large spin systems. The second path of this letter will deal with the case of odd spin chain. In this case spin coherent state path integral formalism fails to give any reasonable result. Thus, our analysis will be based on perturbation theory.

Spin wave theory- We will begin by understanding the excitation spectrum of our model Hamiltonian in Eq.(1). In our model, we expect the spin waves to have a large gap. This is because a spin wave corresponds to introducing a local deviation of the spins away from their respective highest or lowest values of S_z. This incurs energy cost controlled by the free Hamitonian $\hat{H}_0$. Thus the energy cost is proportional to K. Noticing that the classical ground states of our model are locally the fully anti-aligned Neél states, we can introduce small quantum fluctuations in the spirit of Holstein-Primakoff transformation [11]. With a straightforward analysis we obtain that the magnon (spin wave) dispersion is given by [1]

$$\varepsilon_q = \left[\varepsilon_0^2 + \varepsilon_1^2 \sin^2(q)\right]^{1/2} \tag{2}$$

where $\varepsilon_0 = 2s\sqrt{K(K+2\lambda)}$, $\varepsilon_1 = 2s\lambda$ and $-\pi \leq q \leq \pi$. As $K \neq 0$ and in fact large, the magnon dispersion has a large gap.

Even number of sites and spin coherent state path integral- Let us consider our model, Eq.(1) for N even. The ground state of the free theory (K term) is 2^N fold degenerate corresponding to each spin in the highest (lowest) weight states $m = \pm s$. In the degenerate subspace, there are two fully aligned states $|\uparrow,\uparrow,\uparrow,\uparrow,\cdots,\uparrow,\uparrow\rangle$ and $|\downarrow,\downarrow,\downarrow,\downarrow,\cdots,\downarrow,\downarrow\rangle$ and two fully anti-aligned Neél states $|\ p\rangle = |\uparrow,\downarrow,\uparrow,\downarrow,\cdots,\uparrow,\downarrow\rangle$ and $|\ -p\rangle = |\downarrow,\uparrow,\downarrow,\uparrow,\cdots,\downarrow,\uparrow\rangle$ where the arrow denotes the highest (lowest) weight states i.e $m = s \equiv \uparrow (m = -s \equiv \downarrow)$ for each individual spin and the remaining degenerate states are produced by flipping individual spins relative to these extremal states. These two Neél states $|\ \pm p\rangle$ have the lowest energy at first-order in perturbation theory, however they are not exact eigenstate of the quantum Hamiltonian in Eq.(1), thus we expect ground state quantum tunneling coherence between them. Such tunneling is usually mediated by an instanton trajectory, and the exponential of the instanton action (multiplied by a prefactor) yields the energy splitting. A convenient way to obtain this instanton trajectory is via spin coherent state path integral formalism[13, 14, 16], which is the appropriate formalism for large spin systems. In this formalism, the spin operators become unit vectors parameterized by spherical coordinates. The corresponding Lagrangian in this formalism is given by

$$\begin{aligned} L_E = is\sum_i \dot{\phi}_i(1-\cos\theta_i) + K\sum_i \sin^2\theta_i \\ + \lambda\sum_i [\sin\theta_i \sin\theta_{i+1}\cos(\phi_i - \phi_{i+1}) + \cos\theta_i\cos\theta_{i+1}] \end{aligned} \tag{3}$$

The first term is the usual Wess-Zumino [15] term which arises from the non-orthogonality of spin coherent states while the other two terms correspond to the anisotropy energy and the exchange energy. Quantum amplitudes are obtained via the path integral. Solutions of the (Euclidean) classical equations of motion give information about quantum tunnelling amplitudes. The classical equation of motion for ϕ_i yields

$$\begin{aligned} is\frac{d(1-\cos\theta_i)}{d\tau} = \sin\theta_{i-1}\sin\theta_i\sin(\phi_{i-1}-\phi_i) \\ - \sin\theta_i\sin\theta_{i+1}\sin(\phi_i - \phi_{i+1}) \end{aligned} \tag{4}$$

Similar expression holds for the equation of motion for θ_i. Summing both sides of this equation one obtains

$$is\sum_i \frac{d(1-\cos\theta_i)}{d\tau} = 0 \Rightarrow \sum_i \cos\theta_i = l = 0 \tag{5}$$

which corresponds to the conservation of z-component of the total spin $\sum_i S_i^z$, as the full Hamiltonian, Eq.(1), is invariant under rotations about the z axis. A particular solution of Eq.(5) is $\theta_{2k-1} \equiv \theta$, and $\theta_{2k} = \pi - \theta$, $k = 1, 2\cdots, N$. Hence the effective Lagrangian (adding an irrelevant constant) becomes

$$\begin{aligned} L_E^{eff} &= is\sum_{k=1}^{N}\dot{\phi}_k - is\cos\theta\sum_{k=1}^{N/2}(\dot{\phi}_{2k-1} - \dot{\phi}_{2k}) \\ &+ \sum_{i=1}^{N}\left[K + \lambda[1+\cos(\phi_i - \phi_{i+1})]\right]\sin^2\theta \end{aligned} \tag{6}$$

$$= isN\dot{\Phi} - \frac{isN}{2}\dot{\phi}\cos\theta + U_{eff} \tag{7}$$

where $U_{eff} = N[K + \lambda(1+\cos\phi)]\sin^2\theta$ and the last equality is obtained by making the further simplifying ansatz $\phi_i - \phi_{i+1} = (-1)^{i+1}\phi$ effectively reducing to a single spin problem. The instanton that we will find must go from $\theta = 0$ to $\theta = \pi$. Conservation of energy implies $\partial_\tau U_{eff} = 0$, which then must vanish, $U_{eff} = 0$, since it is so at $\theta = 0$. This implies

$$\cos\phi = -\left(\frac{K}{\lambda} + 1\right) \ll 1 \tag{8}$$

since $\sin\theta(\tau) \neq 0$ along the whole trajectory. Thus ϕ is a complex constant which can be written as $\phi = \pi +$

$i\phi_I$ similar to that of two spin case [16]. The classical equation of motion for ϕ gives

$$is\dot{\theta} = -2\lambda \sin\theta \sin\phi = i2\lambda \sin\theta \sinh\phi_I \tag{9}$$

which integrates as

$$\theta(\tau) = 2\arctan\left(e^{\omega(\tau-\tau_0)}\right) \tag{10}$$

where $\omega = (2\lambda/s)\sinh\phi_I$. The instanton is independent of the number of spins and only depends on the initial and the final points. As found in [16] the instanton contributes to the action only through the Wess-Zumino term, as $U_{eff} = 0$ all along the trajectory. The action is given by[16]

$$\begin{aligned} S_c &= S_0 - \frac{isN}{2}\int_0^{\pi+i\phi_I} d\phi \cos\theta|_{\theta=0} - \frac{isN}{2}\int_{\pi+i\phi_I}^{0} d\phi \cos\theta|_{\theta=\pi} \\ &= 0 - isN\pi + Ns\phi_I = -isN\pi + Ns\phi_I \end{aligned} \tag{11}$$

The two Neél states reorganize into the symmetric and antsymmetric linear superpositions, $|+\rangle$ and the $|-\rangle$ as in [16]. The energy splitting is then

$$\Delta = 2\mathscr{D}e^{-S_c} = 2\mathscr{D}\left(\frac{\lambda}{2K}\right)^{Ns}\cos(sN\pi) \tag{12}$$

where $\mathscr{D}$ is a determinantal pre-factor which contains no λ dependence. The factor of λ^{Ns} signifies that this energy splitting arises from $2s\left(\frac{N}{2}\right)$ order in degenerate perturbation theory in the interaction term. The energy splitting, Eq.(12) is the general formula for any even spin N. For $N = 2$ we recover the results obtained previously[12, 16]. The factor sN can be even or odd, depending on the value of the spin. For half odd integer spin, and for $N = 2(2k+1)$ we find Δ is negative which means that $|-\rangle$ is the ground state and $|+\rangle$ is the first excited state. In all other cases, for any value of the spin s and $N = 2(2k)$ we find Δ is positive and then $|+\rangle$ is the ground state, $|-\rangle$ is the first excited state.

Odd spin chain, frustration and solitons- When we consider a periodic chain with an odd number of sites a soliton like defect arises due to the spin frustration. The fully anti-aligned Neél like state cannot complete periodically, as it requires an even total number of spins. Thus there has to be at least one pair of spins that is aligned. This can come in the form up-up or down-down while all other pairs of neighbouring spins are in the up-down or down-up combination. As the total z component of the spin is conserved, these states lie in orthogonal super-selection sectors and never transform into each other. The position of the soliton is arbitrary thus each sector is N-fold degenerate. In the first case the total z component of the spin is s while in the second case it is $-s$. We will without loss of generality consider the s sector. These degenerate states are denoted by $|k\rangle$, $k = 1, \cdots, N$ where

$$|k\rangle = |\uparrow,\downarrow,\uparrow,\downarrow,\uparrow,\cdots, \underbrace{\uparrow,\uparrow,}_{k,k+1^{th}\text{ place}}, \cdots,\uparrow,\downarrow\rangle \tag{13}$$

in obvious notation. These states are not as well the exact eigenstate state of the quantum spin Hamiltonian in Eq.(1), thus we also expect ground state quantum tunneling which lifts the degeneracy and recognizes the soliton states into a band. However, spin coherent state path integral formalism could not give the correct result. From Eq.(12) we saw that energy splitting arises from $2s\left(\frac{N}{2}\right)$ order in degenerate perturbation theory in the interaction term. This gives us a clue that the appropriate formalism for the odd quantum spin chain should be perturbation theory. It is convenient to write the Hamiltonian as

$$\hat{H} = \hat{H}_0 + \hat{V} \tag{14}$$

where $\hat{H}_0$ represents the K (free) term and $\hat{V}$ represents the λ (perturbative) term. The states in Eq.(13) have the same energy $E_s = -KNs^2$ from $\hat{H}_0$ and in first order degenerate perturbation theory $E_s = -KNs^2 - \lambda(N-1)s^2 + \lambda s^2 = (-K-\lambda)Ns^2 + 2\lambda s^2$ and are split from the first excited level, which requires the introduction of a soliton anti-soliton pair, by an energy of 4λ. In each order of perturbation theory less than $2s$, the degenerate multiplet of states mixes with states of higher energy, but due to invariance under translation, the corrections brought to each state are identical and the degeneracy is not split. However, at order $2s$, the degenerate multiplet is mapped to itself. This causes it to split in energy and the states to reorganize into a band. Indeed, $\hat{V}^{2s}$ contains the term $(S^-_{k+1}S^+_{k+2})^{2s}$ and $(S^+_{k-1}S^-_k)^{2s}$. These operators represent quantum fluctuations close to the position of the soliton, when acting on the ket $|k\rangle$ flips the anti-aligned pair of spins at positions $k+1, k+2$ and at $k-1, k$ respectively. It is easy to see that flipping this pair of spins has the effect of translating the soliton $|k\rangle \to |k+2\rangle$ and $|k\rangle \to |k-2\rangle$ respectively. All other terms in $\hat{V}^{2s}$ are quantum fluctuations away from the position of the soliton. They map to states out of the degenerate subspace, either inserting a soliton anti-soliton pair or changing the value of S^z to non extremal values, and hence do not contribute to breaking the degeneracy. To compute the splitting and the corresponding eigenstates, we follow [12], we have to diagonalize the $N \times N$ matrix with components $b_{\mu,\nu}$ given by

$$b_{\mu,\nu} = \langle\mu|\hat{V}\mathcal{A}^{2s-1}|\nu\rangle\,, \quad \mu,\nu = 1,2,\cdots,N \tag{15}$$

where $\mathcal{A}^{2s-1} = \left(\frac{\mathcal{Q}}{E_s - \hat{H}_0}\hat{V}\right)^{2s-1}$, and $\mathcal{Q} = 1 - \sum |\,\mu\rangle\langle\mu\,|$. These matrices are a generalization of the 2×2 matrix in [12]. The calculation of the components is straightforward, looking at $b_{\mu,1}$ we find

$$\begin{aligned} b_{\mu,1} = &\left(\frac{\lambda}{2}\right)^{2s}\langle\mu|S^-_2S^+_3\left(\frac{\mathcal{Q}}{E_s-\hat{H}_0}S^-_2S^+_3\right)^{2s-1}|1\rangle \\ &+\left(\frac{\lambda}{2}\right)^{2s}\langle\mu|S^+_NS^-_1\left(\frac{\mathcal{Q}}{E_s-\hat{H}_0}S^+_NS^-_1\right)^{2s-1}|1\rangle\,. \end{aligned} \tag{16}$$

Applying the operators $2s$ times on the right hand side we obtain

$$b_{\mu,1} = \mathcal{C}[\langle\mu|3\rangle + \langle\mu|N-1\rangle] \tag{17}$$

where $\mathcal{C}$ is given by

$$\begin{aligned}\mathcal{C} &= \pm\left(\frac{\lambda}{2}\right)^{2s}\prod_{m=1}^{2s} m(2s-m+1)\prod_{m=1}^{2s-1}\frac{1}{Km(2s-m)} \\ &= \pm K\left(\frac{\lambda}{2K}\right)^{2s}\left[\frac{(2s)!}{(2s-1)!}\right]^2 = \pm 4Ks^2\left(\frac{\lambda}{2K}\right)^{2s}.\end{aligned} \tag{18}$$

The first product in Eqn.(18) comes from the two square roots that accompany the action of the raising and lowering operators, and the second product is a consequence of the energy denominators. The plus or minus sign arises because we have $2s-1$ products of negative energy denominators in Eq.(16), so if s is integer, $2s-1$ is odd and we get a minus sign while for half-odd integer s, $2s-1$ is even and we get a plus sign. Similarly, one can show that $b_{\mu,\nu} = \mathcal{C}[\langle\mu|\nu+2\rangle + \langle\mu|\nu-2\rangle]$ defined periodically of course. Thus we find that the matrix, $[b_{\mu,\nu}]$, that we must diagonalize is a circulant matrix [17]

$$[b_{\mu,\nu}] = \mathcal{C}\begin{pmatrix} 0 & 0 & 1 & 0 & \cdots & 1 & 0 \\ 0 & 0 & 0 & 1 & \cdots & 0 & 1 \\ 1 & 0 & 0 & 0 & 1 & \cdots & 0 \\ \vdots & 1 & 0 & \ddots & \cdots & \ddots & \\ & & \ddots & & & & \\ 1 & \cdots & \ddots & \cdots & 0 & 0 & 0 \\ 0 & 1 & \cdots & 1\cdots & 0 & 0 & 0 \end{pmatrix}. \tag{19}$$

In this matrix each row element is moved one step to the right, periodically, relative to the preceding row. The eigenvalues and eigenvectors are well known. The j^{th} eigenvalue is given by

$$\varepsilon_j = b_{1,1} + b_{1,2}\omega_j + b_{1,3}\omega_j^2 + \cdots + b_{1,N}\omega_j^{N-1} \tag{20}$$

where $\omega_j = e^{i\frac{2\pi j}{N}}$ is the j^{th} , N^{th} root of unity with corresponding eigenvector $|\ \frac{2\pi j}{N}\rangle = (1, \omega_j, \omega_j^2, \cdots, \omega_j^{N-1})^T$, for $j = 0, 1, 2, \cdots, N-1$. For our matrix, Eq.(19), the only nonzero coefficients are $b_{1,3}$ and $b_{1,N-1}$, thus the one soliton energy bands are

$$\begin{aligned}\varepsilon_j &= \mathcal{C}(\omega_j^2 + \omega_j^{N-2}) = \mathcal{C}(\omega_j^2 + \omega_j^{-2}) \\ &= 2\mathcal{C}\cos\left(\frac{4\pi j}{N}\right).\end{aligned} \tag{21}$$

Introducing the Brillouin zone momentum $q = 2j\pi/N$, the energy bands Eq.(21) can be written as

$$\varepsilon_q = 2\mathcal{C}\cos(2q) \tag{22}$$

which is gapless unlike the magnon dispersion in Eq.(2) but is doubly degenerate as the cosine passes through two periods in the Brillouin zone. The exact spectrum is symmetric about the value $N/2$. With $[x]$ the greatest integer not greater than x, the states for $j = [N/2] - k$ and $j = [N/2]+k+1$ for $k = 0, 1, 2, \cdots, [N/2]-1$ are degenerate as $\cos\left(\frac{4\pi([N/2]-k)}{N}\right) = \cos\left(\frac{4\pi([N/2]+k+1)}{N}\right)$ since $[N/2] = N/2 - 1/2$. However the state with $k = [N/2]$ is not paired, only $j = 0$ is allowed. When s is an integer, $\mathcal{C}$ is negative and the unpaired state $j = 0$ is the ground state which is then non-degenerate, but for s a half odd integer, $\mathcal{C}$ is positive, and the ground states are the degenerate pair with $j = [N/2], [N/2]+1$ in accordance with Kramer's theorem [18]. However, in the thermodynamic limit, $N \to \infty$, the spectrum simply becomes doubly degenerate for all values of the spin and gapless.

Conclusion- We have found the ground state and the low lying spectrum for a periodic spin chain in the limit of large spin, large z-component anisotropy and weak antiferromagnetic exchange coupling between nearest neighbours. For even number of sites, we find that the ground state is unique and corresponds to the symmetric or the anti-symmetric superposition of the two fully antialigned Neél states. Then the other combination is split in energy, proportional to $\left(\frac{\lambda}{2K}\right)^{sN}$. We find this result through an instanton using the spin coherent state path integral. Thus in the thermodynamic limit, the two Neél states are the degenerate ground states, actually allowing for long range order. However, there is no spontaneous symmetry breaking, there is explicit symmetry breaking as the z-component anisotropy explicitly breaks the rotational invariance. There is no massless excitation. The first excited state of this system corresponds to the creation of a soliton anti-soliton pair, with a minimum energy cost of 4λ. The magnons (spin waves) are very highly gapped, due to the large anisotropy, with a minimum energy cost $\sim K$. For an odd number of sites the situation is markedly different. There is no fully aligned Neél state as the system is frustrated. The chain must contain at least one soliton. The soliton can be up-up or down-down giving a total z component of spin s or $-s$ respectively. Since the z-component of the spin is conserved, theses states are in orthogonal super-selection sectors. As the position of the soliton is arbitrary, the ground state in each sector is nominally N fold degenerate. Perturbation to the order $2s$ mixes these states into each other, breaking the degeneracy and creating a gapless band and destroying the possibility of long range order. In the thermodynamic limit, the ground state is doubly degenerate in each sector.

Acknowledgments- We thank NSERC of Canada for financial support.

[1] F. D. M. Haldane, Phys. Rev. Lett. **50**, 1153 (1983)

[2] H. Bethe, Z. Physik **71**, 205 (1931)

[3] L. Hulthén, Arkiv Mat. Astron. Fysik **26**A, 1 (1938)

[4] P. W. Anderson, Phys. Rev. **86**, 694 (1952)

[5] Meier F. and Daniel Loss, Phys. Rev. Lett. **86**, 5373 (2001); Florian Meier, Jeremy Levy, Daniel Loss Phys. Rev. B **68**, 134417 (2003)

[6] Jonathan Simon, Waseem S. Bakr, Ruichao Ma, M. Eric Tai, Philipp M. Preiss and Markus Greiner, Nature **472**, 307 (2011)

[7] J. Villain, Physica **79**B, 1 (1975); F. Devreux and J. P. Boucher, J. Phys. Paris **48**, 1663 (1987); H.-J. Mikesha and M. Steiner, Adv. Phys. **40**, 191 (1991); Hans-Benjamin Braun and Daniel Loss, J. Appl. Phys. **79**, 6107 (1996); S. E. Nagler, W. J. L. Buyers, R. L. Armstrong, and B. Briat, Phys. Rev. Lett. **49**, 590 (1982); N. Ishimura and H. Shiba, Prog. of Theo. Phys., **63**, 743 (1980)

[8] L. Balents, Nature **464**, 199 (2010).

[9] K. Binder and A. P. Young, Rev. Mod. Phys. **58**, 801 (1986).

[10] A. Kitaev, Annals of Physics **321**, 2 (2006).

[11] T. Holstein, and H. Primakoff, Phys. Rev. **58**, 1098 (1940); S. A Owerre, Can. J. Phys. **91**, 542 (2013) .

[12] E. M. Chudnovsky and Javier Tejada, Lectures on Magnetism with 128 problems. Rinton Press, Princeton, NJ, (2006); E. M. Chudnovsky , Javier Tejada , Carlos Calero and Ferran Macia, Solutions to Lectures on Magnetism. Rinton Press, Princeton, NJ, (2006); Gwang-Hee Kim, Phys. Rev. B **67**, 024421 (2003); ibid **68**, 144423 (2003)

[13] John R. Klauder Phys. Rev. D **19**, 2349 (1978)

[14] Alexander Altland and Ben Simons, Condensed Matter Field Theory, Cambridge University Press, New York, (2010); Hagen Kleinert, Path Integrals in Quantum Mechanics, Statistics, Polymer Physics and Financial Markets, World scientific publishing Co. Pte. Ltd (2009)

[15] J. Wess, B. Zumino, Phys. Lett. B **37**:95,1971; S.P. Novikov, Usp.Mat.Nauk, 37N5:3-49,1982; E. Witten, Nucl. Phys., B**160**:57,1979.

[16] S. A Owerre and M.B Paranjape, Phys. Rev. B **88**, 220403(R), (2013).

[17] Davis, Philip J., Circulant Matrices, Wiley, New York, 1970

[18] Kramers H. A., Proc. Amsterdam Acad. **33**, 959 (1930)

[19] Wei Chen, Kazuo Hida, and B. C. Sanctuary, Phys. Rev. B **67**, 104401, (2003).

[20] H. J. Schulz, Phys. Rev. B **67**, 6372, (2003).

[21] Takashi Tonegawa, Kiyomi Okamoto, Hiroki Nakano, Toru Sakai, Kiyohide Nomura, Makoto Kaburagi, J. Phys. Soc. Jpn. 80, 043001 (2011).

[22] Jonas A. Kjäll, Michael P. Zaletel, Roger S. K. Mong, Jens H. Bardarson, Frank Pollmann, Phys. Rev. B **87**, 235106, (2013).

CONCLUSION

A conclusion is the place where
you got tired thinking.

Martin H. Fischer

In this thesis we have lucidly studied recent theoretical and experimental developments on macroscopic quantum tunneling and quantum-classical phase transitions of the escape rate in large spin systems. We employed different theoretical formalisms. We studied biaxial ferromagnetic single molecule magnets and antiferromagnetic exchange-coupled dimer systems using coordinate dependent spin coherent state path integral formalism. For biaxial ferromagnetic system with z-easy axis anisotropy, we found that the real instanton trajectory is in the θ coordinate, while the ϕ coordinate is an complex constant, in contrast to other choices of biaxial ferromagnetic spin systems. As the action for the trajectory is completely determined by the Wess-Zumino term, which in this case is either real or zero; it is not evident how to recover the suppression of tunneling for half-odd integer spins. We showed that in this model there are four complex solutions for ϕ, comprising two instanton paths and two anti-instanton paths. The quantum phase interference is obtained by translating ϕ from zero to these complex solutions and back to zero; the exponentials of the two actions add and give rise to a factor of $(1+\cos(2\pi s))$ in the energy splitting, which obviously vanish for half-odd integer spins, in accordance with Kramers' degeneracy.

We corroborated these results using coordinate independent version of spin coherent state path integral. Indeed, we showed that the suppression of tunneling at zero magnetic field for half-odd integer spin systems, is independent of the coordinate representation. In the presence of a magnetic field applied along the spin hard anisotropy axis direction, tunneling splitting oscillates with the field. We presented the experimental confirmation of this serendipitous theoretical prediction. With the advance in technology, these molecular magnets have been used in the implementation of Grover's

algorithm and magnetic qubits in quantum computing [83, 131]. Recently, experimental and theoretical research on single-molecule magnets are leaning towards the search for new molecular magnets that exhibit tunneling and crossover temperatures. This is an active research area, and it is rapidly expanding. For the antiferromagnetic dimer model with an easy axis anisotropy, we found the low energy eigenvalues and the corresponding eigenstates. We found that the two states $|\downarrow,\uparrow\rangle; |\uparrow,\downarrow\rangle$ reorganize into symmetric and anti-symmetric superposition due to quantum tunneling. The symmetric combination is the lowest-energy state for integer spins, while the anti-symmetric state is the lowest-energy state for half-odd integer spins. These states are respectively the ground states for the dimer. The nature of the low-energy states of this dimer in the perturbative limit, allowed us to map the system onto an entangled pseudospin $1/2$ two-level system. For a dimer which is free to rotate about the staggered easy-axis, we obtained the eigenstates and eigenvalues of this system. The average values of the system observables were calculated and plotted with the parameters of the system. We briefly discussed the environmental influence on the rotating dimer. These results can be applied to a free magnetic dimer clusters in a cavity. It is also useful in quantum computation using entangled two-qubit states.

Furthermore, we employed the effective potential formalism, which paved the way for investigating quantum-classical phase transitions of the escape rate in large spin systems. For the biaxial ferromagnetic system with a magnetic field applied along the medium axis, we obtained the analytical expressions for the instanton trajectories and the crossover temperatures. Indeed, we showed that the boundary between the first- and the second-order phase transitions is greatly influenced by the magnetic field. For the dimer model in the presence of a staggered magnetic field, we derived the exact free energy function, the periodic instanton trajectory, and its corresponding action at zero magnetic field. The regimes of first- and second-order phase transitions, as well as the crossover temperatures were obtained in the presence of the magnetic field. These results are experimentally accessible.

Last but not least, we considered Haldane-like antiferromagnetic spin chain, which comprises the Heisenberg exchange interaction and an easy axis anisotropy. For even number of sites, we found the energy splitting in the perturbative and the non-perturbative limits, using the instanton approach via the spin coherent state path integral. The ground state is unique and corresponds to the symmetric or the anti-symmetric superposition of the two fully anti-aligned Neél states (depending on whether the spin is an integer or half-odd integer). In the perturbative limit, the first excited state is split from the ground state with an energy proportional to $\left(\frac{J}{2D}\right)^{sN}$, where D is large. Thus, in the thermodynamic limit $N \to \infty$, the energy splitting vanishes and the two Neél states become the degenerate ground states, which spontaneously break the discrete translation invariance of the Hamiltonian. However, as this is not a continuous symmetry, we found that there is no massless excitation. For odd number of sites, the situation is markedly different. There is no fully aligned Neél state as the system is frustrated; the cyclic chain must contain at least one soliton. The soliton can be up-up or down-down giving a total z component of spin s or $-s$ respectively. Since the z-component of the spin is conserved, these states are in orthogonal super-selection sectors. As the position of the soliton is arbitrary, the ground state in each sector is nominally N-fold degenerate. In the perturbative limit, order $2s$ in degenerate perturbation theory mixes these states into each other, breaking the degeneracy, and creating a gapless band; thus, destroying the possibility of long range order. For integer spins the ground state is unique and non-degenerate, while for half-odd integer spins the ground state is doubly degenerate in accordance with Kramers' theorem. In the thermodynamic limit, the ground state becomes doubly degenerate for both integer and half-odd integer spins. In the non-perturbative limit, however, no solution has been reported in any literature for the odd spin chain.

BIBLIOGRAPHY

[1] Garg A. Topologically quenched tunnel splitting in spin systems without Kramers' degeneracy. *Europhys. Lett.*, 22:205, 1993.

[2] Garg A. Large transverse-field tunnel splittings in the Fe_8 spin Hamiltonian. *Phys. Rev. B*, 60:6705, 1999.

[3] Garg A. Quenched spin tunneling and diabolical points in magnetic molecules. II. Asymmetric configurations. *Phys. Rev. B*, 64:094414, ibid 094413, 2001.

[4] Garg A., Evgueny Kochetov, Kee-Su Park, and Michael Stone. Spin coherent-state path integrals and the instanton calculus. *J. Math. Phys.*, 44:48, 2003.

[5] M. Abramowitz and Stegun I. A. *Handbook of Mathematical Functions*. New York: Dover, 1972.

[6] Ian Aflleck. Quantum-statistical metastability . *Phys. Rev. Lett.*, 46:388, 1981.

[7] Alexander Altland and Ben Simons. *Condensed Matter Field Theory*. Cambridge University Press, 2000.

[8] P. W. Anderson. An approximate quantum theory of the antiferromagnetic ground state. *Phys. Rev.*, 86:694, 1952.

[9] D. D. Awshalom, J. F. Smyth, G. Grinstein, D. P. DiVencenzo, and D. Loss. Macroscopic quantum tunneling in magnetic proteins. *Phys. Rev. Lett.*, 68:3092, 1992.

[10] L. Balents. Spin liquids in frustrated magnets. *Nature*, 464:199, 2010.

[11] Bernard Barbara and Chudnovsky E. M. Macroscopic quantum tunneling in anti-ferromagnets. *Phys. Lett. A*, 145:205, 1990.

[12] M. V. Berry. Quantal phase factors accompanying adiabatic changes.

[13] H. Bethe. Zur Theorie der Metalle. I. Eigenwerte und Eigenfunktionen der linearen Atomkette. *Z. Physik*, 71:205, 1931.

[14] K. Binder and A. P. Young. Spin glasses: Experimental facts, theoretical concepts, and open questions. *Rev. Mod. Phys.*, 58:801, 1986.

[15] M. Blasone and Petr Jizba. Nambu-Goldstone dynamics and generalized coherent-state functional integrals. *J. Phys. A: Math. Theor.*, 45:244009, 2012.

[16] Hans-Benjamin Braun and Daniel Loss. Chiral quantum spin solitons. *J. Appl. Phys.*, 79:6107, 1996.

[17] Hans-Benjamin Braun, Jiri Kulda, Bertrand Roessli, Dirk Visser, Karl W. Krämer, Hans-Ulrich Güdel, and Peter Böni. Emergence of soliton chirality in a quantum antiferromagnet. *Nature Physics*, 1:159, 2005.

[18] P. F. Byrd and M. D. Friedman. *Handbook of Elliptic Integrals for Engineers and Scientists*. Springer, New York, 1979.

[19] Wei Chen, Kazuo Hida, and B. C. Sanctuary. Ground-state phase diagram of S=1 XXZ chains with uniaxial single-ion-type anisotropy. *Phys. Rev. B*, 67:104401, 2003.

[20] E. M. Chudnovsky. Phase transitions in the problem of the decay of a metastable state. *Phys. Rev. A*, 46:8011, 1992.

[21] E. M. Chudnovsky and D. A. Garanin. First- and second-order transitions between quantum and classical regimes for the escape rate of a spin system. *Phys. Rev. Lett.*, 79:4469, 1997.

[22] E. M. Chudnovsky and D. A. Garanin. Quantum-classical escape-rate transition of a biaxial spin system with a longitudinal field: A perturbative approach. *Phys. Rev. B*, 59:3671, 1999.

[23] E. M. Chudnovsky and D. A. Garanin. Quantum statistical metastability for a finite spin. *Phys. Rev. B*, 63:024418, 2000.

[24] E. M. Chudnovsky and L. Gunther. Quantum tunneling of magnetization in small ferromagnetic particles. *Phys. Rev. Lett.*, 60:661, 1988.

[25] E. M. Chudnovsky and X. Martínez-Hidalgo. Non-Kramers freezing and unfreezing of tunneling in the biaxial spin model. *Europhys. Lett.*, 50:395, 2000.

[26] E. M. Chudnovsky and J. Tejada. *Lectures on magnetism*. Rinton Press, 2006.

[27] E. M. Chudnovsky, D. A. Garanin, and X. Martínez Hidalgo. Quantum-classical transition of the escape rate of a uniaxial spin system in an arbitrarily directed field. *Phys. Rev. B*, 57:13639, 1998.

[28] E. M. Chudnovsky, J. Tejada, Carlos Calero , and Ferran Maci. *Problem solutions to lectures on magnetism*. Rinton Press, 2007.

[29] E.M. Chudnovsky and D.A. Garanin. Rotational states of a nanomagnet. *Phys. Rev. B*, 81:214423, 2010.

[30] E.M. Chudnovsky and Michael F. O' Keeffe. Renormalization of the tunnel splitting in a rotating nanomagnet. *Phys. Rev. B*, 83:092402, 2011.

[31] W. T. Coffey, Yu. P. Kalmykov, and J. T. Waldron. *The Langevin Equation*. Word Scientific, Singapore, 1996.

[32] S. Coleman and C.G Callan. Fate of the false vacuum. II. First quantum corrections. *Phys. Rev. D*, 16:1762, 1977.

[33] Sidney Coleman. Fate of the false vacuum: Semiclassical theory. *Phys. Rev. D*, 15:2929, 1977.

[34] Sidney Coleman. *Aspects of Symmetry*. Cambridge University Press, 1985.

[35] L. N. Cooper. Bound electron pairs in a degenerate Fermi gas. *Phys. Rev.*, 104: 1189, 1956.

[36] J.P. Davis, D. Vick, D.C. Fortin, J.A.J. Burgess, W.K. Hiebert, and M.R. Freeman. Nanotorsional resonator torque magnetometry. *App. Phys. Lett.*, 96:072513, 2010.

[37] Paul Dirac. Quantised singularities in electromagnetic field. *Proc. Roy. Soc. (London) A*, 133:60, 1931.

[38] F. Paul Esposito, L.-P. Guay, R. B. MacKenzie, M.B. Paranjape, and L. C. R. Wijewardhana. Field theoretic description of the Abelian and Non-Abelian Josephson effect. *Phys. Rev. Lett.*, 98:241602, 2007.

[39] R. P. Feynman. Space-time approach to non-relativistic quantum mechanics. *Rev. Mod. Phys.*, 20:367, 1948.

[40] R.P. Feynman and A.R. Hibbs. *Quantum Mechanics and Path Integrals*. McGraw-Hill, Inc, 1965.

[41] I. Firastrau, L. D. Buda-Prejbeanu, B. Dieny, and U. Ebels. Spin–orque nano-oscillator based on a synthetic antiferromagnet free layer and perpendicular to plane polarizer. *J. Appl. Phys.*, 113:113908, 2013.

[42] M. S. Foss-Feig and Jonathan R. Friedman. Geometric-phase-effect tunnel-splitting oscillations in single-molecule magnets with fourth-order anisotropy induced by orthorhombic distortion. *Euro. Phys. Lett.*, 86:27002, 2009.

[43] Eduardo Fradkin. *Field Theories of Condensed Matter Systems*. Addison-Wesley, Redwood City, 1991.

[44] Eduardo Fradkin and Michael Stone. Topological terms in one- and two-dimensional quantum Heisenberg antiferromagnets. *Phys. Rev. B*, 38:7215, 1998.

[45] J. R. Friedman, M. P. Sarachik, J. Tejada, and R. Ziolo. Macroscopic measurement of resonant magnetization tunneling in high-spin molecules. *Phys. Rev. Lett.*, 76: 3830, 1996.

[46] D. A. Garanin. Spin tunnelling: a perturbative approach. *J. Phys. A: Math. Gen.*, 24:L61, 1991.

[47] S. Gider, D. D. Awshalom, T. Douglas, S. Mann, and M. Chaprala. Classical and quantum magnetic phenomena in natural and artificial ferritin proteins. *Science*, 77:268, 1995.

[48] V. I. Goldanskii. The role of the tunnel effect in the kinetics of chemical reactions at low temperatures. *Dokl. Acad. Nauk SSSR*, 124:1261, 1959.

[49] V. I. Goldanskii. Tunnel transitions between systems described by the morse potential curves. *Dokl. Acad. Nauk SSSR*, 127:1037, 1959.

[50] D. A. Gorokhov and G. Blatter. Decay of metastable states: Sharp transition from quantum to classical behaviour. *Phys. Rev. B*, 56:3130, 1997.

[51] Kim Gwang-Hee. Quantum-classical transition of the escape rate of a biaxial spin system in a general magnetic field. *J. Appl. Phys.*, 86:1062, 1999.

[52] Kim Gwang-Hee. Quantum phase interference in nanomagnets with tetragonal symmetry. *J. Appl. Phys.*, 91:3289, 2002.

[53] Kim Gwang-Hee. Level splittings in exchange-biased spin tunneling. *Phys. Rev. B*, 67:024421, 2003.

[54] F. D. M. Haldane. Nonlinear field theory of large-spin heisenberg antiferromagnets: Semiclassically quantized solitons of the one-dimensional easy-axis Néel state. *Phys. Rev. Lett.*, 50:1153, 1983.

[55] F. D. M. Haldane. Continuum dynamics of the 1-d heisenberg antiferromagnet: Identification with the O(3) nonlinear sigma model. *Phys. Lett. A*, 93:464, 1983.

[56] C. Henley and J. von Delft. Destructive quantum interference in spin tunneling problems. *Phys. Rev. Lett.*, 69:3236, 1992.

[57] T. Holstein and H. Primakoff. Field dependence of the intrinsic domain magnetization of a ferromagnet. *Phys. Rev.*, 58:1098, 1940.

[58] A. Honecker, F. Meier, Daniel Loss, and B. Normand. Spin dynamics and coherent tunnelling in the molecular magnetic rings Fe_6 and Fe_8. *Eur. Phys. J. B*, 27: 487, 2002.

[59] L. Hulthén. Uber das austauschproblem eines kristalles. *Arkiv Mat. Astron. Fysik*, 26:1, 1938.

[60] Davis Philip J. *Circulant Matrices*. Wiley, New York, 1970.

[61] Gervais J-L. and Sakita B. Extended particles in quantum field theories. *Phys. Rev. D*, 11:2943, 1975.

[62] Gervais J-L., Jevicki A., and Sakita B. A collective coordinate method for the quantization of extended systems. *Phys. Rep.*, 23:237, 1976.

[63] Liang J-Q, H .J .W. Müller-Kirsten, D. K. Park, and F. Zimmerschied. Periodic instantons and quantum-classical transitions in spin systems. *Phys. Rev. Lett.*, 81: 216, 1998.

[64] R. Jackiw and Rebbi C. Vacuum periodicity in a Yang-Mills quantum theory. *Phys. Rev. Lett.*, 37:172, 1976.

[65] B. D. Josephson. Possible new effects in superconductive tunnelling. *Phys. Lett.*, 1:251, 1962.

[66] Ersin Keçecioğlu and Anupam Garg. Spin tunneling in magnetic molecules: Quasisingular perturbations and discontinuous SU(2) instantons. *Phys. Rev. B*, 67: 054406, 2003.

[67] Michael F. O' Keeffe and Eugene M. Chudnovsky. Renormalization of the tunnel splitting in a rotating nanomagnet. *Phys. Rev. B*, 83:092402, 2011.

[68] A. Khare and M. B. Paranjape. Suppression of quantum tunneling for all spins for easy-axis systems. *Phys. Rev. B*, 83:172401, 2011.

[69] A. Kitaev. Anyons in an exactly solved model and beyond. *Ann. Phys.*, 321:2, 2006.

[70] Jonas A. Kjäll, Michael P. Zaletel, Roger S. K. Mong, Jens H. Bardarson, and Frank Pollmann. Phase diagram of the anisotropic spin-2 XXZ model: Infinite-system density matrix renormalization group study. *Phys. Rev. B*, 87:235106, 2013.

[71] J. R. Klauder. Path integrals and stationary-phase approximations. *Phys. Rev. D*, 19:2349, 1979.

[72] H. A. Kramers. Théorie générale de la rotation paramagnétique dans les cristaux. *Proc. Amsterdam Acad.*, 33:959, 1930.

[73] H. A. Kramers. Brownian motion in a field of force and the diffusion model of chemical reactions. *Physica*, 7:284, 1940.

[74] L. Landau. Zur theorie der energieubertragung. II. *Phys. Z. Sowjetunion*, 2:46, 1932.

[75] L. D. Landau and E.M. Lifshitz. On the theory of the dispersion of magnetic permeability in ferromagnetic bodies. *Phys. Z. Sowietunion*, 8:153, 1935.

[76] L.D. Landau and E.M. Lifshitz. *Quantum mechanics, 3rd ed.* Pergamon, New york, 1977.

[77] L.D. Landau and E.M. Lifshitz. *Statistical Mechanics, Part 1.* Oxford: Pergamon Press, 1991.

[78] J. S. Langer. Theory of the condensation point. *Ann. Phys.*, 41:108, 1967.

[79] A. I. Larkin and Yu. N. Ovchinnikov. Quantum tunneling with dissipation. *Pis'ma Zh. Éksp. Teor. Fiz.*, 37:322, 1983.

[80] A. I. Larkin and Yu. N. Ovchinnikov. Quantum tunneling with dissipation: The prefactor. *Sov. Phys. JETP*, 59(2):490, 1984.

[81] A. J Leggett. *Quantum Tunneling of Magnetization-QTM'94, p. 1.* Kluwer, Dordrecht Press, 1995.

[82] A. J. Leggett, S. Chakravarty, A. T. Dorsey, Matthew P. A. Fisher, Anupam Garg, and W. Zwerger. Dynamics of the dissipative two-state system. *Rev. Mod. Phys.*, 59:1, 1987.

[83] M. N. Leuenberger and Daniel Loss. Quantum computing in molecular magnets. *Nature*, 410:789, 2001.

[84] E. H. Lieb. The classical limit of quantum spin systems. *Commun. Math. Phys.*, 31:327, 1973.

[85] Daniel Loss and David P. DiVincenzo. Quantum computation with quantum dots. *Phys. Rev. A*, 57:120, 1998.

[86] Daniel Loss, David P. DiVincenzo, and G. Grinstein. Suppression of tunneling by interference in half-integer-spin particles. *Phys. Rev. Lett.*, 69:3232, 1992.

[87] Enz M. and R. Schilling. Magnetic field dependence of the tunnelling splitting of quantum spins. *J. Phys. C: Solid State Phys.*, 19:L711, 1986.

[88] Hu J. M., Zhi-De Chen, and Shun-Qing Shen. Quantum tunneling of two coupled single-molecular magnets. *Phys. Rev. B*, 68:104407, 2003.

[89] Richard MacKenzie. Path integral methods and applications. *arXiv:quant-ph/0004090*, 2000.

[90] Gerald D. Mahan. *Many- Particle Physics, 3rd Edition*. Kluwer Academic/Plenum Pulishers, New york, 2000.

[91] F. Matsubara and S. Inawashiro. Simulation of solitons in an Ising-like $S = \frac{1}{2}$ antiferromagnet on a linear chain. *Phys. Rev. B*, 41:2284, 1990.

[92] F. Meier and Daniel Loss. Thermodynamics and spin tunneling dynamics in ferric wheels with excess spin. *Phys. Rev. B*, 64:224411, 2001.

[93] F. Meier and Daniel Loss. Electron and nuclear spin dynamics in antiferromagnetic molecular rings. *Phys. Rev. Lett.*, 86:5373, 2001.

[94] F. Meier, Jeremy Levy, and Daniel Loss Daniel Loss. Quantum computing with antiferromagnetic spin clusters. *Phys. Rev. B*, 68:134417, 2003.

[95] A. Messiah. *Quantum Mechanics. P. 675, 750ff.* Wiley, New York, 1962.

[96] H. J. W. Müller-Kirsten, S.-Y. Lee, D. K. Park, and F. Zimmerschied. Quantum tunneling and phase transitions in spin systems with an applied magnetic field. *Phys. Rev. B*, 58:5554, 1998.

[97] H. J. W. Müller-Kirsten, D.K.Park, and J.M.S. Rana. First-order phase transitions in quantum-mechanical tunneling models. *Phys. Rev. B*, 60:6662, 1999.

[98] H. J. W. Müller-Kirsten, Y.-B. Zhang, J.-Q. Liang, S.-P. Kou, X.-B. Wang, and F.-C. Pu. Quantum-classical phase transition of escape rates in biaxial spin particles. *Phys. Rev. B*, 60:12886, 1999.

[99] H. J. W. Müller-Kirsten, J.-Q. Liang, D. K. Park, and F.-C. Pu. Quantum phase interference for quantum tunneling in spin systems. *Phys. Rev. B*, 61:8856, 2000.

[100] M. A. Novak and Sessoli R. *Quantum Tunneling of the Magnetization -QTM'94, p. 171*. Kluwer, Dordrecht, 1995.

[101] S. A. Owerre. Spin wave theory of XY model with ring exchange interaction on a triangular lattice. *Can. J. Phys.*, 91:542, 2013.

[102] S. A. Owerre. Rotating entangled states of an exchange-coupled dimer of single-molecule magnets. *J. Appl. Phys.*, 115:153901, 2014.

[103] S. A. Owerre and M. B. Paranjape. Macroscopic quantum tunnelling of two interacting spins. *Phys. Rev. B*, 88:220403(R), 2013.

[104] S. A. Owerre and M. B. Paranjape. Coordinate (in)dependence and quantum interference in quantum spin . *ArXiv:1309.6615 (Submitted to Annals of Physics)*, 2014.

[105] S. A. Owerre and M. B. Paranjape. Quantum-classical transition of the escape rate of a biaxial ferromagnetic spin. *J. Magn. Magn. Mater.*, 93:358, 2014.

[106] S. A. Owerre and M. B. Paranjape. Phase transition between quantum and classical regimes for the escape rate of dimeric molecular nanomagnets in a staggered magnetic field. *Phys. Lett. A*, 378:1407, 2014.

[107] S. A. Owerre and M. B. Paranjape. Haldane-like antiferromagnetic spin chain in the large anisotropy limit. *Phys. Lett. A*, 378:3066, 2014.

[108] S. A. Owerre and M. B. Paranjape. Macroscopic quantum tunneling and quantum-classical phase transitions of the escape rate in large spin systems. *ArXiv:1403.4208 (Submitted to Physics Reports)*, 2014.

[109] P. Talkner P. Hánggi and M. Borkovec. Reaction-rate theory: fifty years after Kramers. *Rev. Mod. Phys.*, 62:251, 1990.

[110] Chang-Soo Park and Anupam Garg. Topological quenching of spin tunneling in magnetic molecules with a fourfold easy axis. *Phys. Rev. B*, 65:064411, 2002.

[111] Chang-Soo Park, Sahng-Kyoon Yoo, Dal-Ho Yoon, and D. K. Park. Escape rate of a biaxial nanospin system in a magnetic field: First- and second-order transitions between quantum and classical regimes. *Phys. Rev. B*, 59:13581, 1999.

[112] Chang-Soo Park, Sahng-Kyoon Yoo, and Dal-Ho Yoon. Quantum-classical crossover of the escape rate in a biaxial spin system with an arbitrarily directed magnetic field. *Phys. Rev. B*, 61:11618, 2000.

[113] K. Park, Mark R. Pederson, Steven L. Richardson, Nuria Aliaga-Alcalde, and George Christou. Density-functional theory calculation of the intermolecular exchange interaction in the magnetic Mn_4 dimer. *Phys. Rev. B*, 68:020405, 2003.

[114] C. Paulsen and J.-G. Park. *Quantum Tunneling of the Magnetization -QTM'94, p. 189*. Kluwer, Dordrecht, 1995.

[115] A. Perelomov. *Generalized Coherent States and Their Applications*. Springer, 1986.

[116] A. N. Polyakov. Compact gauge fields and the infrared catastrophe. *Phys. Lett. B*, 59(1):82, 1975.

[117] Dashen R., B. Hasslacher, and A. Neveu. Nonperturbative methods and extended-hadron models in field theory. I. Semiclassical functional methods. *Phys. Rev. D*, 10:4114, ibid; 4130, ibid; 4138, 1974.

[118] I. I. Rabi. Space quantization in a gyrating magnetic field. *Phys. Rev.*, 51:652, 1937.

[119] J. M. Radcliffe. Some properties of coherent spin states. *J. Phys. A: Gen. Phys.*, 4:313, 1971.

[120] M. Razavy. An exactly soluble Schrodinger equation with a bistable potential. *Am. J. Phys.*, 48:285, 1980.

[121] N. Aliaga-Alcalde G. Christou S. Hill, R. S. Edwards. Quantum coherence in an exchange-coupled dimer of single-molecule magnets. *Science*, 302:1015, 2003.

[122] C. Sangregorio, T. Ohm, C. Paulsen, R. Sessoli, and D. Gatteschi. Quantum tunneling of the magnetization in an iron cluster nanomagnet. *Phys. Rev. B*, 78: 4645, 1997.

[123] G . Scharf, W. F Wreszinski, and J. L van Hemmen. Tunnelling of a large spin: mapping onto a particle problem. *J. Phys. A: Math. Gen* ., 20:4309, 1987.

[124] M. O. Scully and M. S. Zubairy. *Quantum Optics*. University Press, Cambridge, 1997.

[125] R. Sessoli, W. Wernsdorfer, D. Gatteschi A. Caneschi, D. Mailly, and A. Cornia. Landau-Zener method to study quantum phase interference of Fe_8 molecular nanomagnets (invited). *J. Appl. Phys.*, 87:5481, 2000.

[126] Jonathan Simon, Waseem S. Bakr, Ruichao Ma, M. Eric Tai, Philipp M. Preiss, and Markus Greiner. Quantum simulation of antiferromagnetic spin chains in an optical lattice. *Nature*, 472:307, 2011.

[127] P. C. E. Stamp, E. M. Chudnovsky, and B. Barbara. Quantum tunneling of magnetization in solids. *Int. J. Mod. Phys. B*, 6:1355, 1992.

[128] M. Stone, Kee-Su Park, and Anupam Garg. The semiclassical propagator for spin coherent states. *J. Math. Phys.*, 41:8025, 2000.

[129] K. L. Taft, C. D. Delfs, G. C. Papaefthymiou, S. Foner, D. Gatteschi, and S. J. Lippard. [Fe(OMe)2(O2CCH2Cl)]10, a molecular ferric wheel. *J. Am. Chem. Soc.*, 116(3):823, 1994.

[130] J. Tejada, X. X. Zhang, E. del Barco, J. M. Hernández, and E. M. Chudnovsky. Macroscopic resonant tunneling of magnetization in ferritin. *Phys. Rev. Lett.*, 79: 1754, 1997.

[131] J. Tejada, E. del Barco, J. M. Hernández, E. M. Chudnovsky, and T. P. Spiller. Magnetic qubits as hardware for quantum computers. *Nanotechnology*, 12:181, 2001.

[132] L. Thomas, F. Lionti, R. Ballou, R. Sessoli D. Gatteschi, and B. Barbara. Macroscopic quantum tunnelling of magnetization in a single crystal of nanomagnets. *Nature*, 383:145, 1996.

[133] R. Tiron, W. Wernsdorfer, N. Aliaga-Alcalde, and G. Christou. Quantum tunneling in a three-dimensional network of exchange-coupled single-molecule magnets. *Phys. Rev. B*, 68:140407(R), 2003.

[134] R. Tiron, W. Wernsdorfer, and N. Aliaga-Alcalde D. Foguet-Albiol, and G. Christou. Spin quantum tunneling via entangled states in a dimer of exchange-coupled single-molecule magnets. *Phys. Rev. Lett.*, 91:227203, 2003.

[135] Takashi Tonegawa, Hiroki Nakano Kiyomi Okamoto, Kiyohide Nomura Toru Sakai, and Makoto Kaburagi. Haldane, large-D and intermediate-D states in an S=2 quantum spin chain with on-site and XXZ anisotropies. *J. Phys. Soc. Jpn.*, 80:043001, 2011.

[136] J. L. van Hemmen and A. Sutő. Tunnelling of quantum spins. *EuroPhys. Lett.*, 1(10):481, 1986.

[137] J. Villain. Propagative spin relaxation in the Ising-like antiferromagnetic linear chain. *Physica B*, 79:1, 1975.

[138] O. Waldmann, C. Dobe, H. U. Gudel, and H. Mutka. Quantum dynamics of the Néel vector in the antiferromagnetic molecular wheel $CsFe_8$. *Phys. Rev. B*, 74: 054429, 2006.

[139] U. Weiss and W. Haeffner. Complex-time path integrals beyond the stationary-phase approximation: Decay of metastable states and quantum statistical metastability. *Phys. Rev. D*, 27:2916, 1983.

[140] W. Wernsdorfer and R. Sessoli. Quantum phase interference and parity effects in magnetic molecular clusters. *Science*, 284:133, 1999.

[141] W. Wernsdorfer, E. Bonet Orozco, K. Hasselback, A. Benoit, D. Mailly, O. Kubo, H. Nakano, and B. Barbara. Macroscopic quantum tunneling of magnetization of single ferrimagnetic nanoparticles of barium ferrite. *Phys. Rev. Lett.*, 79:4014, 1997.

[142] W. Wernsdorfer, R. Sessoli, D. Gatteschi A. Caneschi, and A. Cornia. Nonadiabatic Landau-Zener tunneling in Fe_8 molecular nanomagnets. *Europhys. Lett.*, 50:552, 2000.

[143] W. Wernsdorfer, S. Bhaduri, C. Boskovic, G. Christou, and D. N. Hendrickson. Spin-parity dependent tunneling of magnetization in single-molecule magnets. *Phys. Rev. B*, 65:180403(R), 2002.

[144] W. Wernsdorfer, R. Tiron, D.N. Hendrickson, N. Aliaga-Alcalde, and G. Christou. Quantum dynamics of exchange biased single-molecule magnets. *J. Magn. Magn. Mater.*, 272:1037, 2004.

[145] W. Wernsdorfer, N. E. Chakov, and G. Christou. Quantum phase interference and spin-parity in Mn_{12} single-molecule magnets. *Phys. Rev. Lett.*, 95:037203, 2005.

[146] J. Wess and B. Zumino. Consequences of anomalous Ward identities. *Phys. Lett. B*, 37:95, 1971.

[147] E. Witten. Baryons in the 1N expansion. *Nucl. Phys. B*, 160:57, 1979.

[148] O.B. Zaslavskii. Spin tunneling and the effective potential method. *Phys. Lett. A*, 145:471, 1990.

[149] O.B. Zaslavskii. Quantum decay of a metastable state in a spin system. *Phys. Rev. B*, 42:992, 1990.

[150] O.B. Zaslavskii and V.V. Ulyanov. New methods in the theory of quantum spin systems. *Phys. Rep.*, 214:179, 1992.

[151] C. Zener. Non-adiabatic crossing of energy levels. *Proc. R. Soc. Lond. A*, 137: 696, 1932.

[152] W. M. Zhang, Da Hsuan Feng, and Robert Gilmore. Coherent states: Theory and some applications. *Rev. Mod. Phys.*, 62:867, 1990.

[153] X. X. Zhang, J. M. Hernández, F. Luis, J. Bartolomé, J. Tejada, and R. Ziolo. Field tuning of thermally activated magnetic quantum tunnelling in Mn_{12}-Ac molecules. *Europhys. Lett.*, 35:301, 1996.

[154] Y.-B. Zhang, J.-Q. Liang, H.J.W. Müller-Kirsten, Jian-Ge Zhou, F. Zimmerschied, and F.-C. Pu. Enhancement of quantum tunneling for excited states in ferromagnetic particles. *Phys. Rev. B*, 57:529, 1998.

[155] Y.-B. Zhang, Yihang Nie, J.-Q. Liang, H.J.W. Müller-Kirsten, Supeng Kou, and F.-C. Pu. Periodic instanton and phase transition in quantum tunneling of spin systems. *Phys. Lett. A*, 253:345, 1999.

Appendix I

Computation of derivatives

The derivatives of Eqn.(6.61) and Eqn.(6.60) at the top of the barrier r_b are given by

$$\mu(r_b) = \frac{1-\alpha^2}{4D(1-\alpha^2+\kappa)}; \quad \mu'(r_b) = \frac{-\kappa\alpha^2(1-\alpha^2)}{4D(1-\alpha^2+\kappa)^2};$$
$$\mu''(r_b) = \frac{-\kappa(1-\alpha^2)(1-\alpha^4+\kappa(1-3\alpha^2))}{8D(1-\alpha^2+\kappa)^3}. \tag{I.1}$$

$$U(r_b) = 2D\tilde{s}^2\alpha^2; \quad U'(r_b) = 0;$$
$$U''(r_b) = -D\tilde{s}^2\frac{(1-\alpha^2)^2\kappa}{(1-\alpha^2+\kappa)}; \quad U'''(r_b) = 3D\tilde{s}^2\alpha\frac{(1-\alpha^2)^2\kappa^2}{(1-\alpha^2+\kappa)^2};$$
$$U''''(r_b) = -\frac{D\tilde{s}^2(1-\alpha^2)\kappa[(1+\kappa)(1-2\kappa)+\alpha^4(1+3\kappa)+\alpha^2(-2+\kappa(-2+9\kappa))]}{(1-\alpha^2+\kappa)^3};$$
$$\omega_b^2 = 4D^2\tilde{s}^2\kappa(1-\alpha^2); \quad g_1 = \frac{\alpha\kappa}{2(1-\alpha^2+\kappa)}; \quad g_2 = 0. \tag{I.2}$$

The expansion of the complete elliptic integrals in Eqn.(6.92) near the top of the barrier $Q \to 0$ are given by

$$\mathcal{K}(\lambda) = \frac{\pi}{2}\left[1 + \frac{(1+\kappa)}{4\kappa}Q + \frac{(1+\kappa)(9\kappa-7)}{64\kappa^2}Q^2 + \frac{(1+\kappa)(17+\kappa(25\kappa-22))}{256\kappa^3}Q^3\right]; \tag{I.3}$$

$$\Pi(\gamma^2,\lambda) = \frac{\pi}{2}\left[1 + \frac{(3+\kappa)}{4\kappa}Q + \frac{\kappa(14+9\kappa)-3}{64\kappa^2}Q^2 + \frac{7-\kappa(1-\kappa(25\kappa-33))}{256\kappa^3}Q^3\right]. \tag{I.4}$$